

Advanced Vehicle Concepts and Implications for NextGen

*Matt Blake
Jim Smith
Ken Wright
Ricky Mediavilla*

Sensis Corporation
85 Collamer Crossings
East Syracuse, NY 13057

Michelle Kirby
Holger Pfaender
John-Paul Clarke
Vitali Volovoi
Georgia Institute of Technology

Christopher Dorbian
Akshay Ashok
Tom Reynolds
Ian Waitz
James Hileman
Massachusetts Institute of Technology
Sarav Arunachalam
University of North Carolina

Rosa Weber
Honeywell International

Matt Hedrick
Lakshmi Vempati
CSSI, Inc.

Ryan Laroza
Wim den Braven
ATAC Corporation

Jeff Henderson
Husni Idris
Engility Corporation

Submitted to:
NASA Ames Research Center
Receiving Section, Bldg 255
Moffett Field, CA 94035-1000

NASA STI Program in Profile

Since its founding, NASA has been dedicated to the advancement of aeronautics and space science. The NASA scientific and technical information (STI) program plays a key part in helping NASA maintain this important role.

The NASA STI program operates under the auspices of the Agency Chief Information Officer. It collects, organizes, provides for archiving, and disseminates NASA's STI. The NASA STI program provides access to the NASA Aeronautics and Space Database and its public interface, the NASA Technical Report Server, thus providing one of the largest collections of aeronautical and space science STI in the world. Results are published in both non-NASA channels and by NASA in the NASA STI Report Series, which includes the following report types:

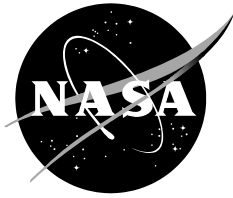
- **TECHNICAL PUBLICATION.** Reports of completed research or a major significant phase of research that present the results of NASA Programs and include extensive data or theoretical analysis. Includes compilations of significant scientific and technical data and information deemed to be of continuing reference value. NASA counterpart of peer-reviewed formal professional papers but has less stringent limitations on manuscript length and extent of graphic presentations.
- **TECHNICAL MEMORANDUM.** Scientific and technical findings that are preliminary or of specialized interest, e.g., quick release reports, working papers, and bibliographies that contain minimal annotation. Does not contain extensive analysis.
- **CONTRACTOR REPORT.** Scientific and technical findings by NASA-sponsored contractors and grantees.

- **CONFERENCE PUBLICATION.** Collected papers from scientific and technical conferences, symposia, seminars, or other meetings sponsored or co-sponsored by NASA.
- **SPECIAL PUBLICATION.** Scientific, technical, or historical information from NASA programs, projects, and missions, often concerned with subjects having substantial public interest.
- **TECHNICAL TRANSLATION.** English-language translations of foreign scientific and technical material pertinent to NASA's mission.

Specialized services also include organizing and publishing research results, distributing specialized research announcements and feeds, providing help desk and personal search support, and enabling data exchange services.

For more information about the NASA STI program, see the following:

- Access the NASA STI program home page at <http://www.sti.nasa.gov>
- E-mail your question via the Internet to help@sti.nasa.gov
- Fax your question to the NASA STI Help Desk at 443-757-5803
- Phone the NASA STI Help Desk at 443-757-5802
- Write to:
NASA STI Help Desk
NASA Center for Aerospace Information
7115 Standard Drive
Hanover, MD 21076-1320



Advanced Vehicle Concepts and Implications for NextGen

*Matt Blake
Jim Smith
Ken Wright
Ricky Mediavilla*

Sensis Corporation
85 Collamer Crossings
East Syracuse, NY 13057

Michelle Kirby
Holger Pfaender
John-Paul Clarke
Vitali Volovoi
Georgia Institute of Technology

Christopher Dorbian
Akshay Ashok
Tom Reynolds
Ian Waitz
James Hileman
Massachusetts Institute of Technology
Sarav Arunachalam
University of North Carolina

Rosa Weber
Honeywell International

Matt Hedrick
Lakshmi Vempati
CSSI, Inc.

Ryan Laroza
Wim den Braven
ATAC Corporation

Jeff Henderson
Husni Idris
Engility Corporation

Submitted to:
NASA Ames Research Center
Receiving Section, Bldg 255
Moffett Field, CA 94035-1000

Contents

1.	Summary and Conclusions.....	24
1.1.	Vehicle Business Cases.....	26
1.2.	Demand Generation	27
1.3.	Vehicle Design.....	29
1.4.	New York Metroplex Analysis	31
1.5.	Washington DC Metroplex Analysis	32
1.6.	Systemwide Delay Results.....	33
1.7.	Weather Impacts	34
1.8.	Analysis of Controller and Pilot Workload.....	34
1.9.	Safety	35
1.10.	Avionics	37
1.11.	Environmental Impacts	37
1.12.	Metrics	38
1.13.	NextGen Observations	39
1.14.	Appendixes.....	40
2.	Introduction.....	41
3.	Previous Work.....	43
4.	Research Method.....	46
5.	Vehicle Business Cases.....	49
5.1.	CESTOL.....	49
5.2.	VLJ.....	52
5.3.	UAS.....	52
5.4.	LCTR	55
5.5.	SST.....	55
6.	Demand Generation	57
6.1.	Baseline demand	57
6.2.	New Vehicle Demand Sets	65
7.	Vehicle Design.....	72
7.1.	CESTOL.....	72
7.2.	VLJ.....	72
7.3.	UAS.....	72

7.4.	LCTR	73
7.5.	SST	73
7.6.	Vehicle Modeling Approaches.....	73
8.	New York Airspace Design	174
8.1.	Background	174
8.2.	Design Principles	175
8.3.	Procedure Design	177
8.4.	Runway Configurations	183
8.5.	Conclusion	185
8.6.	References	185
9.	New York Metroplex Analysis	190
9.1.	SIMMOD	190
9.2.	Airspace Modeling	190
9.3.	Runway Configuration Procedures	197
9.4.	Off-nominal Modeling	203
9.5.	Additional Modeling Details.....	204
9.6.	Metroplex Demand	207
9.7.	Results	211
10.	Washington DC Metroplex Analysis	245
10.1.	Research Method.....	245
10.2.	Reliever Airport Selection	247
10.3.	Simulation Results	252
10.4.	Conclusion	258
11.	Systemwide Delay Results.....	259
11.1.	CESTOL.....	259
11.2.	LCTR	260
11.3.	UAS.....	262
11.4.	VLJ.....	263
11.5.	Comparison of Delay by Scenario	264
12.	Weather Impacts	267
13.	Analysis of Controller and Pilot Workload.....	273
14.	Safety	278
14.1.	System Description	279

14.2.	Identified Hazards	280
14.3.	Qualitative Assessment of Risk	305
14.4.	Certification	316
14.5.	Safety Glossary	321
14.6.	References	325
15.	Avionics	328
15.1.	Avionics to gain access to NextGen Services	329
15.2.	Safety challenges and hazards.....	333
15.3.	Hazards to be mitigated by avionics	333
15.4.	Avionics for Hazard Mitigation	336
15.5.	Advanced Vehicles Avionics Roadmap.....	336
15.6.	Operational Capability: Enhanced Low Altitude Operations	341
15.7.	Operational Capability: Weather Avoidance	345
15.8.	Operational Capability: Terrain, Airspace and Obstacle Avoidance	346
15.9.	Operational Capability: Airborne Collision Avoidance.....	347
15.10.	Operational Capability: Surface Collision Avoidance (Aircraft-based)	351
15.11.	Operational Capability: Wake avoidance & mitigation (Aircraft-based)	357
15.12.	Operational Capability: 3D RNP Arrival and Departure Operations	358
15.13.	Operational Capability: Reduced Oceanic Separation – Altitude Change Maneuvers.	359
15.14.	Operational Capability: Trajectory Clearance with RTA and Downlink	361
15.15.	Aircraft Separation	365
15.16.	Operational Capability: Merging and Spacing.....	365
15.17.	Operational Capability: Delegated Separation in Flow Corridors	367
15.18.	Operational Capability: Self-Separation - Self-Separation Airspace.....	367
15.19.	Operational Capability: Data Link Clearance Delivery and Taxi instructions	372
15.20.	Operational Capability: Increase access and throughput at uncontrolled airports.....	372
15.21.	Operational Capabilities: Low-Visibility Approach, Landing, Take-Off.....	372
15.22.	Avionics Bibliography	375
16.	Environmental Impacts	380
16.1.	APMT-Impacts.....	381
16.2.	Climate Analysis (System-wide Scale).....	382
16.3.	Air Quality Analysis (Metroplex scale).....	389
16.4.	Noise Analysis (Metroplex Scale)	397

16.5.	Caveats on Environmental Analysis	399
16.6.	Summary of Findings and Potential Follow-on Work	399
17.	Metrics	403
17.1.	Previous Research	403
17.2.	Approach	403
17.3.	Key Performance Areas (KPA) and Key Performance Indicators (KPI).....	406
17.4.	Predictability	409
17.5.	High-Level Metrics Framework.....	410
17.6.	Other Trade Studies Proposed to NASA for Future Research.....	430
17.7.	Metric Gaps.....	439
17.8.	Future Research Capabilities Provided to NASA	441
17.9.	Conclusions	441
17.10.	References	441
17.11.	Metrics Definitions	442
17.12.	Complete Metrics Framework	449
18.	Suggested Topics for Future Research.....	462
18.1.	Policy Implementation Studies	462
18.2.	Transition Studies	463
18.3.	Airport Studies	463
18.4.	Safety Studies.....	464
18.5.	Environmental Studies	465
18.6.	Vehicle Studies	465
18.7.	Major Model Improvements / Studies	467
Appendix A.	Acronym List	471
Appendix B.	AEDT Notes.....	474
Appendix C.	ACES Notes	476
C.1.	ACES Configuration	476
C.2.	Flight Trajectory Simulation.....	477
C.3.	Airport Capacities	478
C.4.	Software Issues	478
C.5.	Output Data Anomalies.....	479
C.6.	References	481
Appendix D.	Procedure Analysis Using TARGETS.....	482

D.1.	Spiral Arrival.....	482
D.2.	Spiral Departure	489
D.3.	Applying Wind in TARGETS.....	491
D.4.	TARGETS Aircraft Performance.....	496
Appendix E.	Safety Analysis of the CESTOL Spiral Approach.....	500
E.1.	Introduction.....	500
E.2.	Analytic Approach	500
E.3.	Spiral and Spiral Descents	501
E.4.	Modeling environment and assumptions	502
E.5.	Results	504
E.6.	Conclusions	510
E.7.	Nomenclature	511
E.8.	References	512
Appendix F.	Calculation of Fuelburn and Emissions Using AEDT	513
F.1.	ACES Data Preprocessing	513
F.2.	Database Modifications.....	514
F.3.	FLEET Database	514
F.4.	AIRPORT Database	515
F.5.	MOVEMENTS Database.....	515
F.6.	EVENTRESULTS Database.....	515
F.7.	Workflow	516
F.8.	Scenarios	517
F.9.	Baseline	520
F.10.	VLJ.....	521
F.11.	UAS.....	522
F.12.	LCTR	524
F.13.	SST	525
F.14.	All-Vehicles	526
F.15.	CESTOL Baseline.....	528
F.16.	CESTOL.....	530
F.17.	Lessons Learned.....	531
Appendix G.	Safety Hazards Table	536
Appendix H.	Summary of Contents for Data DVD.....	587

Figures

Figure 1-1. Model infrastructure used this study.....	25
Figure 4-1. Model infrastructure used to conduct the research in this paper	47
Figure 5-1. Passenger departures by airport.....	50
Figure 5-2. LaGuardia airport (left) and simultaneous arrival/departure using CESTOL (right).	51
Figure 5-3. Current-day Cessna cargo routes (ASPM)	53
Figure 5-4. Comparison of transportation costs for ground and air.	54
Figure 6-1. Demand level by year at busiest 500 airports for JPDO demand set.....	58
Figure 6-2. Number of flights in baseline demand sets by year using JPDO trim.	60
Figure 6-3. Average delay versus number of flights for three different trimming methods.	61
Figure 6-4. Comparison of daily flights per airframe.....	62
Figure 6-5. Delay versus average number of flights with and without tail-tracking (ACES).....	63
Figure 6-6. Locations of CESTOL-capable airports within 70-nm of OEP airports.....	65
Figure 6-7. Comparison of flight counts at ATL and satellite airports, with business shift (2025)....	66
Figure 6-8. Scheduled routes for the Large Civil Tiltrotor in 2025.	67
Figure 6-9. UAS cargo routes in 2025.....	68
Figure 6-10. VLJ routes in 2025.....	69
Figure 6-11. SST routes 2,000-4,000 nm (2040).....	70
Figure 6-12. SST longest routes (2040)	70
Figure 6-13. Number of new vehicle flights by scenario (100% trimmed).....	71
Figure 7-1. Performance and fuel burn estimation flow.....	76
Figure 7-2. Runways available at public airports in the United States by runway length.	78
Figure 7-3. CESTOL payload-range design goal.	80
Figure 7-4. CESTOL design mission profiles.	80
Figure 7-5. Effects of slotted wing on transonic air flow.....	81
Figure 7-6. MACW trailing edge designed for a high altitude long endurance aircraft.....	81
Figure 7-7. L/D improvement (Airbus A320) with variable geometry trailing edge ³⁰	82
Figure 7-8. Boeing 787 airframe construction.	83
Figure 7-9. Spiral descent and steep approach concept for CESTOL.....	85

Figure 7-10. Impact of steep approach on landing field length.....	85
Figure 7-11. Interactive design technology trade environment.....	87
Figure 7-12. CESTOL configuration evolution.....	88
Figure 7-13. CESTOL configuration overview.....	89
Figure 7-14. CESTOL cabin arrangement.....	90
Figure 7-15. CESTOL general arrangement.	91
Figure 7-16. Tail volume coefficients correlated with fuselage geometry parameters.	91
Figure 7-17. Schematic of CESTOL engine.....	92
Figure 7-18. High lifting device arrangements and scheduling.	93
Figure 7-19. Lift curves and drag polars for different high lifting device settings.	93
Figure 7-20. CESTOL lift-to-drag ratio at 35000 ft and Mach 0.78.	96
Figure 7-21. Very light jet mission profile.....	100
Figure 7-22. Eclipse 500 general dimensions.....	101
Figure 7-23. VLJ payload range chart.....	104
Figure 7-24. Notional configuration of advanced VLJ.	104
Figure 7-25. FedEx Super CargoMaster ³	107
Figure 7-26. Interior of Super CargoMaster ³	107
Figure 7-27. Standard mission profile of UAS.....	107
Figure 7-28. Three views of Grand Caravan.....	109
Figure 7-29. Comparison of fuel consumption.....	111
Figure 7-30. Comparison of payload-range performance.	111
Figure 7-31. NASA's heavy-lift rotorcraft configurations.....	113
Figure 7-32. LCTR2 design mission profile.....	115
Figure 7-33. LCTR2 geometry model for VASCOMP.....	116
Figure 7-34. LCTR2 weight composition (excluding fuel weight).....	116
Figure 7-35. Figure of merit data.	117
Figure 7-36. Reformation of static MRP/IRP/MCP data.	118
Figure 7-37. MCP and fuel flow model for various mach numbers.....	119
Figure 7-38. Non-optimal power modeling.....	119

Figure 7-39. Hover ceiling comparison.....	120
Figure 7-40. Cruise velocity comparison.	120
Figure 7-41. Detailed mission profile for LCTR2 design mission.....	121
Figure 7-42. Power required, fuel consumption and flow comparison for mission segments.	122
Figure 7-43. LCTR2 weight comparison.....	122
Figure 7-44. Takeoff trajectory.	124
Figure 7-45. Departure trajectory.	124
Figure 7-46. Approach and landing trajectory.	125
Figure 7-47. Forces on tiltrotor aircraft in initial climb.	126
Figure 7-48. Drag models for takeoff (TO), initial climb (IC), and climb (CR) configurations.....	128
Figure 7-49. Forces on tiltrotor aircraft in landing.....	129
Figure 7-50. Drag models for cruise (CR), approach (AP), and landing (LD).	129
Figure 7-51. Thrust models for takeoff, climb, and cruise.	130
Figure 7-52. Thrust models for cruise, descent, approach, and landing.....	130
Figure 7-53. Comparison of takeoff, climb, and cruise.....	131
Figure 7-54. Comparison of cruise, descent, approach, and landing.	131
Figure 7-55. Fuel flow model (comparison with VASCOMP analysis results).....	132
Figure 7-56. Flight trajectory comparison.....	133
Figure 7-57. Total fuel burn comparison.....	133
Figure 7-58. A-weighted sound exposure level (SEL) for LCTR.	138
Figure 7-59. Thrust comparisons between actual thrust and modeled forward thrust.	139
Figure 7-60. SEL contour for departure.	140
Figure 7-61. SEL contour for approach.....	140
Figure 7-62. Left – AE3007 turbofan engine. Right – AE1107C turboshaft engine.	141
Figure 7-63. SST mission profile.	144
Figure 7-64. Concorde dimensions.....	146
Figure 7-65. Conceptual configuration design space.	149
Figure 7-66. Mixed-flow turbofan model.....	150
Figure 7-67. Supersonic transport integrated modeling environment.	151

Figure 7-68. Percentage of composite components in commercial aircraft.	154
Figure 7-69. Sample of SST configurations.	156
Figure 7-70. Engine trade study.	156
Figure 7-71. Jet velocity trade.	157
Figure 7-72. Detailed sonic boom carpet.	159
Figure 7-73. Sonic boom overpressure vs. perceived loudness (MS = Multiple Shock Signature)...	159
Figure 7-74. Boom loudness of various aircraft.	160
Figure 7-75. SST converged geometry.	161
Figure 7-76. Airport noise analysis (Left: departure, right: arrival).	163
Figure 7-77. SST cruise NOx emissions.	164
Figure 7-78. Supersonic transport challenges.	165
Figure 7-79. Mission profile comparison.	166
Figure 7-80. Performance comparison.	167
Figure 7-81. Configuration comparison.	167
Figure 8-1. Overview of procedures.	175
Figure 8-2: CESTOL Spiral.	180
Figure 8-3 LCTR departure location from LGA runway 13.	182
Figure 8-4. Zoomed in view of paths near JFK, LGA, EWR, and TEB.	184
Figure 8-5. Runway Configuration 1.	186
Figure 8-6. Runway Configuration 2.	187
Figure 8-7. Runway Configuration 3.	188
Figure 8-8. Runway Configuration 4.	189
Figure 9-1. N90 current airspace route structure.	191
Figure 9-2. Average departure flight duration.	193
Figure 9-3. Average arrival flight duration.	194
Figure 9-4. Total flight duration comparison.	195
Figure 9-5. Cumulative arrival throughput comparison.	195
Figure 9-6. Cumulative departure throughput comparison.	195
Figure 9-7. NextGen airspace model development.	196

Figure 9-8. CESTOL and VLJ spiral arrival procedure (left) and departure (right).	197
Figure 9-9. Modeled runway configurations at JFK.	198
Figure 9-10. Modeled runway configuration at EWR.	199
Figure 9-11. Modeled runway configurations at LGA.	200
Figure 9-12. Modeled runway configuration at TEB.	200
Figure 9-13. Modeled runway configuration at FRG.	201
Figure 9-14. Modeled runway configurations at HPN.	202
Figure 9-15. Modeled runway configuration at ISP.	202
Figure 9-16. Modeled runway configuration at SWF.	203
Figure 9-17. NextGen airspace flight and storm cell tracks.	204
Figure 9-18. Average delay for 100-iteration simulation.	205
Figure 9-19. VLJ demand.	208
Figure 9-20. Number of flights by airport for the 2040 Baseline and CESTOL scenarios.	209
Figure 9-21. Number of flights by airport for the 2086 Baseline and CESTOL scenarios.	209
Figure 9-22. Number of flights by airport for the 2025 Baseline and CESTOL scenarios.	209
Figure 9-23. Number of flights by airport for the 2040 Baseline and All Vehicles scenarios.	211
Figure 9-24. Number of flights by airport for the 2086 Baseline and All Vehicles scenarios.	211
Figure 9-25. Number of flights by airport for the 2025 Baseline and All Vehicles scenarios.	211
Figure 9-26. Average arrival delay vs. number of flights for all demand years.	212
Figure 9-27. Average departure queue delay vs. number of flights for all demand years.	212
Figure 9-28. Average arrival delay per flight at VLJ airports for 2040.	213
Figure 9-29. Average departure queue delay per flight at VLJ airports for 2040.	213
Figure 9-30. Metroplex operating envelopes for 2086.	214
Figure 9-31. HPN operating envelopes for 2086.	214
Figure 9-32. Percent of total fuel burn versus percent of total flights.	215
Figure 9-33. DNL noise contour comparison at HPN for 2086.	218
Figure 9-34. Average arrival delay vs. number of arrivals for all demand years.	218
Figure 9-35. Average departure queue delay vs. number of departures for all demand years.	218
Figure 9-36. Average arrival delay vs. number of flights at EWR for all demand years.	219

Figure 9-37. Average arrival delay vs. number of flights at JFK for all demand years.	219
Figure 9-38. Average departure queue delay vs. number of flights at EWR for all demand years....	219
Figure 9-39. Average departure queue delay vs. number of flights at JFK for all demand years.	219
Figure 9-40. Metroplex operating envelopes for the 2086 demand.	220
Figure 9-41. Percent of total fuel burn versus percent of flights.	221
Figure 9-42. Percent of total fuel burn versus percent of passengers carried.	221
Figure 9-43. Percent of total NO _x versus percent of flights.	222
Figure 9-44. Percent of total NO _x versus percent of passengers.	222
Figure 9-45. DNL noise contour comparison at EWR for the 2025 demand.	224
Figure 9-46. JFK operating envelopes for Plan 1.	225
Figure 9-47. JFK operating envelopes for Plan 2.	225
Figure 9-48. JFK operating envelopes for Plan 3.	226
Figure 9-49. JFK operating envelopes for Plan 4.	226
Figure 9-50. EWR operating envelopes.	227
Figure 9-51. LGA operating envelopes for Plans 1 and 2.	228
Figure 9-52. LGA operating envelopes for Plan 3 and 4.	228
Figure 9-53. TEB operating envelopes.	229
Figure 9-54. Average arrival delay vs. number of arrivals for all demand years.	230
Figure 9-55. Average departure queue delay vs. number of departures for all demand years.	230
Figure 9-56. Average arrival delay at individual airports.	231
Figure 9-57. Average departure queue delay at individual airports.	231
Figure 9-58. Average arrival delay vs. number of arrivals at EWR for all demand years.	231
Figure 9-59. Cumulative arrival air delay vs. cumulative throughput for 2040.	232
Figure 9-60. Metroplex operating envelopes for 2040.	233
Figure 9-61. Percent of total fuel burn vs. percent of flights.	233
Figure 9-62. Percent of total fuel burn vs. percent of passengers carried.	233
Figure 9-63. Baseline DNL noise contour (left) vs. all-vehicle case (right) for EWR (2086).	237
Figure 9-64. ISP 60-70dB DNL noise contours for all-vehicles scenario.	237
Figure 9-65. Running total of storm intensity affecting JFK.	238

Figure 9-66. Running total of storm intensity affecting SWF.....	238
Figure 9-67. Average arrival delay vs. number of arrivals for all demand years.....	239
Figure 9-68. Average departure queue delay vs. number of departures for all demand years.....	239
Figure 9-69. Average arrival delay and storm intensity for 2025 all-vehicles case.....	239
Figure 9-70. Average departure delay and storm intensity for 2025 all-vehicles case.....	239
Figure 9-71. Average arrival air delay and storm intensity for the 2025 Baseline scenario.....	240
Figure 9-72. Average departure delay and storm intensity for the 2025 Baseline scenario.....	240
Figure 9-73. Cumulative difference in nominal and actual arrivals for 2025.....	241
Figure 9-74. Cumulative difference in nominal and actual departures for 2025.....	241
Figure 9-75. Metroplex operating envelopes for the off-nominal 2025 demand year.....	241
Figure 9-76. Total Fuel Burn for the all aircraft groups in the 2040 demand year.....	242
Figure 9-77. Total NO _x for all aircraft groups in 2040.....	242
Figure 10-1. BWI proposed vertiport location.....	246
Figure 10-2. Potomac TRACON redesigned airspace in 2025.....	248
Figure 10-3. BWI and reliever airport.....	249
Figure 10-4. Example Pareto Curves for IAD.....	250
Figure 10-5. Comparison of the ACES nodal model (left) and runway model (right).....	250
Figure 10-6. Superposition of airport and vertiport.....	251
Figure 10-7. Distribution of BWI operations by runway (fully trimmed case).....	252
Figure 10-8. DC Metroplex flight distribution (fully-trimmed case).....	253
Figure 10-9. Average delay in 2025.....	254
Figure 10-10. Average delay in 2040.....	255
Figure 10-11. DC Metroplex average delay by airport in 2025 (fully-trimmed case).....	256
Figure 10-12. DC Metroplex average delay by airport in 2040 (fully trimmed case).....	256
Figure 10-13. Metroplex average delay comparison by airport in 2025 (fully-trimmed case).....	257
Figure 11-1. Flight volume and delay tradeoff curves for projected traffic in 2025 and 2040.....	260
Figure 11-2. Impact of LCTR shuttle flights between high-density airports.....	261
Figure 11-3. Effect of UAS freight-forwarding operations on the NAS.....	262
Figure 11-4. Effect of VLJ operations on the NAS.....	263

Figure 11-5. Systemwide average delay versus number of flights in 2025.....	264
Figure 11-6. Total systemwide delay versus number of seats in 2025.....	265
Figure 11-7. Systemwide average delay versus number of flights in 2040.....	266
Figure 11-8. Total systemwide delay versus number of seats in 2040.....	266
Figure 12-1. NEXRAD storm cells.	267
Figure 12-2. Storm cells and corresponding rectangles used in ACES.....	268
Figure 12-3. Average delay with and without weather	269
Figure 12-5. Histogram of delays (>30 Minutes) with and without weather	270
Figure 12-4. Arrival counts and capacity at ORD for ACES runs with and without severe weather.	269
Figure 12-6. Average delay by major airport for ACES runs with and without weather.....	271
Figure 12-7. Airborne delays due to weather, 2025, 75% trim.	271
Figure 12-8. Path flown by flight UAL112 to avoid thunderstorms.	272
Figure 13-1. Conflict between aircraft departing from EWR and BWI Airports.....	273
Figure 13-2. Flight from EWR to PHX with seven 3-nm conflicts.....	274
Figure 13-3. Locations of 3-nm conflicts (zoomed).....	275
Figure 13-4. Locations of 3-nm aircraft conflicts.	275
Figure 13-5. Number of 3-nm conflicts per aircraft in the 2025 trimmed	276
Figure 13-6. Number of 5-nm conflicts by scenario.	277
Figure 14-1. Safety risk management process.....	278
Figure 14-2. 5M Model	279
Figure 14-3. Fatal accidents and onboard fatalities by phase of flight, 1999-2008 ⁸	281
Figure 14-4. FAA - Loupe One departure ^{9,10}	282
Figure 14-5. Flow corridors (Source: GA Tech/Google Earth).	286
Figure 14-6. Runback ice ¹²	288
Figure 14-7. Accident trends by segments of aviation industry, 1989–2000.	289
Figure 14-8. Risk matrix.....	307
Figure 14-9. Flight path angle versus approach speed (adapted from J. Hileman by A. Hahn).....	310
Figure 14-10. Go-around analysis results for CESTOL (red dot) and range of current operations. ...	311
Figure 14-11. Minimum decision height as a function of rate of sink	312

Figure 14-12. Flight path angle versus approach speed (adapted from J. Hileman by A. Hahn).....	313
Figure 14-13. Time to collision (example).....	315
Figure 15-1 Future communication study – AP17 Final Conclusions and Recommendations.....	332
Figure 15-2 SVS Display displays the Burbank Airport at 200 feet	343
Figure 15-3 SAM advisories for unstable approach.....	344
Figure 15-4 Deep Landing Advisories	344
Figure 15-5 Dynamic, optimal in-flight rerouting around hazards (Baize, 1999).....	346
Figure 15-6. TCAS Advisory Regions	349
Figure 15-7 Taxi map -- Boeing 787 Navigation Display while on the ground at KORD	352
Figure 15-8 Taxi map display of datalinked taxi routes with traffic	353
Figure 15-9 Ground-based ASDE-X Alerts to Cockpits.....	355
Figure 15-10 Runway Safety: using ADS-B In with RAAS and E-GPWS/TAWS.....	356
Figure 15-11 Runway confusion on take off.....	357
Figure 15-12 Vertical Path Performance Limit (VPPL).....	359
Figure 15-13 4DTRAD negotiation.....	362
Figure 15-14 Enroute Traffic Flow	367
Figure 15-15 CD&R methods and their associated time-to-Loss of separation.....	369
Figure 15-16 Medium term, intent-based Conflict Detection	370
Figure 15-17 Short term, state based conflict detection and resolution maneuvers.....	371
Figure 15-18 IPFD during landing	373
Figure 16-1. FAA Aviation Environmental Tools Suite.....	381
Figure 16-2. Aviation climate impacts pathway (from Wuebbles et al., 2007)	382
Figure 16-3. APMT-Impacts Climate Module (from Marais et al.).....	383
Figure 16-4. Yearly fuel burn and NO _x emissions for new vehicle scenarios.....	384
Figure 16-5. Yearly fuel burn and NO _x emissions for CESTOL scenarios.....	385
Figure 16-6 Difference in time-integrated temperature change (K; policy – baseline).....	387
Figure 16-7 Difference in net present value (2005 US\$; policy – baseline).....	387
Figure 16-8. CESTOL temperature impact (policy – baseline)	388
Figure 16-9. CESTOL monetized damages (policy–baseline).....	388

Figure 16-10 Multi-scale modeling domain used in Arunachalam et al. ¹⁶	391
Figure 16-11. AEDT emissions data for Conventional airspace and NextGen airspace.....	392
Figure 16-12. Contribution to PM Species for Conventional and NextGen airspace.	392
Figure 16-13. Composition of PM in conventional and NextGen airspace scenarios.....	393
Figure 16-14. Ambient concentration of total PM over domain.	394
Figure 16-15. Ambient concentration of PM Ammonium over domain.	395
Figure 16-16. Ambient PM2.5 concentration in baseline (left) vs. NextGen operations (right).....	396
Figure 16-17. Delta (NextGen-Conventional) PM radial concentrations.	396
Figure 16-18. Yearly population exposed (CESTOL case).....	399
Figure 17-1: Simplified representation of the NAS as a system with dynamic behavior	404
Figure 17-2: High level metrics framework	411
Figure 17-3: Metrics classification levels.....	412
Figure 17-4: Simulation design to enable iterative runs to deliver acceptable outcomes	413
Figure 17-5: Cause-effect relationships for Capacity vs. Environment trade study.....	416
Figure 17-6: Experiment design with iterative loops for trade study #1	417
Figure 17-7: Radar graph of Capacity vs. Environment national level impacts (notional).....	421
Figure 17-8: Radar graph of Capacity vs. Environment airport level impacts (notional)	421
Figure 17-9: Capacity vs. Efficiency cause-effect relationships	423
Figure 17-10: Experiment design with iterative loops for trade study #2	425
Figure 17-11: Radar graph of Capacity vs. Efficiency airport level impacts (notional)	426
Figure 17-12: Capacity vs. Predictability cause-effect relationships	427
Figure 17-13: Simulation design with iterative loops for trade study #3	429
Figure 17-14: Capacity vs. Predictability national level impacts (notional)	430
Figure 17-15: Access & Equity cause-effect relationships	450
Figure 17-16: Capacity metrics cause-effect relationships	451
Figure 17-17: Cost Effectiveness cause-effect relationships.....	451
Figure 17-18. Efficiency metrics cause-effect relationship.....	452
Figure 17-19: Efficiency metrics cause-effect relationships	454
Figure 17-20: Predictability metrics cause-effect relationships	455

Figure 17-21: Flexibility metrics cause-effect relationships	455
Figure 17-22: Air Quality metrics cause-effect relationships	456
Figure 17-23: Climate change metrics cause-effect relationships.....	457
Figure 17-24: Noise metrics cause-effect relationships	458
Figure 17-25: Fuel Efficiency metrics cause-effect relationships.....	459
Figure 17-26: Human Performance error metrics cause-effect relationships.....	459
Figure 17-27: Accident Risk metrics cause-effect relationships.....	461
Figure 17-1: Complete metrics framework diagram	462
Figure C-1. Auto-Configure Properties (ACP) settings for simulations.....	476
Figure C-2. IFR Vs. VFR Total Rates	478
Figure C-3. Flight trajectory for flight between BOS and JFK.....	479
Figure C-4. Flight crossing into neighboring ARTCC.....	479
Figure C-5. Aircraft counts for one sector as a function of time.....	480
Figure C-6.Flight Counts in Sample Output Tables.....	481
Figure D-1. Overview of the straight segment TF leg spiral arrival.	483
Figure D-2. Depicts flyability on the straight segment TF leg spiral arrival.	483
Figure D-3. Details of the TF leg spiral arrival with speed and altitude restrictions.	484
Figure D-4. Details of the flyability run on the TF leg spiral approach.....	485
Figure D-5. The TF leg spiral approach flyability in Google Earth.....	485
Figure D-6. Spiral approach implemented using TARGETS Route tool and substituting RF legs. ...	486
Figure D-7. Spiral approach using RF legs viewed in Google Earth.	487
Figure D-8. Spiral approach implemented using the TARGETS SAAAR Prototype tool.	488
Figure D-9. Flyability of five sequential RF legs.....	488
Figure D-10. The pseudo spiral departure constructed with TF legs.	489
Figure D-11. Flyability on the pseudo spiral using the CESTOL aircraft.....	489
Figure D-12. Altitude and speed restrictions on the pseudo spiral departure.	490
Figure D-13. The spiral departure constructed with RF legs.	490
Figure D-14. The RF leg spiral departure in Google Earth.....	491

Figure D-15. Wind definition dialogs.	491
Figure D-16. Setting wind in the flyability parameter set properties dialog.	492
Figure D-17. Command to run the flyability on a user defined flyability parameter set.	492
Figure D-18. A wind heading of 270 at 20 kts pushes the aircraft to the west as expected.	492
Figure D-19. A wind heading of 90 at 20 kts pushes the aircraft to the east as expected.	493
Figure D-20. Wind from 90 at 40 kts fails.	494
Figure D-21. Wind from 90 at 30 kts passes.	494
Figure D-22. Wind on spiral departure from 90 at 40 kts passes.	495
Figure D-23. Wind on spiral departure from 90 at 50 kts fails.	495
Figure D-24. Wind on spiral departure from 270 at 50 kts passes.	495
Figure D-25. Wind on spiral departure from 270 at 60 kts fails.	495
Figure D-26. CESTOL Performance in TARGETS.	496
Figure D-27. VLJ Performance in TARGETS.	497
Figure D-28. UAS Performance in TARGETS.	498
Figure D-29. Tiltrotor Performance in TARGETS.	499
Figure E-1. Decoupled arrival and departure routes for four New York metroplex airports ¹¹	502
Figure E-2. Spiral approach ¹¹	503
Figure E-3. Nominal wind profile.	506
Figure E-4. Planar layout of the landing site.	506
Figure E-5. Conventional and spiral landing trajectories in the presence of varying wind.	506
Figure E-6. Separation violation hazard in the presence of a south-west wind.	507
Figure E-7. Separation violation hazard in the presence of a cross wind.	508
Figure E-8. Separation violation hazard in the presence of a tail wind.	509
Figure F-1. Scenario Annualized Comparison	517
Figure F-2. CESTOL Scenario Annualized Comparison	518
Figure F-3. CESTOL Baseline Number of Flights.	519
Figure F-4. CESTOL Number of Flights	519
Figure F-5. Baseline Categorized Fuelburn and NOx Results	520
Figure F-6. Baseline Fuelburn	520

Figure F-7. VLJ Categorized Fuelburn and NOx Results	521
Figure F-8. VLJ Fuelburn.....	521
Figure F-9. UAS Categorized Fuelburn and NOx Results	523
Figure F-10. UAS Fuelburn.....	523
Figure F-11. LCTR Categorized Fuelburn and NOx Results	524
Figure F-12. LCTR Fuelburn	525
Figure F-13. SST Categorized Fuelburn and NOx Results	526
Figure F-14. SST Fuelburn.....	526
Figure F-15. ALL Vehicles Categorized Fuelburn and NOx Results	527
Figure F-16. All-vehicle fuelburn.....	528
Figure F-17. CESTOL Baseline Categorized Fuelburn and NOx Results	529
Figure F-18. CESTOL Baseline Fuelburn.....	529
Figure F-19. CESTOL Categorized Fuelburn and NOx Results	530
Figure F-20. CESTOL Categorized Fuelburn and NOx Results	531

Tables

Table 6-1. Replacements made to the original IPSA baseline demand.....	59
Table 7-1. Comparison of vehicle performance.....	79
Table 7-2. Values used for technology implementation.....	83
Table 7-3. CESTOL technology suite summary.	86
Table 7-4. CESTOL group weight breakdown.....	94
Table 7-5. CESTOL performance.	95
Table 7-6. Comparison of CESTOL performance with current RJs.	96
Table 7-7. Reference data for the Eclipse 500.	101
Table 7-8. FLOPS VLJ model calibration results.	102
Table 7-9. VLJ converged design vehicle comparison.	104
Table 7-10. Main assumptions and requirements for UAS.	110
Table 7-11. UAS performance summary.....	112
Table 7-12. LCTR2 vehicle overview.	114
Table 7-13. Rotor aerodynamic parameters.	117
Table 7-14. Comparison of LCTR and chosen vehicles for baseline noise characteristics.....	134
Table 7-15. The values of required ratios and resultant dB correction amounts.....	137
Table 7-16. Thrust variation during departure operation.	137
Table 7-17. Thrust variation during approach operation.....	138
Table 7-18. Thrust scheduling for departure operation.	139
Table 7-19. Thrust scheduling for approach operation.	139
Table 7-20. Specifications of AE3007 turbofan engine and AE1107C turboshaft engine.	141
Table 7-21. Supersonic system level metrics'.....	142
Table 7-22. SST reference vehicles and attributes.	145
Table 7-23. Concorde weights ⁷¹	147
Table 7-24. Concorde propulsion characteristics ⁷¹	148
Table 7-25. Concorde noise in terminal area ⁷¹	148

Table 7-26. Summary of modeling assumptions.....	151
Table 7-27. SST design variables.....	153
Table 7-28. Technologies contributing to weight reduction.....	154
Table 7-29. Technology weight assumptions.....	155
Table 7-30. Lifting surfaces geometry.....	161
Table 7-31. SST performance summary.....	162
Table 7-32. SST requirements summary.....	165
Table 7-33: Future challenges to investigate.....	166
Table 8-1. Runways at New York Metro Airports.....	177
Table 8-2. LCTR arrival procedure waypoint restrictions.....	181
Table 8-3. LCTR departure procedure waypoint restrictions.....	183
Table 9-1. Arrival lateness probability distribution.....	206
Table 9-2. Minimum Turn-around times in minutes with the cumulative probability distribution. ...	206
Table 9-3. Number of flights by vehicle type in the baseline and VLJ demand sets.....	207
Table 9-4. Number of daily flights by vehicle type in the baseline and CESTOL demand sets.....	208
Table 9-5. Number of flights by vehicle type and airport for the mixed-vehicle demand set.....	210
Table 9-6. Number of flights by vehicle type in the baseline and all-vehicles demand sets.....	210
Table 9-7. Fuel burn gradient.....	216
Table 9-8. CO ₂ gradient.....	216
Table 9-9. NO _x gradient.....	216
Table 9-10. PM gradient.....	217
Table 9-11. Comparison of area (sq. miles) within the 60 dB DNL noise level contour for 2086. ...	217
Table 9-12. Fuel burn gradient.....	221
Table 9-13. CO ₂ gradient.....	222
Table 9-14. NO _x gradient.....	222
Table 9-15. PM gradient.....	223
Table 9-16. Comparison of area (sq. miles) within the 60 dB DNL noise level contour for 2025. ...	223
Table 9-17. Comparison of area (sq. miles) within the 60 dB DNL noise level contour for 2040. ...	224
Table 9-18. Comparison of area (sq. miles) within the 60 dB DNL noise level contour for 2086. ...	224

Table 9-19. Mixed Vehicle (Capacity Experiment) summary.	229
Table 9-20. Fuel burn gradient.	234
Table 9-21. CO ₂ gradient.	234
Table 9-22. NO _x gradient.	235
Table 9-23. PM gradient.	235
Table 9-24. Comparison of area (sq. miles) within the 60 dB DNL noise level contour for 2025. ...	236
Table 9-25. Comparison of area (sq. miles) within the 60 dB DNL noise level contour for 2040. ...	236
Table 9-26. Comparison of area (sq.miles) within the 60 dB DNL noise level contour for 2086.	236
Table 9-27. Comparison of area within 60 dB DNL contour for the All Vehicles demand for 2086.	243
Table 10-1. Major DC airport runway configuration from ASPM for July 13, 2006.	245
Table 10-2. DC Metro area runway configuration for 2025 redesigned airspace.	247
Table 10-3. Driving times between DC Metro airports.	247
Table 14-1. Hazard severity classification.	306
Table 14-2. Likelihood definitions.	306
Table 15-1 NextGen ATS utilization due to unique vehicle missions & capabilities.	328
Table 15-2. Advanced vehicles and the hazards they are especially susceptible to.	334
Table 15-3 Advanced Vehicles Avionics Roadmap.	337
Table 16-1. Environmental impact metrics.	380
Table 16-2. Climate assumptions for new vehicle study.	386
Table 16-3. Mid-range noise input assumptions.	398
Table 17-1: Capacity vs. Environment performance outputs for system-wide and regional analysis	418
Table 17-2: Capacity vs. Efficiency performance metrics for trade study #2.	424
Table 17-3: Capacity vs. Predictability performance metrics for system-wide and regional analysis	428
Table 17-4: Safety performance metrics for system-wide and regional analysis.	432
Table 17-5: Flexibility, access and equity, and predictability metrics for various levels of analysis.	436
Table 17-6: Noise vs. Emissions performance metrics for system-wide and regional analysis.	439
Table 17-7: Identified gaps in metrics.	440

1. Summary and Conclusions

This report presents the results of a major NASA study of advanced vehicle concepts and their implications for the Next Generation Air Transportation System (NextGen). Comprising the efforts of dozens of researchers at multiple institutions, the analyses presented here cover a broad range of topics including business-case development, vehicle design, avionics, procedure design, delay, safety, environmental impacts, and metrics.

The study is motivated by parallel developments that are occurring in air traffic management and vehicle design. Advances in ATM are being driven by improvements in information technology, whereas advances in vehicle design are primarily being driven by breakthroughs in material science, such as the development of lightweight composites that promise to make aircraft lighter and more energy-efficient.

The study focuses on the following five new vehicle types:

- Cruise-efficient short takeoff and landing (CESTOL) vehicles
- Large commercial tiltrotor aircraft (LCTRs)
- Unmanned aircraft systems (UAS)
- Very light jets (VLJs)
- Supersonic transports (SST)

The timeframe of the study spans the years 2025–2040, although some analyses are also presented for a “3X” scenario that has roughly three times the number of flights as today. Full implementation of NextGen is assumed.

Our modeling of NextGen has been necessarily generic because the definition of NextGen is still somewhat hazy, its implementation still only partially determined and described by the FAA. Therefore, specific conclusions, such as the value of one aspect of NextGen over another, are difficult to make and are subject to interpretation. Section 1.14 of this summary gives some observations regarding NextGen. Because NextGen and the new vehicles have not yet been implemented, we relied on expert opinion as well as a variety of models for this study. Figure 1-1 shows the model infrastructure used in this research. Vehicle design was performed at the Georgia Institute of Technology’s Airspace System Design Laboratory (ASDL) using the ASDL Environmental Design Space (EDS) toolkit. EDS was used to compute tradeoffs among different vehicle design variables—weight, fuel burn, noise, emissions, and range—to produce economically feasible and aerodynamically efficient vehicles that would satisfy mission requirements.

To evaluate the efficiency of terminal area procedures, we used the Airport and Airspace Simulation Model (SIMMOD) to compute the trajectories in the terminal area. SIMMOD output includes precise aircraft position and altitude information that are passed to the Aviation Environmental Design Toolkit (AEDT) for noise and emissions analysis. System-wide assessments of throughput and delay were performed using the Airspace Concepts Evaluation System (ACES). The aircraft tracks from ACES, along with the aircraft BADA data created by ASDL, were passed to AEDT to compute emissions and fuel burn. Other models that were used include the FAA’s Terminal Area Route Generation Evaluation & Traffic Simulation (TARGETS) for flyability analysis; the Performance Data Analysis and Reporting System (PDARS), for safety metrics; the Aviation Environmental Portfolio Management Tool (APMT),

for assessing environmental impacts, the Transportation Systems Analysis Model (TSAM), for V LJ demand forecasting; AvDemand for schedule generation; and the Future Air Traffic Management Concepts Evaluation Tool (FACET), for system-wide traffic flow management analysis.

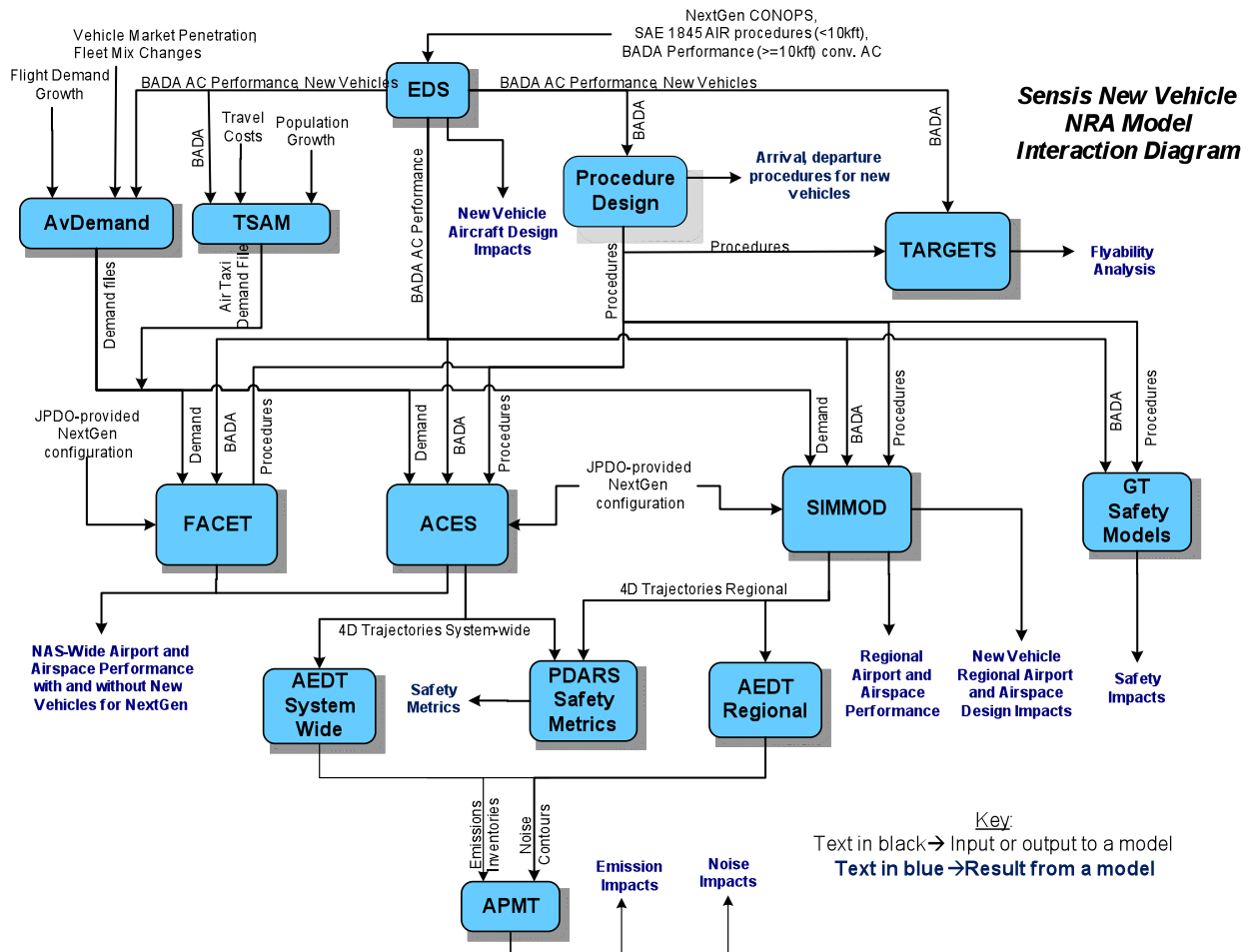


Figure 1-1. Model infrastructure used this study.

The set of models selected and the method for integrating them was highly successful in analyzing performance (e.g. capacity/efficiency), environmental impact, and many aspects of safety for new vehicles in a NextGen world. Moreover, substantial knowledge was gained regarding areas that need to be improved to provide more accurate and capable analyses in the future. These suggested improvements are documented in Section 18.7 as well as in the various detailed sections of the report. One area that is worth emphasizing is the need to do frequent intermediate analysis of results at various points of data exchange within the infrastructure. In a large and complex simulation such as this, there are many opportunities for one model to generate erroneous data, and if the erroneous outputs are used as inputs at successive stages of the process, a lot of time and resources are wasted.

1.1. **Vehicle Business Cases**

Expert opinion was most valuable in defining high-level vehicle performance parameters, vehicle production rates, and realistic missions. The primary external experts for each vehicle included:

- CESTOL: Andy Hahn (NASA)
- VLJ: Bruce Holmes (Holmes Consulting, LLC; formerly of DayJet Corporation, NASA, JPDO)
- UAS: Steve Vail (FedEx)
- LCTR: Larry Young (NASA), Doug Boyd (NASA)
- SST: Jon Seidel (NASA), Jeff Berton (NASA), Bob Welge (Boeing)

Together these experts and the study team developed the following new vehicle missions.

1.1.1. CESTOL

Because of the CESTOL's unique characteristics—its ability to land and take off using a 3,000 foot runway, its slow (103 knot) approach speed, and its 100-passenger size—there are several ways it can be used to enhance throughput in a NextGen environment. It can be used by airlines to offload traffic from congested hubs to nearby reliever airports. Additionally, its short takeoff and landing (STOL) characteristics enable it to utilize underused runways at some existing hubs.

Combined with precise independent approach/departure paths in Metroplexes, the CESTOL could provide a major boost in NAS passenger capacity by flying additional terminal area routes independent of conventional aircraft. The unique ability to fly unconventional (e.g., steep, spiral) approaches is enabled by the NextGen precision routing capability and improved controller information and automation to monitor the more complex airspace. CESTOLs will always have some economic disadvantage and some additional safety and environmental concerns over an equivalent conventional aircraft; so the question is whether the unique flight profiles enabled by NextGen outweigh the greater costs of the CESTOL.

1.1.2. VLJ

For VLJs, the business model assumes that carriers would provide on-demand air taxi service between relatively uncongested airports. The socioeconomic TSAM model was used to estimate future demand for VLJs in the 2025–2040 timeframe, as well as the airports that flights would depart from and arrive to. By avoiding major hub airports, the VLJ business model ends up having little impact on other traffic. The viability of the VLJ is then only a function of the profitability of its business model. If there is demand for a premium priced point-to-point on-demand service between smaller airports in a region, then the VLJ/air taxi seems viable. A significant NextGen improvement for enabling on-demand VLJ operations is VFR-like operations in IFR conditions at non-towered airports.

1.1.3. UAS

The application we chose to examine for the UAS is that of a cargo operator (such as Federal Express) forwarding freight from a spoke airport to a more distant airport. The size of the UAS was

assumed to be similar to that of a Cessna Caravan. It was also assumed that “see and avoid” technology for UASs would be perfected by the timeframe of the study.

By avoiding congested airports, the UAS freight-forwarding mission ends up having no significant impact on capacity or delay. Two key issues are the cost-effectiveness of the business model, and the requirement to address all safety concerns for operating unmanned aircraft throughout the lower density NAS environment. This second issue is common to many UAS missions in the NAS and therefore may be solved in the next few years for government UAS operational purposes. Because the UAS business model replaces ground vehicles with UAS vehicles, a useful environmental analysis would compare the total environmental footprint of the two approaches: future ground vehicles vs. future UAS vehicles for package delivery. The ground alternative was not evaluated in this study; therefore, it is not possible to provide insights on this environmental impact comparison.

1.1.4. LCTR

Because a 90-passenger LCTR has many moving parts it is assumed that it will be more costly to acquire and maintain than a 90-passenger fixed-wing aircraft. Therefore airlines flying LCTRs would have to charge passengers more per seat. The LCTR business model assumes that travelers would pay a premium fare for a flight between popular city pairs that provided much more reliable departure and arrival performance. Because LCTRs utilize vertiports that are separate from an airport’s main runways, LCTRs can get into and out of heavily congested airports more reliably than fixed-wing aircraft.

Combined with precise independent approach/departure paths and new landing pads at congested hubs, the LCTR adds capacity to the busiest short-haul city-to-city routes. However, the drawbacks identified for the CESTOL—increased operating costs, safety, and environmental concerns—are even more pronounced for the LCTR. If NextGen ends up adding significantly more conventional capacity and predictability, then the LCTR business model described here seems unlikely to succeed. If NextGen fails to enable reliable service for conventional aircraft then LCTRs seem much more viable.

1.1.5. SST

For the SST, NASA directed us to look at a 100-passenger aircraft that cruises at Mach 1.6. To meet airport noise requirements we selected an aircraft with a range of 4,000 nm. After consultation with Boeing, we decided that the minimum flight distance that a passenger would be willing to pay a premium fare would be 2,000 nautical miles. Our simulations show that the effect on delay for the SST is negligible because of its small fleet size of 400 to 800 airframes. Despite the small number of airframes, the environmental impact of the SST is quite large, and the current prohibition on sonic booms over land remains unresolved. Moreover, the previous SST airliner (Concorde) was never a financial success, so it remains unclear whether a new SST airliner would be a viable business choice even under NextGen.

1.2. Demand Generation

The study used baseline demand sets that were created by the JPDO's Interagency Portfolio and System Analysis (IPSA) group in 2008. Two were for the years 2025 and 2040; the third was the 3X demand set. The airframes in the JPDO demand sets were the same as today, except for two substitutions made by the JPDO—the super jumbo A380 and the new Boeing 787. Because we expect many of the

older aircraft in the demand set to be replaced by quieter and more fuel-efficient aircraft in the future, we further modified the JPDO baseline demand set, substituting newer airframes for these older ones. These newer airframes include two NASA-envisioned vehicles, the N150 and the N301. The N150 is a single-aisle replacement for aircraft like the B737 and the A320, while the N301 is a twin-aisle replacement for aircraft like the B767 and B777.

The initial schedules that JPDO created using the Terminal Area Forecast (TAF) are based on relatively unconstrained consumer demand. In general they do not account for the finite capacities of airports or airspace (there are some limits on a few major congested airports). When the schedules are flown using ACES, or any other simulator, the delays that result are much longer than would be tolerable in practice. To obtain schedules with reasonable delays, flights are removed from the unconstrained schedules using a process known as trimming. To trim the schedules, JPDO runs the unconstrained demand sets through LMInet, a queuing simulation developed in the late 1990s¹. The flights to be deleted are those that LMInet identifies as having the highest congestion scores; that is, the flights that flew through the most crowded sectors and arrived at or departed from the most crowded airports. Deleting all of the flights from a JPDO list of most congested flights produces a schedule that induces only mild average delay per flight—on the order of two minutes per flight. We refer to the resulting schedule as the 100% trimmed schedule. Deleting half the flights in the list gives what we refer to as the 50% trimmed schedule. The number of flights trimmed from the 2086 schedule is much greater than the number trimmed from the 2025 schedule. To understand the effect of varying demand, we used demand sets at five trim levels: 0%, 25%, 50%, 75% and 100%.

1.2.1. CESTOL

The CESTOL schedules were created by modifying the baseline schedules for 2025, 2040, and 2086. Specifically, whenever the demand-capacity ratio within a 15-minute time-bin at a major airport exceeded 90% of the airport's visual meteorological conditions (VMC) capacity, the excess flights were shifted to a satellite airport that was within 70 nm of the original airport. The equipment type of the shifted flights, all of which had stage lengths less than 600 nm, was converted to CESTOL.

1.2.2. LCTR

As with the CESTOL, the tiltrotor would relieve congestion at major airports by shifting traffic away from runways with high demand at congested airports. Specifically, we identified city pairs having at least fifteen flights in one direction during a single day. Tiltrotors replaced the large aircraft using these routes in a way that preserved the number of aircraft seats. For example, two 150-seat aircraft would be replaced by three tiltrotors. It was assumed, based on expected production rates, that the 2025 scenario would have 300 tiltrotors, the 2040 scenario would have 800, and the 2086 scenario would have 2,300.

1.2.3. UAS

The UAS schedules developed for the New Vehicle NRA assumed 4,000 daily flights between known cargo hubs and spoke airports located 30 to 150 nm away.

1.2.4. VLJ

Using projected demand between city-pairs, the TSAM model computed the number of flights that could be flown in an economically competitive manner by a 4-passenger VLJ given certain assumptions regarding airline operating costs, the price of jet fuel, and the cost of auto travel. Future VLJ demand was created for the 2025 and 2040 datasets but was not created for the 3X dataset. No VLJs fly into major hubs.

1.2.5. SST

Two scenarios were modeled for the SST, a 90-seat aircraft with a maximum range of 4,000 nm. In the first scenario, the SST replaced conventional aircraft on the longest commercial routes having stage lengths under 4,000 nm. In the second scenario, the SST randomly replaced conventional aircraft on randomly selected routes with stage lengths between 2,000 and 4,000 nm. No SSTs were assumed to have been built by 2025; the 2040 and 2086 schedules assumed 400 and 800 SST flights, respectively.

1.3. Vehicle Design

The purpose of developing new vehicle models for the NextGen research task was to provide the capability to represent the new vehicle concepts in the procedure-design, simulation, and analysis tool-sets shown in Figure 1-1. These tools primarily use one of two performance models. The first of these is Eurocontrol's Base of Aircraft Data (BADA)ⁱⁱ, the second is that described in SAE AIR-1845ⁱⁱⁱ.

The five vehicle models specified by NASA for investigation were split into two groups. The first group included the CESTOL, LCTR, and the SST; the second included the VLJ and the UAS. The approach for the first group involved creating detailed performance and sizing models of the aircraft using high fidelity tools to capture the range of performance and then create BADA and AIR-1845 models that approximate the vehicles behavior as closely as possible. The second group was modeled using a relatively high-level characterization approach that was based on directly representing the aircraft in BADA and AIR-1845 using simplified engineering approaches. Both approaches relied on the FAA's Environmental Design Space (EDS) and other NASA tools. When EDS executes an analysis for any aircraft, the required AEDT and ACES information are automatically created in terms of the BADA and AIR 1845 data.

For this study, design of the CESTOL and SST utilized standard EDS capabilities. The SST design required additional EDS analysis capabilities for the aerodynamics and boom signature, and the LCTR design required a separate analysis capability that was specific to rotorcraft sizing and synthesis. Vehicle class models for VLJ and UAS were developed by altering existing BADA and AIR-1845 performance models. The development of new vehicle models starting from these baseline models was a three-part process: (1) Determine or match performance fuel burn over a range of missions; (2) Adjust emissions indices to match engine emissions improvements, and (3) Adjust noise power distance and spectral information to obtain noise benefits.

1.3.1. CESTOL

For this study, the CESTOL aircraft was proposed to be a 100 passenger regional jet cruising at Mach 0.78. It was envisioned to be able to take off and land on a 3000-foot runway—substantially shorter than

a conventional runway—but still cruise at fuel efficiency comparable with a similar-sized existing aircraft. To improve efficiency, the CESTOL design employed a number of innovative technologies including a high-speed slotted wing, a mission-adaptive compliant wing, ultra efficient engine technology, and new composite materials for the airframe. The final design evolved through an iterative design and analysis process involving trade-offs of the major design variables.

1.3.2. VLJ

Currently, air taxi trips for light jets average about 300 nm and range up to 600 nm, but a future VLJ will need to fly slightly longer ranges, to cover more routes. A design range of 750 nm was considered reasonable for this aircraft. Aircraft speed is important for air taxi aircraft, but is not as big a driver as availability and serviceable airfield proximity to destinations, so a modest minimum cruise speed of Mach 0.6 was set. Because air taxi operations will place a higher priority on their on-demand flexibility and less on payload capability, a future VLJ will be smaller than most current light jets, needing to carry at most 4 passengers. We assumed that advances in remote piloting technologies would make a single pilot configuration feasible in the future, however, by allowing a second ‘reserve’ pilot to monitor a flight from the ground and assume control in an emergency. A single remote pilot could even monitor multiple aircraft simultaneously, reducing the number of required salaried pilots by an operator thereby lowering costs. The Eclipse 500 was chosen as the baseline aircraft because of its relative similarity to the anticipated future VLJ and because of the desire to select an aircraft that is currently flying and that has available data.

1.3.3. UAS

A derivative of the Cessna Super CargoMaster was used to model a UAS vehicle that would have an impact on NextGen. Now FedEx is operating more than 250 of these aircraft. This aircraft would need autonomous navigation, sense-and-avoid capability, ground pilot monitoring, and would fly generally like a piloted aircraft. The Cessna Caravan was designed to fly by two pilots. When it is converted to a UAS, however, its operational empty weight cannot benefit much from the weight saving of the pilots, since more avionic equipment is needed for environmental sensing, auto flight, remote control and communication, and actuators. For this study, the fuel consumption of was reduced by 20% from the Grand Caravan, while its range was improved more than 40% for the same payload. Based on the results of Ultra Efficient Engine Technology (UEET) and considering the 40 years improvement in the year of 2025, three assumptions were made on the emissions characteristics of the UAS: 20% reduction in fuel burn, 50% reduction in nitrogen oxide (NO_x), and 8% reduction in all other emissions indices as each throttle setting.

1.3.4. LCTR

Unlike the aircraft discussed above, the LCTR design was dictated completely by NASA. The LCTR concept used was NASA’s LCTR2, a short-haul regional transport entering service in 2018. It can transport 90 passengers (in 32-inch pitch, single class 2-2 seating layout) to the maximum range of 1,200 nm with cruising speed of 300 knots. It has a wing spanning 107 ft and blade folding mechanism with assumed weight penalty of 1,000 lb for each rotor blade. Four advanced 7,500-lb class turbo-shaft engines drive two 65-ft diameter prop-rotors. Because the LCTR design came from NASA, our goal was to create a comparable model with public domain analysis tools such that the required ACES and AEDT analyses

could be completed. This translation is more straightforward in cases of conventional fixed-wing aircraft than the case of tiltrotor aircraft which requires unique interpretations of elementary physical components such as lift and thrust to fit the airspace modeling equations appropriately. During the current work, considerable effort was invested into this translation. Because AEDT cannot simulate vertical thrust of the helicopter mode, the LCTR is modeled as a conventional turboprop aircraft during takeoff and landing.

1.3.5. SST

The environmental impacts of the SST include sonic boom, high altitude cruise, high fuel consumption per passenger, and high level of noise in arrival and departure areas—all of which make the design of the SST a great challenge for its inclusion into NextGen, but also a great source of research opportunities. Commercial supersonic flights over land are currently prohibited by the Federal Aviation Administration (FAA) because of the sonic boom. For the SST, it is more efficient to cruise at higher altitudes (~50,000 ft) for aerodynamics reasons; however, doing so increases the amount of high altitude emissions, which may cause ozone destruction and consequently affect the global climate. To reduce the level of noise in the terminal areas, current commercial transports use large bypass ratio engines to reduce the jet velocity there; however, the SST mission is not well suited for high-bypass ratio engines because of the heavy aerodynamics penalty during supersonic cruise. In addition, the FAA anticipates that “any future Notice of Proposed Rulemaking issued by the FAA affecting the noise operating rules would propose that any future supersonic airplane produce no greater noise impact on a community than a subsonic airplane.”^{iv} Because of the tradeoff between the vehicle performance and the environmental impacts of combustion emissions at high altitudes the maximum cruising altitude of the SST was fixed at 53,000 ft. Based on the selection criteria, the Concorde was selected as the SST reference vehicle. Starting from this reference vehicle, a rich trade space of SST designs was explored based on tradeoffs between range, noise, and environmental impact.

1.4. New York Metroplex Analysis

To address congestion in the New York airspace, we redesigned procedures into and out of New York using a gridded layout that provides all aircraft paths to and from landing and departing runways. The redesign relies on Area Navigation (RNAV) procedures, Required Navigational Performance (RNP), and metering to increase throughput. Conventional aircraft use continuous descent arrival (CDA) procedures but depart in the same manner as today. For almost all the airports, CESTOL aircraft, due to their unique performance characteristics, use spiral paths to arrive and depart. VLJ aircraft also utilize the spiral procedures. LCTR aircraft arrive at constant altitude toward their destination after which they descend to the airport in segments to reduce noise; they depart in the same manner, ascending in segments followed by a constant altitude until they exit the metro area airspace. Supersonic transports use the same paths as conventional aircraft but are metered to maintain separation between aircraft.

Using SIMMOD and AEDT, we compared throughput, delay, emissions and noise for the redesigned New York airspace and today’s airspace. Four runway configuration plans were included in the model which also included spiral approaches for CESTOL and VLJ aircraft. An off-nominal scenario with convective storm cells moving through the NY Metroplex was also studied.

Because VLJs were added to less-congested satellite airports, their addition to the metroplex did not change the overall delay. Additionally, the slow speeds of VLJs had little impact on throughput because

most of the aircraft using the satellite airports were also flying at slow speeds. On a per-flight, per-distance, and per-time basis, VLJs performed better than business jets and regional jets in the terminal airspace. Due to the VLJs limited seating capacity, their performance in fuel burn per passenger is worse than that of regional jets, but better than business jets. Emissions results are similar to those for fuel burn because there is a direct correlation between fuel burn and CO₂. Farmingdale Airport (FRG) had the largest increase in noise contour area (5.4%), but it also had the biggest increase in VLJ flights (23.5%).

The CESTOL scenario showed a substantial reduction in delay compared to the baseline, primarily due to the offloading of flights from Newark International Airport (EWR) to satellite airports. Although CESTOLs operate at slower speeds, their impact on metroplex throughput is minimal. Spiral departure procedures combined with midfield takeoff procedures help mitigate the negative impacts CESTOLs have on departure throughput. Furthermore, the use of underutilized runways for CESTOL operations contributes to an overall increase in the metroplex arrival throughput. Comparing CESTOL vehicles to commercial jets, the CESTOLs have less fuel burn on a per-flight and on a per-passenger basis in the terminal airspace. CESTOL vehicles perform similar to regional jets on a per-flight basis, while carrying more passengers. Except for the relative fuel burn performance in terms of distance, the CESTOL have a better fuel burn performance in the terminal airspace when compared to commercial and regional jets. The relative fuel burn performance in terms of distance is slightly higher for the CESTOL when compared against regional jets. Again CO₂ emissions performance is directly correlated to fuel burn and thus follows the same trends. The day-night average noise level (DNL) noise contours are observed to increase where CESTOLs operate. However, the shift in the number of flights at the different airports, combined with the different aircraft types in the different demand years, make it difficult to isolate the noise impacts of the CESTOL aircraft at the different airports.

A mixed-vehicle capacity experiment was also performed to analyze the effects of the CESTOL and LCTR procedures on airport capacity. The four airports included in this experiment were JFK, EWR, LGA, and TEB. The demand set for this experiment was created to maximally test throughput at the four airports. The experiment showed a significant increase in throughput at EWR due to the CESTOL arrivals to runway 11 and the LCTR arrivals to a nearby landing strip. This increase in throughput offsets a drop in throughput due to the CESTOL's slow arrival speed whenever the aircraft makes a conventional landing on EWR's runway 22. (Airspace constraints prevent the CESTOL from landing using a spiral approach on this runway.) When LCTRs are able to operate on underutilized runways, as is the case at TEB, increased departure throughput is observed. However, when LCTR departures are mixed with other vehicles, their slower operating speeds cause negative impact on throughput and delay.

1.5. *Washington DC Metroplex Analysis*

As with the NY airspace, to assess the impact of NextGen and new vehicles on the Washington DC metroplex we redesigned the DC airspace, creating independent routes to and from all of the runways. The major features of this reorganization include separate arrival and departure fixes and paths for each runway, paths within the terminal area that are separated by at least 1000' vertically and/or 3 nm laterally, no interdependence between airports within the terminal area, and flight paths that avoid current restricted airspace around the DC metropolitan area. We also assumed that all aircraft would be equipped for RNP approaches to accurately fly arbitrary paths. Detailed fix-to-runway paths for each airport and runway were designed, giving particular attention to avoiding conflicts between airports, as well as separating the

CESTOL and LCTR paths from other aircraft. The enhanced terminal modeling capability (or Runway Model) of ACES was used to model the metroplex. Results are consistent with those of for the redesigned New York airspace. They again reveal that CESTOL aircraft have the potential to increase throughput and reduce delay when used with reliever airports and underutilized runways. Moreover, LCTR aircraft reduce delay by utilizing corridors into and out of vertiports, flying routes that do not conflict with conventional aircraft flows. The results also show that adding VLJ and UAS vehicles to the fleet mix does not adversely affect average delay.

1.6. Systemwide Delay Results

This section presents system-wide delay results that were generated using Version 5.0 of ACES. This version of ACES includes a high-fidelity physics-based trajectory integrator that computes the trajectory of each aircraft every half-second from 40 nm of the departure airport to 40 nm of the arrival airport. The baseline capacities provided by JPDO assume NextGen to be fully implemented by 2025, with only small capacity increases after that year. These capacities include all known new and planned runway construction, as well as all JPDO operational improvements. Airport capacities under NextGen have been modeled in detail by JPDO, with NextGen operational improvements increasing average capacity for the top 35 airports by approximately 45%, although there is considerable variation around that average for the individual airports. Similarly, en route sector capacities increased by a factor of 1.7 when all NextGen en route operational improvements were modeled.

1.6.1. CESTOL

The ACES results show an exponential tradeoff between flight volume and system delay. The CESTOL scenario (which shifts many flights to less congested regional airports) shows a substantial reduction in delay compared to the baseline scenario. Or equivalently, at the same level of delay—approximately 6 minutes per flight—the CESTOL scenario can handle approximately 2,500 more flights per day than the baseline in 2025, and 5,000 more flights per day in 2040.

1.6.2. LCTR

The LCTR shuttle flights increase system capacity substantially, although the effect of replacing shuttle flights with LCTRs is smaller than the effect of the CESTOL business-shift strategy. At a constant average NAS-wide delay of 6 minutes the LCTR scenario can handle 1,100 more flights than the baseline scenario in 2025, and 2,700 more flights than the baseline in 2040. Regardless of the state of technology of LCTRs in particular, it remains true that any vehicle capable of landing in a very short (600 feet or shorter) landing pad and capable of flying arrival and departure routes that are procedurally separated from those on the main runways, will increase the capacity of the NAS significantly. Whether airlines are willing to invest in a more costly vehicle like the LCTR remains less clear.

1.6.3. UAS

The volume-delay tradeoff curve for the UAS freight forwarding scenario is essentially flat. This is because the UAS business model adds many small aircraft to the system, but those aircraft depart from uncongested spoke airports and arrive at small remote airports with little traffic. As a result, the entire volume/delay tradeoff curve is simply shifted to the right.

1.6.4. VLJs

Because few VLJs fly into major hubs, their impact on delay is also small. As in the UAS scenario, the VLJ scenario shows a slight decrease in average delay because many aircraft were added without a significant increase in total delay. At a constant average delay of 6 minutes per flight, the VLJ scenario adds 4,000 flights in 2025 and 7,000 flights in 2040. Because the VLJ only carries 4 passengers, it does not substantially increase the capacity of the NAS for carrying passengers.

1.6.5. SST

The effect of the SST on systemwide delay is negligible because, although passengers benefit because the SST flies faster than a conventional aircraft, the simulation adjusts the SST's scheduled arrival time to account for this difference. Moreover, only a subset of the 400 SST aircraft actually fly CONUS routes, and the international SST flights fly like a conventional aircraft during their initial and final phases of flight.

1.7. Weather Impacts

Convective thunderstorms are a major source of disruption in the NAS. Delays during the convective weather months—June, July, and August—are the highest of the year, exceeded only by delays during the worst winter storms. Although NextGen is expected to raise airport capacity in instrument meteorological conditions (IMC), aircraft will not have the ability to fly through severe thunderstorms. To examine the interaction of NextGen and new vehicles in the presence of convective thunderstorms, we ran a small number of ACES simulations incorporating the weather from the day 27 June 2007—a day in which a line of thunderstorms blocked heavily-traveled routes between Chicago and New York.

We found that the addition of weather significantly increased the number of flights with long delays. For example, weather increased average delay per flight at Chicago O'Hare (ORD) from 2 minutes to 12 minutes, at Newark (EWR) from 2 minutes to 11 minutes, and at LaGuardia (LGA) from 4 minutes to 11 minutes. Although most of the increase in delay was caused by the drop in airport capacity when thunderstorms pass directly over an airport, there is also an increase in en route delay due aircraft travelling longer routes to avoid thunderstorms. More than 1,000 flights in the 2025 baseline scenario gained 5 minutes or more of airborne delay due to weather. The data contained 1,156 flights whose airborne times increased by more than 5 minutes in the weather scenario; 216 of these flights gained more than 30 minutes of airborne delay. The longest airborne delay for any flight was two hours; this is a reasonable maximum delay and comparable to the longest airborne delays that aircraft absorb in practice. There was no significant difference in delay response to weather between the baseline cases and the cases with the new vehicles.

1.8. Analysis of Controller and Pilot Workload

A conflict occurs when two aircraft flying at the same altitude are separated by less than 3 nm in terminal airspace or 5 nm in en route airspace. To avoid potential conflicts, an air traffic controller will take action to adjust the speed or heading of either or both aircraft well in advance of the conflict. Therefore the number of conflicts that a scenario produces should be a good indicator of workload for controllers and pilots. To assess the effects of NextGen and new vehicles on controller and pilot workload

we ran our ACES simulation, specifying that the software not maneuver the aircraft to avoid conflicts. From the simulation output we then tabulated the number of conflicts at both 3 and 5 nm. We found that there were three main types of conflict: (1) an aircraft overtaking a slower aircraft using the same jet route, (2) jet routes that cross, and (3) aircraft converging to the same metering fix. Roughly half of all conflicts are of this third type. We found that although delay increased exponentially with the number of scheduled flights, the number of conflicts, and hence workload, increased linearly with schedules operations. When delay was very high, however, the number of conflicts increased at a rate that was less than linear, due to so many aircraft being held on the ground. We found no difference in the conflict rate for the scenarios that introduced new vehicles.

1.9. **Safety**

Our approach to safety analysis was to identify the hazards associated with each element of the system—vehicles, rules and procedures, operating environments—while also keeping in mind stakeholder goals, and tradeoffs. One product of this research is a reusable analysis infrastructure that includes a set of publicly-available safety models and analysis methods for qualitatively evaluating the safety impact of new vehicle concepts on NextGen and vice-versa. The scope of the assessment was limited to the operation of each new vehicle in the New York Metroplex. All nominal phases of flight including taxi, takeoff, climb, cruise, descent, approach, and landing were examined. Specific attention was paid to human interaction among air traffic controllers and flight crews as well as with each new vehicle and its environment—the New York metroplex and weather conditions.

The safety risk methodology determines the potential severity and likelihood of each hazard, identifies mitigation strategies for the hazards that pose the unacceptable risk, and evaluates the effectiveness of any mitigation strategies used.

The safety analysis for each vehicle is composed of the following three components:

- Identification of Known Hazards – identification of historical hazards and risks which may be exacerbated by the integration of the vehicle into NextGen.
- Identification of New Hazards – identification of new hazards peculiar to the new vehicle and its operations within NextGen.
- Analysis of Risk – an assessment that determines whether the new vehicle and its operations introduce more or less risk than is acceptable with current aircraft.

We evaluated historical (or known) hazards through discussions with subject matter experts, examination of problem statements from the Commercial Aviation Safety Team (CAST), and examination of a safety issue database compiled from multiple stakeholders by the JPDO Safety Working Group. We also evaluated new hazards by reviewing areas of change identified by the Future Aviation Safety Team (FAST), safety concerns contained in the JPDO Safety Working Group safety database, and subject matter expert input. For each vehicle, hazards were identified and grouped into five areas: performance, automation, procedures, environment, and training. A small sample of the identified hazards is listed below. For the complete list see the main document.

1.9.1. CESTOL

The phases of flight that distinguish the CESTOL from its conventional aircraft counterparts—spiral approaches, steep descents—also pose safety risks. Hazards related to spiral descents, similar to spiral departures, are also associated with maintaining trajectory both vertically and laterally, which can be affected by wind conditions, equipment capability and failures, and crew situational awareness. Due to the low wing-loading, the CESTOL is susceptible to wind gusts that could result in lower passenger quality-comfort ratings resulting from increased sudden jolts, excessive ups and downs, or side-to-side motions. Also, its slower approach speed may significantly reduce the margin of error particularly when operating in high-density airspace.

1.9.2. VLJ

The safety concerns that VLJs exacerbate mainly reside in the operational domain and are associated with flight crew experience and size. It is anticipated that the majority of the VLJs will be operated as corporate jets or air taxis with professional pilots at the controls; there may also be a significant number of owner operators (non-professional pilots). While the hazards would be the same, the risks they pose would generally be higher for the non-professional pilots than for the professional pilots. While the operational hazards listed below could be associated with most jet aircraft, the merging of the commercial and GA worlds (along with dynamic pilot skill sets) exacerbates these hazards when the VLJ is exposed to this operational environment.

1.9.3. LCTR

The phase of flight that is of particular concern with the LCTRs is transitioning from the airplane mode to rotorcraft mode on approach to landing. Other hazards association with the LCTR include: The flight crew's failure to maintain proper approach speed and sink rate could result in the LCTR developing a high sink rate at slow airspeed which could result in the LCTR entering a vortex ring state (VRS) due to the relatively high disk loading. In addition, merging from above or too close to other small and slow general aviation aircraft could create a wake turbulence hazard for the trailing aircraft.

1.9.4. UAS

Hazards associated with the UAS include a remote pilot's loss of situational awareness while operating multiple UASs that could result in possible near mid-air, mid-collision with other aircraft, terrain or objects. Moreover, loss of command and control data link function might cause the UAS to make an unpredictable maneuver with the remote pilot unable to control UAS, resulting in possible near mid-air, mid-air collision with other aircraft, terrain, or objects.

1.9.5. SST

An issue with the SST is its ability to have adequate visibility out the forward flight deck windscreen. A lack of visibility restricts a pilot's ability to transition from instrument flight to visually identifying the runway environment for landing and also from maintaining visual separation from other aircraft. Moreover, the supersonic Concorde that operated in the past was restricted from overland operation and was also waived from having to be equipped with a TCAS. Little has been accomplished in the development of TCAS for SSTs. Also, the SST of the future will be operating en route with subsonic

aircraft as well as in the high density arrival/departure traffic areas. This will require the supersonic aircraft to pass the subsonic aircraft both laterally and vertically. Research needs to be conducted to determine adequate safe passing distance between SSTs and other aircraft.

1.10. ***Avionics***

Significant avionics upgrades are necessary to handle advanced vehicle operations in the NextGen Air Transportation System. In this study, we identified the on-board technology for manned and unmanned aircraft that are anticipated to be available for our advanced vehicles around 2018 to 2025, the timeframe that our advanced vehicles will first be introduced into the NAS. We describe the services and infrastructure that will be available in the NextGen Air Transportation System (ATS) and identify the airborne technology enhancements that can mitigate many of the potential hazards generated by the utilization of advanced vehicle performance capabilities on missions within the future NextGen ATS. Similar to the NextGen avionics roadmap developed by the JPDO Aircraft Working Group, we map the required hazard-mitigation avionics against the operational capabilities listed in the NextGen Implementation plan.

Both government and industry investment strategies for the advancement of ground-based and onboard technologies will determine if and when the listed avionics functionality will be available for installation and use on our advanced vehicles. Airborne technology and research initially dedicated to military aircraft, in time, can be hosted on avionics platforms used for civil transport aircraft and vice versa. Technology developed for fixed wing aircraft is often adapted for use in rotorcraft. The latest trend in avionics development is the adaptation of avionics for manned aircraft, to unmanned aircraft systems. Market demands will determine if these technology developments and transfers are cost effective for the Original Equipment Manufacturers (OEMs), aircraft suppliers and the vehicle operators. In addition, government investment, standards and mandates can significantly influence the time to market of these new avionics capabilities.

1.11. ***Environmental Impacts***

New vehicle concepts in the NextGen airspace can be evaluated in terms of environmental impact at three levels of resolution: vehicle, regional, and national. For this study, regional and national can alternatively be thought of as metroplex and system-wide, respectively. The environmental impact areas we consider are noise, air quality, and climate. It is important to account for the different categories of environmental impacts as the mix of effects and stakeholders impacted varies across them. Climate impacts, for example, are realized globally whereas noise impacts are mostly felt by people who live in the immediate vicinity of airports. The metrics and assessment tools of relevance also vary across the different categories. For instance, calculating climate impacts at the system-wide level requires an integrated climate model capable of evaluating impacts on the global scale, whereas impacts at the vehicle level can be determined from aircraft characteristics and first principles.

Although all of these metrics could be determined using the modeling tools available, time constraints required that a reduced subset be examined. We therefore focused on system-wide climate (only combustion emissions); metroplex air quality in terms of changes to ambient particulate-matter concentration; and metroplex noise. To calculate the target metrics and to monetary impacts, we used

APMT-Impacts, which was developed at the Massachusetts Institute of Technology (MIT). The primary inputs for APMT are the noise and emissions inventories produced by AEDT. Because uncertainty with many aviation effects is high, Monte Carlo analyses was performed to bound output values.

Systemwide climate impacts were assessed for scenarios for each the new vehicle scednario. Each of the new vehicle scenarios caused greater damage to the global climate relative to the relevant baseline scenario in terms of both time-integrated surface temperature change and monetized damages due to the higher fuel burn and emissions. The SST, LCTR, and all-vehicles scenarios were particularly detrimental due to fuel burn levels much greater than the baseline case. The SST had an increased adverse impact on climate due to effects unique to flight in the stratosphere. The remaining cases—VLJ, UAS, and CESTOL—had smaller impact on climate because they account for a small percentage change in total fuel burn relative to the baseline.

A metroplex-scale air quality analysis was performed over the NYC region, for the conventional current airspace as well as for the NextGen airspace. The NextGen scenario produced fewer emissions from the airspace activity compared to the conventional airspace, and the effects of this reduction in emissions manifest themselves in an overall decrease in particulate matter (PM) concentrations in the NYC region. In particular, the reduction in PM Ammonium is observed far beyond the local NYC metroplex area, extending further along the coasts and inland. The reduction in PM due to the NextGen airspace has the greatest effect close to the airports, the decrease becoming less pronounced as the distance from the metroplex increases.

Noise was analyzed at the NYC metroplex level in order to independently assess the impacts of the advanced technologies of the CESTOL vehicle, along with the airspace design enabled through NextGen (without any advanced vehicle concepts). Both scenarios led to a reduction in total population exposed to a given noise level and in monetized damages in the form of housing value depreciation.

1.12. **Metrics**

An approach was developed for assessing the impact of integrating new vehicle concepts into the NAS. This approach, based on control theory, utilizes International Civil Aviation Organization (ICAO) Key Performance Areas (KPAs), and can be extended to a wide range of performance and trade-off assessments at varying levels of fidelity. To illustrate the approach, three key trade studies between two performance areas of system performance, environment and safety are utilized. An array of trade-offs and potential research goals that might be of interest to NASA in the future are also summarized. The method is generic and can be used to investigate other operational impact assessments as well as for system-wide, regional, or local analysis. It also accounts for fine-tuning of demand characteristics, airspace procedures, and vehicle performance/design characteristics that may be required for achieving desired performance outputs.

For the most part, our research indicates that system performance, safety, and environmental impacts can be captured using well understood metric specifications and existing tools. In some cases, however, we were able to identify metric gaps that stem from a lack of understanding of underlying processes (example: supersonic noise/boom), a lack of modeling capabilities that would facilitate their evaluation (example: flexibility/number of options), or from a lack of both of these elements.

Our research indicates that cause-effect relationships between metrics can be effectively used for capturing impact propagation and enabling trade-off analyses between different performance aspects. Furthermore, the metrics framework is more than just an effective means of capturing impact propagation across performance areas: the concept also can be helpful in rolling up performance outcomes from lower- to higher-levels of performance assessment. Examples of this latter capability might involve rolling-up outcomes from the regional to national, the vehicle to the operational, or the operational to societal levels.

Further research is needed to better understand the complexities involved with using iterative run-scenarios and analyses that enable fine-tuning of demand characteristics, airspace procedures, or vehicle performance/design characteristics to deliver desired performance outcomes; however, the necessary foundation was developed and successfully used to support low fidelity assessments.

1.13. ***NextGen Observations***

The goal of this study has been to analyze the new vehicles in a NextGen environment and evaluate whether NextGen makes the new vehicles more or less viable. Although beyond the specific scope of the current contract, we now present a few conclusions here regarding NextGen, independent of the new vehicles, in areas where we have gleaned some insight.

The ability of NextGen aircraft to reliably fly precise routes in the terminal area can be utilized significantly improve performance in congested metroplex environments. The improved performance is accomplished by eliminating dependencies between routes and adding routes, thus increasing capacity and predictability. The amount of increased capacity and predictability for conventional aircraft was not specifically analyzed in this study, but it appears to be significant. In addition to providing precise navigation, a NextGen environment would need to provide increased information sharing and improved automation for controllers to safely manage this increased traffic.

The same precise navigation and improved controller information and automation will enable better access to underutilized airports in congested areas for business jets, air taxis, and potentially new scheduled air carrier operations, assuming community acceptance of significantly increased commercial operations.

Provision of negotiated 4D contracts would be expected to further increase capacity and predictability by more efficiently utilizing every slot on every independent route to every runway. This 4D trajectory capability was not analyzed in this study, so it is not possible to give even a subjective sense of the magnitude of this benefit.

As demonstrated for the new vehicles, independent routes can enable different approach configurations (e.g., different speeds, glide-slope angles). This technique could be highly advantageous even with more conventional aircraft by having conventional aircraft certified for slightly different approach profiles and then assigning them to precise independent routes, thus getting much of the benefits of decoupling the approaches. As per the NextGen ConOps, this idea could be taken a step further by combining with 4D contracts that provide a conflict-free new approach course for every aircraft thus optimizing (minimizing) the fuel burn. Again this was outside the scope of the current study and was not analyzed to determine quantitative benefits.

Currently non-towered airports operate under IFR conditions at significantly reduced rates (e.g., one-in/one-out rates). The NextGen ability for non-towered airports to operate under IFR conditions at VFR rates will have the same benefits to conventional commercial and general aviation users as it does for VLIJ or CESTOL aircraft operators. The unknown is whether there is a significant business case for growth in commercial (or GA) operations at individual non-towered airport and whether surrounding communities want air traffic growth at these airports. Again this was not analyzed as it is beyond the scope of this contract.

NextGen contains ideas representing a tremendous amount of technology and procedural change. There are a wide variety of possible mixes of NextGen concepts that could be analyzed to gain insight into the best combination of technology and procedures to achieve significant improvements in the air traffic system with a reasonable investment. Section 18 provides additional ideas for potential studies that would provide some additional insight into NextGen.

1.14. **Appendixes**

This report also includes a number of appendixes. Appendix A is a glossary of acronyms. Appendix B summarizes lessons learned and workarounds that were developed in using the beta version of AEDT. Similarly, Appendix C summarizes assumptions, lessons learned, and workarounds associated with ACES. Appendix D describes experiments that were conducted to see whether TARGETs could model spiral approaches (It could). Appendix E gives a fairly technical analysis of the hazards induced by trajectory drift during the CESTOL spiral approach. Appendix F describes in detail our process for using AEDT to calculate of fuelburn and emissions from ACES data. (The AEDT output is discussed in the Environmental Impacts of the report. In that section we also present monetized environmental impacts that were derived using the APMT-Impacts model.). Appendix G presents a large table of hazards that were identified for each of the new vehicles. Finally, Appendix H contains a description and listing of directories in the data DVD that was produced as part of this report.

i Peter F. Kostiuk, Eric M. Gaier, and Dou Long, “The Economic Impacts of Air Traffic Congestion,” *Air Traffic Control Quarterly*, Vol. 7(2), 1999, pp. 123–145.

ii European Organisation for the Safety of Air Navigation, “User Manual for the Base of Aircraft Data (BADA) Revision 3.6,” EEC Note No. 10/04, September 2004.

iii SAE Committee A-21, Aircraft Noise, “Procedure for the Calculation of Noise in the Vicinity of Airports,” Aerospace Information Report No. 1845, Warrendale, PA: Society of Automotive Engineers, Inc., March 1986.

iv Federal Register: October 22, 2008 (Volume 73, Number 205), Rules and Regulations, pp. 62871-62872, From the Federal Register Online via GPO Access, wais.access.gpo.gov

2. Introduction

NextGen represents a transformation of the air traffic control system from its present highly manual, analog, ground-centric state into one in which digital technology, information sharing, and automation is ubiquitous. This transformation has implications across the gamut of aviation activity, from air transport services business-models through airspace rulemaking. The Federal Aviation Administration's (FAA) Joint Planning and Development Office (JPDO)^v is responsible for coordinating this transformation among multiple government organizations with collaboration from industry.

In addition to the transformation occurring in air traffic management, a technology and business driven transformation is occurring in aircraft design, production, and manufacture. Advances in materials science, such as the development of carbon composites for use in airplane fuselages and wings, promise lighter, stronger, and more fuel efficient vehicles. Engine design technology will produce quieter engines for next generation aircraft. Engine manufacturers have also recently begun building small, lightweight, and energy-efficient turbofan engines,^{vi} which spurred the manufacture of very light jets, as well as a follow-on generation of personal and light jets, and the opening of an on-demand air taxi market.^{vii} Advancements are accelerating in digital, networked avionics systems that lead to widespread implementation of performance-based communication, navigation, and surveillance capabilities throughout the air transport, business, corporate, and general aviation fleets. Unmanned aircraft systems (UASs), widely used by the military, are expected to enter civilian service once a reliable and cost-effective sense-and-avoid capability is developed.^{viii}

Given that both the air traffic management system and aircraft design are currently undergoing significant transformations, an interesting research question arises. To what extent does the NextGen transformation either constrain or promote new vehicle designs, new operating capabilities, and new business models? Conversely, to what extent should the possible new vehicles and business models influence the NextGen specification? Closely related to these questions are issues concerning the aspects of NextGen that are critical to realize the full performance capability of these new aircraft, as well as the overall throughput, capacity, delay, environmental, access, and safety impacts of the combination of these new vehicles with the NextGen transformations.

Recognizing the importance of these questions, NASA's Aeronautics Research Mission Directorate (ARMD) started two parallel research efforts aimed at analyzing the deployment of new vehicles with the advanced concepts in the NextGen specification. The study scope includes the interactions, safety tradeoffs and environmental implications among operational procedures, new vehicle technologies, and the performance of NextGen. One of the two ARMD studies is being conducted by Sensis Corporation, and is the focus of this report.

This study is important for several reasons. First, inconsistencies between the NextGen definition and the capabilities of the new vehicles are more easily rectified if identified early. Second, the types of aircraft that are expected to be available in the future influence the performance and environmental targets that are specified by NextGen. Third, the NextGen terminal area procedures will be highly influenced by the performance capabilities of the vehicles that operate in the airspace. Finally, the specification of NextGen itself can be changed, if needed, to accommodate the capabilities and performance of the new vehicle designs.

The project considered five specific types of future advanced vehicles: large civil tiltrotors (LCTRs), unmanned aircraft systems (UASs), supersonic civil transports (SSTs), very light jets (VLJs), and cruise-efficient short takeoff and landing vehicles (CESTOLs). These five vehicles represent only a fraction of those currently being studied by industry, but they do represent vehicles that have a reasonable probability of being utilized in the decade of the 2020's and beyond. Two of the aircraft—VLJs and UASs—are available today. UASs are limited to flight in controlled airspace primarily due to their lack of sense-and-avoid technology, but that restriction is likely to be eliminated by the 2020's, if technology matures as expected. A first generation of multi-engine VLJs (and light ject) is being manufactured today, with a new generation of single-engine jets on the horizon. The Bell/Agusta Aerospace is currently developing Tiltrotor aircraft for civilian use. Their model BA609, a nine-passenger vertical-takeoff vehicle with a cruise speed of 275 knots and a range of 1,000 nautical miles (nm) is expected to receive certification in 2010^{ix}. By the decade of the 2020's, much larger LCTRs, such as the 90-passenger version studied here, may be in service. Although CESTOL aircraft are not available today, they are under active consideration by aircraft manufacturers as a replacement for a single-aisle large commercial transport. Although not nearly as STOL as this study, some Airbus A320 and Boeing 737 class aircraft have been modified and certified for steep glideslope approaches and shorter runway utilization. Finally, the SST, the vehicle requiring the most technological improvements among the five studied here, is nevertheless within the possibility of production in the next twenty years (and of course a previous SST, the Concorde, has provided limited commercial airline service in decades past).

v www.jpdo.gov/

vi Black, Sara, "Very Light Jets Creating a Demand for Composites," High Performance Composites, 1 January 2006, <http://www.compositesworld.com/articles/very-light-jets-creating-a-demand-for-composites2.aspx> (accessed February 2009).

vii Bonnefoy, P.A., R.J. Hansman, 2007. Potential Impacts of Very Light Jests on the National Airspace System. *Journal of Aircraft*, (44) 4: 1318–1326 .

viii Lacher, A.R, D.R. Maroney, A.D. Zeitlin. 2007. Unmanned Aircraft Collision Avoidance – Technology Assessment and Evaluation Methods, The MITRE Corporation, http://www.mitre.org/work/tech_papers/tech_papers_08/07_0095/07_0095.pdf

ix "BAAC 609 Flight Test Continues Development Pace," 18 June 2007, http://www.bellhelicopter.com/en/company/pressReleases/PR_07_0618-04_609_TestPace.cfm

3. Previous Work

A summary of project progress through January of 2009 is given in a recently-published paper.^x Studies of specific new vehicle technologies, independent of NextGen, have been ongoing for many years. For example, NASA has studied civil tiltrotor (LCTR) operations over the last two decades, both analytically and through very high fidelity human-in-the-loop (HITL) motion simulation studies. Analytical studies have shown the feasibility of LCTR for short-haul (< 500 nm) operations, diverting short-haul travelers to the LCTR's vertiport, thereby freeing arrival and departure slots on the main runway for more efficient longer-haul transport aircraft.^{xi} This result suggests that overall passenger throughput at vertiport-enabled airports can be increased with minimal impact on flight delays. HITL simulators have shown that LCTR conversion from "turboprop mode" to "helicopter mode" on arrival is best achieved before acquiring the glideslope when instrument meteorological conditions (IMC) prevail.^{xii} This result has implications for the design of LCTR instrument approaches.

In the UAS world, much attention is being devoted to the "sense and avoid" technology necessary to integrate them into the National Airspace System (NAS) as well as best practices for UAS use prior to the availability of the sense-and-avoid capability.^{xiii} Proposed UAS missions are plentiful: cargo systems operating continuously for guaranteed next-day service for all freight,^{xiv} humanitarian and disaster relief operations,^{xv} high altitude long endurance missions for communication support or surveillance,^{xvi} and meteorological sensor platforms, among many others. Even without civilian applications, the military is growing their fleet of UAS vehicles at a tremendous rate and needs routine access to civilian airspace.

Because VLJs are in commercial use today, there have been several studies focusing on the impact of VLJs operating in the NAS. A study using the Transportation System Analysis Model (TSAM) at Virginia Tech showed that VLJ on-demand air-taxi service becomes economically competitive with commercial air service if the VLJ cost drops below \$1.85 per passenger mile (2006 dollars).^{xvii} Although not targeting VLJs specifically, a recent paper on the NextGen early implementation effort in Florida suggests that VLJs might help climate change by avoiding altitudes that cause cirrus-inducing contrails^{xviii}

In the SST world, studies have focused on producing a "quiet" sonic boom so that SST flights over land become commonplace. Studies have also focused on the business case for such vehicles. Initially it is envisioned that small SST business jets will be produced,^{xix} although there is some work on large commercial SSTs as well.^{xx}

There have been numerous studies of CESTOL technologies in the last decade. Of particular importance is a study of the short takeoff and landing (STOL) technology on a hypothetical single-runway airport.^{xxi} The study affirmed the commonly-held belief that differences in approach velocities negatively impact runway capacity, unless the slower-moving aircraft can be separated from the rest of the arrival flow. Because of their short runway landing capability, CESTOL vehicles tend to have much slower approach speeds than conventional aircraft.

Of particular note are previous studies focusing on the performance implications of a fully-implemented NextGen system. The JPDO has studied the future with and without the NextGen transformation using only traditional aircraft types. Their studies include aircraft such as the Boeing 787

and Airbus A380, but do not include any of the vehicle technologies included in this study. The JPDO results show that the projected future travel demand (in 2025) is only approximately 30% satisfied without NextGen, but approximately 80% satisfied if NextGen is fully implemented.^{xxii} An interesting question arises as to whether these new vehicles, with new and different flight profiles and arrival/departure requirements, can help bridge the remaining 20% gap in 2025 and the even larger gaps in 2040 and beyond.

x Wieland, F., Smith, J. A., and Clarke, J. P., “Implications of New Aircraft Technologies on the Next Generation Air Transportation System,” Proceedings of the 2009 USA/Europe Air Traffic Research and Development Seminar, Napa, California, July 2009.

xi “Civil Tiltrotor Missions and Applications, Phase II: The Commercial Passenger Market,” Boeing Commercial Airplane Group, Bell Helicopter Textron Inc, and Boeing Helicopters, Summary Final Report for NASA/FAA, NASA-CR-177576, February, 1991.

xii J. V. Lebacqz and B. C. Scott, “Ground-Simulation Investigation of VTOL Airworthiness Criteria for Terminal-Area Operations,” Journal of Guidance, 8(6), Nov-Dec 1985.

xiii “Best Practice for Small Unmanned Aircraft Systems Operations,” RTCA document W1-S2-001-b-SAPP_Best Practices, September 2006.

xiv K. Han, A. L. Garcia, I. M. Leo, M. Martin del Campo, C. Muhammad, L. Ortez-Valles, and G. L. Donohue, “Unmanned Aerial Vehicle Cargo System,” Proceedings of the 2004 Systems and Information Engineering Design Symposium, Matthew H. Jones, Stephen D. Patek, and Barbara E. Tawney, eds.

xv L. A. Young, “Enhanced Rescue Lift Capability,” Proceedings of the 63rd Annual Forum of the American Helicopter Society, Virginia Beach, VA, May 1-3 2007.

xvi L. A. Young, J. A. Yetter, and M. D. Guynn, “System Analysis Applied to Autonomy: Application to High Altitude Long Endurance Remotely Operated Aircraft,” Proceedings of the AIAA Space 2006 Conference, San Jose, CA, September 2006.

xvii A. A. Trani, H. Baik, N. Hinze, S. Ashiabor, J. K. Viken, S. Dollyhigh, “Nationwide Impacts of Very Light Jet Traffic in the Future Next Generation Air Transportation System (NGATS),” Proceedings of the 6th AIAA Technology, Integration, and Operations Conference (ATIO), 25-27 September 2006, Wichita, Kansas.

xviii B. Holmes, “Implementing Next-Generation Air Transportation System Technologies,” Proceedings of the 26th International Conference on the Aeronautical Sciences, 14-19 September 2008, Anchorage, Alaska.

xix P. Henne, “The Case for Small Supersonic Aircraft,” Proceedings of the AIAA/ICAS International Air and Space Symposium and Exposition: The Next 100 Years, 14-17 July 2003, Dayton, OH.

xx D.M. Mavris, M.R. Kirby, and S. Qiu, “Technology Impact Forecasting for a High Speed Civil Transport,” Proceedings of the 1998 AIAA World Aviation Conference, 28-30 September 1998, Anaheim, CA.

xxi P. Phelps, P. Bock, C. Gologan, A. Kuhlmann, TU Munchen, Barhaus Luftfahrt, “Impact of ESTOL Capability on Runway Capacity—An Analytical Approach,” Proceedings of the 8th AIAA ATIO Conference, 14-19 September 2008, Anchorage, AK.

xxii Gawdiak, Y., Director, Integrated Portfolio and System Assessment (IPSA) group at JPDO, private communication.

4. Research Method

Conducting a study such as this one requires that the aircraft and airspace system be defined well enough to allow quantitative models to extract usable results. Because the five new vehicles and the airspace concept (NextGen) have not yet been implemented, the study relied on expert opinion in addition to a variety of models. For each vehicle, a series of telecons were conducted with NASA and industry experts to establish the desired capabilities, the technology assumptions based on year of introduction to the fleet, and the departure point for each vehicle. The external experts for each vehicle included:

CESTOL: Andy Hahn (NASA)

VLJ: Bruce Holmes (Holmes Consulting, LLC; formerly of DayJet Corporation, NASA, JPDO)

UAS: Steve Vail (FedEx)

LCTR: Larry Young (NASA), Doug Boyd (NASA)

SST: Jon Seidel (NASA), Jeff Berton (NASA), Bob Welge (Boeing)

The first step is to define vehicle performance and mission requirements. These two concepts are intertwined: the mission is difficult to define unless the vehicle performance has been identified, and vice-versa. Therefore, mission definition and vehicle specification need to proceed in concert with each other.

After the high-level vehicle performance is specified, detailed vehicle design can be performed. In this study, the Georgia Institute of Technology's Airspace System Design Laboratory (ASDL) designed the vehicles using the ASDL Environmental Design Space (EDS) toolkit. EDS was used to compute tradeoffs among different vehicle design variables—weight, fuel burn, noise, emissions, and range—to produce economically feasible and aerodynamically efficient vehicles that would satisfy mission requirements.

Eurocontrol's Base of Aircraft Data (BADA) is a standard for describing vehicle performance. For conventional aircraft, BADA performance data already exists. For the new vehicles, ASDL used EDS to project each new vehicle's performance as needed for the BADA standard. When projecting the vehicle's performance, its noise and emissions profiles were also estimated. These profiles are needed to drive the Aviation Environmental Design Toolkit (AEDT), a standard suite of tools used to generate noise contours and emissions profiles around airports.

The second step is to generate a demand set, or schedule, for each new vehicle. Some of the new vehicles would be expected to replace aircraft on existing routes, while other new vehicles would add new routes to the system. For example, the ASDL-designed CESTOL would operate much like a Boeing 737-class aircraft, and thus would replace existing aircraft in future scheduled service. Similarly, CTRs could replace flights between heavily trafficked city pairs within the range of a typical shuttle operation (500 nm). The VLJ mission would be largely an air-taxi service; the experience of DayJet indicates that air taxi flights would largely substitute for ground transportation (as opposed to diverting air carrier passengers),

and thus VLJ use would add flights to the system. LSSTs would replace certain long-haul flights, while the UAS missions would add flights to the system.

The third step is to define arrival and departure procedures for the new vehicles, particularly for those vehicles with performance substantially different from conventional aircraft. For example, CESTOL aircraft, as designed by ASDL, would have an approach speed of 103 knots, suggesting that the CESTOL arrival streams would need to be segregated from conventional aircraft, which have approach speeds around 115–140 knots. Additionally, CTRs operate from different parts of the airport than other aircraft, and therefore would require different approach and departure paths. To evaluate the efficiency of terminal area procedures the project used the Airspace Simulation Model (SIMMOD) to compute the trajectories, in the terminal area, of the conventional aircraft with the new procedures. Metrics from the SIMMOD analysis include the traditional delay/capacity/throughput numbers, as well as precise aircraft position and altitude information that can be passed to AEDT for environmental impact (noise and emissions) analysis.

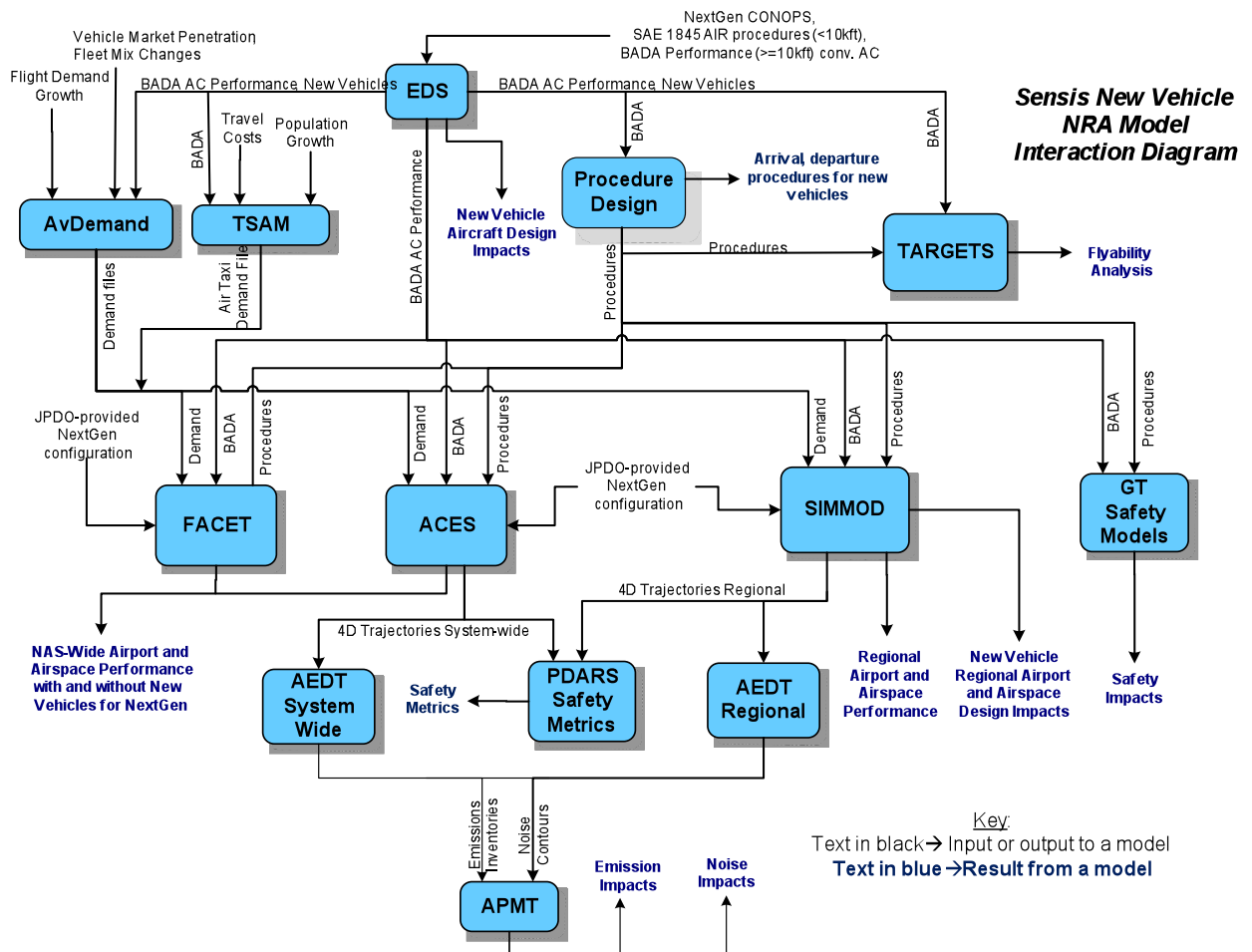


Figure 4-1. Model infrastructure used to conduct the research in this paper

The fourth step is to evaluate these procedures, from flyability, operational, and safety perspectives. “Flyability” refers to the degree to which the procedure avoids obstacles, conforms to acceptable aircraft performance standards, and does not subject passengers to any extreme forces. “Operational” refers to the ability to achieve the planned activities and schedule, and “safety” includes the personnel, vehicles, and

other airborne and ground based systems. Flyability is primarily assessed through expert opinion and with some quantitative analysis; operational evaluation is typically done through discrete event simulation, and the safety of the procedures is evaluated using a combination of expert opinion and quantitative analysis. The procedures evaluations were performed for several complex airspace/airport regions, often called a Metroplex. The safety analysis consists of two parts. The first part is determining the safety margin in the current system as compared to the margin in a NextGen system. The second part is determining the safety margin of a NextGen system with the new vehicles. For this step, human factors models from the Georgia Institute of Technology, as well as expert opinion and historical data, are used to determine the safety margins.

The final step is to roll up the results from the individual procedure and Metroplex evaluations into a system-wide assessment of the performance of the new vehicles. The system-wide assessment includes quantitative capacity and delay improvements as well as environmental impacts. The demand file (consisting of both the new vehicles and existing conventional aircraft), the BADA performance of all vehicles, and the terminal area procedures are combined to compute the expected system-wide impact of the new vehicles. Capacity and delay metrics as well as environmental metrics (using AEDT) can be computed at this point, along with some level of controller workload based on dynamic density of the airspace. The Airspace Concepts Evaluation System (ACES) software is used to evaluate system performance at this step. These steps are aided by a model-based infrastructure. Figure 4-1 shows the model infrastructure used in this research. Each model in the figure represents a specific computation based on the steps listed above. Other models used in this study include the FAA's Environmental Design Space (EDS), for aircraft design; the FAA's Terminal Area Route Generation Evaluation & Traffic Simulation (TARGETS) for flyability analysis; the Performance Data Analysis and Reporting System (PDARS), for safety metrics; the Aviation Environmental Portfolio Management Tool (APMT), for assessing environmental impacts, the Transportation Systems Analysis Model (TSAM), for demand forecasting; AvDemand for schedule generation; and the Future Air Traffic Management Concepts Evaluation Tool (FACET), for system-wide simulation.

5. Vehicle Business Cases

This section discusses the business case for each vehicle. Although airline cost and revenue data were generally unobtainable, the project benefitted from several discussions with representatives from the airline industry. These discussions enabled business cases for each vehicle to be determined with enough detail to generate flight demand sets to input into models.

5.1. *CESTOL*

Because of the CESTOL's unique characteristics—its ability to land and take off using a 3,000-foot runway, its slow (103 knot) approach speed, and its 100-passenger size—there are several ways it can be used to enhance throughput in a NextGen environment. First, it can be used by airlines to offload traffic from congested hubs to nearby reliever airports, improving passenger metrics for doorstep-to-destination speed and convenience in many cases. Second, its short takeoff and landing (STOL) characteristics enable it to use some existing airports more efficiently. Third, CESTOLs can utilize nonstandard procedures to utilize unused terminal airspace and thus increase airspace capacity. This section will outline the business case for all three of these uses. Section 6 presents in greater detail the manner in which schedules were created for each of the new vehicle types.

Offloading Traffic to Reliever Airports

The CESTOL vehicle designed by Georgia Tech's Aerospace Design Laboratory (ASDL) is similar to a class of next-generation narrow-body aircraft that industry is considering producing in the 2018–2020 period. It can carry 100 passengers and is capable of taking off and landing on runways as short as 3,000 feet. The CESTOL's range depends on how the aircraft is configured: when taking off from a conventional 7,000-foot runway it has a range of 2,000 nm. To take off from a 3,000 foot runway the aircraft must be lighter, and thus must carry less fuel, which reduces its range to 600 nm.

To measure benefits of using reliever airports to absorb excess demand, the baseline demand files were modified by offloading flights from the top 35 major airports whenever their demand to capacity ratio exceeded 90% in any 15-minute interval. The capacities used were provided by the JPDO and are for the year 2025. The selected flights—all of which had stage lengths less than 600 nm—were offloaded to reliever airports within 70 nm of the primary airport, provided that the reliever possessed a paved runway at least 3,000 feet long with a width of at least 100 feet.

The justification for this approach is that it represents an extension of the current low-cost carrier (LCC) operating model. LCCs routinely service otherwise underutilized airports near major metropolitan areas, and with an expected 2X–3X traffic growth, it is reasonable to expect more such airports will be utilized in the future. However, there are clearly many other business and policy factors that would need to be addressed to consider initiating commercial service at many of these small airports however that was outside the scope of this study. For one thing, most of the reliever airports currently lack infrastructure and supporting services: on-site emergency crews, passenger security checkpoints, and luggage handling facilities, to name a few. Therefore significant airport infrastructure development will be needed to prepare reliever airports for commercial flights.

More importantly, for a commercial flight to be profitable there must be sufficient demand to and from each airport to warrant service. Most large airports today are hubs; which means that a significant portion of their passengers are connecting passengers, rather than local demand. Figure 5-1 was made using passenger ticket data for the first quarter of 2009 (www.bts.org). The number of departing passengers whose itinerary originates at a given airport is shown in red; the number who are only at the airport to make a connection is shown in blue. Connecting passengers are a very large percentage of total passengers at most hubs: ATL (80%), DFW (75%), ORD (64%). On the other hand, a small airport such as Allentown Airport in Pennsylvania (25% of passengers connecting) that is a large distance from a hub draws passengers from surrounding neighborhoods. A reliever airport that is near a hub has the disadvantage of not being able to offer service to many destinations and having to share its passenger base with a hub.



Figure 5-1. Passenger departures by airport.

Using existing airports more efficiently

It is possible to exploit the short landing and takeoff characteristics of CESTOL to improve the capacity of existing airports, without infrastructure development and with a minimal impact on aviation rules. An example is New York's LaGuardia airport (LGA), currently one of the most congested airports in the nation. In a typical configuration, LGA uses runway 22 (RW22) for arrivals and runway 13 (RW13) for departures. The two runways intersect at right angles, as shown in Figure 5-2. Aircraft on RW13 must wait for arrivals on RW22 to pass the intersection before they can take off. On the arrival side, controllers must separate aircraft more than is nominally necessary to create a gap for the interleaved departures.

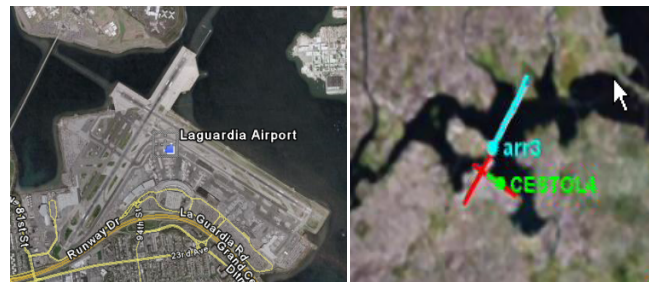


Figure 5.2 LaGuardia airport (left) and simultaneous arrival/departure using CESTOL (right)

Neither of these procedures is necessary with CESTOL operations. CESTOL departures can taxi to the center of RW13 and depart using only the southern half of RW13, while arrivals (conventional or CESTOL) occur on RW22 behind the departing CESTOL. The right-hand side of Fig. 1 shows a snapshot of this procedure, where a CESTOL aircraft is executing an intersection departure while an arrival occurs simultaneously, but behind, the departure.

If an all-CESTOL fleet is assumed at LGA, then this procedure increases its throughput by a factor of 1.9 relative to current operations. This capacity increase occurs without adding any additional infrastructure, and is compatible with existing FAA rules and therefore costly and time-consuming rulemaking procedures are avoided. All that is necessary to realize this capacity increase is the production and use of new vehicle types that possess short takeoff and landing capability at LGA.

LaGuardia is not alone in its ability to exploit CESTOL technology; in fact most busy airports can realize a capacity gain. For example, CESTOL can land and depart on the underutilized existing runway 18 (RW18) at Newark Liberty Airport (EWR). Although RW18 is 6,800 feet long, because it crosses two other main runways (runways 22L and 22R) at approximately the 4,800-foot mark, the usable part of RW18 (allowing for go-around procedures) is a little over 3,000 feet. Thus CESTOL aircraft can land and depart RW18 while operations are occurring on 22L and 22R simultaneously, whereas conventional aircraft cannot use RW18. As a result, RW18 is underutilized at EWR. An existing study using the ACES model suggests a 35-40% increase in capacity at EWR alone when CESTOL operations occur at RW18 while conventional aircraft use 22L and 22R. When extrapolated to other congested airports with similar runway constraints, the study estimated that the use of CESTOL aircraft nationwide could reduce NAS system delays by up to 20%.

Ability to Fly Nonstandard Approaches

Due to their unique design and low approach speed, CESTOL aircraft are capable of flying nonstandard approaches. Two such nonstandard approaches are steep approaches (5.5 degree glide slope) and spiral approaches. Steep approaches are in use today; in fact, they are mandatory at London City Airport for noise abatement purposes. Spiral procedures are also in use today. Norman Y. Mineta San Jose International (SJC) airport has a spiral procedure for departures and Palm Springs International (PSP) airport has a spiral procedure for arrivals. The existing procedures are all compatible with conventional aircraft, resulting in spirals of a fairly large radius with a limited number of turns.

In contrast, the CESTOL is capable of tight spiral approaches, with a radius of 1.5 nm and a load factor not exceeding 1.15 times the force of gravity (1.15 G). Both capabilities—that of executing a steep approach as well as a tight spiral—can be utilized to design procedures in dense airspace to maximize the utilization of the airspace and the throughput of the runways, while simultaneously minimizing the noise footprint and fuel burn. These factors could provide significant arrival and departure airspace capacity gains providing the business incentive to acquire and utilize CESTOL vehicles.

To create a CESTOL scenario that could be modeled, we assumed, based on rough CESTOL production rates, that the 2025 schedule would have approximately 10,000 daily CESTOL flights. We also assumed that there would be 50,000 daily CESTOL flights in 2040 and 80,000 daily CESTOL flights by 2086.

5.2. VLJ

For VLJs, the business model assumes that carriers would provide on-demand air taxi service between relatively uncongested airports. A socioeconomic model, called the Transportation Systems Analysis Model, (TSAM) was run to estimate what that demand would be, and what airports the flights would depart from and arrive to. The resulting set of flights was added to the baseline demand to create the VLJ demand set. Existing air-taxi operations already exist in parts of the country and some are continuing to survive even in the current bad economic climate; and there are strong reasons to believe they will thrive when the economy picks up. VLJs and similar technologically advanced light transportation aircraft will possess the avionics and crew capabilities to fly virtually all envisioned performance-based navigation procedures in the time frames studied. The TSAM model estimated that there would be demand for 4,000 daily VLJ flights in 2025, and 8,000 daily flights in 2040. TSAM was not run for 2086, so for modeling purposes, the 2086 used the same 4,000 flights as the 2040 schedule.

5.3. UAS

Unlike the other new vehicle technologies studied by this project, the UAS represents a level of technology, as opposed to a specific vehicle. The level of technology can be applied to a small surveillance system, as is common today especially in the military world. But the technology, when mature, could also be applied to control a large aircraft. Because the project assumes a 2025–2040 time-frame as well as full implementation of NextGen, it is also reasonable to assume that “see and avoid” technology will be perfected by that date and that UAS aircraft will operate routinely in the NAS. Debate

about this point abounds, of course, but that debate is the subject of other projects and other investigations. Here we concentrate on the expected effect if UAS-equipped aircraft are available during the study period.

The requirements for the UAS mission given to us by NASA are: (1) that we investigate a civilian application of UAS technology; (2) that we investigate an aircraft weighing 100 pounds or more; and (3) that the application must have an impact on the NAS. These requirements rule out almost all current UAS uses, which primarily involve surveillance or data collection. These missions typically fly in restricted airspace through which civilian flights are prohibited.

After considerable discussion we decided on the following UAS mission. First, when UAS technology becomes widely available, our belief is that it will be applied to cargo operations before passenger-carrying operations, because of the reluctance of passengers to fly on a pilotless aircraft. Second, we believe that the technology will be applied to small aircraft before it is applied to large aircraft. Therefore, the application we chose to examine is that of a cargo operator (such as Federal Express, or FedEx) forwarding freight from a “spoke” airport to a more distant airport. Currently large cargo operators, like FedEx, operate a hub-and-spoke network. The hub for FedEx happens to be Memphis airport (MEM). Typically packages are flown into Memphis, moved to another airplane, and then flown onwards to one of the spoke airports in the network. At the spoke airport, the packages are offloaded. Local packages are placed on local delivery trucks, while packages for more distant cities can be routed either by air or by truck. To forward freight by air, FedEx today (in 2009) utilizes a fleet of 250 Cessna Super CargoMaster aircraft. Figure 5-3 shows the routes flown by these aircraft on December 20, 2007. An example route is between Dulles Airport (IAD) to Cumberland MD (CBE). Because the cargo volume to CBE is not large enough to justify a flight from their hub in MEM, FedEx flies the packages to IAD, and then offloads them to a Cumberland-bound CargoMaster.



Figure 5-3. Current-day Cessna cargo routes (ASPM)

We asked Steve Vail, our NUAC FedEx member, the circumstances under which they would use a small aircraft versus a truck. His answer was simple: “whichever costs less.” We therefore did a cost comparison of truck forwarding and aircraft forwarding. The analysis is relatively straightforward. For intercity trucks, FedEx contracts all the delivery to independent operators. On the FedEx site are all the parameters you need—the size of the truck you need to buy, maintenance requirements, insurance requirements, and cost per mile that FedEx reimburses their operators.

The Cessna website gives the price of the Super CargoMaster as well as the operating cost per flight-hour and per flight-mile. Assuming that the airplane could be sold privately at the end of its useful life, the actual cost of purchasing the aircraft is the original purchase price minus the cost of a 10-year-old used CargoMaster plus the cost of conversion from a UAS to a conventional aircraft. This resale cost can be found on numerous websites featuring used aircraft for sale.

Given these assumptions, we found that because the fixed cost of an aircraft is higher than a truck, for small distances the truck is preferred. However, the variable costs of the aircraft are lower than for the truck, especially when you consider that an aircraft can get to a remote city faster. Based upon the data we could find, we developed the linear cost model for each mode shown in the figure below.

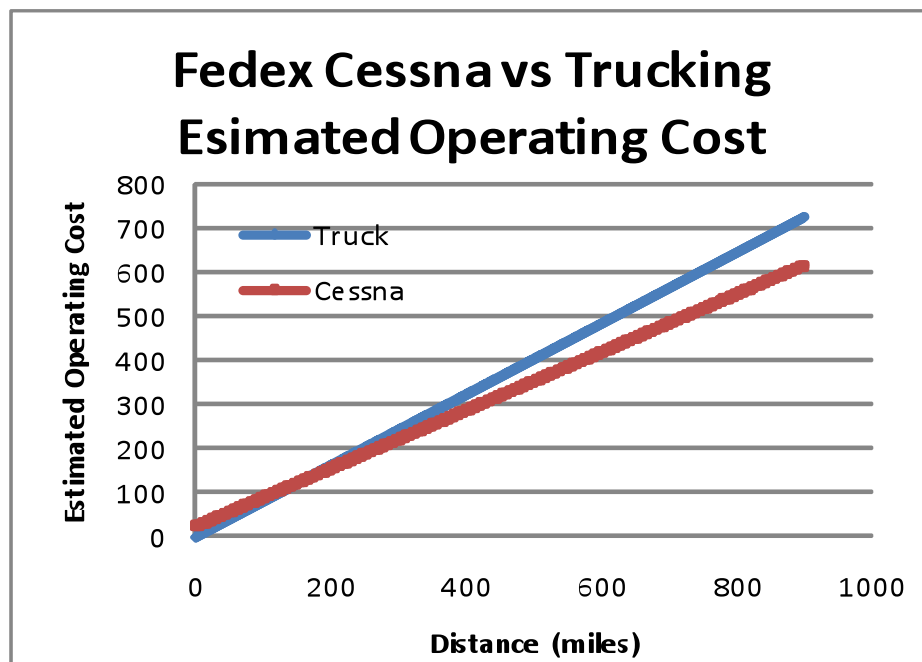


Figure 5-4. Comparison of transportation costs for ground and air.

The two lines cross at about 125-150 miles, meaning that if the truck has to travel more than 125 miles or so to its destination, then the aircraft is less expensive and FedEx would prefer flying to driving. Note that the distance represents truck travel distance, not the great circle distance from one city to the other. For example, if the remote city is in the mountains, the great circle distance might only be 90 miles, but because the truck has to travel a circuitous route its distance might be more like 130 miles. In that instance the aircraft would be preferred to the truck.

We assume that the introduction of UAS technology on the CargoMaster will drop its operating cost substantially, so that in the future FedEx would be motivated to use more UAS-equipped small aircraft than they do today. We had no accurate way to judge the cost savings in use of a UAS CargoMaster over a piloted system so we performed a sensitivity study. We ran a set of results where the breakeven distance was 120 miles, similar to today. Then we ran another set where the breakeven distance was 90 miles (i.e. use the airplane when the truck has to travel more than 90 miles from the spoke airport). Then we ran a third one where the breakeven distance was 60 miles, and for completeness we ran another one where the breakeven distance was reduced to 30 miles. For the majority of the analysis we utilized the most optimistic UAS replacement strategy where future UAS CargoMaster class aircraft are used for routes as short as 30 miles. The UAS schedules that were modeled assumed 4,000 daily flights between known cargo hubs and spoke airports located 30 to 150 nm away.

5.4. **LCTR**

Because a 90-passenger LCTR has many moving parts it is assumed that it will be more costly to acquire and maintain than a 90-passenger fixed-wing aircraft. Therefore airlines flying LCTRs would have to charge passengers more per seat. The LCTR business model assumes that travelers would pay a premium fare for a flight between popular city pairs that was much more reliable in departing and arriving on time. Because LCTRs utilize vertiports that are separate from an airport's main runways, LCTRs can get into and out of heavily congested airports more reliably than fixed-wing aircraft. LCTRs would have few delays and a high volume of flights between popular city pairs would enable passengers to reliably leave for a remote city in the morning and reliably return home the same evening. For the LCTR demand set, flights between heavily trafficked city pairs within the range of a typical shuttle operation (500 nm) were identified in the baseline demand set and replaced with LCTRs, travelling between the same city pair. It was assumed, based on expected production rates, that the 2025 scenario would have 300 tiltrotors; the 2040 and the 2086 scenarios would have 800

5.5. **SST**

The SST business case is tied into the vehicle design. NASA directed us to look at a 100-passenger SST that cruises at Mach 1.6. The vehicle design team could not meet the airport noise requirements unless they de-rated the engines, which means that the maximum range becomes 4,000 nm. That range does not allow the SST to fly from California to Asia, but it does allow the SST to fly to Europe from the East Coast, as well as to Hawaii and Alaska from the continental US.

It is clear that the business case for SST relies on time-sensitive travelers paying a premium price for the shorter duration flight. To justify that, the flights should be as long a distance as possible, because short distance flights are dominated by taxi times and terminal wait times, and do not benefit from the supersonic cruise speeds of the SST. We decided that the minimum flight distance that a passenger would be willing to pay a premium fare would be 2,000 nautical miles; industry experts from Boeing confirmed this decision. The farther the flight, the easier the business case for the SST, so flights just below 4,000 nautical miles are preferred.

To develop the business case, we first estimated SST production rates. Boeing told us that there would be none in 2025. In 2040, we can expect about 400 such aircraft and 800 in 2086. Next, we

identified flights in our baseline demand set with stage lengths between 2,000 and 4,000 nm. We considered two business models. The first consisted of the flights having the longest stage lengths, which were exclusively oceanic flights to Europe, Alaska, and Hawaii. However, Boeing noted that an actual SST day would include some repositioning flights within the Continental United States (CONUS). To get that effect, we considered a second case in which flights in the 2,000 to 4,000 nm range were randomly replaced with SSTs. The second and final demand set includes considerably more flights within the CONUS.

6. Demand Generation

6.1. *Baseline demand*

The study used three baseline demand sets that were created by the JPDO's Interagency Portfolio and System Analysis (IPSA) group in 2008. The years 2025 and 2040 were chosen for two of the demand sets because these years bracket the timeframe in which the JPDO-planned NextGen system is expected to be in widespread use. The third, “3X,” demand set has traffic levels that are three times what they are today. This demand set is sometimes referred to as the 2086 demand set because that is the year the JPDO estimated traffic would reach that level. It is also worth noting that a slight increase in the forecasted growth rate can move the year that 3X will be reached from 2086 to sometime in the decade of the 2050's.

To generate a future demand set, the JPDO first selects a representative “seed” day from which to extrapolate traffic patterns. Thursday, July 13, 2006, was chosen because summer is a busy season for air travel and Thursdays are a busy day of the week. Also, July 13 is not associated with a holiday weekend and can therefore be reasonably assumed to be representative of a busy travel day in the summer of 2006. The JPDO grows the seed-day schedule using the expected passenger growth rates that are published annually in the FAA's Terminal Area Forecast (<http://aspm.faa.gov/main/taf.asp>). These growth rates extend 15 to 20 years into the future and are based on factors such as expected growth rates for population and income. Because the TAF forecasts do not, as of this writing, extend beyond 2025, the final year's growth rate for each airport is used to project traffic growth to 2040 and 2086. As with any long-range forecast, the TAF is an extremely coarse estimate of traffic demand significantly far out in the future however it provides a reasonable baseline to start from.

Expected passenger counts are converted into scheduled flights between city-pairs by using what's known as a Fratarling algorithm. When additional flights are needed to handle extra enplanements in the future, the JPDO will duplicate an existing flight in the seed day, slightly offsetting its departure and arrival times from those of the original flight. This process replaces individual flights in the seed day with multiple flights in the future demand set. The added flights are only offset from each other by a minute or so in order to replicate the operators existing business model. For instance, there are often many flights between certain city pairs early in the morning and late in the afternoon but not in the middle of the day as that is when airlines believe passengers want to fly. The JPDO method preserves this business model, however it also means that the forecasted demand sets probably contain slightly more delay than might actually be realized in the future as the operators might change schedules to avoid congested peaks of arrivals or departures. This approach generates future demand sets that look very similar to today's demand, where traffic is concentrated at 30-40 major hubs. Figure 6-1 shows the number of flights by airport and year for the three demand sets.

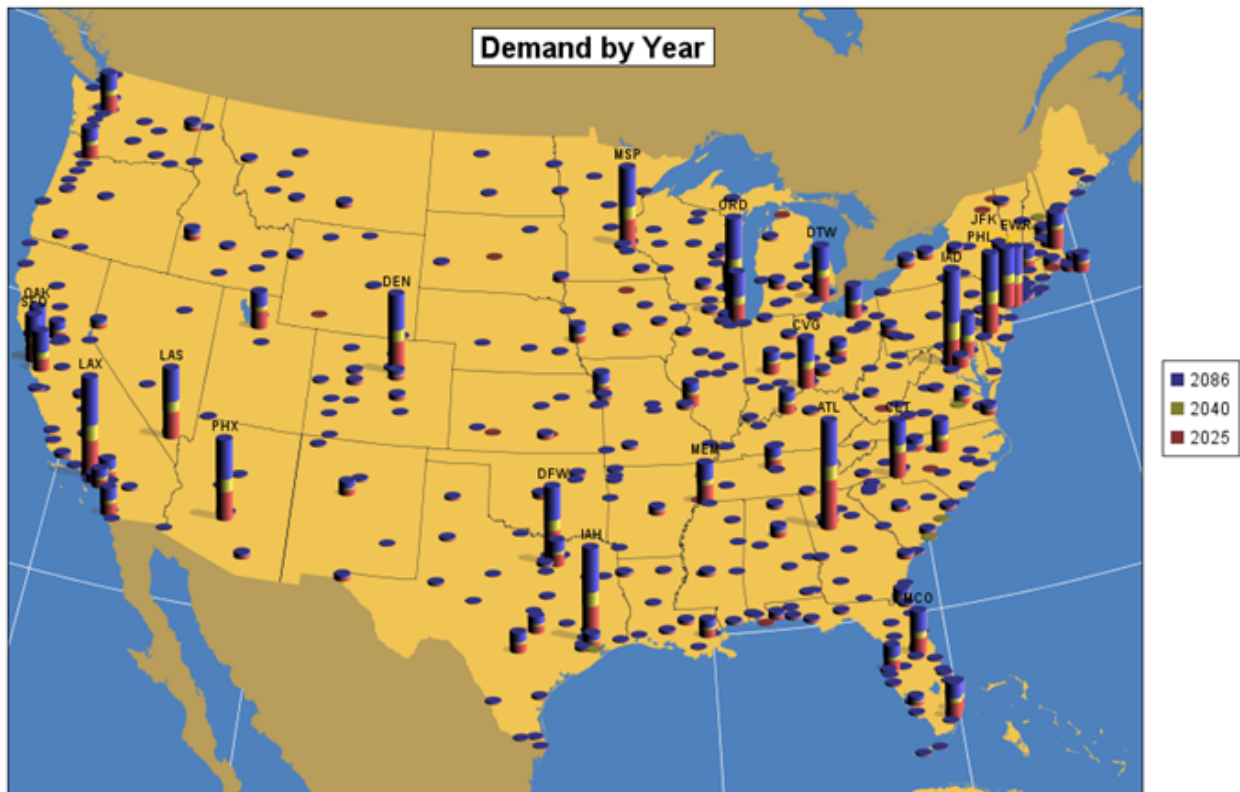


Figure 6-1. Demand level by year at busiest 500 airports for JPDO demand set.

6.1.1.

6.1.2. *Airframe substitutions*

The airframes in the JPDO demand sets were the same as those in the seed day, except for two substitutions made by the JPDO—the super jumbo A380 and the new Boeing 787 Dreamliner. However, aircraft such as the MD8 and DC10 that remained in the demand set are not likely to be flying in large numbers in 2040 and 2086. And keeping those aircraft in the demand set yields an overly noisy, fuel-inefficient, and polluting future NAS. Because we expect many of these older aircraft to be replaced by quieter and more fuel-efficient aircraft in the future, we modified the JPDO baseline demand set, substituting newer airframes for these older ones. We further modified the demand sets using two NASA-envisioned vehicles, the N150 and the N301. The N150 is envisioned as a single-aisle replacement for aircraft like the B737 and the A320, while the N301 is a twin-aisle replacement for aircraft like the B767 and B777. The NASA envisioned performance for these vehicles is an extremely aggressive research target.

Figure 6-1 summarizes the vehicle substitutions we made to the JPDO baseline. For the A306, the number of flights contained in the original IPISA file was 237 in 2025; 201 in 2040; and 376 in 2086. None of these flights were replaced in the modified file in 2025; however, all were replaced with B787s in 2040 and 2086. Half of the B742s in the demand set were replaced by the B748s, and half by A388s. Many of the flights were replaced by the NASA envisioned N150 and N300 as noted in Table 6-1. All

other data for these modified flights—departure and arrival airports, departure and arrival times, and route—were unchanged.

Table 6-1. Replacements made to the original IPSA baseline demand.

AC Type	ORIGINAL IPSA FILE			REPLACED BY . . .		
	2025	2040	2086	2025	2040	2086
A306	237	201	375		B787	B787
A30B	9	12	24		B787	B787
A310	161	126	236		B787	B787
A342	10	15	25		B787	B787
A36	2	2	2		N301	N301
B701	1	1	1	B739	N150	N150
B712	684	423	763		N150	N150
B721	3	3	3	B737		
B722	66	88	162	B738		
B727	419	8	19	B738		
B72Q	2	3	5	B737		
B742	245	330	581	B748/A388	B748/A388	B748/A388
B743	72	117	269	B748/A388	B748/A388	B748/A388
B757	2	4	9		N150	N150
B772	224	332	673			N301
B773	49	75	175			N301
DC10	74	46	83	B772	B787	B787
DC8	4	5	10	B752	N150	N150
DC87	4	6	11	B752	N150	N150

6.1.3. *Trimming*

The initial schedules that JPDO creates using the TAF are based on relatively unconstrained consumer demand; in general they do not account for the finite capacities of airports or airspace (there are some limits on a few major congested airports). When the schedules are flown using ACES, or any other simulator, the delays that result are much longer than would be tolerable in practice. To obtain schedules with reasonable delays, flights are removed from the unconstrained schedules using a process known as trimming.

To trim the schedules, JPDO runs the unconstrained demand sets through LMInet, a queuing simulation developed in the late 1990s.^{xxiii} The flights to be deleted are those that LMInet identifies as having the highest congestion scores; that is, the flights that flew through the most crowded sectors and arrived at or departed from the most crowded airports. Deleting all of the flights from a JPDO list of most congested flights to create a schedule that induces only mild average delay per flight (on the order of two minutes per flight) produces what we refer to here as the 100% trimmed schedule; deleting half the flights in the list gives the 50% trimmed schedule. As shown in Figure 6-2, the number of flights trimmed from the 2086 schedule is much greater than the number trimmed from the 2025 schedule. To understand the

effect of varying demand, the project used demand sets at five trim levels: 0%, 25%, 50%, 75% and

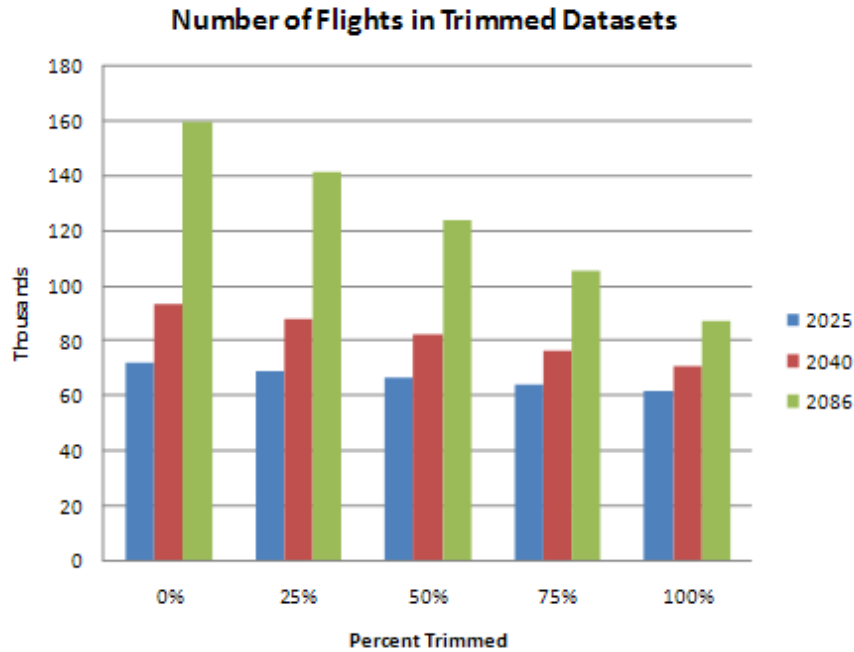


Figure 6-2. Number of flights in baseline demand sets by year using JPDO trim.

100%.

Because the flights in the JPDO trim list come from highly congested airports and fly during the busiest hours of the day, removing these flights causes a substantial decrease in delay. The middle curve in Figure 6-3 shows average NAS-wide delay, as computed by ACES, as a function of the number of scheduled flights for the 2025 schedule. The right endpoint of this curve is the untrimmed demand set, which has 79,000 flights. For this schedule ACES computes an average delay per flight just below 20 minutes. When all of the flights in the JPDO list are removed, the resulting schedule has 69,000 flights and an average delay of just two minutes. In other words, this 13% reduction in flights leads to a 90% reduction in delay.

To understand the relationship between delay and trimming, we experimented with two other trimming methods. The top curve in Figure 6-4 shows delay versus the number of flights if one simply deletes flights at random from the demand set. This method is much less efficient at reducing delay than the JPDO method. The bottom curve shows a trimming approach that is more efficient than the JPDO method. For this approach we modeled the delay at each major airport in the NAS as a simple deterministic queue. We then successively removed the flights from the demand set that caused the most delay. Targeting flights based on the amount of delay they cause clearly reduces delay very rapidly when delays are high. In addition, this figure demonstrates that the method chosen for trimming flights has a big

impact on delay. For consistency with other studies, the method used for the rest of this project was the JPDO trimming method.

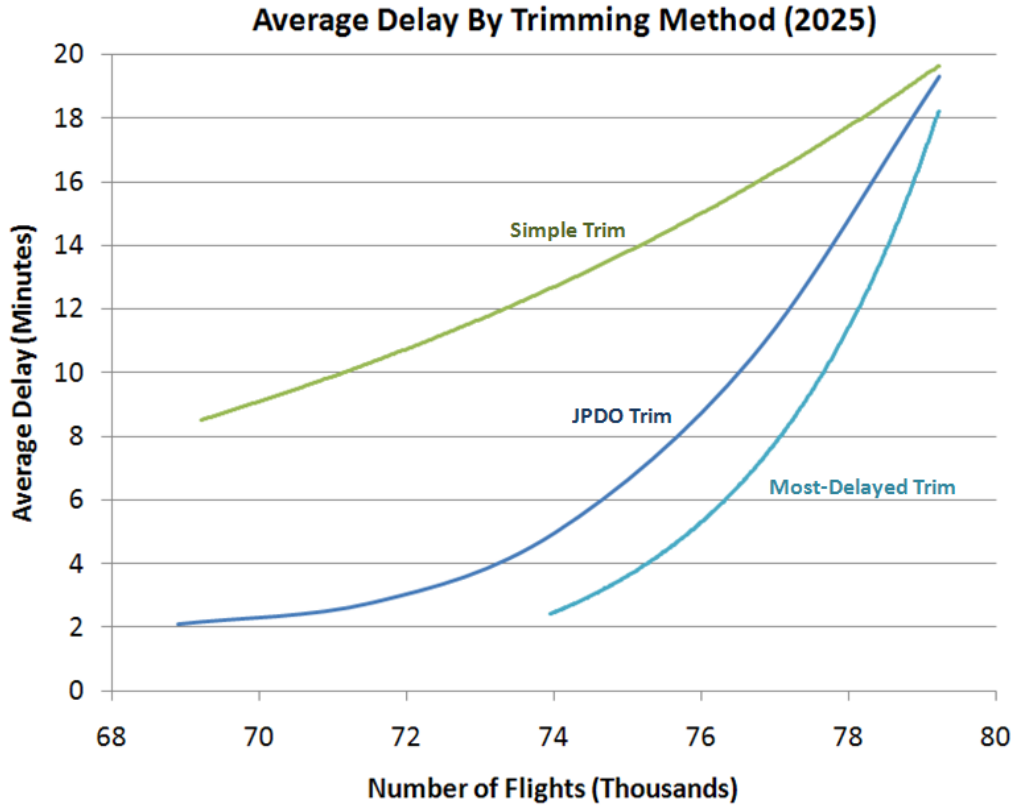


Figure 6-3. Average delay versus number of flights for three different trimming methods.

6.1.4. Tail tracking

In a demand set that is not tail-tracked, every aircraft is at the airport and ready to take off at its scheduled departure time; it is only delayed because of congestion at the departure airport, destination, or in the airspace it must fly through to reach its destination. In reality, however, aircraft travel on itineraries between multiple city pairs and flights often take off late because the aircraft was delayed at some bottleneck earlier in the day. For example, an aircraft that departs an hour late from one airport will arrive an hour or so late at its destination. Depending on how much slack is in an airline's schedule, this aircraft will likely depart late to its next destination, and so on throughout the day. Therefore, demand sets that are not tail-tracked can drastically underestimate delay.

There is no source of data available on existing tail connectivity for the various operators and obviously there is no source for the new flights we created in the future. To account for the propagation of delay, we added tail numbers to the flights in the JPDO-provided demand set using what's known as a greedy algorithm. Assuming a turn-around of 45 minutes, each flight that arrives at an airport is paired with the earliest possible departing flight having the same equipment type and airline. This method results in an average of about 1.8 flights per day per airframe with about 15% of airframes flying more than three or more legs per day. This is about half the number of legs per day per airframe than is found in actual schedules. For example, Figure 6-4 shows that tail-tracking the flights for Southwest airline in our 2025 untrimmed demand set results an average of about 3-4 flights per day per airframe, whereas Southwest's actual schedule averages 6 to 7 flights per airframe per day (Bureau of Transportation Statistics, 8 June 2009).

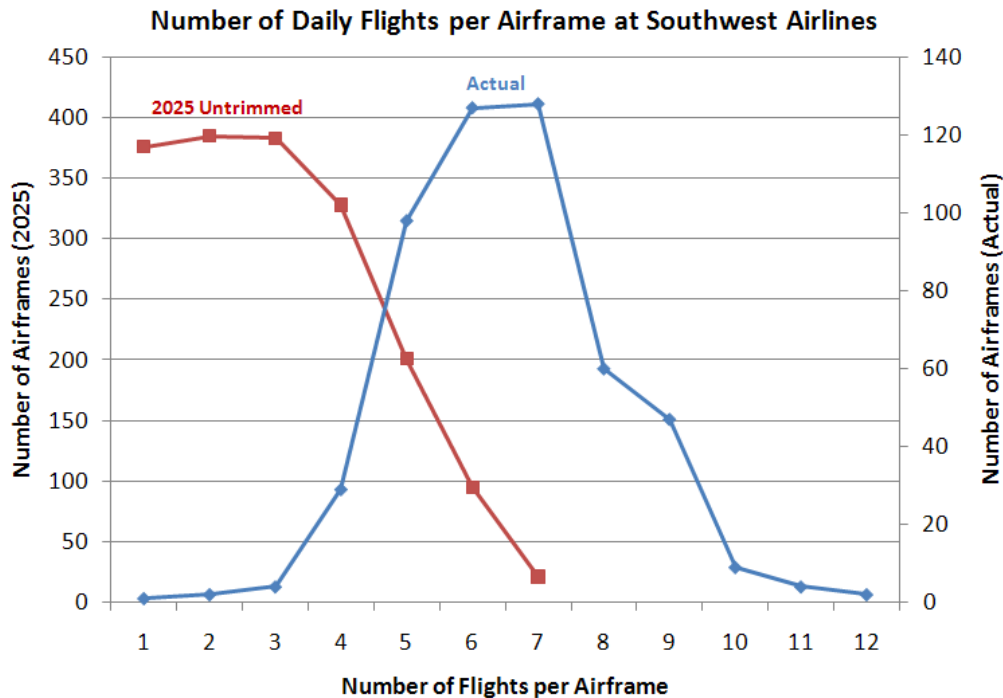


Figure 6-4. Comparison of daily flights per airframe.

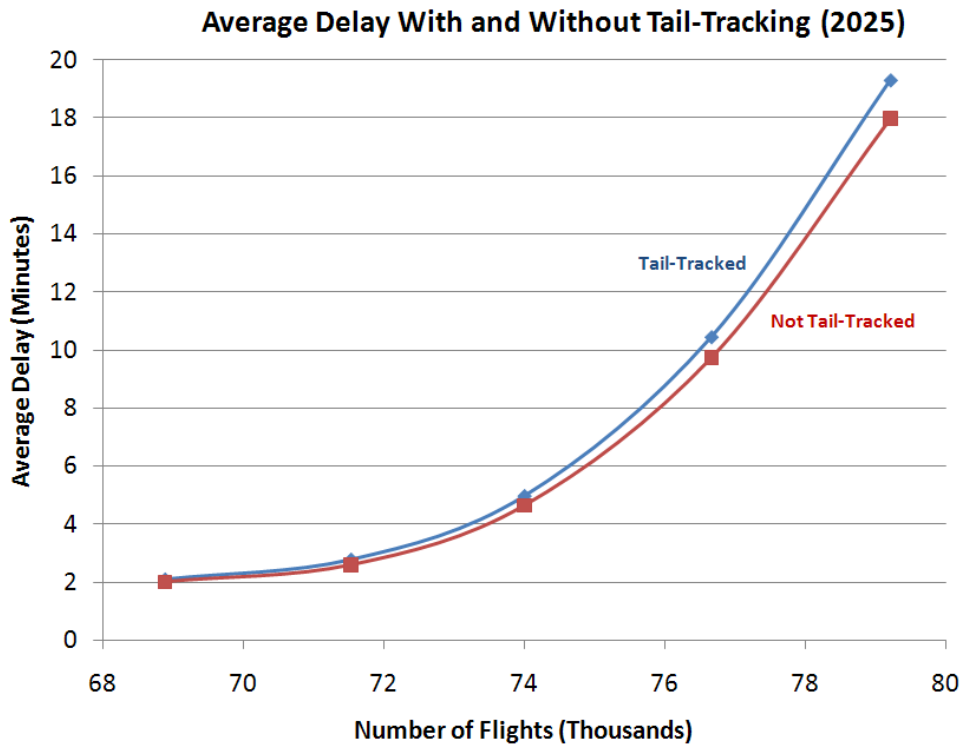


Figure 6-5. Delay versus average number of flights with and without tail-tracking (ACES).

Figure 6-5 presents ACES results for the 2025 baseline demand set, with and without tail-tracking. It shows that tail-tracking raises average NAS-wide delay by about 7%. Late in the study we identified a bug in ACES that causes tail-tracked airframes to occasionally take off before their previous leg has landed—meaning that a single airframe can sometimes be in two places at the same time. The occurrence of this bug is rare, affecting only about 1-2% of the aircraft in the simulation. We estimate that it leads to an underestimation of average delay by about 3.5%. Were this bug corrected we would expect that maximum delay with tail-tracking shown in Figure 6-5 to be 19.7 minutes rather than the 19.3 minutes shown.

A demand set with a higher number of flights per airframe than we were able to achieve with our tail-tracking algorithm would see a significant increase in delay, perhaps on the order of a 20-30% increase in delay compared to a not tail-tracked demand set. It should be possible to devise a better algorithm for creating itineraries that better resemble actual airline itineraries. Doing so would require modifications to the replication process that is used to generate future demand sets. The addition to the schedule of trains of aircraft that are slightly offset in time might be leading to schedules that cannot be optimized as efficiently as real-world schedules. Schedules with too few legs per airframe per day require more airplanes than real-world schedules and produce less than the expected amount of propagated delay.

6.1.5. Lessons learned in developing demand sets

In developing demand sets, we found that we sometimes overlooked details that required us to go back and rerun ACES with corrected demand sets. These problems consumed resources for the study because ACES requires several hours to run with large demand sets.

The most costly problem in terms of time, and one of the most difficult to uncover, came about because the scheduled arrival and departure times in the demand set we were given did not include taxi-in and taxi-out times. For a schedule that was not tail-tracked, this would not be a problem because ACES ignores the arrival times that are in the schedule and only uses the departure times. ACES creates its own scheduled arrival times by flying the flight unimpeded through the airspace. Because we assumed that the scheduled times in the demand set were gate-to-gate times instead of wheels-off to wheels-on times, our tail-tracked demand set sometimes ended up with aircraft being scheduled to depart before the time that their previous leg was scheduled to arrive. This error gave results with too much delay and many of our early ACES runs had to be discarded and rerun with corrected schedules.

We found that to properly calculate delay for a tail-tracked demand set we need to run the demand set through ACES twice; the first time to obtain the scheduled arrival times for the different flights using the unimpeded flight times determined by ACES. We then used our algorithm to tail-connect the demand set, which was then run through ACES a second time.

6.2. New Vehicle Demand Sets

6.2.1. CESTOL

The main advantage of CESTOL aircraft is that they can take off and land on runways as short as 3,000 feet. When taking off from a short runway the range of the aircraft is limited to about 600 nm. The

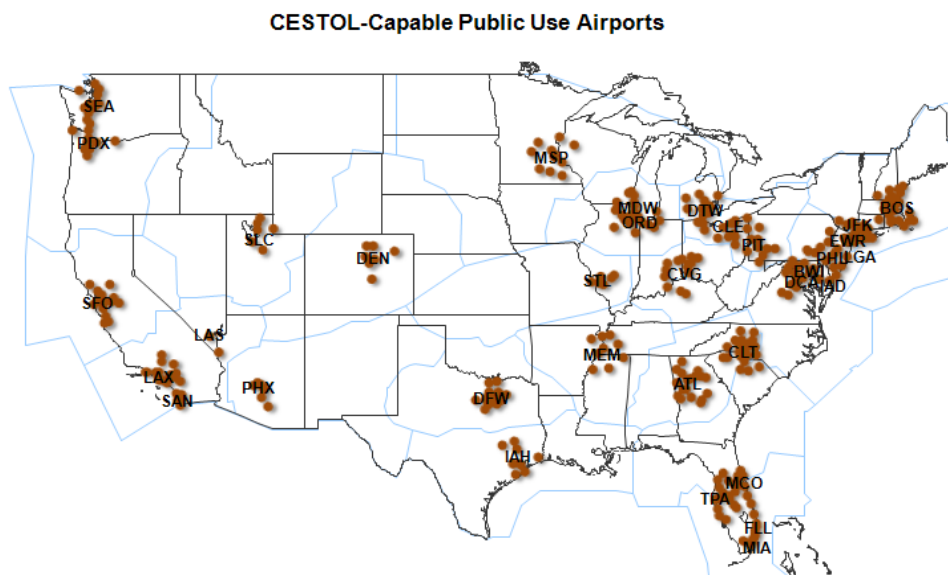


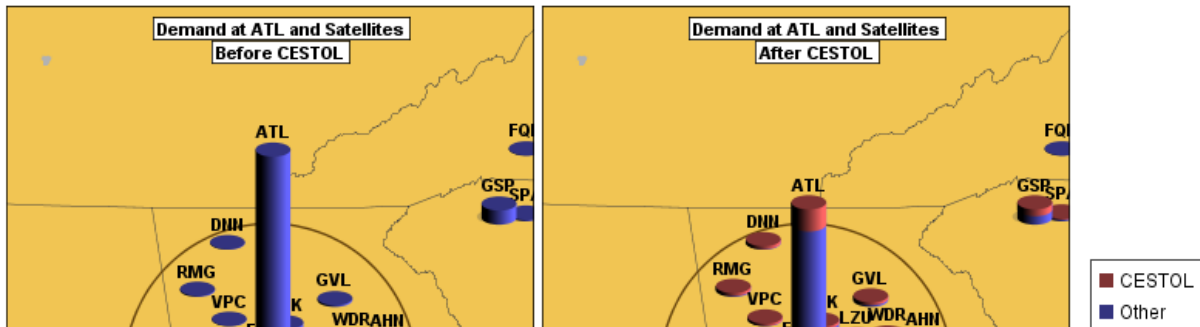
Figure 6-6. Locations of CESTOL-capable airports within 70-nm of OEP airports.

CESTOL concept of operations replaces excess flights at congested airports with flights operating out of nearby satellite airports. Figure 6-6 shows the locations of 469 public-use airports with runways that could support CESTOL operations and that are within 70 nm of a major airport.

The CESTOL schedules were created by modifying the untrimmed baseline schedules for 2025, 2040, and 2086. Specifically, whenever the demand-capacity ratio within a 15-minute time-bin at a major airport exceeded 90% of the airport's visual flight rules (VFR) capacity, the excess flights were shifted to a satellite airport that was within 70 nm of the original airport. The equipment type of the shifted flights, all of which had stage lengths less than 600 nm, was converted to CESTOL. Trimming for the CESTOL worked as follows: Flights that were on the JPDO list were removed from the schedule excluding those flights that had been shifted to satellite airport.

Applying the CESTOL reassignment algorithm to the untrimmed 2025 baseline schedule caused 2,490 flights to be shifted, resulting in a 5% reduction in traffic at the busiest 35 airports. Using estimated CESTOL production rates, it was assumed that the 2025 schedule would have approximately 5,000 daily CESTOL flights. To make up the difference, a random number generator was used to substitute CESTOLs for conventional aircraft flying routes with stage lengths less than 600 nm. Figure 6-7 shows a comparison of the number of flights at Atlanta-Hartsfield International Airport (ATL) before and after the offloading of the CESTOL flights. Schedules with CESTOLs were created in a similar manner for 2040

and 2086. It was assumed that there would be 12,000 daily CESTOL flights in 2040 and 30,000 daily CESTOL flights by 2086.



6.2.2. LCTR

As with the CESTOL, the tiltrotor would relieve congestion at major airports by shifting traffic away from runways with high demand at congested airports. A short-haul aircraft with 90 seats and a 500 nm range, the tiltrotor can take off and land from a 600 ft. landing pad, freeing up an airport’s main runways for longer-haul transports. Because of high expected production and operations costs, it was assumed that tiltrotor operations would be confined to profitable high-frequency shuttle routes. Specifically, we identified city pairs having at least fifteen flights in one direction during a single day. Tiltrotors replaced the large aircraft using these routes in a way that preserved the number of aircraft seats. For example, two 150-seat aircraft would be replaced by three tiltrotors. It was assumed, based on expected production rates, that the 2025 scenario would have 300 tiltrotors, the 2040 scenario would have 800, and the 2086 scenario would have 2,300. Figure 6-8 shows the routes flown by the tiltrotor in the 2025 schedule. The tiltrotor replacement algorithm was applied to each baseline dataset after it had been trimmed.

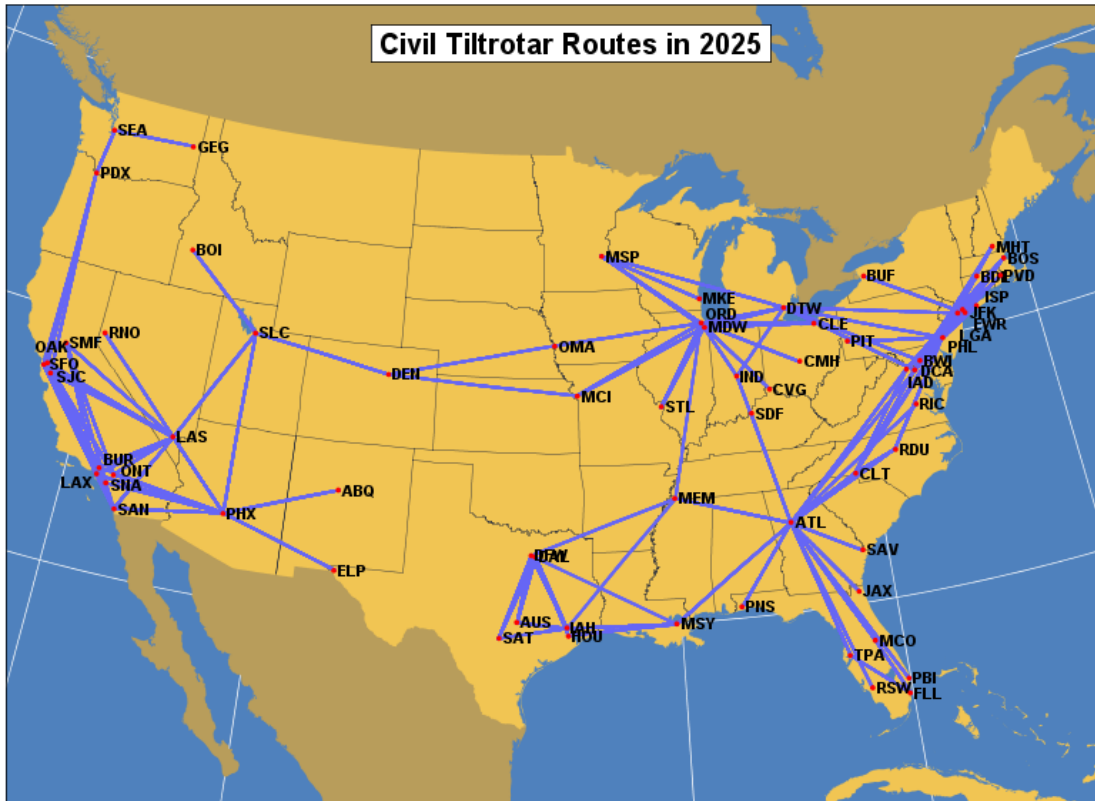


Figure 6-8. Scheduled routes for the Large Civil Tiltrotor in 2025.

6.2.3. UAS

UASs are interesting because they describe a level of technology, not a particular aircraft. UAS technology, if perfected, could feasibly be used in any aircraft from light reconnaissance activities (for which they are used today) through large commercial airliners. UAS requirements on this project included (1) a vehicle that weighed over 100 pounds; (2) a civilian mission; (3) a mission that impacts traffic levels in the NAS. To satisfy these three requirements, a mission involving freight forwarding using small aircraft was analyzed.

Rapid freight delivery today involves large aircraft flying to many spoke airports. When packages arrive at a spoke airport, if they are destined to a remote area, they can be forwarded by truck or by small aircraft. Which mode is chosen is strictly a matter of cost. On one of the days analyzed—December 20, 2007—two-hundred fifty three small-aircraft cargo flights were identified serving city pairs that began at a freight carrier’s “spoke” airport and ended at a smaller airport, usually in a rural area. The preferred vehicle for these freight-forwarding flights was a “Cessna Caravan Super Cargo Master” (C208) and its variants.

Were UAS technology to be installed on C208 aircraft, it would have the following effects. First, all material related to pilot comfort and safety—seats, seat belts, yokes, rudders, air conditioning, and most avionics—could be removed from the aircraft. However, extra avionics required to securely communicate between a pilot on the ground (remotely monitoring the flights) and the on-board flight control system would be needed as well as enhanced automation. The project estimated that the weight

savings from removal of pilot necessities approximately balanced the weight gain from additional communication avionics, resulting in no net increase in weight or cargo capacity.

The UAS would have some cost savings because one ground-based pilot could remotely monitor several vehicles. Thus the breakeven point between using a truck and using a C208 for freight forwarding is likely to change in favor of the C208. The project estimated that currently the breakeven point is roughly 120 miles, meaning that if a truck must travel more than 120 miles along roads then the C208 is more cost effective. Because precise cost estimates of UAS technology are difficult to forecast, the project developed UAS demand sets with distance ranges 30-60 miles, 60-90 miles, 90-120 miles, and 120-150 miles.

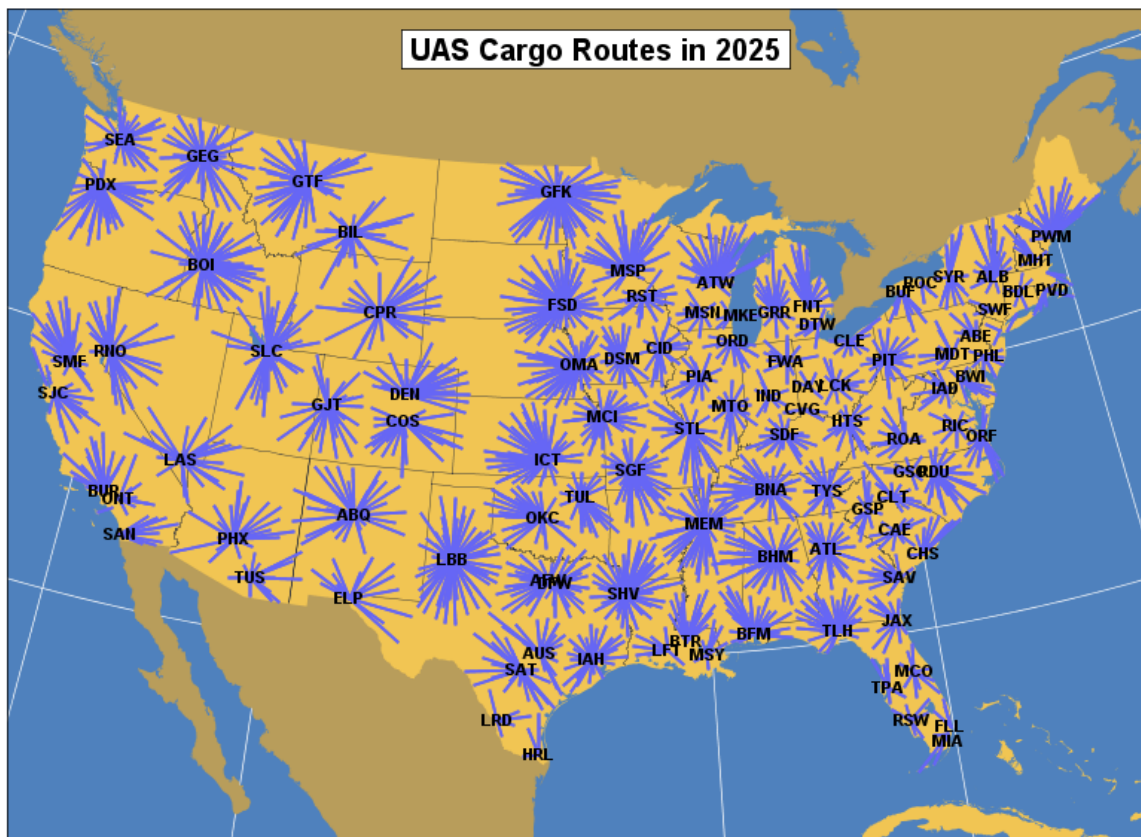


Figure 6-9. UAS cargo routes in 2025.

6.2.4. VLJ

VLJs are in commercial use today. Expanded use of VLJs assumes decreasing operating costs relative to other forms of transportation and increases in delay and unreliability of other forms of transportation. The VLJ schedules shown in Figure 6-10 were created by researchers at NASA's Langley Research Center using Virginia Tech's Transportation Systems Analysis Model (TSAM).¹⁶ Using projected demand between city-pairs, the model computes the number of flights that could be flown in an economically competitive manner by a 4-passenger VLJ given certain assumptions regarding airline operating costs, the price of jet fuel, and the cost of auto travel. Under this study's assumptions very few

VLJs fly into major hubs. Future VLJ demand was created for the 2025 and 2040 datasets but was not created for the 3X dataset. Roughly 4,000 VLJ flights were added to the 2025 datasets (at all trim levels); and roughly 7,000 VLJ flights were added to the 2040 and 2086 datasets.

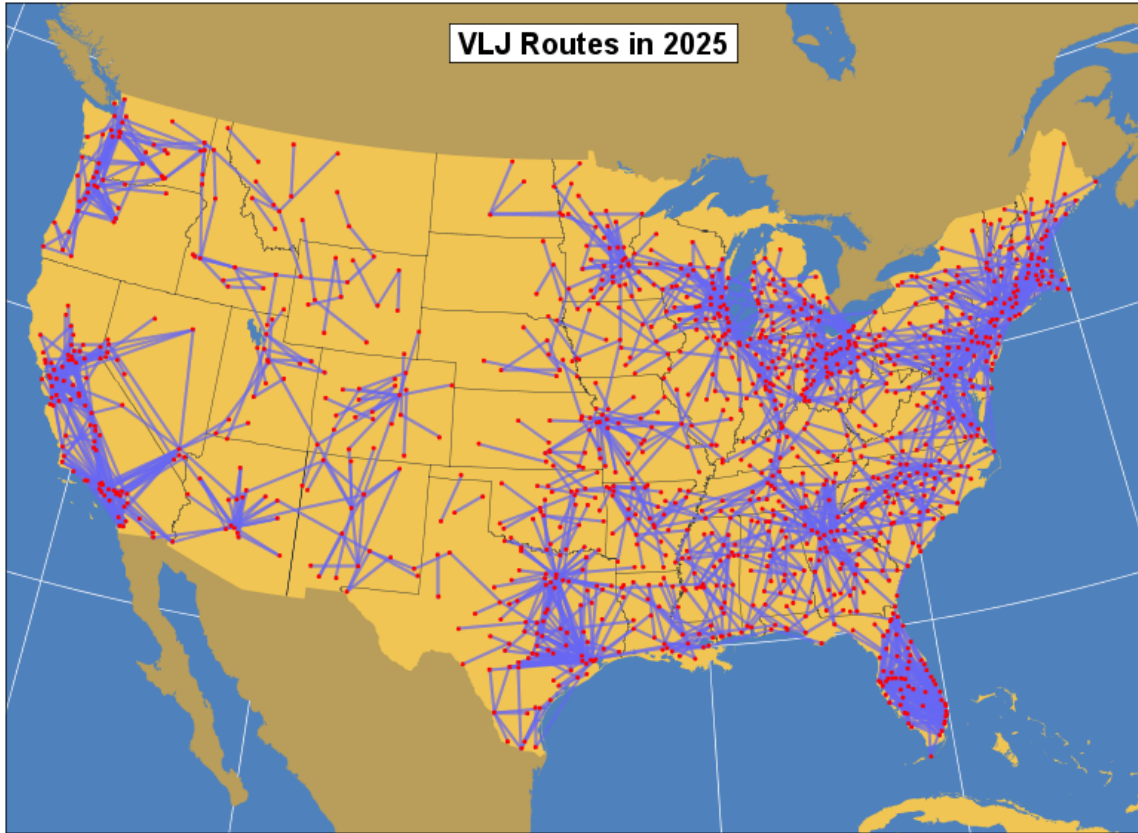


Figure 6-10. VLJ routes in 2025.

6.2.5. SST

Two scenarios were modeled for the SST, a 90-seat aircraft with a maximum range of 4,000 nm. In the first scenario, shown in Figure 6-11, the SST randomly replaced conventional aircraft on routes with stage lengths between 2,000 and 4,000 nm. In the second scenario, shown in Figure 6-12, the SST replaced conventional aircraft on long commercial routes having stage lengths under 4,000 nm. No SSTs were assumed to have been built by 2025; the 2040 and 2086 schedules assumed 400 and 800 SST flights respectively.

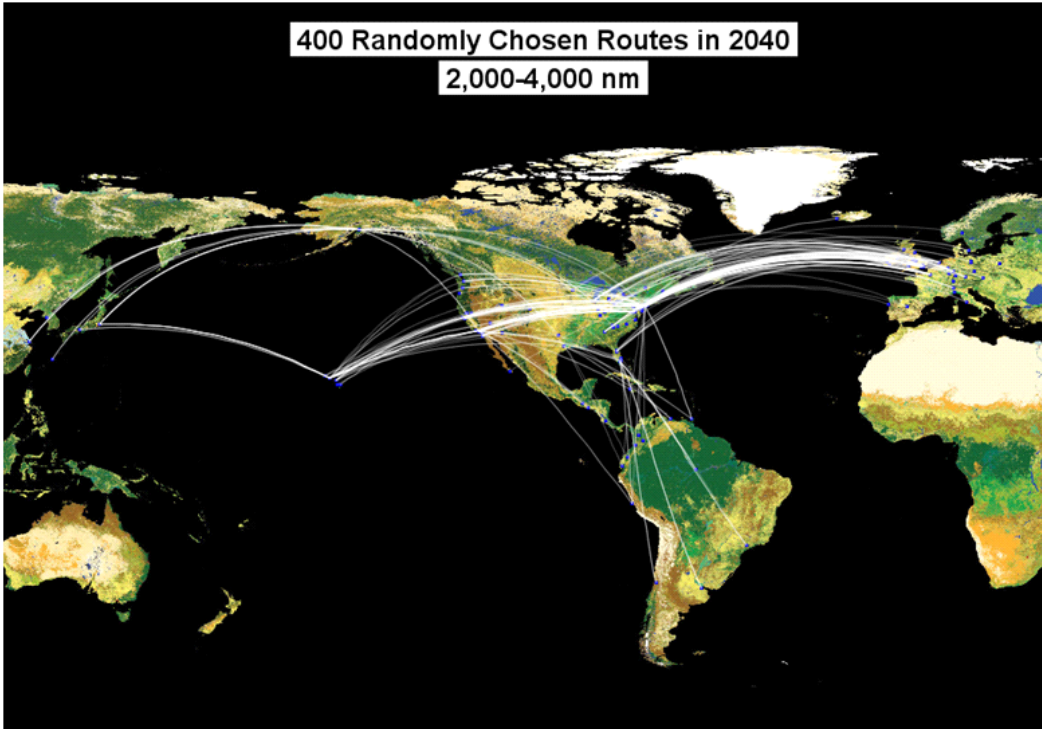


Figure 6-11. SST routes 2,000-4,000 nm (2040).

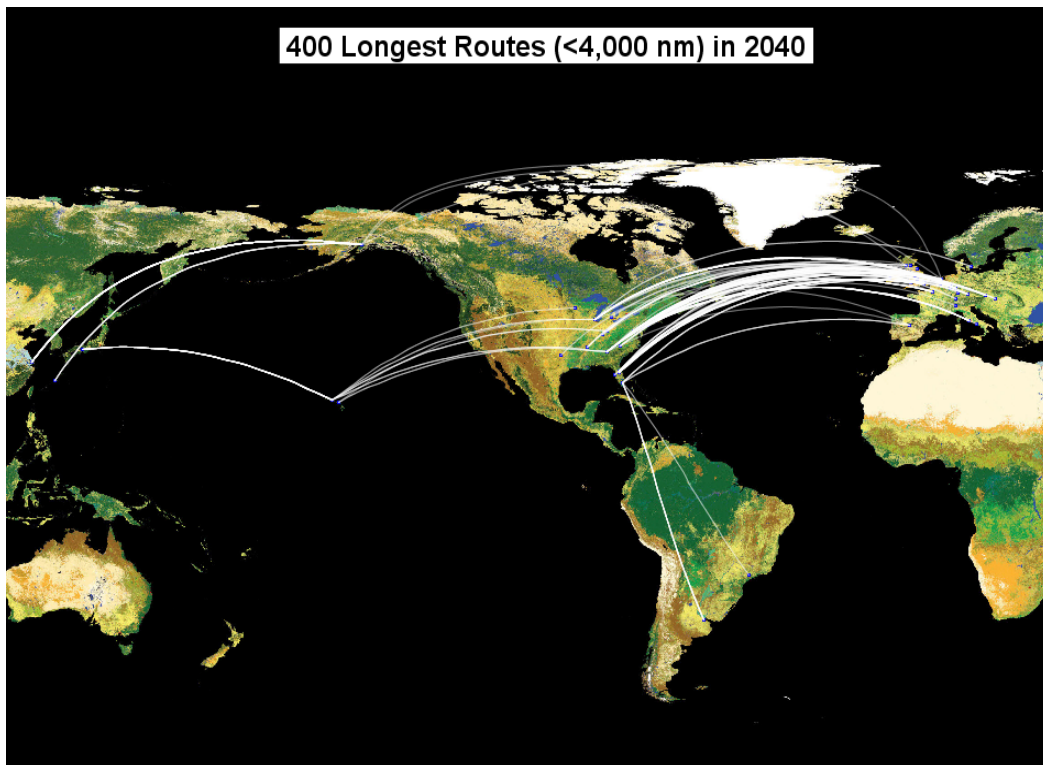


Figure 6-12. SST longest routes (2040)

6.2.6. All-Vehicle

Demand sets were also created for an all-vehicle scenario that included all five vehicles. The numbers of each type of new vehicle in the trimmed version of these demand sets is shown in Figure 6-13. Although the total number of vehicles varied across scenarios, all scenarios had the same passenger demand.

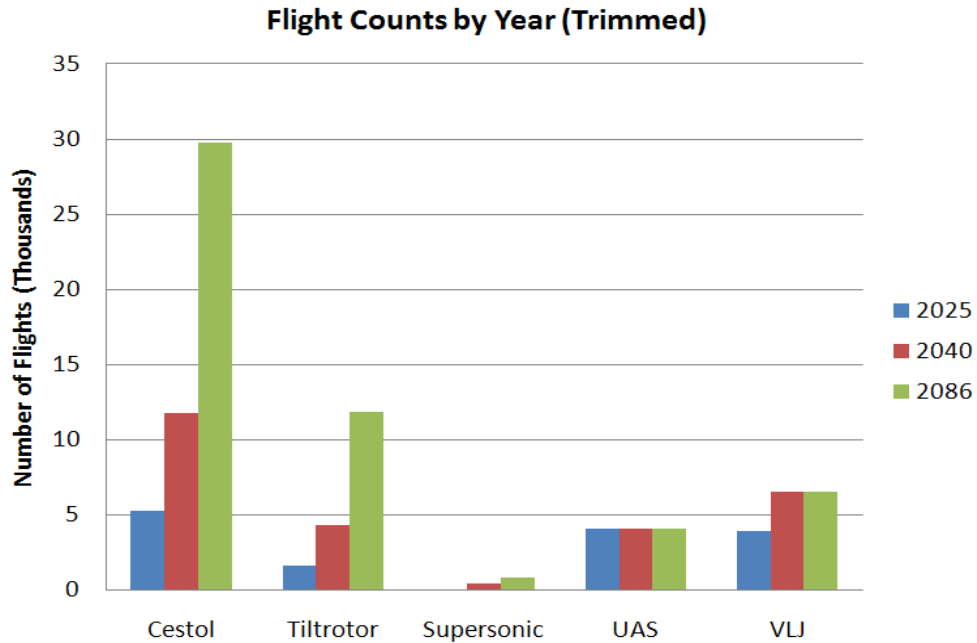


Figure 6-13. Number of new vehicle flights by scenario (100% trimmed).

xxiii Peter F. Kostiuik, Eric M. Gaier, and Dou Long, “The Economic Impacts of Air Traffic Congestion,” *Air Traffic Control Quarterly*, Vol. 7(2), 1999, pp. 123–145.

7. Vehicle Design

The focus of this section is to identify and categorize the potential attributes of a selection of several classes of advanced vehicles as they affect operation in NextGen projected for 2025 and beyond. The following sections will present an overview of each advance vehicle concept, focusing on their mission and operational capabilities in the NextGen context. The approach used to design each of the vehicles will be provided and, subsequently, the final designs will be discussed.

7.1. **CESTOL**

The CESTOL aircraft was envisioned to be a new class of civil transport that can take off and land on substantially shorter than conventional runways but can still cruise at fuel efficiency comparable with similar size existing aircraft. For this study, the CESTOL aircraft was proposed to be a 100 passenger regional jet cruising at Mach 0.78. The introduction of such an aircraft was anticipated to revitalize the currently underutilized airports within a Metroplex and underutilized runways at congested hub airports (such as Newark), thus alleviating traffic congestion at hub airports. Leveraging on unparalleled low speed performance, the CESTOL platform can serve as an excellent test bed for investigation of innovative terminal area procedures, such as steep approach, spiral descent, and Simultaneous Non-Interfering closely spaced parallel runways envisaged in NextGen.

7.2. **VLJ**

There have been predictions of very light jets (VLJ) dominating the future air transportation system for several years now. While a fewer than 500 aircraft in the VLJ and light jet category exist today, and cause minor issues in the current airspace, the prospect of ubiquitous VLJ usage raises significant issues for the performance of NextGen. While some of the pioneering VLJ on-demand air carriers were unable to survive in the current economic climate, there remains the probability that an economically viable equilibrium could be achieved. The experiences gained by on-demand carriers in the 2006 to 2009 time period proved the existence of the market, illustrated the value of networked fleet management (as contrasted with traditional out-and-back charter operations), and revealed the value of low-cost, modest performance aircraft to serve on-demand markets that are too thin for scheduled service. Conversations with Bruce Holmes, formerly of DayJet, a VLJ operator, indicated that, at the time, DayJet anticipated that the VLJ refresh cycle would be on the order of every five years instead of the more typical 20-25 years for current commercial aircraft^{xxiv}. As such, the advanced VLJ described in this section is four generations past those that are currently in service or in the process for being certified. The VLJ was anticipated to be a single crew, 4-passenger aircraft that can operate out of airports with a minimum 3,000 ft runway length with steep approach procedures. Additionally, it is anticipated that single-engine VLJ aircraft could offer a significant reduction in on-demand air carrier operational costs compared to the first generation of multi-engine VLJs.

7.3. **UAS**

Unmanned Aircraft Systems (UAS) have been proposed for a multitude of missions from high altitude measuring and communication, through persistent urban surveillance, and carrying time critical cargo to remote locations where it is not cost effective to provide crewed service. Thus, depending on the

application of an UAS, the design can be substantially different. One business model of its civilian application is freight forwarding, operating continuously for next-day delivery service. FedEx has long been using small cargo airplanes for this application. In 1986, Cessna developed a cargo version of the Cessna 208 Caravan for FedEx, called the CargoMaster; later, a bigger cargo version by stretching the fuselage by 4 feet, installing a ventral cargo pod, and upgrading to a more powerful engine, which is the Super CargoMaster^{xxv}. Now FedEx is operating more than 250 Super CargoMaster^{xxvi} aircraft. As a basis of this NRA, a UAS vehicle that would have an impact on NextGen was desired. As a result, this latter business model was assumed for the UAS developed herein. The UAS was designed to carry a couple of thousand pounds of payload from a larger transshipment point to closer to the point of final delivery.

7.4. **LCTR**

Civil rotorcraft have the potential to relieve air traffic congestion by utilizing runway independent, vertical terminal operations and providing point-to-point travel. However, the meaningful integration of this potential capability into NextGen presumes overcoming limits of current rotorcraft technologies. Enhanced throughput capability (higher speed, longer range, and more payload capability), operational and environmental (especially noise) acceptance will be the key drivers towards the air transportation system level operation of rotorcraft. In the late 80's, the Boeing company showed that a large commercial tiltrotor fleet derived from the V-22 Osprey technology could partially fulfill these challenges in an economically viable manner^{xxvii}. More recently, NASA's comparative research for future heavy lift rotorcraft systems concluded that "Large Civil Tiltrotor had the best cruise efficiency, hence the lowest weight and cost and were economically competitive, with the potential for substantial impact on the air transportation system^{xxviii}." For the current study, NASA's up-to-date concept of large civil tiltrotor, LCTR2, was chosen as the baseline rotorcraft vehicle. LCTR2 was designed for the short-haul regional market with entry into service of 2018 or later; it carries 90 passengers for 1,000 nm with 300 knots cruise speed^{xxix,xxx} and can operate from under utilized vertiports. The choice of this particular vehicle concept is necessary and useful because LCTR2's vehicle characteristics reflect the relevant technological challenges and their resolution for the future of high-speed and long-range rotorcraft.

7.5. **SST**

A commercial supersonic aircraft would significantly reduce trip time and consequently pave the way for rapid travel all over the world. The vehicle analyzed in this study was a 100 passenger aircraft with a range of 4,000 nm and that cruises at Mach 1.6. The SST design was subjected to several noise and emissions constraints. In terms of noise, the vehicle was desired to have a low boom signature (65-70 PLdB) over land and also meet the 20-30 EPNdb noise constraint in terminal areas. In terms of emissions, the aircraft in cruise was desired to produce less than 5 grams of nitrous oxides per kilogram of fuel, while at the same time mitigating the water vapor in the high atmosphere. The SST concept was the most technically challenging vehicle for this study.

7.6. **Vehicle Modeling Approaches**

The purpose of developing new vehicle models for the NextGen research task was to provide the capability to represent the new vehicle concepts in the procedure design and analysis tools described in other sections of this report. These tools, primarily, use one of two performance models. The first of these

is Eurocontrol's Base of Aircraft Data (BADA)^{xxxii}, the second is that described in SAE AIR-1845^{xxxiii}. Due to the data requirements of the other analysis tools, any representation of future vehicle concepts must be made compatible with these approaches. This process implies that advanced levels of aircraft modeling will be appropriate when proposed new vehicle concepts are dramatically different than existing BADA or AIR-1845 entries.

The five vehicle models specified by NASA for investigation were split into two groups. The first group included the CESTOL, LCTR, and the SST; the second included the VLJ and the UAS. The first group approach was to create detailed performance and sizing models of the aircraft using higher fidelity tools to capture the range of performance and then create BADA and AIR-1845 models that approximate the vehicles behavior as closely as possible. The two approaches are the FAA's Environmental Design Space (EDS) and other NASA tools and the AEDT High-Level approaches, respectively. The reader is directed to Reference xxxiii for more detail regarding EDS developments and capabilities. The second group was modeled using a relatively high-level characterization approach, which was based on directly representing the aircraft in BADA and AIR-1845 using simplified engineering approaches.

EDS/NASA Tools Approach

The EDS/NASA tools approach enabled ASDL to construct a vehicle model accounting for interdisciplinary couplings across key aircraft sizing and synthesis components as well as detailed engine design and performance aspects. EDS is a numerical simulation based on physics rather than expert opinion or inventory analysis that is capable of estimating source noise, exhaust emissions, and performance for potential future aircraft designs under different technological, operational, policy, and market scenarios. The detailed EDS modules, originally developed by NASA, are seamlessly integrated to provide vehicle level emissions, noise, and performance characteristics required by ACES and AEDT and include the tools listed below.

- a. CMPGEN – Compressor performance map generator^{xxxiv}
- b. Numerical Propulsion System Simulation (NPSS) – calculates the engine thermodynamic analysis^{xxxv,xxxvi}
- c. Weight Analysis of Turbine Engines (WATE) – estimates component weights and dimensions based on cycle parameters calculated in NPSS^{xxxvii}
- d. Emissions correlations – Method based on a P3-T3 methods^{xxxviii}
- e. FLight OPTimization System (FLOPS) – calculates aircraft weights and performance results based on mechanical model from WATE and cycle performance from NPSS^{xxxix}
- f. Aircraft Noise Prediction Program (ANOPP) – predicts certification noise levels and noise power distance curves, based on aircraft dimensions from FLOPS and engine information from NPSS and WATE^{xl}
- g. Arnie McCullers' version of WAVE drag (AWAVE) – calculates supersonic wave drag^{xli}
- h. WING DESign (WINGDES) – calculates induced drag^{xlii}

- i. Boeing Design and Analysis Program (BDAP) – calculates skin friction drag^{xliii}
- j. Two Surface Aerodynamics (AERO2S) – calculates low speed aerodynamics^{xliv}
- k. PBOOM^{xlv} and PCBOOM^{xlvi} – In this study PBOOM is used specifically to optimize the fuselage shape by optimizing the area rule distribution of the vehicle, where PCBOOM is used to calculate the boom loudness.

When EDS executes an analysis for any aircraft, the required AEDT and ACES information are created in terms of the BADA and AIR 1845 data. For this study, the CESTOL and SST utilized elements of EDS, specifically items “a” through “f”. The SST required additional analysis capability for the aerodynamics and boom signature adding the “g” through “k” analysis tools listed above. The LCTR model required a separate analysis capability that was specific to rotorcraft sizing and synthesis. Specifically, based on the detailed descriptions on LCTR vehicle provided by NASA, VASCOMP II^{xlvii} was utilized to obtain compact and reasonably accurate model for the baseline. VASCOMP II is a first order sizing and performance analysis program for generic vertical takeoff and landing aircraft.

AEDT High-Level

Some of the new vehicle concepts are, from a performance point of view, substantially similar to or are evolutions of aircraft types that currently exist. Given that the goals of the NextGen project were to evaluate the system level impacts of these new aircraft concepts, it was not necessary to produce highly detailed vehicle models with EDS for the systems that could be represented using lower fidelity approaches. The vehicle class models that were developed using deviations from existing BADA and AIR-1845 performance models included the VLJ and UAS. The process of developing new aircraft performance models started with the identification of one or more similar aircraft models that currently exist in either the BADA and/or the SAE-1845 data sets. At the same time, technology and future performance data was collected to determine performance, noise, and emissions improvements for the future aircraft. The development of new vehicle models from the baseline models was a three-part process.

- Determine or match performance fuel burn over a range of missions
- Adjust emissions indices to match engine emissions improvements
- Adjust noise power distance and spectral information to obtain noise benefits

The first step of the process is the most important as it determines the overall performance of the vehicle concept for use in the ACES analysis tool to quantify the impact in the airspace. The second two steps were necessary to capture the full range of environmental improvements measured using AEDT. The general process flow is depicted in Figure 7-1. The iteration for drag-polar, specific fuel consumption and payload-range were performed using a simple Breuet range equation basis or for more detail, a simplified model in FLOPS. Regardless of the approach, the performance coefficients, both BADA and AIR-1845, were investigated using AEDT’s performance model, which implements both BADA and AIR-1845. This approach ensured that field, departure, enroute, and arrival performance meet both the needs of the vehicle concept and provide sufficient margin to ensure safe operation through a variety of airspace concepts. Once the vehicle performance and fuel burn were determined, the resulting BADA

coefficients and general performance metrics were passed to other team members for the procedure development and ACES analysis. The second and third steps in the high-level characterization process were specific to the environmental impact-modeling portion, specifically AEDT. AEDT implements both BADA and AIR-1845 equations to determine aircraft performance and fuel burn throughout the full range of the flight envelope. It also implements the Boeing fuel flow method^{xlviii} to determine emissions and AIR-1845 and ECAC Doc. 29^{xxxii,xlix} to estimate noise impact.

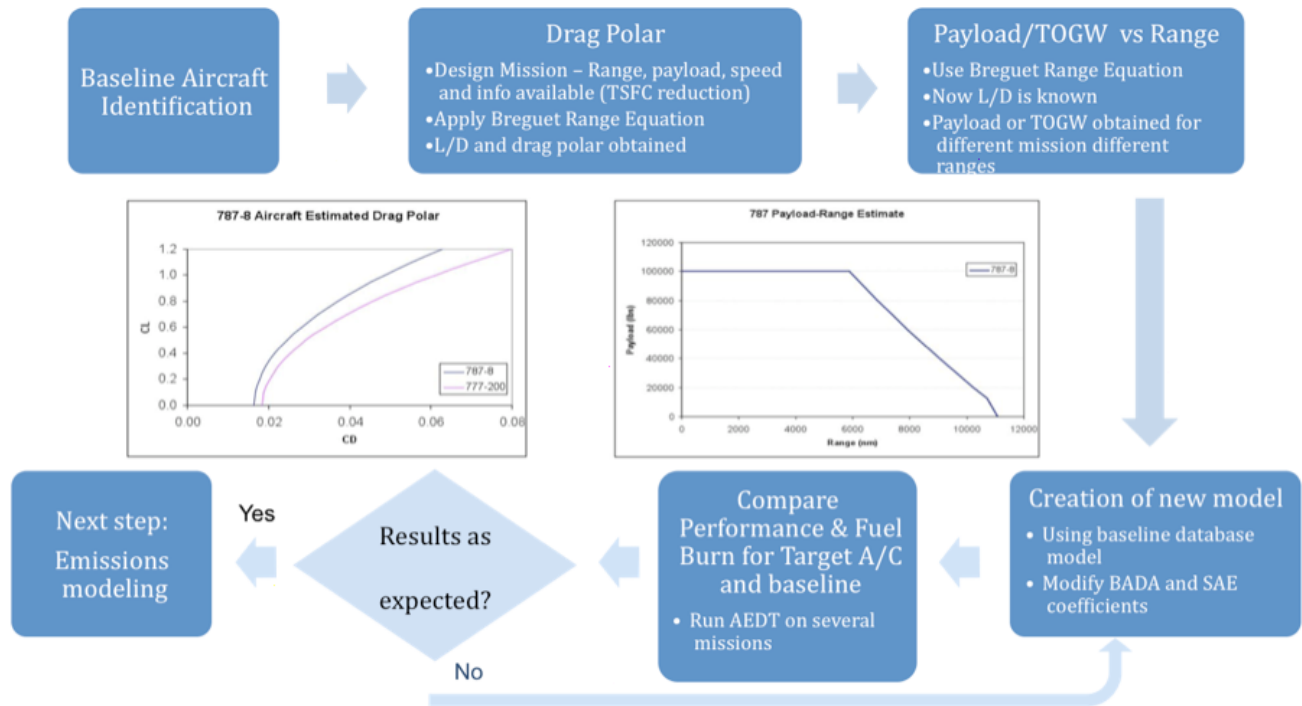


Figure 7-1. Performance and fuel burn estimation flow.

The development of new emissions indices (EI) was based upon what technology improvements were expected for each of the engine types. The improvements were classified in one of two key ways: a direct reduction in the specific EI or often an adjustment of the EIs to meet a change in margin to the certification limits. The specific limits and means of determining the certification values for each of the regulated emissions are contained in Volume II of Annex 16 to the Convention on International Civil Aviation¹. In the case of a direct improvement to the emissions, the EIs were changed accordingly. At the same time, the reference fuel flows that correspond to each of the EIs were adjusted to reflect any fuel burn improvements for the new vehicle concept. This prevents the case where the fuel flow during the simulation either exceeds the maximum value or is less than the minimum value contained in the data. In both the direct reduction and margin based approaches, the changes in EI were uniformly applied across all fuel flows. Simultaneous to the alteration of the emissions values, the noise power distance (NPD) curves of the UAS and VLJ were altered to achieve changes in noise footprint. The process assumed that the spectral profile of the noise for the new vehicles remains essentially unchanged, but the certification noise values were modified. A quick overview of the NPD alteration process is given below:

Step 1: Using the SAE-AIR-1845 simplified method of NPD generation, and the associated spectral class information in AEDT, iterate to determine the desired sound pressure level (SPL) values, which give the current EPNL values in the existing database.

Step 2: Using the new SPL values, calculate the associated A-weighted metrics.

Step 3: Iterate on reducing the SPL values until the associated EPNL is reduced to the desire level, respectively.

Step 4: Using the SPL values from Step 3, calculate the associated A-weighted metrics.

Step 5: Apply the difference in the A-weighted values found in Step 4 and Step 2 to the respective NPDs.

Once the performance and the emissions and noise information for the UAS and VLJ were validated, the detailed information for each was passed on to the other members of the research project.

CESTOL

One of focal questions in regards to establishing CESTOL performance goals was what would be the correct combination of the target range and field performance to successfully launch the aircraft in NextGen, in light of advanced technologies available within the CESTOL timeline. The CESTOL field length performance is crucial in its ability to access underutilized airports within any given metropolitan area. An examination of the FAA Form 5010 Master Airport Records database^{li} indicates that a Balanced Field Length (BFL) of 3,000 ft will allow operations to 83% of public airports with asphalt or concrete runways in the United States as depicted below. This percentage drops to 58% for aircraft that require runways of at least 4000 ft. Thus, the initial goal of balanced field length was set to be 3000 ft. Other target performance metrics were established through benchmarking existing aircraft and relevant conceptual designs, such as the Extremely Short Takeoff and Landing (ESTOL) aircraft, one of experimental configurations identified by NASA's Vehicle Systems Program (VSP). The initial primary

performance metrics of the NASA suggested CESTOL aircraft compared to other aircraft are listed in Table 7-1. Comparison of vehicle performance. Table 7-1. The capabilities served as a starting point for the detailed design modeling of the ASDL CESTOL.

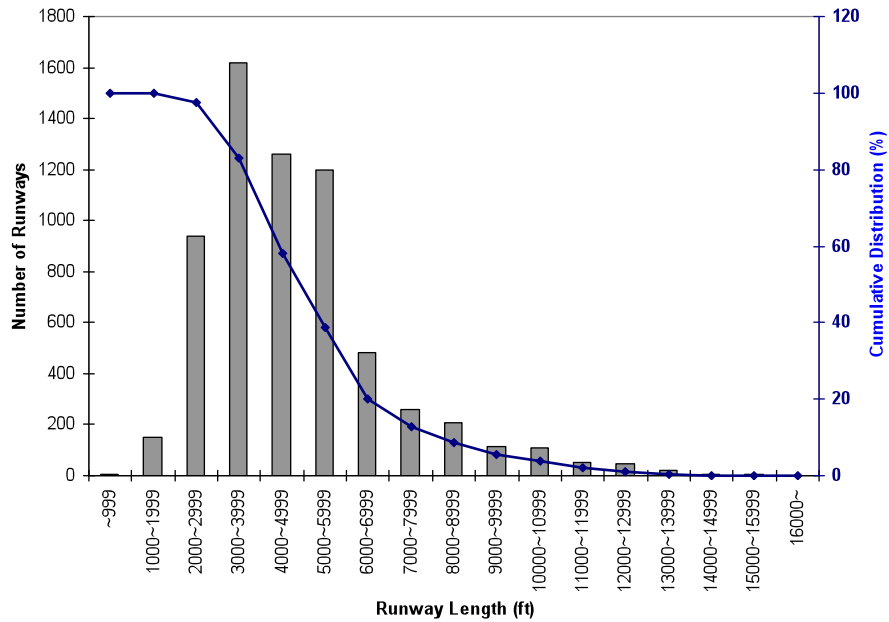


Figure 7-2. Runways available at public airports in the United States by runway length.

Table 7-1. Comparison of vehicle performance.

	Current NASA Suggestion	VSP ESTOL	B737-800
IOC	2021	-	1997
Mach No.	0.78	0.8	0.78
Range	2000 nm with CTOL, 600 nm with STOL	1400 nm	2700 nm
Balanced field length	3000 ft for Shorter Range (600 nm)	2000 ft	9100 ft
No. of passengers	80~120 for jet <80 for Prop	90	162

Shorter range requirements may facilitate the integration of Short Take-Off and Landing (STOL) capabilities. Furthermore, it might be more sensible to optimize the aircraft design for the shorter regional routes that the aircraft is intended to primarily serve. On the other hand, a NASA expert pointed out that attaining a comparative range capability is very likely to be crucial for market penetration. Airlines would prefer to have a family of aircraft of the same type rather than having different aircraft optimized for different operational capabilities because of the increased overhead costs associated with maintaining different families of aircraft in their inventories. Such considerations led the team to embrace a comparable range capability of state-of-the-art regional jet (RJ) aircraft in order to successfully introduce CESTOL into the future RJ market. The two competing goals of field performance and range performance can be balanced by restricting its STOL operation boundary, or adopting Conventional TakeOff and Short Landing (CTOSL) for long-range (2000 nm) operations and STOL (600 nm) for short-range operations. Figure 7-3 depicts the target payload-range capabilities of CESTOL for two operational modes. The aircraft is to be designed to take off from a 3000 ft runway at the TOGW equivalent to a full cabin loading of 21,000 lbs with 600 nm range fuel loading. If it were loaded with more fuel for a longer range, the aircraft would use a conventional take-off. Figure 7-4 illustrates the mission profiles that were used to quantify the mission fuel quantities for economic and design range missions. A reserve mission segment including a 200 nm diversion to an alternative airport and a 30 min hold are applied to the calculation of mission fuel for both missions.

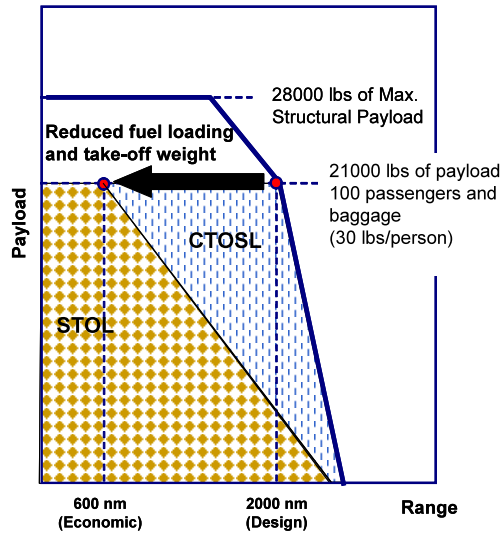


Figure 7-3. CESTOL payload-range design goal.

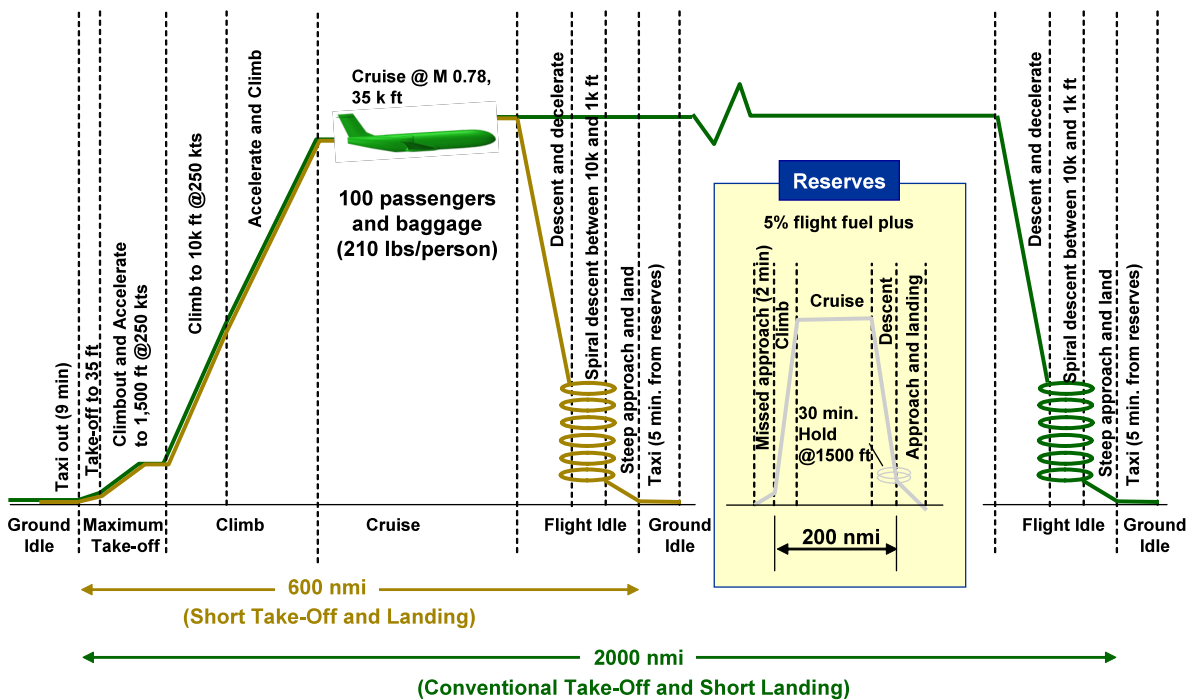


Figure 7-4. CESTOL design mission profiles.

Detailed CESTOL Design

There was consensus within the team and NASA that the initial operational capability (IOC) date should be no later than 2021 in order to start impacting the market around 2025. This, thereby, narrowed down a lengthy technology portfolio into a subset that can reach TRL 6 by 2014 and TRL 8 by 2021. The selected technologies are described below.

High Speed Slotted Wing (HSSW)

One of the key technologies identified by the team was targeted to the cruise efficiency, specifically a high speed slotted wing (HSSW), pursued by Boeing and NASA since 1999. The cruise slot along the span shifts the transonic shock aft and increases the divergence Mach number. This high speed performance benefit is traded off with low speed performance enhancement by de-sweeping wing or increasing wing thickness, which also reduces wing weight. Despite these benefits, the wind tunnel tests^{lii} done by NASA and Boeing indicated that the HSSW test configuration exhibits a considerable increase in drag below the divergence Mach number. It is assumed that the HSSW offsets the drag divergence Mach number by 0.03 based on previous research conducted by ASDL for NASA. The team estimated the reduction in wing sweep angle equivalent to the offset of the divergence Mach number, and then incorporated a de-swept wing planform into the CESTOL configuration.

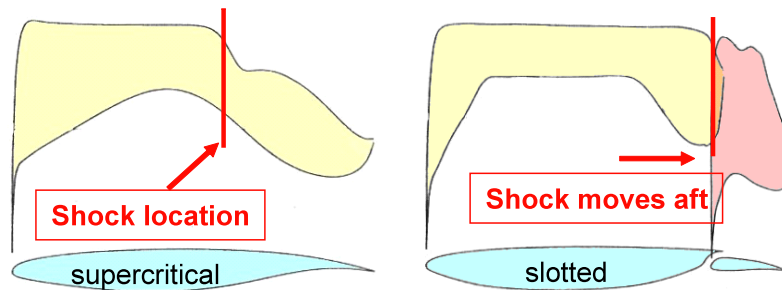


Figure 7-5. Effects of slotted wing on transonic air flow.

Mission Adaptive Compliant Wing (MACW)

The mission adaptive compliance wing (MACW) has been developed by Flexsys with support from Airforce. The MACW can enhance aerodynamic efficiency, continuously optimizing wing section geometry in flight^{liii}. Figure 7-6 illustrates a MACW designed for a high altitude and long endurance aircraft. The morphing trailing edge structure, seamlessly attached to wing box, can undergo +/- 10 degree flap deflection. This technology is also applicable to hinged flap system of commercial transport aircraft^{liii}. According to Flexsys and others' study^{liv,lv}, the application to Airbus 320 flap would result in a minimum 3% L/D improvement throughout a range of CL. It was assumed that the improvement offsets the degradations in L/D due to pressure drag increase at off-design points by adapting HSSW.

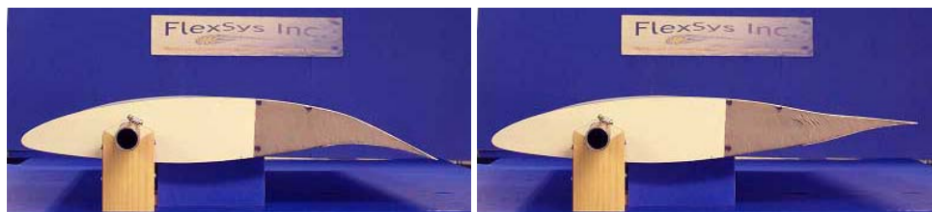


Figure 7-6. MACW trailing edge designed for a high altitude long endurance aircraft.

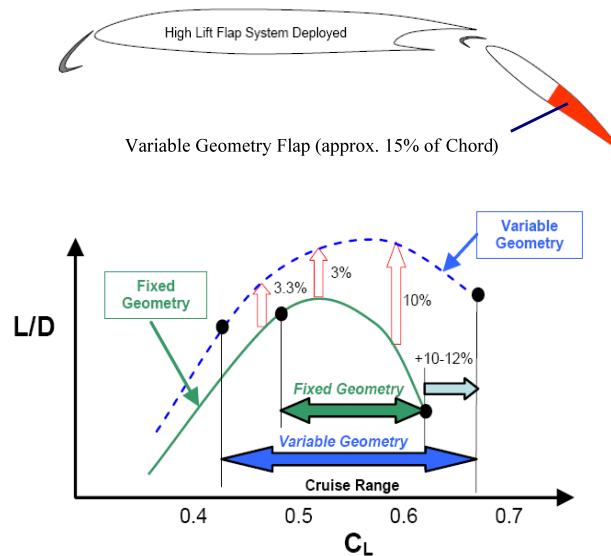


Figure 7-7. L/D improvement (Airbus A320) with variable geometry trailing edge^{liii}.

Ultra Efficient Engine Technology (UEET)

The propulsion system is enhanced by infusing a series of Ultra Efficient Engine Technologies (UEETs). These enhancements are anticipated to collectively result in 9% reduction in fuel consumption and 5% engine weight reduction. The UEET program was set up by NASA in the late 1990s to identify and develop new technologies to enhance the performance of future gas turbine engines. The program goal was to select technologies with the potential to contribute to reducing fuel burn for large subsonic aircraft by 15%, reducing fuel burn for small subsonic aircraft by 8%, and reducing LTO NOx by 70% from CAEP/4 standards, all by 2015. Once these technologies were developed to a TRL of 5 or 6, it was envisioned that they would be transferred to the commercial sector and contribute to enabling a safe, secure, and environmentally friendly air transportation system.^{lvi} As part of Georgia Tech's involvement in UEET, a physics-based vehicle design environment was developed to evaluate technologies in the UEET portfolio, and information on these technologies was collected through interaction with NASA leads. This environment was a previous version of EDS.

Five of the engine technologies from the UEET portfolio were selected for implementation on the CESTOL project and were selected based on their applicability to engines with similar thrust capabilities as desired for CESTOL. The five selected engine technologies are the Highly Loaded high pressure turbine (HPT), the advanced low pressure turbine (LPT) with aggressive transition ducting, lightweight single crystal blade alloy for turbine rotors, low conductivity ceramic thermal barrier coatings (TBC) for HPT airfoils, and ceramic matrix composite (CMC) vane materials for the HPT. As engine technologies, these are all modeled in EDS.

Table 7-2 lists the input metrics and values used to simulate each of the selected technologies from a reference engine used for the CESTOL development. The highly loaded HPT is modeled by an increase in efficiency and a decrease in number of blades, which is the result of higher loading in a single stage HPT, as is expected for an engine in the thrust class expected for CESTOL. The advanced LPT with aggressive ducting is modeled with an increase in allowable LPT stage loading. The Lightweight Single Crystal Blade Alloy is modeled with an increase in HPT vane and blade temperatures and a decrease in

HPT stator and blade densities. The low conductivity TBC is modeled only with increases in allowable HPT vane and blade temperatures. The CMC vane is modeled as an increase in allowable vane temperature, and also an increase in maximum allowable turbine inlet temperature (T4).

Table 7-2. Values used for technology implementation.

Tech Metric	Highly Loaded HPT	Advanced LPT with Aggressive Ducting	Lightweight Single Crystal Blade Alloy	Low Conductivity TBC	CMC Vane
Max T4 (deg R)					3650
HPT Adiabatic Efficiency (delta)	0.005				
HPT # of blades (delta, %)	-21				
HPT 1st Vane Rel. Temp (delta, deg R)			100	300	700
HPT Blade Rel. Temp (delta, deg R)			100.00	300	
HPT Stator Density (delta, %)			-4.15		
HPT Blade Density (delta, %)			-4.15		
LPT Stage Loading (delta, %)		30			

Composite Airframe

Since the introduction of carbon fiber composites in the 1960's, composite materials have proven their merit in military aircraft applications that can justify a significant cost penalty for the enhanced composite structure^{lvii}. Prodigious development in advanced material and manufacturing methods has continued to curtail “both manufacturing cost and damage tolerance barriers to the application to commercial transport primary structures”. The Boeing 787 makes greater use of advanced nonmetallic material in its airframe and primary structure than any previous Boeing commercial airplane. Half of the airframe, including the wing, fuselage, and empennage, is constructed with composite materials^{lviii} as shown in Figure 7-8. It was assumed that applying a Boeing 787 level of advanced airframe technologies would result in 15, 20, and 12 percent reduction in weight, respectively, to the fuselage, wing, and empennage over conventional metallic structures^{lix}.

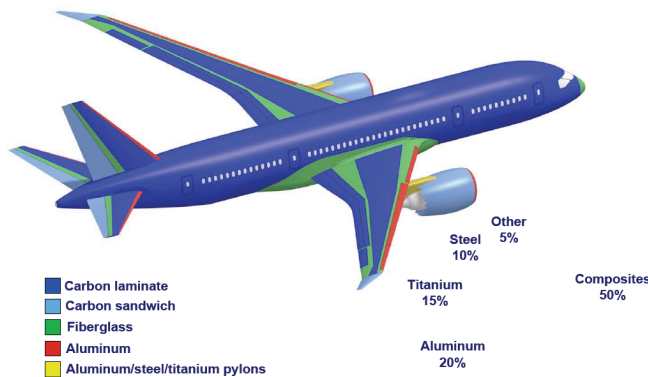


Figure 7-8. Boeing 787 airframe construction^{lx}.

Natural Laminar Flow

The principle behind natural laminar-flow (NLF) designs and materials is to optimize the shape of the aircraft external configuration and to improve surface quality through the application of advanced material and fabrication method, delaying the transition of the boundary layer from a laminar state to a turbulent state. Such a delay of transition to turbulence serves to reduce skin friction drag, thereby reducing fuel burn. “On a typical transonic wing, a 25% run of laminar flow on the upper and lower surfaces will result in roughly a 25% reduction in profile drag.”^{lxix} Despite such a significant benefit,

laminar flow design has not been broadly introduced to commercial transport aircraft. One of the principle impediments is the heightened sensitivity of laminarity to surface irregularities or imperfections, incurring an increase in manufacturing costs and/or maintenance costs, which must be traded against the drag benefits of laminar flow.^{lxi} While NLF has been widely applied in business, corporate, and general aviation aircraft over the past two decades, it is only recently that NLF implementation to commercial fleet has been undertaken^{lxii}. The natural laminar-flow nacelle on the Boeing 787 is reportedly the first application of laminar flow to large commercial transport. It was anticipated that more extensive use of the technology, including wing and tails, would become economically viable for the CESTOL aircraft. It was assumed that the wing upper surface could maintain laminar flow up to 50% of its chord length at Mach 0.78 and 16 degrees of wing sweep. Wing lower surface was not expected to benefit from this technology since a Kreuger flap was installed on the wing leading edge. Both the tail and nacelle are assumed to maintain laminar flow up to 20 percent of their characteristic length.

Spiral Descent and Steep Approach

The identified airframe and engine technologies facilitate incorporating unconventional terminal area procedures, such as spiral descent and steep approach, which are pictorially described in Figure 7-9. The spiral descent procedure adopted by CESTOL is an unconventional descent technique, with which the airplane continuously flies along a circular and descending path from a certain altitude over the airport. The aircraft is intended to use a steep approach technique that maintains a glide slope of 5.5 degrees, as opposed to the standard 3.0 degrees. Implementation of this higher angle approach would reduce terminal area noise and landing field length. Figure 7-10 illustrates the amount of reduction in landing field length due to steep approach technique. An increase in flight path angle by 2.5 degree results in a 343 ft reduction. An additional 152 ft reduction can be obtained by reducing obstacle height to 30 ft. Note that reduction of screen height is subject to approval by local airworthiness authorities.

There are several in-service commercial jets that are capable of steep approach. Avro RJ and the Fokker 70 jets have routinely exercised steep approaches at London City airport in UK,^{lxiii} where all aircraft must be capable of at least a 5.5 deg approach angle for noise abatement issues and obstacles. ERJ 135, Airbus 318, and ERJ 170 were also certified for the steep approach at London City airport in 2003, 2006, and 2007. ERJ 190 is being assessed for approval as of June 2009. However, steep approaches introduce an important aerodynamic performance constraint that must be taken into account in the aircraft sizing and synthesis process. Approaching at higher glide slope angle requires a substantially higher drag as compared with normal 3-degree slope approach. Some aircraft, such as ERJ 170 and Airbus 318, use spoilers to augment drag, while Avro RJs deploy airbrakes installed in the tailcone. However, the use of flight spoilers trims down wing lift and subsequently may increase approach speed in order to maintain a similar level of lift coefficient margin. For instance, the Airbus 318 increases approach speed by 8 knots, which is unfavorable for CESTOL design heavily constrained with field performance and approach speed. The team decided to use tailcone airbrakes for the CESTOL baseline configuration to avoid lift loss due to deploying spoilers.

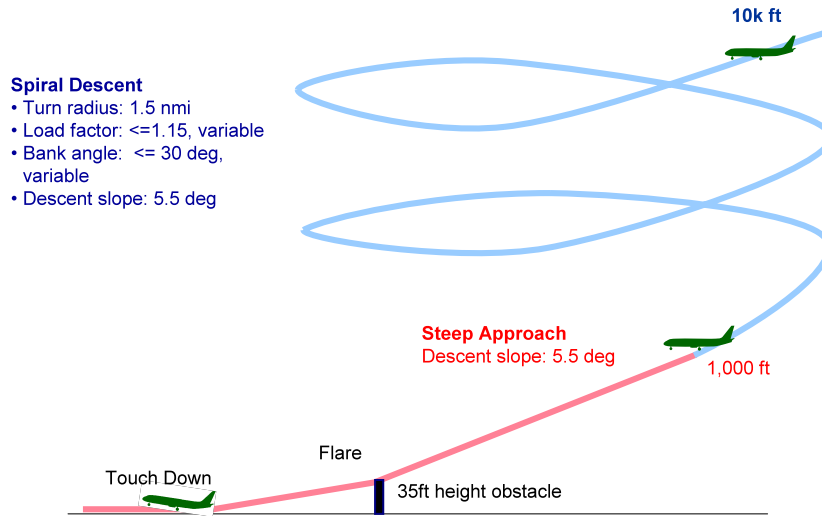


Figure 7-9. Spiral descent and steep approach concept for CESTOL.

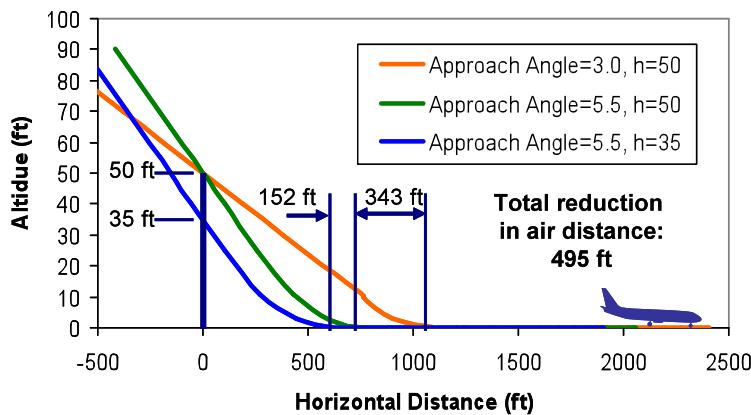


Figure 7-10. Impact of steep approach on landing field length.

Technology Characterization and Simulation

The technology assumptions applied to the construction of the CESTOL model are summarized in Table 7-3. The assumptions associated with UEET, composite material, steep approach, and NLF are incorporated through adjustment of technology factors in EDS. For instance, the benefit of composite material technology can be incorporated by adjusting weight correction factors according to the values listed in the table. The HSSW technology was incorporated in a more complex way. The benefit of delaying drag divergence Mach number by 0.03 was traded with de-sweeping the wing because of stringent low speed requirements. Basically, the performance assumptions are based on relative cruise performances to a conventional baseline. Therefore, the reduction in sweep angle equivalent to the transonic drag reduction benefit was estimated with the baseline aircraft wing configuration from empirical data.^{lxiv} Then, a transonic drag adjustment factor was attuned such that the resulting transonic drag at cruise Mach number was close enough to the baseline configuration drag. Another effect of the slotted supercritical airfoil is a considerable increase in profile drag, which was assumed to be canceled out by the benefit of MACW technology.

Table 7-3. CESTOL technology suite summary.

Simulation Factor Technology	Mdd	Engine SFC	Laminar Flow				Weight					App Slope (deg)	Screen height (ft)
			Wing*	Fuselage	Nacelle	Tail	Wing	Fuselage	Tail	Engine	Hydraulic		
HSSW	(+) 0.03												
MACW	Cancel out drag rise at off-design due to the incorporation of HSSW (~2.5% compared to conventional wing)												
UEET		(-) 9%									(-) 5%		
Composite Fuselage/Wing							(-) 15%	(-) 20%	(-) 12%				
Steep Approach											(+) 8%	5.5	35
Natural Laminar Flow			50%	10%	20%	20%							
Total	(+) 0.03	(-) 9%	50%	20%	20%	20%	(-) 15%	(-) 20%	(-) 12%	(+) 5%	(+) 8%	5.5	35

* upper wing surface only.

Convergence of CESTOL Design

The CESTOL vehicle model was developed in a phased approach. The first phase was aimed at developing a high level AEDT model. To this end, an interactive environment that has been created with surrogated models derived from a notional CESTOL FLOPS model. The initial design identified by the first phase efforts was further matured during the second phase. The converged configuration was elaborated through the EDS environment and established as an EDS detailed model, and was incorporated into the AEDT fleet database to support subsequent airspace impact analyses.

Although exhaustive design optimization was deemed out of the scope of this study, significant design variables such as wing area and engine thrust must be determined through assessment of critical vehicle system metrics in order to produce a feasible vehicle design that can perform the Concept of Operations (CONOPS) and requirements formulated for CESTOL. It was also desired that the resultant aircraft design exploit most of benefits of the technology set described in the previous section. In order to support such a dynamic, the team developed an interactive design space exploration environment that allows rapid design evaluations in concert with evolving technology assumptions.

The CESTOL model was developed based on a representation of Boeing 737-800 with a CFM56-7B27. A number of Design of Experiments (DoE) simulations around the reference aircraft were performed using Phoenix Integration ModelCenter[®]. The results were regressed to produce a set of surrogate models with a neural network regression technique. The user interface (Figure 7-11) created with JMP[®] software drives the surrogate models and estimates system metrics in response to user inputs

on design variables and technology assumptions in a real time fashion. Interested readers in the theoretical background and examples of this technique are referred to Kirby^{lxv} and Biltgen^{lxvi}. As a first cut wing loading, thrust to weight ratio and required lift coefficients at takeoff and landing were determined with preliminary establishment of technology assumptions and performance targets.

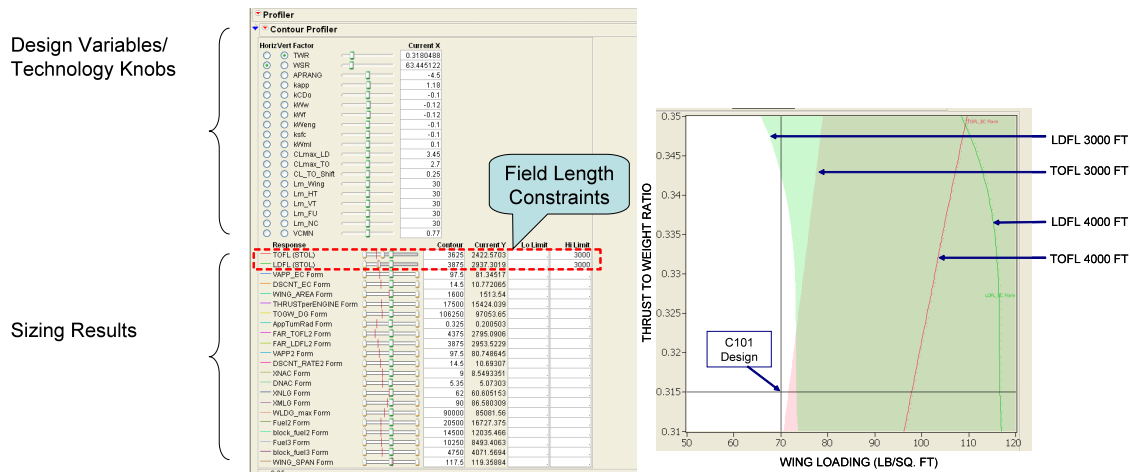


Figure 7-11. Interactive design technology trade environment.

Configuration Development Overview

The CESTOL model was matured through an iterative design and analysis process that rigorously involved experienced man-in-the-loop design decisions at each configuration update. The model evolution is depicted in Figure 7-12. Through the trade-off study described previously, the values of a set of major design variables were determined with initial convergence of technology characterization. A FLOPS model representing the reference aircraft was morphed into the first CESTOL model, labeled Configuration 100 or C100, which was evolved into C101 incorporating updated technology assumptions and group weight corrections. C101, identified through the first generation modeling efforts, served as a basis of a high level model for fleet analysis.

The C101 configuration evolved through several major updates into the C109, the final configuration within this study, including a higher fidelity low speed aerodynamic analysis that incorporated HSSW wind tunnel data^{lxvii} produced by NASA. In addition, the scheduling of high-lifting devices, spoilers, and speed brakes were established through in depth investigation on its impacts on field performance and climb performance requirement. An initial concept and requirement study consistently indicates that approach and landing performance is one primary drivers of this aircraft design. Thus, a trade study was performed to increase maximum lift coefficient while maintaining cruise Mach number comparable to state of the art RJs, leveraging on the aerodynamic advantage of the HSSW technology. Tails were resized as wing and engine location changed.

Once the configuration was converged into C109, the FLOPS model was transferred into the EDS toolset to develop a higher fidelity engine model that replaces a rubberized engine model derived from a CFM56 engine representation. The impacts of the selected UEET suite were accounted for in an engine component level within the EDS toolset. Subsequently, the EDS tool, rigorously assessing both air-vehicle and engine performance, iterated the engine design and analysis process, establishing physics-based interdependencies across environmental metrics, which the first generation model lacks. All CESTOL vehicle data shown hereafter are pertinent to C109 unless mentioned otherwise.

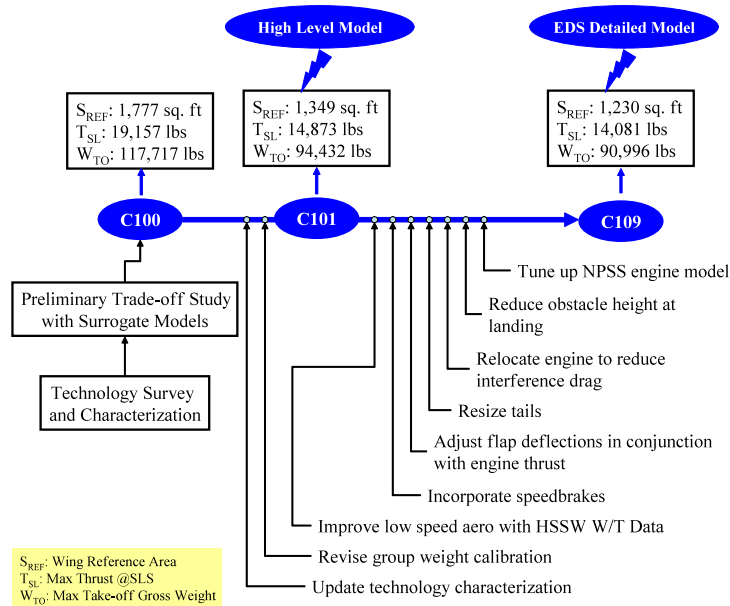


Figure 7-12. CESTOL configuration evolution.

Summary of CESTOL Design

In general appearance, the converged CESTOL aircraft has a traditional tube-wing configuration as illustrated in Figure 7-13. Low-wing, T-tail, and engines over the wing arrangement are the most noticeable features of the external configuration. The wings outfitted with HSSW are considerably less swept, at 16 degrees, than modern civil subsonic transports. Two advanced high bypass turbofan engines are installed over the wing. Pylons are added between the engines and wing to minimize adverse effects from wing-engine interactions. This layout was selected primarily to shield fan noise, which is one of the dominant sources at approach. This arrangement also assuages the kinematic constraints associated with main landing gear integration. Although an experimental investigation suggests that this engine integration would offer a reduction in drag as compared with conventional under-wing engine integration, this benefit was not accounted for in the aircraft performance estimation. Another outstanding feature of this aircraft is large speed brakes at the tail cone, which is similar to that of BAe 146. These speed brakes allow the aircraft to reach adequate lift-to-drag ratio required to maintain 5.5 deg slope angle at steep approach.

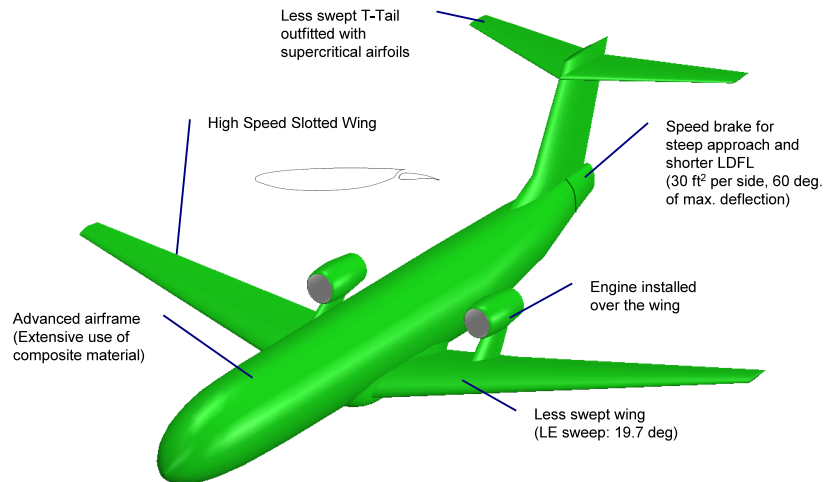


Figure 7-13. CESTOL configuration overview.

Configuration Description

The CESTOL fuselage geometry was initially determined in conjunction with its cabin arrangement as shown in Figure 7-14, which compares the Boeing 737 and the CESTOL cabin arrangement. CESTOL cabin has 5 seats per row as compared with the 6 seats per row found in the B737. This arrangement resulted in a 10% reduction in the width and height of the CESTOL fuselage section from those of B737, which allows it to keep the fineness ratio of the fuselage in a favorable range in spite of 20% reduction in its length. A three-view of the CESTOL is depicted in Figure 7-15. The length of the aircraft is 110.4 ft with a wing span of 105.8 ft. When the aircraft is resting on its landing gear in a static condition at design take-off gross weight, the overall height is 32.6 ft. The C109 wing planform was derived through a series of sizing procedures described previously. It represents a balance of features that provides good cruise efficiency and superb low speed characteristics for takeoff and landing. The planform area of the wing is 1229.9 sq. ft, the aspect ratio is 9.1, the taper ratio is 0.22, and the quarter chord sweep is 15.7 deg. The wing platform has a break at 30% of semi-span. Airfoil thickness varies along the span: 15.4% at the root, 12.6% at the break, and 11.0% at the tip.

The C109 has a conventional T-tail arrangement sized with a tail volume coefficient method^{lxviii} that accounts for fuselage width and height effects. Figure 7-16 indicates that CESTOL horizontal and vertical tail designs well agree with the empirical relationships. For the horizontal tails, the area of the two-surface tail planform is 287.3 sq. ft, the span is 41.52 ft, the aspect ratio is 6, and the taper ratio is 0.4. The quarter chord line is swept back 21.8 deg. The horizontal tails are mounted to the tip of vertical tail. The horizontal tail has a volume coefficient of 0.88. The cross-section of the horizontal tail is a supercritical biconvex airfoil that has the thickness ratio of 0.1. The vertical tail features a swept-back planform with the sweep angle of 28.8 deg. at the leading edge. The reference area of the planform is 190 sq. ft, the span is 15.72 ft, and the aspect ratio is 1.3. The root chord is 18.27 ft and 13.82 ft long, with and without the leading edge extension, respectively. The tip chord length was selected such that it is slightly longer than the horizontal tail root chord to provide sufficient structural interface between them. This arrangement results in taper ratio of 0.75. The vertical tail has a volume coefficient of 0.06, which was estimated from an empirical equation for T-tail volume coefficient. The cross-section of the vertical tail is also a supercritical biconvex airfoil that has the thickness ratio of 0.1.

The fuselage, lofted with elliptical sections, is shaped similar to a conventional civil transport. It has a landing gear pod blended under each side of its belly, where the wings are attached to fuselage. The aft-fuselage is upswept to maintain a reasonable tail-strike clearance. The tailcone at the aft-fuselage functions as speedbrakes to provide a sufficient amount of drag increase required for 5.5 degree steep approach. The panels of 30 sq. ft per side can be deflected outward up to 60 degrees. The landing gear is in a tricycle arrangement and was located to achieve a balance of features that provides appropriate ground clearance, tip-back angle, turnover angle, and load distribution between nose and main gears.

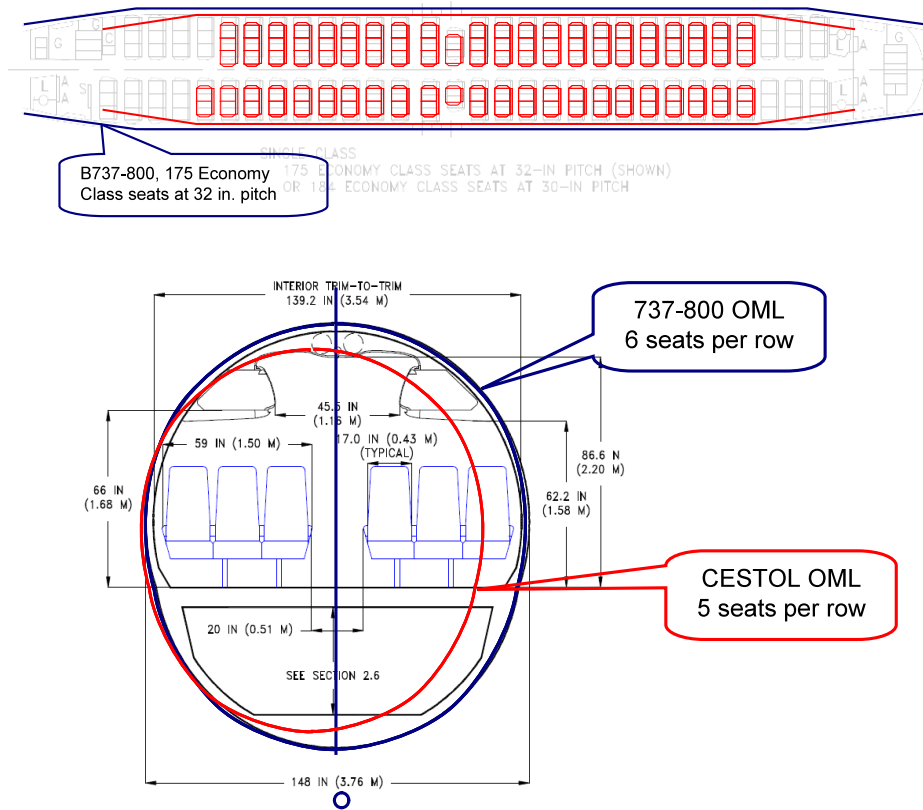


Figure 7-14. CESTOL cabin arrangement.

LIFTING SURFACES	WING	HT	
AREA, FT ²	1229.9	287.3	
SWEEP (C/4), DEG	15.7	21.8	
AR	9.1	6.0	
TR	0.22	0.4	
DIHEDRAL ANGLE, DEG	6.0	0	

WEIGHT	DESIGN (1995 nm)	ECONOMIC (600 nm)
OEWS, LBS	52,314	52,314
PAYLOAD, LBS	21,000	21,000
FUEL, LBS	17,682	7,986
TOGW, LBS	90,996	81,300

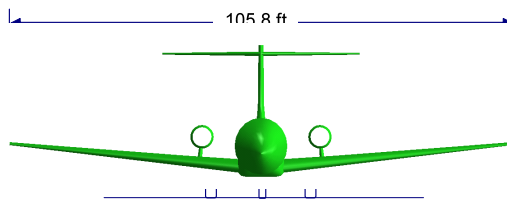
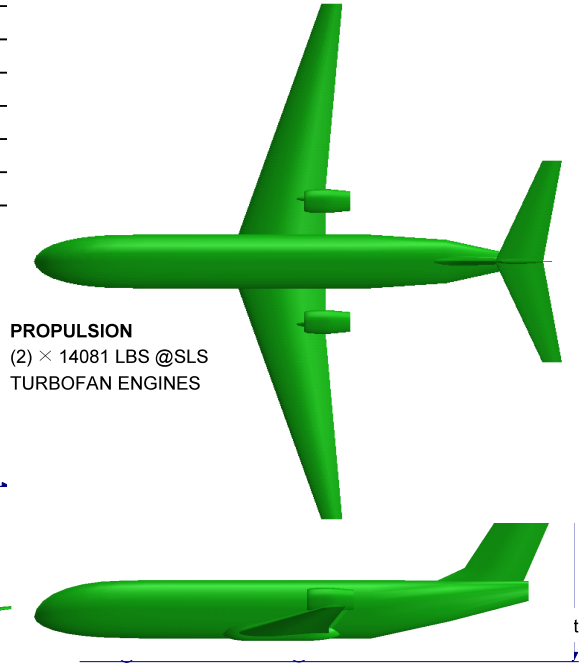


Figure 7-15. CESTOL general arrangement.

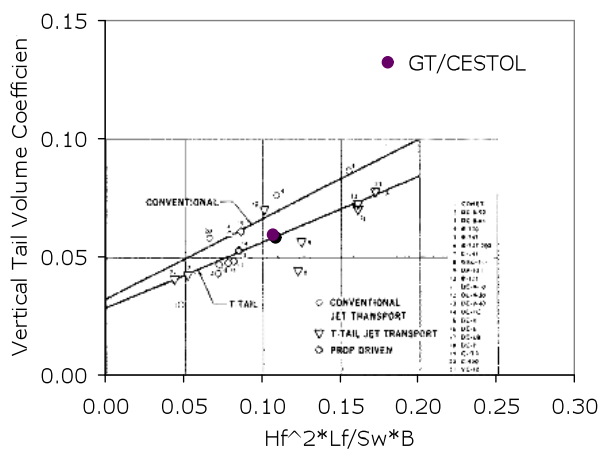
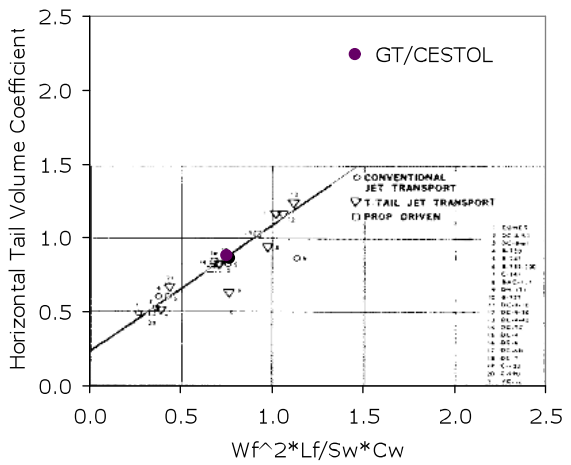


Figure 7-16. Tail volume coefficients correlated with fuselage geometry parameters.

Propulsion System

CESTOL is powered by two high bypass turbofan engines installed over the wing. Each engine has a maximum installed sea-level static thrust of 14,081 pounds. The engine has an uninstalled sea level static (SLS) overall pressure ratio (OPR) of 28.5, an uninstalled SLS fan pressure ratio (FPR) of 1.72, an uninstalled SLS BPR of 5.45, an uninstalled SLS extraction ratio of 1.12, and a maximum T4 of 3350°R. Figure 7-17 shows a schematic diagram of the engine. The engine has a three stage LPC, a nine stage HPC, a single stage HPT, and a four stage LPT. The overall length of the engine pod is 114.1 inches and

the maximum nacelle diameter is 59.1 inches. The inlet is designed to have a total capture area of 1826.7 sq. in. and a total projected area of 1378 sq. in, giving a contraction ratio of 0.754. This inlet is sized to a throat Mach number of 0.63. The bare engine weight is 2,782.5 lbs.

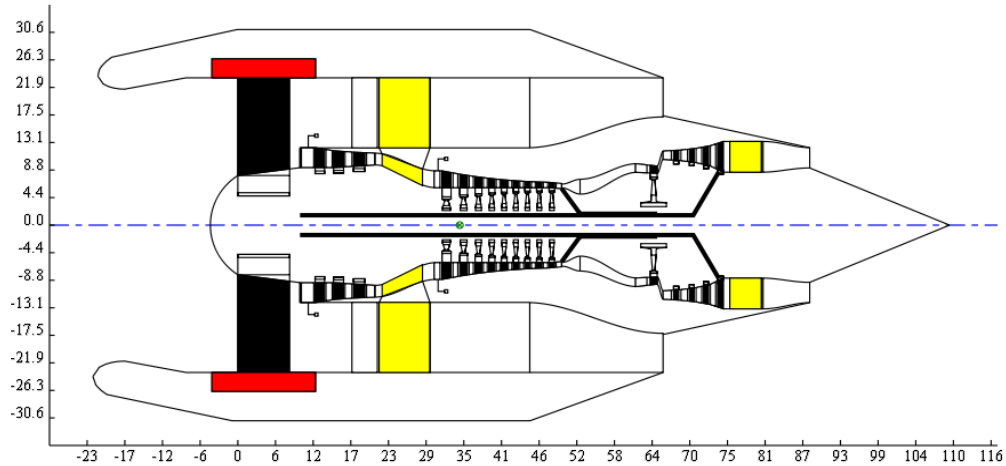


Figure 7-17. Schematic of CESTOL engine.

High Lifting Devices

The design of CESTOL was heavily driven by the landing field performance goal: 3000 ft field length for the economic range mission. Hence, the integration of high lifting devices was one of the critical design aspects. The final CESTOL aircraft is outfitted with full span variable camber Kreuger (VCK) flaps at the leading edge and double slotted flaps running from the exposed root to 98% of semi-span as illustrated in Figure 7-18, which also illustrates airfoil configurations at cruise and high lifting configurations. A VCK was selected over a slat because it allows for a smooth, continuous upper wing surface, which is crucial in maintaining natural laminar flow over the wing. It also serves as an insect shield during takeoffs and landings.

The lift coefficient curves and drag polars of clean, take-off, and landing configurations are estimated by a low speed aerodynamics estimation tool with several modifications. These modifications were required to replace two dimensional airfoil data estimated by empirical equations embedded in the code with the wind tunnel test data^{lxvii} for HSSW airfoils. The resulting CESTOL lift coefficient curves and drag polars are depicted in Figure 7-19. The maximum lift coefficient was found to be 1.5 for the clean configuration and to reach up to 3.1 at the landing configuration. The lift curves and drag polars were incorporated into FLOPS to estimate field performance for STOL and CSTOL operations.

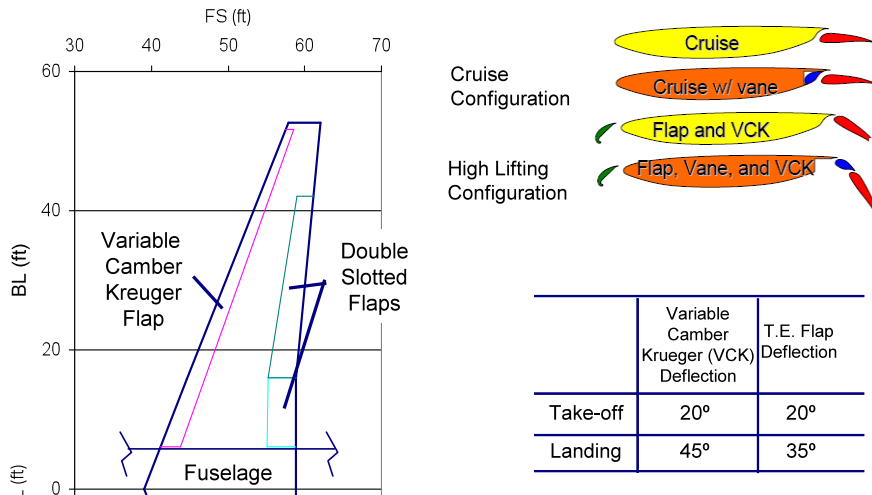


Figure 7-18. High lifting device arrangements and scheduling.

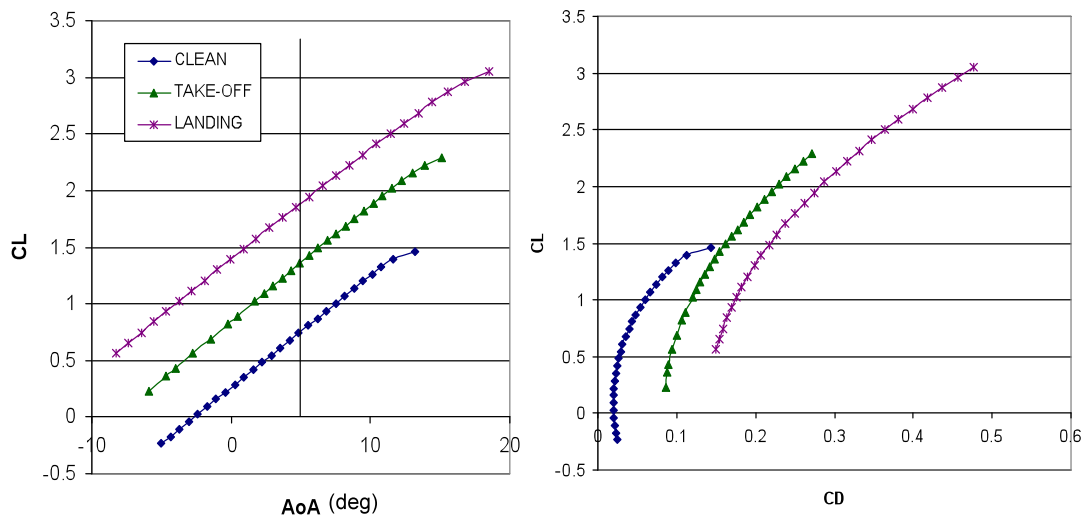


Figure 7-19. Lift curves and drag polars for different high lifting device settings.

Weight Estimation

The CESTOL component weights are estimated within FLOPS. As the configuration converged, the propulsion system weight was updated with WATE. It was assumed that the CESTOL structure is designed to withstand a g-limit of +2.5/-1 g. In order to account for the benefits of using advanced materials, the wing, fuselage, and tail weight were adjusted with a reduction of 20, 15, and 12%, respectively, to all metallic fabrications. The operating empty weight was 52,364 lbs, which results in 73,364 lbs of zero fuel weight for the full cabin-loading configuration, which includes 100 passengers at 210 lbs per passenger. The maximum take-off gross weight is 90,993 lbs, including 17,629 lbs of fuel required to complete 2000 nm design range flight and a reserve. A detailed group weight breakdown is listed in Table 7-4.

Table 7-4. CESTOL group weight breakdown.

Mass And Balance Summary	Percent	Pounds
Wing	9.5	8,653
Horizontal Tail	1.3	1,183
Vertical Tail	1.0	936
Fuselage	9.8	8,956
Landing Gear	4.6	4,194
Structure Total	26.3	23,922
Engines*	7.9	7,225
Thrust Reversers	1.1	959
Fuel System-Tanks And Plumbing	0.8	693
Propulsion Total	9.8	8,878
Surface Controls	1.6	1,483
Auxiliary Power	0.9	784
Instruments	0.4	403
Hydraulics	0.8	739
Electrical	1.8	1,626
Avionics	1.2	1,121
Furnishings And Equipment	9.3	8,413
Air Conditioning	1.3	1,200
Anti-Icing	0.2	165
Systems And Equipment Total	17.5	15,935
Weight Empty	53.6	48,735
Crew And Baggage	1.0	915
Unusable Fuel	0.5	470
Engine Oil	0.1	82
Passenger Service	1.6	1,462
Cargo Containers	0.8	700
Operating Weight	57.6	52,364
Passengers, 100	19.8	18,000
Passenger Baggage	3.3	3,000
Zero Fuel Weight	80.6	73,364
Mission Fuel	19.4	17,629
Ramp (Gross) Weight	100.0	90,993

* Includes nacelle and air-induction system weight

Aircraft Performance

The performance metrics of the converged CESTOL configuration are summarized in Table 7-5. The configuration selected through the preliminary trade-off study met the take-off field length (TOFL) and landing field length (LDFL) goals of 3000 ft with the economic mission range fuel loading. However, the final configuration was found to be short of meeting the target. This shortcoming is mainly due to the update of the initial technology assumptions on the maximum lift coefficient values with the high-speed





slotted wing (HSSW) low speed wind tunnel data. Because we only missed the desired takeoff field length by 20 feet or so, we felt the result was acceptable.

The final CESTOL is compared to other RJ capabilities in Table 7-6. Despite the assumptions of considerable structural weight reduction, CESTOL is only slightly lighter than the current fleet. This is primarily because of its substantially larger wing driven by the aggressive field performance requirements. Its wing loading at the maximum take-off gross weight is computed to be 74 lbs/sq. ft, which is approximately 34% less than other RJs wing loading values, which range from 111 to 112 lbs/sq. ft. Thanks to such a low wing loading and other technology assumptions including steep approach technique, CESTOL aircraft outperforms the current RJ in field performance. However, the CESTOL wing is substantially oversized for cruise as shown in Figure 7-20. With a full cabin loading, the CESTOL operates in a range of CL between 0.32 at the end of cruise and 0.34 at the beginning of cruise, achieving 17.5 to 18.5 L/D, which is about 20% less than the maximum L/D value that the original CESTOL aerodynamic design due to the compromise for the takeoff and landing performance.

Table 7-5. CESTOL performance.

Parameter	Value
Mission Range (100 pax)	1,995 nm
Max Payload	28,000 lbs
Max Landing Weight	86,266 lbs
Max Fuel Quantity	17,682 lbs
Operating Cruise Mach	0.78
Approach Speed	102 ktas
TOFL @ Design Mission	3,795 ft
TOFL @ Economic Mission	3,067 ft
LDFL @ Design Mission	3,188 ft
LDFL @ Economic Mission	3,171 ft

Table 7-6. Comparison of CESTOL performance with current RJs.

	BAE 146-200	Embraer 190	Bombardier CRJ 1000	GT/CESTOL
				
Passenger Seats	100	88 -114	100-104	100
Maximum Take Off Weight (lbs)	93,000	110,892	91,800	90,846
Maximum Landing Weight (lbs)	81,000	94,799	?	86,266
Wing Area (ft²)	832	996	817	1,228
Thrust (lbs)	27,888	37,000	27,260	28,367
Max Payload (lbs)	?	28440	26,800	28,000
Design Cruise Mach	0.73	0.78	~0.83	0.78
Design Range (nm)	1,328	2,400	1,691	1,985
Take Off Field Length @ MTCW (ft)	~4,800	6,745	6,995	3,785
Take Off Field Length @ 500 nm range	3,772	4,157	?	3,020
Landing Field Length (ft)	3,405 (100 Pax @210 lbs/person)	4,341 (Maximum Landing Weight)	5,823 (?)	3,188 (100 Pax @210 lbs/person)

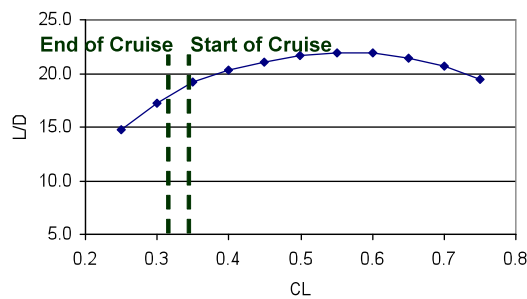


Figure 7-20. CESTOL lift-to-drag ratio at 35000 ft and Mach 0.78.

AEDT and ACES connectivity

With the CESTOL final design established, the BADA and Air 1845 performance data was needed for the ACES and AEDT analysis. The final design was simulated in EDS, which is capable of generating the full set of input coefficients required by ACES and AEDT^{lxix}. Most of the AEDT coefficients are calculated from using engine and vehicle performance generated in the FLOPS output files; however the

engine deck and ANOPP outputs are used for the coefficients needed by AEDT for TSFC and noise calculations. The equations to generate the ACES and AEDT coefficients as a function of aircraft and engine parameters are given in References xxxi and xxxii and also the Integrated Noise Model (INM) Version 7.0 Technical Manual^{lxx} for the terminal area noise calculations.

CESTOL Summary, Lessons Learned, and Potential Further Research

The CESTOL configuration was the first vehicle that the team modeled and the process developed for the design provided guidance for the development of subsequent vehicles. Many lessons were learned, assumptions were made to progress the NRA objectives, such that the oceans were not boiled during the effort. As a result, a number of further research areas were identified.

Since an extremely in depth and high fidelity design optimization of the NextGen vehicles was out of the scope of this study, CESTOL aircraft design space was not re-examined once the initial vehicle definition was passed to the other tools. Far-reaching optimization of the vehicle configuration and engine cycle would yield additional benefits for the integration of CESTOL aircraft into NextGen based on a feedback loop from the system wide analysis. A future research goal for the CESTOL would be to revise the design requirements and reevaluate a modified design reflecting the lessons learned from all the subsequent fleet analysis. Such a study that closes the loop would offer more insights of the complex interactions between vehicle designs, vehicle operational capabilities, and system-of-systems impacts.

In this sense, this study also illuminated the need for new capabilities that allow rapid assessment on the dynamics between future vehicle capabilities and future airspace system behavior. In the case of CESTOL, for example, alleviating the field performance constraint from 3000 ft to 4000 ft would improve substantial improvement fuel efficiency at the vehicle level through resizing the wing area and thus improving cruise L/D. However this trimmed capability would reduce the number of airports that CESTOL can access, and thereby the rolled up benefits at the fleet level may not be proportional to vehicle level improvement. It was envisaged that surrogate models harnessing multiple layers of parametric spaces including technologies, vehicle designs, vehicle operational capabilities, and airspace performance metrics could create an environment that allows users to rapidly assess the impacts of future vehicle capabilities on future airspace system performance, environmental efficiency, and safety assurance.

In addition to the need of further design space exploration and methodological enhancement, a couple of technologies were identified to be worth further investigation. Powered lift technologies, such as upper surface blowing and circulation control on the wing, were conceived to be well suited for CESTOL application from the vehicle integration standpoint during the technology selection process. Nevertheless those technologies ended up being excluded mainly because subsequent analysis tools, such as AEDT, are not readily applicable to such unconventional concepts. The vehicle analysis indicates that integration of powered lift technology could provide an improvement in usable maximum lift coefficient (CL_{max}) and would assist in improving the efficiency of CESTOL that is outfitted with a wing sized for low speed performance. For instance, achieving a CL_{max} of 4.0, when compared to the CESTOL that achieved about 3.1, would yield a 25% improvement in L/D through cruise wing sizing alone.

The other technology that warrants a further study is the feasibility of an intelligent flight control algorithm that enables fly-by-wire (FBW) system to control spoilers to increase drag. The ERJ 170 uses flight spoilers to increase the drag as required for a steep approach. Unlike the Airbus 318, the aircraft

does not increase its speed in spite of reduced CL_{max} due to the deployment of spoilers.^{lxxi} The FBW system moves the spoilers in and out in response to pilot inputs, allowing the reduction of CL margin. To maintain a conservative approach, this scheme was not applied to the CESTOL. The CESTOL approach speed is significantly lower than that of the ERJ 170, implying the absolute difference between the approach speed and the stall speed is also much less than the ERJ 170. Therefore, this difference would place higher requirements for precision and stability on the handling and speed of the aircraft. If such a system can replace the current tailcone speed brakes, however, there would be weight and cost savings.

There are also areas that require higher fidelity analyses. The benefits from HSSW and MACW technologies were assumed without any detailed analysis to quantify possible interactions between HSSW and MACW technologies. The noise shielding effect of the engine-over-the wing arrangement needs to be quantified with physics-based analysis or experiments.

The spiral descent approach was investigated from the aircraft sizing and synthesis perspective, to see if turn performance can support this unconventional operation concept with a quasi-static motion analysis. Changes in descent segment fuel burn due to adapting spiral descent were considered to be insignificant in the aircraft sizing standpoint. However, its fleet level impacts could be significant, requiring a more detailed analysis.

Very Light Jet (VLJ)

Due to the anticipated increasing market for on-demand air taxi transportation services, a Very Light Jet (VLJ) was included in this research to analyze their potential impact on air transportation. Designed to operate mainly at smaller reliever airports, VLJs are anticipated to be smaller and less expensive than typical business jets. Numerous companies have begun to develop these small, versatile aircraft in response to anticipated high demand, and some air taxi service providers have already begun using these in their fleets. Due to this popularity, this research endeavored to include advanced VLJs to analyze their potential impacts in NexGen.

Design Requirements for the VLJ

The next generation VLJ will primarily be used for on-demand air taxi services, a function which strongly influences its design characteristics. Current light jets serve the business market very well, but as the market for on-demand services continues to grow, the required capabilities of future aircraft will shift toward a design which best suits the operational characteristics of the network it serves. Specific aircraft requirements can be refined by analyzing the potential network which a future VLJ might serve. These requirements must consider advances in performance-based navigation, communication, surveillance, and trajectory management in addition to airports served and speed desired. By matching the aircraft capabilities to the network it serves, aircraft operators will best ensure profitability and a reasonable revenue stream.

The design requirements for the future VLJ in this research were driven by considerations appropriate for an introduction date of 2020, a 4th generation capability from today's VLJ technology level. In this time frame, demand for air taxis will have grown, and VLJs will need to be capable of a broader range of operations. Currently, on-demand carrier trips for light jets average about 350 nm and range up to 600 nm. Future VLJ designs for personal and commercial use may need to fly slightly longer ranges, to cover more routes as scheduled air-carrier service contracts away from thinner markets. A design range of 750

nm was considered reasonable for an on-demand operator of this future aircraft. Aircraft speed is important for air taxi aircraft, but is not as big a driver as availability and serviceable airfield proximity to destinations, so a modest minimum cruise speed of Mach 0.6 was set. Because air taxi operations will place a higher priority on their flexibility to service thin, on-demand markets, a future VLJ will be smaller than most current light jets, needing to carry 4 to 6 passengers.

On-demand air travel needs to be affordable and competitively priced compared to alternate means of transportation. Thus, a major requirement for aircraft that serve the air taxi market is a low direct operating cost (DOC). Current light jets (such as the Cessna CitationJet class) tailored mainly to private businesses operate between \$2.50 and \$4.00 per nmi DOC (depending on fuel and other costs variables). The introduction of the VLJ offered operators a DOC of between \$1.25 and \$1.75 per nmi, resulting in an ability to reach new markets. The goal for future air taxi operations is around \$0.50/nmi DOC, based on aircraft and fuels technology advancements. While this figure represents a target for an economically attractive transportation service, it also has a significant influence on vehicle design. First, it appears likely that a future VLJ for on-demand service will benefit from a single engine configuration in order to substantially reduce operating costs. The absence of a reserve engine will have direct impacts on the reliability requirements of any engine used, as well as on regulatory requirements for low speed performance of the aircraft. Another major consideration that may be required to achieve the DOC target is having only a single pilot in the aircraft. Many current on-demand air carrier business models incorporate two-pilot crews, largely due to passenger perceptions and insurance considerations. Advances in remote piloting technologies may make a single pilot configuration more acceptable to the marketplace in the future, however, by allowing a second 'reserve' pilot to monitor a flight from the ground and assume control in an emergency. A single remote pilot could even monitor multiple aircraft simultaneously, effectively reducing the number of pilots salaried by an operator and dramatically reducing operating costs. The weight savings related to carrying 5 people (4 passengers + 1 pilot) compared to 6 (4 passengers + 2 pilots) will also translate to a smaller, lighter, more efficient aircraft.

In summary, a future, next generation very light jet will be considered in this research. It should be capable of traveling 750nm while carrying 4 passengers and 1 pilot at a cruise speed of at least Mach 0.6. The design mission profile for this aircraft is shown in Figure 7-21. This VLJ will be introduced around the year 2020, and will incorporate technology improvements appropriate for that time frame, especially advances in propulsion, aerodynamics, and avionics.

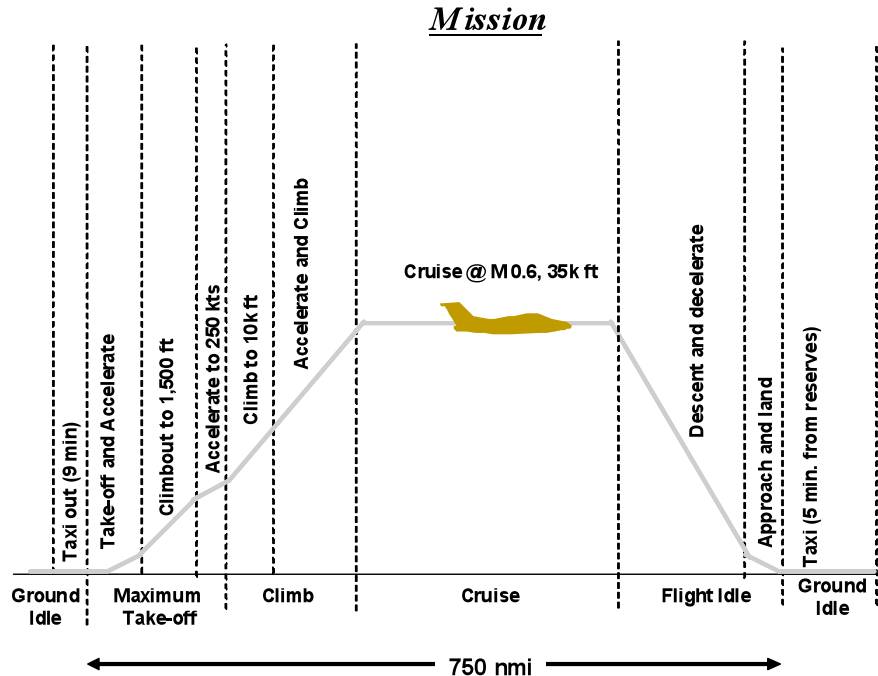


Figure 7-21. Very light jet mission profile.

Detailed VLJ Design

The VLJ design considered for this research is an evolution of the current SoA systems and the high level modeling approach was used. Thus, it was determined that an appropriate model could be constructed by selecting a baseline aircraft representation within AEDT and modifying it according to the technology and performance goals associated with a 4th generation VLJ. The first step in the design process, then, was to select and model the baseline concept. Specific technology and performance improvements were then assumed to represent a technology level appropriate for an introduction date of 2020. The technology improvements and assumptions were then applied to the calibrated model, to capture the tradeoffs and interdependencies of the various design decisions as described in the Vehicle Modeling Approaches previously.

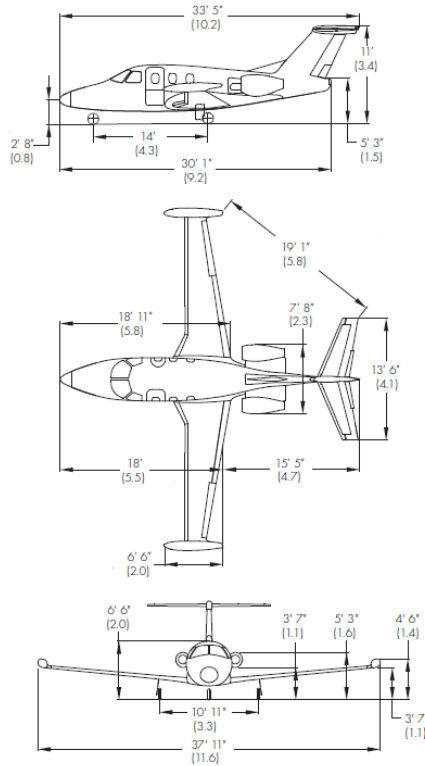
The Eclipse 500 was chosen as the baseline aircraft because of its relative similarity to the anticipated future VLJ and because of the desire to select an aircraft that is currently flying and has available data. The general dimensions of the Eclipse 500 are shown in Figure 7-22. A calibrated model of the Eclipse 500 was constructed using FLOPS, to use as a benchmark for the future VLJ. Basic characteristics of the Eclipse 500 used for calibration are listed in Table 7-7.

The baseline VLJ model was calibrated to match the Eclipse 500 using publically available information. An airframe model was created using FLOPS and an engine deck model was created to match the known performance data. Geometry of the Eclipse 500 was matched, as were weights, fuel use, and thrust-to-weight ratio, for particular mission conditions. The calibration results are listed in Table 7-8.



ECLIPSE 500 DIMENSIONS

ECLIPSE
AVIATION



- NOTES:
1. Eclipse 500 with performance improvement package
 2. All dimensions are in feet and inches (meters)
 3. Dimensions are rounded to the nearest inch (nearest decimeter)
 4. Length includes horizontal stabilizer static wicks
 5. Heights are measured using nominal empty weight

© 2007 Eclipse Aviation Corporation, All Rights Reserved

Figure 7-22. Eclipse 500 general dimensions^{lxxii}.

Table 7-7. Reference data for the Eclipse 500^{lxxiii}.

Parameter	Eclipse 500	Units
Maximum Ramp Weight	6,034	lb
Maximum Takeoff Weight	6,000	lb
Maximum Landing Weight	5,600	lb
Operating Empty Weight	3829	lb
Wing Area	114	ft ²
Passengers	5	-
Sea Level Static Thrust Per Engine	900	lbf
Number of Engines	2	-
Takeoff Field Length (Std Day)	2,345	ft
Landing Field Length (Std Day)	2,250	ft
Design Range	900	nmi
Cruise Mach	0.64	Mach
Maximum Altitude	41,000	ft

Table 7-8. FLOPS VLJ model calibration results.

Parameter	Eclipse 500 Values	Calibrated Values	Units
Maximum Takeoff Weight	6,000	6,000	lb
Operating Empty Weight	3,829	3,829	lb
Sea Level Engine Thrust	900	900	lbf
Takeoff Field Length (Std Day)	2,345	2,564	ft
Landing Field Length (Std Day)	2,250	2,505	ft
Cruise Mach	0.64	0.638	Mach
Maximum Altitude	41,000	40,985	ft
Range of the Long Range Trip [3] (1,100 nm @ 41,000 ft with 710 lbs payload, 100 nm reserve flight and 30 minute holding time)	1,100	1,107	nmi
Block Fuel of the Long Range Trip	1,281	1,135	lb
Block Time of the Long Range Trip	203	218	min

When designing the next generation very light jet, there were several assumptions and tradeoffs that needed to be considered. First, as already mentioned, there was the desire to include only a single pilot on the aircraft, which would reduce total operating costs that must be priced into the seat fare. The effect of the single-pilot model is to reduce the pilot staffing for an air carrier from about 4.5 pilots per plane to about 2.2. With current technology levels, the consequent reduction in safety and high insurance costs associated with the loss of redundancy of pilot control makes this alternative undesirable. For a future VLJ, therefore, reliable remote pilot technology is assumed, enabling a reduction in DOC without the same reduction in safety. This aspect will be further addressed in other sections of this report.

Another design tradeoff that was considered for the future VLJ revolved around maximum cruise altitude and fuselage weight. Currently, light jets used for air taxi operations often cruise at fairly low altitude, around 25,000ft or less, due to relatively short range of average routes. If a future VLJ was designed for a similar mission, the aircraft would need less cabin pressurization because of the lower altitude and thus could gain significant weight savings. However, since the design range is longer, it was determined that the greater efficiency of cruising at higher altitudes for longer-range missions outweighed the potential benefits of reductions in fuselage weight. Thus the normal cruise altitude for the VLJ was assumed to a relatively typical 35,000 ft.

Because the future VLJ is intended to serve small local and regional airports, a takeoff and landing field length requirement was expected to be stringent. A 4,000ft balanced field length requirement was chosen as a target, because a very high portion of current demand is served at airports with runways of that length. According to the FAA Airport Planning and Programming Office (data from 2001), 2,454 (or almost half) of the nation's 5,025 public use airports have runway lengths of 4,000 feet length or more. Another 1,390 public use airports have runways of 3,000 feet or more (for a total of 3,884, or 76%). No tradeoff was conducted to evaluate the effect of accessibility of runways shorter than 4,000 feet on market penetration for the on-demand air carrier business model. Such an evaluation in future NextGen studies would be valuable.

Many specific aerodynamic and propulsion assumptions were required for modeling the future VLJ. The engine powering this aircraft was assumed to have behavior similar to the engines that power the

Eclipse 500. The engine model used for this aircraft was thus calibrated to the PW610F, but was then rubberized to allow scaling for single engine performance. Since the single engine was expected to scale to a larger size, the noise characteristics used to represent this engine were for the larger PW530A.

The future VLJ was designed to enter into service in the year 2020, which implied a technology level equivalent to approximately 2015. Technologies expected to mature in that time frame included aerodynamic and propulsion advances that improve the overall efficiency of the aircraft, similar to the assumptions used for the CESTOL. Engine performance improvements of 8% were considered appropriate based on UEET assumptions with associated scaling for small engines utilized by this aircraft. Aerodynamic improvements included natural laminar flow airfoil and body design. Current technology estimates achievable in conjunction with wing chord, cruise speed, and adverse pressure gradient limitations garner 50% laminar flow assumption on wing and stabilizers. No leading edge devices were assumed for this aircraft, although high-lift devices were assumed to meet the field length requirement. The movement from two engines to a single engine accounted for approximately a 3% decrease in empty weight, a net reduction accounting for a reduction in total engine and pylon weight and a slight increase in vertical tail weight associated with the single engine configuration.

Summary of VLJ Design

After all design decisions and technology improvement assumptions were made, a converged solution for the next-generation VLJ was reached. Although it was initially based on an Eclipse 500, the passenger capacity, single-engine configuration, and performance characteristics of the future VLJ greatly resembled the newer Eclipse 400. This aircraft weighed slightly less than the reference Eclipse 500, owing mainly to the single engine and technological improvements. The future VLJ also had a slightly longer takeoff field length, and was designed for fewer passengers at a shorter range. A basic comparison showing the design characteristics of the Eclipse 500 and the converged VLJ is listed in Table 7-9. A payload-range chart highlighting the capabilities of the future VLJ is shown in Figure 7-23.

A notional view of the future VLJ is shown in Figure 7-24. Because of its design mission, desired payload, and design decisions, the advanced VLJ is a small, lightly swept-wing monoplane, with a single engine mounted on the rear fuselage, and a 'V' tail surrounding the engine. The final configuration resembles the basic layout of the Eclipse 400.

Table 7-9. VLJ converged design vehicle comparison.

Parameter	Eclipse 500	ASDL-GT VLJ	Units
Maximum Ramp Weight	6,034	5,626	lb
Maximum Takeoff Weight	6,000	5,600	lb
Maximum Landing Weight	5,600	5,600	lb
Operating Empty Weight	3829	3748	lb
Wing Area	114	138	ft ²
Passengers	5	4	-
Sea Level Static Thrust Per Engine	900	1,690	lbf
Number of Engines	2	1	-
Takeoff Field Length (Std Day)	2,345	3,875	ft
Landing Field Length (Std Day)	2,250	2,250	ft
Design Range	900	750	nmi
Cruise Mach	0.64	0.6	Mach
Maximum Altitude	41,000	41,000	ft

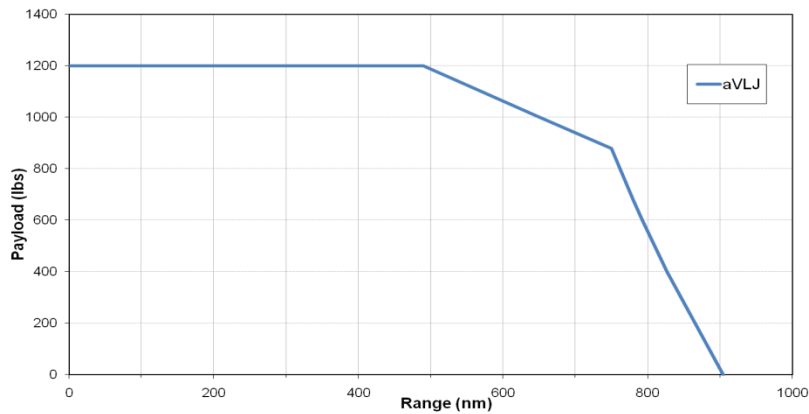


Figure 7-23. VLJ payload range chart.



Figure 7-24. Notional configuration of advanced VLJ^{lxxiv}.

AEDT and ACES Connectivity

Although the VLJ model was created in FLOPS, the BADA and AIR 1845 performance data were needed for ACES and AEDT. Once again, since the VLJ model was not high-fidelity, it was deemed appropriate to utilize a baseline AEDT representation and modify it to accurately resemble the future VLJ. In this process, the FLOPS model of the VLJ provided information on the weight and performance trades resulting from the design decisions.

The converged FLOPS results were translated directly into modifications of the AEDT coefficients representing the baseline Eclipse 500. Specifically, the converged FLOPS VLJ model provided information for aerodynamic and drag polar data, engine thrust levels and lapse rates, fuel consumption, and basic weights. The emissions indices were scaled down from the AEDT information used for the Eclipse 500. The Noise Power Distance (NPD) information for the PW530A was substituted for the VLJ, as it was assumed to have similar noise characteristics to the advanced VLJ's larger scale single engine. The performance of the AEDT VLJ model was validated for appropriate and reasonable weight, climb rate, cruise speed, cruise altitude, thrust, and fuel burn on a design range mission.

VLJ Summary, Lessons Learned, and Potential Further Research

The converged design for the future VLJ seemed very reasonable and appropriate for the purposes of this research. By incorporating modest technology improvement assumptions, the converged VLJ design met all the requirements dictated by its anticipated mission. Since the scope of the research involved air transportation system level impacts, a detailed, high-fidelity VLJ design was not necessary, especially since similar vehicles exist currently. A future challenge would be to develop a high-fidelity model of this aircraft, especially one including future technologies. If a follow-on study focused more on vehicle-level trends and impacts, a higher-fidelity analysis would have to be done to appropriately model this future light jet.

Unmanned Aircraft Systems

Unmanned Aircraft Systems (UAS) have been proposed for a multitude of missions from high altitude measuring and communication, through persistent urban surveillance, and carrying time critical cargo to remote locations where it is not cost effective to provide crewed service. Thus, depending on the application of an UAS, the design can be substantially different. NASA has discussed 7 possible applications of UAS during the 2025 to 2040 timeframe, and finally identified 2 applications that could have an impact on NextGen. This section summarizes the design, modeling and performance of one application, i.e., mid-size cargo delivery UAS.

Design Requirements for the UAS

There is a wide range of possibilities for a UAS configuration depending on what the Initial Operational Capability (IOC) date would be and how it would be used. NASA envisions that a UAS would operation in the 2025 to 2040 timeframe. Projecting the technology level that can be reached during that time frame, 7 possible applications of UAS were suggested and discussed.

1. UAS passenger aircraft;
2. UAS large cargo aircraft;

3. UAS mid-size cargo aircraft, for freight forwarding, taking packages from large airports to smaller communities;
4. UAS small (VTOL) cargo aircraft, about 200 lbs of weight, carrying about 50 lbs of packages, for delivering such as FedEx/UPS small package to an office or home within a metropolitan area;
5. UAS local surveillance aircraft, about 50 lbs of weight, for reporting, police, closed-circuit television camera in the sky, border patrol, etc;
6. UAS bush fire fighting aircraft;
7. UAS high altitude long endurance aircraft, cruising for a week or longer at above 65,000 ft, for communication relay, disaster response, hurricane tracking, etc.

Applications 1 and 2 would probably have the same missions as the pilot controlled aircraft that they would replace; thus no apparent special impact on NextGen. Application 7 would take off and land during the leisure time of NAS operation; thus also no apparent special impact. Application 6 would be viable only outside of the metropolitan area; thus its impact would be very limited and ignorable. Application 4 is too risky to have many such aircraft flying in congested cities; thus it is ruled out as a possible application. Since Application 5 is studied by the sister project managed by Raytheon, Application 3 became the focus of the current effort.

The success of Application 3, or mid-size cargo aircraft (UAS later on), would need autonomous navigation, sense-and-avoid capability, ground pilot monitoring, and would fly generally like a piloted aircraft. FedEx has long been using small cargo airplanes. In 1986, Cessna developed a cargo version of the Cessna 208 Caravan for FedEx, called the CargoMaster; later, a bigger cargo version by stretching the fuselage by 4 feet, installing a ventral cargo pod, and upgrading to a more powerful engine, which is the Super CargoMaster. Now FedEx is operating more than 250 Super CargoMaster. As a basis of this NRA, a derivative of the Super CargoMaster would be used to model a UAS vehicle that would have an impact on NextGen. The CargoMaster is depicted in Figure 7-25.

Super CargoMaster is a dedicated cargo airplane, which has proven itself time after time for legendary and unparalleled reliability and dependability. It has large cargo load capacity of 3,500 lbs and cargo volume of 450 cubic feet,^{lxxv} and a host of cargo-ready features, including front-to-back loading, durable interior sidewalls, a replaceable flat wood-floor, a cargo barrier aft of the pilot seats, and pre-marked loading zones, depicted in Figure 7-26.



Figure 7-25. FedEx Super CargoMaster^{xxvi}.



Figure 7-26. Interior of Super CargoMaster^{xxvi}.

It would be natural to select Super CargoMaster as the baseline for the UAS of freight forwarding mission for its established performance reputation. Based on the experience of FedEx with Super CargoMaster and distributions of airports in the United States, the typical flight range of UAS is about 150 nm with one end being a large airport and the other end being a small general aviation (GA) airport. Considering some small GA airports may not have fuelling capability, the design range of UAS is at least two times 150 nm. Therefore, the design range is selected as 400 nm. The cruise altitude and speed of UAS should be similar to those of Super CargoMaster. Considering the shorter design range of UAS than Super CargoMaster and some weight saving because of pilotless, the payload should not be less than 3,000 lbs. As a result, the mission profile assumed for the UAS is depicted in Figure 7-27.

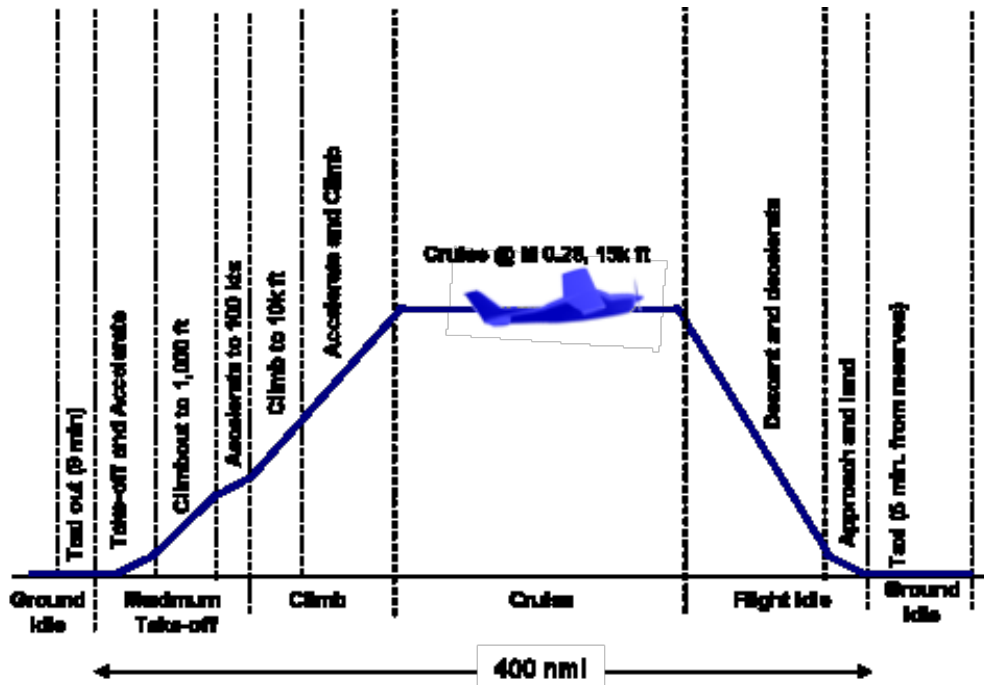


Figure 7-27. Standard mission profile of UAS.

Detailed UAS Design

The UAS design considered for this research is an evolution of the current SoA systems and the high level modeling approach was used, as was done with the VLJ. Thus, the detailed design process of UAS

includes collecting the baseline data, establishing the modeling environment, making modeling assumptions and tradeoffs, calibrating the baseline aircraft model, and convergence of the design.

Although it would be natural to select Super CargoMaster as the baseline for UAS, limited public performance data of Super CargoMaster was available. The performance data are very useful for model calibration purpose. On the other hand, there are plenty such data of Cessna Grand Caravan, which is a passenger variant of Super CargoMaster, developed in 1990. The two versions have the same geometric dimensions, engine, takeoff gross weight, and stall speed, and almost the same other performance parameters such as cruise speed. The main difference is that Grand Caravan has cabin windows and slightly better mission performance. Therefore, Grand Caravan was selected as the departure point for the UAS modeling. Unless indicated otherwise, the performance data are from Reference^{lxxvi}, which is the specification and description manual of Grand Caravan, published by Cessna Company in 2007. The manual provided detailed information regarding performance and geometric information for which the high level modeling approach could be validated, as described previously.

Cessna Grand Caravan is an unpressurized, single-engine, braced high wing, turboprop aircraft, with fixed landing gear, depicted in Figure 7-28. The aircraft can accommodate up to 14 persons including pilots. Suitable allowance for luggage is provided. It is certified with single pilot but has equipment for two pilots. The powerplant is a Pratt & Whitney PT6A-114A turboprop engine, mounted in the nose of the fuselage. It is equipped with a metal, three-blade, anti-ice, constant speed, full feathering, reversible pitch propeller, manufactured by McCauley. Wing airfoils are NACA 23017.424 at root, NACA23012 at tip; incidence is 2°37' at root, -0°36' at tip.^{lxxv}

Grand Caravan was designed to fly by two pilots and has device for two pilots. When it is converted to a UAS, however, its operational weight empty can not benefit much from the weight saving of two pilots and device, since more avionic equipment is needed for environmental sensing, auto flight, remote control and communication, and actuators. Considering the operational weight empty is often calculated with only one pilot since Grand Caravan is certified with one pilot, no weight saving from replacing human pilots seems a reasonable assumption for operational weigh empty of UAS. Since Grand Caravan was already designed for takeoff and landing at small GA airports, there is no need to improve the takeoff and landing performance.

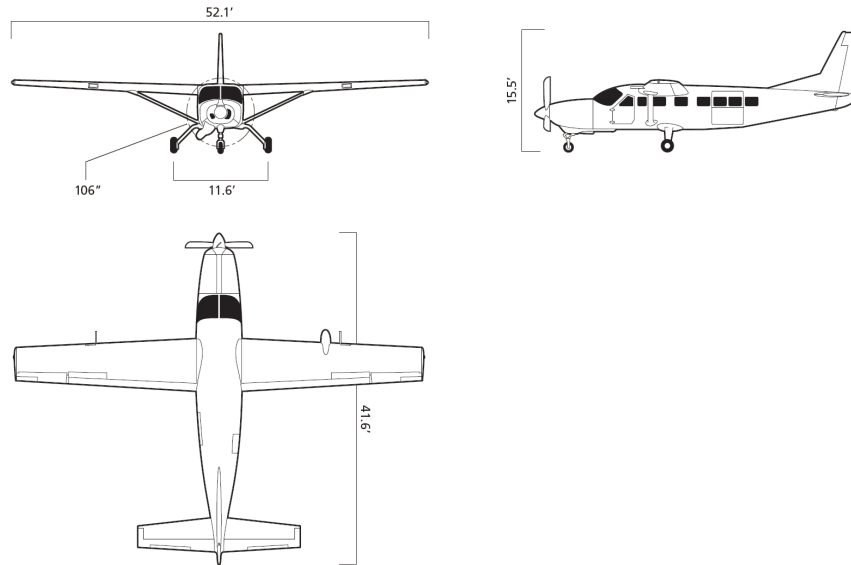


Figure 7-28. Three views of Grand Caravan^{lxxvii}.

The UAS was assumed to enter into service in 2025. Based on the technology assumptions made for the CESTOL and the VLJ, similar technological advances were considered applicable for the UAS. The engine PT6A-114A of Grand Caravan was certified in 1980s; therefore the new engine will have 40 years of technology improvements, leading to reduction of SFC and emission. The noise level may not change much since the current noise level of Grand Caravan is relatively low and not a concern. Grand Caravan has all metal, fail-safe two spar wings, and conventional fuselage made of sheet metal.^{lxxvi} It was deemed not economically viable to make wing and fuselage of mainly composite material due to scale issues as noted by Mitsubishi.^{lxxviii} However, some parts of UAS structures can be made of composite material and save some weight. Summarizing the above, the main assumptions and requirements made for UAS are listed in Table 7-10. The most significant advancements for the UAS were with respect to engine performance and payload-range improvements. For this study, the fuel consumption of was reduced by 20% from the Grand Caravan, while its range was improved more than 40% for the same payload, depicted in Figure 7-29 and Figure 7-30, respectively.

Table 7-10. Main assumptions and requirements for UAS.

Category	Assumptions
Engine	Adoption of UEET, resulting in the following: a. 20% reduction of SFC; b. 50% reduction of NOx; c. 8% reduction of other emissions such as CO, HC, and Smoke. Noise: the same as the current level, proportional to thrust level of UAS.
Operational Weight Empty	Adoption of composite material and removal of human pilots, resulting in a 120 lbs of weight saving, i.e., new operational weight empty is 4,394 lbs (originally 4,514 lbs).
Mission	Design range: 400 nm; Design payload: no less than 3,000 lbs; Flight reservation: 45 minutes at 10,000 ft; Design cruise altitude: 15,000 ft; Design cruise speed: about M0.28; Maximum altitude: 25,000 ft; Takeoff and landing performance: the same as Grand Caravan; Ramp weight: 8,785 lbs (the same as Grand Caravan) Maximum landing weight: 8,500 lbs (the same as Grand Caravan)

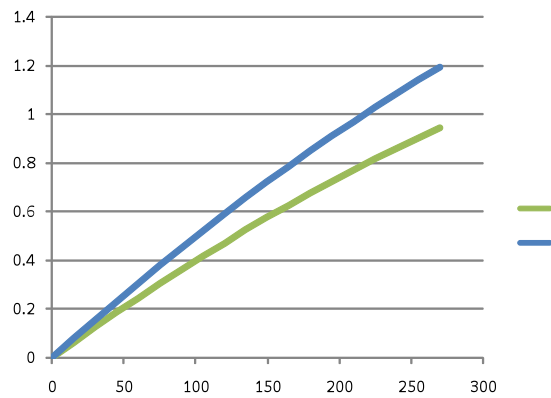


Figure 7-29. Comparison of fuel consumption.

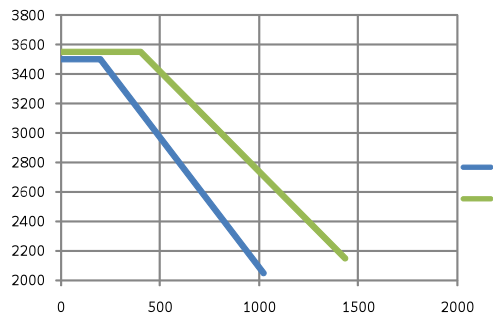


Figure 7-30. Comparison of payload-range performance.

Summary of UAS Design

Based on the above assumptions and performance objectives desired for the UAS, a converged solution was obtained. As with the VLJ approach, the focus of the UAS design was to enable the NextGen systemwide impact analysis. Thus, the level of detail of the design of the UAS was limited in scope. The final performance characteristics for the UAS developed for this study are listed in Table 7-11.

Table 7-11. UAS performance summary.

Item	Value
Crew	Uncrewed
Passengers	Freighter
Design Range (nm)	400
Maximum Take-off Weight (lb)	8,785
Maximum Landing Weight (lb)	8,500
Maximum Payload (lb)	3,550
Empty Weight (lb)	4,274
Design Cruise Mach Number	0.283
Design Cruise Altitude (ft)	15,000
Take-off Field Length, Std. Day (ft, 50 ft obstacle)	2,420
Landing Field Length, Std Day (ft, 50 ft obstacle)	1,795
Engine Take-off Thrust (shp)	675
Number of Engines	1

AEDT and ACES Connectivity

The converged UAS model, which is based on FLOPS, can be used to calculate the performance characteristics for ACES and AEDT, as with the VLJ approach. However, the noise curve and emission indices required by AEDT and ACES were not straight forward. Thus, the team used an equivalency approach by identifying similar aircraft within the AEDT database. The Raytheon T-6A Texan II^{lxxxix} is a military trainer with one turboprop engine. The engine is PT6A-68, which has similar power as the PT6A-114A of the UAS. Therefore, the Texan's NPD curves were used as the approximation for the UAS, assuming the noise level of those engines would have minor changes in the future. The noise spectra are obtained by first looking up the noise group ID's for the PT6A-68 engine from the spectral class document,^{lxxx} and then finding the spectra curves of those ID's from the database. The emission indices of the PT6A-114A in the database were used as the baseline for the new engine of UAS. Based on the results of UEET and considering the 40 years improvement in the year of 2025, three assumptions were made on the emissions characteristics of the UAS, specifically, 20% reduction in fuel burn, 50% reduction in NOx, and 8% reduction in all other emissions indices as each throttle setting.

UAS Summary, Lessons Learned, and Potential Further Research

NASA made the fundamental requirements for the UAS, while the other design requirements were suggested by this research. All in all, the UAS model was very straightforward in the development. Among the challenges remaining to be met are further analyses of noise and emission. Another major challenge, and assumption for this analysis, is the development of see-and-avoid technology. The noise characterization will require higher fidelity analyses of propeller noise, turbine engine noise, and airframe noise such as high lift device and landing gear noise. In addition to calculation of noise level, the more difficult analysis of noise is to determine the noise spectra, which are now measured instead of calculated. The emission characterization will require higher fidelity analyses of the engine combustion process to improve the emission prediction, given the design parameters of the turbine engine.

Large Civil Tiltrotor (LCTR)

Rotorcraft have a unique capability of runway independent operation which can substantially impact the congested terminal area operation. But to combine this potential into NextGen, operational performance of rotorcraft system has to be projected into the competent level with the current turboprop fleet as a valid means of regional transport. Considering the fundamental limits of conventional helicopters' throughput capability, especially in flight speed aspect, rotorcraft with the relatively higher disk loading have greater potential to achieve this level of performance. NASA has performed in-depth conceptual study for three heavy lift rotorcraft configurations designed to probe their validity as large civil transports.^{xxviii} These configurations are depicted in Figure 7-31. Major vehicle configurations benchmarked were 'Large Civil Tiltrotor', 'Large Civil Tandem Compound', and 'Large Advancing Blade Concept'. Boeing Aircraft Company also has performed the commercialization study for civil tiltrotor which resulted in technologically feasible and economically viable fleet extension based on currently operating V-22 Osprey tiltrotor aircraft.^{xxvii} Each of the NASA vehicles has been sized to meet similar goals. As one of the primary results of this study, Large Civil Tiltrotor (LCTR) had the best cruise efficiency, hence the lowest weight and showed economically competitiveness, with the potential for substantial impact on the air transportation system. Based on the findings of these researches, LCTR aircraft was chosen for this study. This section describes the modeling and validation results for the baseline LCTR which represents the dominant rotorcraft system in the future regional airspace.



Figure 7-31. NASA's heavy-lift rotorcraft configurations

Design Requirements for the LCTR

NASA's LCTR2 (Large Civil Tiltrotor 2) is the refined tiltrotor concept originated from NASA Heavy Lift Rotorcraft Systems Investigation program^{xxviii} and designed for the short-haul regional transport market of 2018.^{xxix} NASA utilized the rotorcraft design software (RC) and aerodynamic analyzer (CAMRAD II) in conjunction with the blade and wing structural model to obtain refined and optimized vehicle. This LCTR2 has been selected as the baseline aircraft model because it provides both the reasonable requirements for future regional transport and the feasible technological solution for those requirements based on high-fidelity analyses. This section summarizes the primary requirements, notional design mission, key vehicle characteristics and important technological assumptions of LCTR2 based on NASA studies.

NASA's LCTR has been designed for short-haul regional transport entering service in 2018. It can transport 90 passengers (in 32-inch pitch, single class 2-2 seating layout) to the maximum range of 1,200 nm with cruising speed of 300 knots. It has a wing spanning 107 ft and blade folding mechanism with assumed weight penalty (1,000 lb for each rotor blade) to satisfy the gate compatibility limited by FAA Aircraft Design Group III regulation (118 ft) currently applied for Boeing 737 and Airbus 320 aircraft. It adopts high-wing structure and sponsons containing the main landing gear systems. Advanced four 7,500-lb class turboshaft engines drive two 65-ft diameter proprotors. Two engines and one rotor driving system are packaged into each engine nacelle and tilted together. Each rotor consists of four blades. These rotors also control yaw maneuver and the V-tail is used without independent vertical tail in empennage part.

The primary characteristics of the LCTR used to develop the detailed model are listed in Table 7-12 and the mission profile for the validation of the model is depicted in Figure 7-32. These requirements were explicitly defined in the NASA report and are just provided herein for completeness. Unlike the previous aircraft discussed, the LCTR design was dictated completely by the NASA experts. Thus, the objective herein was to create a comparable model with public domain analysis tools such that the required ACES and AEDT models could be established.

Table 7-12. LCTR2 vehicle overview.

Parameter	Value
Structural design gross weight (SDGW)	107,104 lb
Operating empty weight	67,652 lb
Installed power	4 x 7,500 hp
Design payload	19,800 lb (90 passengers)
Main cabin	Single class 2-2 seating
Overall length	108.9 ft
Overall width	142.0 ft
Wing span	107.0 ft
Number of rotors	2
Rotor radius	32.5 ft
Number of blades	4
Tip speed, hover	650 ft/sec
Tip speed, cruise	350 ft/sec
Cruise speed	300 knots
Service ceiling	30,000 ft
Wing loading (SDGW)	107.4 lb/ft ²
Disk loading (SDGW)	16.14 lb/ft ²

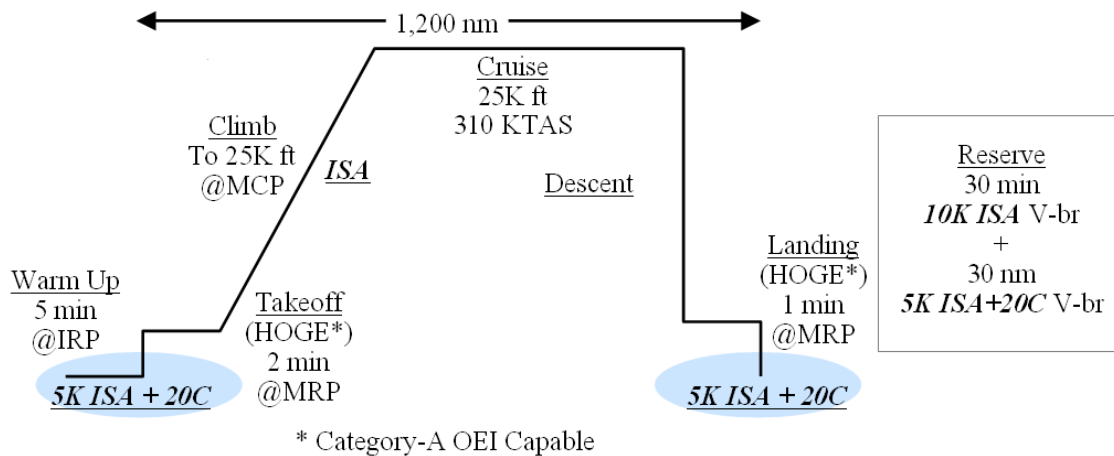


Figure 7-32. LCTR2 design mission profile.

Detailed LCTR Design

Based on the detailed descriptions on NASA’s LCTR2 vehicle characteristics and high fidelity modeling,^{xxix,xxx} approximated remodeling of LCTR2 was performed to facilitate system-wise fleet operation analysis. VASCOMP II was utilized to obtain compact and reasonably accurate model for the baseline vehicle within its own limit to simulate the vehicle’s performance in the dissimilar operational mission profiles to the original design mission. We used a conventional departure and approach in a propeller mode rather than using the vertical capability due to safety reasons. VASCOMP II is the first order sizing and performance analysis program for generic vertical-takeoff-and-landing (VTOL) aircraft and has been successfully utilized for high-speed rotorcraft modeling tasks.^{lxxxi,lxxxii} For the current modeling and analysis work, the VASCOMP II with a modified conventional takeoff module was used considering the non-vertical takeoff and initial climb procedures.

The strategy for VASCOMP modeling for the baseline vehicle was to translate geometry, fixed weights (excluding fuel weight), and propulsion data into VASCOMP input parameters as closely as possible to the NASA’s data and, then, to adjust the aerodynamic input parameters to match the resultant performance metrics and mission fuel burn amounts. This approach was chosen because VASCOMP performs only simplified first-order aerodynamic calculations contrast to the detailed aerodynamic modeling data provided by NASA,^{xxx} which cannot be translated directly into the limited set of VASCOMP’s aerodynamic input parameters.

VASCOMP requires the minimal set of vehicle geometric parameters approximating actual vehicle geometry into the set of primitive geometric entities such as cylinder, hemisphere, and rectilinear objects. Two major modifications from the actual geometry of LCTR2 were for the empennage and the outer section of the main wing. V-tail has been replaced with the separated vertical and horizontal tails based on their projected areas. Main wing has been modeled by the single planform parameters while the outer section of the main wing had been designed to tilt with engine nacelle reducing downloading effect during the axial flight mode in original LCTR2 design. The effect of this modification to download increase has been described in later part of this section. Figure 7-33 shows the most important geometric parameters represented in the VASCOMP input data.

All the weight components except the fuel weight have been fixed with the LCTR2 data. Empty weight, fixed useful weight, and payload weight has constant values as shown in Figure 7-34. Payload weight of 19,800 lb corresponds to the 90 passengers and their baggage weight and fixed useful weight consists of weight of crew, unusable fuel, and rafts, per the reference NASA configuration.^{xxx} Unless otherwise noted, all LCTR data generated herein was compared to the NASA data quoted in Reference xxx.

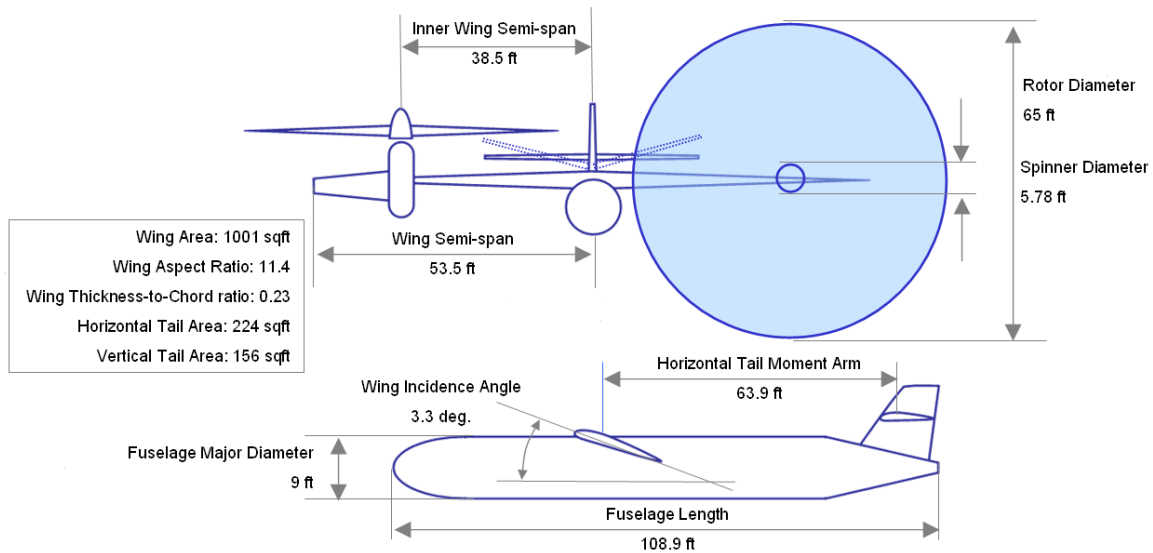


Figure 7-33. LCTR2 geometry model for VASCOMP.



Figure 7-34. LCTR2 weight composition (excluding fuel weight).

Among the various options for rotor aerodynamic models of VASCOMP, the Boeing-Vertol proprotor model was used. The model requires hover figure of merit table, representative drag divergence Mach number for blade (value for 75% radial position), and reference power coefficient (C_{po}) value as input parameters and calculates power and thrust coefficients for given flight conditions. Figure 7-35

shows the figure of merit data^{xxix} and symbolized the values that were used as VASCOMP input corresponding to LCTR2's rotor airfoil at hover tip speed. A comparison between NASA and VASCOMP's estimation for major rotor performance metrics, which are in a reasonable agreement, are listed in Table 7-13. Both results are based on the simulation for the design mission described in the previous section.

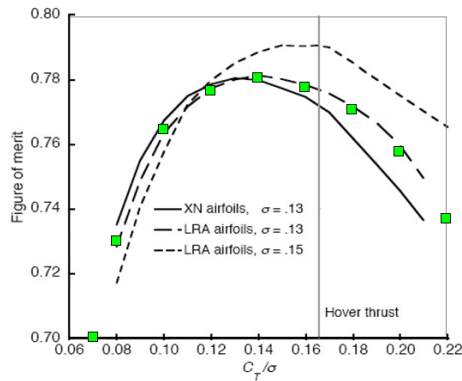


Figure 7-35. Figure of merit data.

Table 7-13. Rotor aerodynamic parameters.

Parameter	NASA	VASCOMP
Hover tip speed	650 fps	650 fps
Cruise tip speed	350 fps	350 fps
Solidity (σ)	0.13	0.128
Hover figure of merit	0.78	0.784
Hover CT/σ	0.166	0.1678
Cruise CT/σ	0.0867	Max* 0.0878 Min* 0.0778
Cruise propulsive efficiency	0.84	Max* 0.836 Min* 0.816

*Max and Min correspond to the start and end condition of cruise segment in design mission analysis result

Total vehicle drag in cruise is the sum of parasite and induced drag. Parasite drag has been modeled using the provided flat plate drag area of 34.18 ft² with additional 1.58 ft² for engine leakage and cooling at cruise condition. To model the lift-dependent induced drag, aerodynamic span efficiency (Oswald efficiency factor) has been estimated by VASCOMP based on the given rotor and wing configuration. Vertical download in hover has been estimated as 8.7% of takeoff gross weight by VASCOMP contrast to the 7.4% from NASA's results. This difference originated from neglecting the outer wing tilt in hover but the effect of this on hover performance was very little in terms of required hover power as shown in the later section on performance validation.

To model available power and fuel flow for the entire flight regime, detailed engine performance data provided by NASA were translated into VASCOMP's engine deck format. This implementation was broken down to following three sub tasks;

- Reformatting static MRP (Maximum Rating Power), IRP (Intermediate Rating Power), and MCP (Maximum Continuous Power) data into referred power as function of the power setting (referred turbine inlet temperature)
- Reformatting MCP (and corresponding fuel flow) data into referred power (and referred fuel flow) as functions of Mach number and power setting
- Validation of off-design (non-optimum) engine performance data with built-in calculation logic of VASCOMP

VASCOMP's engine deck format requires that power and fuel flow are non-dimensionalized and tabularized by power setting (referred turbine inlet temperature, T/θ , where θ is the ambient temperature ratio to 518.69°R). Left chart of Figure 7-36 corresponds to the given NASA engine data in for a static condition. Assuming the reference turbine inlet temperatures of 2400°R, 2550°R, and 2600°R for MCP, IRP, and MRP conditions, respectively, one can obtain collapsed single static power curve shown in right chart of Figure 7-36, as required by VASCOMP's engine deck format.

For non-static flight conditions including conversion and cruise segments, MCP and corresponding fuel flow data had to be input as functions of flight Mach numbers. VASCOMP uses available power and fuel flow for 100% power turbine speed to estimate the non-optimum values for corresponding conditions. Because LCTR2 uses significantly reduced tip speed in cruise (350 fps, corresponding to 54% of 650 fps for hover), proper non-optimum engine performance modeling is important for cruise performance evaluation. To model non-static engine performance, the provided engine performance data for 100% power turbine speed in various flight speeds were fitted by the least-square method as shown in Figure 7-37.

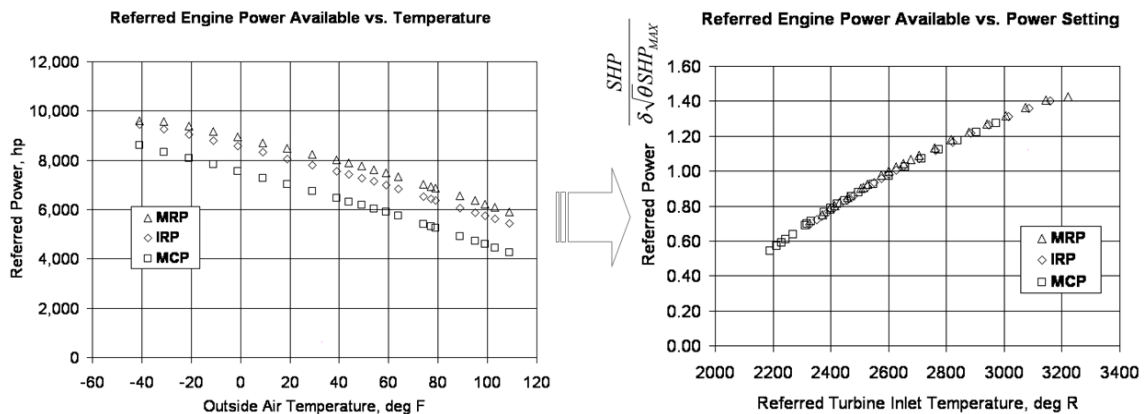


Figure 7-36. Reformation of static MRP/IRP/MCP data.

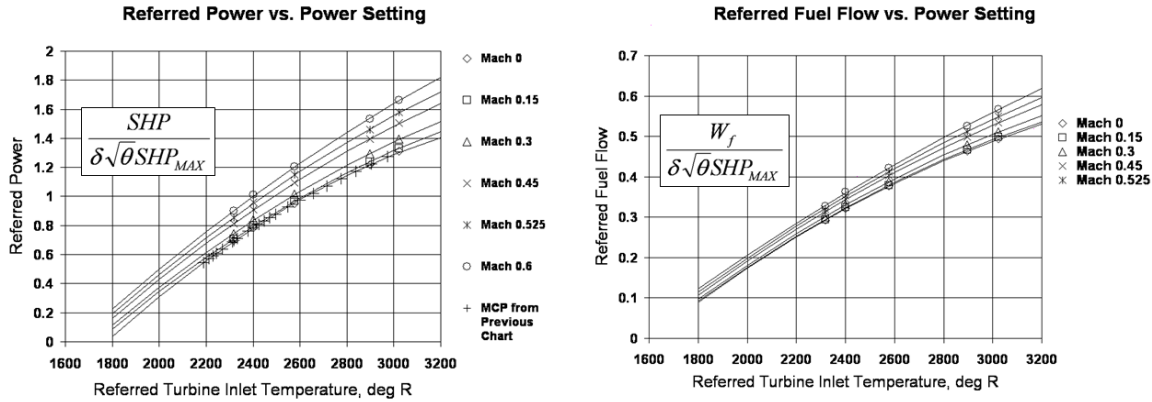


Figure 7-37. MCP and fuel flow model for various mach numbers.

Figure 7-38 validates the non-optimum power modeling by VASCOMP referenced to corresponding 100% power turbine speed value. Within a reasonable range, all data points are clustered to the modeling curve confirming that the built-in logic of VASCOMP for the calculation of available power for reduced power turbine speed gives satisfactory modeling results matching provided engine data.

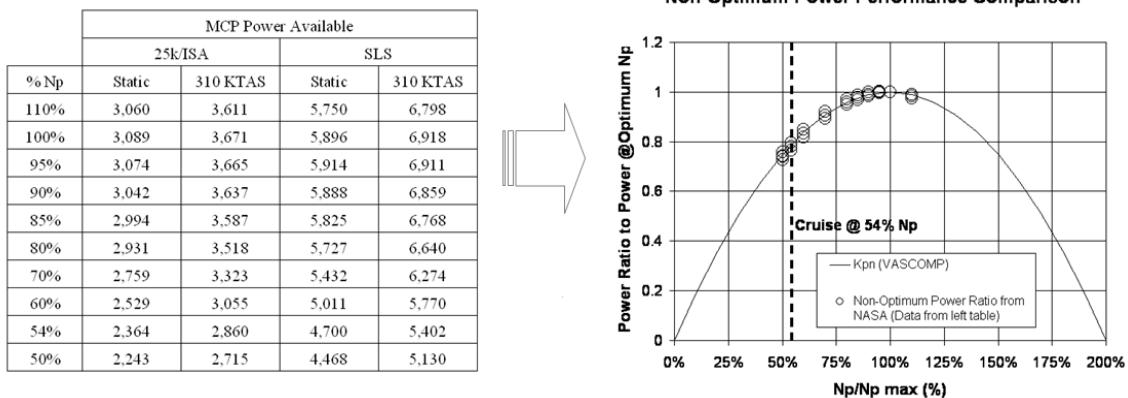


Figure 7-38. Non-optimal power modeling.

Summary of LCTR2 Design

The validity of previously described VASCOMP model for LCTR2 was measured by modeled vehicle performances and segment-by-segment mission fuel burn amounts. For vehicle performance evaluation, hover and cruise performance were calculated to reproduce the hover ceiling and cruise velocity data provided by NASA.

Hover Performance Validation

Independent of the design mission, hover ceiling was estimated for multiple takeoff gross weight conditions. For each takeoff gross weight condition, required hover power at varying hover altitude was calculated by VASCOMP. The comparison of two takeoff gross weight conditions are provided in Figure 7-39 for standard and increased temperature conditions, which shows a reasonable agreement with the high fidelity modeling result. The power versus altitude chart for takeoff gross weight of only 107,104 lb

is shown in the left chart of this figure. All calculations were performed for out-of-ground effect (OGE) conditions.

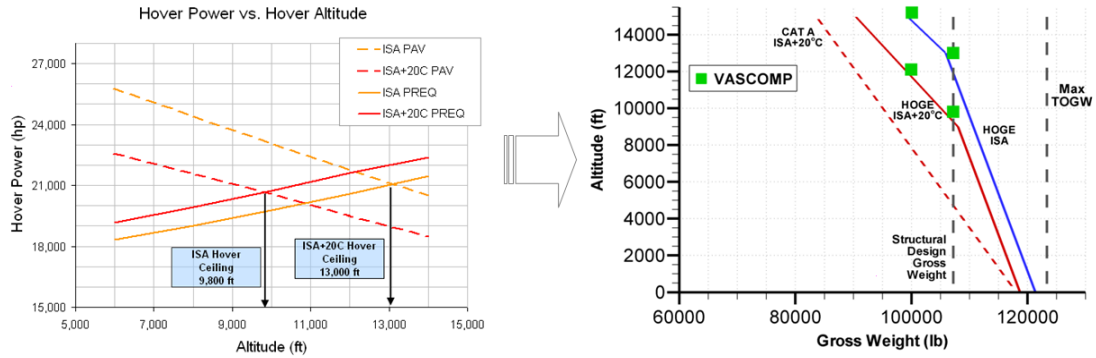


Figure 7-39. Hover ceiling comparison.

Cruise Performance Validation

Using the design takeoff gross weight of 107,104 lb, cruise performances were evaluated for different cruising altitudes. For each altitude, speed for best endurance, speed for best range, and the maximum speed have been calculated by VASCOMP and compared to NASA data. The speeds correspond to the specific position in the speed versus required power curve and represent the required power model for each flight condition defined by altitude and cruise speed. Figure 7-40 shows a reasonable agreement between VASCOMP's calculation results (indicated with symbols in graph) and high-fidelity modeling results (indicated with lines in graph) except the best range speed, which is very sensitive to the power-to-speed gradient. But all the best range speeds of high fidelity model are bound between VASCOMP's best range speeds and 99% of these values.

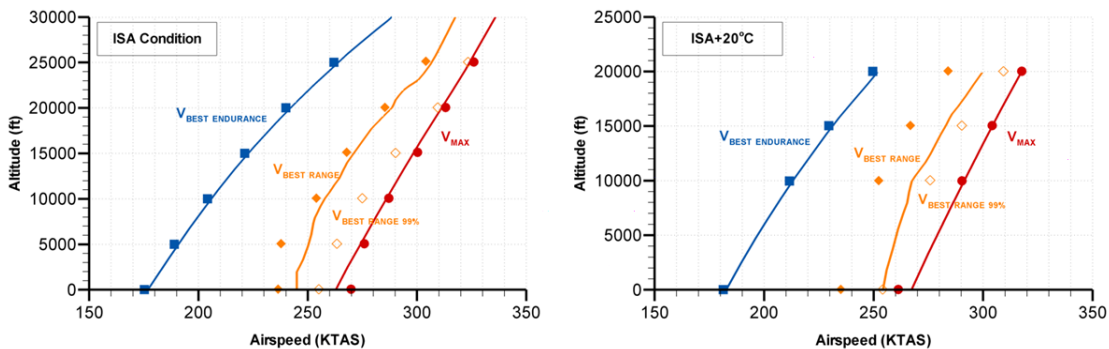


Figure 7-40. Cruise velocity comparison.

Mission Performance Validation

Based on the key performance model matching high-fidelity analysis results for hover and cruise flights, detailed mission performance analysis has been performed using previously described VASCOMP model to compare vehicle behaviors in the segment-by-segment manner for the design mission summarized in Figure 7-41. This detailed mission profile is basically identical to previously described design mission profile in Figure 7-32 except the explicit inclusion of conversion and reserve mission segments. In usual vehicle sizing analysis the engine power is assumed ‘rubberized’ and estimated for enough power for the given OEI (one engine inoperable) condition and the most demanding power condition. But for current mission performance validation, the total engine power capacity has been fixed with the 30,000 hp (four times of 7,500 hp) based on the closely matching engine performance model described in previous section to ensure direct fuel burn comparisons for each and every mission segments. As a reference, the ‘rubberized engine sizing’ for LCTR2 design mission resulted in the smaller value than 30,000 hp for the OEI takeoff condition, also with the decreased takeoff gross weight than constant 30,000 hp-engine power case.

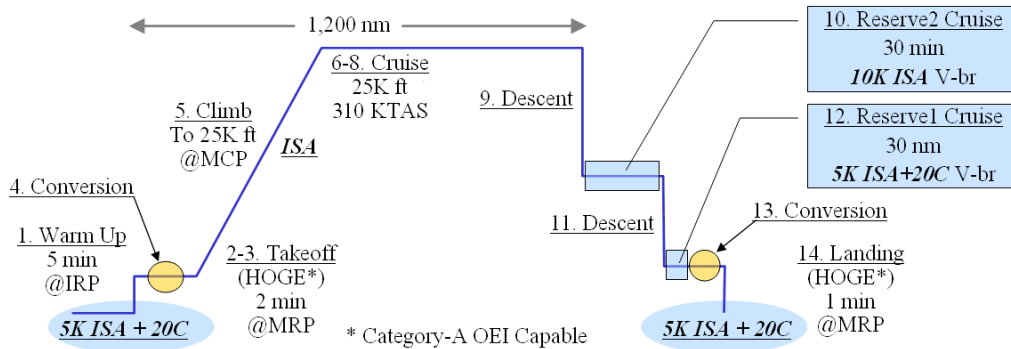


Figure 7-41. Detailed mission profile for LCTR2 design mission.

As a result of the VASCOMP modeling, the final results were compared side by side to the NASA data. As shown in Figure 7-42 the required power and fuel consumption for each and every major mission segments are similar in magnitude and the resultant takeoff gross weight was 107,382 lb by VASCOMP modeling compared to the reference 107,104 lb. The difference between these is lower than 0.5%. Figure 7-43 shows the vehicle weight composition of LCTR2 for the design mission.

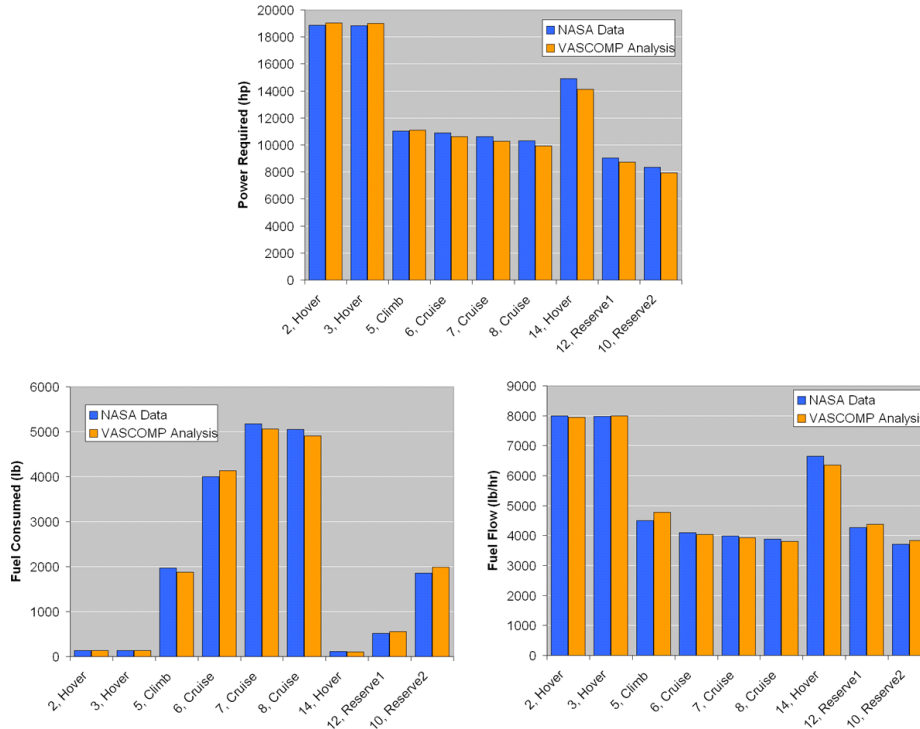


Figure 7-42. Power required, fuel consumption and flow comparison for mission segments.

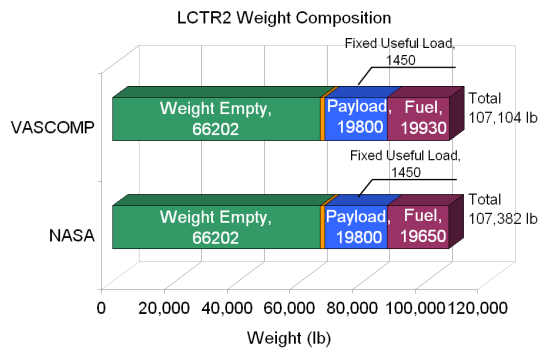


Figure 7-43. LCTR2 weight comparison.

LCTR2 Terminal Operation Modeling

One of the key integration challenges of the LCTR to NextGen is the interoperability in the terminal area with consideration of passenger comfort and aircraft safety. Despite the axial flight capability of the LCTR, short rolling takeoff and landing is preferred due to the better flying quality and the easier rejection procedure in case of emergency.^{lxxxiii} The construction of the terminal operation scenario of LCTR was greatly facilitated by the documents^{lxxxiii,lxxxiv} by and communications with NASA's tiltrotor experts^{lxxxv} who coordinated and analyzed tiltrotor flight tests because there is no firmly established terminal operation conventions and regulations for large civil tiltrotor aircraft yet. To properly assess the operational performance of LCTR2, a notional operation profile had been setup and VASCOMP was utilized to estimate operational mission performance. In addition, the procedures developed herein were driven by the operational and terminal airspace redesign that will be discussed in later sections. The

procedures here are notional and could be modified for future studies, but a stake was put in the ground to assess the broader effects of the LCTR2 interactions at the system level. More extensive work on more realistic procedures is on-going within NASA and were not incorporated within the time frame of this study.

As a result of previous studies, a short rolling takeoff with 75°-nacelle tilt using approximately 60% of maximum continuous power in the takeoff procedure was assumed. Transition from 'airplane' to 'helicopter mode' was performed using a moderate flight path angle (0~3°) because the steeper angles often result in too much loss of mechanical energy during decelerating conversion. The final 1,000-ft approach was constrained by the rate of descent and flight path angle limits. Minimum speed during the final approach was not allowed to fall below 50-knots considering the inaccuracy of flight speed measurement under this flight velocity. 50-knots approach speed also provided a safe cushion in case of the single engine failure. Another important reason for non-vertical descent was to ensure the absence of the fatal vortex ring status susceptible in vertical descent with the high rate of sink. This procedure was modeled in VASCOMP. Only airports at sea level static condition were assumed and the entire flight was flown in ISA atmospheric condition. Design takeoff gross weight of 107,104 lb was used for departure and 85% of this weight was assumed at the start of approach procedure corresponding to notional 1,000-nm cruise operation.

The nacelle tilt angle of 75° and 55% of power setting was assumed for takeoff. This short running takeoff model resulted in the lift-off after 240-ft ground run with acceleration to 34-knots lift-off speed. The typical takeoff practice described in Reference lxxxiii shows the lift-off within 300-ft, with 20~30 knots speed. Figure 7-44 shows the altitude and the velocity during takeoff procedure. During the takeoff and the initial climb, flap deployment (assumed as 15% of the inboard wing area) was assumed and vehicle drag has been adjusted to match the parasite drag corresponding to 75° nacelle tilt configuration interpolated from the known flat plate drag areas of 0° and 90° nacelle tilt configurations of LCTR2. The transition to 'airplane mode' are initiated at 1,000-ft altitude and vehicle is accelerated to nominal climb speed of 225-knots maintaining 3°-flight path angle. Entire departure trajectory up to 6,000 ft is shown in Figure 7-45.

After a hold at 6,000 ft, vehicle descends adjusting speed. At 2,000 ft altitude, transition from 'airplane' to 'helicopter mode' is initiated with the approximately 1.3 times of aircraft stall speed. Decelerating transition is executed with 0°-flight path angle. During the final landing approach, 50-knots forward flight speed in 'helicopter mode' has been assumed with 500-fpm descending rate. Figure 7-46 shows the trajectory for approach and landing procedures.

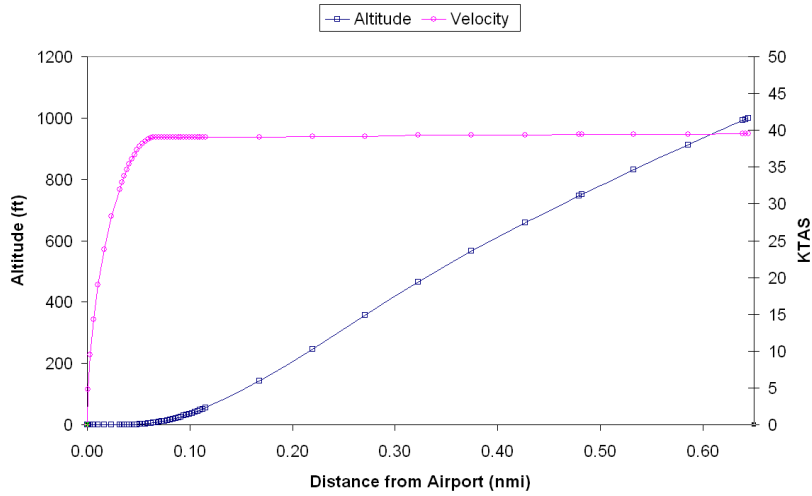


Figure 7-44. Takeoff trajectory.

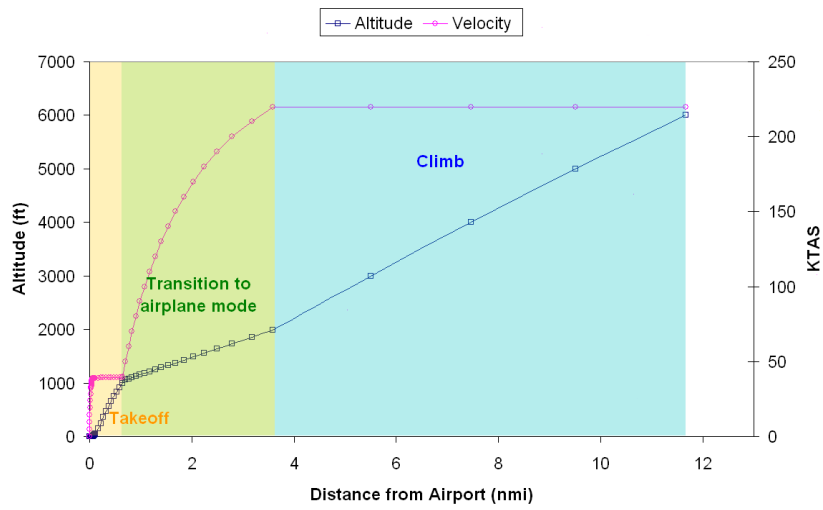


Figure 7-45. Departure trajectory.

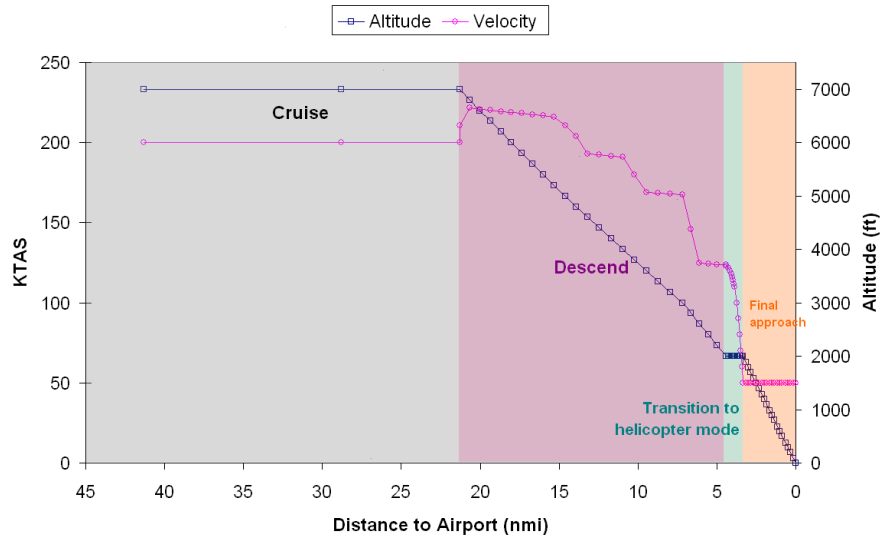


Figure 7-46. Approach and landing trajectory.

AEDT and ACES Connectivity

The VASCOMP model for the large civil tiltrotor aircraft has been constructed using and validated for NASA LCTR2 vehicle and has been extended for the notional operation procedures. This model should also be translated to facilitate the ACES and AEDT system wide analysis. This translation is more straightforward in cases of conventional fixed wing aircraft than the case of tiltrotor aircraft which requires unique interpretations of elementary physical components such as lift and thrust to fit the airspace modeling equations appropriately. During the current work, considerable effort was invested into this translation and the primary assumptions and their validities are described in detail at this section.

The most elementary building block for the current airspace modeling work is BADA. Basically, BADA characterization consists of physics-based energy method to simulate vehicle behavior in diverse flight phases and conditions. At the heart of this method is:

$$(T - D) \times V_{TAS} = mg \frac{dh}{dt} + mV_{TAS} \frac{dV_{TAS}}{dt}$$

where

- T thrust acting parallel to the aircraft velocity vector
- D aerodynamic drag
- m aircraft mass
- h altitude
- G gravitational acceleration
- VTAS true airspeed

d/dt time derivative

To make this model work properly, the correct component from the total force generated by proprotors has to be used as the thrust. Figure 7-47 depicts the force vectors and thrust components for typical initial climb flight of tiltrotor aircraft characterized by large tilt angle measured from the flight direction. Note that the force vectors are not necessarily in force equilibrium and the aircraft is gaining or losing mechanical energy by the net action of these forces.

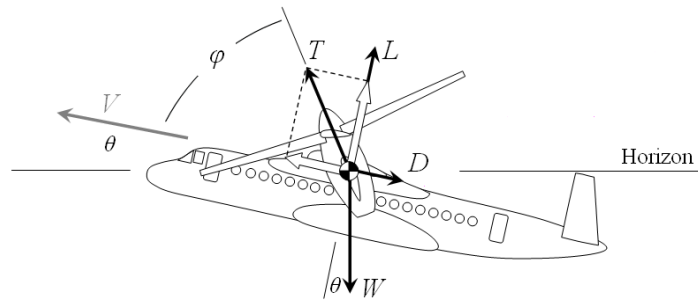


Figure 7-47. Forces on tiltrotor aircraft in initial climb.

The lift of tiltrotor aircraft is generated by two separated sources; lifting surfaces and proprotors. During the ‘helicopter mode’ flight phase and the transition phase, considerable portion of total lift is produced by the proprotors and the proprotors are also the main thruster during the entire flight regime. This division into the lift and the thrust components from the total force generated by proprotors is governed by the nacelle tilt angle (φ in Figure 7-47). Therefore, both the lift and the thrust of tiltrotor aircraft are the functions of nacelle tilt angle, which is, in general, incompatible with the modeling convention assuming only small constant thrust angle or neglecting it. Because BADA modeling parameter set doesn’t include the thrust angle explicitly, the ‘thrust’ had to be defined as the component of total thrust aligned to flight velocity vector and required coefficients for thrust model were obtained for this forward thrust component based on predetermined nacelle tilting schedule, given as:

$$T_{Forward} = T_{Total} \times \cos \varphi$$

But, independent of this redefinition of thrust as the forward component of total thrust, the fuel consumption still depends on the absolute total thrust. BADA equations model the fuel consumptions differently for all flight phases. Idling (or minimum) fuel consumption is directly fit by the fuel consumption amount independent of thrust but the fuel consumptions for climb and cruise involve thrust values via TSFC (thrust specific fuel consumption) model. Thus, in the fuel consumption equations for climb and cruise, the specific fuel consumption has to be based on the forward component of total thrust, instead of the total thrust, to provide legitimate fuel consumptions. For the turboprop aircraft category, the TSFC and the fuel flow equations for climb phase are given as:

$$\eta = C_{f1} \times \left(1 - \frac{V_{TAS}}{C_{f2}} \right) \times \frac{V_{TAS}}{1000} \quad \text{and} \quad f_{nom} = \eta \times T$$

Because modified thrust model provides the forward thrust only, the TSFC has to be the fuel flow per forward component of total thrust, such that

$$\eta' = \eta \times \frac{T_{Total}}{T_{Forward}} = \frac{fuel\ flow}{T_{Forward}} \quad \text{and} \quad f_{nom} = \eta' \times T_{Forward}$$

The aerodynamic drag of the vehicle is modeled by following equations in BADA. The lift coefficient is determined assuming that the flight path angle is zero and a correction for a bank angle is made. Based on this lift coefficient, C_{D0} and C_{D2} for each flight phase are used to calculate corresponding drag coefficient.

$$C_D = C_{D0,TO/IC/CR/AP/LD} + C_{D2,TO/IC/CR/AP/LD} \times (C_L)^2 \quad \text{where} \quad C_L = \frac{2m \cdot g}{\rho \cdot V_{TAS}^2 \cdot S \cdot \cos \phi}$$

This formulation is based on the quadratic dependency of drag coefficient to the lift coefficient which is suitable only for cruise (CR) and approach (AP) configurations of tiltrotor aircraft when it is in the ‘airplane mode’ with small tilt angle. When tiltrotor aircraft operates in ‘helicopter mode’ with large tilt angle, the significant portion of lift force is generated by the thrust of proprotors and this portion of lift force doesn’t directly affect the drag force. Therefore, the values of C_{D2} for takeoff (TO), initial climb (IC) and landing (LD) configurations had to be determined to be very small to ensure this independency of drag coefficient on the lift coefficient. Due to the numerical difficulty occurred in the processing of BADA-related modules,^{lxv} the smallest possible value was found to be 0.0005 and this caused discrepancy between the VASCOMP analysis result and the BADA modeling although the effect of this discrepancy is negligible due to the relatively large magnitude of thrust acting in the same line of action (also due to the small values of dynamic pressure in this low speed flight regime.)

Modeling of landing phase of tiltrotor aircraft required artificial increase in drag coefficient for landing configuration (LD) to prevent the occurrence of the negative thrust which is incompatible with the predetermined range of thrust modeling coefficients. Figure 7-48 shows the drag coefficients calculated from above (based on the notional operational mission described in the previous section compared with the VASCOMP analysis results). Note that this chart includes the taxi segment of the initial 5 minute duration. During the running takeoff and the initial climb, the drag coefficient is varying nonlinearly and is overestimated by BADA equation.

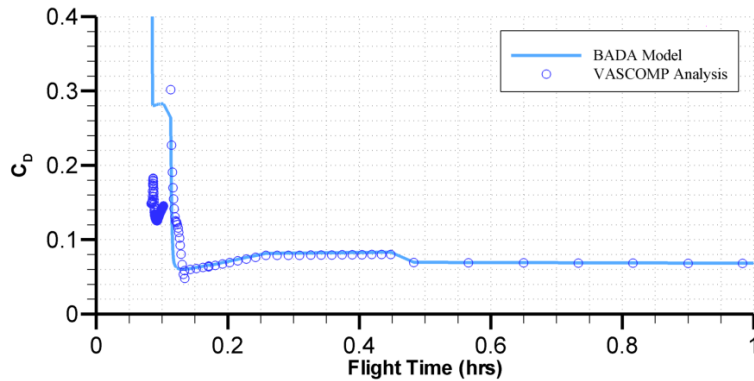


Figure 7-48. Drag models for takeoff (TO), initial climb (IC), and climb (CR) configurations.

During the final approach and landing phase of tiltrotor flight, the vehicle descends with the large tilt angle (near 90°) maintaining relatively low forward speed and moderate rate of sink. The current notional analysis is based on 50-knots forward speed and 500-fpm rate of descent as described in the previous section. This flight behavior of ‘helicopter mode’ is similar to the forward flight of conventional helicopters, which is far from the conventional fixed-wing aircraft’s. Figure 7-49 depicts the forces acting in the landing phase of the tiltrotor aircraft.

The thrust component parallel to the flight direction can be in the same direction of drag force contrast to all the other flight segments but this ‘negative’ thrust is incompatible with the ranges of coefficients for thrust modeling, which assumes only the positive values of thrust for entire flight regimes. The equation below is used to calculate landing thrust in BADA where T_{\max} means the maximum climb thrust for corresponding altitude and speed in landing phase. The multiplying coefficient in this equation is limited as the positive value.

$$T_{des,ld} = C_{T_{des,ld}} \times T_{\max}$$

To guarantee the correct vehicle behavior in landing with large tilt angle within the limit of the range of descending thrust coefficient, a constant amount of drag coefficient was artificially added to the lift-independent drag coefficient for landing configuration, whose increase was matched by the thrust increase changing the magnitude of the thrust to the positive from the negative value. Figure 7-49 also shows the concept of this adjustment. Based on the vertical landing analysis results produced by VASCOMP, approximated landing model for tiltrotor aircraft had been made and used for BADA model generation and comparison because the current VASCOMP program cannot perform analysis for non-vertical landing. Assuming the vertical thrust component of proprotors is same as the vertical landing, the forward thrust was modeled from the drag force corresponding to the given forward speed and the flat plate drag area of the ‘helicopter mode’ vehicle (140.99 ft^2) and the required energy loss corresponding to the given rate of sink. The drag coefficient includes the artificial increment by 1.5 due to the reason which has been previously described. This adjustment results in the positive forward thrust maintaining the correct forward flight speed and descending rate.

Figure 7-50 shows the modeled drag coefficient with the VASCOMP analysis results and the approximating model for landing segment. The cluster of symbols appearing ahead of landing segment corresponds to the conversion segment which could not be fully captured by the BADA drag model.

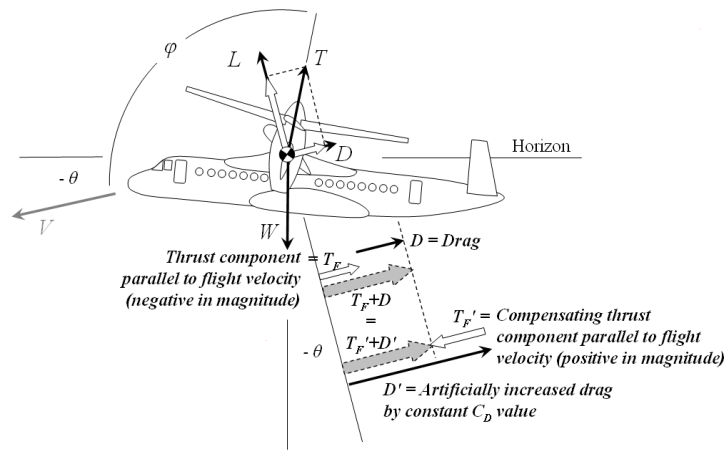


Figure 7-49. Forces on tiltrotor aircraft in landing.

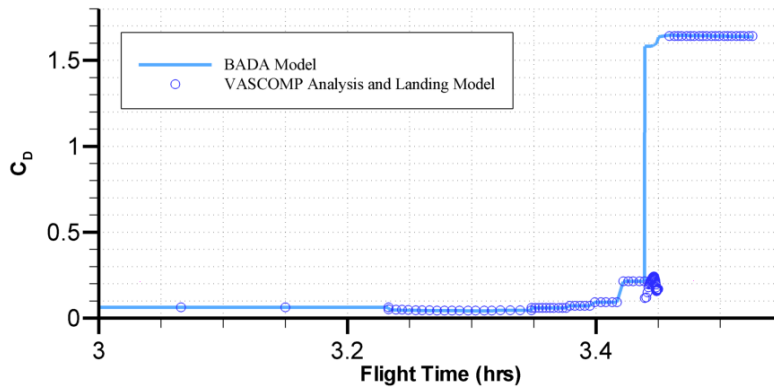


Figure 7-50. Drag models for cruise (CR), approach (AP), and landing (LD).

The thrust component which is parallel to the flight velocity has been used to calculate the thrust coefficients for BADA model. For the turboprop category aircraft, the maximum climb and takeoff thrust is defined by:

$$(T_{\max})_{ISA} = C_{Te1} \times \left(1 - \frac{h}{C_{Te2}} \right) / V_{TAS} + C_{Te3}$$

which is the function of flight altitude and velocity. The actual variation of thrust during the takeoff and climb shows significant nonlinearity due to the variation of the fuselage angle during the takeoff and initial climb-out and the variation of the nacelle tilt angle during the conversion phase to ‘airplane mode,’ which make the general thrust variation hard to be fitted to the functional form above. The best fit obtained for takeoff and climb thrust has been compared with VASCOMP data in Figure 7-51. For the visual clearness, the abscissa has been log scaled. The suitability of this thrust model has to be analyzed in

terms of power determining vehicle acceleration in conjunction with the drag model, which is discussed later in this section.

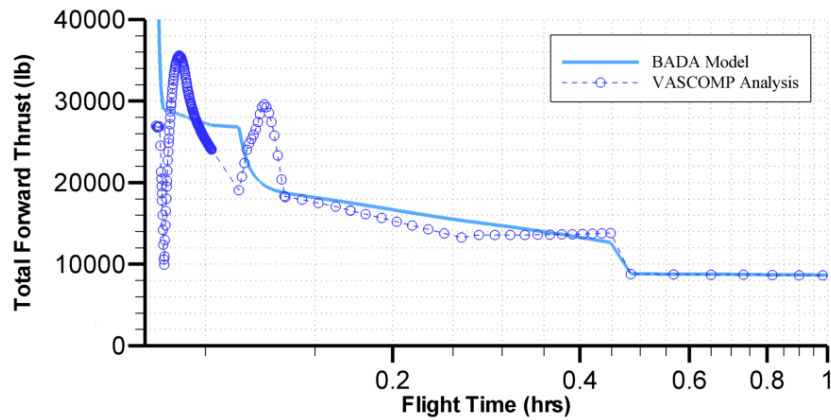


Figure 7-51. Thrust models for takeoff, climb, and cruise.

Cruise thrust is equated to drag as long as the thrust is below the maximum climb thrust and the descending thrusts are calculated using multiplying coefficients for corresponding descent phases which are defined by predetermined altitudes and minimum speeds. Therefore, the descending thrusts are constrained by the variation of climb thrust for the corresponding altitude. Figure 7-52 shows the modeled descending thrust compared with the VASCOMP analysis data which contains large nonlinear variation for the decelerating conversion segment. Overall model fits to the VASCOMP data except conversion behavior. The landing segment contains the positive thrust as a result of the additional drag described in the previous section, which should be negative value extended from the thrust value at the end of conversion segment in case of no adjustment.

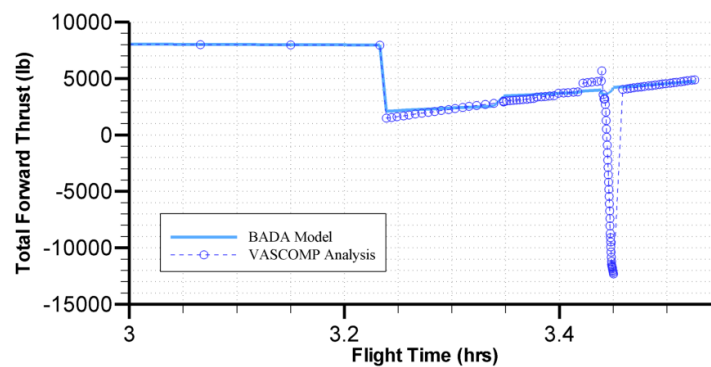


Figure 7-52. Thrust models for cruise, descent, approach, and landing.

The thrust and drag models described so far are combined with the flight trajectory to determine the vehicle acceleration. The effect of over- and under-estimation should be bound to follow general trend of this term. Figure 7-53 and Figure 7-54 show the comparison of VASCOMP data, which confirms that the general trend is in reasonable agreement except the conversion segments. The large difference between VASCOMP and BADA models in the final conversion (to ‘helicopter mode’) originates from the combination of the artificial drag increase and ‘flattened out’ thrust (shown in Figure 7-52) for that

segment. Considering the limited flexibility of the thrust and drag models, the detailed matching for conversion behaviors was not possible.

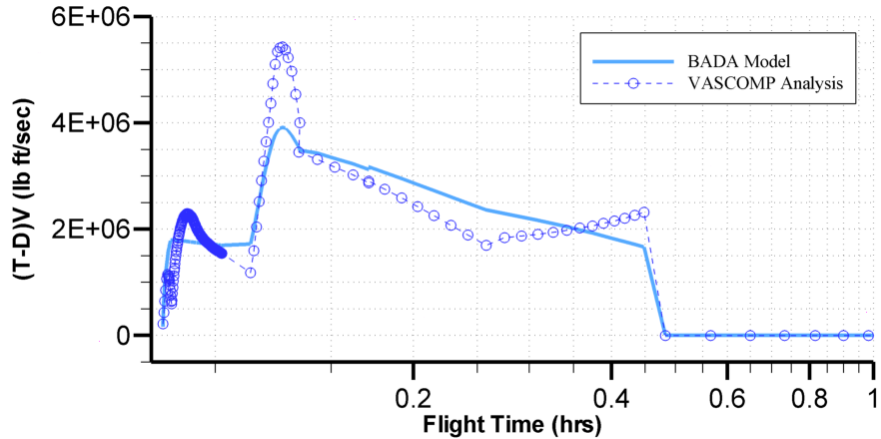


Figure 7-53. Comparison of takeoff, climb, and cruise.

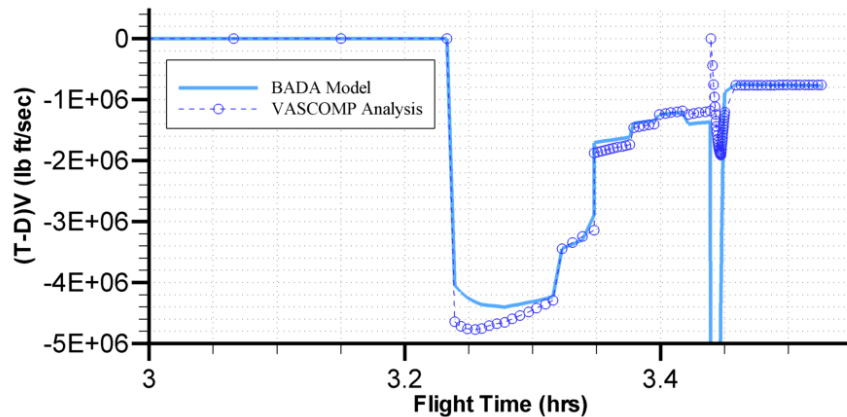


Figure 7-54. Comparison of cruise, descent, approach, and landing.

As described previously, the fuel flow for climb segment is modeled as the function of flight velocity only and the fuel flow is calculated as zero in case of zero velocity. The fuel flow data from VASCOMP shows that it is hard to be correlated to flight velocity only and the significant amount of fuel is consumed when the flight velocity is near zero. Additional to this dissimilarity of the actual fuel consumption and the functional form of the model, there were two challenges to fit the fuel flow model to the VASCOMP analysis result. The first was the narrow range of coefficients allowable in and the other was the fact that the fuel flow model for the cruise segment is also dependent on the climb fuel flow via η term:

$$f_{cr} = \eta \times T \times C_{f_{cr}}$$

In other words, the closer fit in climb fuel flow resulted in violation of the range of C_{fl} (<10.0) and/or negative value of C_{fer} (>0.0) as defined in Reference lxxxvii. The best fit under these limitations are provided in Figure 7-55 for the climb segment. The minimum fuel flow is the function on altitude only, which has been comprised using the over- and under-estimations for descent and landing segments, respectively, and also shown in Figure 7-55. Inevitably, there exists possibility of over-estimation of fuel flow during the climb of arbitrary flight mission due to the limitation of the functional form and the coefficients' range of the current fuel flow equations adopted in BADA but the selections of coefficients have been made to preserve the accuracy of the cruise fuel flow amount.

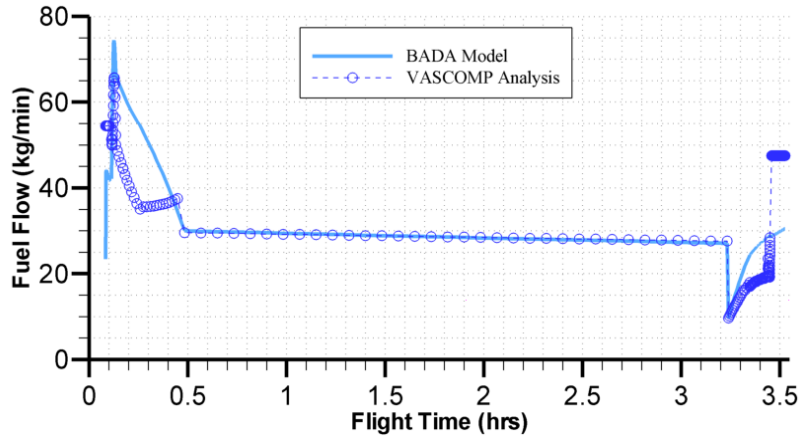


Figure 7-55. Fuel flow model (comparison with VASCOMP analysis results).

BADA model development described in detail in this section was based on the data requirements for ACES. The performance of this combined model has been checked using test module developed in ASDL to simulate the actual AEDT output data. The flight trajectory up to cruise segment has been compared for multiple arbitrary missions and is shown in Figure 7-56. Acceleration profile and the resultant velocity trajectories show a reasonable agreement with the notional mission profile obtained as the VASCOMP analysis result. The fuel burn amounts from the diverse flight scenarios have also been compared with the two VASCOMP analysis results for the 1,000-nm notional operational mission and for the 1,200-nm design mission, which shows the matching trend for different flight distances.

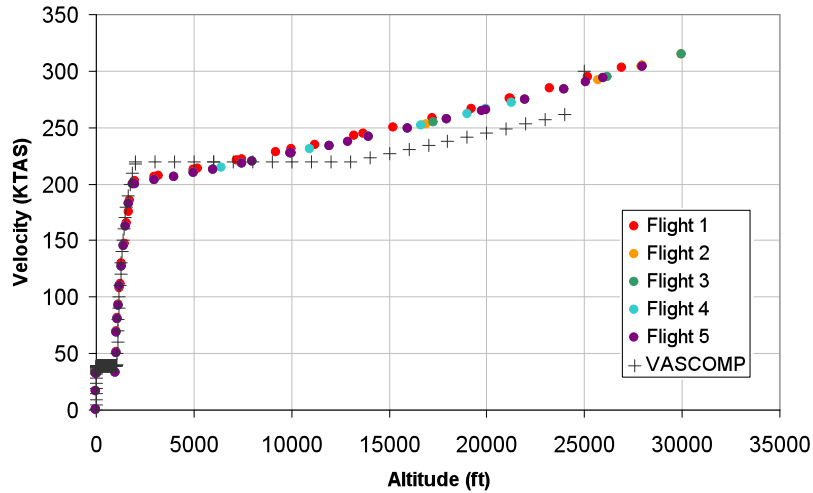


Figure 7-56. Flight trajectory comparison.

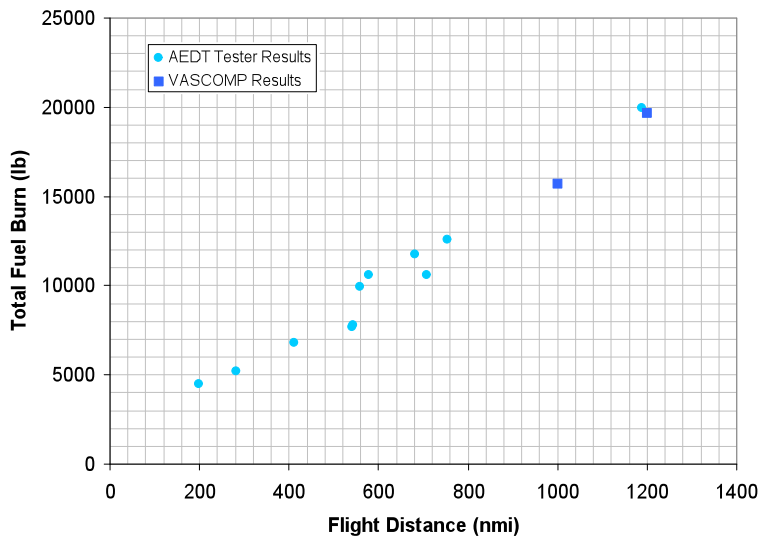


Figure 7-57. Total fuel burn comparison.

In order to accurately generate noise and emission characteristics of future tiltrotor aircraft, experimental data or physics-based tools for each characteristic is definitely required to generate NPD curves and raw emission indices. It is hard to obtain experimental data of noise and emission characteristics especially for future tiltrotor aircraft of this size. Thus, proper physics-based analysis tools would be good candidates to obtain accurate noise and emission characteristics. However, generating the noise and emission characteristics by physics-based tools was beyond the scope of the current study. Rather, first-order methods for generating required noise and emission data would suffice in light of current project purpose and scope, the key issue of which is not the new vehicles themselves, but the new

operations. More accurate data generation for noise and emission characteristics for the future tiltrotor aircraft should be an issue for further research. The strategy of modeling noise and emission characteristics for the LCTR was to use existing characteristics data of similar vehicles or engines and modify them based on appropriate physical theories and reasonable assumptions.

First step for modeling noise characteristics was to choose similar vehicles of which the noise characteristics are available in the database. The LCTR can be thought of having two flight modes such as helicopter mode in the vicinity of the airport, i.e., during terminal operations, and turboprop mode in other flight segments. This leads to select an appropriate vehicle for each mode.

There are not many helicopters in the database which can be comparable with LCTR in size. Fortunately, there is CH-47 in the database. Although CH-47 has half of LCTR in gross weight and one engine power, its vehicle length and rotor radius are very similar to those of LCTR. Furthermore, the effects of differences in gross weight and engine power on noise characteristics can be adjusted using proper physics-based formula which will be explained later.

For the turboprop mode, P-3C is in the database which comparable to LCTR in size. However, P-3C has 4 rotors. Thus, among available turboprop vehicles in the database, Convair CV 580 and DHC-8 have been chosen as similar vehicles to obtain baseline noise characteristics of LCTR for the turboprop mode. Convair CV580 and DHC-8 have similar geometric dimensions in their sizes and propeller characteristics as well as power plant characteristics. Although their gross weight and engine power are also half of LCTR and their propeller radiuses are much smaller, their effects on noise characteristics can be adjusted in the same manner as would be done for CH-47. Table 7-14 shows comparisons of LCTR and chosen baseline vehicles for general dimensions, weights, powerplants, and rotor or propeller characteristics.

Table 7-14. Comparison of LCTR and chosen vehicles for baseline noise characteristics.

Vehicle	Dimensions				Weights (lb)	
	Max. Length (ft)	Max. Height (ft)	Wing Span (ft)	Wing Area (ft ²)	Empty Weight	Gross Weight
LCTR	108.9	27.44	107	1001	-	107,500
CH-47	99	18.7	-	-	24,000	50,000
CV 580	81.5	29.16	105.3	920	30,275	58,140
DHC-8	84.25	24.57	90	605	25,743	43,000
Vehicle	Powerplant			Rotor or Propeller Characteristics		
	Class	No. Engines	One Engine Power (hp)	No. Rotors or Props.	Radius (ft)	No. Blades
LCTR	turboshaft	4	7500	2	32.5	2*4
CH-47	turboshaft	2	3750	2	30	2*3
CV 580	turboprop	2	3750	2	6.75	2*4
DHC-8	turboprop	2	2413	2	6.5	2*4

The baseline noise characteristics from chosen similar vehicles must be adjusted to obtain reasonable noise characteristics estimation for LCTR. Before doing this, it is worthwhile to investigate what noise source components contribute the overall tiltrotor aircraft noise, which include.

Rotor noise = vortex noise + rotational noise

Primary jet noise

Core & turbine noise

Compressor (inlet) noise

From the fact that the noise source components of helicopter and turboprop aircraft are the same as those of tiltrotor aircraft, the noise characteristics of chosen similar vehicles can be taken and adjusted for each mode of LCTR. Since the major noise source component of helicopter and turboprop aircraft is rotor or propeller noise, thus, primary jet, core and turbine, and compressor noise differences are assumed to be neglected. It was further assumed that rotor and propeller noises have the same noise characteristics, i.e., the sum of vortex noise and rotational noise. The physical difference between rotor and propeller noises comes from rotational noise. As seen in Table 7-14, since the number of engines is different between LCTR and chosen vehicles, the noise correction for multiple engines must be also included. Following a similar approach proposed by Dunn,^{lxxxviii} the overall sound pressure level for the vortex noise has the relationship as

$$L_0 \propto 20 \log_{10}(V_{tip} \times T)$$

where L_0 is the overall sound pressure level, V_{tip} is the rotor or propeller tip speed, and T is the thrust. This relationship assumes that other parameters are the same such as total blade area on one side of rotor or propeller and related angles.

The overall sound pressure level for rotational noise has the relationship as

$$L_0 \propto 10 \log_{10}(SHP^{1.55} \times D^{-2.265}) - 2.2N_B$$

where SHP is the shaft power, D is the rotor or propeller diameter, and N_B is the number of blades and assumes that other parameters are the same such as angle between flight path and sound propagation path, Doppler Effect correction, and directivity correction.

The noise correction for multiple engines can be obtained as

$$\Delta dB \propto (10 - 20/N) \log_{10}(N)$$

where ΔdB is the noise level difference in dB unit and N is the number of engines.

Total noise correction for baseline noise characteristics from chosen vehicles can be done by calculating ratios for each required noise correction parameters. Then the resultant total noise correction formula in dB unit is given as follows.

$$\Delta dB_{tot} = 20 \log_{10}(V_{tip_R} \times T_R) + 10 \log_{10}(SHP_R^{1.55} \times D_R^{-2.265}) - 2.2N_{B_R} + (10 - 20/N_R) \log_{10}(N_R)$$

where the subscript R means the ratio of parameter between LCTR and chosen vehicle.

The noise table formats for helicopter and turboprop required for AEDT are slightly different.^{lxxxvii} The noise type, operational mode and concerned sound level locations are the same. While the helicopter noise table in AEDT requires side type which is classified as 4 different types such as Left (L), Center (C), Right (R), and Static (S). Here, Static means the static operations such as idling and hovering. Basically, 3 different NPD curve (L/C/R) must be provided for the helicopter noise characteristics to account for the asymmetrical directivity. For the turboprop aircraft, the thrust setting field takes the place of side type in helicopter noise table. Thus, different NPD curves should be provided for different thrust settings, which can be set in percentage thrust. Due to the terminal area procedure assumptions described previously, the LCTR behaves as a conventional aircraft, not the helicopter, during terminal area procedures and thus, noise table format of the turboprop aircraft was used for NPD development.

The raw baseline noise characteristic tables from CH-47, CV 580 and DHC-8 were modified to set up the baseline noise characteristics for the LCTR. The operational modes of hovering in ground effect, hovering out of ground effect, departure, and arrival are extracted from the noise characteristics of CH-47. All noise characteristics are assumed to be those at 100% thrust setting. For departure and arrival operations, the noise characteristics of all side types are averaged to give one NPD curve at 100% thrust setting. The resultant noise table becomes the baseline noise characteristic table for the helicopter mode of LCTR. For the turboprop mode, the raw noise characteristic tables from CV 580 and DHC-8 were averaged at the same thrust settings or just added in the table for the different thrust settings, which results in the baseline noise characteristic table for the turboprop mode of LCTR.

The next step is to adjust the baseline noise characteristic tables as described previously. To use the correction formula, the values of required ratios should be calculated. Those ratios and the amounts of resultant sound level corrections in dB are listed in Table 7-15. The noise level for the helicopter mode of LCTR was increased by 11.46 dB from CH-47 noise level and decreased by 6.82dB from the average noise level of CV 580 and DHC-8. Each amount of adjustments was applied to all the noise levels in the baseline noise tables, which results in the adjusted noise characteristics. The adjustments for helicopter mode were based on 100% thrust setting; the NPD curves at other thrust settings for the helicopter mode are required. This can be done by considering the LCTR mission profile. Since the transition from the helicopter mode to the turboprop mode and reverse are done by tiltrotor conversion process, the thrust variation from takeoff at helicopter mode to climb with turboprop mode is known. The mode during conversion process is assumed to be the helicopter mode. The conversion process is divided into 4 intervals for departure and approach operations. For the departure operation, the rotor angle is varied from 70° to 0°. For the approach operation, it is varied from 0° to 90°. The thrust variations for departure and approach are listed in Table 7-16 and Table 7-17, respectively.

The thrust settings in Table 7-16 and Table 7-17 are used for final noise characteristic table of LCTR based on its actual thrust whatever its direction is. Based on the thrust setting schedule, the adjusted noise characteristic tables can be used to generate noise levels for other thrust settings by interpolating on thrust settings. After this step, the complete noise characteristic table for the SEL is obtained. Figure 7-58 shows the adjusted SEL of LCTR based on actual thrust. Although there have been other studies that have considered more detailed assessment of the noise characteristics of this type of vehicle, it was beyond the scope of the current study to go into that level of detail on every vehicle. Thus, simplifications were made for the LCTR2 that could be improved upon in future studies.

Table 7-15. The values of required ratios and resultant dB correction amounts.

Vehicle	LCTR	CH-47	Average of CV 580 & DHC-8	Ratio	
Mode	Tiltrotor	Helicopter	Turboprop	Helicopter	Turboprop
Rotor Tip Speed (knots)	650 at hover 350 at cruise	416.72	416.72	1.56	0.84
Thrust (lb)	107,500 at helicopter mode 17,158.36 at turboprop mode	50,000	8,071.6	2.15	2.13
Engine Power (hp)	7,500	3,750	3081.5	2.00	2.43
Rotor Radius (ft)	32.5	30	6.625	1.08	4.91
Number of Blades	4	3	4	1.33	1.00
Number of Engines	4	2	2	2.00	2.00
Δ B for helicopter mode = + 11.46dB Δ B for turboprop mode = - 6.82dB					

Table 7-16. Thrust variation during departure operation.

Step	Rotor Angle	Mode	Thrust for One Engine	% Thrust
Takeoff		Helicopter	29,132	100.0
Conversion	75 – 60	Helicopter	26,014	89.3
	60 – 45	Helicopter	20,033	68.8
	45 – 20	Helicopter	14,051	48.2
	20 – 0	Helicopter	8,070	27.7
Climb		Turboprop	2,100	7.2

Table 7-17. Thrust variation during approach operation.

Step	Thrust or Rotor Angle	Mode	Thrust for One Engine	% Thrust
Descend	1200 – 2600 lb	Turboprop	475	1.6
	2600 – 3300 lb	Turboprop	738	2.5
Conversion	0 – 20	Helicopter	4,206	14.4
	20 – 45	Helicopter	9,990	34.3
	45 – 60	Helicopter	15,774	54.1
	60 – 90	Helicopter	21,558	74.0
Final Approach		Helicopter	24,450	83.9

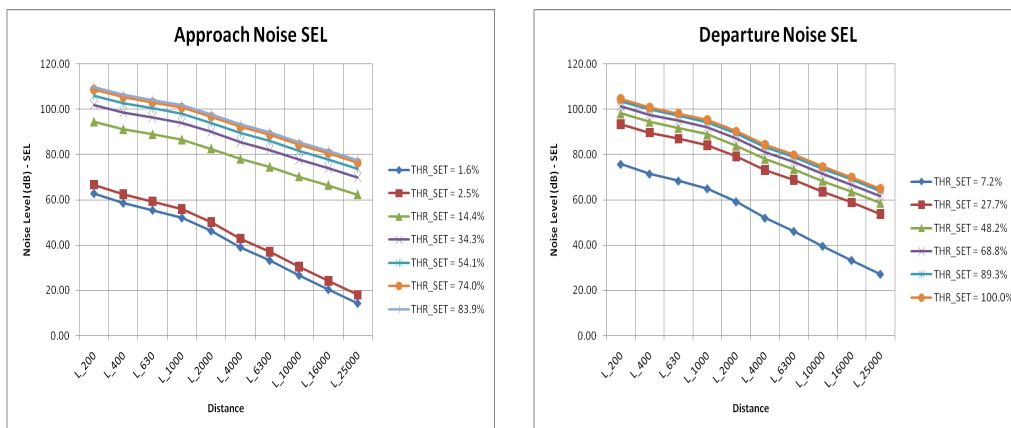


Figure 7-58. A-weighted sound exposure level (SEL) for LCTR.

At this step, all the required noise characteristics for LCTR have been obtained within the accuracy of assumptions made. However, these noise characteristics are those obtained based on actual thrust of LCTR. Because AEDT cannot simulate vertical thrust of the helicopter mode, the LCTR is modeled as a conventional turboprop aircraft. If the actual thrust of the helicopter mode were to be used in AEDT, it would treat it as the forward thrust aligned with vehicle x axis. This will cause significant errors and the flight simulation results of LCTR in AEDT will indicate a quite different vehicle. Thus, as seen in the previous section, the thrust related tables are made based only on the forward thrust which is extracted from the actual thrust. For this purpose, comparisons between actual thrust and modeled forward thrust was conducted and shown in Figure 7-59. As a result, thrust schedules for the modeled forward thrust for departure and approach were established and are listed in Table 7-18 and Table 7-19. Finally, the adjustments for the noise characteristics of LCTR were made based on actual thrust values listed in Table 7-18 and Table 7-19 using the same method as in previous thrust correction method. The resultant noise

contours of SEL for departure and approach operations are shown in Figure 7-60 and Figure 7-61, respectively.

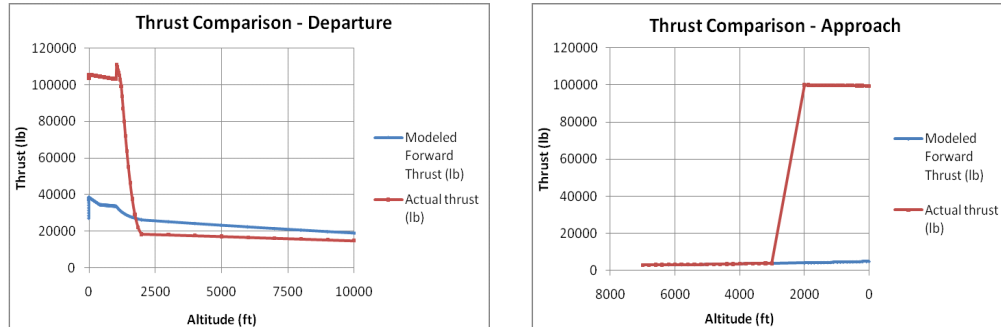


Figure 7-59. Thrust comparisons between actual thrust and modeled forward thrust.

Table 7-18. Thrust scheduling for departure operation.

Mode	Forward Thrust for One Engine	% Thrust	Actual Thrust for One Engine	% Thrust
Helicopter	9,639	100.0	26,377	95.1
Helicopter	8,750	90.8	26,092	94.1
Helicopter	7,500	77.8	24,270	87.6
Helicopter	6,250	64.8	4,477	16.1
Turboprop	3,750	38.9	3,415	12.3
Turboprop	2,500	25.9	3,458	12.5

Table 7-19. Thrust scheduling for approach operation.

Mode	Forward Thrust for One Engine	% Thrust	Actual Thrust for One Engine	% Thrust
Turboprop	726	7.5	726	2.6
Turboprop	955	9.9	955	3.4
Helicopter	1,009	10.5	24,985	90.1
Helicopter	1,072	11.1	24,949	90.0
Helicopter	1,157	12.0	24,902	89.8
Helicopter	1,219	12.6	24,866	89.7

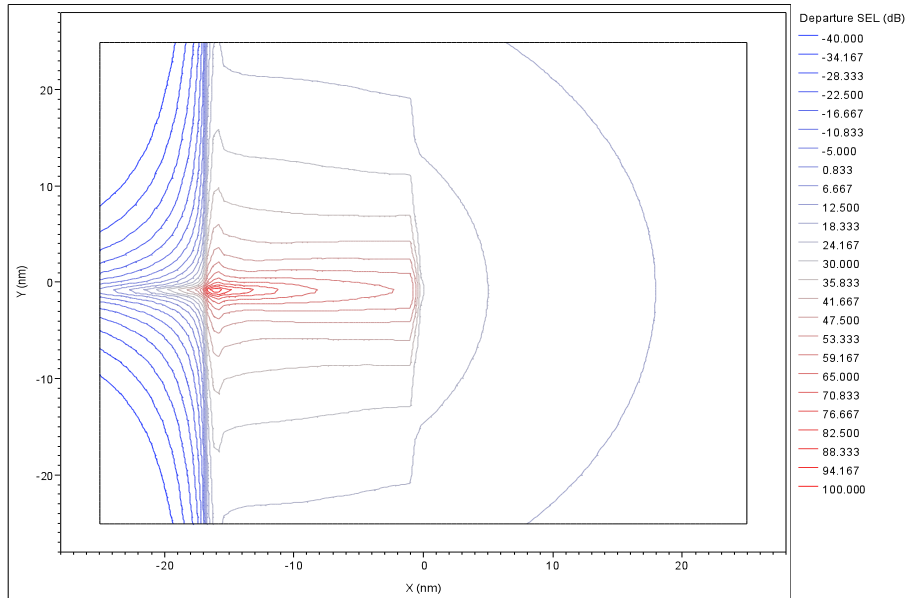


Figure 7-60. SEL contour for departure.

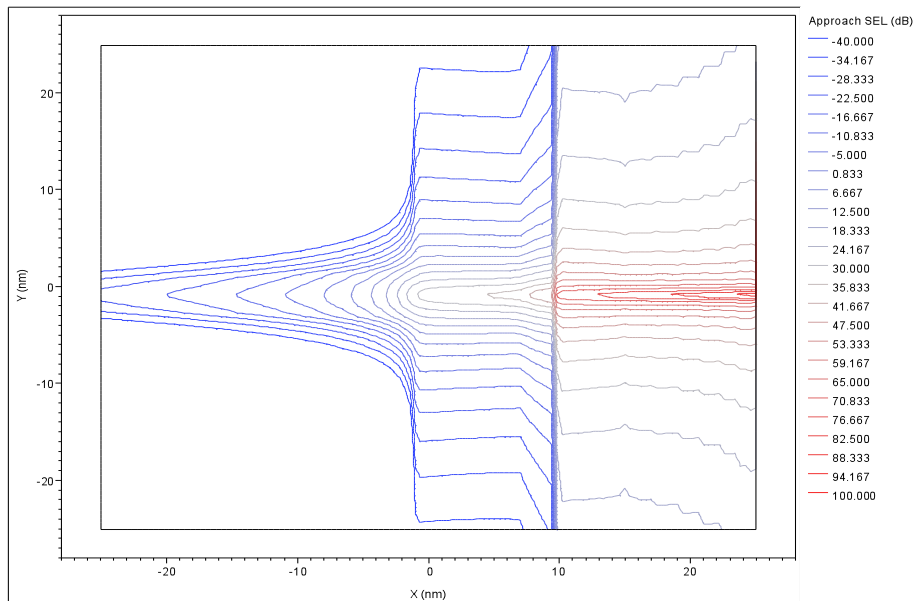


Figure 7-61. SEL contour for approach.

LCTR is expected to use the advanced version of AE1107C Liberty engine. AE1107C Liberty engine has been used for V-22 Osprey tiltrotor aircraft. From the fact that AE 1107C turboshaft engine and AE3007 turbofan engine share a common core, the combustion characteristics are expected to be similar. Furthermore, since the emission characteristics are determined mainly by the combustion process itself, the emission characteristics of AE 1107C are also expected to be similar to those of AE3007. Table 7-20 lists the specification of two engines and Figure 7-62 shows their pictures.

The overall pressure ratio of AE3007 is slightly higher than AE1107C, although they share the common core. From the basic combustion theory, the higher pressure-ratio tends to result in higher combustion temperature. Since combustion temperature is a main factor of generating emissions, the higher combustion temperature it produces, the higher emissions result. However, because higher pressure also prevents dissociations, fewer radicals, which are the sources of emissions, are generated. As a result, the effects of higher pressure-ratio of AE3007 than AE1107C seem to be cancelled. From this discussion, if the same oxidizer to fuel ratio is assumed to be used, the differences in emission characteristics between AE3007 and AE1107C engines might be small. Thus, the emission data of AE3007 was used for that of LCTR without modification. Although the effect of technology development can be included here with proper assumption, it is moved to further research issue for now.

Table 7-20. Specifications of AE3007 turboprop engine and AE1107C turboshaft engine.

Engine	Power (shp)	Thrust (kN)	Pressure Ratio	Length (in)	Diameter (in)	Weight (lbf)	Bypass Ratio
AE3007	-	33.54	17.45	106.5	38.5	1650	4.86
AE1107C	6150	38.16	16.7	78.1	34.2	971	-

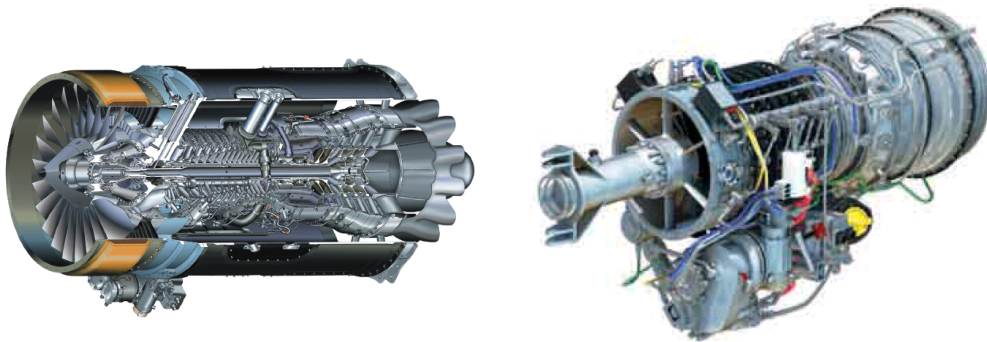


Figure 7-62. Left – AE3007 turboprop engine^{lxxxix}. Right – AE1107C turboshaft engine^{xc}.

LCTR Summary, Lessons Learned, and Potential Further Research

Although the baseline LCTR was successfully modeled for BADA and AEDT using the various assumptions and adjustments as described previously, considerable research is still needed to more accurately represent this configuration within the other tools (ACES and AEDT). For example:

Explicit inclusion of tilt angle (thrust angle, in general) as the flight description parameter

Refinement in drag formulation allowing independency of lift for large tilt angles and/or permission of zero value for CD2 coefficient

Refinement of the current fuel flow equation for turboprop aircraft and/or insertion of new fuel flow equation for tiltrotor aircraft

Adjustment of allowable ranges for relevant modeling coefficients mentioned in this report

The noise and emissions are and will surely be hot topics for future aircraft operations in NextGen for this type of system. Although the key focus of current research is not the future vehicle itself, but the new operation, higher fidelity tools based on physics-based means should be incorporated to generate required noise and emission tables for AEDT. The approaches of generating those described herein should be only reasonable for current purpose. However, it is recommended that these should be done in further research to improve accuracy and reliability of results on new vehicle operations. It is also recommended that the impact of technology development at target time should be also included in further research.

Supersonic Transport (SST)

The environmental impacts of the SST include: sonic boom, high altitude cruise, high fuel consumption per passenger, and high level of noise in arrival/departure areas. Commercial supersonic flights over land are currently prohibited by the Federal Aviation Administration (FAA) because of the sonic boom. This constitutes a major drawback for the SST business case as it drastically limits its operation. It is deemed critical to have the next SST capable of supersonic flight over land in order to be economically viable.^{xcii} High altitude cruise and high fuel consumption imply emissions challenges. For the SST, it is more efficient to cruise at higher altitudes (~50,000 ft) for aerodynamics reasons; however this increases the amount of high altitude emissions, which may cause ozone destruction and consequently affect the global climate.^{xcii} Additionally, the SST has local environmental challenges related to the level of noise in arrival and departure areas. Current commercial transport aircrafts use large bypass ratio engines to reduce the jet velocity in the terminal areas; however the SST mission is not well suited for high-bypass ratio engines because of the heavy aerodynamics penalty during supersonic cruise. Therefore all of these environmental impacts make the design of the SST a great challenge for its inclusion into NextGen, and also a great source of research opportunities.

Based on the 2008 NASA Research Announcement (NRA), there are three phases planned for supersonic research: N+1 (starting in 2015), N+2 (starting in 2020), and N+3 (starting in 2030). For each of these research phases, NASA is targeting different vehicles. Table 7-21 is listing the different types of aircraft with specific characteristics for each of these supersonic programs. Based on the scope of this research and discussions with the systems experts, it was deemed appropriate to aim for a vehicle in the N+2 & N+3 ranges, which is listed in the last column as the GT ASDL suggestion.

Table 7-21. Supersonic system level metrics^{xcii,xciii}

Design Characteristic	N+1 Supersonic Business Class Aircraft	N+2 Small Supersonic Airliner	N+3 Efficient Multi-Mach Aircraft	GT ASDL Suggestion
IOC	2015	2020	Beyond 2030	2021
Cruise Speed (Mach)	1.6-1.8	1.6-1.8	1.3-2.0	1.6
Range (n.mi.)	4000	4000	6000	4000
Payload (pax)	6-20	35-70	100-200	100
Sonic Boom (PLdB)	65-70	65-70	65-70 (low boom)	65-70

			75-80 (unrestricted)	
Airport Noise (Below stage 3 EPNdB)	10	10-20	20-30	10
Cruise Emissions (Cruise NOx g/kg of fuel)	Equivalent to current subsonic aircraft	<10	<5 and particulate and water vapor mitigation	<10
Fuel Efficiency (passenger-mi./lb of fuel)	1.0	3.0	3.5-4.5	1-3

The SST mission profile, illustrated in Figure 7-63 represents a key assumption to the SST design. The process of selecting the SST mission profile involved the participation of governmental and industrial experts in the field. Two founding assumptions were used to create the mission profile: (1) the SST shall behave exactly like any subsonic transport aircraft within the terminal areas, and (2) the SST shall only fly supersonic on trans-oceanic routes and not over land. The first assumption establishes the takeoff, climb, approach, landing and reserves segments of the mission profile. The main consequence of the second assumption is the 200 nm subsonic cruise required for the aircraft to reach the ocean shore before initiating the supersonic cruise-climb. This assumption was also based on a current FAA regulation prohibiting commercial supersonic flight over land. To overcome this limitation the SST will have to greatly reduce its sonic boom signature to demonstrate that supersonic flights over land do not create nuisance for the public or have negative environmental impacts on the Fauna and Flora. For this study, this assumptions was reasonable considering the time required to overcome the technical challenges and the time required to append the regulation; more than likely the overall time needed will exceed the time frame established for this study, hence the assumption. Another bounding assumption of the mission profile is the SST cruise altitude. As discussed earlier, there is a tradeoff between the vehicle performance and the environmental impacts of combustion emissions at high altitudes. Therefore the maximum cruising altitude of the SST was fixed at 53,000 ft.

The final iteration on the requirements also involved the choice of reference vehicle. Three types of reference vehicles were considered: concepts built, concepts discontinued, and design concept in progress. From these three types, eleven reference vehicles were identified and listed, with their respective attributes, in Table 7-22. The final selection of the reference vehicle was based on two criteria: (1) amount of publicly available data, and (2) the how close the vehicle attributes are compared to the N+2 & N+3 requirements.

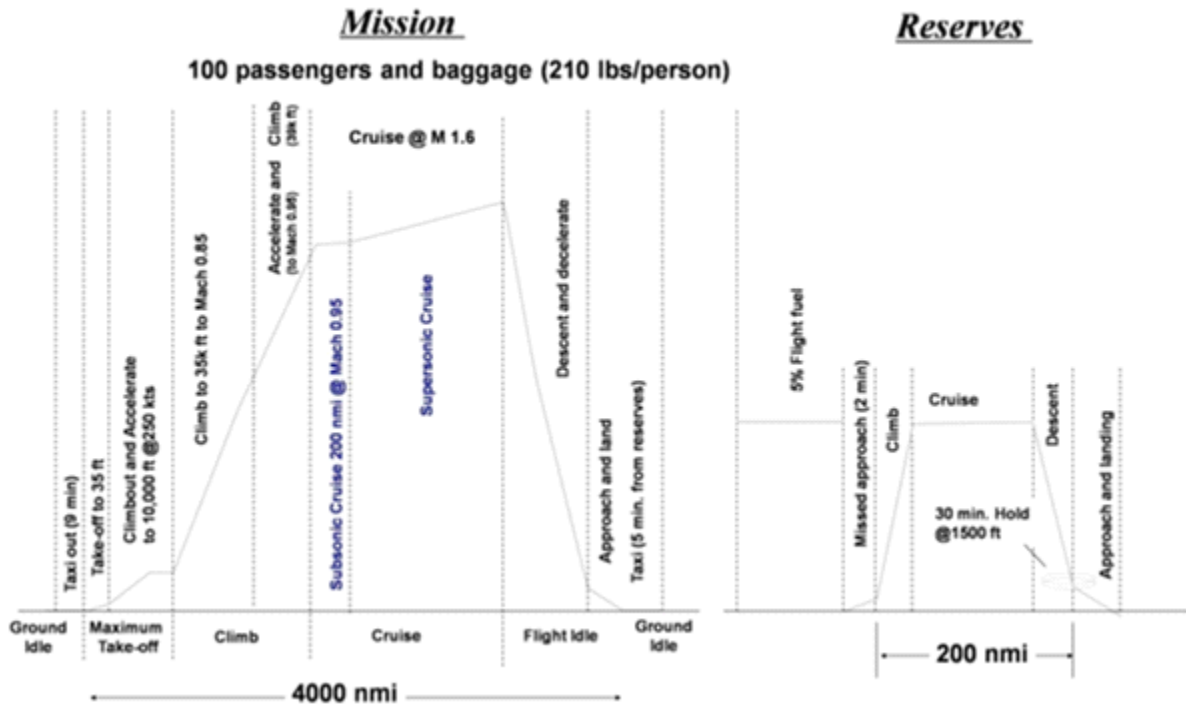


Figure 7-63. SST mission profile.

Table 7-22. SST reference vehicles and attributes.

Year	Vehicle		Mach	TOGW (1000 lbs)	# of Pax	Range (nm)	Noise (psf)
1947	Bell X-1 (Ref.Vehicle)	Built	1	12.2	1		
1968	Tupolev 144	Built	1.84	397	130	3500	2
1969	Boeing 2707	Discontinued	2.7	750	275	4000	2
1969	Concorde	Built	2.04	408	128	3900	1.94
1990	High Speed Civil Transport	Discontinued	2.4	645	250	5000	2.5
1999	Dassault	Discontinued	1.8	86	8	4000	
1999	Sukhoi S-21	In progress	2.3	114	10	4000	
2003	F-5 low	Built	1.4	25	1	760	
2003	Gulfstream SBJ	In progress	1.8	160	8	4000	0.15
2009	Aerion	In progress	1.7	90	12	4200	0.5
2009	SAI QSST	In progress	1.7	153	12	4600	0.3

Based on the team selection criteria, it became evident that the Concorde should be the SST reference vehicle. Although it flies faster than the required Mach number, its range and number of passengers are very similar to the requirements listed in Table 7-21. The relatively high Takeoff Gross Weight (TOGW) and over-pressure are not deemed to be an obstacle considering the year that the Concorde came into service. Furthermore, these attributes are also considered to be great research opportunities for the analysis of technological infusion to the vehicle. In terms of operational mission, the Concorde received its FAA certification January 9, 1979. The aircraft could carry up to 128 passengers over 3,900 nm at a maximum operating cruise speed of Mach 2.04 and maximum operating altitude of 60,000 ft.

During its service life, the major markets for the Concorde were Paris to New York and London to Washington; however, considering the current market growth, the Asian market would probably be one of the most dominant markets for the future SST. It should be noted that the range required to tap into that market is more in the order of the N+3 phase (i.e. ~6000 n.mi.). In terms of dimensions, the Concorde provides a good reference for the fuselage required to carry 100 passengers. The 3 view drawings of the Concorde are illustrated in Figure 7-64.

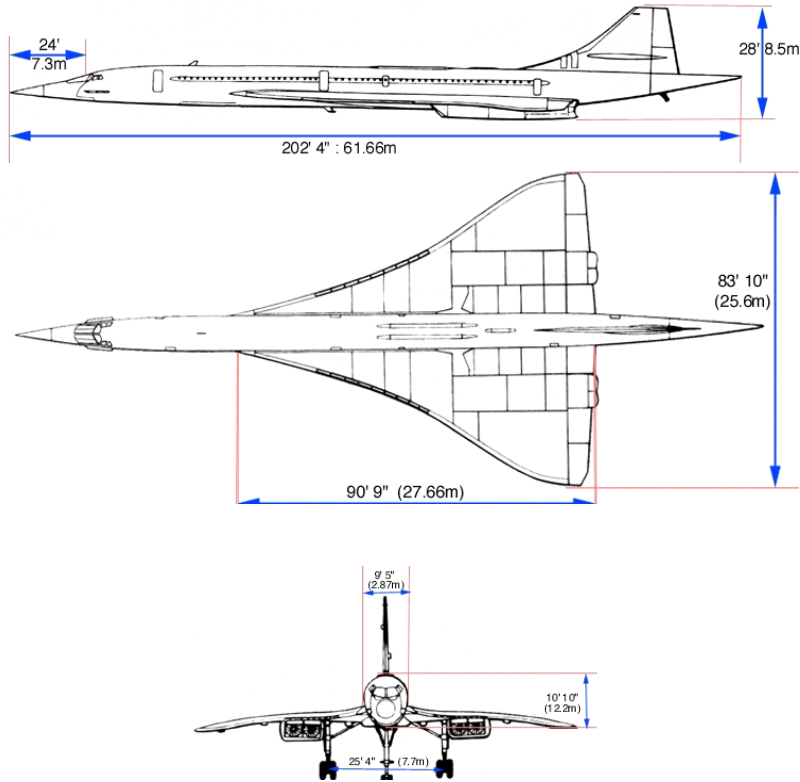


Figure 7-64. Concorde dimensions^{xciv}.

Since the TOGW of the SST will be smaller than the Concorde, due to the new advancement in material and manufacturing technologies, the wing will be smaller; however the other key geometric characteristics of the Concorde can still be used as baseline values for the analysis. In addition, the weight breakdown of the Concorde was used to benchmark the development of the SST. The Concorde weight breakdown is listed in Table 7-23. It can be noticed that the maximum fuel weight is more than half of the maximum TOGW of the aircraft. The Concorde was using four turbojet engines with afterburner to provide more thrust during critical segment of the mission profile. The propulsion characteristics of the Concorde are listed in

Table 7-24. Using the maximum thrust of the engine and the maximum TOGW, that gives a Thrust to Weight ratio (T/W) of approximately 0.37. This value will be useful as a reference for the preliminary sizing of the SST.

Table 7-23. Concorde weights^{xciiv}.

Parameter	Weight (lbs)
Maximum Take Off Weight	413,000
Operating Empty Weight	175,500
Maximum Payload Weight	29,500
Maximum Landing Weight	245,000
Maximum Fuel Weight	210,900

Table 7-24. Concorde propulsion characteristics^{xv}.

Maximum thrust produced at takeoff (per engine)	38,050 lbs (with post-combustion)
Maximum thrust produced during supersonic cruise (per engine)	10,000 lbs
Fuel Consumption (at Idle Power)	302 gallons/hr
Fuel Consumption (at Full Power)	2885 gallons/hr
Fuel Consumption (at Full Re-heated power)	6180 gallons/hr

The Concorde engines were also a major contributor to the airport noise, and more particularly the jet velocity. The Concorde noise values in the terminal area are listed in Table 7-25. The Stage II & III limits are based on the TOGW of the Concorde. With the information provided in Table 7-25, it is evident that the reduction of noise in the terminal areas will be a considerable challenge for the future SST.

Table 7-25. Concorde noise in terminal area^{xv}.

	Noise (EPNdB)	Stage II Limit (EPNdB)	Stage III Limit (EPNdB)
Takeoff	119.5	105.3	101.8
Landing	116.7	106.9	103.6
Sideline	NA	106.9	100.2

In summary, the Concorde will be used as a reference vehicle for the design of the SST. The historical information listed in this section will be used for two main purposes: (1) as baseline values for the sizing of the SST, and (2) to establish the boundaries of the design space by varying the baseline values. The next section describes the modeling and simulation environment used to explore the design space.

Detailed SST design

The modeling and simulation environment is used to explore the technical feasibility of various SST concepts. Consequently, it will be used to reduce the number of potential SST configurations from a large number to a handful of concepts that can be analyzed in more detail. The process starts by creating a geometric representation of the vehicle. The main geometric tradeoff is between the time of creating the model and its fidelity. Since one of the objectives is to have a rapid exploration of the design space, the level of fidelity was traded for a conceptual geometry modeler, the NASA's Vehicle Sketch Pad (VSP). In this case, lower fidelity implies that no internal structural details (e.g. spar, stringers, etc) are taken into account, and that only external geometry is modeled for further analysis. Nevertheless, VSP allows for an extensive parametric representation of the geometry, which offers a graphical user interface that can be automated in batch mode. The user can then input ranges for the parametric variables and multiple SST configurations can be created in a matter of seconds. Figure 7-65 shows a sample of the configurations that can be created with the design environment. As is evident, various discrete settings can be obtained by the modeling environment.

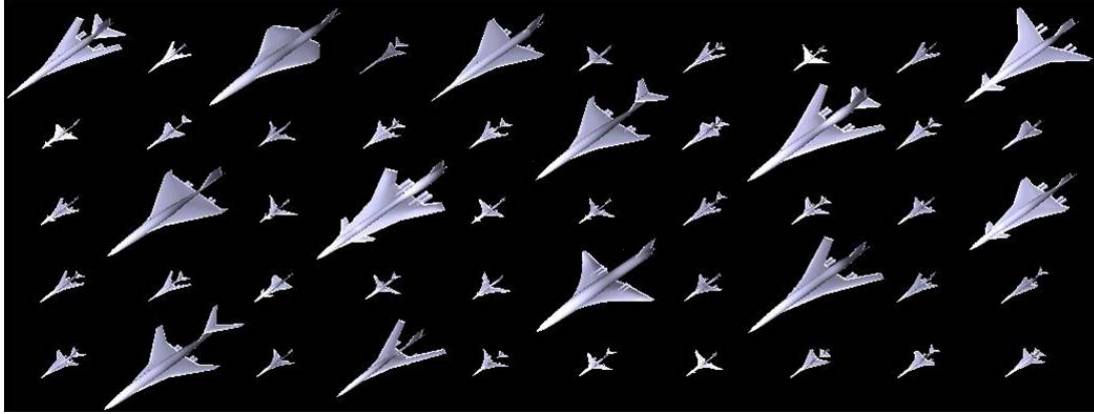


Figure 7-65. Conceptual configuration design space.

Based on the potential geometric differences in configurations, the next step is to analyze the associated aerodynamics. There is an important tradeoff for aerodynamics model between the accuracy of the responses and the time required to obtain the responses. Given the current objectives of the modeling environment, faster linearized approaches were selected over higher fidelity analysis tools. Consequently the aerodynamics characteristics of the potential configurations are calculated using the following programs:

AWAVE for supersonic wave drag^{xli}

WINGDES for induce drag^{xlii}

BDAP for skin friction drag^{xliii}

AERO2S for low speed aerodynamics^{xliv}

WINGDES is also used to calculate the SST lift coefficients. The aerodynamics coefficients are then calculated for multiple flight conditions, which are used by the mission analysis code, FLOPS.

Another objective of the SST modeling environment is to enable the engine-airframe optimization. This implies providing the best engine cycle for a given airframe configuration.^{xcv} This is achieved by optimizing simultaneously the SST geometry and engine cycle variables. The cycle variable ranges are based on the engine type used and a mixed-flow turbofan (MFTF) was used in this study. The MFTF is one of the most common engines for modern military aircraft. Figure 7-66 illustrates the main components of the MFTF: inlet, fan, high-pressure combustor (HPC), burner, bypass, high pressure turbine (HPT), low pressure turbine (LPT), mixer and a variable nozzle. It is important to note that the LPT powers the fan whereas the HPT drives the HPC. The MFTF NPSS model is taking as inputs the engine cycle variables with an estimate of the required sea level thrust, and it optimizes the core of the engine to meet the desired thrust. The main output of the NPSS model is an engine deck that is passed to FLOPS for the mission analysis.

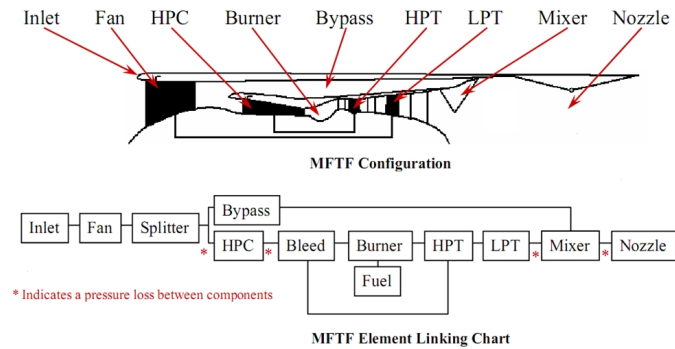


Figure 7-66. Mixed-flow turbofan model.

The drag polars from the aerodynamic module and the engine deck from the propulsion module are then used by FLOPS to calculate the mission performance. For the SST study the FLOPS weights module is used to calculate the empty weight breakdown of the vehicle. On the propulsion side, FLOPS also offers the ability to “scale the engine” if the thrust required is greater than the thrust available defined by the engine deck. The engine weight predictions are based on the WATE.^{xxxvii} This weight module is embedded within NPSS and it is strongly depended on the following four engine cycle parameters: (1) Fan Pressure Ratio (FPR), (2) Overall Pressure Ratio (OPR), (3) Extraction Ratio (ExtR), and (4) Throttle Ratio (ThR). This weight information is then added to the FLOPS input file to complete the operational empty weight of the SST. The results of FLOPS provide extensive mission analysis information that will be used as reference data to create the BADA files.

The modeling of the SST would be incomplete without a sonic boom analysis. For this task, two models are selected in this study: PBOOM^{xliv} and PCBOOM.^{xlvi} In this study, PBOOM was used specifically to optimize the fuselage shape by optimizing the area rule distribution of the vehicle, where PCBOOM was used to calculate the boom loudness. To simulate the atmospheric absorption of the shock, Needleman et al. regressed an empirical model by assuming a rise time of 3 ms for a shock strength magnitude of 1 psf.^{xcvi} This value is assumed in this study for all boom analyses.

Figure 7-67 summarizes the flow of information of the SST integrated modeling environment. Most of the programs are in executable format, and they are linked together with MATLAB scripts that automatically create the input files and parse the output files. This integrated environment allows the design team to rapidly explore the design space by either running some design of experiments on a specific set of variables or by launching a multi-objective genetic algorithm based on the work of Buonanno^{xcvii} and enhanced by Mavris, et.al.^{xcv}

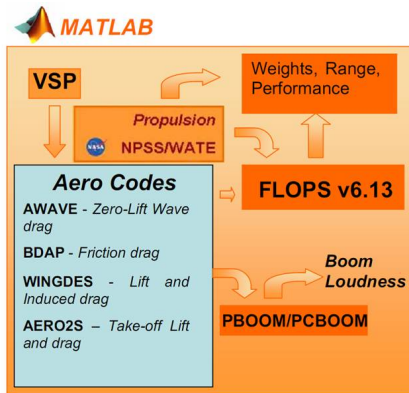


Figure 7-67. Supersonic transport integrated modeling environment.

Table 7-26 summarizes the assumptions made for the modeling environment. Some of these assumptions were made to minimize the computational time needed to converge on a final configuration given the conceptual nature of the study, whereas other assumptions were based on expert advice and current state-of-the-art technologies (e.g. the choice of using the MFTF engine). The design of the propulsion system is extremely important. For this study, the MFTF engines are designed using a unique design point, which corresponds to the pinch point of the mission profile. The pinch point represents the minimum difference between the thrust available and thrust required of the SST. The pinch point can vary depending on the aircraft configuration and desired mission performance; for the SST it can occur during the transonic regime, at the top of climb or as the SST transitions to supersonic cruise. This one point assumption is reasonable for the MFTF because it is based on a fixed cycle. On the other hand, if a variable cycle engine would be considered for a future study, a multi-design point approaches would be preferred to optimize the engine with the aircraft mission.

Table 7-26. Summary of modeling assumptions.

Geometry	Subset of discrete alternative (i.e. V tail was not consider)
	No structural elements included in geometry
	Assume clean external surface (i.e. no antenna)
Aerodynamics	Use linearized models
	Use empirical models for form drag and transonic wave drag
	No Aeroelastic effects have been considered
Propulsion	Assume MFTF as engine type
	Engine is design and scale with 1 design point
Weight	Use empirical model for weight prediction
Boom	Assume 3ms of shock rise time during boom analysis
Stability & Control	Only calculate static stability

The next set of assumptions is to define the ranges of the continuous design variables. These ranges will determine the overall size of the design space. Two approaches are taken to determine the ranges: (1) assume a percentage deviation from the Concorde (i.e. $\pm 20\%$), and (2) perform preliminary analyses using the environment. By setting the ranges of the design variables, the end-users are seeking to capture the variability of the responses; small ranges can result in capturing none or little variability, whereas large ranges can get outside of the model assumptions and result in singularities.

The first set of variables considered is related to the geometry of the vehicle. They include the fuselage, wing and stabilizer variables. From the requirements established in Table 7-26 the fuselage shall carry 100 passengers, which is similar to the Concorde fuselage. Consequently a deviation from the Concorde fuselage is with the length varying between 190 and 200 feet and the diameter between 9 and 12 feet.

For supersonic aircraft, it is desired to have a high fineness ratio, which is the ratio of the body length over its maximum width. On the one hand, high fineness ratio is used to minimize wave drag, which also has an impact on the sonic boom footprint; hence, one of the Gulfstream concepts attaches a boom spike to the nose of the aircraft.^{xcviii} On the other hand, high fineness ratio can also introduce instability problem, which can be solved by stability augmentation systems, which add weight. Regarding fuselage diameter, this variable is linked to the passengers comfort and the ride quality of the SST since larger diameters imply more space for the passengers. The fuselage dimensions are important design characteristics for the SST, as some of the fuel needs to be carried within the fuselage because of the large volume of fuel required and the smaller thickness of the supersonic wing.

The design variables utilized in this study are listed in Table 7-27. The initial definition of the wing variable ranges started with a deviation from the Concorde, but further refinement were performed based on preliminary analyses using the SST environment. All of the wing variables have strong impact on the aerodynamics of the vehicle. The variables are not independent since the wing area is used to calculate both wing loading and aspect ratio. From the lift equation, the wing area has a strong impact on the weight that can be lifted by the vehicle. That creates a starting point for the sizing algorithm. Then, supersonic aircrafts tend to have high wing loading and low aspect ratio in order to minimize the supersonic drag. These variables will then be used to calculate the other wing characteristics like the span and taper ratio. Note that these variables are calculated differently depending on the type of wing platform used. The stabilizer variables are similar to the wing variables but they also include the sweep, thickness to chord ratio, and the horizontal volume coefficient.

As the name suggest, stabilizers are meant to stabilize the aircraft and to provide control for maneuverability and trim. The size of the stabilizers is function of their position on the vehicle and the type of stabilizer. As listed in Table 7-27, four discrete types of stabilizer are used in this study: (1) tailless, (2) horizontal/vertical tail, (3) T tail and (4) canard with a vertical stabilizer. The main trade for stabilizer is between control, additional drag and weight. A larger stabilizer can be associated with more control but also more structural weight and more drag because of the additional weighted area. Consequently for the SST, it is desired to minimize the size of the stabilizer to reduce the structural weight and drag.

The next set of design variables are for the MFTF engine cycle. The ranges for the engine cycle parameters are based on the experience of resident experts on the NPSS model since the model is quite sensitive to large variation.

In the modeling and simulation environment, the algorithm is trying to optimize the engine-airframe configuration. The engine cycle is first picked and then the baseline thrust is scaled depending on the pinch point of the mission. The genetic algorithm then tries many different variations of the design variables in order to find the best engine-airframe configuration. The initial weight estimates are based on the suggestions of subject matter expert and preliminary analysis using the FLOPS empirical weight

models. The starting guess for the takeoff weight was 300,000 lbs with a fixed cargo weight of 15,000 lbs.

Table 7-27. SST design variables.

Design Parameter	Min	Max
Wing Area, (ft ²)	3400	4700
Wing Loading (lb/ft ²)	65	80
Wing Aspect Ratio	2.3	6.2
Stabilizer Aspect Ratio	1.2	4
Stabilizer Taper Ratio	0.1	0.5
Stabilizer Sweep (deg)	45	60
Stabilizer Thickness to Chord Ratio	0.03	0.05
Stabilizer Horizontal Volume Coefficient	0.04	0.35
Fan Pressure Ratio @ SLS	1.8	3.2
Overall Pressure Ratio @ SLS	25	35
Throttle Ratio	1.0	1.1
Extraction Ratio @ SLS	0.95	1.05
T41 Max	3000	3800

The entry date of service of the Concorde was 1976, while the tentative date of entry to service of the SST considered in this study is 2021. In this time, there will be significant technological improvements in every discipline, and one of the most important improvements occurs by the introduction of new material to reduce the overall vehicle weight. As illustrated in Figure 7-68, the percentage of composite component in commercial aircraft has significantly increased during the last few decades.^{xcix} This shift is not only due to the material advancements, but also due to the manufacturing processes which have made the new material more reliable and predictable. A sample set of technologies are listed in Table 7-28 with associated qualitative impacts on the aircraft weight breakdown that we considered for application to the design of the SST herein. Based on the literature surrounding these technologies, more quantitative weight assumptions were made in this study and are listed in Table 7-29. The ranges of the technology impacts were used in the modeling and simulation environment to ensure that the vehicle could close the mission analysis loop and at the same time not overdesign the vehicle assuming the integration of the new technologies.

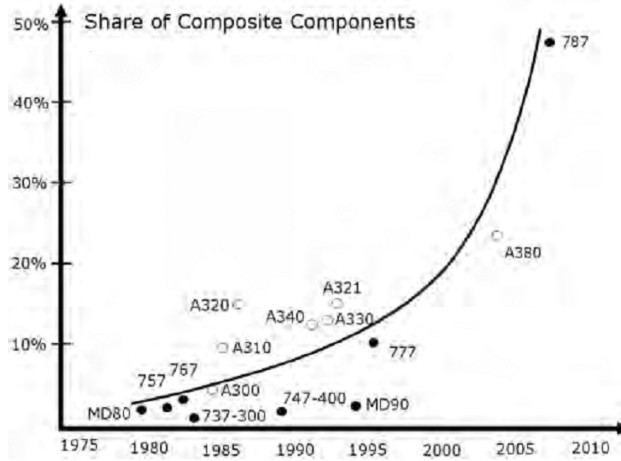


Figure 7-68. Percentage of composite components in commercial aircraft.

Table 7-28. Technologies contributing to weight reduction.

Category	Technology	Wing	Fuselage	Engine	Empty Weight
Material	Advanced Alloys	Medium	Low	Low	Medium
	Advanced Composite	High	High	Low	High
Cabin Interior	Panel - Glass Microsphere				Low
	Lighter seats – plastic fasteners				Low
	Advanced Flight Entertainment				Low
Manufacturing	Friction Stir Welding	Low	Low		Low
Other	Advanced Auxiliary Power Units				Low

Table 7-29. Technology weight assumptions.

Component	Weight Reduction
Wing	10-20%
Fuselage	5-10%
Engine	5-10%
Operating Empty Weight	15-25%

The design space exploration started with the modeling assumptions discussed above and the information gathered by performing off-line preliminary analyses. The design team then launches the genetic algorithm to explore the design space. The convergence criteria of the optimization scheme included the mission range (4,000 nm.), the engine jet velocity (minimize the noise during takeoff) and the boom loudness (minimize). The main challenges encountered during the design space included: (1) the engine-airframe optimization, (2) the minimization of the jet velocity at takeoff, and (3) the boom loudness.

The SST modeling environment provided with a wide range of aircraft configurations, as illustrated in Figure 7-69, however the engine-airframe optimization convergence often required further sub-optimizations. Consequently, from each set of simulation runs the “best” configurations were selected based on the convergence criteria and the geometry was fixed to further optimize the engine cycle parameters. The first step conducted in the refinement of the engine cycle parameter was to determine the relative importance of the cycle parameters on the mission range. It was noticed that the FPR and the OPR had the greatest impact on the variability of meeting the design range. Figure 7-70 presents a graphic illustrating the relationship of the range as a function of the FPR and OPR. Although the relationship is highly non-linear, clear trends can be extracted from the chart. Lower FPR tends to maximize the range; however the trends are not as evident regarding the OPR. The study objective was not necessarily to maximize the range, but to meet the design range specified by the requirements. Consequently, it can be seen that multiple values of the OPR could provide the desired range of 4,000 nm. Since higher OPR implies more compressor stages and therefore more weight, the lower value of the OPR was selected.

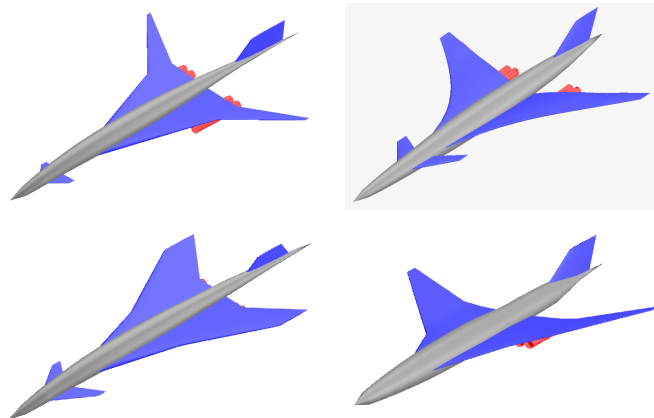


Figure 7-69. Sample of SST configurations.

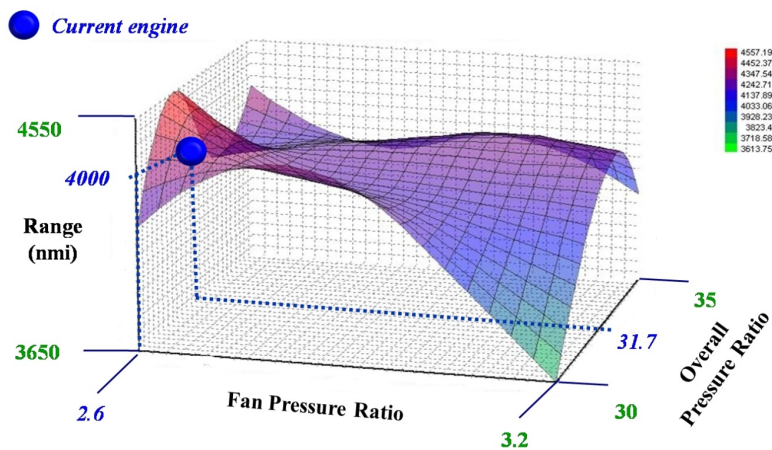


Figure 7-70. Engine trade study.

The second major trade considered in this study also involves the MFTF engines. Assuming more stringent noise regulation in future terminal areas, high jet velocity during takeoff constitutes a major obstacle for the SST integration into the NAS due to community noise implications. There are multiple design and operational alternatives that are considered to deal with this problem. From the design perspective, one can think of adding a noise suppression system, whereas from the operational perspective it is possible to takeoff at lower thrust settings to minimize the jet velocity. Due to the lack of noise suppression systems data for this sized aircraft, the operational perspective was assumed in this study.

From a series of discussions with subject matter experts, two constraints were imposed on the jet velocity analysis. The first constraint was that the engine jet velocity shall be smaller than 1,300 feet per seconds, and the second constraint was that the SST must takeoff within a 10,000-foot runway. Consequently, once the engine was sized for the mission, the jet velocity analysis would start by verifying that the takeoff field length is smaller than 10,000 ft. If it is the case, the engine thrust setting at takeoff would be reduced until the SST would takeoff within the allowable 10,000 ft. This trade can be visualized in Figure 7-71. If the SST jet velocity is still higher than 1300 fps within the 10,000 ft runway, the engine sea level static thrust is increased and the NPSS model calculates a new engine deck. Using this method

the engine is oversized which creates a non-negligible weight penalty to the design. The 10,000 ft constraint is also a limiting factor for the operation of the SST since the aircraft is now limited to airport with relatively long runway.

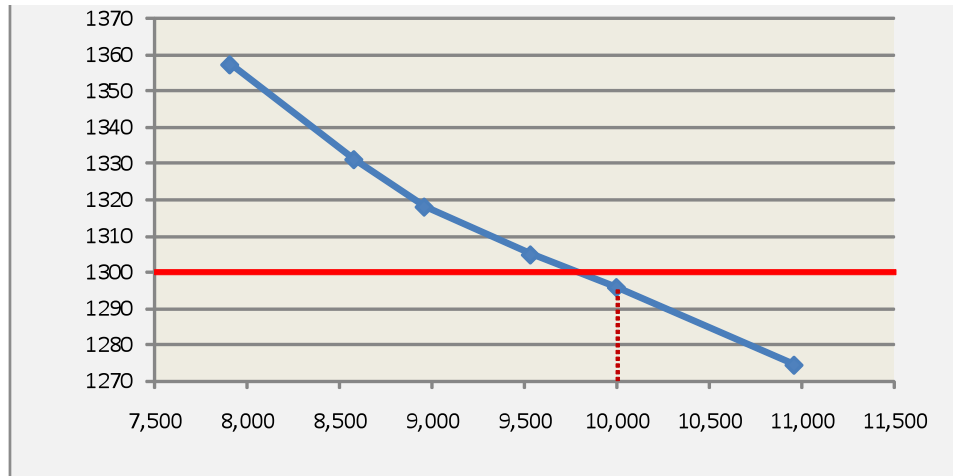


Figure 7-71. Jet velocity trade.

The last analysis to be discussed is the sonic boom analysis. The SST must abide by laws that prohibit supersonic flight over land, so it is essential to conduct a sonic boom analysis to verify overpressure levels by means of a contour plot over the entire trajectory. By using the AEDT executable that generates the mission profile data, the output also contains enough trajectory information to conduct a sonic boom analysis by using PCBoom. PCBoom is a sonic boom propagation tool that is based on linear theory. Linear theory is composed of the following 3 steps:

Area distribution of aircraft due to volume and area distribution due to lift are added to obtain total area distribution^{c,ci}

Total area distribution used to generate Whitham's F-function^{ci}

F-function used to propagate pressure signature to the ground by means of Thomas's Waveform Parameter Method^{ci}

To conduct the analysis, the program needs data about the atmosphere, aircraft (shape factor, weight, and length), and trajectory of the mission. The atmosphere data is based on a standard atmosphere and assumes calm conditions (no wind). In a standard atmosphere, the temperature profile throughout the atmosphere is the default, with no variation due to local conditions. The aircraft data uses a shape curve factor to determine the area distribution of the aircraft being analyzed, which was assumed to be a value of 6. This assumption is limiting the accuracy of the analysis since the area distribution of the aircraft is the most important data in terms of linear theory. The aircraft's weight and length however, are directly input and were assumed to be 282,000 lbs and 200 ft, respectively.

The trajectory file is where most of the mission profile information is utilized to generate a contour plot of the pressure signature during supersonic flight. The file requires the following inputs:^{cii}

- Initial longitude and latitude coordinate of the mission
- The x and y locations from the initial coordinate
- Mach number
- Altitude
- Time profile of the mission
- Change in Mach number with respect to time
- Acceleration of aircraft in terms of Mach number
- Heading
- Change in heading with respect to time
- Derivative of change in heading
- Flight path angle
- Change in flight path angle with respect to time
- Derivative of change in flight path angle

Requirement numbers 1, 3, 4, 5 and 11 are given from the mission profile outputs, and they are used to calculate all the other requirements. The x and y locations during the mission are also given, but they are in the terms of latitude and longitude. PCBoom requires the x and y locations to be in units of feet, so the latitude and longitude coordinates need to be converted.^{ciii} The latitude conversion is constant, but the longitude conversion depends on the latitude coordinate. To calculate the longitude, the conversion data is used to create a trend line in Excel, and the equation of the trend line is used as a conversion factor to calculate the changes in longitude in terms of feet. This data is added together throughout the mission to calculate the exact location of the aircraft along the trajectory. The equation used for conversion purposes is given below. Variable x is the latitude coordinate, and y is the distance per change in longitude in units of feet.

$$y = -39.062x^2 - 944.71x + 380187$$

The heading is assumed to be 0 degrees when heading north, and the heading increases when rotated clockwise [cii]. The heading is calculated using the x and y locations and trigonometry, given by:

$$h = \tan^{-1} \left(\frac{y_2 - y_1}{x_2 - x_1} \right)$$

The derivatives and second derivatives of the Mach number, heading, and flight path angle with respect to time are all found by using the forward difference calculations. Once all the required information is calculated, PCBoom can generate the pressure contour on the ground. Figure 7-72 shows the details of the sonic boom carpet. With the trajectory in the center of the carpet, the overpressure

decreases as one moves laterally away from the trajectory. The faint grey curved lines within the carpet represent the ray cones during the flight; therefore the aircraft is traveling from the upper right corner to the lower left corner of the figure. The ray cone is plotted instead of the wave cone because the ray cone (generated from Ray Tracing Theory) portrays the path that the energy takes from a set location of the aircraft, which is not distorted when the aircraft is doing maneuvers (unlike the wave cone).^{cii} The wave cone is just the combination of different ray cones at different times. Figure 7-73 shows the perceived loudness given the signature overpressure. The variation of the signature's shape can alter the perceived loudness of the signature, even if various signatures share the same overpressure.^{civ}

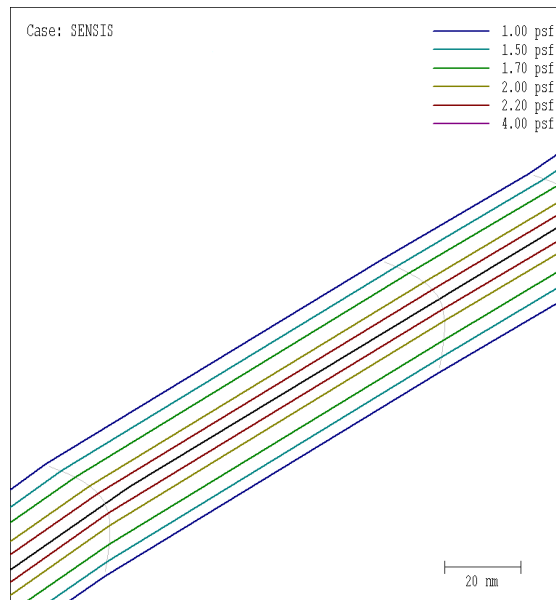


Figure 7-72. Detailed sonic boom carpet.

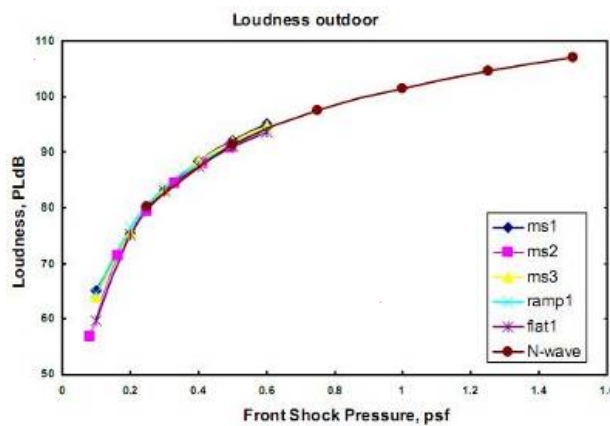


Figure 7-73. Sonic boom overpressure vs. perceived loudness (MS = Multiple Shock Signature).

PCBoom is a useful tool that gives reasonable linearized estimates of the sonic boom footprint on the ground, but future work is required in generating more accurate boom carpets. The next step is to utilize PCBoom in batch mode by means of an executable, which not only automates the process, but also permits use of the specific total area distribution curve of the aircraft to generate a boom carpet. The inability to use the specific area distribution curve is one potential explanation why the overpressure

levels in the boom carpet are high. Currently any specific modifications to the area distribution curve to decrease the overpressure are not being captured. Furthermore, the mission itself needs to be more refined in order to reduce sudden changes in trajectory. These sudden changes cause focused booms to occur, which may double or even triple the overpressure in specific locations within the carpet. The sonic boom problem is the most challenging issues to close both the SST business and technical cases. The boom loudness strongly depends on the shape, size and cruising velocity of the aircraft. During the design space exploration, the average boom loudness was around 100 PLdB. The perceived level of sound measured in PLdB is different from actual sound intensity. Figure 7-74 compares the boom loudness of the Concorde with other vehicle studies.^{cv}

The High Speed Civil Transport (HSCT) was part of a study conducted by NASA whereas the Supersonic Business Jet (SBJ) and Quiet Supersonic Jet (QSJ) are in reference to the Gulfstream company research studies. From Figure 7-74, it can be noticed that even though there is a great difference in shape and size between the Concorde and the SBJ, the boom loudness is not that much different. In the figure, PLdB is a measure of the perceived loudness of a sound, specifically the boom. It takes into account the over- and under-pressure of the passing boom, the frequency, etc. On the other hand, dB(A) is a scale that adjusts frequency content to approximate how the ear hears. It is implemented using A-weighted decibels (dBA). The dBA is the most common unit used for measuring environmental sound levels. It adjusts, or weights, the frequency components of sound to conform to the normal response of the human ear at conversational levels and is an international metric that is used for assessing environmental noise exposure of all noise sources. Providing dBA and PLdB, which is specific to the boom of a supersonic aircraft, the chart shows how the two different metrics of noise are related in regards to supersonic aircraft.

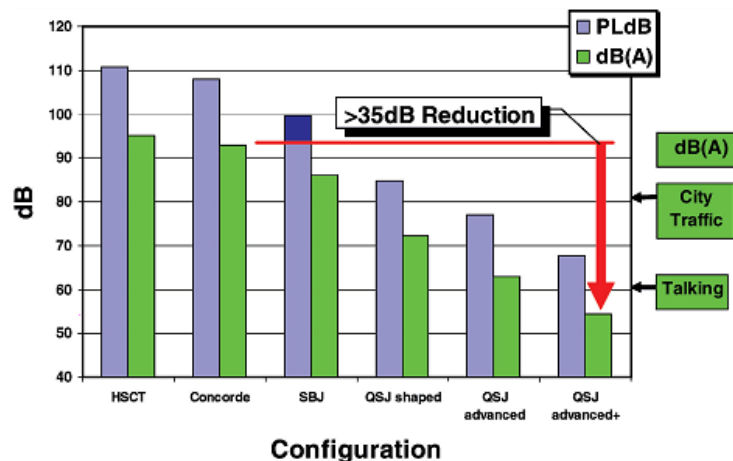


Figure 7-74. Boom loudness of various aircraft.

The QSJ shaped is referring to the vehicle shape optimization, since it was demonstrated to have an impact on the boom loudness through the F5 Shaped Sonic Boom Demonstration (SSBD).^{cvii} The “advanced” concepts include shape optimization as well as new configuration, such as the integration of a boom spike the can be extended from the nose of the aircraft. In this study limited shape optimization has been conducted on the SST, which only included the fuselage shape optimization in order to optimize the area ruling of the vehicle. The choice was based on the desired to have a broader exploration of the design space, which implied a lower level of fidelity from an aerodynamics perspective. In order to capture

detailed shape optimization, the modeling environment would need higher fidelity tools like Computational Fluid Dynamics (CFD), to better capture the near field pressure distribution around the vehicle. This is assumed to be a future trend to explore for the SST in a subsequent study.

Summary of SST Design

From all the configurations analyzed during the design space exploration and based on the trades discussed in the previous section, the SST converged to the configuration illustrated in Figure 7-75. The vehicle configuration selected is a canard with a swing wing. This configuration proves to be the best compromise between high speed cruise and low speed performance in the terminal area. As previously discussed, no aeroelastic phenomena were taken into account for the design space exploration. This type of analysis, requiring higher fidelity tools, would however be critical for further refinement of the vehicle. Table 7-30 lists the lifting surfaces geometry and the weight breakdown of the final configuration. A summary of the vehicle performance characteristics is listed in Table 7-31.

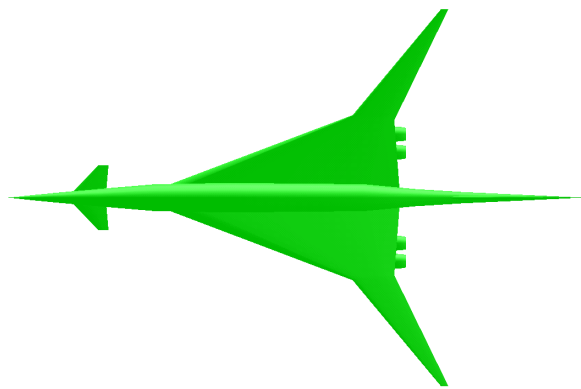


Figure 7-75. SST converged geometry.

Table 7-30. Lifting surfaces geometry.

Parameter	Wing	HT	VT
Surface Area, (ft ²)	3589.6	161	390
Sweep (C/4), (deg)		45	55.2
Wing Upswept (deg)	64		
Wing Swept (deg)	38		
Aspect Ratio	4.44	2.4	0.4
Taper Ratio	0.1	0.29	0.6
Dihedral Angle (deg)	4.1	0	0

Table 7-31. SST performance summary.

Characteristic	Value
Crew	2
Passengers	100
Range (nm)	4,000
Cruise Mach Number	1.6
Max Altitude (ft)	53,000
Operating Empty Weight (lbs)	110,344
Total Payload (lbs)	35,400
Fuel (lbs)	137,756
Takeoff Gross Weight (lbs)	282,000
Take-off Field Length, Std. Day (ft)	10,000
Landing Field Length, Std Day (ft)	7,154
Engine Take-off Thrust (lb)	~25,000
Number of Engines	4
Boom Loudness (PLdB)	104.6

AEDT and ACES Connectivity

With the converged SST vehicle, the next element needed was the connectivity to AEDT and ACES. This section will describe the assumptions and AEDT results related to the SST noise and emissions analyses. These analyses can only be viewed as the best approximation since no physical model exists of the MFTF engines in this thrust class.

The noise analysis required the Noise Power Distance (NPD) curves of an airframe-engine configuration. The curves present the noise level as a function of the engine thrust settings and the distance from the runway. Since no NPD curves exist for the MFTF-SST configuration and the analysis tool utilized for community noise is at best skeptical, the next best option is to select NPD curves from an existing aircraft resembling the MFTF-SST configuration. That means an airframe with 4 engines with a sea level thrust of approximately 25,000 lbs each, and a TOGW as close to 282,000 lbs as possible. The closest aircraft from the Integrated Noise Model (INM) database is the McDonnell Douglas DC-08-71. The DC-08-71 has 4 engines producing 22,000 lbs of thrust each and the TOGW of the aircraft is 325,000 lbs. Figure 7-76 shows the noise contours of the SST airframe with the DC-8 NPD curves from the AEDT analysis. The approach of equivalency used for the SST was identical to the analogy conducted for the LCTR.

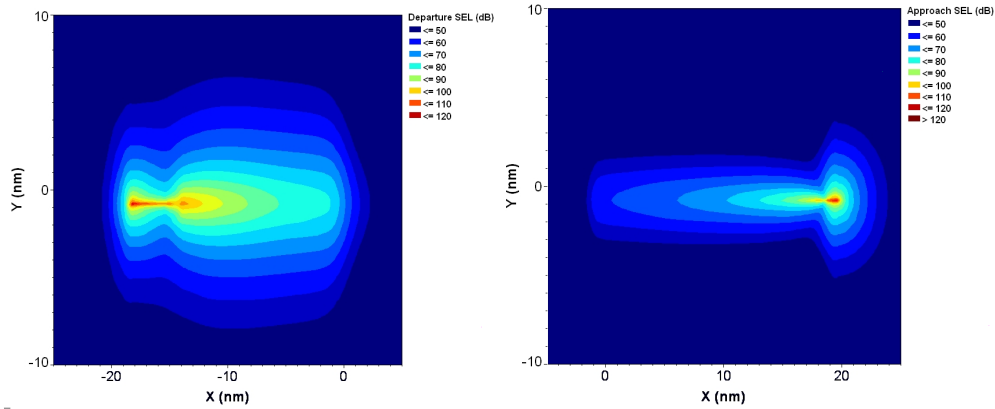


Figure 7-76. Airport noise analysis (Left: departure, right: arrival).

The emissions design requirement stated that the NOx emissions shall be smaller than 10 NOx g/kg of fuel during cruise. As with the noise representation, there was no existing NOx emissions model for the MFTF engine and the combustor, consequently the team relied on NASA subject matter expert to provide an approximation of the Emission Index of NOx (EINO_x); specifically:

$$EINO_x = a_0 \times (Pt_3^{a_1}) \times e^{\left(\frac{Tt_3 - 459.67}{a_2}\right)} \times a_3$$

$$a_0 = 0.025, a_1 = 0.370, a_2 = 0.370$$

$$a_3 = \left(1 + \frac{1}{(10 \times \%F_n)!}\right) \times \left(\frac{FAR}{delPhi}\right)^{-\frac{1}{3}}$$

where, Pt₃ and Tt₃ represent the total pressure and total temperature at the compressor exit; %F_n corresponds to the thrust setting; FAR corresponds to the Fuel to Air Ratio; delPhi corresponds to the combustor cooling percent. A good assumption for the delPhi value was suggested by the subject matter expert at 20%. This equation was then coded into the NPSS MFTF models to calculate the EINO_x emissions as the aircraft is flying the mission. Figure 7-77 illustrates the NOx emissions produced during cruise as a function of the engine thrust settings. It can be seen that all the cruise altitude of the SST are meeting the emission requirements of having smaller than 10 NOx g/kg of fuel during cruise.

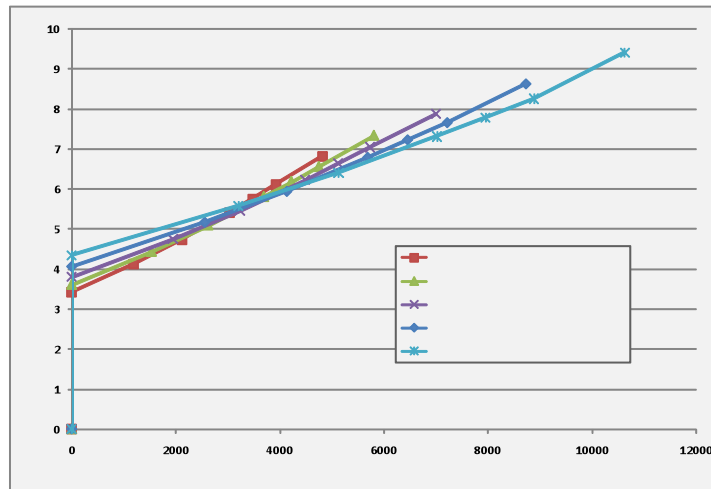


Figure 7-77. SST cruise NOx emissions.

SST Summary, Lessons Learned, and Potential Further Research

The main challenges remaining to be achieved include further analysis of the sonic boom, noise and emissions. The sonic boom problem will require the use of higher fidelity analysis tools in conjunction with new vehicle configurations. The noise model will require better acoustic prediction of NPD curve for conceptual engine, since NPD curves are generally created based on experimental test results. The NOx emissions will require higher fidelity analysis of the engine combustion process to improve the NOx prediction of conceptual engine. To summarize the results section of the study, Table 7-32 presents a summary of the main SST requirements status.

The main lesson learned through this study is the high complexity caused by the multiple constraints surrounding the design of the SST aircraft. A summary of the constraints encountered in this study are listed as follows:

- Boom loudness;
- High jet velocity at takeoff;
- Weight sensitivity of the aircraft;
- Airframe optimization for both low and high speed;
- Engine cycle optimization for both low and high speed;
- Fuel efficient engine in all regime;
- Emissions level reduction;
- Noise level reduction.

In order to meet these constraints it was important to explore a large design space including both continuous and discrete variables. Following the design exploration, even the best designs needed further propulsion analyses to optimize the engine cycle and to meet the jet velocity constraints. These refinements were necessary because of the multi-modal nature of the design space. This means that the

genetic algorithm used in this study had some difficulty converging toward a global minimum, which would have corresponded to a truly optimized aircraft meeting all the convergence criteria. An initial design was developed for this study, but numerous challenges still exist and warrant further research. For example, the future design analyses to explore for the SST aircraft are well documented in the research literature and were also encountered herein. A summary of these challenges are presented in Figure 7-78.^{cvi} More specifically for based on this study, Table 7-33 lists the potential challenges that should be investigated in order to close the supersonic technical and business cases.

Table 7-32. SST requirements summary.

Design Requirement	GT ASDL Suggestion	Verification
Cruise Speed (Mach)	1.6	OK
Range (n.mi.)	4000	OK
Payload (pax)	100	OK
Sonic Boom (PLdB)	65-70	104.6
Airport Noise (Below stage 3 EPNdB)	10	Approximation OK, but need better estimates of NPD curves
Cruise Emissions (Cruise NOx g/kg of fuel)	<10	Approximation OK, but need better estimates of engine emissions
Fuel Efficiency (passenger-mi./lb of fuel)	1-3	3.34



Figure 7-78. Supersonic transport challenges.

Table 7-33: Future challenges to investigate.

Research Area	Challenges
Design Analysis	Global optimization scheme Complete technology impact analysis
Geometry	Additional discrete configuration (e.g. V-tail, boom spike) Morphing surfaces
Aerodynamics	Higher fidelity analysis of the near pressure field Overall shape optimization of the vehicle
Aeroelasticity	Flutter analysis Wing structure interactions
Propulsion	Additional engine types (e.g. FLADE, variables cycle engine) Inlet design integration Noise suppression systems
Stability and Control	Supersonic trim Fuel distribution management Dynamics S&C analysis
Noise and Emission	NPD curve modeling Emission (combustion) modeling for different engine cores

Compiled Vehicle Comparison

The focus of this NASA sponsored research was to investigate the impact of advanced vehicle concepts within NextGen. This section discussed the five advanced vehicles that were modeled by ASDL for use in the broader research effort lead by Sensis. The selection of the vehicles considered was based on unique aircraft types and operations that differ from the existing commercial fleet and would potentially have an impact on NextGen. As a summary of the unique vehicle capabilities, Figure 7-79 through Figure 7-81 depicts the mission profile, performance, and configuration comparison. As evident, the vehicles selected for consideration span a wide range of capabilities. The impact that each vehicle has within NextGen are discussed in later sections of this report.

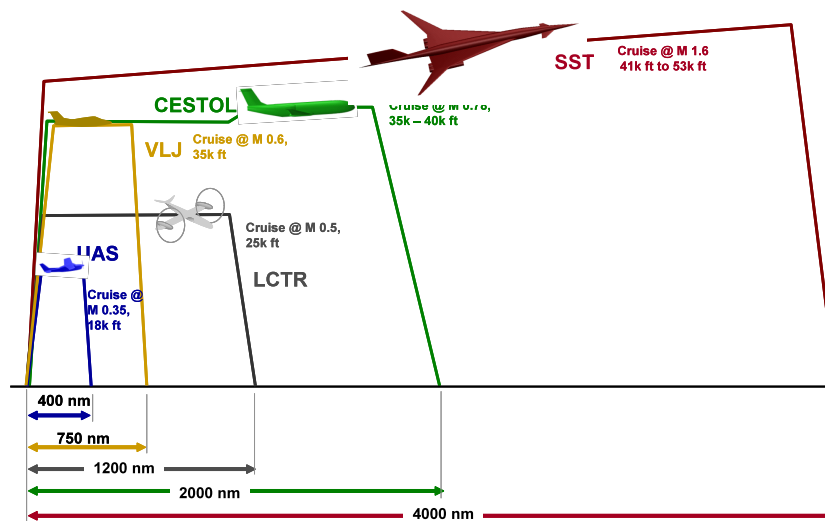


Figure 7-79. Mission profile comparison.

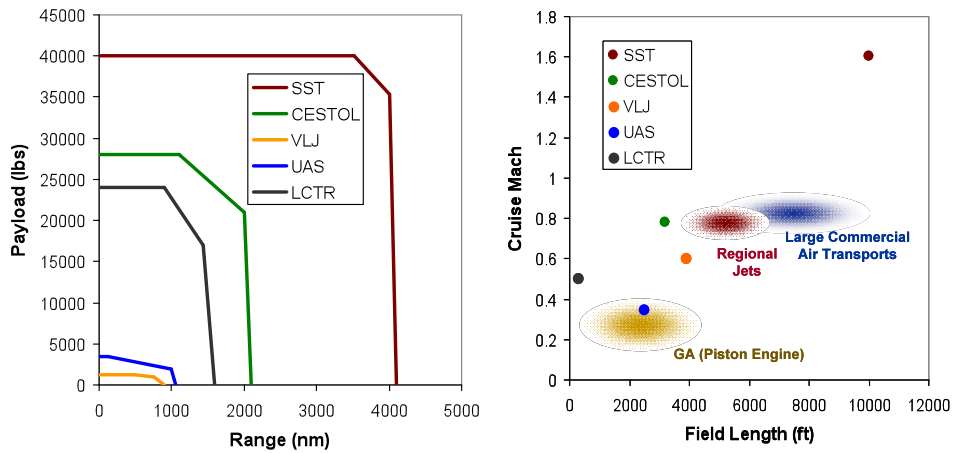


Figure 7-80. Performance comparison.






	CESTOL 	VLJ 	UAS 	LCTR 	SST 
Passenger Seats	100	4	0	90	100
Maximum Take Off Weight (lbs)	90,846	5,600	8,750	107,382	282,000
Design Fuel Burn (lbs)	17,682	1,287	840	19,930	137,756
Max Cruise Altitude (ft)	40,000	41,000	24,500	25,000	53,000
Thrust per engine (lbs)	14,081	1,690	675 shp	7,500 shp	~25,000
Max Payload (lbs)	28,000	1,200	3,550	19,800	35,400
Cruise Mach	0.78	0.6	0.28	0.5	1.6
Design Range (nmi)	2,000	750	400	1,200	4,000
Take Off Field Length @ MTOW (ft)	3,795	3,875	2,420	0 - 600	10,000
Approach Speed (kts)	102	90	78	50	148
Landing Field Length (ft)	3,188	2,250	1,795	0 - 600	7,154

Figure 7-81. Configuration comparison.

xxiv Holmes, B., Discussion about VLJ Design Requirements and Refresh Cycle. October 7, 2008.

xxv http://en.wikipedia.org/wiki/Cessna_Caravan, cited in June 2009.

xxvi <http://www.cessna.com/caravan/super-cargomaster.html>, cited in June 2009.

-
- xxvii Thompson, P., Neir, R., Reber, R. Scholes, R., Alexander, H., Sweet, D. Berry, D., "Civil Tiltrotor Missions and Applications Phase II: The Commercial Passenger Market Summary Final Report," NASA CT 177576, January 1991.
- xxviii Johnson W., Yamauchi, G.K., Watts, M.E., "NASA Heavy Lift Rotorcraft Systems Investigation," NASA/TP-2005-213467.
- xxix Acree, C.W., Yeo, H., Sinsay, J.D., "Performance Optimization of the NASA Large Civil Tiltrotor," NASA TM 2008-215359, June 2008.
- xxx "LCTR2 Configuration Report (Draft v7)," NASA, December 2008.
- xxxi European Organisation for the Safety of Air Navigation, "User Manual for the Base of Aircraft Data (BADA) Revision 3.6," EEC Note No. 10/04, September 2004.
- xxxii SAE Committee A-21, Aircraft Noise, "Procedure for the Calculation of Noise in the Vicinity of Airports," Aerospace Information Report No. 1845, Warrendale, PA: Society of Automotive Engineers, Inc., March 1986.
- xxxiii Kirby, M., Mavris, D., "The Environmental Design Space," ICAS 2008, 14-19 September 2008, Anchorage, AK.
- xxxiv Converse, G.L.; Giffin, R.G., "Extended Parametric Representation of Compressors Fans and Turbines. Vol. I - CMGEN User's Manual," NASA CR-174645, 1984.
- xxxv "NPSS User Guide," Software Release: NPSS_1.6.4; REV: Q; Doc. #: NPSS–User; Doc Revision: W in progress; Revision Date: November 5, 2006.
- xxxvi "NPSS Reference Sheets," Software Release: NPSS_1.6.4 V; Doc. #: NPSS–Ref Sheets Doc Revision: W in progress; Revision Date: January 05, 2007.
- xxxvii Tong, M. T., Ghosn, L. J., Halliwell, I., "A Computer Code for Gas Turbine Engine Weight and Disk Life Estimation," ASME Paper No. GT-2002-30500, ASME Turbo Expo: Land, Sea & Air 2002, June 2002, Amsterdam, The Netherlands.
- xxxviii Norman, P.D., et.al., "Development of the technical basis for a New Emissions Parameter covering the whole AIRcraft operation: NEPAIR," NEPAIR/WP4/WPR/01 Final Report, EC Contract Number G4RD-CT-2000-00182, September 2003.
- xxxix McCullers, L.A., "Flight Optimization System, Release 6.12, User's Guide," revised 14 October 2004.
- xl Zorumski, W.E., "Aircraft Noise Prediction Program Theoretical Manual," NASA TM 83199, revised December 2006.
- xli Harris, R. V. Jr., "An Analysis Correlation of Aircraft Wave Drag," NASA TMX-947, March 1964.

xlii Carlson, H., Chu, J., Ozoroski, L., Mccullers, A., “Guide to AERO2S and WINGDES Computer Codes for Prediction and Minimization of Drag Due to Lift,” NASA TP 3637, November 1997.

xliii Middleton, W. D., Lundry, J. L., “A System of Aerodynamic Design and Analysis of Supersonic Aircraft,” NASA CR-3351, 1980.

xliv Harris, Roy V. Jr., “An Analysis Correlation of Aircraft Wave Drag,” NASA TMX-947, March 1964.

xlv Coen, P., “Development of a Computer Technique for the Prediction of Transport Aircraft Flight Profile Sonic Boom Signatures,” Master’s Thesis, The George Washington University, 1991.

xlvi Plotkin, K. J., “PCBoom3 Sonic boom prediction model – Version 1.0c,” AFRL-HE-WP-TR 2001-0155, Wyle Research Laboratories, Arlington, VA, May 1996.

xlvii Schoen, A.H., Rosenstein, H., Stanzione, K., Wisniewski, J.S., “VASCOMP 2. The V/STOL Aircraft Sizing and Performance Computer Program, Volume 6: User’s Manual, Revision 3,” NASA CR 163639, May 1980.

xlviii Dubois, D.P., Paynter, G.C., “Fuel Flow Method 2’ for Estimating Aircraft Emissions,” SAE 2006-01-1987.

xlix ECAC, “Standard Method of Computing Noise Contours around Civil Airports,” ECAC Document 29, 1986 (2nd edition 1997).

l International Civil Aviation Organization, “Annex 16 to the Convention on International Civil Aviation — Environmental Protection Volume II — Aircraft Engine Emissions,” 1993.

li FAA, 2004, Airport Master Records, Form 5010, http://www.faa.gov/airports/airport_safety/airportdata_5010/menu/index.cfm.

lii Krist, S. E., “High Speed Slotted Wing,” presented at Applied Aerodynamics Peer Review October 19-21, 2004.

liii Hetrick, J. A., Osborn, R. F., Kota, S., “Flight Testing of Mission Adaptive Compliant Wing,” 48th AIAA/ASME/ASCE/AHS/ASC Structures, Structural Dynamics, and Materials, Honolulu, Hawaii, AIAA, 2007.

liv Greff, E., “The Development and Design Integration of a Variable Camber Wing for Long/Medium Range Aircraft,” *Aeronautical Journal*, November 1990.

lv Austin, F., Siclari, M. J., Van Nostrand, W., Kottamasu, V., Volpe, G., “Comparison of Smart-Wing Concepts for Transonic Cruise Drag Reduction,” SPIE Smart Structures and Materials Conference, San Diego, CA, 4-6 March 1997.

lvi Shaw, J., Peddie, C., “NASA Ultra Efficient Engine Technology Project Overview,” NASA/CP-2004-212963, 2004.

lvii Karal, M., "AST Composite Wing Program-Executive Summary," NASA/CR-2001-210650, 2001.

lviii Hale, J., "Boeing 787 from the Ground Up," *Aero*, No. 6, 2004.
http://www.boeing.com/commercial/aeromagazine/articles/qtr_4_06/AERO_Q406.pdf, Accessed 2009 June 9.

lix Teresko, J., "Boeing 787: A Matter of Materials - Special Report: Anatomy of a Supply Chain," 2007. http://www.industryweek.com/articles/boeing_787_a_matter_of_materials_-_special_report_anatomy_of_a_supply_chain_15339.aspx, Accessed 2008 August 14.

lx Hawk, J., "The Boeing 787 Dreamliner: More Than an Airplane," AIAA Aircraft Noise and Emissions Reduction Symposium (ANERS), 24 - 26 May 2005, Monterey, California, 2005.

lxi Crouch, J., "Modeling Transition Physics for Laminar Flow Control," 38th Fluid Dynamics Conference and Exhibit, Seattle, Washington, June 23-26, AIAA, 2008.

lxii Sacco, G.: Natural Laminar Flow Technology: 20 Years of Piaggio P.180 Experience. Symposium on Applied Aerodynamics and Design of Aerospace Vehicles (SAROD 2009), Bengaluru, India.

lxiii Everts, R., "Steep Approach at Londoncity Airport," *Flightline*, published by Fokker Service, No. 6, June 2001.

lxiv Raymer, D., "Aircraft Design: A Conceptual Approach," AIAA Education Series, 3rd ed., 1999.

lxv Kirby, M., "A Methodology for Technology Identification, Evaluation, and Selection in Conceptual and Preliminary Aircraft Design," Ph.D Thesis, Georgia Institute of Technology, 2001.

lxvi Biltgen, P., "A Methodology for Capability-Based Technology Evaluation for Systems-of-Systems," Ph.D Thesis, Georgia Institute of Technology, 2007.

lxvii Chaffin, M. S., Morgan, H. L., Johnson, P. L., Courtney, J. M., "High-Lift Wind Tunnel Test Measurements on a Cruise-Slotted Airfoil," NASA/TM-2005-213788, 2005.

lxviii Morris, J., Ashford, D. M., "Aircraft Fuselage Configuration Studies Point to Use of Multideck Fuselages," SAE 670370, 1967.

lxix De Luis, J., "A process for the quantification of aircraft noise and emissions interdependencies," PhD Dissertation, Georgia Institute of Technology, 2008.

lxx Boeker, E. R., Dinges, E., He, B., Fleming, G., Roof, C.J., Gerbi, P.J., et al. "Integrated Noise Model (INM) Version 7.0 Technical Manual," U.S. Department of Transportation, Federal Aviation Administration, Office of Environment and Energy, January 2008.

lxxi Lutz, T., "City Lights: The E-170 steep approach programme," IFALPA The Global Voice of Pilots News, June 2006.

-
- lxxii http://www.eclipseaviation.com/files/pdf/Eclipse_500_Dimensions.pdf, cited in July 2009.
- lxxiii <http://www.eclipseaviation.com/eclipse500/operation/specifications.php>, cited in July 2009.
- lxxiv <http://www.eclipseaviation.com/jet.php#/eclipse400/style/gallery/>, cited in July 2009.
- lxxv Jane's All the World's Aircraft (1992-93), Cessna Aircraft, Jane's Information Group Limited, 1993.
- lxxvi http://www.atlantic-aero.com/103_Aircraft%20Sales/103_Docs/2008_Grand_Caravan_Specs_Models.pdf, specification and description manual of Grand Caravan by Cessna, cited June 2009.
- lxxvii www.tomsaircraft.com/udocs/20080104093832_2008%20Caravan%20FULL%20brochure.pdf, airplane introduction brochure by Cessna, cited in June 2009.
- lxxviii <http://www.flightglobal.com/articles/2009/09/09/332045/aa09-mitsubishi-unveils-major-changes-to-mrj-programme.html>, cited in September 2009.
- lxxix http://en.wikipedia.org/wiki/T-6_Texan_II, cited August 2009.
- lxxx John A. Volpe National Transportation Systems Center, Acoustics Facility, Spectral Classes for FAA's Integrated Noise Model Version 6.0, DTS-34-FA065-LR1, 1999.
- lxxxi Schoen, A.H., Rosenstein, H., Stanzione, K., Wisniewski, J. S., "VASCOMP 2. The V/STOL Aircraft Sizing and Performance Computer Program, Volume 6: User's Manual, Revision 3," NASA CR 163639, May 1980.
- lxxxii Tai, J., Mavris, D., Schrage, D., "A Comparative Assessment of High-Speed Rotorcraft Concepts (HSRC) – Reaction Driven Stopped Rotor/Wing and Variable Diameter Tiltrotor," AIAA and SAE, 1997 World Aviation congress, Anaheim, CA, October 1997.
- lxxxiii Decker, W.A., Conversations regarding tiltrotor terminal operations, November 18, 2008.
- lxxxiv Hindson, W. S., Hardy, G. H., Tucker, G. E., Decker, W. A., "Piloting Considerations for Terminal Area Operations of Civil Tiltwing and Tiltrotor Aircraft," Piloting Vertical Flight Aircraft: A Conference on Flying Qualities and Human Factors, July 1993.
- lxxxv E-mail Communications between ASDL and NASA, March 2009.
- lxxxvi E-mail Communications between ASDL and Sensis Corp., May, June 2009.
- lxxxvii Hall, C., Smith, D., Soucacos, P., Hansen, A., Nwokeji, P., Regan, G., "AEDT Database Description Document, Fleet Database, Version 2.2.2," Prepared for FAA, August 2008.

-
- lxxxviii Dunn, D.G., Peart, N. A., "Aircraft Noise Source and Contour Estimation," NASA CR-114649, July, 1973, pp.148–175.
- lxxxix http://www.rolls-royce.com/civil/products/smallaircraft/ae_3700/index.jsp, as of 7/19/2009.
- xc http://www.rolls-royce.com/defence/products/helicopters/ae_1107C_liberty.jsp, as of 7/19/2009.
- xcii NASA Aeronautics Research Mission Directorate, "The Supersonic Project," <http://www.aeronautics.nasa.gov/fap/supersonic.html#boom>, cited June 2009.
- xciii Alonso, J. J., "Overview of NRA Solicitation," N+3 Pre-Proposal Conference, NASA, Washington, D.C., 29 Nov. 2007 (downloadable from www.aeronautics.nasa.gov/pdf/overview_solicitation_alonso_11_29_07.pdf, cited June 2009).
- xciv *Research Opportunities in Aeronautics – 2008*, NRA NNH08ZEA001N, Aeronautics Research Mission Directorate, NASA, Washington, D.C., 2008, <https://nspires.nasaprs.com/external/>, cited June 2009.
- xcv Concorde website, <http://www.concordesst.com/>, cited June, 2009.
- xci Mavris, D., N., Rallabhandi, S. K., "Supersonic Concept Selection using Advanced Genetic Algorithms," Final Report NASA Contract No. NAS1-02117, March 2007.
- xcvi Needleman, K. E., Darden, C. M., Mack, R. J., "A Study of Loudness as a Metric for Sonic Boom Acceptability," AIAA Paper No. 91-0496.
- xcvii Buonanno, M., "A Method for Aircraft Concept Exploration Using Multicriteria Interactive Genetic Algorithms," Georgia Institute of Technology, December 2005.
- xcviii Henne, P., A., "Small Supersonic Civil Aircraft," Gulfstream presentation given at the Aircraft Noise and Emissions Reduction Symposium, Monterey, CA, 2005.
- xcix Committee on Durability and Life Prediction of Polymer Matrix Composites in Extreme Environments, *Going to Extremes*, Washington, D.C., National Academy Press, 2005.
- c Carlson, H. W., "Simplified Sonic Boom Prediction," NASA, Hampton, VA., 1978.
- ci Cohen, P. G., "Development of a Computer Technique for the Prediction of Transport Aircraft Flight Profile Sonic boom Signatures," 1991.
- cii Plotkin, K. J., "Computer Models for Sonic Boom Analysis," 2002.
- ciii "The Sentinel," "Latitude Longitude Conversion to Feet," *Hyper News*, 2001.
- civ Plotkin, K.J., Morgenstern, J.N., "Examination of Sonic Boom Signatures experienced Indoors," AIAA, 2008.

cv Henne, P. A., “Case for Small Supersonic Civil Aircraft,” Journal of Aircraft 42.3 (2005) 765-774.

cvi Pawlowski, J., Graham, D., Shaped Sonic Boom Demonstration, Program Overview, <http://www.sonicbooms.org>, 2004.

cvii Coen, P., “Supersonic Project Overview,” NASA presentation at the Fundamental Aeronautics Annual Meeting, Atlanta, GA, Oct. 2008, www.aeronautics.nasa.gov/fap/PowerPoints/SUP_ATL_Overview.pdf, cited November 2008.

8. New York Airspace Design

8.1. *Background*

Airports in the vicinity of New York City are extremely congested. John F. Kennedy International (JFK), Newark International (EWR), LaGuardia (LGA) and Teterboro (TEB) airports are some of the busiest in the United States, with JFK, EWR and LGA ranking 12th, 14th and 18th respectively in 2007 in terms of number of takeoffs and landings by air carriers, air taxis, general aviation and military aircraft.¹ These four airports may be circumscribed by a circle that is 20 nm in diameter, leading to high levels of congestion and with traffic numbers set to grow with the introduction of new vehicles, an entire redesign of the airspace and its procedures is necessary.

This redesign effort also includes the following airports in the New York metropolitan area: Stewart International (SWF), Long Island Mac Arthur (ISP), Westchester County (HPN), and Farmingdale Republic Airport (FRG). When all of these airports are in operation, the multiple runway usage leads to interactions between the various flows of traffic arriving and departing each airport. An image of the current procedures into the aforementioned airports can be seen in Figure 8-1. Many of the airports share the same procedures, and numerous intersecting tracks result in coupling between the procedures. Unlike the procedures proposed for this redesign, almost all aircraft are vectored onto the final approach to their landing runways, whereas the redesigned airspace features a gridded layout that provides all aircraft paths to and from landing and departing runways. As traffic increases at the satellite airports, interactions will become more numerous leading to increased congestion in the airspace.

This section looks at the redesign of airspace and flight procedures to accommodate new vehicles and environmental impacts in the New York Terminal Radar Approach Control (TRACON), otherwise known as N90. In it we describe the principles used in the design of the procedures that have been created for current aircraft (referred to as 'nominal aircraft' in this paper), as well as CESTOL, LCTR, VLJ and SST aircraft.

8.2. Design Principles

8.2.1. Terminal Area Throughput

Terminal area throughput is a function of both runway throughput and airspace throughput. Runway throughput depends on the runway configuration in use at the various airports, the fleet mix operating at these airports, and the inter-operation spacing (or timing rules). For example, JFK airport has many wide-bodied aircraft arriving in the afternoon which would result in a 4 nm runway threshold spacing between successive aircraft, but at TEB airport, the fleet mix is made up of mostly general aviation traffic which are classified as 'small' and require a 2.5 nm spacing between successive aircraft. Airspace throughput depends on the distribution of aircraft speeds and the length of the common path. Due to the large variety of aircraft in the New York airspace—from the Cessna 172 to the A380—and differing separation requirements between these aircraft, congestion should worsen as traffic levels increase, severely reducing airport and airspace capacity. We address these problems by using different runways and new procedures for existing and new aircraft concepts.

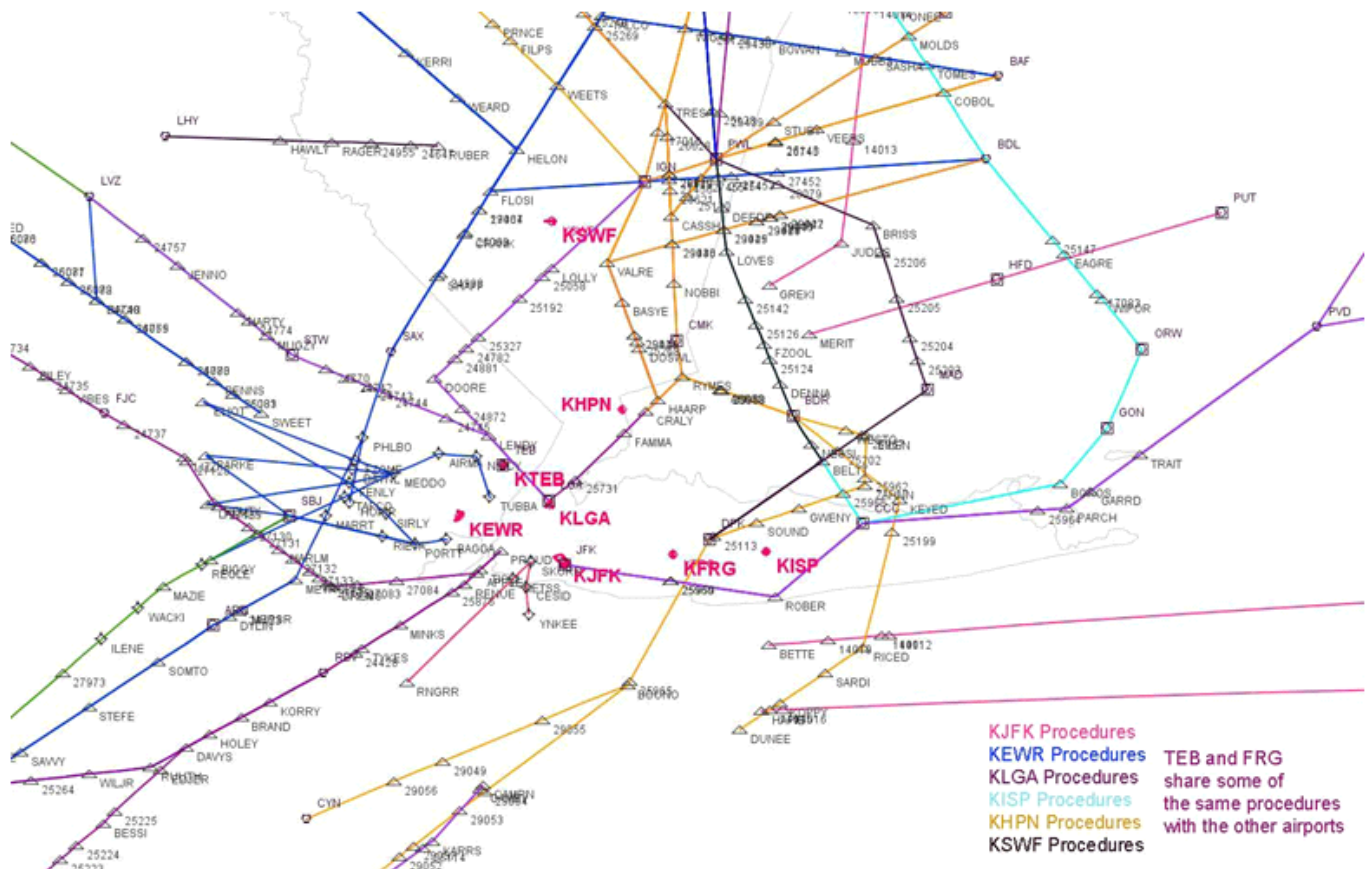


Figure 8-1. Overview of procedures

8.2.2. Maximization of Runway Throughput

Runway throughput can be maximized by optimizing the runway configuration at each airport. This is done by taking into account the stochastic demand and capacity of the airport and weather variability. It is also beneficial to optimize the aircraft schedule so the average inter-operation time for a given runway configuration is minimized. For example, in Atlanta, the new runway, 10/28, is designated mainly for regional jets and large jets; this has resulted in lower periods of time between successive aircraft, increasing the airport's capacity. Like terminal throughput, this issue has been addressed in this redesign effort by assigning certain vehicles certain runways or procedures.

8.2.3. Maximization of Airspace Throughput in an RNAV/RNP operating environment

The New York airspace being studied is being designed assuming Area Navigation (RNAV) procedures and Required Navigation Performance (RNP) that provide many options to increase throughput. One such method involves metering, used when the spacing required between aircraft is less at the runway threshold than upstream of the threshold. As a pair of aircraft descends towards the runway, the trailing aircraft travels at a faster groundspeed than the leading aircraft at a certain point in time (as a function of distance from the airport, altitude and winds aloft). Due to this, compression occurs between the leading and trailing aircraft, resulting in the need for a larger spacing between two aircraft further from the airport compared to at the runway threshold. For example, in order for 2 B767's to be separated by 4 nm at the runway threshold, at a point 65 nm from the airport, they may need to be 18 nm apart (for a given wind condition). To take into account this compression, metering may be used. Implementing metering may involve issuing aircraft Requested Time of Arrivals (RTAs) or ATC issuing speed changes to keep aircraft a certain distance or time apart at a specific waypoint. Ultimately, if metering is done correctly, the distance between aircraft will gradually decrease from what is required at the metering fix to the spacing needed at the runway threshold, avoiding the need for vectoring. This method is dependent on the acceptable upper bounds in upstream spacing and the constraints at the origin. Metering has been successfully used by Memphis Center (ZME) during the fall 2008 CDA flight trials and can also be used if the trailing aircraft is at a faster speed than that of the leading aircraft. Metering will be used in this redesign effort for supersonic transport flights and CDA procedures involving nominal aircraft.

Airspace throughput can also be maximized by segregating slower and faster aircraft onto separate arrival paths, provided that it is possible to merge the two flows just prior to touchdown. For example, two parallel flows could be created, one for faster aircraft, the other for slower and before the turn onto final approach, these two flows could be merged. This method would be subject to stabilized approach criteria such that aircraft would have enough time to be configured for landing.

As done with arrivals, slower aircraft could also be taken out of nominal departure flows as soon as possible after takeoff. This would enable faster aircraft to accelerate quickly to their faster climb speed and exit the congested airspace as soon as possible, without being impeded by slower aircraft.

These design principles were also adapted into the design of new procedures for the New York airspace.

8.3. Procedure Design

The aircraft being considered for the NRA new vehicle integration project, nominal aircraft, CESTOL, VLJ, LCTR and supersonic transports, all have different performance characteristics making it possible to devise procedures which will be optimal for each flying machine. These are detailed below along with general procedure information.

8.3.1. General Procedure Information

The general layout for the redesigned New York Airspace was based on the runway layout of the major New York airports: JFK, EWR, LGA and TEB. The available runways at all of the airports in this

Table 8-1. Runways at New York Metro Airports

Airport	Runways
JFK	4L/22R, 4R/22L, 13L/31R, 13R/31L
EWR	4L/22R, 4R/22L, 11/29
LGA	4/22, 13/31
TEB	1/19, 6/24
ISP	6/24, 10/28, 15L/33R, 15R/33L
HPN	11/29, 16/34
FRG	1/19, 14/32
SWF	9/27, 16/34

study can be seen in Table 8-1.

Due to the predominant runway directions of 13/31 and 4/22 for the three airports with the highest traffic density (JFK, LGA and EWR), the arrival and departure paths were aligned with these runways, creating a grid like structure. The tool used for mapping the procedures was FAA's Terminal Area Route Generation Evaluation & Traffic Simulation (TARGETS) tool. All

waypoints used are new waypoints and are not charted, allowing for maximum flexibility while designing the lateral paths for the new procedures.

8.3.2. Nominal Arrivals and Departures

Nominal Arrivals

Nominal arrivals will fly paths incorporating Continuous Descent Arrivals (CDA). CDAs have already been implemented at Los Angeles International Airport and a flight test involving over 400 flights has been recently completed at Atlanta's Hartsfield-Jackson International Airport. Further studies are underway to introduce CDAs at Charleston Air Force Base, Eglin Air Force Base and Jacksonville Airport. Aircraft will descend at a flight path angle between 2.5 and 3.5 degrees and will maintain a descent speed of 300 knots till 10000 ft, at which point they will slow to 240 kts. By creating a 'steep' descent profile (3.5 degree descent angle) and a 'shallow' descent profile (2.5 degrees), a window was created to show the upper and lower range of the possible descent profiles. While designing the CDA paths, in order to comply with TARGETS criteria, it was assumed that for every 10 kts of deceleration, 1 nm was required, and to descend 318 ft, 1 nm was needed. If an arrival path involves a downwind leg, a baseleg and a turn onto final, aircraft would be required to turn onto the baseleg at 210 kts and onto final at 180 kts. Such restrictions would ensure that all aircraft would be able to comfortably make these turns regardless of their size. For most arrivals, the Final Approach Fix (FAF) is located 5 nm from the runway threshold, at which point the aircraft is established on the ILS glideslope.

Nominal Departures

To account for the different take-off weights of aircraft and also different performance characteristics, takeoff calculations were performed using two different vertical speeds: 2500 ft/min and 1000 ft/min. Using these two vertical speeds, 'shallow' and 'steep' paths were constructed to depict a tube that aircraft would fly within. The restriction of maintaining an airspeed of less than 250 kts below 10000 ft was taken in to account.

8.3.3. CESTOL Aircraft

Cruise Efficient Short Take-Off Landing (CESTOL) vehicles will prove to be beneficial to the NAS in the future, enabling flights served by A320/B737 passenger sized aircraft to depart and arrive on shorter runways at less congested airports. These aircraft have a unique set of performance characteristics, including a lower landing speed and the ability to fly an approach at a steeper flight path angle. These characteristics provide the opportunity to design unique approach and departure procedures utilizing the spiral. The properties of the spiral approach/departure procedures are as follows:

1. Radius of 1.5 nm
2. On approach, vehicle enters spiral at 180 knots and 10000 feet and exits spiral at approach speed (100-110 kts) and 1000 ft, approximately 1.5 nm or 3 nm from the runway threshold.²
3. The aircraft will initially maintain the spiral at a bank angle of 25 degrees, and will roll out onto the final approach segment with a bank angle of around 5.5 degrees. As the aircraft slows to its final approach speed, its bank angle will gradually decrease in order to maintain the 1.5 nm radius spiral.
4. A descent angle between 2.5 and 5.5 degrees will be flown while in the spiral. This is dependent on the CESTOL aircraft and its performance characteristics.
5. For departures, the vehicle will climb as steeply as possible to 10000 feet and then exit the spiral and continue on its filed flight plan.

There are many benefits to including spiral procedures in the redesigned New York airspace, but the most important aspect is the amount of airspace such a procedure saves. By employing a spiral, instead of protecting a large, angled tube (which increases in radius as distance from the airport increases), all that is needed is a cylinder with radius 1.5 nm from the ground extending up to 10000 ft. Also, as previously mentioned, with spiral approaches slower aircraft such as the CESTOL can be kept out of the path of aircraft requiring a faster approach speed. For this reason, CESTOL aircraft will be operating using procedures ending on dedicated runways. Allowing for a 1.5 nm or 3 nm final approach segment ensures the pilot has enough time to stabilize the aircraft on the runway heading before landing. This also means that the spiral is not directly over the airport which eliminates the possibility of conflict between arrival paths to other runways. By not having the spiral over the airport, one concern is the amount of noise that will be generated by aircraft flying over communities; but the CESTOL aircraft in this study are not equipped with blown flaps and will be at an idle power setting while in the spiral Engine thrust will only be increased while the aircraft is on the final approach in order to maintain the glideslope, similar to procedures being used today. All airports with the exception of FRG (space constraints) have unique CESTOL spiral approaches.

A graphic representation of the CESTOL spiral is shown in Figure 8-2. Note that the descent profile is not to scale.

8.3.4. VLJ Aircraft

Very Light Jet (VLJ) vehicles will be able to cater to the potential increase in demand for smaller passenger aircraft. We envision these aircraft to have roughly similar performance characteristics as the CESTOL aircraft, but to be more maneuverable due to the smaller size of the aircraft. With these characteristics in mind, the VLJs will be using the same spiral procedures as the CESTOL aircraft. A significant difference to the CESTOL procedures involves the VLJ rolling out with wings level at a speed of 80 knots at the end of the spiral instead of 100 knots and a bank angle of 5.5 degrees for the CESTOL aircraft.

8.3.5. LCTR Vehicles

LCTR will also be integrated into the newly designed New York airspace with procedures solely developed for these vehicles. These flying machines have unique procedures for landing at JFK, EWR, LGA, ISP, HPN airports and will be sharing the same CESTOL departure lateral track. Only FRG does not have individual LCTR procedures due to space constraints.

LCTR Arrival Procedures

The LCTR arrival procedures involve flights coming into the New York airspace at 6000 or 7000 ft and will descend (or ascend for departures) along continuously segmented vertical paths while avoiding Blade Vortex Interaction (BVI). The maximum descent or ascent flight path angle for these vehicles would be limited to 15 degrees due to safety issues, but to achieve such a high flight path angle, a level segment is required where the vehicle transitions between aircraft and helicopter mode.

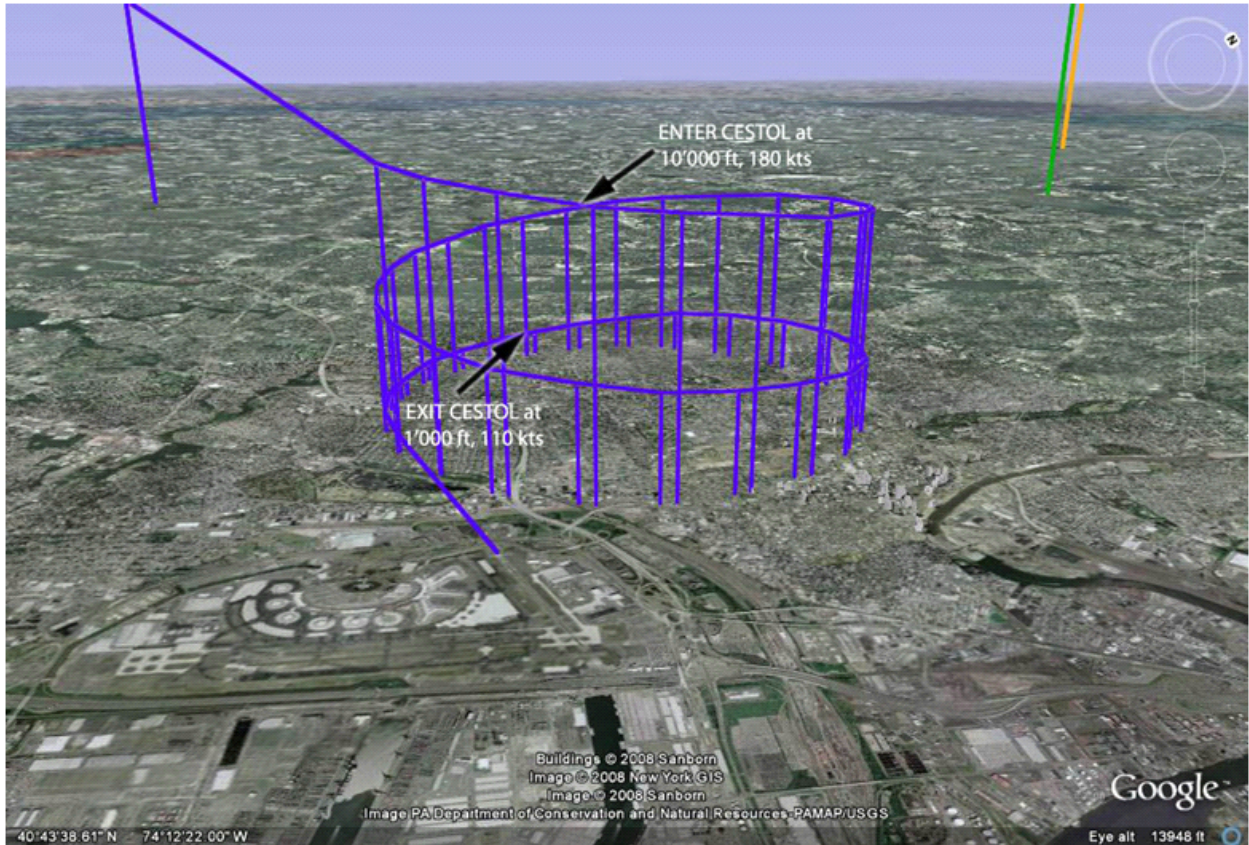


Figure 8-2: CESTOL Spiral

As determined by NASA and the aircraft design, the most optimum descent profile is not a vertical descent, but a conventional approach involving forward motion while descending, followed by a rollout segment on the runway. For the particular designed LCTR, the touchdown speed would be close to 50 knots and would require 300 ft to slow down. This profile is optimal as the aircraft is louder when hovering down to the runway than when compared to descending at some forward airspeed down to the landing strip.

In light of this new requirement, a landing strip of dimensions 200 ft by 600 ft was created at each airport, either on the property or close to the property. All runway headings are dependent on the direction of the arrival procedures already designed.

Table 8-2 shows the various waypoints and restrictions on most LCTR arrival procedures and was created using a trajectory analysis undertaken by the designers of the LCTR aircraft. The distances are from the touchdown point.

Table 8-2. LCTR arrival procedure waypoint restrictions

Waypoint	Distance (nm)	Altitude (ft)	Speed (kts) (IAS)
1	25	7000	180
2	5	2000	125
3	3.3	2000	50
4	0	0	0

LCTR Departure Procedures

Departing flights have their own departure paths and climb to 6000 ft, then continue to the edge of the defined New York metro airspace, after which, they would be able to climb to their assigned cruising altitude. These aircraft depart from existing runways which are not heavily utilized such as runway 24 at TEB and runway 15R at ISP. At JFK, LGA, HPN, and TEB, LCTR aircraft share the same runway as either CESTOL, conventional or both types of aircraft, but still have independent departure paths.

Even though these aircraft share the same runway as CESTOLs and conventional aircraft, in most cases, the LCTRs depart very close to the end of the runway. Another possibility is that if conventional aircraft are departing at LGA using runway 13, the LCTRs will depart at a point opposite taxiway T. Refer to Figure 8-3.

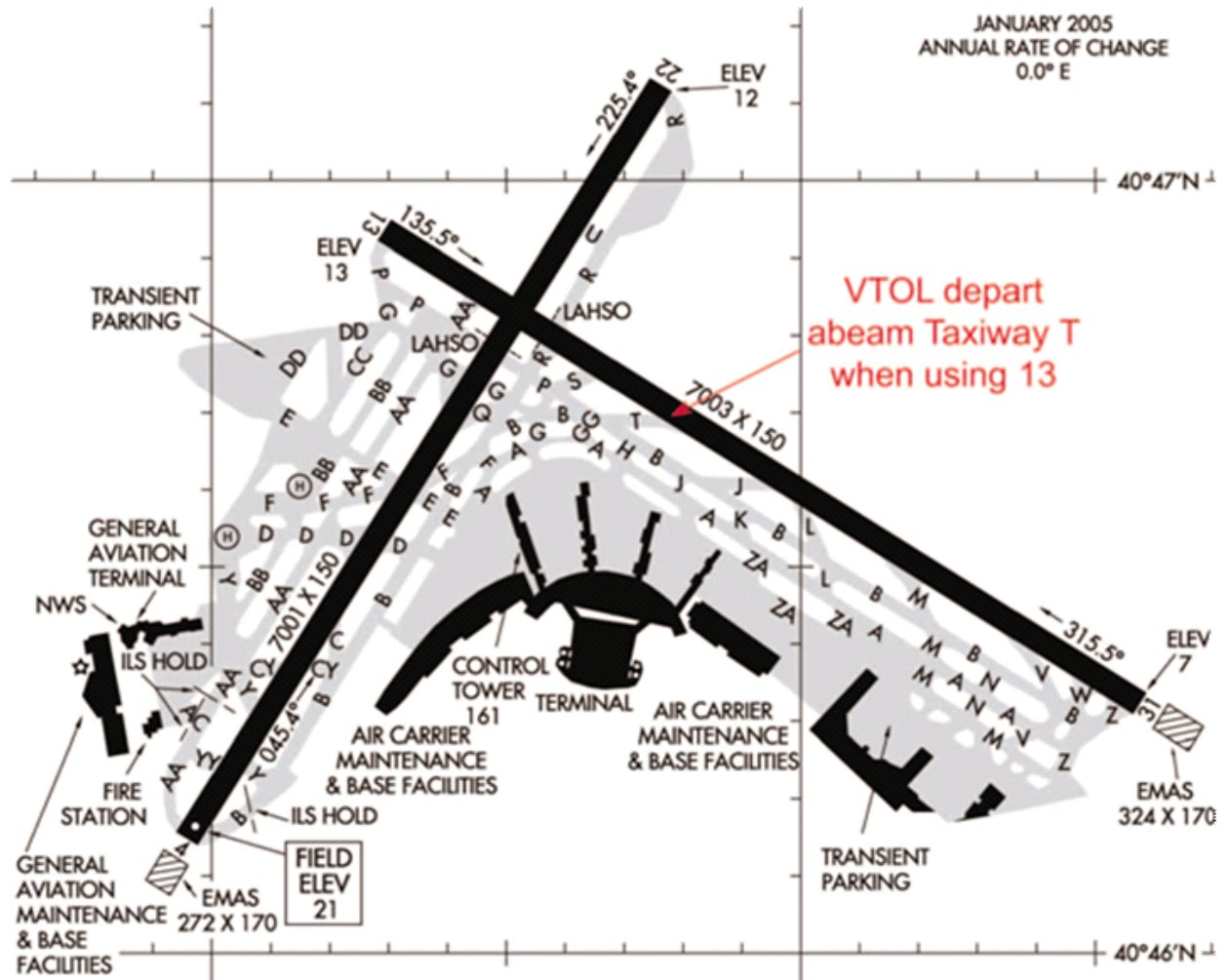


Figure 8-3 LCTR departure location from LGA runway 13

If LCTR aircraft are required to depart from a runway which is used for conventional aircraft or CESTOL for landing, depending on the length of the runway, spacing techniques will need to be used to ensure a safe operation. From calculations, it will take a LCTR aircraft 1.11 minutes to travel 3 nm from the start of its takeoff run. At this distance, it will be at an altitude of 2000 ft. The minimum time at the runway threshold between departures, considering two large category aircraft following each other, 2.5NM between them, at an approach speed of 130 knots, is 1.15 minutes. If it is certain a conventional/CESTOL aircraft will stop before the LCTR departure point, a simultaneous LCTR departure and conventional/CESTOL operation may be possible. More studies of this joint operation will be done through simulation.

Table 8-3 shows the various waypoints and restrictions on most LCTR departure procedures and was created using a trajectory analysis undertaken by the designers of the LCTR aircraft. The distances are from the beginning of the take-off roll.

Table 8-3. LCTR departure procedure waypoint restrictions

Waypoint	Distance (NM)	Altitude (ft)	Speed (kts) (IAS)
1	0.036	0	34
2	0.65	1000	40
3	3.6	2000	180
4	12	6000	180

8.3.6. *Supersonic Transports*

Supersonic Transports (SSTs) will be flying the same arrival and departure procedures as nominal aircraft, but due to their high descent and approach speeds they will need to be metered in order to maintain the required amount of spacing.

8.4. *Runway Configurations*

With regards to runway configurations, a separate project involves determining the optimum set of runway configurations based on a certain set of assumptions; but initially, the study will be based on configurations that are seen today (based data from the Performance Data Analysis and Reporting System [PDARS] that was provided by the ATAC Corporation). With this in mind, most configurations have separate runways for CESTOL aircraft and nominal aircraft, mainly due to the different types of arrival and departure procedures for each type as described later in this section. The main traffic flow pattern into each airport accounts for arrivals and departures from the Northwest, Northeast and Southwest as these directions represent the majority of traffic that is seen arriving into the New York airspace. Figure 8-4 shows a birds-eye view of the redesigned airspace; it can be seen that most of the tracks are near the four major airports: JFK, LGA, EWR and TEB.

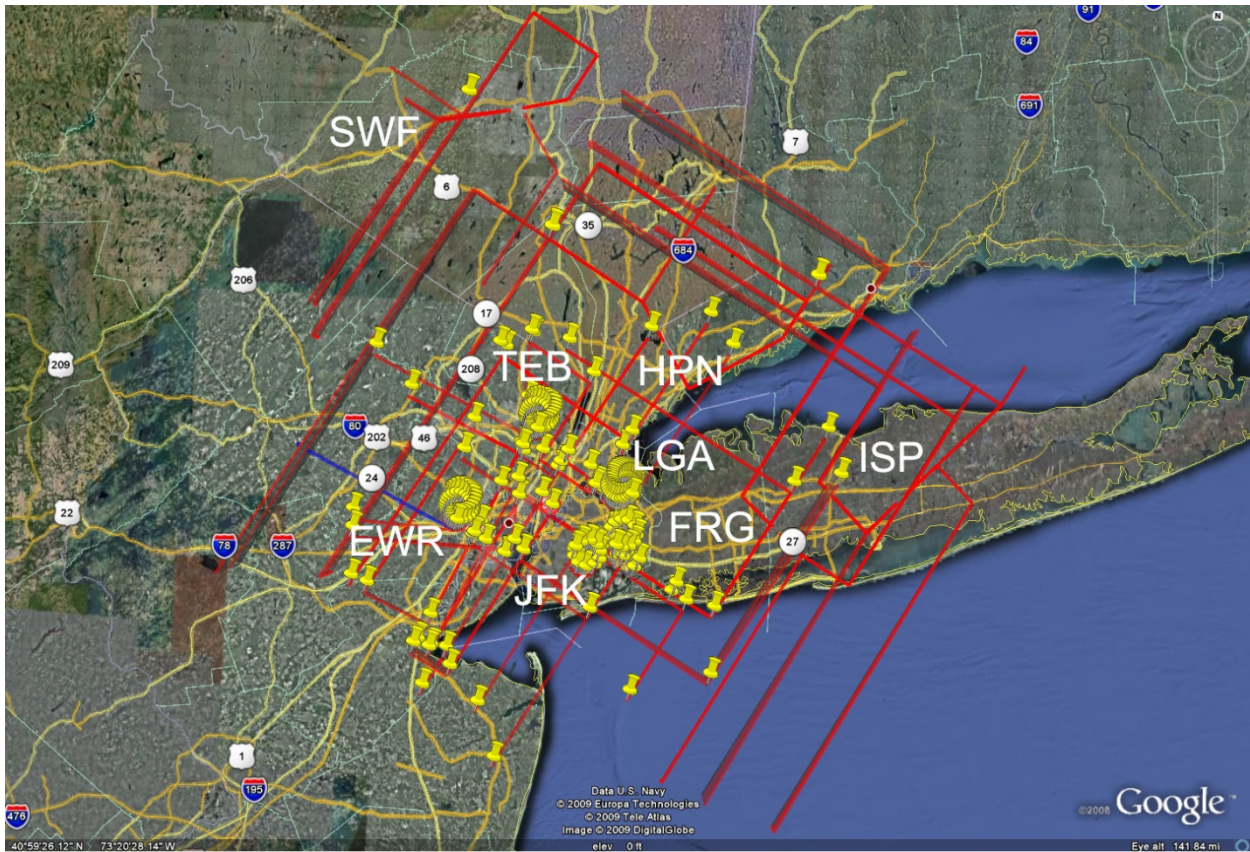


Figure 8-4. Zoomed in view of paths near JFK, LGA, EWR, and TEB

The four main configurations provided by ATAC are shown on the following two pages. If today's runway usage trends are followed, CESTOL operations for EWR will be primarily from runway 11. The balanced field length of the proposed CESTOL aircraft with a 500 nm range is 3020 ft, while the landing field length for an aircraft with 100 passengers at 210 lbs each is 3188 ft.² The length of runway 11 is 6800 ft, so it is theoretically possible to have one CESTOL aircraft to be cleared for departure while the other is on final approach to runway 11, requiring arriving and departing traffic to be spaced accordingly. At LaGuardia airport, CESTOL and nominal aircraft operations will be arriving and departing from the same runways, resulting in ATC having to space the flights appropriately. The same principle applies to JFK for runways 13L and 13R. At TEB and HPN airports, CESTOLs will have to use nominal departure paths due to space constraints, while for TEB, they will be arriving on the same runway as nominal traffic, and, like in LaGuardia's case, will need to be spaced properly. JFK, EWR, LGA, TEB, and SWF all required additional landing strips due to congestion at the airports, while LCTRs landing at HPN, ISP and FRG use existing runways. For departures, all LCTRs use existing runways, but have routes independent of other aircraft. As mentioned before, VLJs will use CESTOL procedures and supersonic aircraft will use nominal aircraft arrival and departure paths.

8.5. **Conclusion**

With new vehicles forecast to enter the NAS in the very near future, it is important to determine how all these vehicles will impact the NAS. To minimize this impact, it is essential to develop procedures such that all new vehicles will be able to fly in the most efficient manner. The New York metro area is one of the most congested today and is in dire need of an airspace redesign and for this reason, procedures have been developed incorporating these new vehicles with the goal to maximize airspace or runway throughput. A grid-like structure of procedures was created so as to be either parallel or perpendicular with the runways of the airports in New York which have the highest traffic density. Nominal aircraft arrivals would use a CDA procedure and would depart in the same manner they do today. For almost all the airports, CESTOL aircraft, due to their unique performance characteristics, will use spiral paths to arrive and depart. VLJ aircraft will also utilize the spiral procedures and LCTR aircraft will be at constant altitude toward their destination after which they will descend in segments to the airport, avoiding BVI at all times and will depart in the same manner (ascending in segments followed by a constant altitude till they exit the metro area airspace). Supersonic transports will fly on the same paths as nominal aircraft but will be metered in order to maintain the required separation between successive aircraft. The current runway configurations are being used, but it is possible that after the completion of another part of the project, a different set of configurations will be in use.

8.6. **References**

- 1 Administration, F. A., "Top 50 Busiest U.S. Airports 2007," January 2007.
- 2 Nam, T. and Ran, H., editors, PowerPoint Presentation -*CESTOL Concept and Initial Sizing Revision B*. ASDL, Ga. Tech, Atlanta, GA. 2008.

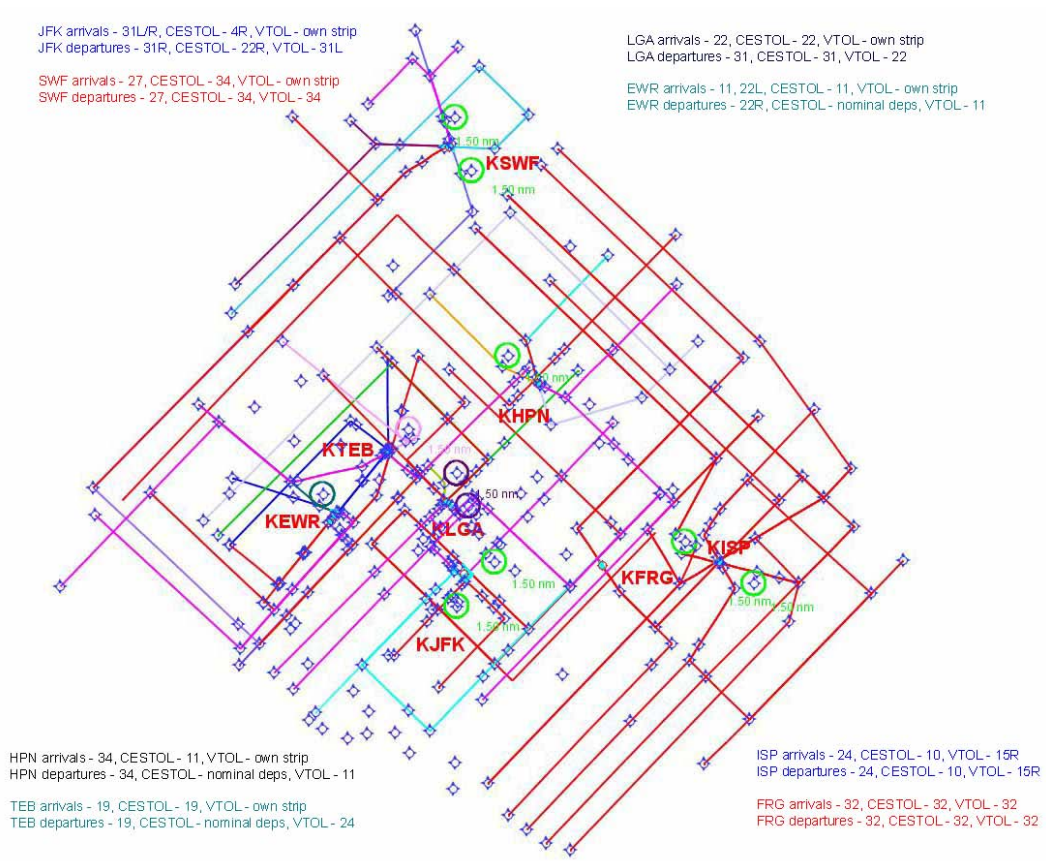


Figure 8-5. Runway Configuration 1

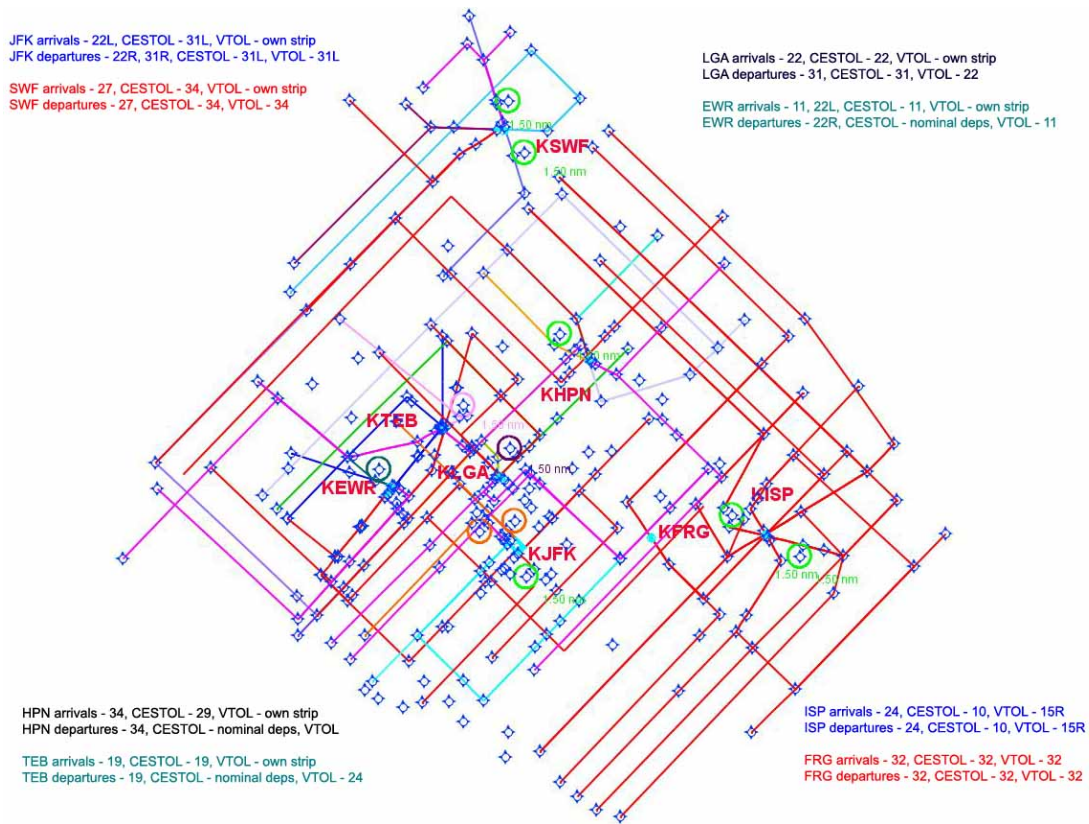


Figure 8-6. Runway Configuration 2

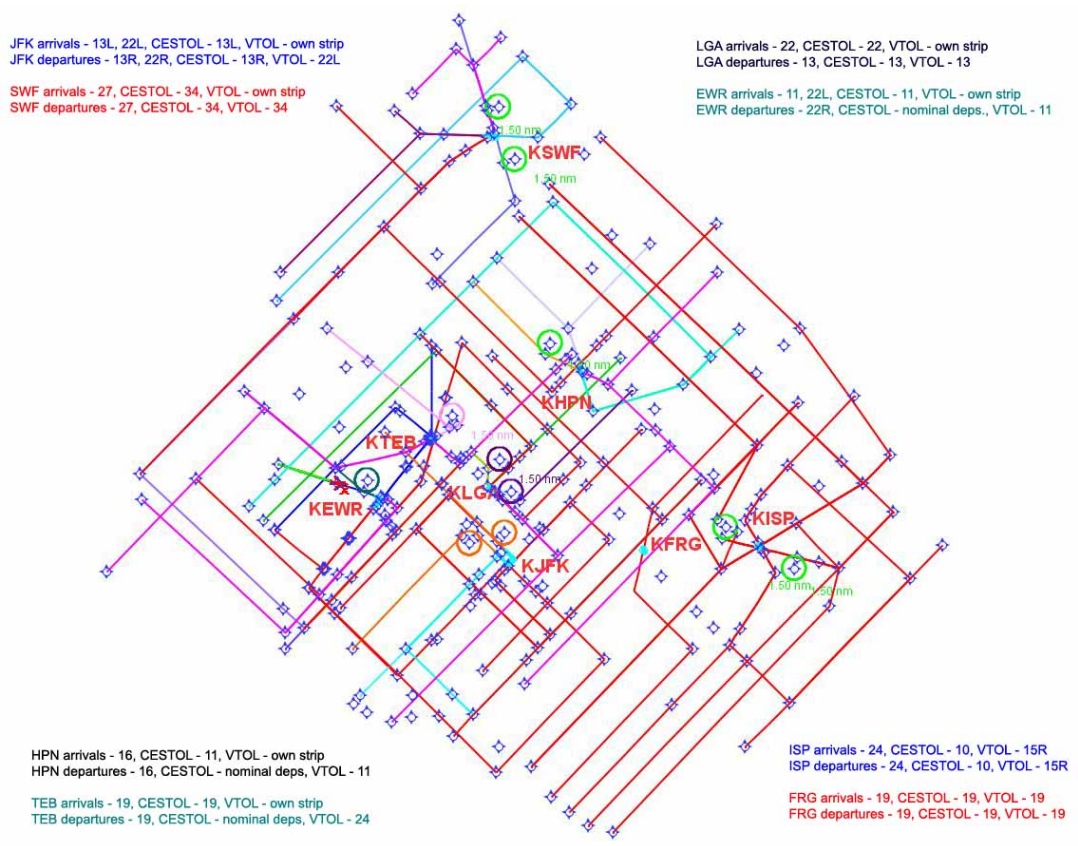


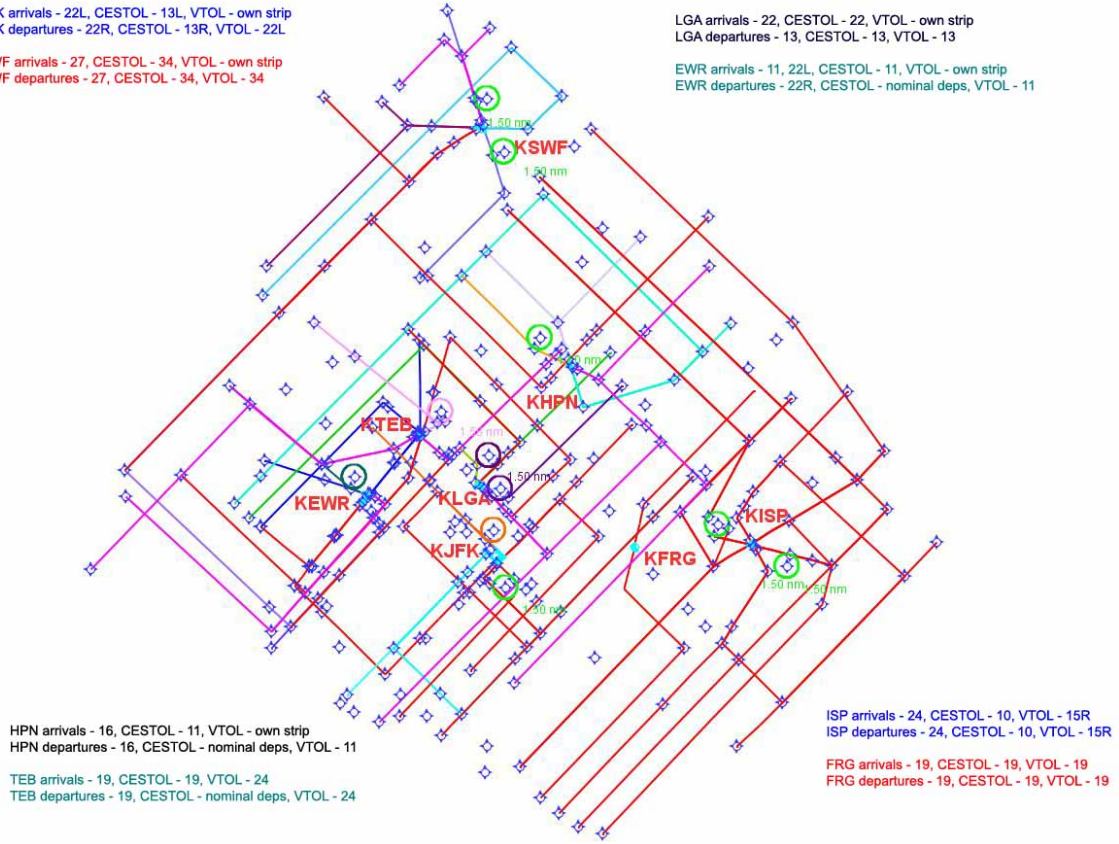
Figure 8-7. Runway Configuration 3

JFK arrivals - 22L, CESTOL - 13L, VTOL - own strip
JFK departures - 22R, CESTOL - 13R, VTOL - 22L

SWF arrivals - 27, CESTOL - 34, VTOL - own strip
SWF departures - 27, CESTOL - 34, VTOL - 34

LGA arrivals - 22, CESTOL - 22, VTOL - own strip
LGA departures - 13, CESTOL - 13, VTOL - 13

EWR arrivals - 11, 22L, CESTOL - 11, VTOL - own strip
EWR departures - 22R, CESTOL - nominal deps, VTOL - 11



HPN arrivals - 16, CESTOL - 11, VTOL - own strip
HPN departures - 16, CESTOL - nominal deps, VTOL - 11
TEB arrivals - 19, CESTOL - 19, VTOL - 24
TEB departures - 19, CESTOL - nominal deps, VTOL - 24

ISP arrivals - 24, CESTOL - 10, VTOL - 15R
ISP departures - 24, CESTOL - 10, VTOL - 15R

FRG arrivals - 19, CESTOL - 19, VTOL - 19
FRG departures - 19, CESTOL - 19, VTOL - 19

Figure 8-8. Runway Configuration 4

9. New York Metroplex Analysis

This section presents the results of an analysis of the New York Metroplex terminal airspace. It describes the modeling tools, the development of the airspace structure, modeled NextGen runway and terminal airspace procedures, and additional details about an off-nominal scenario. The analysis was conducted using the publicly available Airport and Airspace Simulation Model (SIMMOD) version 3.1^{cvi} and the FAA's Aviation Environmental Design Tool (AEDT). SIMMOD was used to compute the airspace, airport and vehicle operating performance while AEDT was used to compute the environmental impacts.

9.1. *SIMMOD*

SIMMOD is a fast-time, Monte-Carlo, discrete-event simulation model that tracks the movement of individual aircraft as they travel through the airspace and on the ground. The ability of the model to provide realistic results under complex operating conditions has been confirmed repeatedly in a number of airport and airspace simulation studies^{cix}. SIMMOD uses a node-link structure to represent the gate/taxiway and runway/airspace route system. Input parameters include traffic demand and fleet mix, route structures (both in the airspace and on the airport surface), runway use configurations, separation rules and control procedures, aircraft performance characteristics, airspace sectorization, and interactions among multiple airports.

Based upon a user-input scenario, SIMMOD tracks the movement of individual aircraft through an airport/airspace system, detects potential violations of separations and operating procedures, and simulates air traffic control actions required to resolve potential conflicts. The model properly captures the interactions within and between airspace and airport operations, including interactions among multiple neighboring airports.

The 4-D aircraft trajectories produced by SIMMOD are then used as input to compute fuel burn and the full complement of emissions results, including CO₂, CO, NO_x, and particulate matter, as well as noise contours in the vicinity of the airports. Airspace delay in the SIMMOD trajectories were captured for the fuel burn and emissions calculations. However, the airspace delay close to the airports was assumed to be minimal, and was not included in the noise contour calculations.

9.2. *Airspace Modeling*

Two airspace route structures were developed for this research. The first structure reflects current day operations and includes the numerous interactions between the arrival and departure procedures for eight modeled airports. This structure was calibrated against historical operations and was incorporated into the second configuration as described later in the paper. The second airspace structure is a fully decoupled system where each arrival fix and airport combination has unique procedures so that only aircraft going to or departing from the same airport interact with each other. It should be noted that the airspace representation and procedures outlined herein are hypothetical and not representative of any actual airspace design underway or planned to be implemented. These procedures serve as an example of how

new vehicles might operate in the distant future when NextGen is fully implemented and are therefore useful for research purposes. The NextGen configuration was the basis for all operating comparisons presented in this paper.

9.2.1. Current-Day Airspace Modeling

The current-day airspace route structure was developed in SIMMOD using radar flight track and flightplan data extracted from the FAA's Performance Data Analysis and Reporting System (PDARS)^{cx}. The selected day (19 March 2007) represents typical flight operations in the Metroplex. Four runway plan changes made during the day were included in the overall simulation model. Although this significantly increased the model's complexity, it was necessary to include them to better reflect the noise impacts of the advanced vehicles in the vicinity of the airport. The airports modeled in SIMMOD include the four primary airports: JFK, Newark (EWR), LaGuardia (LGA) and Teterboro (TEB); and four secondary airports, including Farmingdale (FRG), White Plains (HPN), Islip (ISP) and Stewart (SWF). The details of each airport's runway configuration will be discussed in further detail in later sections.

The airspace boundary of the SIMMOD model encompasses all of the airspace within the radar coverage of the N90 TRACON. The PDARS flight paths of all aircraft were grouped by their runway-fix combination. Then, a route which is representative of the nominal flight trajectory was defined. Routes for turbojet and turboprop aircraft were segregated and routes were built for each group. Special attention was paid to route convergence and divergence points in order to capture airspace interactions. In order to accurately represent the 4-D trajectories in SIMMOD, the aircraft speeds by weight class were also considered. This was done by incorporating the PDARS aircraft speeds by weight class for each of the routes into the model. Locations of holding patterns and regions where aircraft were vectored to absorb delay were included in the model. Figure 9-1 presents the arrival and departure route structure modeled in SIMMOD for the current day conditions (arrival - green and departure - red).

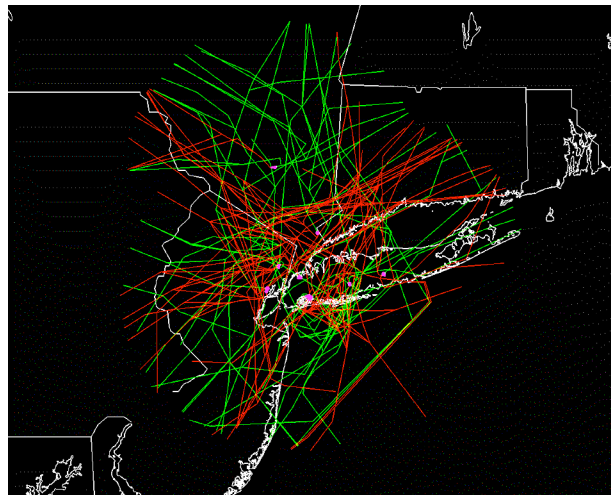


Figure 9-1. N90 current airspace route structure.

The modeled flight demand used for calibrating the model was based on flights that occurred on the representative day. Only arriving and departing flights for the eight modeled airports were considered in the demand schedule.

Aircraft arriving to one of the eight modeled airports were injected into the simulation based on the time they first appear in the radar data. For departures within the Metroplex, radar flight paths typically begin when an aircraft is above approximately 200 feet AGL. To account for this, departure injection times were adjusted for the time it takes to taxi from the gate to the departure queue, perform the takeoff and climb to 200 feet AGL.

9.2.2. Current-Day Airspace Calibration

After the current-day airspace model was developed, its performance was calibrated against the PDARS radar data. The primary metrics used for calibration were runway throughput, and arrival and departure transit times. The transit times and runway throughput for each runway-departure/arrival fix combination were compared between the simulated results and what was observed in the radar data. As a secondary comparison, transit times by aircraft weight class were made to ensure that any differences were accurately accounted for in the model.

Figure 9-2 presents the average departure flight duration per route on the most commonly used routes on the left axis. The number of flights for each route is also provided as reference on the right axis. The error bars shown in Figure 9-2 represents the half-sigma standard deviation from the average. As the chart shows, the departure transit times for the most commonly used routes are within a half-sigma from the PDARS radar data. Average flight durations in SIMMOD that fall outside of the PDARS range are generally the routes that are least flown.

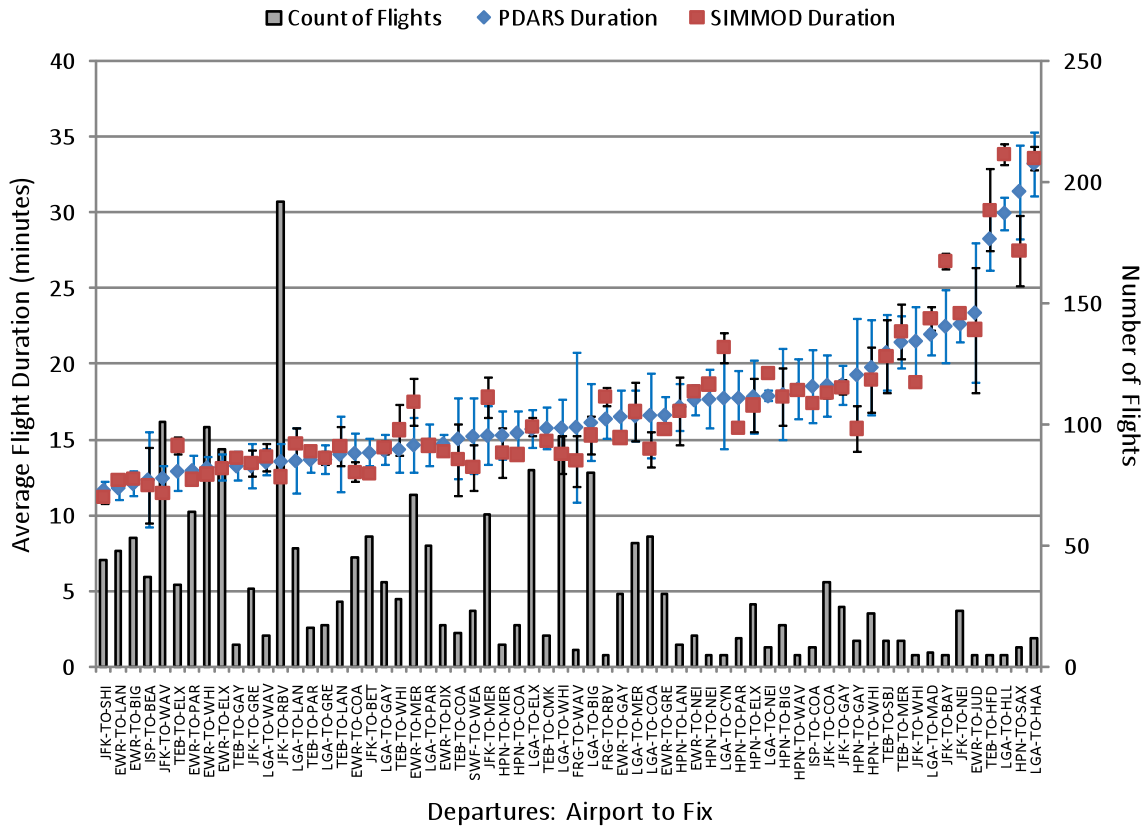


Figure 9-2. Average departure flight duration.

Similarly for arrivals, Figure 9-3 presents the average arrival flight duration per route on the most commonly used routes. The number of flights for each route is provided as reference.

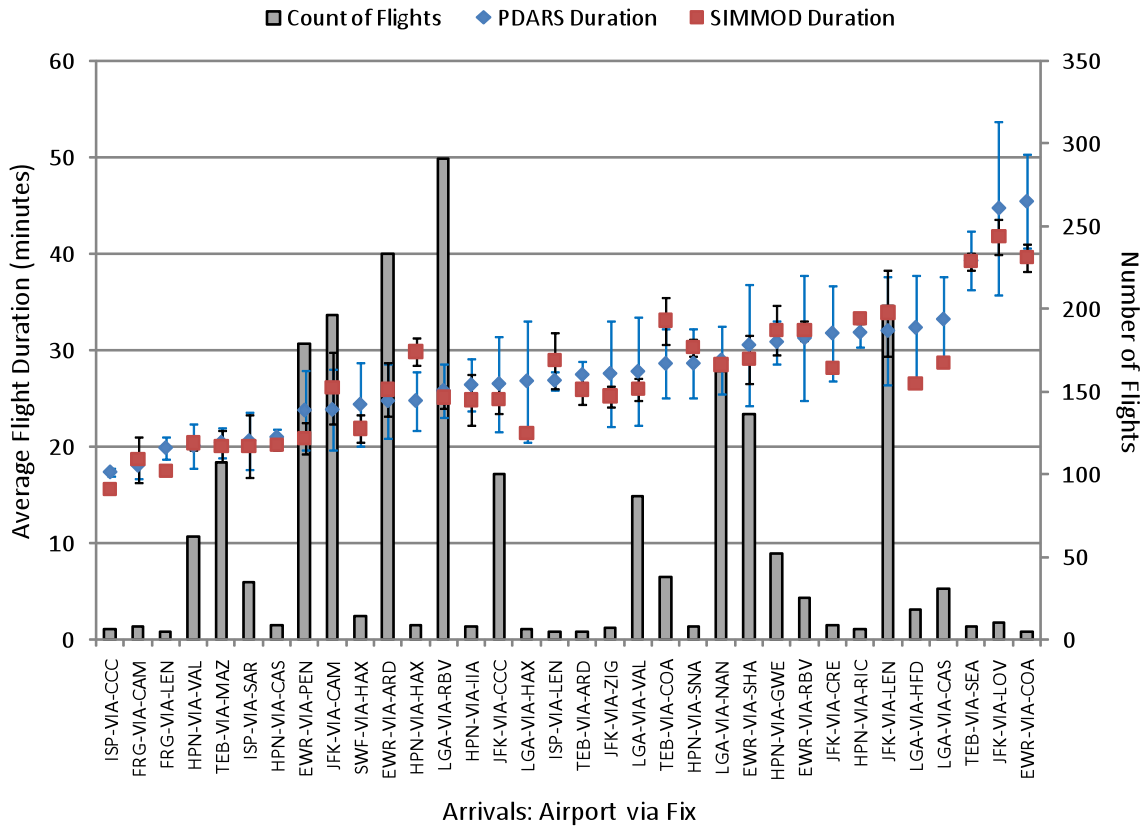


Figure 9-3. Average arrival flight duration.

For the four busiest airports in the metroplex (EWB, JFK, LGA, and TEB), the flight duration was also measured in terms of weight class. Figure 9-4 presents a comparison between the PDARS radar data and the SIMMOD simulation of the total flight duration per weight class in each of the airports.

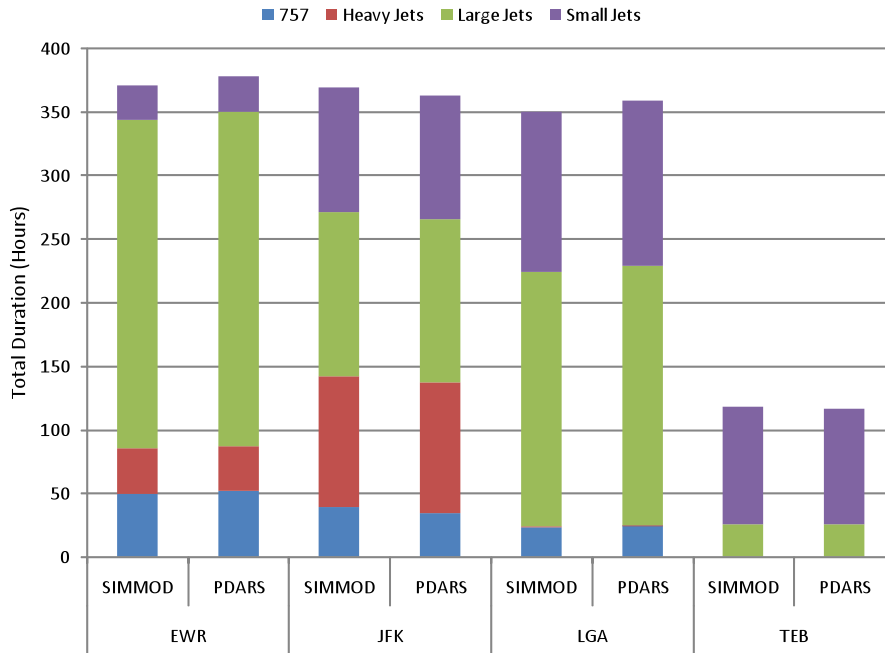


Figure 9-4. Total flight duration comparison.

In addition to flight duration, the runway throughput was also calibrated. Figure 9-5 and Figure 9-6 present the SIMMOD cumulative arrival and departure throughput for the four busiest airports compared against the cumulative throughput in the PDARS radar data respectively. As can be observed from the charts, there are no significant differences between the actual and modeled runway throughput.

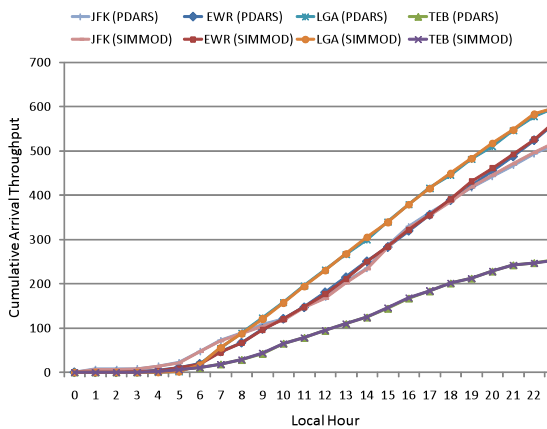


Figure 9-5. Cumulative arrival throughput comparison.

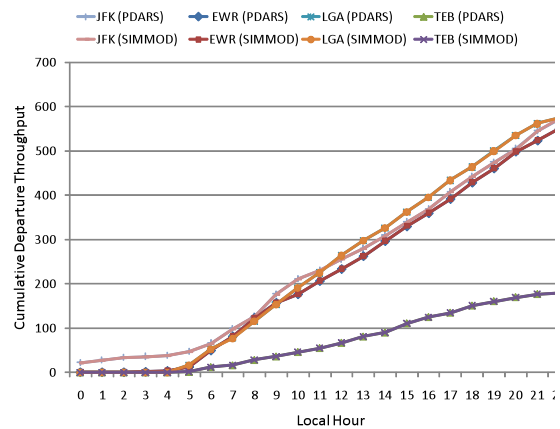


Figure 9-6. Cumulative departure throughput comparison.

Additional calibration data are available in the Electronic Appendix of Results included with this paper.

9.2.3. NextGen Airspace Modeling

A second simulation model was developed to study the potential impacts of NextGen technologies and procedures. The SIMMOD NextGen airspace structure was constructed by combining the current-day airspace structure with the local NextGen airspace designed by Georgia Tech University.

The geographic coverage of the local NextGen airspace was limited to within approximately 20 nm of the eight modeled airport. This design provided the “inner” airspace of the model while the current day routes were connected to the various entry and exit points of the inner airspace to provide coverage for the entire Metroplex airspace. In addition, all routes outside of the inner airspace were decoupled, thus eliminating any airspace interactions between airports. Speed and altitude profiles were adjusted to reflect a continuous descent and deceleration for arrivals and continuous ascent and acceleration for departures. Figure 9-7 presents the modeling steps involved in the development of the NextGen airspace model.

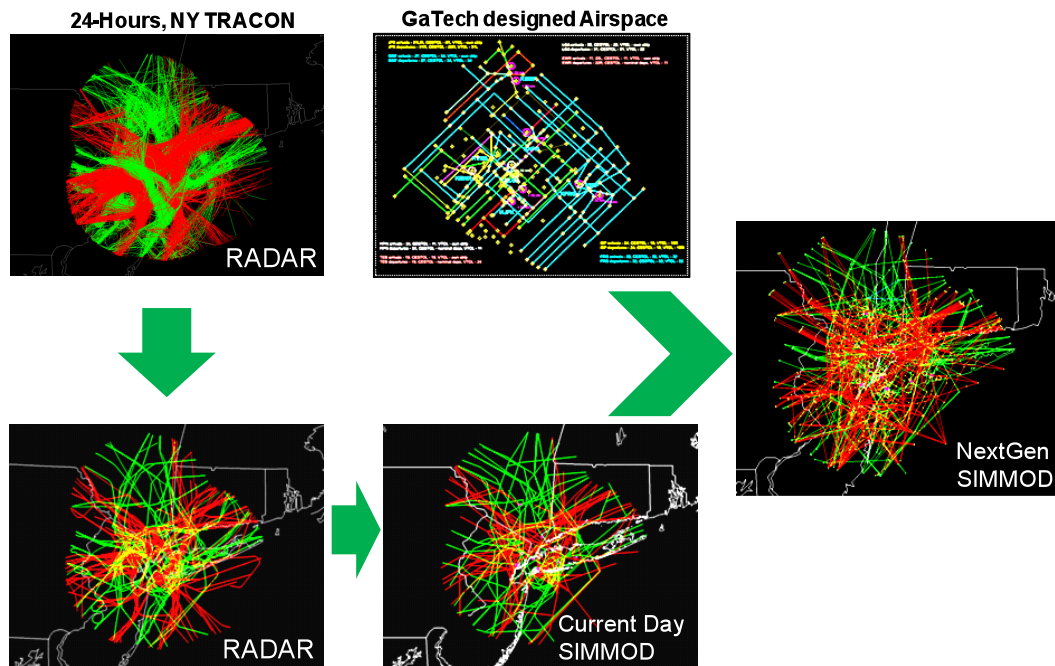


Figure 9-7. NextGen airspace model development.

Overall, the most important characteristic of the NextGen airspace is that all routes are decoupled from each other. Procedures associated with each airport-arrival/departure fix combination do not interact with each other. This significantly simplifies the airspace operations since flights at one airport do not affect the operations at another airport.

9.2.4. NextGen Procedures

In addition to the decoupled airspace, new procedures are included to exploit the capabilities of the advanced vehicles to fly unconventional approaches and departures. The first example of these are the spiral departure procedures developed for the CESTOL and VLJ aircraft as shown in Figure 9-8. The spiral departures allow CESTOL and VLJ aircraft to climb quickly after takeoff, which permits trailing

departures to takeoff sooner. The CESTOL and VLJ departure procedure begins its spiral climb approximately 3 nm away from the end of the runway and ends at 10,000' MSL. The climb is accomplished by turning within a 1.5 nm radius circle, and requires approximately 1.5 turns to reach 10,000'. After this spiral climb, the aircraft continue their climb unimpeded to cruise altitude and the enroute airspace. Furthermore, CESTOL and VLJ aircraft use their capability to takeoff in shorter distances allowing the use of midfield departures in certain circumstances which further minimize their interaction with conventional traffic. These procedures are essential in minimizing the impact of CESTOL and VLJ aircraft on the rest of the conventional aircraft fleet.

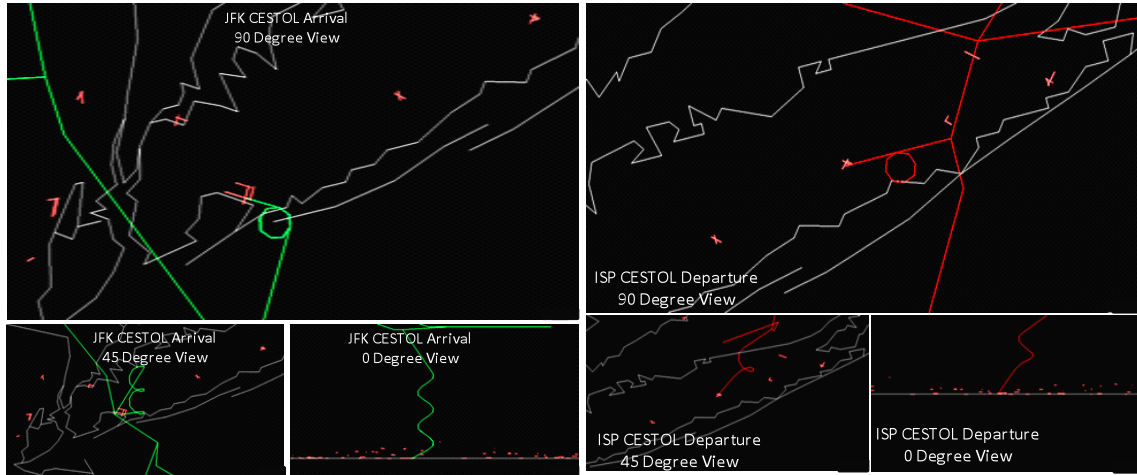


Figure 9-8. CESTOL and VLJ spiral arrival procedure (left) and departure (right).

CESTOL and VLJ aircraft also use spiral arrival procedures. These arrival procedures are nearly identical to the departure procedures, just flown in reverse. They start at 10,000' and utilize a 1.5 nm radius spiral that ends within 3 nm of the runway at 1,000' where it merges with the conventional approach procedure. With a 5.5 degree glide slope, it takes the aircraft approximately two turns to complete its descent in the spiral. Although this procedure provides a benefit by segregating the slower moving CESTOL and VLJ aircraft from the rest of the traffic, the aircraft are penalized by having to travel an additional 20 nm during their spiral descent.

The procedures developed for the LCTR aircraft are also designed to limit their interaction with other traffic. During forward flight, LCTRs fly similarly to turboprop aircraft. However, during their transition from forward flight to vertical flight they significantly interfere with conventional aircraft procedures. Since the vertical flight mode does provide the LCTR with minimal takeoff and landing rolls, departure procedures were designed to use the very end of runways, away from conventional operations. To further segregate LCTRs from conventional traffic, 600 foot landing strips were added, where space permitted, at modeled airports.

9.3. Runway Configuration Procedures

As previously mentioned, four runway configuration plans were included in this model. Plan changes occur at 01:00 (Plan 1), 09:00 (Plan 2), 13:00 (Plan 3), and 18:00 (Plan 4). This section provides a detailed description of the different runway configurations in the eight modeled airports.

9.3.1. JFK

Figure 9-9 presents the four runway configurations at JFK using a color-coded legend (the same legend is used for all subsequent runway configuration figures). During Plan 1, conventional aircraft arrivals to 31R block conventional departures to the same runway, as well as CESTOL departures from 04L. CESTOL departures from 04L are also sequenced with departures from 31R. It is also important to note that due to the CESTOL's ability to depart midfield from Taxiway H, arrivals to 31L do not block its operations. CESTOL arrivals to 04R, however, are sequenced with conventional arrivals to 31L. Lastly, LCTR arrivals to the landing strip are unimpeded by other traffic throughout the simulation day.

During Plan 2, conventional departures from 31R and 22R are sequenced, while conventional arrivals use 22L. CESTOL and VLJ departures are mixed on runway 31L. Again, taking advantage of the capabilities of the advanced vehicles, CESTOL departures take off from Taxiway N, which allows for simultaneous departures from 22R and 31L.

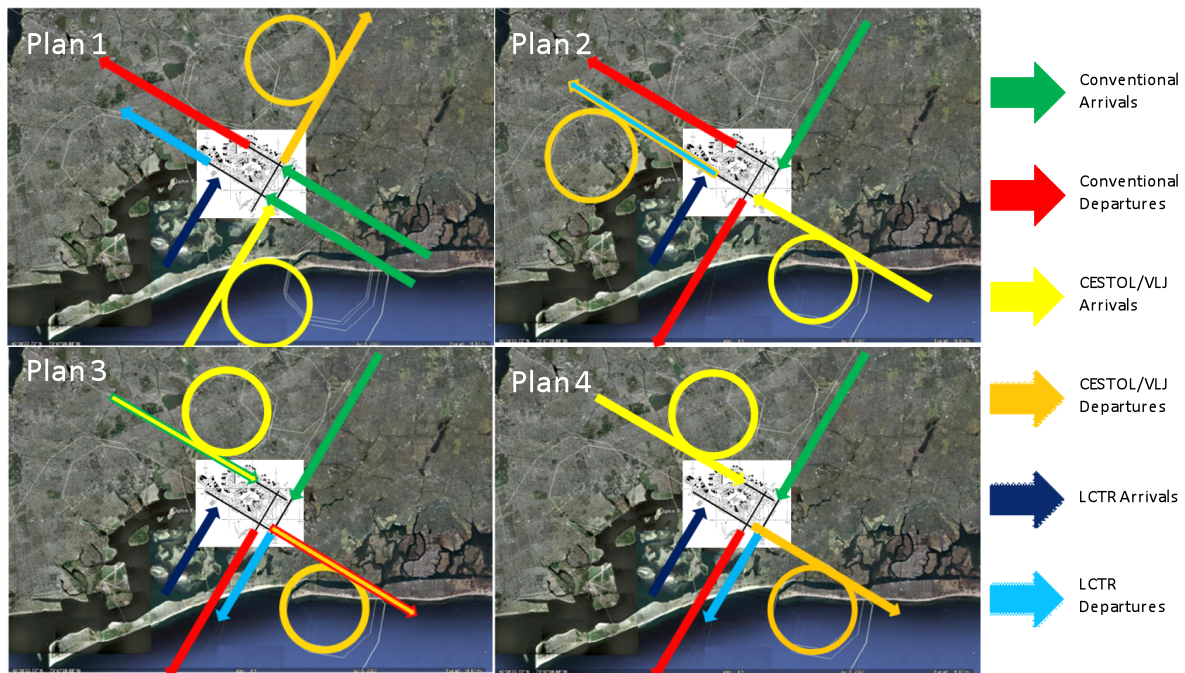


Figure 9-9. Modeled runway configurations at JFK.

During Plan 3, there are mixed CESTOL and conventional arrival and departure procedures on 13L and 13R respectively. As previously mentioned, CESTOL spiral procedures allow for minimized interaction with conventional traffic. CESTOL arrivals to 13L are merged with conventional traffic about 1.5 nm from the runway threshold. Similarly, for departures from 13R, CESTOLs depart midfield from Taxiway N, and turn into the spiral 3 nm away from the runway threshold. LCTR departures are now moved to 22L, where they are segregated from other traffic soon after takeoff.

Plan 4 is similar to Plan 3, but 13L and 13R are limited to CESTOL operations only.

9.3.2. EWR

EWR's runway configuration remains constant throughout the simulation day. Conventional departures use runway 22R, while arrivals use runways 11 and 22L as shown in Figure 9-10.

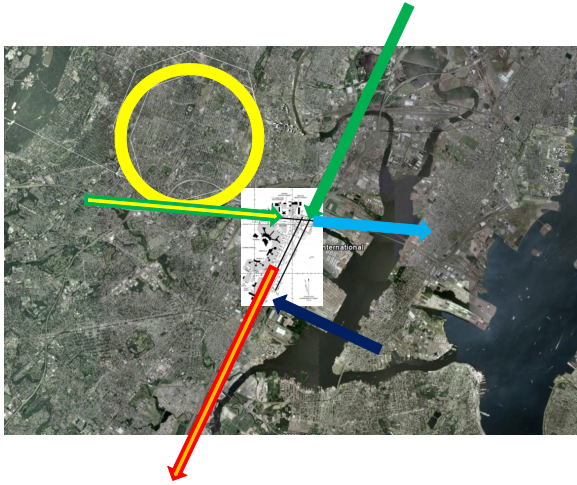


Figure 9-10. Modeled runway configuration at EWR.

Due to runway 11's short length, arrivals to this runway are limited to small aircraft only. Arrivals to this runway land and hold short allowing for unimpeded departure operations on Runway 22R. Runway 22L is the main arrival runway, accounting for more than 90% of all conventional arrival operations. Runway 22L is independent of the other runways, allowing for continuous arrival operations.

With the addition of advanced vehicles, Runway 11 is more utilized. CESTOL arrivals use this runway without hindering 22R departures. LCTR departures also use runway 11, but they are sequenced with 22R departures and blocked by 22L arrivals. The advantage of LCTRs using this runway, however, is that they are segregated from all other traffic after takeoff. It is also important to note that due to airspace constraints, CESTOL departures from 22R do not utilize spiral procedures. The CESTOL's slower takeoff speeds add some extra delay to operations to ensure that there is proper aircraft separation after takeoff.

9.3.3. LGA

LGA has two modeled runway configurations as shown in Figure 9-11. As can be observed in the figure, LGA does not have underutilized runways, which forces more interaction between conventional and advanced vehicles. Since advanced vehicle procedures are mixed with conventional traffic, the CESTOL spiral arrival and departure procedures become essential in minimizing delay caused by their slower takeoff and landing speeds. Additionally, CESTOL departures on Runway 13 during Plan 3 and Plan 4 take off midfield on Taxiway T to avoid interaction with arrivals to Runway 22. LCTR departures on Runway 13 also take off midfield on Taxiway W.



Figure 9-11. Modeled runway configurations at LGA.

Although LCTR arrivals to LGA are segregated from other arrivals, they block departures from Runway 31 during Plan 1 and Plan 2. Furthermore, during Plan 3 and Plan 4, the mixed LCTR, CESTOL and conventional vehicle departure procedures on Runway 13 increase departure queue delay.

9.3.4. TEB

TEB has a single runway configuration throughout the simulation day as shown in Figure 9-12. Similar to EWR, airspace constraints do not allow for spiral departure procedures for advanced vehicles. CESTOLs and VLJs depart using conventional procedures, which causes some added delay due to their slower takeoff speeds. In contrast, LCTR departures utilize Runway 24, and are completely independent of other operations.

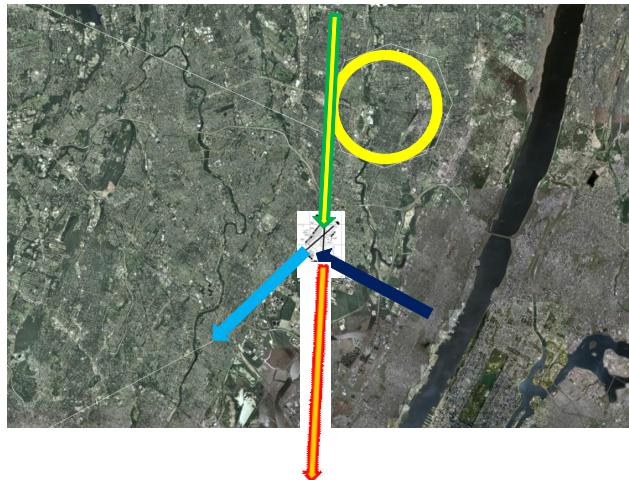


Figure 9-12. Modeled runway configuration at TEB.

For arrivals, CESTOLs and VLJs use spiral arrival procedures, and are merged in with conventional traffic 3NM away from the runway threshold. Since LCTR arrivals to the landing strip overfly Runway 19, their arrival procedure blocks Runway 19 departures, which adds to the departure queue delay.

9.3.5. FRG

FRG has two runway configurations as shown in Figure 9-13. Unlike the other modeled airports, no added procedures for advanced vehicles were added to this airport. All aircraft operate under conventional procedures on Runway 32 during Plan 1 and Plan 2, and Runway 19 during Plan 3 and Plan 4.

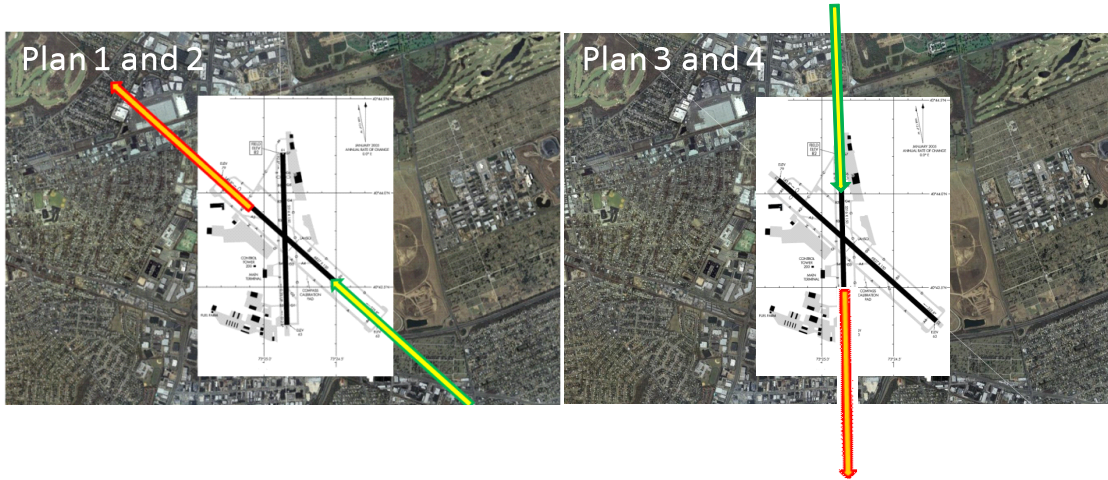


Figure 9-13. Modeled runway configuration at FRG.

FRG has very little demand in all future scenarios, and FRG's close proximity to JFK limits the available airspace for additional advanced vehicle procedures.

9.3.6. HPN

Figure 9-14 presents the modeled runway configurations at HPN. CESTOL and VLJ departures use conventional procedures and are mixed with conventional traffic. LCTR departures use Runway 11, but must be sequenced with traffic on Runway 16 and 34.



Figure 9-14. Modeled runway configurations at HPN.

For arrivals, CESTOLs and VLJs use runway 11, but must be sequenced with other arrivals due to the crossing runway. Additionally, LCTR arrivals to the landing strip, located north of the airport, are sequenced with CESTOL and conventional vehicle traffic.

9.3.7. ISP

ISP is the best example of the benefits of exploiting the capabilities of advanced vehicles. All conventional and advanced vehicle operations are segregated in the airspace, and many runways are utilized as shown in Figure 9-15. LCTR operations on Runway 15 are independent of conventional vehicle operations on Runway 24.

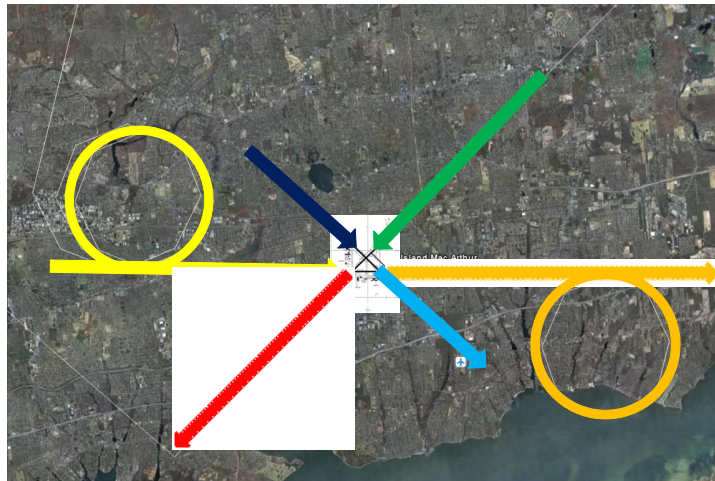


Figure 9-15. Modeled runway configuration at ISP.

CESTOL and VLJ operations on Runway 10 have some interaction with conventional vehicle and LCTR traffic, but are unimpeded in the airspace.

9.3.8. SWF

Lastly, SWF has one runway configuration throughout the simulation day as shown in Figure 9-16. Like the ISP runway configuration, advanced vehicle traffic is segregated from conventional traffic by using Runway 34 and an added landing strip for LCTR arrivals. The LCTR landing strip is located south of Runway 27.

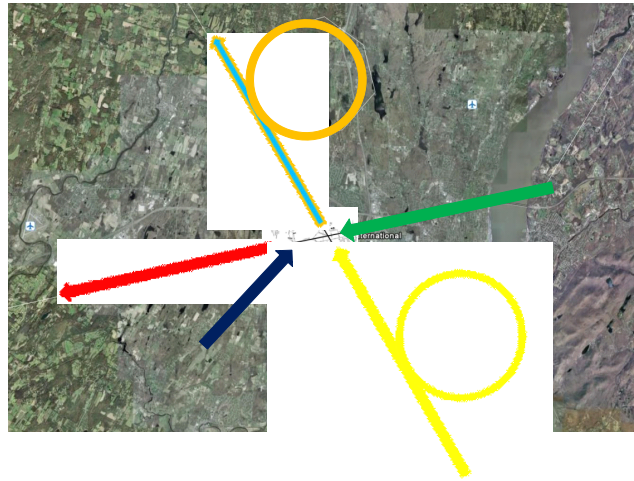


Figure 9-16. Modeled runway configuration at SWF.

CESTOL and VLJ arrivals to Runway 34 block conventional departures from Runway 27, and are sequenced with conventional arrivals. The mixed CESTOL, VLJ, and LCTR departures from Runway 34 are sequenced with conventional departures from Runway 27, but are segregated after takeoff.

9.4. *Off-nominal Modeling*

The purpose of modeling off-nominal operations within the metroplex was to determine if the advanced vehicles provide any benefit during the off-nominal conditions or during the recovery from them. The off-nominal conditions modeled for this effort are convective storm cells moving through the NY Metroplex.

Modeling the dynamics of the movement of storm cells through a block of airspace and the corresponding effects on flight operations is exceptionally complex. In addition, SIMMOD does not have any direct way to model the movement of the storm cells or their impacts. However, through various simplifying assumptions and clever implementations of the capabilities of SIMMOD, a reasonable representation of the storm cell impacts was developed. The modeling of the storm cells started with the actual storm cell tracks (time and position) during a 24-hour period from 27 June 2005. The main assumption was that any aircraft traveling towards a storm cell on a route that passes through a 10 nm by 10 nm region encompassing the center of a storm cell are blocked and incur airspace delay until the cell passes far enough away such that the route no longer falls within the cell's impact zone. This airspace delay is representative of aircraft holding or vectoring due to the storm cell. As the storm cells move across the terminal airspace, different flights paths are blocked and correspondingly unblocked, which

frees up the movement of holding aircraft and forces others to hold. Aircraft already below 3,000' MSL and close to final approach are allowed to land.

Aircraft that are on the ground, awaiting departure, are blocked if a storm cell is currently blocking their planned flight path. Using this method, departure ground delay and arrival air delay can be tracked separately for analysis. Figure 9-17 presents the NextGen airspace flight tracks along with the modeled storm cell tracks.

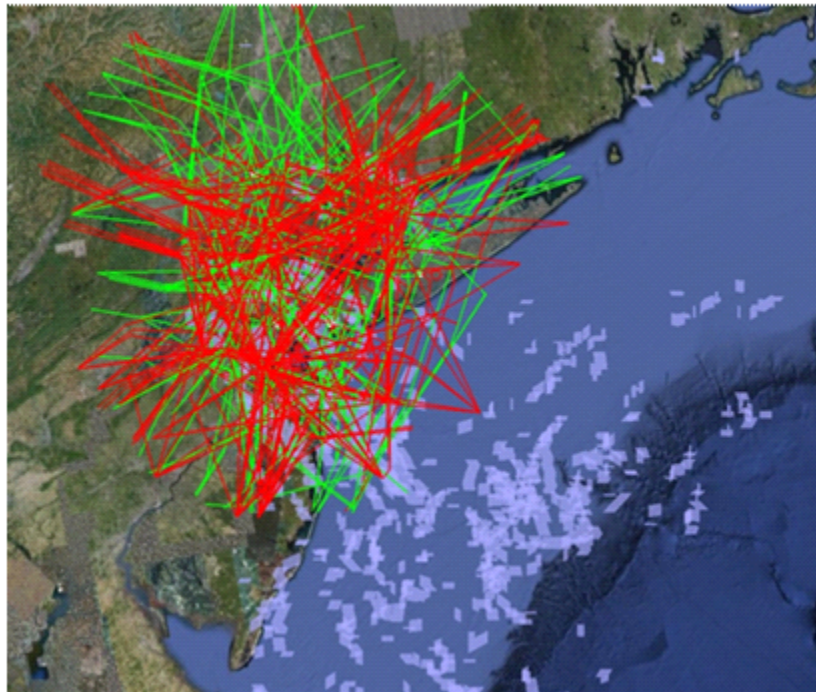


Figure 9-17. NextGen airspace flight and storm cell tracks.

9.5. Additional Modeling Details

This section presents additional modeling parameters that affect the simulation results.

9.5.1. Effects of Multiple Iterations

As previously mentioned, SIMMOD is a Monte-Carlo simulation model. In order to observe the variability in the output of multiple iterations, a 100-iteration simulation was run, and the average overall delay was calculated for each of the iterations as shown in Figure 9-18. The range in the average delay in all 100 iterations was 9 seconds.

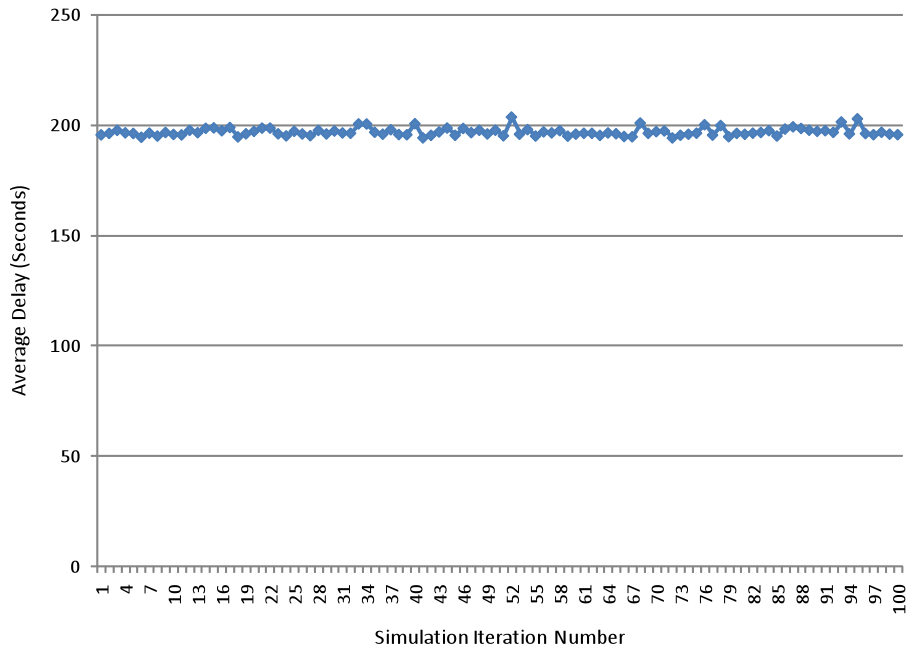


Figure 9-18. Average delay for 100-iteration simulation.

It was found that although the delay for a single flight varied from one iteration to another, the average delay does not vary significantly. It was thus decided that five iterations would be adequate in the analysis. All results presented in this paper are from 5-iteration simulation runs. For AEDT flight trajectories however, only the first iteration was used as input.

9.5.2. Lateness Distribution

Utilizing SIMMOD’s Monte Carlo simulation capabilities, an arrival lateness distribution, taken from the *Portland International Airport Data Package Number 3 Airport Capacity Enhancement Plan Phase II Terminal Location Study*^{cx1}, was included in all simulation runs. This lateness distribution allows for arrivals to appear in the TRACON boundary up to 20 minutes early or as late as 60 minutes, as shown in the probability distribution shown in Table 9-1.

Table 9-1. Arrival lateness probability distribution.

Number of minutes by which actual arrival time would exceed scheduled arrival time	Distribution of aircraft lateness (cumulative %)
-20	0.0%
-15	4.7%
-2	31.5%
0	52.6%
5	70.3%
10	83.6%
15	94.3%
30	95.9%
45	98.4%
60	100.0%

This table reads as follows:

- 0% arrive at the boundary more than 20 minutes early
- 4.7% (4.7% - 0%) arrive between 15 and 20 minutes early
- 26.8% (31.5% - 4.7%) arrive between 2 and 15 minutes early

This lateness distribution allows for variability in the sequence of arriving aircraft, which is important in the analysis of the interactions between advanced and conventional vehicles.

9.5.3. Turn-around Time for Tail-Connected Flights

Leveraging data from the same Portland Study, the turn-around time for each aircraft group was included in the model. Tail-connected arrivals taxi to a gate and hold for a length of time representative of the average turn-around time for their aircraft group using the distribution shown in Table 9-2, before they allowed to depart. Late arrivals resulting in subsequent late departures are accounted for in the model.

Table 9-2. Minimum Turn-around times in minutes with the cumulative probability distribution.

Heavy		757		Large Jet		Large Turboprop		Small +		Small	
min.	cum. prob.	min.	cum. prob.	min.	cum. prob.	min.	cum. prob.	min.	cum. prob.	min.	cum. prob.
60	0.79	45	0.92	20	0.20	20	0.07	20	1.00	10	0.16
90	1.00	50	1.00	25	0.25	30	0.97			15	0.56
				30	0.50	40	1.00			20	0.64
				35	0.64					25	1.00
				40	1.00						

9.6. *Metroplex Demand*

The following sections describe NY Metroplex demand in the modeled airports for each of the scenarios. The demand for the eight Metroplex airports was taken from the systemwide demand sets described in the Demand Generation section of this report. The trajectory for each flight was assigned based on their origin-destination pair and aircraft type.

9.6.1. *VLJ Demand*

As described in Section 6, the VLJ demand sets were generated by adding VLJ flights directly to the baseline demand. The additional VLJ demand constitutes approximately 2.5% of all demand in the metroplex and is located at smaller airports (TEB, HPN, FRG, and SWF) where demand is below their maximum capacity. Table 9-3 presents the number of conventional and VLJ aircraft in the baseline and VLJ demand sets.

Table 9-3. Number of flights by vehicle type in the baseline and VLJ demand sets.

	Baseline Demand			VLJ Demand		
	2025	2040	2086	2025	2040	2086
Conventional Vehicles	5,221	5,544	6,014	5,221	5,544	6,014
VLJ	0	0	0	130	154	154
Total	5,221	5,544	6,014	5,351	5,698	6,168

Figure 9-19 presents the VLJ demand in the small airports. For the flights at the individual airports, the VLJ demand constitutes between 2% and 30% increase. The airport that showed the greatest percentage increase was at FRG in the 2040 demand schedule, which had a 30% increase in the number of flights. The airport that received the most VLJ flights overall was HPN, with a total of 60 VLJ flights. The airport with the most VLJ flights was TEB in the 2086 demand year.

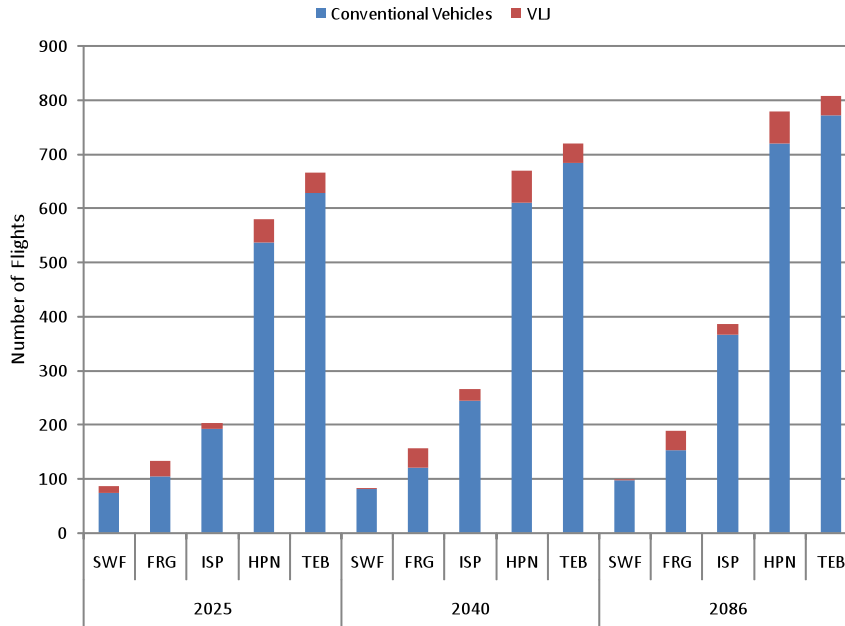


Figure 9-19. VLJ demand.

9.6.2. CESTOL Demand

The CESTOL demand sets consist of a similar number of overall flights in the Metroplex as the baseline scenario, but with 5% - 8% of the flights as CESTOL aircraft, mostly added to EWR, JFK, and LGA, as shown in Table 9-4. The CESTOL demand set has fewer flights than the baseline demand set because the CESTOL business shift algorithm moved a number of flights to satellite airports outside of the metroplex.

Table 9-4. Number of daily flights by vehicle type in the baseline and CESTOL demand sets.

	Baseline Demand			CESTOL Demand		
	2025	2040	2086	2025	2040	2086
Conventional Vehicles	5,357	5,967	7,266	5,025	5,723	6,729
CESTOL	0	0	0	454	373	358
Total	5,357	5,967	7,266	5,479	6,096	7,087

Although the number of flights on a metroplex basis is relatively similar, the number of flights at individual airports varies considerably in the 2086 demand, as shown in Figure 9-20 and Figure 9-21.

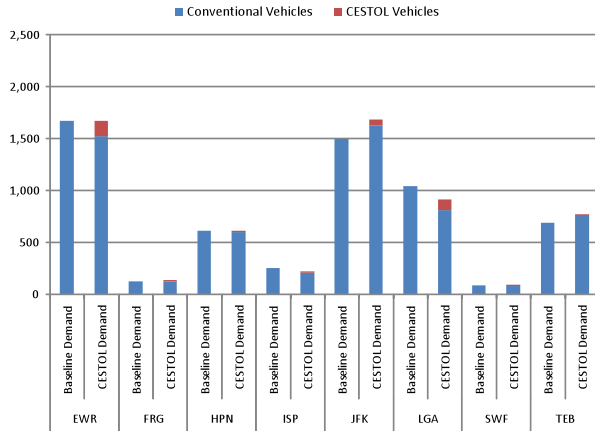


Figure 9-20. Number of flights by airport for the 2040 Baseline and CESTOL scenarios.

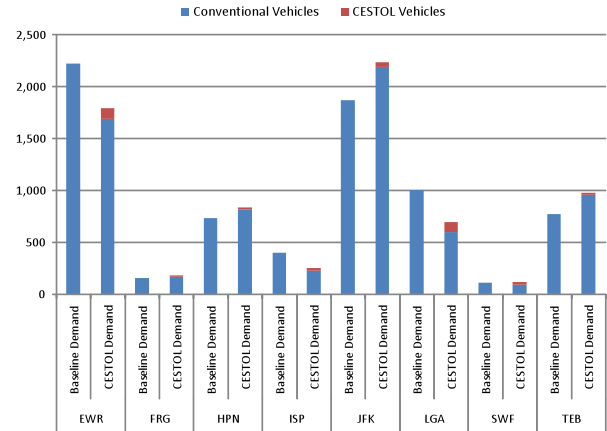


Figure 9-21. Number of flights by airport for the 2086 Baseline and CESTOL scenarios.

It is also important to note that the number of CESTOL vehicles decreases in the metroplex over time. This decrease is due to the shifting of CESTOL flights into other airports that were not modeled in this terminal airspace study. Figure 9-22 presents the number of flights by airport for the 2025 baseline and CESTOL scenarios.

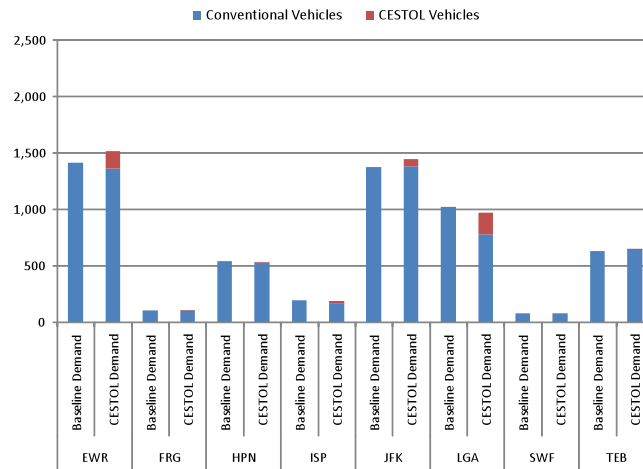


Figure 9-22. Number of flights by airport for the 2025 Baseline and CESTOL scenarios.

9.6.3. Mixed-Vehicle Demand

In order to analyze the effects of CESTOL and LCTR vehicles on the NY Metroplex airports, a notional demand set was engineered to exceed the capacity of each airport. Only the four busiest airports in the metroplex (JFK, EWR, LGA, and TEB) were analyzed for this experiment. This controlled experiment compared the maximum runway throughput for the same flights with and without advanced

vehicles. The first case was run with the mixed-vehicle demand, as shown in Table 9-5, while the second case was run with the advanced vehicles being replaced with comparable conventional aircraft. The CESTOLs were replaced with A320s and the LCTR were replaced with DHC8s.

Table 9-5. Number of flights by vehicle type and airport for the mixed-vehicle demand set.

	Mixed Vehicles Demand				Conventional Vehicles Only Demand			
	KEWR	KJFK	KLGA	KTEB	KEWR	KJFK	KLGA	KTEB
Conventional Vehicles	1,260	1,260	660	1,065	1,800	1,710	1,470	1,185
CESTOL	420	330	690	0	0	0	0	0
LCTR	120	120	120	120	0	0	0	0
Total	1,800	1,710	1,470	1,185	1,800	1,710	1,470	1,185

9.6.4. All Vehicles Demand

Table 9-6 presents the number of flights in the baseline and all-vehicle demand sets by vehicle type. While the total number of flights in the metroplex in the different demand years is similar, the distribution of flights in the different airports varies over time.

Table 9-6. Number of flights by vehicle type in the baseline and all-vehicles demand sets.

	Baseline Demand			All Vehicles Demand		
	2025	2040	2086	2025	2040	2086
Conventional Vehicles	5,357	5,967	7,266	4,930	4,919	5,145
CESTOL	0	0	0	270	532	893
VLJ	0	0	0	130	154	154
LCTR	0	0	0	90	210	380
UAS	0	0	0	12	12	12
SST	0	0	0	0	115	185
Total	5,357	5,967	7,266	5,432	5,942	6,769

Figure 9-23 and Figure 9-24 present the number of flights in each airport for the 2040 and 2086 demand years respectively. EWR and JFK have a decrease in overall demand as demand is shifted to surrounding satellite airports. In addition, their fleet mix has evolved to include a significant percentage of advanced vehicles. In 2040, EWR was modeled to have a fleet mix that includes 20% advanced vehicles. All of the small airports in the Metroplex have increased demand during this time. However, most of the increased demand is from advanced vehicle operations rather than conventional aircraft.

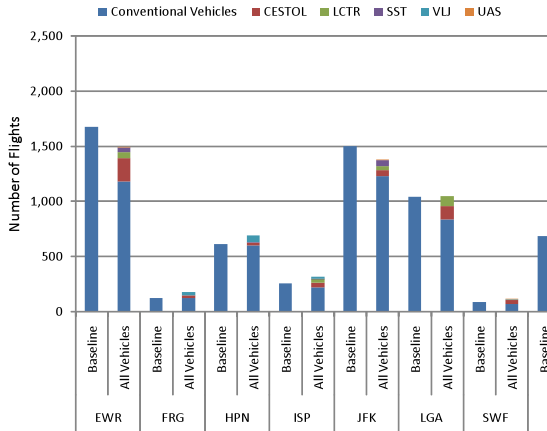


Figure 9-23. Number of flights by airport for the 2040 Baseline and All Vehicles scenarios.

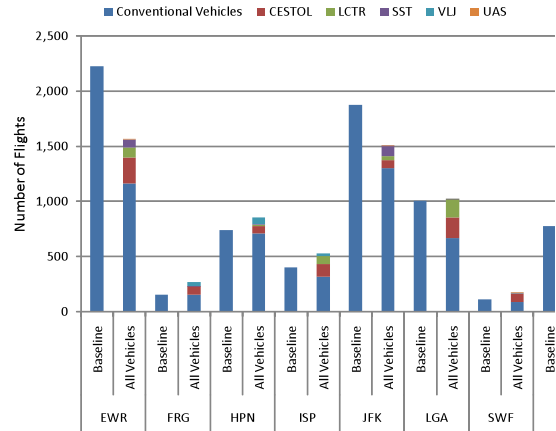


Figure 9-24. Number of flights by airport for the 2086 Baseline and All Vehicles scenarios.

Figure 9-25 presents the number of flights in each airport for the 2025 Baseline and All Vehicles scenarios.

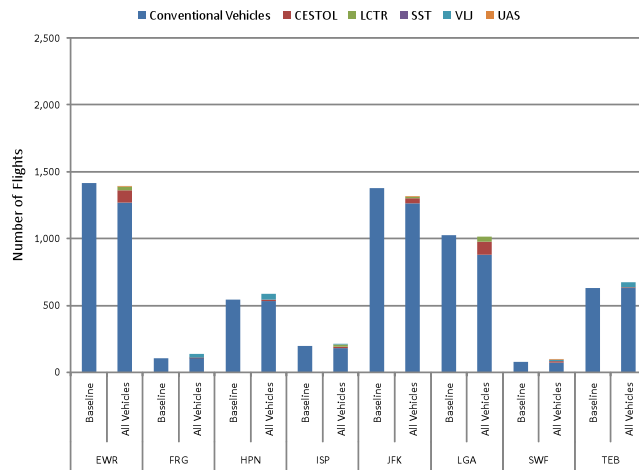


Figure 9-25. Number of flights by airport for the 2025 Baseline and All Vehicles scenarios.

The shifting of demand from the large airports to the smaller airports is possible due to the adoption of advanced vehicles. Furthermore, the added flight demand to the satellite airports comprises advanced vehicles that are able to utilize runways that conventional aircraft would not otherwise use.

9.6.5. Off-nominal Demand

The All Vehicles demand sets and the 2025 Baseline demand set, shown in Table 9-6, were used for the analysis of the Off-nominal scenario.

9.7. Results

This section presents results and analysis of the effects of advanced vehicles and their associated procedures, as well as the effects of off-nominal weather in the terminal airspace. The effects are analyzed

in terms of airspace and ground delay, runway capacity and throughput, emissions performance, and noise contours.

9.7.1. VLJ

This section presents the results and analysis for the VLJ demand compared against the baseline demand.

Delay

Figure 9-26 and Figure 9-27 compare average arrival air delay and average departure queue delay respectively. The VLJs were added to the less congested satellite airports and their addition to the metroplex demand does not change the overall average delay. For an increased number of flights, the same amount of average delay was observed.

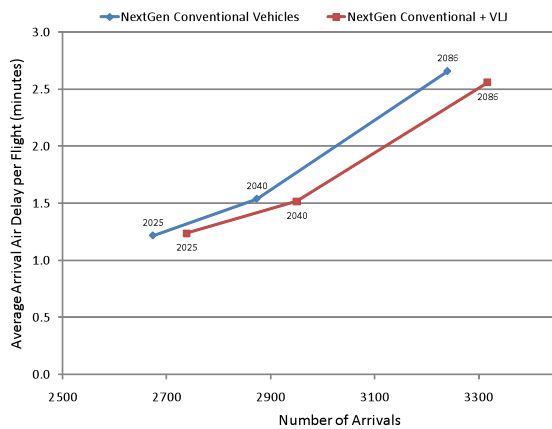


Figure 9-26. Average arrival delay vs. number of flights for all demand years.

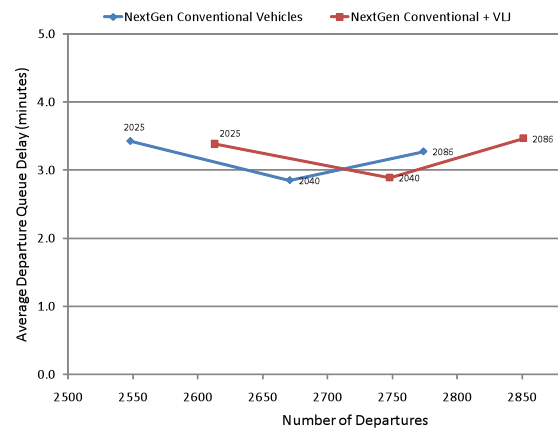


Figure 9-27. Average departure queue delay vs. number of flights for all demand years.

Looking more closely at the average delay at the airports where VLJ demand was added, there is a slight increase in the average arrival delay, as shown in Figure 9-28. The increase in average arrival air delay is influenced by the number of flights in each airport as shown in Figure 9-19. FRG received the greatest percentage increase in the number of flights from the VLJ demand, and therefore shows the greatest percentage increase in arrival air delay. Furthermore, FRG does not have any additional VLJ procedures that may help mitigate interactions with conventional traffic. HPN had the greatest number of flights added to its demand, and it shows the greatest total increase in average arrival air delay. Although VLJ arrival procedures at HPN use Runway 11 exclusively, they must still be sequenced with conventional arrivals due to crossing runways. Additionally, VLJ arrivals to Runway 11 also block departures, which cause some added departure queue delay.

Although the increases in delay at the smaller airports are observable, they do not affect the overall metroplex average in any significant way. Since the increases in delay at these airports only affect a small number of flights when compared to the number of flights at the main airports, their affect to the overall metroplex results are minimal.

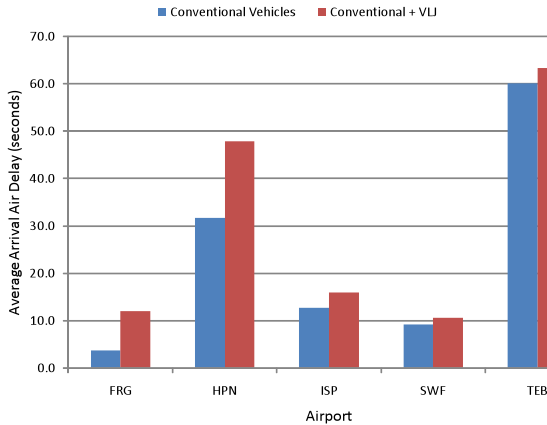


Figure 9-28. Average arrival delay per flight at VLJ airports for 2040.

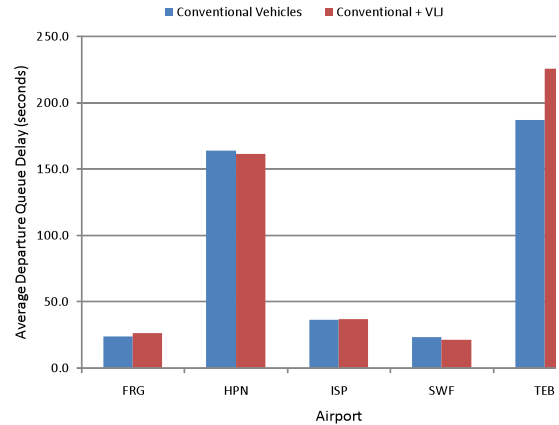


Figure 9-29. Average departure queue delay per flight at VLJ airports for 2040.

Similarly for departures, the fluctuations in delay due to the addition of the VLJs are minor when looking at the metroplex as a whole. It must also be noted that departure queue delay is more of a function of the runway demand. If VLJ departures were added during busy time periods, a slight increase in average delay is observed, as shown in Figure 9-29 for TEB. However, if demand is added during off-peak hours, a slight decrease in average delay is observed, as shown for HPN. The decrease on average departure queue delay is due to an increase in the number of flights without adding to the total delay.

Capacity

Since the VLJs only added less than three percent more flights to the metroplex demand, no significant impact was observed in the metroplex throughput as shown in Figure 9-30. This figure presents the number of arrivals and departures in a 15-minute time increment in the metroplex. The outer boundary of this plot represents the peak throughput in a given 15-minute time increment given the demand.

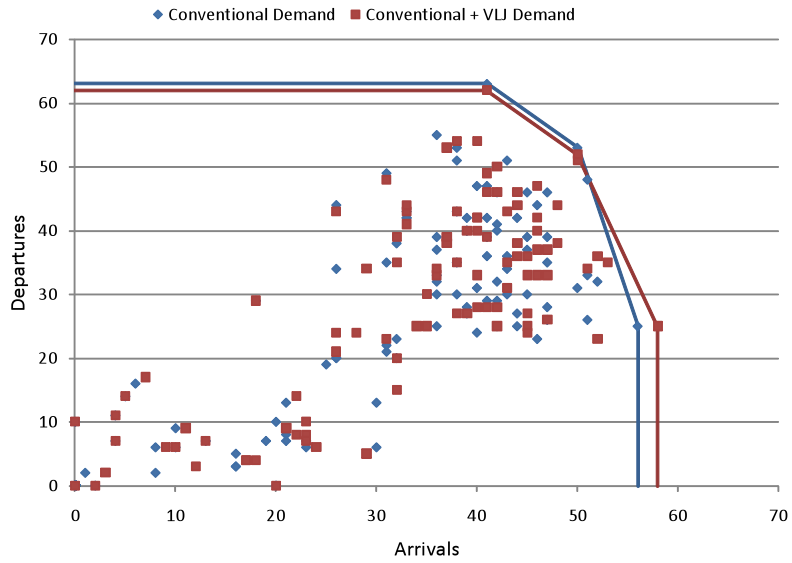


Figure 9-30. Metroplex operating envelopes for 2086.

Additionally, limited impact was observed for individual runway throughput as shown in Figure 9-31. This figure presents the operating envelopes for HPN in the 2086 demand, which had the highest number of VLJs in the modeled airports.

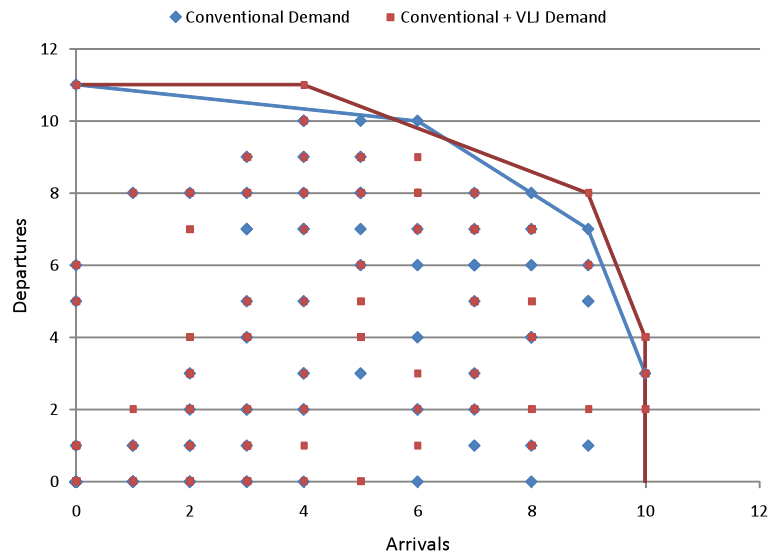


Figure 9-31. HPN operating envelopes for 2086.

Although VLJs operate at slower speeds, no decrease in throughput was observed. This is due to the smaller aircraft that typically operate at HPN, which also operate at slower speeds similar to the VLJs. Furthermore, the use of Runway 11 for arrivals helps mitigate impact to throughput.

Fuel Burn and Emissions

In order to compare the impacts of the advanced vehicles to the conventional vehicles in terms of fuel burn and emissions, relative environmental performance metrics were generated to show the advanced vehicles' relative performance to the other vehicles. Figure 9-32 presents the fuel burn of seven conventional aircraft categories and the VLJ relative to the number of flights for each category, in each of the six scenarios. When comparing two vehicles in this way, a vehicle category with a steeper slope performs worse on a relative basis than one with a more horizontal slope. In other words, an aircraft group with a higher slope value leaves a greater emissions footprint than aircraft groups with a lower slope value. This chart was created by summing the total fuel burn for each aircraft category and dividing it by the total fuel burn for all categories. The percent of flights was computed in a similar way.

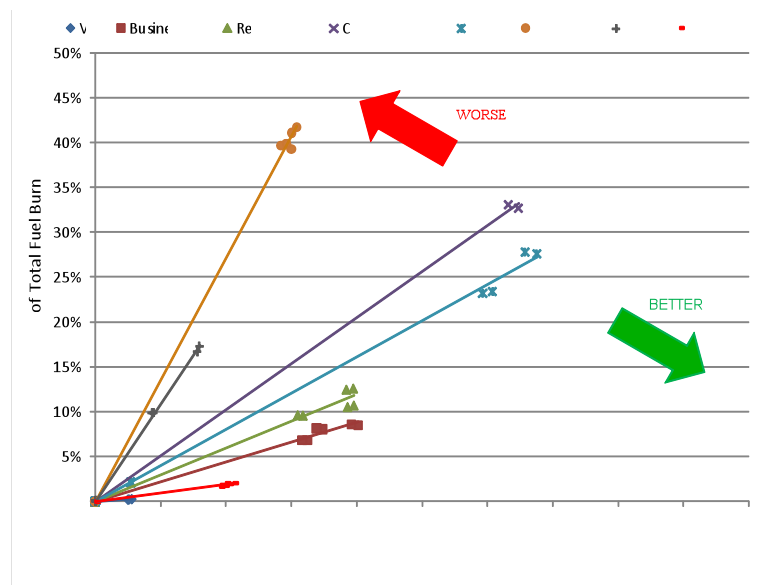


Figure 9-32. Percent of total fuel burn versus percent of total flights.

In addition to comparing fuel burn to the number of flights, comparisons against distance flown, flight duration, and number of passengers were also generated. In addition to fuel burn, emissions results for CO₂, NO_x, and particulate matter (PM) were also analyzed in a similar way. All emissions results for the other scenarios are presented in the same manner.

Because the VLJs constitute such a small percentage of the total fleet mix, the slope values for the VLJ compared against the business jets and regional jets are presented in Table 9-7 to Table 9-10. Table 9-7 presents the percent of total fuel burn versus the percent of the total flights, distance, time, and passengers. Lower values indicate better environmental performance.

Table 9-7. Fuel burn gradient.

Percent of Total Fuel Burn /	VLJ	Business Jet	Regional Jet
Percent of Total Flights	0.077	0.441	0.597
Percent of Total Distance	0.069	0.447	0.626
Percent of Total Time	0.057	0.468	0.645
Percent of Total Passengers	2.604	8.548	1.200

On a per-flight, per-distance, and per-time basis, VLJs performed better than business jets and regional jets in the terminal airspace. Due to the VLJs limited seating capacity, their relative performance in fuel burn per passenger is worse compared to regional jets, but still performs better than business jets.

Since there is a direct correlation between fuel burn and CO₂, the results for CO₂, shown in Table 9-8, reveal the same trends.

Table 9-8. CO₂ gradient.

Percent of Total CO ₂ /	VLJ	Business Jet	Regional Jet
Percent of Total Flights	0.077	0.441	0.597
Percent of Total Distance	0.069	0.447	0.626
Percent of Total Time	0.057	0.468	0.645
Percent of Total Passengers	2.604	8.548	1.200

For NO_x, the VLJs perform better than business jets and regional jets in the terminal airspace, as shown in Table 9-9.

Table 9-9. NO_x gradient.

Percent of Total NO _x /	VLJ	Business Jet	Regional Jet
Percent of Total Flights	0.017	0.414	0.504
Percent of Total Distance	0.015	0.420	0.528
Percent of Total Time	0.013	0.439	0.544
Percent of Total Passengers	0.577	8.047	1.018

Table 9-10 compares the relative particulate matter emissions for VLJ, business jets, and regional jets. PM results follow similar trends as fuel burn.

Table 9-10. PM gradient.

Percent of Total PM/	VLJ	Business Jet	Regional Jet
Percent of Total Flights	0.083	0.445	0.584
Percent of Total Distance	0.074	0.452	0.611
Percent of Total Time	0.062	0.473	0.630
Percent of Total Passengers	2.800	8.636	1.173

Noise

The primary metric used for noise comparisons is the area within the 60 dB Day-Night Average Sound Level (DNL) noise contour. Table 9-11 compares the area, in square miles, within the 60 dB DNL noise level contour for the airports with added VLJ flights in the 2086 demand year. The size and shape of the noise contour area are influenced by the number of flights in each runway and the location of their operations.

Table 9-11. Comparison of area (sq. miles) within the 60 dB DNL noise level contour for 2086.

	ISP	FRG	SWF	HPN	TEB
Conventional	2.680	3.197	0.285	6.114	7.913
Conventional + VLJ	2.817	3.380	0.292	6.251	7.989
Sq. Mile Change	0.137	0.183	0.007	0.137	0.076
Percent Change	4.90%	5.40%	2.40%	2.20%	0.90%

The airport that had the largest increase in noise contour area, at 5.4%, is FRG, which is also the airport that had the biggest increase in the percentage of VLJ flights added (23.5%). In addition to the percentage increase in the number of flights, the location of the operations also impacts the overall shape of the 60 dB DNL noise contour area. Figure 9-33 presents the DNL noise contour for HPN in the 2086 demand with and without the additional VLJ flights.

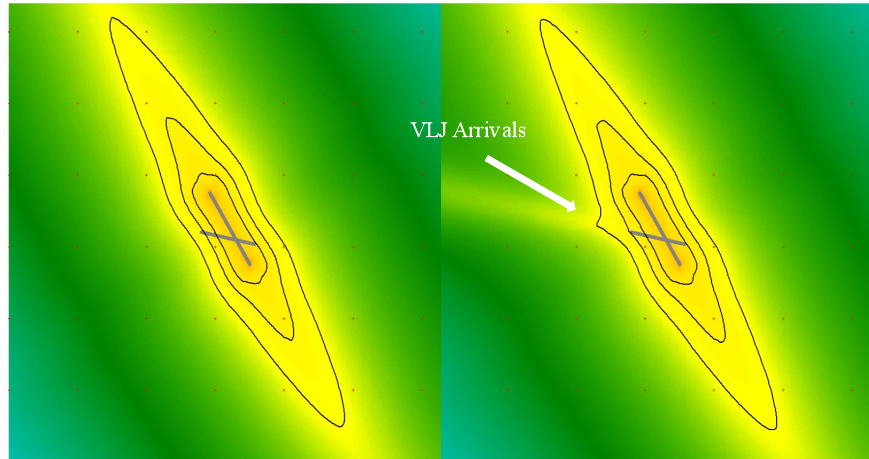


Figure 9-33. DNL noise contour comparison at HPN for 2086.

As can be observed from the figure, there is a noticeable bulge towards Runway 11 due to VLJ arrival operations. Furthermore, there is a 2.2% increase in the area within the 60 dB DNL noise contour.

9.7.2. CESTOL

This section presents the results and analysis for the CESTOL scenario compared against the baseline scenario, in terms of airspace and ground delay, runway capacity, emissions, and noise.

Delay

Figure 9-34 presents the average arrival air delay in the metroplex for the CESTOL and baseline scenarios. Similarly, Figure 9-35 presents the average departure queue delay for the same scenarios. Both arrival and departure queue average delay results are primarily driven by the two airports in the metroplex that have the greatest number of flights, JFK and EWR.

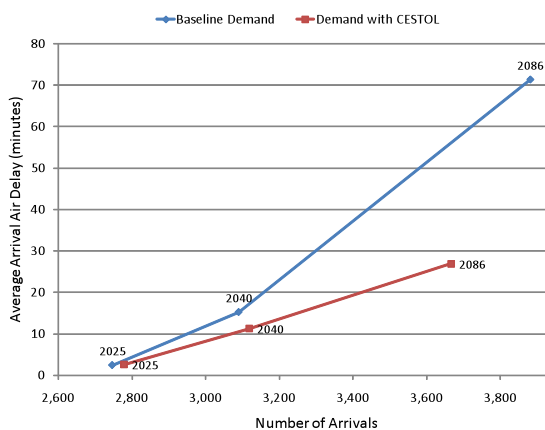


Figure 9-34. Average arrival delay vs. number of

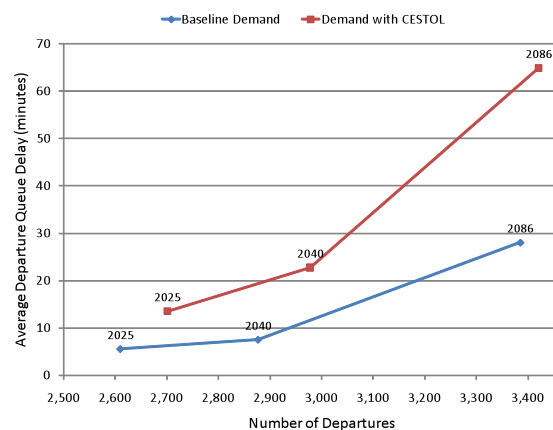


Figure 9-35. Average departure queue delay vs.

arrivals for all demand years.

number of departures for all demand years.

Looking closer at the average arrival air delay at these two airports, as shown in Figure 9-36 and Figure 9-37, it is clear that the average arrival air delay at EWR is the primary driver for all arrival air delay in the metroplex. Since there are significantly more arrivals at EWR in the baseline scenario during the 2040 and 2086 demand years, the average arrival air delay for the metroplex becomes skewed.

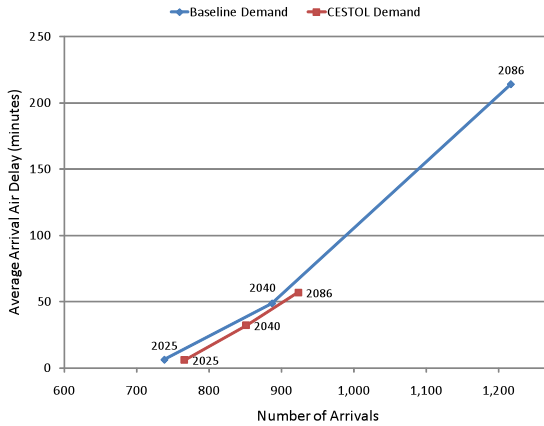


Figure 9-36. Average arrival delay vs. number of flights at EWR for all demand years.

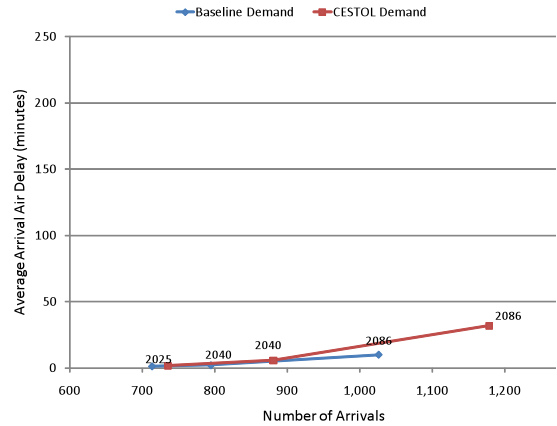


Figure 9-37. Average arrival delay vs. number of flights at JFK for all demand years.

Looking at departure queue delay at EWR and JFK, shown in Figure 9-38 and Figure 9-39, it is apparent that the average departure queue delay at JFK is the primary driver for all departure queue delay in the metroplex. In this case, the greater number of departures at JFK in the CESTOL demand skews the overall average departure queue delay in the metroplex.

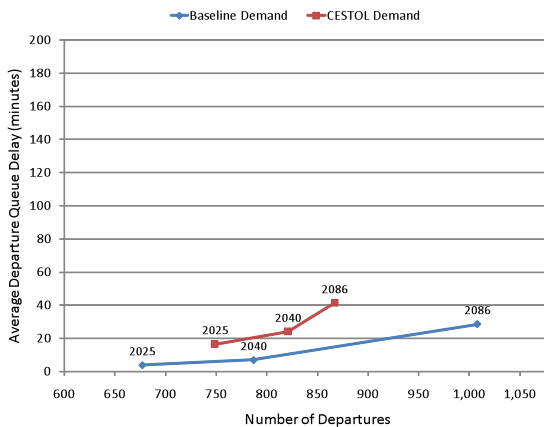


Figure 9-38. Average departure queue delay vs. number of flights at EWR for all demand years.

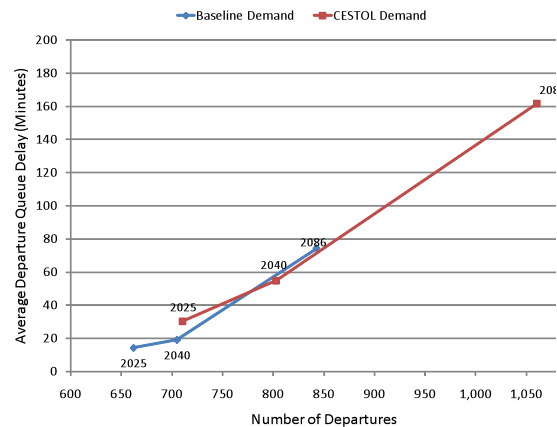


Figure 9-39. Average departure queue delay vs. number of flights at JFK for all demand years.

The skewed average arrival air delay per flight at EWR, along with the skewed average departure queue delay at JFK, make it challenging to isolate the impact of CESTOL vehicles, and to make meaningful comparisons against the baseline scenario in terms of delay. Although the total number of flights in the metroplex is comparable in the baseline and CESTOL scenarios, there are still many demand differences in the individual airports. Furthermore, if demand is added to already congested airports, the impact to delay becomes more significant to the metroplex-wide results.

Capacity

Although the varying distribution of flights in the individual airports makes it difficult to analyze the CESTOL impact in terms of delay, when considering the throughput for the metroplex, the variation is of less consequence. As long as adequate demand for the runways exists, the maximum throughput for the metroplex is still reached. The 2086 demand was selected to analyze the impact of the CESTOL and its associated procedures on metroplex throughput. Figure 9-40 presents the operating envelopes for the 2086 demand.

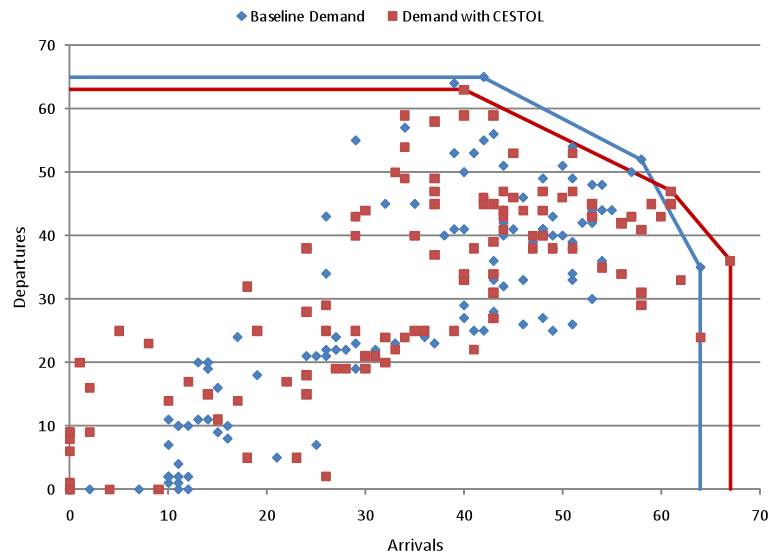


Figure 9-40. Metroplex operating envelopes for the 2086 demand.

The figure shows a slight increase in peak arrival throughput, and a slight decrease in peak departure throughput. These differences can be attributed to the CESTOL and its associated procedures.

Since the spiral procedures and midfield departure procedures are implemented to individual airports in varying degrees, and since the number of CESTOL flights added to each airport also varies, it is difficult to measure the effects of the CESTOL procedures on an airport level. However, the overall effects of these procedures can be analyzed on a metroplex level. Although CESTOLs operate at slower speeds, their impact to metroplex throughput is minimal. Spiral departure procedures combined with midfield takeoff procedures help to mitigate negative impacts CESTOLs have on departure throughput. Furthermore, the use of underutilized runways for CESTOL operations contributes to an overall increase in the metroplex arrival throughput.

Fuel Burn and Emissions

The CESTOL fuel burn and emissions performance are analyzed in the same manner as the VLJs. Figure 9-41 presents the percentage of total fuel burn versus the percentage of fleet mix for the aircraft groups in the CESTOL scenario. Figure 9-42 presents the same data using the number of passengers as the basis for comparison. As previously stated, steeper slopes indicate worse performance.

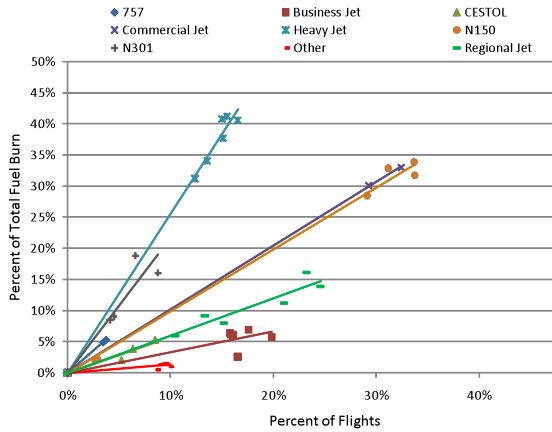


Figure 9-41. Percent of total fuel burn versus percent of flights.

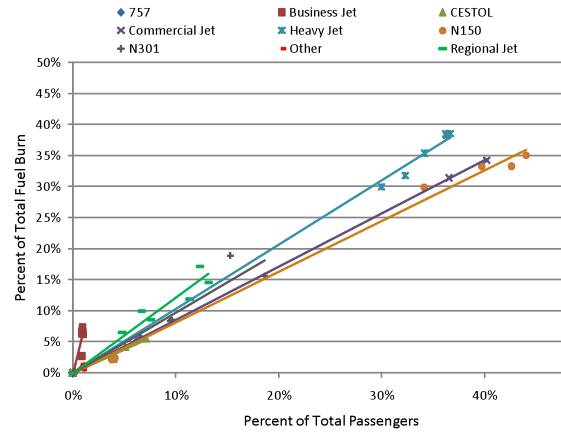


Figure 9-42. Percent of total fuel burn versus percent of passengers carried.

Comparing CESTOL vehicles to commercial jets, the CESTOLs have less fuel burn on a per-flight and on a per-passenger basis in the terminal airspace. CESTOL vehicles perform similar to regional jets on a per-flight basis, as shown in Figure 9-41, while carrying more passengers, as can be observed from Figure 9-42. The relative fuel burn performance is presented in Table 9-12 in terms of slope.

Table 9-12. Fuel burn gradient.

Percent of Total Fuel Burn /	CESTOL	Commercial Jet	Regional Jet
Percent of Total Flights	0.570	1.023	0.598
Percent of Total Distance	0.606	1.069	0.591
Percent of Total Time	0.572	1.096	0.601
Percent of Total Passengers	0.750	0.856	1.213

Except for the relative fuel burn performance in terms of distance, the CESTOL have a better fuel burn performance in the terminal airspace when compared to commercial and regional jets. The relative fuel burn performance in terms of distance is slightly higher for the CESTOL when compared against regional jets.

CO₂ emissions performance is directly correlated to fuel burn and follows the same trends, as shown in Table 9-13.

Table 9-13. CO₂ gradient.

Percent of Total CO ₂ /	CESTOL	Commercial Jet	Regional Jet
Percent of Total Flights	0.570	1.023	0.598
Percent of Total Distance	0.606	1.069	0.591
Percent of Total Time	0.572	1.096	0.601
Percent of Total Passengers	0.750	0.856	1.213

For NO_x, CESTOLs perform better than both commercial and regional jets on a per-flight and on a per-passenger basis, as shown in Figure 9-43 and Figure 9-44.

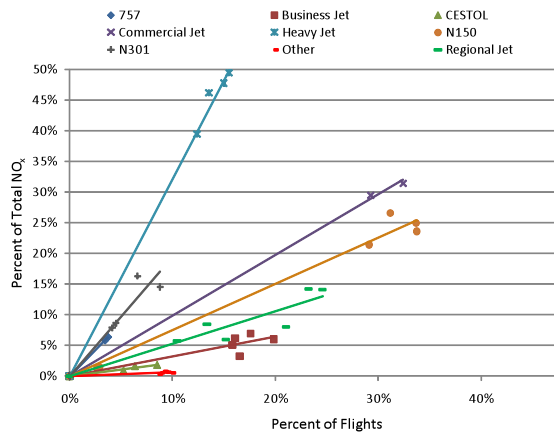


Figure 9-43. Percent of total NO_x versus percent of flights.

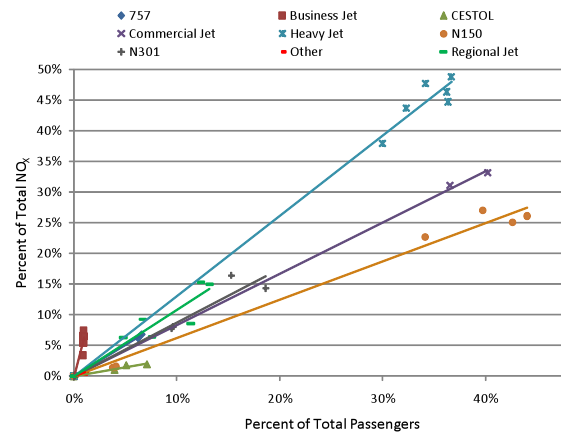


Figure 9-44. Percent of total NO_x versus percent of passengers.

The other emissions performance metrics, NO_x and PM, are presented in Table 9-14 and Table 9-15 in terms of gradient.

Table 9-14. NO_x gradient.

Percent of Total NO _x /	CESTOL	Commercial Jet	Regional Jet
Percent of Total Flights	0.213	0.985	0.526
Percent of Total Distance	0.224	1.030	0.521
Percent of Total Time	0.211	1.056	0.531
Percent of Total Passengers	0.284	0.835	1.076

Table 9-15. PM gradient.

Percent of Total PM/	CESTOL	Commercial Jet	Regional Jet
Percent of Total Flights	0.551	1.035	0.595
Percent of Total Distance	0.587	1.082	0.589
Percent of Total Time	0.555	1.109	0.599
Percent of Total Passengers	0.725	0.866	1.207

In terms of NO_x and PM, CESTOLs have better emissions performance than commercial jets and regional jets in the terminal airspace.

Noise

As mentioned in the demand section, the number of CESTOL aircraft in the metroplex decreases from the 2025 demand to the 2086 demand. To best visualize the noise effects of the CESTOL aircraft in comparison with conventional aircraft, contour areas from the 2025 demand year where the number of CESTOL aircraft is greatest are shown in Table 9-16. Negative values in the change in square miles indicate that the CESTOL scenario covered a smaller 60 dB DNL noise contour area.

Table 9-16. Comparison of area (sq. miles) within the 60 dB DNL noise level contour for 2025.

	JFK	LGA	ISP	EWR	FRG	SWF	TEB	HPN
Baseline	32.662	7.238	1.447	17.936	2.197	0.475	8.953	4.202
Demand with CESTOL	31.777	6.831	1.263	18.174	2.203	0.358	8.831	4.222
Sq. Mile Change	-0.885	-0.407	-0.185	0.238	0.006	-0.117	-0.123	0.020
Percent Change	-2.7%	-5.6%	-12.8%	1.3%	0.3%	-24.6%	-1.4%	0.5%

This data shows varying changes in the noise contour areas for the individual airports, which are not necessarily explained by the changes in the number of flights. Meaningful interpretations of the data becomes challenging because the noise contour areas are influenced by many variables including, the number of flights, the aircraft types, the procedures flown, and the time the flights are scheduled (due to a 10 dB penalty for night operations). For example, JFK shows a 3% decrease in the 60 dB noise contour area, while it had 5% more flights in the CESTOL demand, as shown in Figure 9-22. SWF had 5.4% more flights in the CESTOL demand, but had a 25% decrease in noise contour.

Other airports did show some connection between the noise contour and number of flights. For example, LGA had a 6% decrease in the number of flights, and a 6% decrease in the noise contour area. EWR had a 7% increase in the number of flights, and a 1% increase in the noise contour area. Figure 9-45 presents the 60 dB, 65 dB, and 70 dB DNL noise contour for EWR in the 2025 demand.

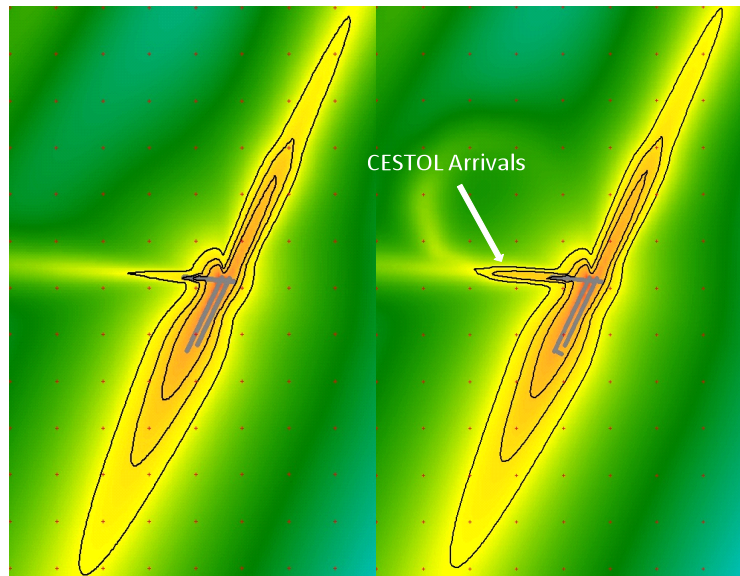


Figure 9-45. DNL noise contour comparison at EWR for the 2025 demand.

As can be observed from the figure, the CESTOL arrival procedures on Runway 11 extend the noise contour farther out in this direction. The noise contour for the departures from Runway 22R is observed to decrease slightly in the CESTOL scenario.

Table 9-17 and Table 9-18 present the 60 dB DNL noise contour areas for the 2040 and 2086 scenarios.

Table 9-17. Comparison of area (sq. miles) within the 60 dB DNL noise level contour for 2040.

	JFK	LGA	ISP	EWR	FRG	SWF	TEB	HPN
Baseline	33.442	6.856	1.904	18.210	2.397	0.301	8.995	4.890
Demand with CESTOL	33.388	5.814	1.400	19.179	2.456	0.317	8.914	5.106
Sq. Mile Change	-0.054	-1.042	-0.504	0.969	0.058	0.016	-0.081	0.215
Percent Change	-0.2%	-15.2%	-26.5%	5.3%	2.4%	5.4%	-0.9%	4.4%

Table 9-18. Comparison of area (sq. miles) within the 60 dB DNL noise level contour for 2086.

	JFK	LGA	ISP	EWR	FRG	SWF	TEB	HPN
Baseline	41.899	6.955	3.069	26.183	3.167	0.443	7.510	6.087
Demand with CESTOL	49.489	5.053	1.686	21.577	2.997	0.578	10.657	6.885
Sq. Mile Change	7.590	-1.902	-1.383	-4.606	-0.170	0.134	3.147	0.798
Percent Change	18.1%	-27.3%	-45.1%	-17.6%	-5.4%	30.4%	41.9%	13.1%

A more controlled demand schedule, where the number of flights and the scheduled operation times are constant, while changing the number of CESTOLs in the fleet mix, might help isolate the noise impacts of the CESTOL and other advanced vehicles in individual airports.

9.7.3. Mixed Vehicle (Capacity Experiment)

This section presents the results of the mixed-vehicle capacity experiment. The purpose of this experiment is to analyze the effects of the CESTOL and LCTR procedures on airport capacity. The four airports included in this experiment are JFK, EWR, LGA, and TEB. All operating envelopes presented in this section are for 15-minute time increments.

JFK

Figure 9-46 and Figure 9-47 present the operating envelopes for JFK during Plan 1 and Plan 2 respectively. During Plan 1 CESTOL arrivals use Runway 04R exclusively, but must still be sequenced with conventional vehicle arrivals to 31L, as shown in Figure 9-9. LCTR arrivals are segregated from all other traffic when arriving to the landing strip. These added procedures for the advanced vehicles results in a slight increase in the maximum arrival throughput.

CESTOL departures from 04L during Plan 1 are sequenced with conventional vehicle departures from 31R, while LCTR departures from 31L takeoff between conventional vehicle arrivals to 31L. Since both CESTOLs and LCTRs depart from runways not used by conventional vehicles, an increase in the maximum departure throughput is observed.

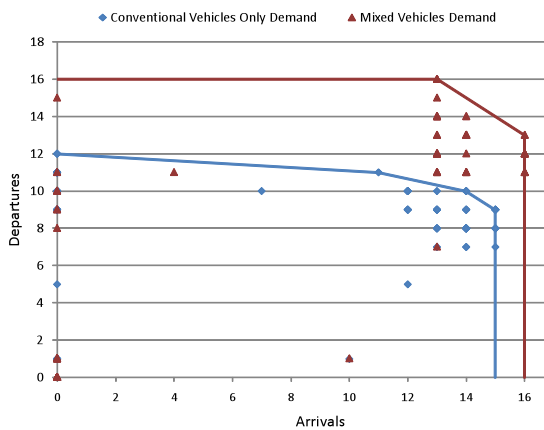


Figure 9-46. JFK operating envelopes for Plan 1.

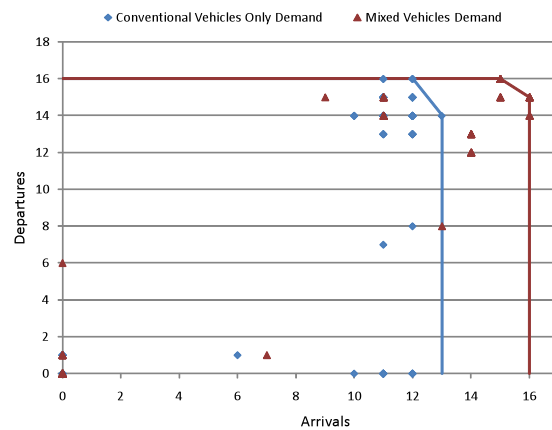


Figure 9-47. JFK operating envelopes for Plan 2.

During Plan 2, independent CESTOL arrivals to Runway 31L combined with independent LCTR arrivals to the landing strip, results in an increase in the maximum arrival throughput. LCTR and CESTOL departures from Runway 31L are mixed, and must take off between CESTOL arrivals. Since the CESTOL and LCTR are segregated from conventional traffic, no significant differences were observed in departure throughput.

Figure 9-48 and Figure 9-49 present the operating envelopes for JFK during Plan 3 and Plan 4 respectively. A slight increase in arrival throughput is observed during Plan 3, which is primarily due to the independent LCTR arrivals to the landing strip. The CESTOL spiral arrival procedures on Runway 13L help minimize negative impacts to arrival throughput.

Similarly, CESTOL spiral and midfield departure procedures on Runway 13R help mitigate negative impacts to departure throughput. LCTR departures on Runway 22L takeoff between arrivals to 22L, and

must also be sequenced with CESTOL departures from 13R. The LCTR departure procedures during Plan 3 have limited impact to the overall throughput.

Since the Plan 4 runway configuration is similar to the Plan 3 configuration with the exception of exclusive CESTOL operations on Runways 13L and 13R, no significant differences in throughput are observed in the Mixed Vehicle demand. However, there is an increase in throughput when compared against the Conventional Vehicles demand because conventional vehicles traffic in this runway configuration is limited to Runway 22L and 22R only.

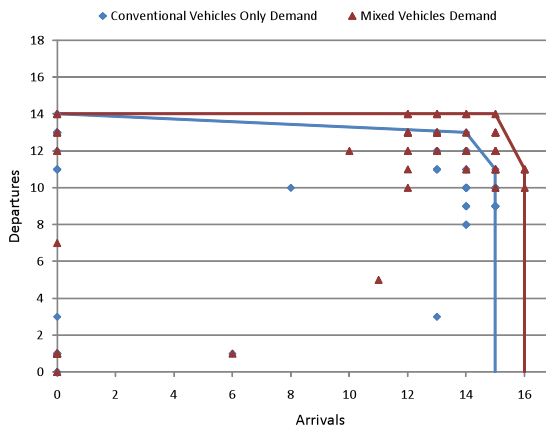


Figure 9-48. JFK operating envelopes for Plan 3.

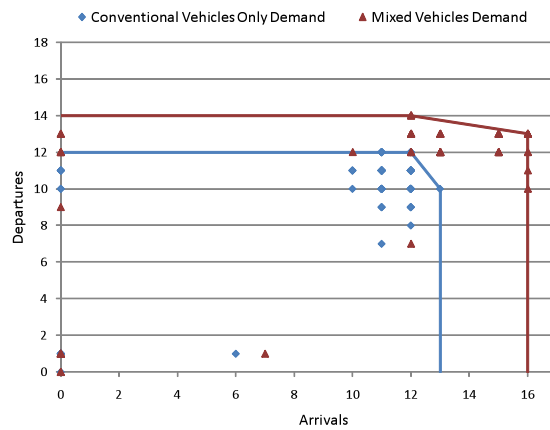


Figure 9-49. JFK operating envelopes for Plan 4.

EWR

EWR operates under a single runway configuration throughout the simulation day, as shown in Figure 9-10. Figure 9-50 presents the operating envelopes at EWR for the Mixed Vehicle and Conventional Vehicles Only demands.

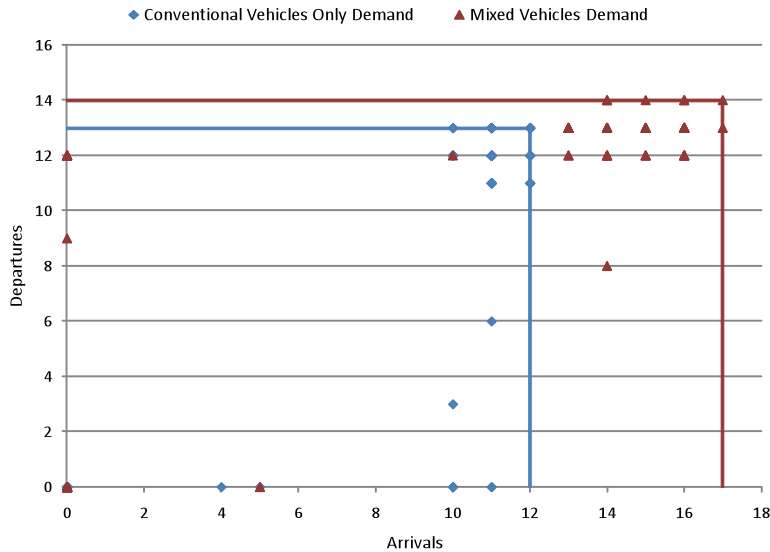


Figure 9-50. EWR operating envelopes.

The figure shows a significant increase in the arrival capacity at EWR. The reason for this increase is due to the CESTOL arrivals to Runway 11 and the LCTR arrivals to the landing strip as shown in Figure 9-10. It must be noted that although the CESTOL arrivals are shown to be mixed with conventional traffic on Runway 11, the amount of conventional vehicles using this runway is limited to only a few turboprop aircraft. The addition of CESTOL arrivals to EWR increases the utilization of Runway 11, which increases the maximum arrival throughput at this airport. Since CESTOLs require a shorter runway, CESTOL arrive to Runway 11 without blocking conventional departures from Runway 22R. Moreover, the addition of LCTR arrivals to EWR increases arrival capacity without impeding other operations due to the use of the landing strips.

Due to airspace constraints, CESTOL departures use conventional procedures to take off from Runway 22R. Their slower takeoff speeds slow down conventional traffic, which decreases runway throughput. The LCTR departures on Runway 11, although sequenced with other departures from 22R and arrivals from 22L, provide some additional departure throughput, which offsets some of the decrease in throughput caused by the CESTOL departures. Overall, there is a slight increase in the maximum departure throughput at EWR.

The ability of the advanced vehicles to land on shorter runways increases the maximum arrival throughput at EWR through the use of Runway 11 and the landing strip. Airspace constraints prevent the implementation of spiral departure procedures for the CESTOL aircraft, which decreases departure throughput. However, the utilization of Runway 11 for LCTR departures offsets the decrease in throughput caused by the CESTOLs.

LGA

LGA has two runway configurations as shown in Figure 9-11. Since LGA does not have extra runways where advanced vehicles can operate, the use of spiral arrival and departure procedures by CESTOL traffic to mitigate any negative impact on throughput is essential. During Plan 1 and Plan 2, only a slight decrease in arrival throughput is observed due to the application of spiral arrival procedures

on Runway 22, as shown in Figure 9-51. Moreover, the use of the additional landing strip for LCTR arrivals also helps increase arrival throughput.

The use of the landing strip for LCTRs, however, blocks departures from Runway 31. This causes a decrease in the departure throughput, as shown in Figure 9-51. The LCTR departures from Runway 22 increase departure throughput, but is not enough to offset the decrease in throughput from Runway 31.

During Plan 3 and Plan 4, a similar trend is observed, as shown in Figure 9-52.

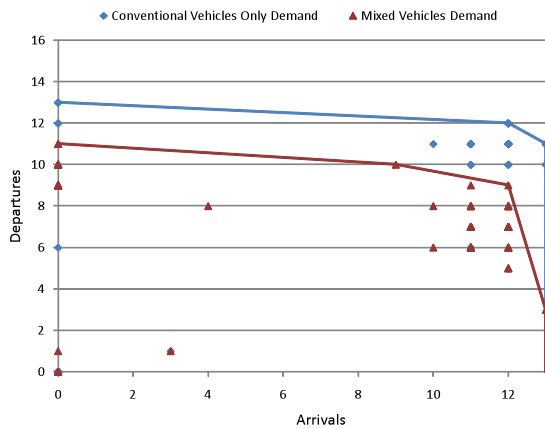


Figure 9-51. LGA operating envelopes for Plans 1 and 2.

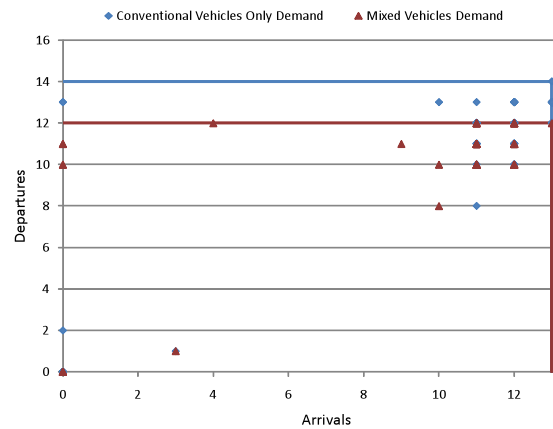


Figure 9-52. LGA operating envelopes for Plan 3 and 4.

CESTOL spiral arrivals to Runway 22 and LCTR arrivals to the landing strip help lessen any negative impacts to arrival throughput. For departures, the mixture of all departure procedures from Runway 13 decreases overall throughput. Spiral and midfield departure procedures help mitigate some of the CESTOL and LCTR impacts to throughput, but it does not eliminate them.

TEB

For TEB, only LCTR vehicles were included in the engineered demand as shown in Table 9-5. Therefore, only the impacts of the LCTRs are analyzed. Figure 9-53 presents the operating envelopes at TEB for the Mixed Vehicle and Conventional Vehicles Only demands.

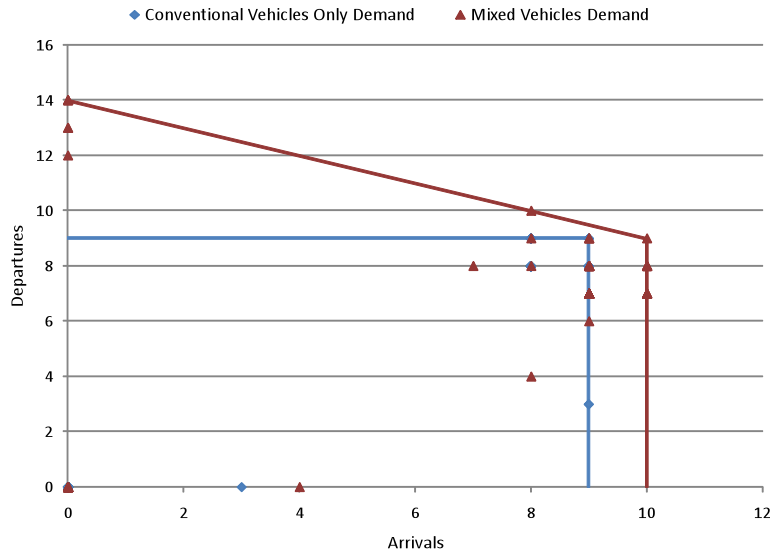


Figure 9-53. TEB operating envelopes.

The maximum arrival throughput at TEB is observed to increase slightly due to the addition of the landing strip used by LCTR arrivals, as shown in Figure 9-12. Similar to the landing strip added at LGA, the landing strip added to TEB blocks departure traffic. The independent use of Runway 24 for LCTR departures more than offsets the decrease in departure throughput.

Summarized Results

In general, if CESTOL and LCTR procedures can be segregated from conventional vehicle traffic, then an increase in the maximum throughput is observed, as observed with CESTOL arrival procedures at EWR and departure procedures at JFK during Plan 1. If CESTOL and LCTR procedures are mixed with, or impede conventional vehicle traffic, then a decrease in the maximum throughput is observed as observed with LGA procedures. Spiral and midfield procedures help mitigate negative impacts to throughput during mixed conventional and advanced vehicle procedures, but it does not eliminate them. Table 9-19 presents a summary of the results for the capacity experiment.

Table 9-19. Mixed Vehicle (Capacity Experiment) summary.

Airport	Runway Configuration	Arrival Throughput	Departure Throughput
JFK	Plan 1	+	++
	Plan 2	++	O
	Plan 3	+	O
	Plan 4	+	+
EWR	All Plans	++	+
LGA	Plan 1 and Plan 2	O	-
	Plan 3 and Plan 4	O	-
TEB	All Plans	+	+

“O” = limited impact, “+” = increase in throughput, “-” = decrease in throughput

9.7.4. All Vehicles

This section presents the results and analysis for the all-vehicle scenario compared against the baseline scenario, in terms of airspace and ground delay, runway capacity, emissions, and noise.

The all-vehicles demand includes UASs and SSTs. UASs have flight characteristics similar to the Cessna Caravan and therefore use conventional procedures. The number of modeled UAS flights in the Metroplex is less than 1%. SSTs are direct replacements for other large jets and have similar flight characteristics in the terminal airspace. The benefits and impact of the SST aircraft are more prevalent in the enroute airspace and its operational impacts in the modeled airspace are not expected to be significant.

Delay

The primary factor that increases air delay in the Metroplex terminal airspace is the amount of demand placed on arrival runways during any given period. The airspace configuration used for all of the advanced vehicle comparison is the decoupled NextGen airspace, which eliminates any interaction between airports or runways at an airport. The impact of this is that the usage of underutilized or unused runways by advanced vehicles increases throughput and decreases air delay.

Figure 9-54 presents the impact to the average arrival air delay of the demand shift caused by the advanced vehicles operating from underutilized, unused, and even new landing strips. This chart presents the average arrival air delay per flight in the baseline and all-vehicle scenarios for the three demand years. Figure 9-55 presents the average departure queue delay for the same three years. As these results show, trends over the three demand years indicate significant advantages in scenarios with advanced vehicles included in the fleet mix. For reference, today these airports see average arrival delays between 6 and 8 minutes on good-weather days and average departure delays between 8 and 12 minutes.

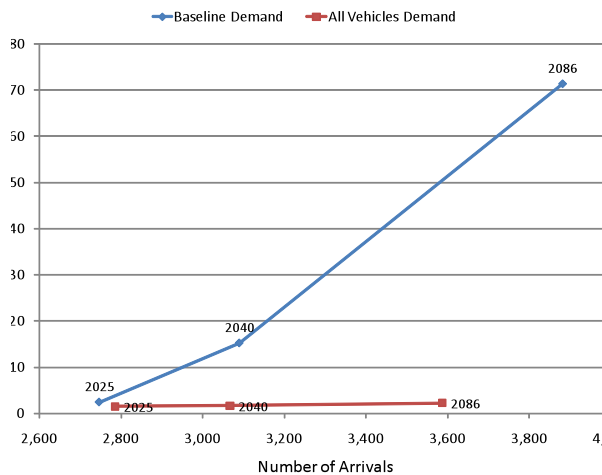


Figure 9-54. Average arrival delay vs. number of arrivals for all demand years.

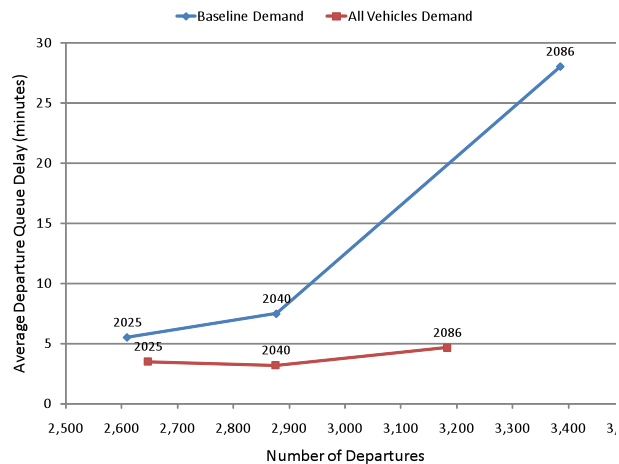


Figure 9-55. Average departure queue delay vs. number of departures for all demand years.

Looking more closely at the delay at the individual airports, Figure 9-56 and Figure 9-57 present the average arrival air delay and average departure queue delay in the 2040 demand year. The decrease in the number of flights at EWR and JFK show a corresponding decrease in both arrival and departure delay.

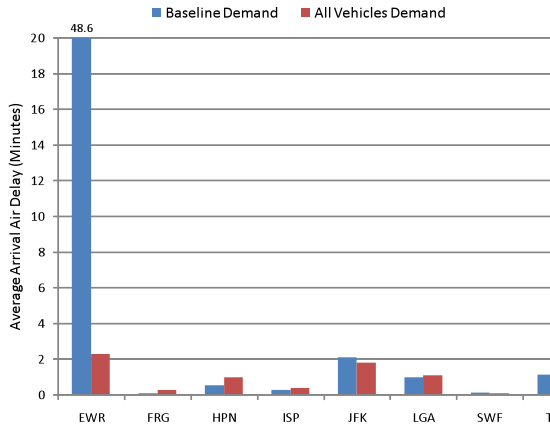


Figure 9-56. Average arrival delay at individual airports.

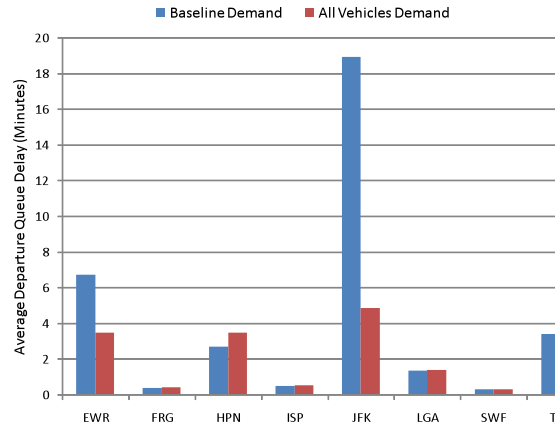


Figure 9-57. Average departure queue delay at individual airports.

Note that the substantial decrease in arrival air delay at EWR from the Baseline to the All Vehicles demand is primarily driven by two factors. The first factor is the 12.5% decrease in the number of total arrivals at EWR. The second factor is the advantages that the advanced vehicles provide. The utilization of Runway 11 by the CESTOL aircraft along with the LCTR arrivals to the landing strip provides increased throughput and decreases arrival air delay. Figure 9-58 presents the average arrival air delay at EWR.

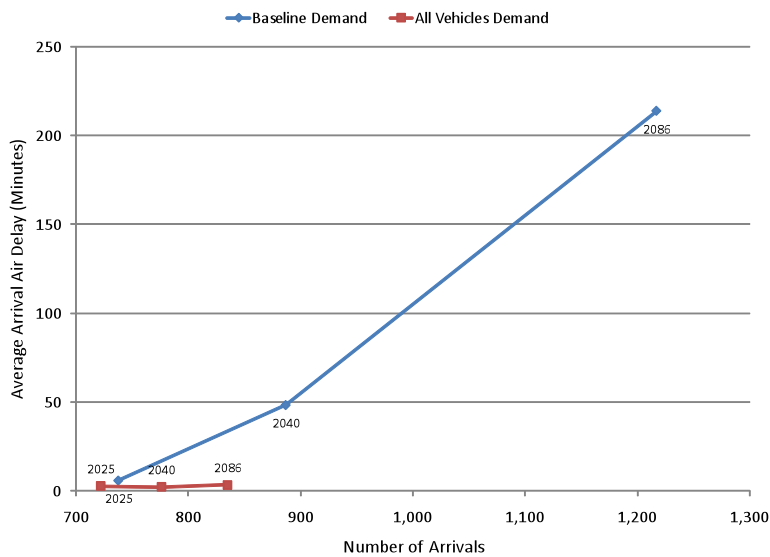


Figure 9-58. Average arrival delay vs. number of arrivals at EWR for all demand years

Similarly, the substantial decrease in the departure queue delay at JFK is driven by the same two factors. The advanced vehicles' utilization of runways not used by conventional vehicles, and the decrease in the number of total flights at JFK are contributing factors to the decrease in delay.

Since flights are shifted to the smaller airports, a corresponding increase in delay at these airports is observed. As previously mentioned, if demand is added to less congested airports, the impact to delay is less significant to the metroplex-wide results.

Capacity

Figure 9-59 presents a comparison of throughput and delay between the Baseline and All Vehicles scenarios for 2040. This chart clearly shows the significant impact the advanced vehicles can have on the operations of the Metroplex. For the demand year 2040, the Baseline and All Vehicle scenarios have nearly the same number of flights. Figure 9-59 presents the cumulative arrival air delay versus the arrival throughput. It is obvious that the arrival airspace in the Baseline scenario is fully saturated causing unacceptable levels of delay exceeding 15 minutes per flight. With the introduction of the advanced vehicles, delay is reduced to less than 2 minutes per flight.

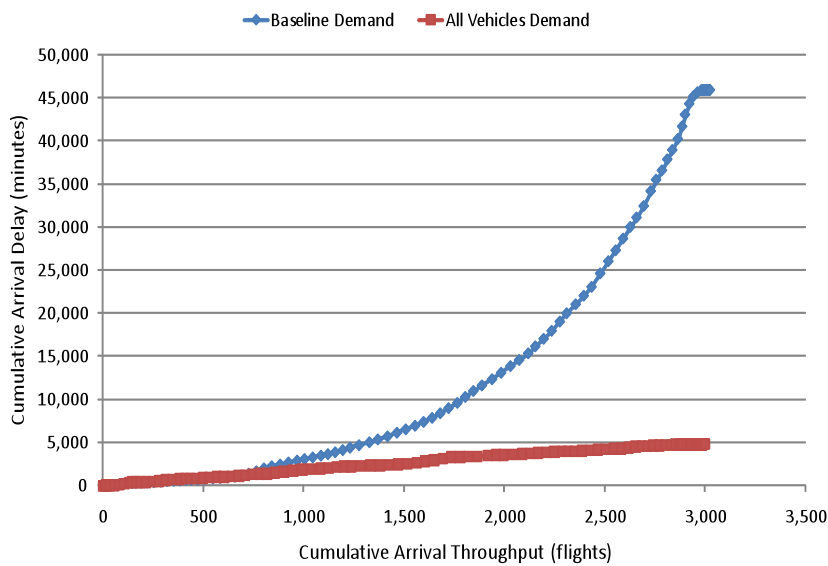


Figure 9-59. Cumulative arrival air delay vs. cumulative throughput for 2040.

Correspondingly, this decrease in delay occurred along with an increase in maximum arrival and departure throughput. Figure 9-60 presents the metroplex-wide operating envelopes for the Baseline and All Vehicles scenarios. This chart uses 15-minute time increments from five-iteration simulation runs. Increases in both arrival and departure throughput are observed.

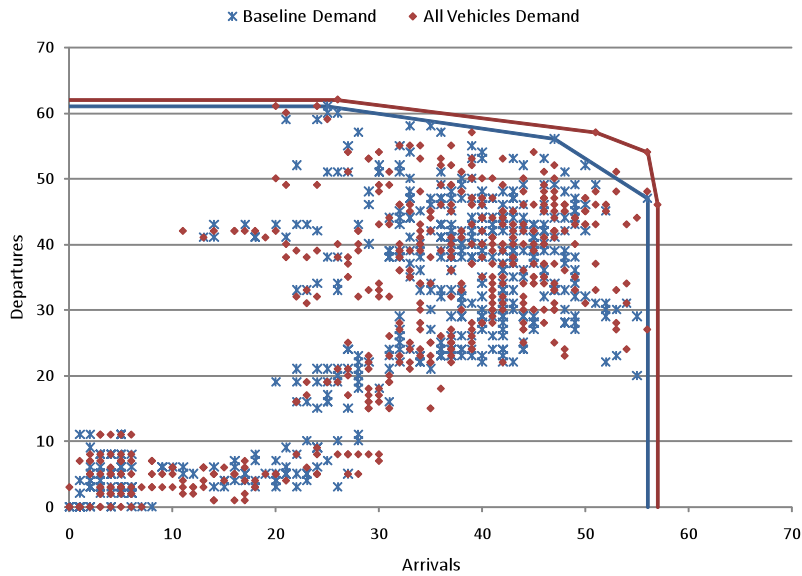


Figure 9-60. Metroplex operating envelopes for 2040.

Fuel Burn and Emissions

The fuel burn and emissions for the All Vehicles scenario are analyzed in the same manner as the CESTOL and VLJ scenarios. Relative emissions performance is plotted as the percentage of emissions by aircraft group versus the percentage of flights, distance traveled, flight duration, and number of passengers, and is provided in the Electronic Appendix of Results. Figure 9-61 and Figure 9-62 present the percent of fuel burn versus the percent of flights and versus the percent of passengers carried respectively.

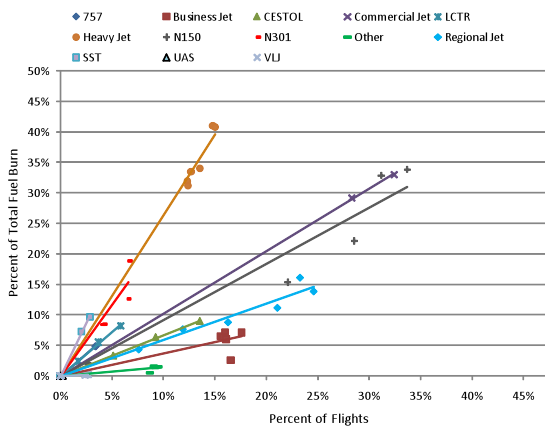


Figure 9-61. Percent of total fuel burn vs. percent of flights.

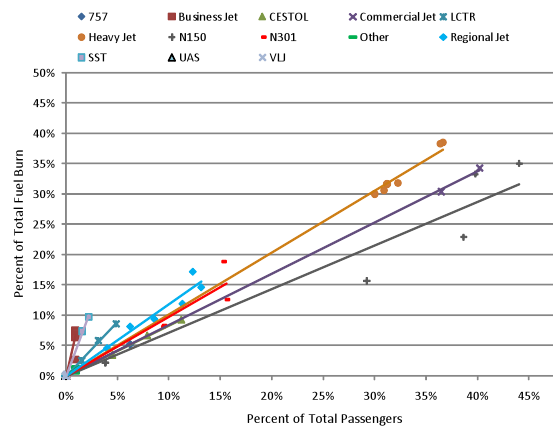


Figure 9-62. Percent of total fuel burn vs. percent of passengers carried.

In order to observe the relative emissions performance of the advanced vehicles, the slopes of the advanced vehicles along with a comparable aircraft group are presented in tabular form in Table 9-20 through Table 9-23.

Table 9-20. Fuel burn gradient.

Percent of Total Fuel Burn /	CESTOL	Commercial Jet	VLJ	Business Jet	LCTR	Regional Jet	UAS	SST
Percent of Total Flights	0.667	1.023	0.072	0.368	1.428	0.595	0.181	3.492
Percent of Total Distance	0.650	1.077	0.065	0.432	1.233	0.594	0.220	3.178
Percent of Total Time	0.640	1.112	0.055	0.458	0.909	0.606	0.181	3.541
Percent of Total Passengers	0.830	0.843	3.545	6.943	1.778	1.182	--	4.504

CESTOLs compared against commercial jets, and VLJs compared against business jets follow the same trends as discussed in the CESTOL and VLJ results sections. This section focuses on the other three advanced vehicles, LCTR, UAS, and SST.

Table 9-21. CO₂ gradient.

Percent of Total CO ₂	CESTOL	Commercial Jet	VLJ	Business Jet	LCTR	Regional Jet	UAS	SST
Percent of Total Flights	0.667	1.023	0.072	0.368	1.428	0.595	0.181	3.492
Percent of Total Distance	0.650	1.077	0.065	0.432	1.233	0.594	0.220	3.178
Percent of Total Time	0.640	1.112	0.055	0.458	0.909	0.606	0.181	3.541
Percent of Total Passengers	0.830	0.843	3.545	6.943	1.778	1.182	--	4.504

As seen in Table 9-20 and Table 9-21, in terms of fuel burn and CO₂, LCTRs perform worse in the terminal airspace on a per-flight, per-distance, and per-time basis when compared to regional jets. SSTs are also observed to perform worse when compared against commercial and regional jets. UAS aircraft are modeled to have similar characteristics as the Cessna Caravan, and have similar emissions performance as other small aircraft. Note that UAS aircraft are excluded from comparisons on a per-passenger basis. The trends in the relative emissions performance for the LCTR, SST, and UAS aircraft follow similar trends in terms of NO_x and PM, as shown in Table 9-22 and Table 9-23.

Table 9-22. NO_x gradient.

Percent of Total NO _x	CESTOL	Commercial Jet	VLJ	Business Jet	LCTR	Regional Jet	UAS	SST
Percent of Total Flights	0.286	0.985	0.017	0.353	1.349	0.521	0.081	1.421
Percent of Total Distance	0.278	1.036	0.015	0.407	1.164	0.522	0.098	1.293
Percent of Total Time	0.273	1.070	0.013	0.432	0.858	0.534	0.081	1.441
Percent of Total Passengers	0.359	0.823	0.833	6.704	1.696	1.045	--	1.838

LCTRs perform worse when compared against regional jets, and SSTs perform worse than other commercial vehicles.

Table 9-23. PM gradient.

Percent of Total PM	CESTOL	Commercial Jet	VLJ	Business Jet	LCTR	Regional Jet	UAS	SST
Percent of Total Flights	0.655	1.033	0.078	0.366	1.542	0.590	0.193	3.585
Percent of Total Distance	0.638	1.087	0.070	0.432	1.331	0.590	0.234	3.264
Percent of Total Time	0.628	1.123	0.060	0.458	0.981	0.602	0.193	3.636
Percent of Total Passengers	0.815	0.851	3.825	6.910	1.921	1.172	--	4.628

Note that this data only includes the flight operations within the metroplex and does not represent the relative efficiency for the entire flight.

Noise

The advanced vehicles have several impacts on the noise contours around the airports. The first is that these vehicles may have a different noise footprint compared to conventional vehicles. Also, their unique operating characteristics allow the use of unconventional procedures, which has the potential to change the shape of the noise contours.

Overall, the impact of the advanced vehicles on the noise in the vicinity of the eight modeled airports was quantified by the change in area within the 60, 65, and 70 dB DNL noise contours. Table 9-24, Table 9-25, and Table 9-26 present the area, in square miles, contained within the 60 dB DNL noise contour for the Baseline and All Vehicles scenarios and the percent difference relative to the Baseline scenario. This data shows the varying levels of change in the noise contour areas at the modeled airports for the 2025, 2040, and 2086 demand years.

Table 9-24. Comparison of area (sq. miles) within the 60 dB DNL noise level contour for 2025.

	JFK	LGA	ISP	EWR	FRG	SWF	TEB	HPN
Baseline	32.662	7.238	1.447	17.936	2.197	0.475	8.953	4.202
All Vehicles Demand	32.685	6.997	1.853	17.818	2.293	0.562	9.175	4.374
Sq. Mile Change	0.023	-0.241	0.406	-0.118	0.097	0.087	0.222	0.172
Percent Change	0.07%	-3.34%	28.02%	-0.66%	4.40%	18.42%	2.48%	4.09%

Table 9-25. Comparison of area (sq. miles) within the 60 dB DNL noise level contour for 2040.

	JFK	LGA	ISP	EWR	FRG	SWF	TEB	HPN
Baseline	33.442	6.856	1.904	18.210	2.397	0.301	8.995	4.890
All Vehicles Demand	40.535	10.536	4.637	18.982	2.727	0.446	9.375	5.289
Sq. Mile Change	7.093	3.680	2.732	0.772	0.330	0.145	0.380	0.399
Percent Change	21.21%	53.68%	143.5%	4.24%	13.76%	48.12%	4.23%	8.15%

Table 9-26. Comparison of area (sq.miles) within the 60 dB DNL noise level contour for 2086.

	JFK	LGA	ISP	EWR	FRG	SWF	TEB	HPN
Baseline	41.899	6.955	3.069	26.183	3.167	0.443	7.510	6.087
All Vehicles Demand	49.351	13.774	7.006	26.074	3.978	0.846	8.083	6.920
Sq. Mile Change	7.452	6.819	3.936	-0.109	0.810	0.403	0.573	0.833
Percent Change	17.79%	98.05%	128.25%	-0.42%	25.59%	91.02%	7.62%	13.69%

Comparing the eight airports, EWR shows the least change by percent when compared against the Baseline scenario throughout the three demand years. Figure 9-63 presents the noise contour area at EWR for the 2086 Baseline and All Vehicles scenarios. Although it can be observed that there are noticeable increases in areas where advanced vehicles operate, there is also a decrease in the regions used by conventional vehicles and procedures. The 60 dB noise contour area for the 2086 Baseline scenario is 26.2 square miles while the 2086 All Vehicles scenario is 26.1 square miles. This difference in area is less than one percent.

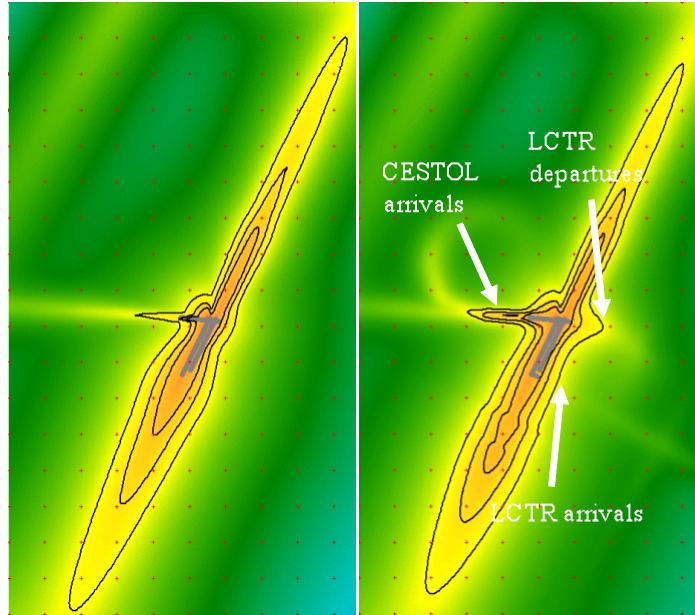


Figure 9-63. Baseline DNL noise contour (left) vs. all-vehicle case (right) for EWR (2086).

Alternatively, ISP shows the most dramatic change in the size of the noise contour area from the Baseline scenario throughout the three demand years.

Similar to the DNL noise contours in the CESTOL results, the contour areas are influenced by more than just the number of flights, but are also influenced by the aircraft types, the procedures flown, and the time the flights are scheduled. ISP has a consistent increase in the number of flights, along with an increase in the use of advanced vehicles and their corresponding procedures in the All Vehicles scenario. Figure 9-64 illustrates the impacts of all of these factors on the 60-70 dB noise contours at ISP.

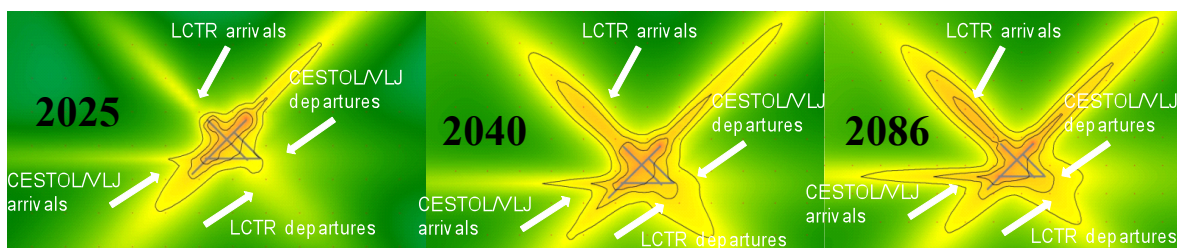


Figure 9-64. ISP 60-70dB DNL noise contours for all-vehicles scenario.

As can be observed in the figure, the noise contour areas continually grow where the advanced vehicles operate. The area within the 60 dB noise contour grows from 1.8 square miles in the 2025 demand year to 7.0 square miles in the 2086 demand year, which are 28% and 128% larger than the Baseline scenario, respectively.

9.7.5. Off-nominal

This section presents the results of the Off-nominal scenario. As stated in the Model Development section, the modeled weather data covers a 24-hour period; however, the first storm cells to affect the Metroplex terminal airspace do not start until 10 AM. Throughout the day, the number, intensity, and location of the storm cells vary and therefore have a significant and highly variable impact on the flight operations in the Metroplex. Figure 9-65 presents the running total of all storm intensities, the storm intensities affecting the modeled NY Metroplex airspace, and those affecting only JFK. Figure 9-66 presents the same information for SWF.

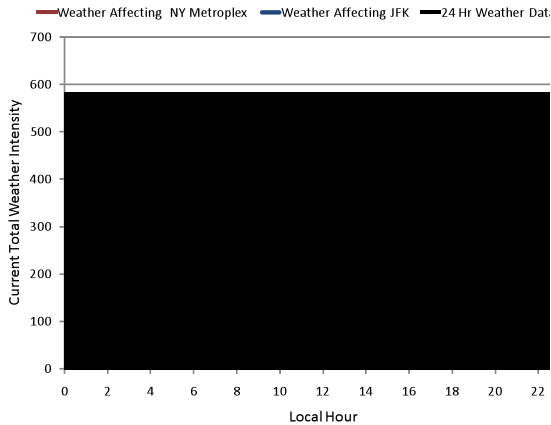


Figure 9-65. Running total of storm intensity affecting JFK.

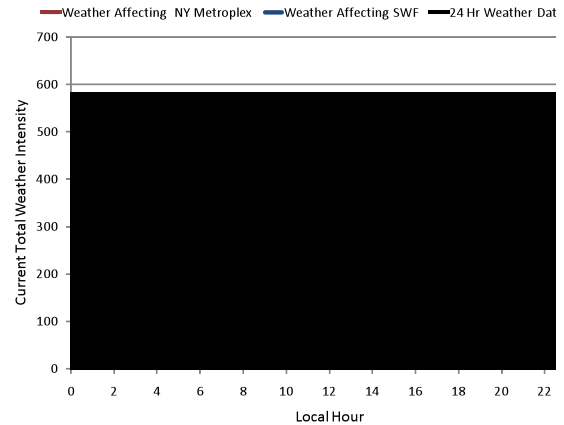


Figure 9-66. Running total of storm intensity affecting SWF.

As the chart shows, the storm intensities affecting each airport vary considerably. At JFK, for example, the storm cells affect flights between 10:00 and 24:00. Operations at SWF, however, are not significantly affected by the storm until 19:00. Therefore, the weather effects on each airport are dependent on the varying distribution of the time and location of individual storm points.

Delay

Figure 9-67 presents the average arrival air delay against the number of arrivals. Figure 9-68 presents the average departure queue delay against the number of departures. In the off-nominal weather conditions, arrival air delay was an average of 9 minutes higher than in the nominal weather conditions. In the off-nominal weather conditions, departure queue delay was an average of 4 minutes higher than in the nominal weather conditions.

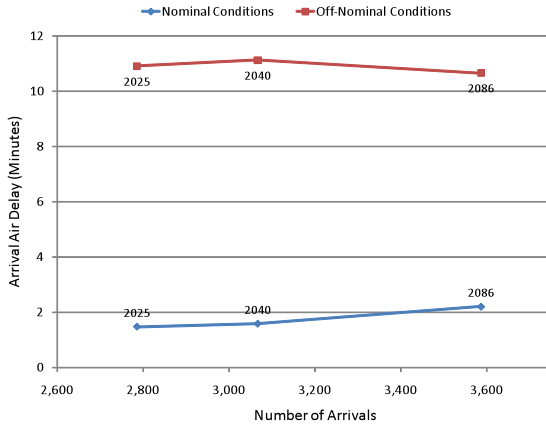


Figure 9-67. Average arrival delay vs. number of arrivals for all demand years.

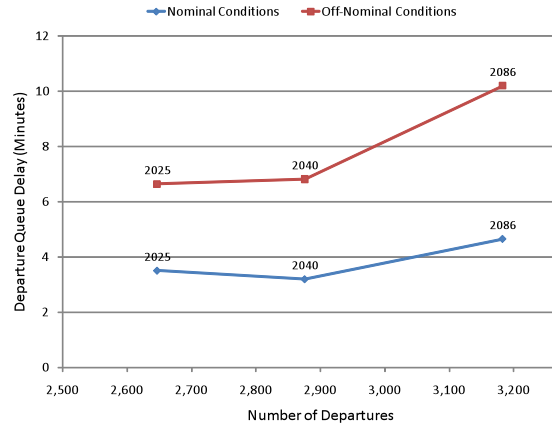


Figure 9-68. Average departure queue delay vs. number of departures for all demand years.

The increase in delay due to the convective storm cells occurs during peaks in storm intensity. Figure 9-69 presents the average arrival air delay for aircraft landing during each 15-minute time bin throughout the day. The sum of all storm intensity during the corresponding 15-minute time bin is included as a reference. The arrival air delay presented in this chart is associated with each flight’s runway touchdown time and reflects all delay that occurred during the flight. This explains why the peak of the delay occurs after the greatest storm intensity.

Figure 9-70 presents the average departure ground delay and departure air delay for aircraft held on the ground during each 15-minute time bin. The same storm intensity is plotted as a reference. Similar to the arrival air delay, the peak for the reported ground delay occurs once the aircraft are finally able to depart. Departures incur limited airspace delay since once they depart they continue unimpeded through the terminal airspace unless a new storm cell appears along their route.

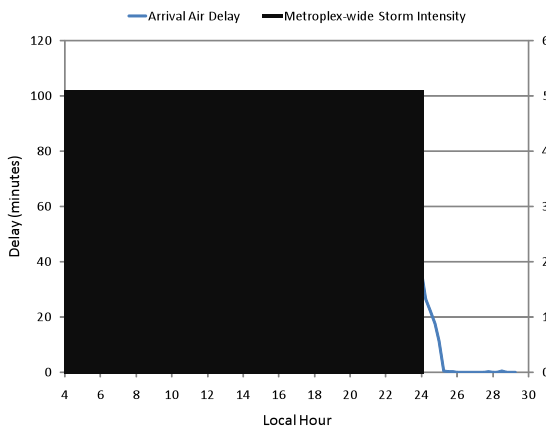


Figure 9-69. Average arrival delay and storm intensity for 2025 all-vehicles case.

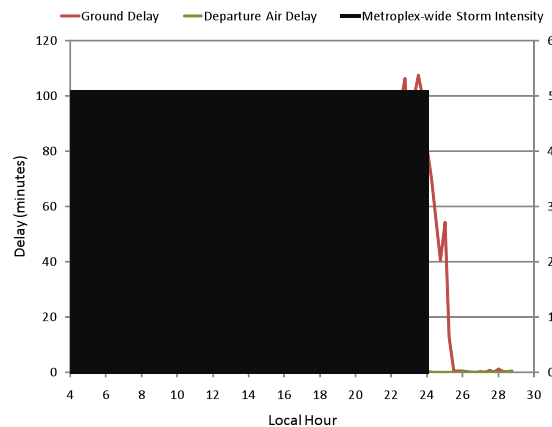


Figure 9-70. Average departure delay and storm intensity for 2025 all-vehicles case.

In order to observe the effect of the advanced vehicles during off-nominal weather conditions compared to demand with only conventional vehicles, the 2025 Baseline and 2025 All Vehicles demand were simulated using the same modeled off-nominal weather input. The 2025 demand year was chosen because both the Baseline and All Vehicle scenarios have a similar number of flights by airport, as shown in Figure 9-25, and approximately the same amount of overall delay under nominal conditions, as shown in Figure 9-54.

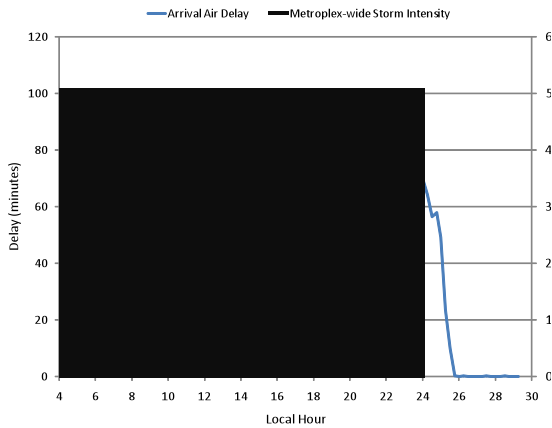


Figure 9-71. Average arrival air delay and storm intensity for the 2025 Baseline scenario.

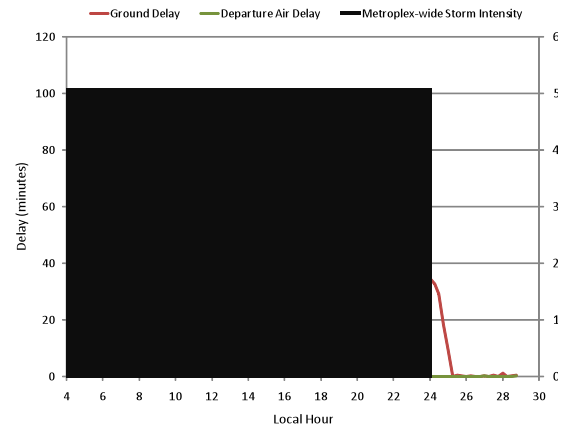


Figure 9-72. Average departure delay and storm intensity for the 2025 Baseline scenario.

Comparing the 2025 Baseline and All Vehicles scenarios under off-nominal conditions, the peak in average air delay is higher for the Baseline scenario. However, the average ground delay is higher in the All Vehicles scenario. The amount of delay incurred in each case is dependent on the scheduled times of operations and the planned flight path with respect to the time and location of the convective storm cell tracks. The primary driver for these results is the distribution of storm cell tracks and intensities throughout the metroplex rather than the unique characteristics of the advanced vehicles.

Capacity

Figure 9-73 and Figure 9-74 present the cumulative difference in the number of nominal and actual arrivals and departures in the metroplex respectively. These charts were created by first taking the difference between the number of expected arrivals/departures and the number of actual arrivals/departures in one-hour increments, and then taking a cumulative sum of this difference. Negative values indicate the number of flights that are held, and have not yet landed due to the blocking by convective storm cells. Positive values indicate early arrivals.

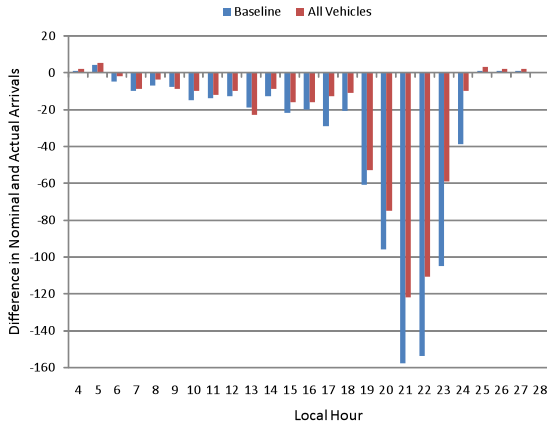


Figure 9-73. Cumulative difference in nominal and actual arrivals for 2025.

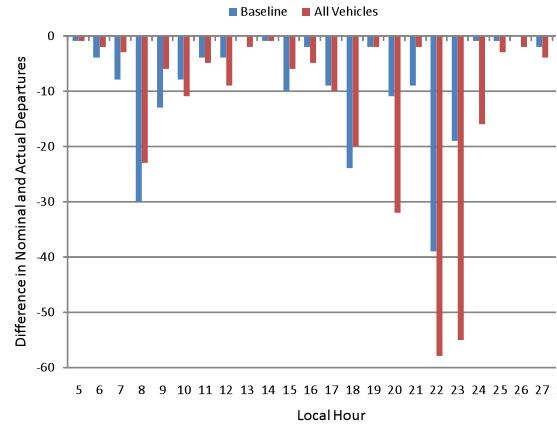


Figure 9-74. Cumulative difference in nominal and actual departures for 2025.

There is an increase in the number of held flights between the hours of 18:00 and 23:00, which corresponds with the peak storm intensity times, as shown in Figure 9-65. In the Baseline scenario, more arrivals are held by the convective storm cell tracks, while more departures are held in the All Vehicles scenario.

Figure 9-75 presents the operating envelopes for the metroplex in the Baseline and All Vehicles scenario for the 2025 Off-nominal conditions. The All Vehicles scenario show a slight increase in maximum throughput, which may be due to the increased utilization of runways by advanced vehicles during recovery from the convective storms.

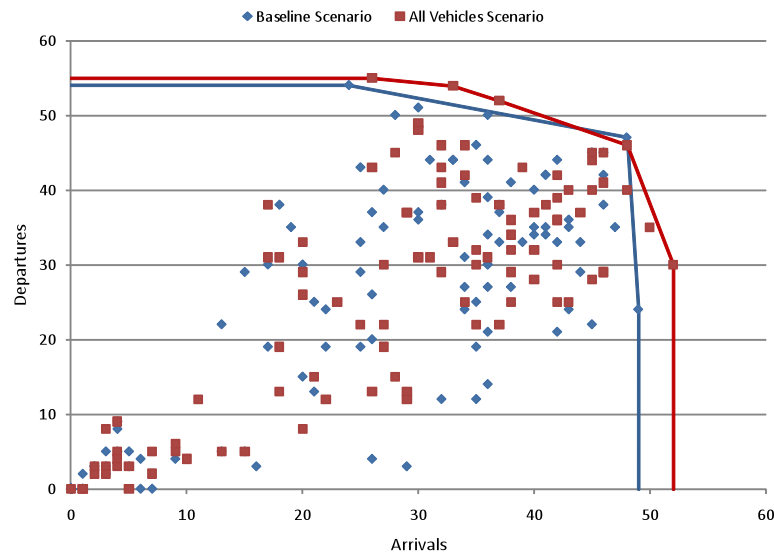


Figure 9-75. Metroplex operating envelopes for the off-nominal 2025 demand year.

Fuel Burn and Emissions

Due to the increase in delay in the Off-nominal scenario, increases in total fuel are observed as shown in Figure 9-76. CESTOLs and VLJs show an 8% increase in fuel burn between the nominal and off-

nominal scenarios. Business jets have a 10% increase, and regional jets have a 39% increase in fuel burn. These percent increases are more primarily driven by the distribution of the storm cell tracks, as opposed to characteristics that can be attributed to the advanced vehicles.

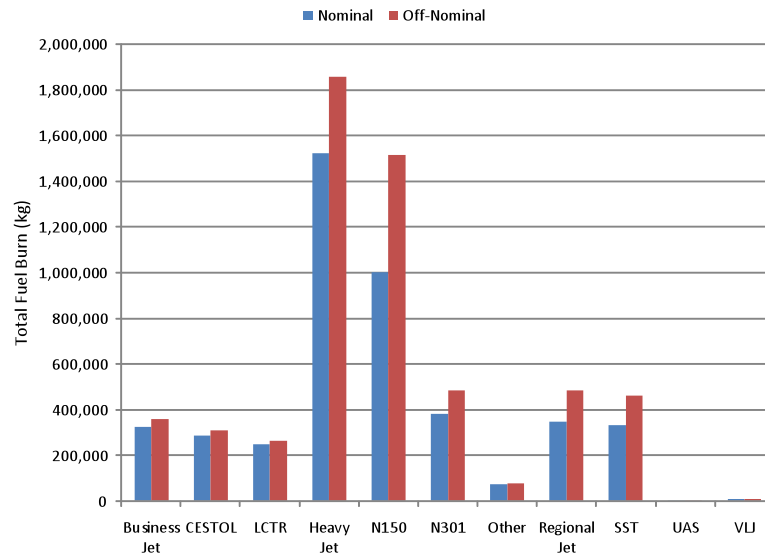


Figure 9-76. Total Fuel Burn for the all aircraft groups in the 2040 demand year.

Similar trends are observed for other emissions metrics. Figure 9-77 presents the increases in NO_x in the 2040 demand year.

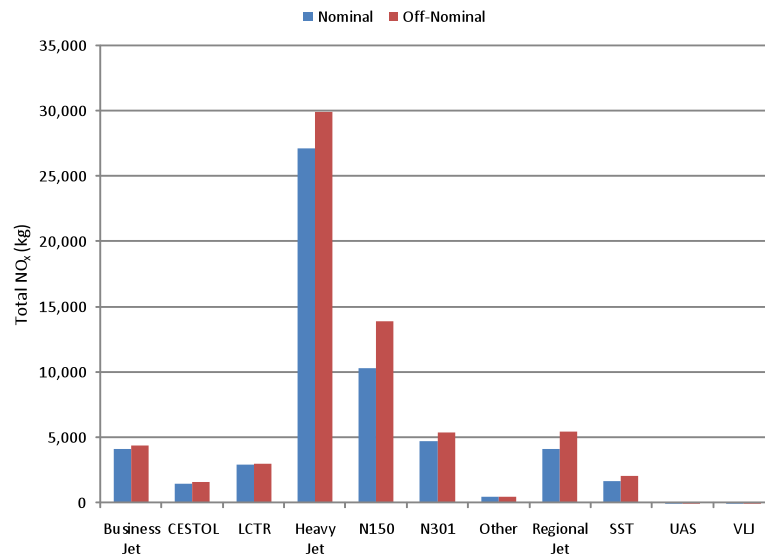


Figure 9-77. Total NO_x for all aircraft groups in 2040.

Noise

Due to model limitations, delay was removed from flights for AEDT noise calculations. Nevertheless, increases in the 60 dB DNL noise contour areas are observed for the off-nominal scenario, as shown in Table 9-27.

Table 9-27. Comparison of area within 60 dB DNL contour for the All Vehicles demand for 2086.

	JFK	LGA	ISP	EWR	FRG	SWF	TEB	HPN
Nominal	49.351	13.774	7.006	26.074	3.978	0.846	8.083	6.920
Off-Nominal	50.237	14.125	7.247	26.276	3.977	0.846	8.102	7.443
Sq. Mile Change	0.886	0.351	0.241	0.202	0.000	0.000	0.020	0.523
Percent Change	1.80%	2.55%	3.44%	0.77%	-0.01%	0.00%	0.24%	7.56%

This increase in the noise contour areas are due to flights held by the convective storm cells. Flights that are pushed past 10 PM incur a 10 dB penalty, which causes this increase in the off-nominal scenario.

9.7.6. Conclusion

The direct addition of VLJs to smaller and less congested airports has minimal impact on overall delay in the metroplex. VLJs perform better than business jets in terms of fuel burn and emissions in the terminal airspace, due to their smaller size and weight. Although the VLJs exhibit less effect on airspace delays than regional jets on a per-flight basis, their relative performance in fuel burn and emissions per passenger is worse than that of regional jets. As expected, the direct addition of VLJs to the small airports increases the 60 dB DNL noise contour areas around the airports. The location of the increases in the noise contour area is dependent on the runways where VLJs operate.

Since the CESTOLs have been added to the modeled airports in various ways, their specific impacts to metroplex operations are difficult to isolate. However, the benefits of the CESTOL's ability to land and take off from shorter runways, which allow them to operate on runways not fully utilized by conventional aircraft, allow for added capacity at particular airports. Furthermore, the CESTOL aircraft's ability to climb quickly, which allows the use of spiral departure procedures at particular airports, helps mitigate their impact on conventional vehicle traffic. For fuel burn and emissions, CESTOLs perform better than commercial jets in the terminal airspace. The DNL noise contours are observed to increase where CESTOLs operate. However, the shift in the number of flights at the different airports, combined with the different aircraft types in the different demand years, make it difficult to isolate the noise impacts of the CESTOL aircraft at the different airports.

Taking advantage of the LCTR's ability to land on short runways allow for the use of landing strips, which help segregate LCTR arrival traffic from other conventional vehicles. The use of the landing strips increases arrival throughput, and eliminates negative impacts to arrival air delay. However, the placement of LCTR landing strips that cross departure runways causes negative impacts to departure throughput, as can be observed for LGA. Furthermore, when LCTRs are able to operate on underutilized runways, as is

the case at TEB, increased departure throughput is observed. However, when LCTR departures are mixed with other vehicles, their slower operating speeds cause negative impact on throughput and delay. For fuel burn and emissions, the LCTRs are observed to perform worse than regional jets in the terminal airspace. The noise impact of the LCTR is highly sensitive to their flight trajectories, which affect the overall noise contours at individual airports differently. In general, the LCTRs have a bigger noise footprint than other vehicles.

Since the UAS and SST aircraft operate similar to conventional vehicles in the terminal airspace, their impact on the metroplex in terms of delay and capacity is not analyzed. In terms of fuel burn and emissions, the UAS perform similar to other small aircraft in the terminal airspace. SSTs are observed to have a higher relative fuel burn and emissions when compared to other large commercial jets in the terminal airspace.

In the All Vehicles scenario, the increase in the adoption of advanced vehicles allows for the shift of flights from the major airports to the smaller satellite airports in the metroplex, and increased runway utilization.

cviii Federal Aviation Administration, "SIMMOD Manual Version 3.1," September 2008.

cix Bobick, J. C., "Validation of the SIMMOD Model," ATAC Corporation, Mountain View CA, Contract No. DTFA03-85-C- 00043

cx den Braven, W., Schade, J., "Concept and Operation of the Performance Data Analysis and Reporting System," SAE Advances in Aviation Safety Conference (ACE), Montréal, 8 - 12 September, 2003, paper number 2003-01-2976.

cxi Miller, C., Monk, H., "Portland International Airport Data Package Number 3 Airport Capacity Enhancement Plan Phase II Terminal Location Study," FAA William J. Hughes Technical Center Library, Atlantic City International Airport, NJ, June 2003, Report No. DOT/FAA/CT-TN03/17.

10. Washington DC Metroplex Analysis

This section investigates a reorganization of the airspace in the Washington DC metroplex to accommodate the unique performance capabilities of the new vehicle types for the years 2025 and 2040. The redesigned airspace takes advantage of expected NextGen airport and sector capacity improvements projected for these years. The DC metroplex includes three large airports—Washington Dulles International Airport (IAD), Baltimore-Washington International Airport (BWI), Washington National Airport (DCA)—as well as six satellite airports. Landing and takeoff areas for LCTR aircraft, known as vertiports, were identified at each of the three major airports.

Results show that CESTOL aircraft have the potential to increase throughput and reduce delay when used with reliever airports and underutilized runways. LCTR aircraft reduce delay by utilizing corridors into and out of vertiports, flying routes that do not conflict with conventional aircraft flows. We also found that adding VLJ and UAS vehicles to the fleet mix does not adversely affect average delay.

10.1. *Research Method*

To take advantage of the capabilities of the CESTOL and LCTR aircraft as well as NextGen features (e.g. RNAV/RNP, Continuous Descent Arrivals), the Potomac TRACON airspace was redesigned with the goal of maximizing airport and airspace throughput. This was accomplished by 1) making use of reliever airports and underutilized runways for the CESTOL aircraft, 2) adding vertiports for the LCTR, and 3) separating the arrival and departure flows of conventional, CESTOL, and LCTR aircraft to ensure non-interfering operations.

The enhanced terminal modeling capability (or Runway Model^{cxiii}) of the Airspace Concept Evaluation System (ACES)^{cxiii, cxiv} was used to model the metroplex. The Runway Model allows users to define each runway in an airport, define the runway's role (departure, arrival, or both), assign runways to specific departure and arrival fixes, and characterize the rules governing the use of these runways, such as through separation and crossing runway limitations.

10.1.1. Major DC Area Airports

We used ASPM to find the predominant runway configuration on our base day, July 13, 2006, at the three major DC airports. See Table 10-1. Although airport runway configurations typically change throughout the day based on weather and other reasons, we used a single runway configuration in this study.

Table 10-1. Major DC airport runway configuration from ASPM for July 13, 2006.

Airport	Arrival Runway	Departure Runway
KIAD	1L, 1R	30
KBWI	33L, 33R	28, 33R
KDCA	15, 19, 22	15, 19, 22

We also identified planned runway additions at these airports. On November 20, 2008, a new parallel runway, 1L/19R, began operating at IAD. In addition, the Metropolitan Washington Airports Authority

has plans to add a fifth runway at IAD, parallel to the current 12/30 runway^{cxv}. For the purposes of this study, it is assumed that this fifth runway would be in operation by 2025.



Figure 10-1. BWI proposed vertiport location.

To take advantage of the helicopter like approach and landing capability of LCTR aircraft we looked at the land around IAD, BWI, and DCA to find potential areas to add LCTR vertiports. Because the LCTR only requires a small landing area (approximately 600 ft.) the cost of adding this vertiport would be substantially lower than adding a longer runway. Due to the small size requirement there is much more flexibility in locating the vertiport on the airport grounds. A possible vertiport location for BWI is shown in Figure 10-1. Vertiport locations were also chosen for IAD and DCA.

The CESTOL aircraft has the ability to operate from runways as short as 3000', allowing it to use smaller reliever airports as well as existing smaller runways at large airports. Both BWI and DCA currently have runways that are not suitable for large commercial airliners; however, they would be usable by the CESTOL aircraft in this study. At BWI, runway 33R is 5000' x 100' and DCA runway 22 is 4911' x 150'. In redesigning procedures for the Potomac TRACON airports, we make use of these runways for the CESTOL.

Accounting for the planned runway and potential vertiport additions, and looking at runway usage in our redesigned airspace we revised the runway configurations in 2025 for the three major Potomac TRACON airports as shown in Table 10-2.

Table 10-2. DC Metro area runway configuration for 2025 redesigned airspace.

Airport	Arrival Runway	Departure Runway
KIAD	1L, 1C, 1R, TR	30L, 30R, 1L, TR
KBWI	33L, 33R, 28, TR	28, 33R, TR
KDCA	15, 19, 22, TR	15, 19, 22, TR

Note: TR is the LCTR vertiport runway designation

10.2. **Reliever Airport Selection**

To maximize the use of the CESTOL capabilities we selected a number of small reliever airports in the DC metropolitan area that could be used to offload short haul traffic from IAD, BWI and DCA. The airports selected as relievers had to meet the following initial criteria: 1) airport must be within 70 nm radial distance of the origin or destination OEP-35 airport, 2) possess at least one paved runway greater than or equal to 3,000 feet in length and having a width greater than or equal to 100 feet. For simplicity, we did not consider the costs of airport enhancements such as runways and taxiways improvements to accommodate larger aircraft. Other important cost factors to consider are added security requirements, environmental impact mitigation, and safety enhancements (e.g. surface monitoring systems).

The last qualifying factor was driving time from the satellite airport to the original airport. In our study, driving time was limited to 90 minutes or less. Driving times were obtained from Google Maps (<http://maps.google.com>). Note that driving times during busy traffic periods were not considered for simplicity. The selected reliever airports for this study are: Carroll County Regional/Jack B. Poage Airport (DMW), Manassas Regional/Harry P. Davis Airport (HEF), Frederick Municipal (FDK), Eastern West Virginia Regional Airport/Shepherd Field (MRB), Martin State Airport (MTN), and Stafford Regional Airport (RMN). See Table 10-3 for the reliever airport assignments.

Table 10-3. Driving times between DC Metro airports.

Primary Airport					
KIAD		KBWI		KDCA	
Reliever	Drive Time (min)	Reliever	Drive Time (min)	Reliever	Drive Time (min)
KMRB	85	KFDK	54	KFDK	65
KFDK	55	KDMW	53	KMTN	78
KMTN	88	KMTN	36	KRMN	54
KRMN	73	KHEF	87	KHEF	53
KHEF	38				

Drive times from Google Maps, checked on 1/7/09

Note: drive times do not take into account traffic delays

10.2.1. Procedure Design

Having selected the runway configurations and reliever airports, we determined the arrival and departure fixes and assignments to the runways. The criteria used in the design were 1) each runway should have separate arrival and departure fixes and paths, 2) paths within the terminal area should be separated by at least 1000' vertically and/or 3 nm laterally, 3) there should be no interdependence between airports within the TRACON, 4) all aircraft are assumed to be equipped for RNP approaches to accurately fly arbitrary paths, and 5) flight paths will avoid current restricted airspace around the DC metropolitan area.

Detailed fix-to-runway paths for each airport and runway were designed, giving particular attention to avoiding conflicts between airports as well as separating the CESTOL and LCTR paths from other aircraft. An overview of the redesigned airspace with the arrival and departure paths for the 9 airports selected for this study is shown in Figure 10-2.

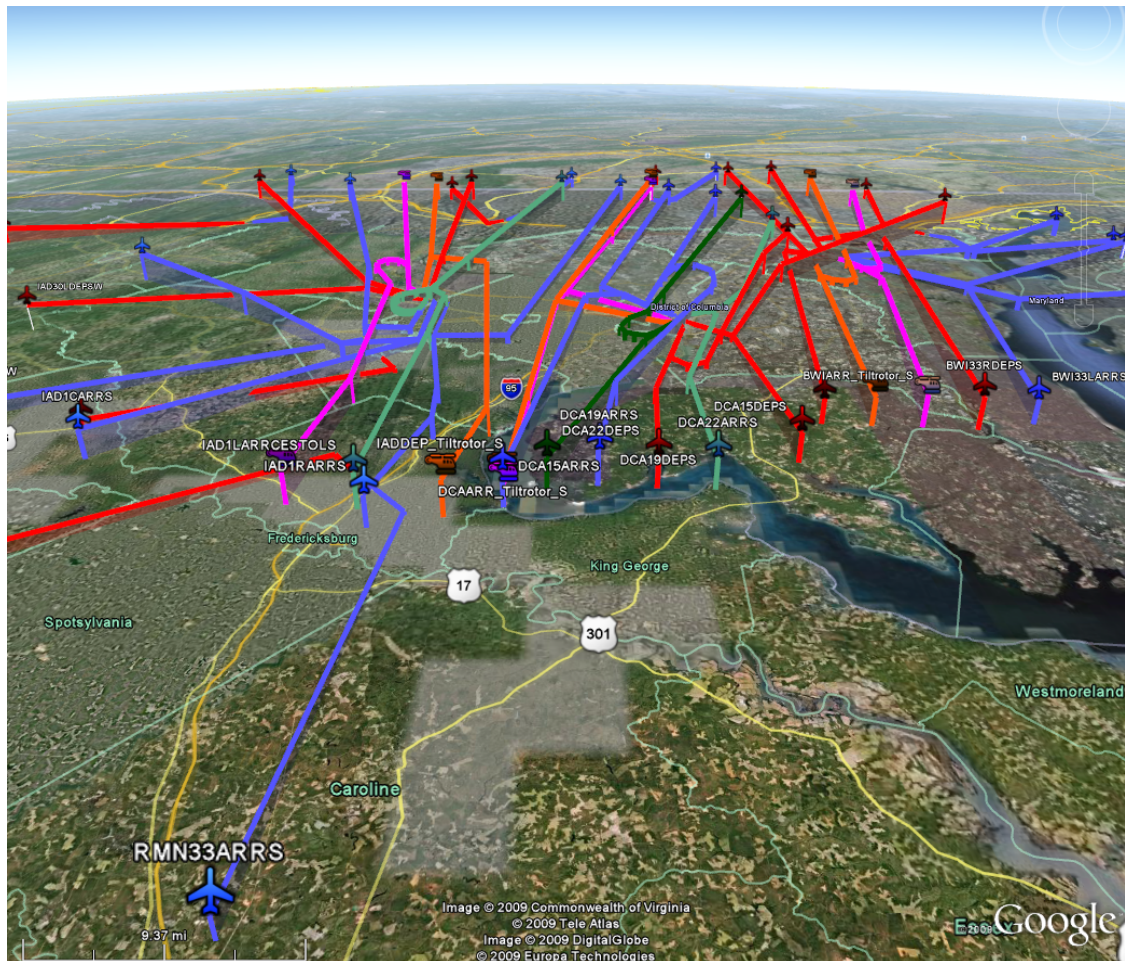


Figure 10-2. Potomac TRACON redesigned airspace in 2025.

An example of a reliever airport for BWI can be seen in Figure 10-3. In this case Martin State Airport (MTN) is used to offload some CESTOL flights from BWI. The arrival and departure paths for traffic between the two airports have been separated to allow for non-interfering operations.



Figure 10-3. BWI and reliever airport.

The redesigned airspace produced a set of arrival and departure fixes as well as runway assignments for each airport being modeled. This new airspace design was then implemented in ACES using the enhanced terminal model feature described above.

10.2.2. ACES Simulation

The default terminal area model in ACES is the nodal model. In this model, airports are represented as points surrounded by a circular terminal area of user-defined radius, (normally 40 nm). The terminal area boundary contains eight equidistant fixes alternating in function between arrival and departure (left diagram in Figure 10-5). The arrival and departure rates of each airport are obtained from Pareto curves which represent the composite arrival and departure rates for all runway configurations. A sample Pareto curve used in the ACES nodal model is shown in Figure 10-4. Unlike the nodal model, the ACES runway model allows the user to define each runway in an airport, its role (departure, arrival, or both), and assign the runway specific departure and arrival fixes (right diagram in Figure 10-5). In addition, the user can define rules governing the use of the runways, such as aircraft separation and crossing runway restrictions. The runway model allows for a large number of runway configurations that can be modified during the simulation to reflect airport configuration changes that typically occur throughout the day.

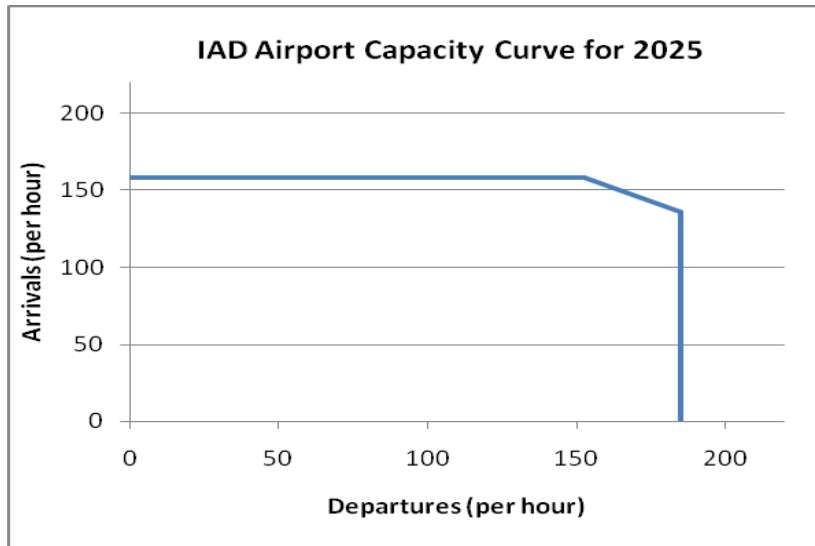


Figure 10-4. Example Pareto Curves for IAD.

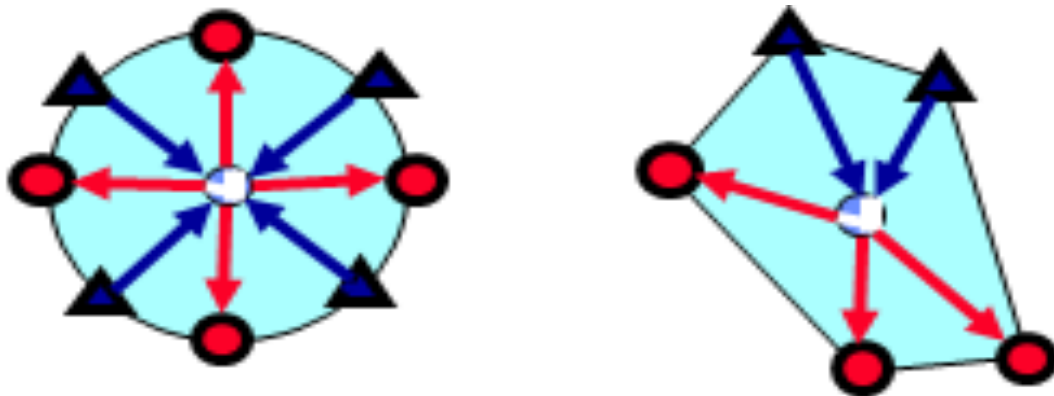


Figure 10-5. Comparison of the ACES nodal model (left) and runway model (right).

10.2.3. Runway Model Verification

A simulation of IAD was performed using the airport configuration for July 13–14, 2006, as a first-level verification of the ACES Runway Model. The actual flight data set schedule for those days was obtained from Aircraft Situation Display to Industry (ASDI) data and formatted for ACES input. Data from the Aviation System Performance Metrics (ASPM) system was used to compare against ACES results. ASPM data has been used in a previous study to validate ACES results^{cxvi}. It is worth noting that the ASPM database contains only a subset of scheduled air carrier operations while the ACES flight schedule includes all scheduled air carrier flights as well as other non-scheduled IFR flights.

The ASPM data showed that the airport configuration for IAD was 19L/19R for arrivals, and 19L/30 for departures during a 24-hour period starting on 13 July 2006, 5:00 AM. The flight schedule for the simulation consisted of approximately 1,150 flights originating or arriving at the IAD airport. Two simulations were conducted with this data set: 1) IAD nodal model and 2) IAD runway model. The weighted average delay computed for the IAD Runway Model simulation was within one minute of the weighted ASPM average delay value (4.60 vs. 3.89 minutes). From these results, we concluded that the ACES model approximates IAD operations well enough to continue the analysis.

10.2.4. Simulation Configuration

We made special provisions in the ACES configuration to ensure that the CESTOL and LCTR vehicles were simulated according to our experimental assumptions. These steps were necessary because ACES only allows differentiation of traffic in the terminal area based on engine type (piston, turboprop, and jet) instead of aircraft type. CESTOL aircraft were designated as piston in the aircraft characteristics table in ACES. This allowed ACES to route these vehicles to short runways designated specifically for piston aircraft. CESTOLs were also able to use longer runways as these were designated for use by all aircraft types. LCTR operations were assumed to be independent from the rest of the traffic flowing into and out of airports. This was accomplished by superimposing vertiports on the original airport in the terminal model management table in ACES. For example, a vertiport DC1 was added to airport DCA. Although both were geographically identical, the vertiport featured only one landing area (or pad). The flight schedule was modified to ensure only LCTR aircraft were routed to and from these vertiports (see Figure 10-6).

ACES provides a wide array of simulation options; however, the most relevant functionality was limited to 1) departure and arrival aircraft separation within the terminal area, and 2) increasing the sector Monitor Alert Parameters values for all sectors by a factor of 1.7 from 2006 values. This factor is the expected capacity increase derived from the implementation of NextGen concepts of operations and tools around the 2025 timeframe^{cxvii}.

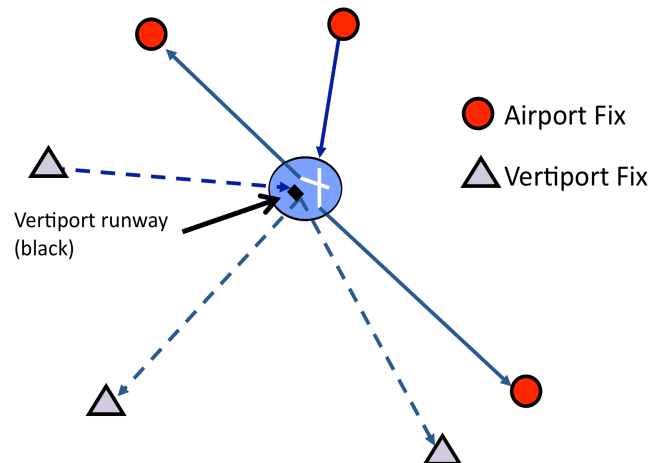


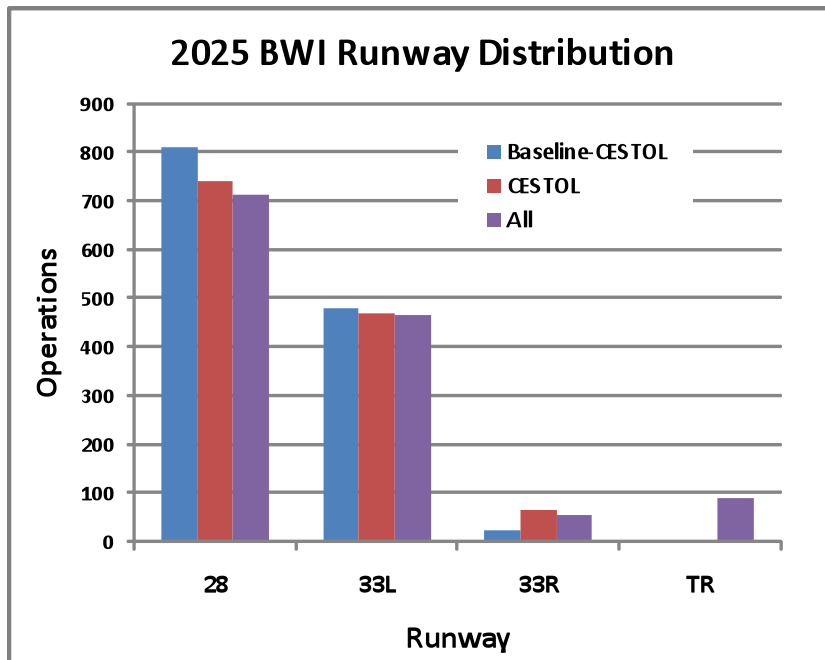
Figure 10-6. Superposition of airport and vertiport.

The flight schedules used were those provided by the Joint Planning and Development Office (JDPO) and that were described in the demand generation section of this report. The schedules for the DC metroplex simulations included only flights into or out of the DC metropolitan airports.

10.3. *Simulation Results*

This section presents the results from our ACES runway model simulation of the DC Metroplex for the years 2025 and 2040. The new vehicle cases analyzed were baseline (no new vehicles), CESTOL replacement, LCTR replacement, and a case that includes a mix of all new vehicle types, including CESTOL, LCTR, VLJ, UAS, and SST.

The design of the new procedures, which takes advantage of new vehicle capabilities, allows for the use of reliever airports, underutilized runways at large airports, and additional vertiports. The intent of



these changes is to offload operations from the primary, highly used runways with the ultimate goal of reducing delays and/or increasing throughput of flights and passengers.

At BWI and DCA the CESTOL can make use of shorter runways typically used for general aviation (GA) operations. The effect of the primary runway offloading at BWI in 2025 can be seen in Figure 10-7, which depicts runway distribution from the ACES simulations. The Baseline-CESTOL schedule that is referred to in this figure needs some explanation. As described in the Demand Generation section of this report, the CESTOL schedule was created by shifting flights in the untrimmed schedule from busy airports to satellite airports. To trim this schedule, specific flights were then deleted from the schedule; however, flights that had business-shifted were not deleted. The Baseline-CESTOL schedule contains no CESTOLs. The Baseline-CESTOL schedule is the same as the baseline schedule, but with the same

flights removed that were removed from the CESTOL schedule. Except where specified we use the fully (100%) trimmed schedules in this analysis.

In the Baseline-CESTOL case the two primary runways (28 and 33L) are used for 98% of the total operations. In the CESTOL replacement schedule case, some CESTOL operations are shifted to the shorter runway, 33R, dropping the primary runway usage to 95% of total operations. In the all-vehicles case, where all five new vehicle types are simulated, a further shift of flights to the vertiport (runway TR) is observed, dropping the primary runway use to 89% of total operations. There is a similar effect in the 2040 results, with the all-vehicles case reducing the primary runway usage to 79% of total operations.

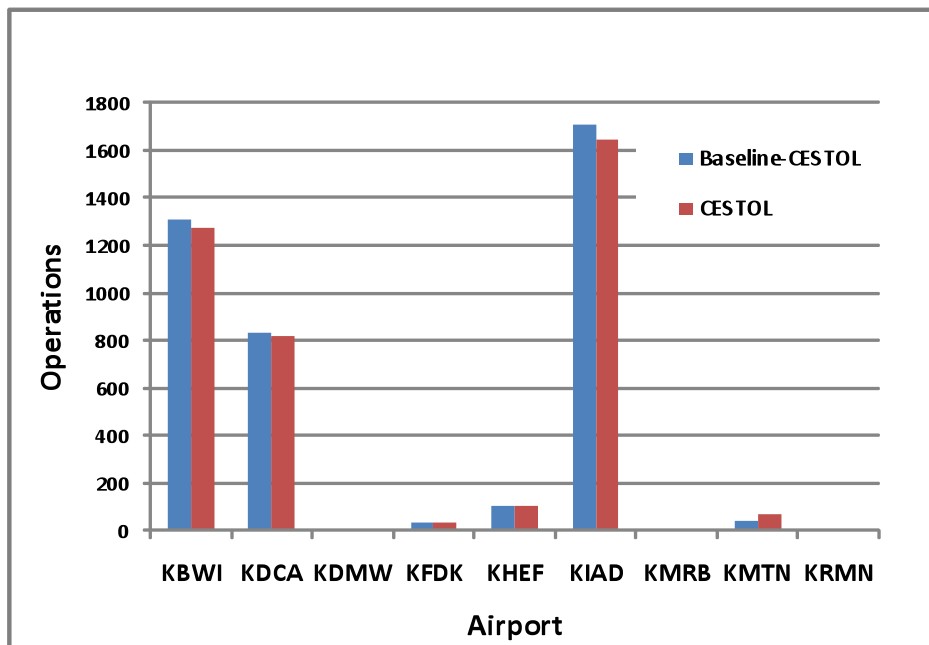


Figure 10-8. DC Metroplex flight distribution (fully-trimmed case).

The effect on airport loading due to the use of reliever airport for the CESTOL can be seen by looking at the change in distribution of operations between the airports in the DC Metroplex for the baseline, CESTOL and all-vehicles cases shown in Figure 10-8. Compared to the baseline, the CESTOL case reduces the number of flights at the three major airports in the Potomac TRACON (IAD, BWI and DCA). This is due to the use of smaller reliever airports by the CESTOL aircraft. An increase in flights can be seen at MTN, a reliever airport for the CESTOL aircraft.

The effect on the average delay of all airports included in the DC Metroplex in 2025 is shown in Figure 10-9. This plot shows the tradeoff between the number of flights and average delay per flight in the DC Metroplex for three trim levels: 0%, 50%, and 100%. In the baseline case (with no new vehicle types) at about 4,000 flights the average delay per flight is 3.5 minute. When the CESTOL aircraft is introduced into the fleet mix, and there is a shift of flights to the reliever airports, the average delay per flight at the 4,000 flight baseline point drops to about 2 minutes. Another way of looking at this is that one could choose an operating point of 3.5 minutes average delay and increase the volume of flights to about 4,400 per day by using CESTOL aircraft and reliever airports.

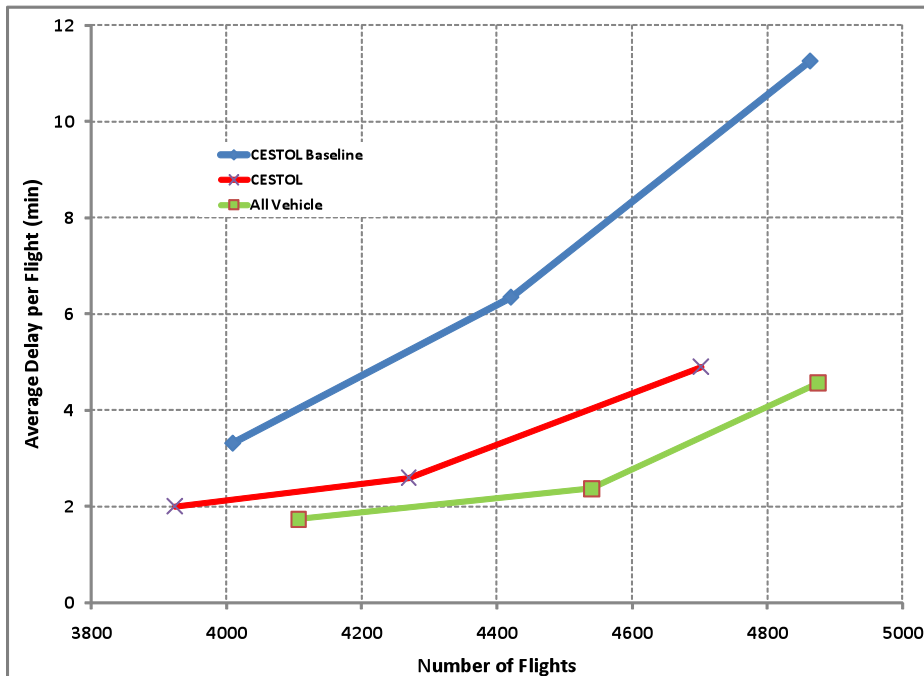


Figure 10-9. Average delay in 2025.

When all new vehicle types are included, there is a more pronounced reduction in delay (or increase in flight volume for a given delay) due to the CESTOL reliever airports, the LCTR vertiports, and the addition of VLJ and UAS flights that make use of the smaller airports in the Metroplex. In this case, choosing an operating point of 3.5 minutes of average day allows for an increase in flight volume to about 4,700 flights per day.

The 2040 simulation results, shown in Figure 10-10, are similar to those for 2025. The all-vehicle schedule for includes SSTs; however, SST performance in the terminal airspace is the same as for conventional vehicles.

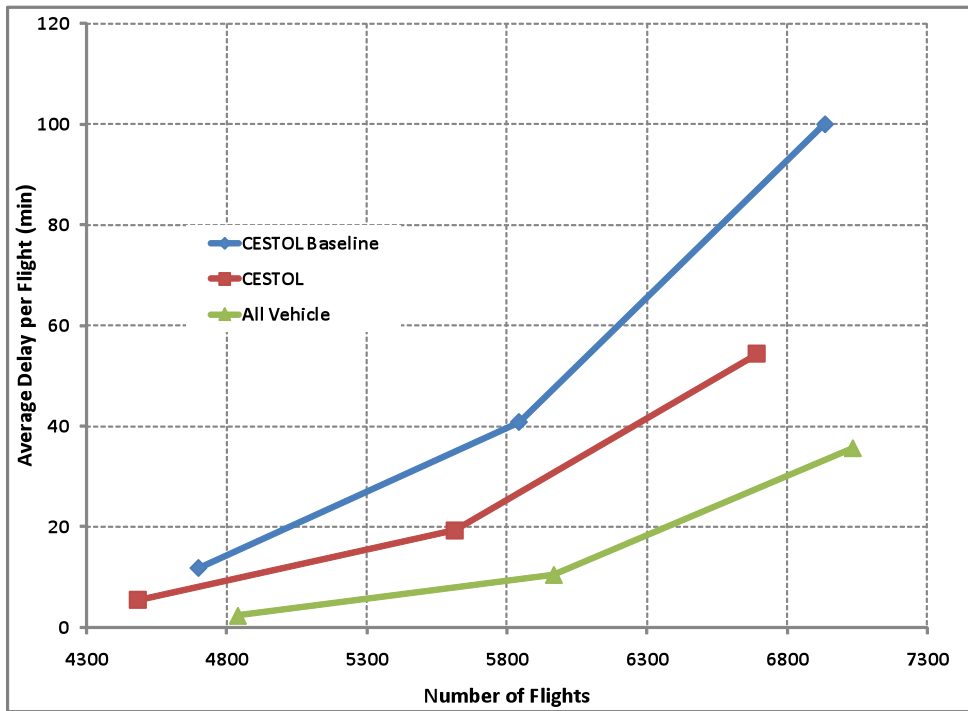


Figure 10-10. Average delay in 2040.

The delay per flight shown in Figure 10-9 and Figure 10-10 is the overall average for all flights arriving or departing at the nine DC Metroplex airports, for the three trim levels 0%, 50%, and 100%. Because we shifted flight volume away from the three major airports it would be expected that the delays at those airports would decrease, and it is of interest to investigate the effect of adding flights to the reliever airports. The distribution of delay among the DC Metroplex airports included in this study for 2025 is shown in Figure 10-13. Of the three major DC airports, BWI has the largest average delay. Looking at the effect of the CESTOL reliever airports we see that BWI also experiences the largest decrease in average delay—from about 6 minutes in the baseline case to just over 3 minutes when reliever airports (and an additional short BWI runway) are used. IAD and DCA also exhibit a similar trend to a lesser degree than BWI. In addition, the reliever airports show very little change in average delay—their average delay per flight is less than 1 minute in all cases. When all new vehicles are included in the fleet mix there is an even larger decrease in average delay, with BWI showing an all-vehicle average delay of about 2.5 minutes per flight.

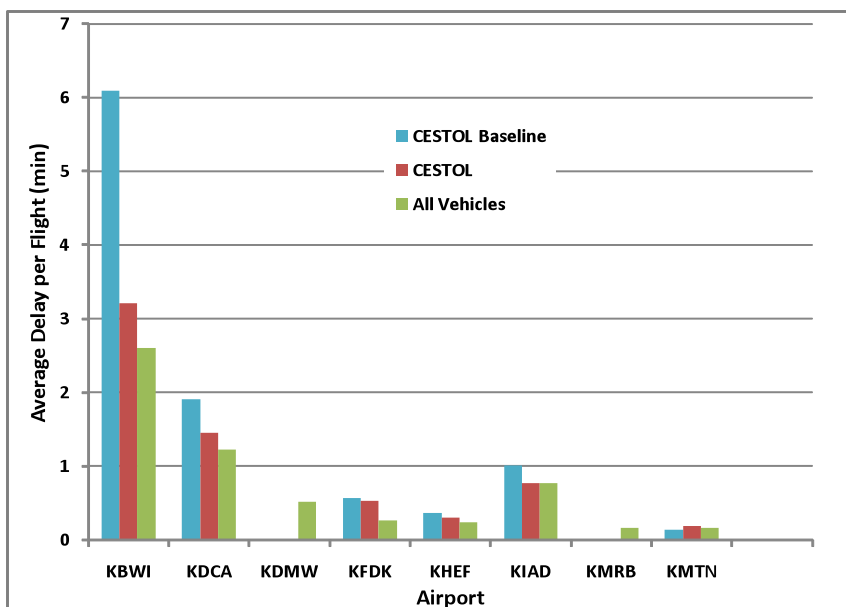


Figure 10-11. DC Metroplex average delay by airport in 2025 (fully-trimmed case).

The distribution of average delay by airport for airports included in the 2040 fully trimmed case is shown in Figure 10-12 for the CESTOL and all-vehicles cases. BWI had the biggest decrease in delay (over 45%) of all the airports. These are not surprising results given that flight demand is largely being shifted to reliever airports.

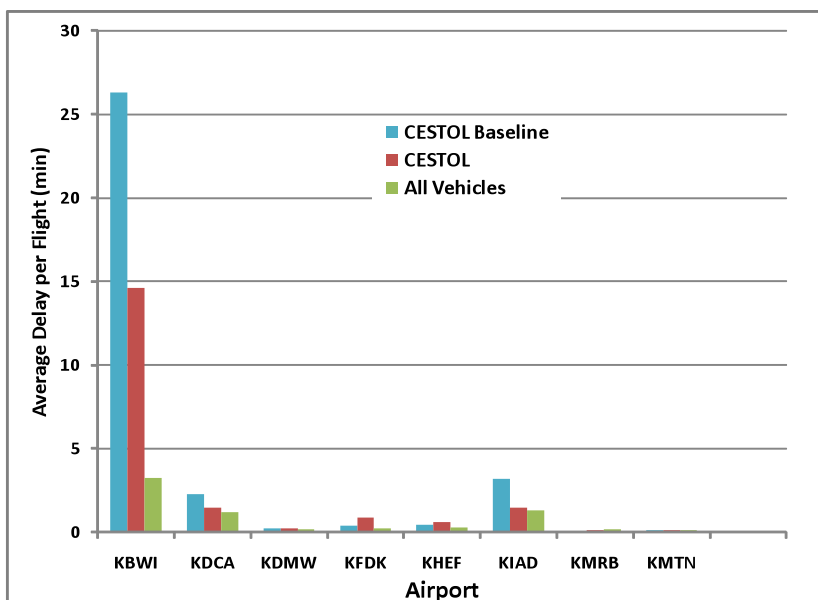


Figure 10-12. DC Metroplex average delay by airport in 2040 (fully trimmed case).

The reliever airports show very little change in average delay with some possible increase in the CESTOL case. When all new vehicles are included in the fleet-mix, the average delay at BWI decreases to about 2.5 minutes per flight.

The average delay by airport for the 2025 fully trimmed case can be seen in Figure 10-13 for the LCTR schedule. BWI benefited from the added vertiport capacity, resulting in a decrease in average delay from 5.5 minutes to 3.7 minutes; however, DCA appears to have experienced a slight increase in delay. Upon further analysis, we traced the source of delay to held flights departing from LaGuardia airport.

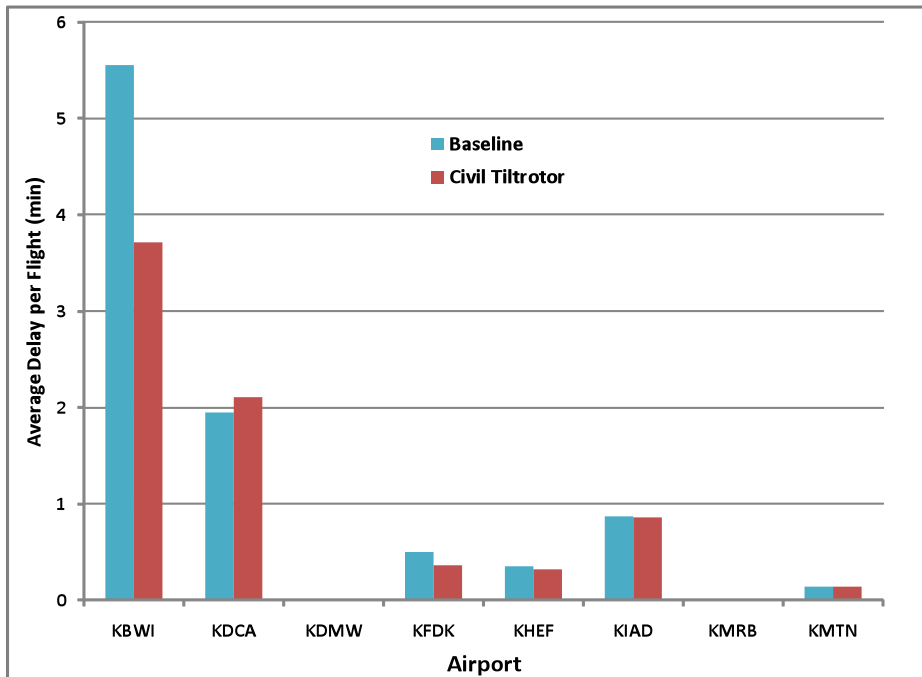


Figure 10-13. Metroplex average delay comparison by airport in 2025 (fully-trimmed case).

Detailed reviewed of the data highlighted some instances of improper aircraft separation during takeoff and landings. No software fixes for this problem were made at the time of this study. Our analysis indicates this anomaly affects approximately 10% of the total flights.

10.4. **Conclusion**

The results presented here show that the addition of the CESTOL and LCTR aircraft provide an overall benefit to the DC Metroplex operation in terms of throughput and average delay, whereas the addition of the VLJ and UAS vehicles in the fleet mix do not appear to adversely affect delay. In the 2025 timeframe the use of CESTOL could increase the throughput in the DC Metroplex from 4,000 to 4,400 flights per day while maintaining the same metroplex-wide average delay of 3.5 minutes per flight. In 2025 BWI showed a decrease in average delay from 5.5 minutes to 3.7 minutes. The all-vehicles case includes CESTOL, LCTR, VLJ, UAS and SST. For the all-vehicle case, the total DC Metroplex throughput in 2025 increases from 4,000 to about 4,700 flights per day while maintaining the same average delay of 3.5 minutes per flight.

cxii G. Couluris, G. Carr, L. Meyn, K. Roth, A. Dabrowski, and J. Phillips, Terminal Area Modeling Complexity Alternatives in a NAS-wide Simulation, AIAA-2004-5435, AIAA Guidance, Navigation, and Control (GNC) Conference and Exhibit, August 2004, Providence, Rhode Island

cxiii G. Couluris, C.G. Hunter, M. Blake, K. Roth, D. Sweet, P. Stassart, J. Phillips, and A. Huang, National Airspace System Simulation Capturing the Interactions of Air Traffic Management and Flight Trajectories, AIAA-2003-5597, AIAA Guidance, Navigation, and Control (GNC) Conference, August 2003, Austin, Texas

cxiv L Meyn, T. Romer, K. Roth, L. Bjarke, and S. Hinton, Preliminary Assessment of Future Operational Concepts Using the Airspace Concept Evaluation System, AIAA-2004-6508, AIAA Aviation Technology, Integration, and Operations (ATIO) Forum, September 2004, Chicago, Illinois

cxv Metropolitan Washington Airports Authority, "Dulles Development Projects," URL: http://www.metwashairports.com/dulles/d2_dulles_development_2/d2_home [cited 28 August 2009]

cxvi S. Zelinski, Validating The Airspace Concept Evaluation System Using Real World Data, AIAA-2005-6491, Modeling and Simulation Technologies Conference and Exhibit, August 2005, San Francisco, California

cxvii Gawdiak, Y., "IPSA NextGen Portfolio Analysis: Benefits Assessment Overview," Joint Planning and Development Office, May 2009 (unpublished).

11. Systemwide Delay Results

This section presents system-wide delay results that were generated using the Airspace Concepts Evaluation System (ACES), Version 5.0. This version of ACES includes a high-fidelity physics-based trajectory integrator that computes the trajectory of each aircraft every half-second from 40 nm of the departure airport to 40 nm of the arrival airport. Within the departure and arrival airspace, ACES computes a simple trajectory transit time from the runway to the departure fix and from the arrival fix to the runway and uses standard arrival-departure capacity curves, called Pareto curves, to add delay as needed to ensure airports do not exceed their maximum arrival or departure rates.

Baseline capacities were provided by JPDO. The baseline capacities assume NextGen will be fully implemented by 2025, with only small capacity increases after that year. The baseline capacities include all known new and planned runway construction, as well as all JPDO operational improvements. Airport capacities under NextGen have been modeled in detail by JPDO, with NextGen operational improvements increasing average capacity for the top 35 airports by approximately 45%, although there is considerable variation around that average for the individual airports. Similarly, en route sector capacities increased by a factor of 1.7 when all NextGen en route operational improvements were modeled. In the current study, these JPDO-provided assumptions are generally used without significant modification. The study did modify specific aircraft types assigned to the flight timetable, procedures by which the new aircraft accessed runways at large airports, and the overall traffic volume changes implied by the operation of new aircraft types. Examples of these changes are outlined below.

11.1. *CESTOL*

A primary application for CESTOL technology is to offload flights from heavily congested airports. The 100-passenger CESTOL aircraft is capable of arriving and departing at airports whose runways are 3,000 feet long or greater. Most aircraft of that size require at least 5,000 foot runways, and sometimes longer. As a result, the CESTOL aircraft can arrive and depart at many more airports than conventional aircraft of the same size. This characteristic can be exploited to relieve larger airports of flights in excess of their capacity. This business case is motivated by a generalization of a network-based approach to airline scheduling, as opposed to the hub-and-spoke method of scheduling. In this scenario, travelers would be routed more directly to their ultimate destinations by offering them a myriad of choices to airports other than the dominant one in each metropolitan area.

To explore this concept, projected future traffic demand was modified by offloading flights from the top 35 major airports whenever their demand to capacity ratio exceeded 90% in any 15-minute interval. The selected flights must have a stage length less than 600 nm, which is the maximum range of the CESTOL aircraft. The flights were offloaded to reliever airports within 70 nm of the primary airport, provided that the reliever possessed a paved runway at least 3,000 feet long with a width of at least 100 feet.

Figure 11-1 shows the ACES performance for the future traffic projected for the years 2025 and 2040 using standard FAA traffic growth rates. The performance is presented as a tradeoff curve between flight volume and system delay. As flight volume grows, the system delay grows exponentially. The

exponential relationship is not surprising given that airports operate similar to a queuing system, in which the runways operate as servers and the flights operate as customers using the servers.

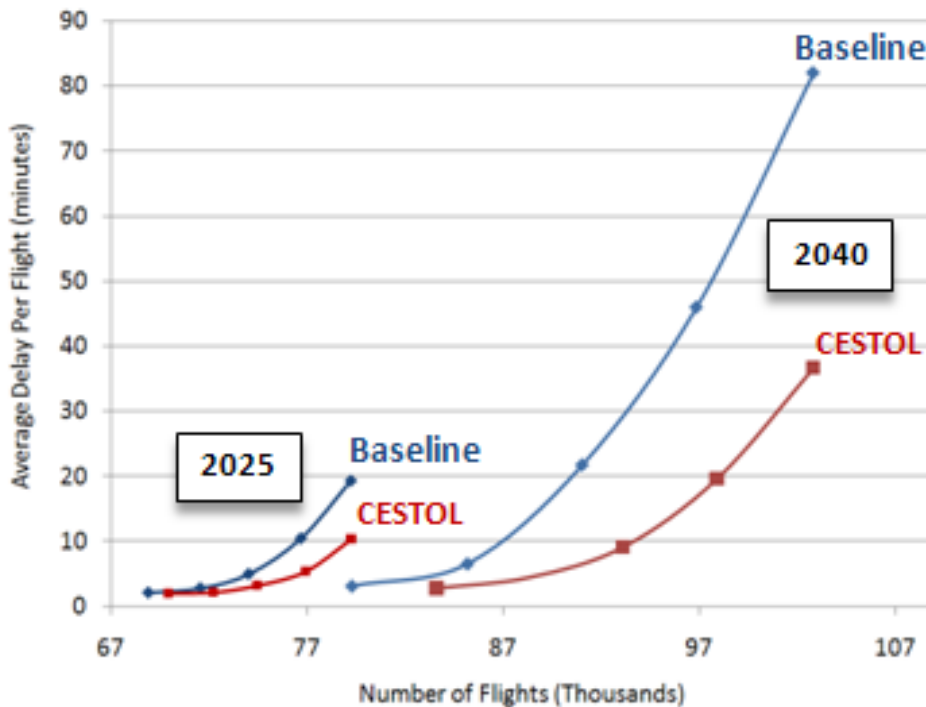


Figure 11-1. Flight volume and delay tradeoff curves for projected traffic in 2025 and 2040.

Figure 11-1 contains many points that are operationally infeasible, because average delays and variances are unacceptably large. It is therefore important when interpreting Figure 11-1 to establish an operationally feasible point on the volume/delay tradeoff curves. One such method is to select an operating point where the average system-wide delay was about equal to a recent actual year. In 2006, the ASPM data set records an average delay at the 35 largest airports around 6 minutes per flight, with three airports operating as high as 9 minutes per flight. Using that criteria, there are approximately 2,500 more flights per day with CESTOL in 2025 and 5,000 more flights per day in 2040.

11.2. LCTR

A second strategy for increasing operations without proportionally increasing delay is to use vertical takeoff and landing aircraft, such as LCTRs, to arrive and depart at areas of an airport independent of the dominant runways. If independent LCTR arrival/departure routes are procedurally separated from fixed-wing aircraft arrival/departure procedures, then the LCTRs can perform runway-independent operations, thus adding capacity without adding to delay. But because LCTRs have higher operating costs than their fixed-wing counterparts (the project herein analyzed a 90-passenger tiltrotor), they become economically feasible only in high-density markets where fixed-wing service is somewhat unreliable due to high congestion-related delays. City pairs that have “shuttle” operations were targeted for LCTR service.

Shuttle operations are defined here as having more than fifteen flights per day in one direction. After making reasonable assumptions about LCTR production rates per year, 1,600 flights were identified as being candidates for LCTR usage in 2025 and 4,300 flights were identified in 2040.

The impact of LCTR replacement for these flights is as follows. The original fixed-wing aircraft that serve these high-density markets must compete with other fixed-wing aircraft for both airspace and runway slots (both departure and arrival). When replaced by LCTRs, they can use the runway-independent arrival and departure procedures to service the airport with little, or no, impact on the fixed-wing aircraft operations. The LCTR operations will potentially interfere with each other, but will not

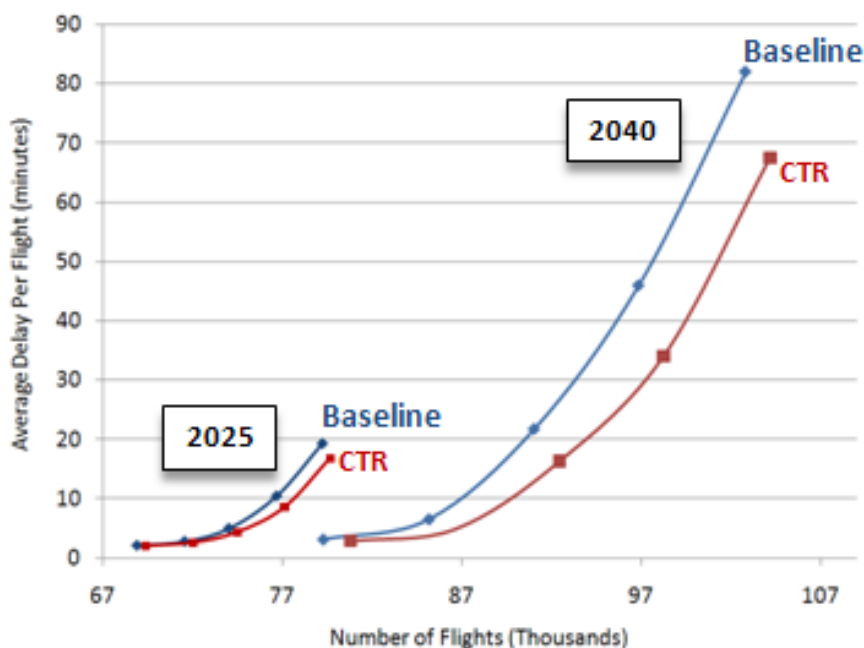


Figure 11-2. Impact of LCTR shuttle flights between high-density airports.

impact fixed-wing operations at the airport. The result of such a shift for the future demand years 2025 and 2040 is shown in Figure 11-2.

Figure 11-2 shows that the LCTR shuttle flights increase system capacity substantially, although the effect of replacing shuttle flights with LCTRs is smaller than the effect of the CESTOL business-shift strategy shown in Fig. 2. At a constant average NAS-wide delay of 6 minutes the LCTR scenario can handle 1,100 more flights than the baseline scenario in 2025, and 2,700 more flights than the baseline in 2040. Regardless of the state of technology of LCTRs in particular, it remains true that any vehicle capable of landing in a very short (600 feet or shorter) landing pad and capable of flying arrival and departure routes that are procedurally separated from those on the main runways, will increase the capacity of the NAS significantly. Whether business is willing to invest in a more costly vehicle like the LCTR remains less clear.

11.3. UAS

The scenario created for the UAS involved forwarding freight using Cessna Caravan-sized aircraft flying mainly autonomously but with a pilot overseeing the flight from the ground. Today private air carriers make limited use of piloted Cessna Caravans to move mail from hub to spoke airports; trucks are most often used for this task. The UAS schedules developed for the New Vehicle NRA assumed 4,000 daily flights between known cargo hubs and spoke airports located 30 to 150 nm away. See Figure 6-9. The impact of the UAS on delay is small because only small numbers of UAS flights were added at passenger hubs.

The UAS would have some cost savings because one ground-based pilot could remotely monitor several vehicles. Thus the breakeven point between using a truck and using a C208 for freight forwarding is likely to change in favor of the C208. The project estimated that currently the breakeven point is roughly 120 miles, meaning that if a truck must travel more than 120 miles along roads then the C208 is more cost effective. Because precise cost estimates of UAS technology are difficult to forecast, the project developed UAS demand sets with distance ranges 30-60 miles, 60-90 miles, 90-120 miles, and 120-150 miles. Adding all four of these UAS demand sets to the 2025 and 2040 baseline demand sets gives the results shown in Figure 11-3.

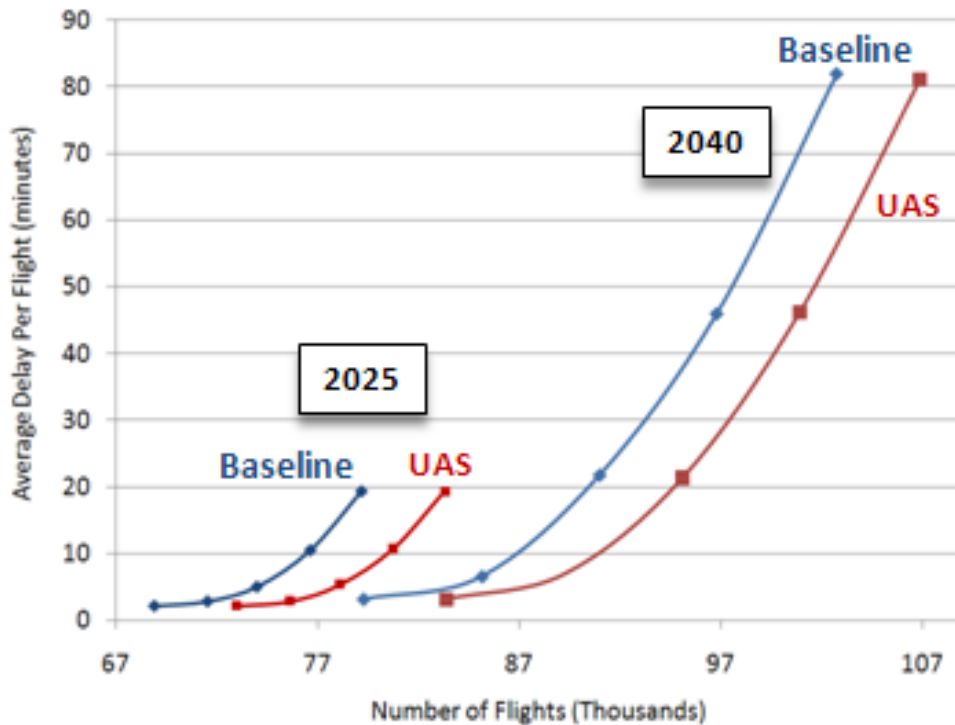


Figure 11-3. Effect of UAS freight-forwarding operations on the NAS.

The volume-delay tradeoff curve for the UAS freight forwarding scenario is essentially flat. This is because the UAS business model adds many small aircraft to the system, but those aircraft depart from relatively uncongested spoke airports and arrive at small remote airports with little traffic. As a result, the entire volume/delay tradeoff curve is simply shifted to the right. There is a slight downward trend in the

average delay for the UAS curve due entirely to mathematics: The UAS scenario adds flights without increasing total delay, resulting in a slight decrease in average delay.

11.4. **VLJ**

Very Light Jets are in commercial use today. Expanded use of VLJs assumes decreasing operating costs relative to other forms of transportation. The VLJ schedules used in the New Vehicle NRA were created by researchers at NASA’s Langley Research Center using Virginia Tech’s Transportation

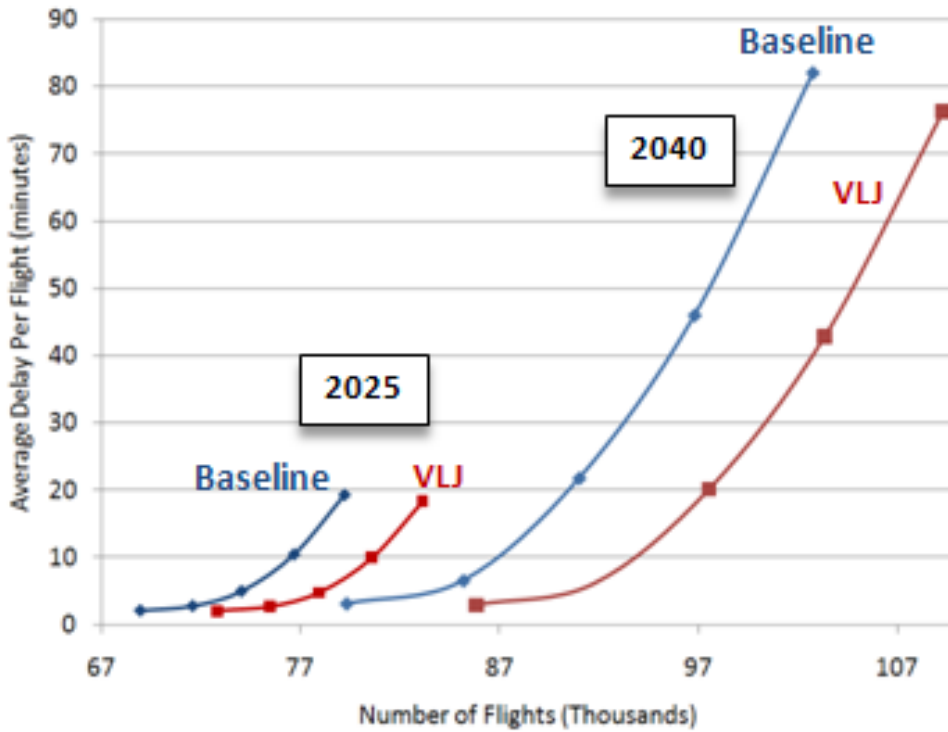


Figure 11-4. Effect of VLJ operations on the NAS.

Systems Analysis Model (TSAM). Using projected demand between city-pairs, the model computes the number of flights that could be flown in an economically competitive manner by a 4-passenger VLJ given certain assumptions regarding airline operating costs, the price of jet fuel, and the cost of auto travel. Figure 11-4 shows the results of adding 3,900 VLJ flights to the 2025 baseline schedule and 6,500 VLJ flights to the 2040 baseline schedule.

Because few VLJs fly into major hubs, their impact on delay is small. Like in the UAS scenario, the VLJ scenario shows a slight decrease in average delay because many aircraft were added without a significant increase in total delay. At a constant average delay of 6 minutes per flight, the VLJ scenario adds 4,000 flights in 2025 and 7,000 flights in 2040. Carrying four passengers, the VLJ fulfills purposes distinct from increasing NAS capacity between major hubs. Those purposes include providing commercial service in markets too thin to support scheduled service. The analysis indicates that because

the VLJs utilize smaller airports and related airspace, their contribution to these markets comes with little effect on delays in the major hub operations

11.5. **Comparison of Delay by Scenario**

Figure 11-5 compares the demand-delay trade-off curves for the baseline scenario, with no new vehicles, to the trade-off curves for the four new vehicle scenarios (it was assumed the SST would not be in use by 2025). Because the Cestol scenario removed flights from the most congested airports during the most congested hours of the day, it naturally shows the largest reduction in delay. The tiltrotor scenario shows a smaller, but still significant reduction in delay. In the tiltrotor scenario, flights on the most popular routes were offloaded to vertiports. The VLJ and UAS scenarios added a substantial number of flights without causing an appreciable change in systemwide delay. On the other hand, the VLJ increases the passenger-carrying capacity of the NAS by only a miniscule amount; the UAS not all. Because the tiltrotor and Cestol scenarios assume the same level of passenger demand as baseline, neither increases actual passenger throughput. Figure 11-6, shows total minutes of systemwide delay for each of the scenarios in 2025.

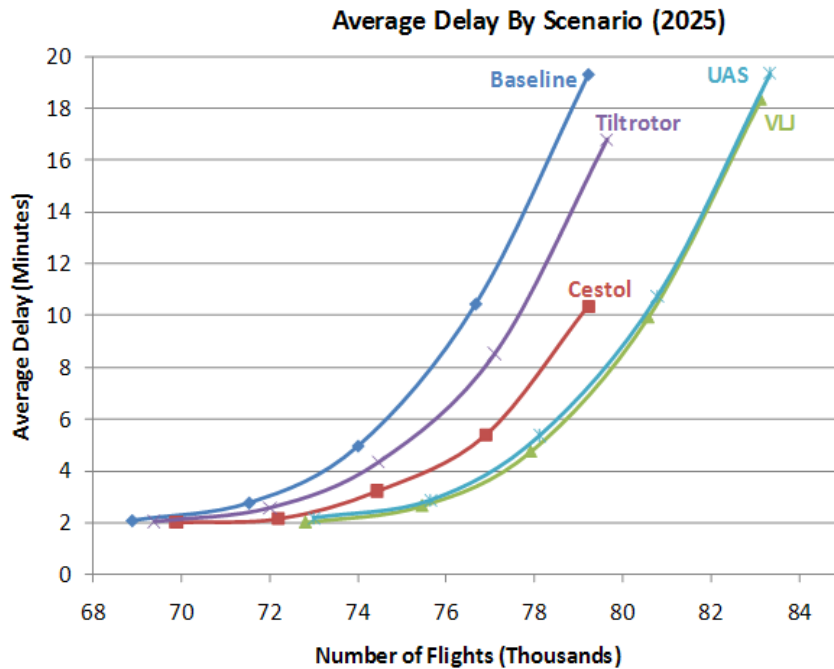


Figure 11-5. Systemwide average delay versus number of flights in 2025.

The results for the 2040 scenario, shown in Figure 11-7, are similar to those for the 2025 scenario. Because demand in 2040 is expected to be greater than in 2025 the delay seen using the untrimmed schedule is much greater—about 80 minutes per flight in 2040 as opposed to 20 minutes per flight in 2025. Although passengers benefit because the SST flies faster than a conventional aircraft, the simulation adjusts the SSTs scheduled arrival time to account for this difference. Moreover, only a subset of the 400 SST aircraft actually fly CONUS routes, and the international SST flights fly like a conventional aircraft during their initial and final phases of flight. The affect of the SST on systemwide

delay is therefore negligible. Figure 11-8 shows that the VLJ and UAS scenarios in 2040 differ very little from the baseline: they add substantial numbers of aircraft to the system, but because they don't add flights to busy hubs, the affect on overall delay and passenger counts is small.

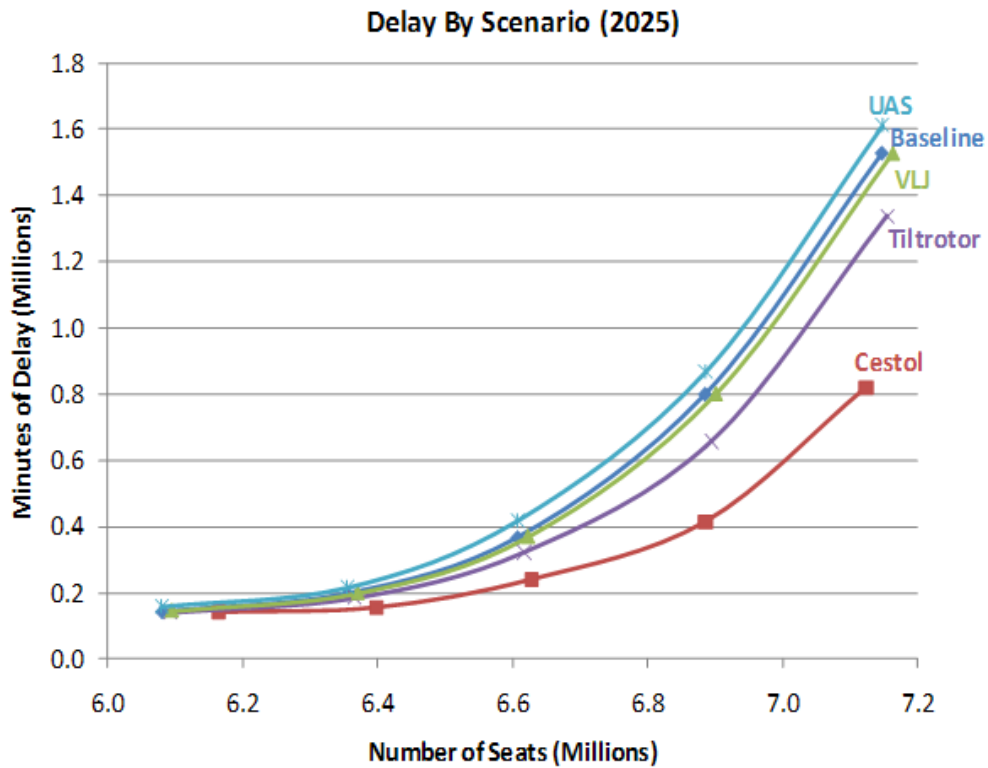


Figure 11-6. Total systemwide delay versus number of seats in 2025.

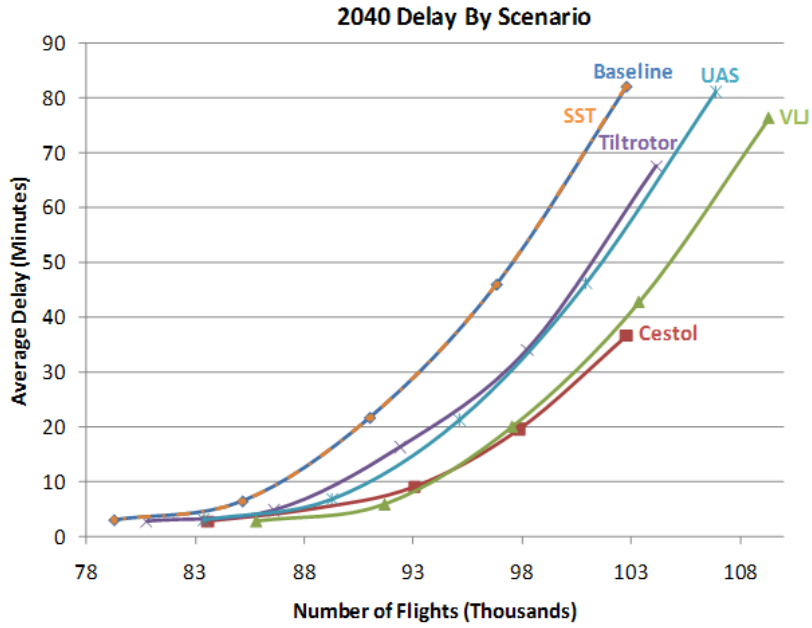


Figure 11-7. Systemwide average delay versus number of flights in 2040.

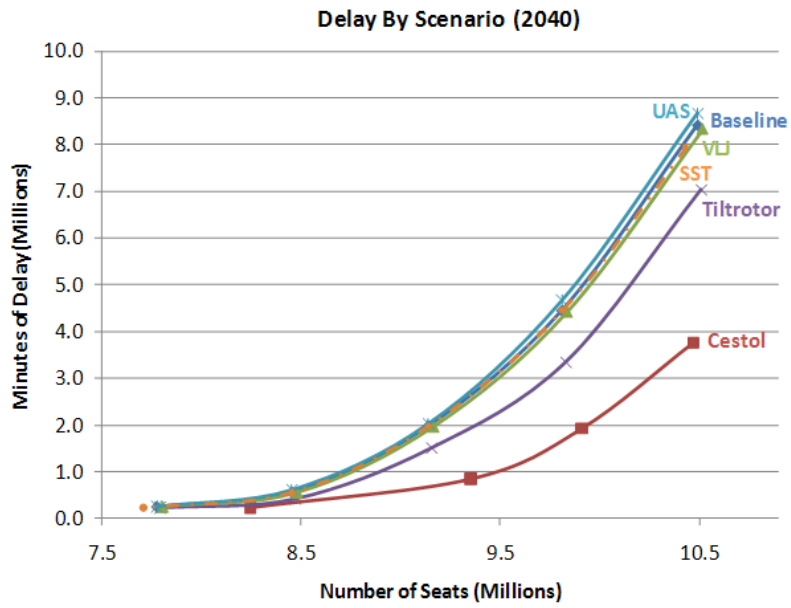


Figure 11-8. Total systemwide delay versus number of seats in 2040.

12. Weather Impacts

Convective thunderstorms today are a major source of disruption in the NAS. Delays during the convective weather months—June, July, and August—are the highest of the year, exceeded only by delays during the worst winter storms. Although NextGen is expected to raise airport capacity in instrument meteorological conditions (IMC), aircraft will not have the ability to fly through severe thunderstorms. In this section of the report we examine the interaction of NextGen and new vehicles in the presence of convective thunderstorms.

Our approach was to rerun a small number of ACES simulations incorporating the weather from the day 27 June 2007. On this day a line of thunderstorms blocked heavily-traveled routes between Chicago and New York. Storms also passed directly over airports in Dallas, Chicago and New York, resulting in the second highest delay total for any day in the summer of 2007.

To simulate the weather for this day, we created capacity timelines for the airports where thunderstorms passed directly overhead. For the hours in which Metar data indicated that the most severe part of the storm was directly over the airport we set the airport's capacity to one-quarter of its capacity in Visual Meteorological Conditions (VMC). To model en route thunderstorms we created moving rectangles of approximately the same size and in the same locations as the actual thunderstorms on 27 June 2007.

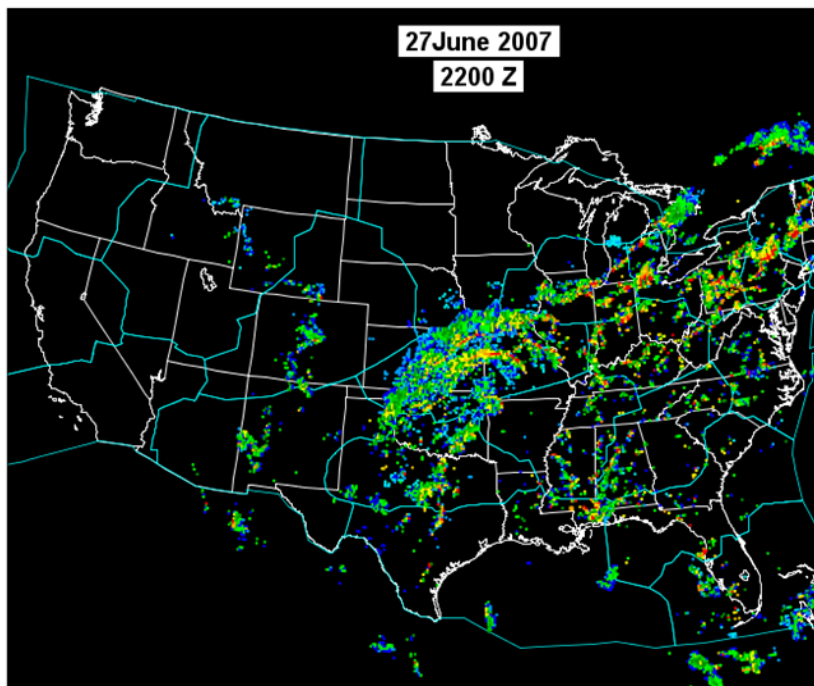


Figure 12-1. NEXRAD storm cells.

En route weather data was obtained from radar images provided online by the National Climatic Data Center (NCDC), an example of which is shown in Figure 12-1. From these images we extracted storm

cells with reflectivity greater than 50 dBZ. These are the red and purple pixels in Figure 12-1. To incorporate en route weather into our simulation, we used an experimental ACES model, known as the Constrained Airspace Re-routing Planner (CARP), which forces the aircraft in the simulation to maneuver around a user-provided set of obstacles.

We succeeded in making ACES steer aircraft around storm cells. Unfortunately we found that, due to a lack of memory, ACES could not be programmed to run with shapes representing the thousands of weather pixels in a day's worth of weather images. To reduce the number of unique en route storms in our simulation we created an algorithm that replaced clusters of adjacent storm cells with rectangles of approximately the same size. See Figure 12-2.

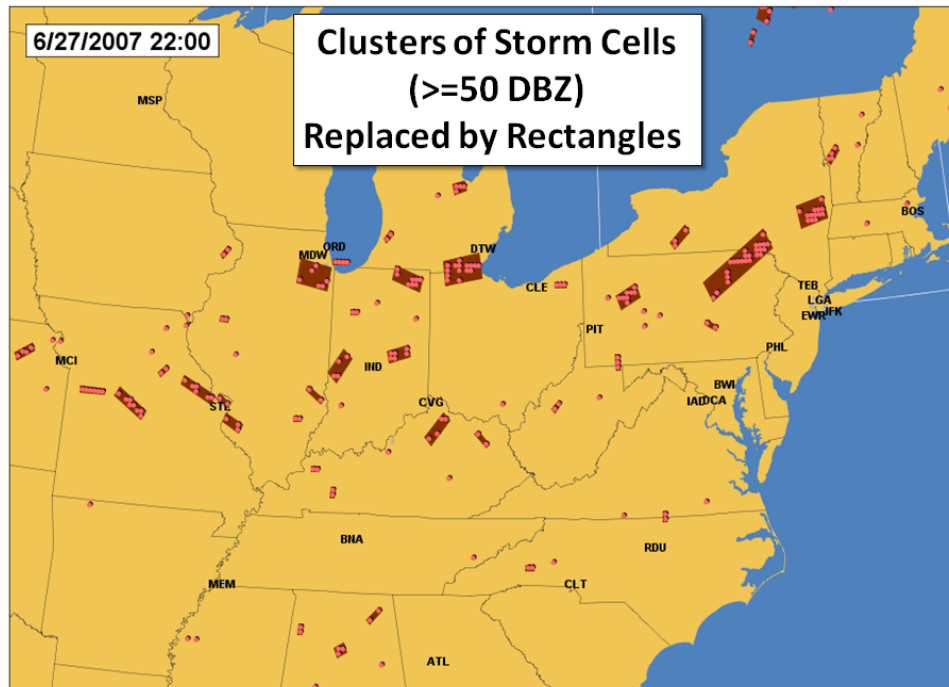


Figure 12-2. Storm cells and corresponding rectangles used in ACES

A single weather image was used to define the weather for every hour of the day; individual rectangles therefore were active only for a single hour. Replacing clusters of storm cells with rectangles and ignoring storms that consisted of a single pixel resulted in 2000 unique obstacles that aircraft needed to avoid. This number still caused an out-of-memory error in ACES. In response we deleted the smallest storm clusters until—through trial and error—we found a configuration with 243 rectangles that ran successfully.

12.1.1. Simulation Results

To measure the effect of weather on delay we ran two 2025 baseline demand sets and two 2025 all-vehicle demand sets through ACES. Simulations were run for each demand set, both with and without weather. The trim level for the demand sets were 75% and 100%, which means that we removed from the demand sets three-quarters and all of the flights on the JPDO's trim list respectively. At trim levels of

75% and 100% the demand sets had low delays. Figure 12-3 shows average delay versus the number of scheduled operations for these simulations. Hollow markers show the results without weather; solid markers show the results with weather. The overall effect of weather is to increase the average delay per flight by about 1 minute. The increase in delay is slightly higher for the 75% trimmed demand sets than for the 100% trim demand sets.

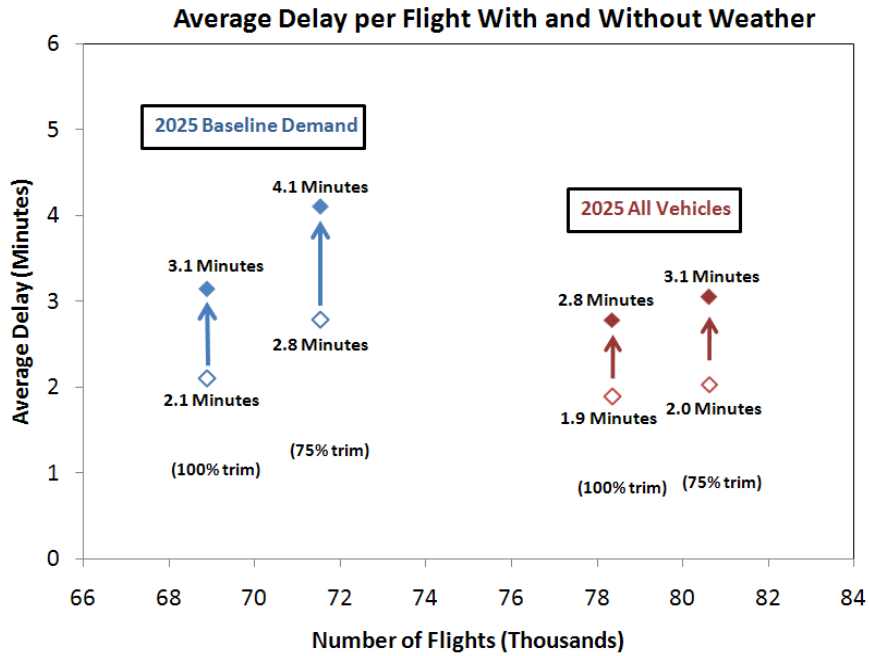
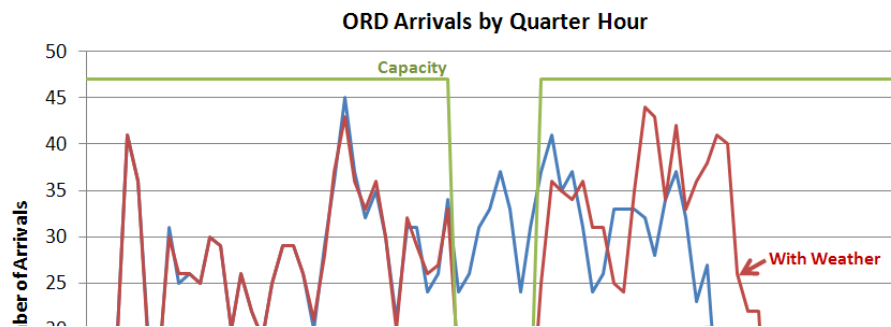


Figure 12-3. Average delay with and without weather

As expected, delays increased most at the airports that were directly impacted by thunderstorms. Figure 12-4 shows the number of arrivals at ORD by quarter hour, along with the airport's arrival capacity in the bad-weather scenario. Before 15:00, arrival capacity is well above the scheduled demand at the airport. During the time when thunderstorms pass over the airport, 15:00 - 17:00, capacity is reduced to one-fourth of the airport's good-weather capacity, causing a large number of flights to be delayed.



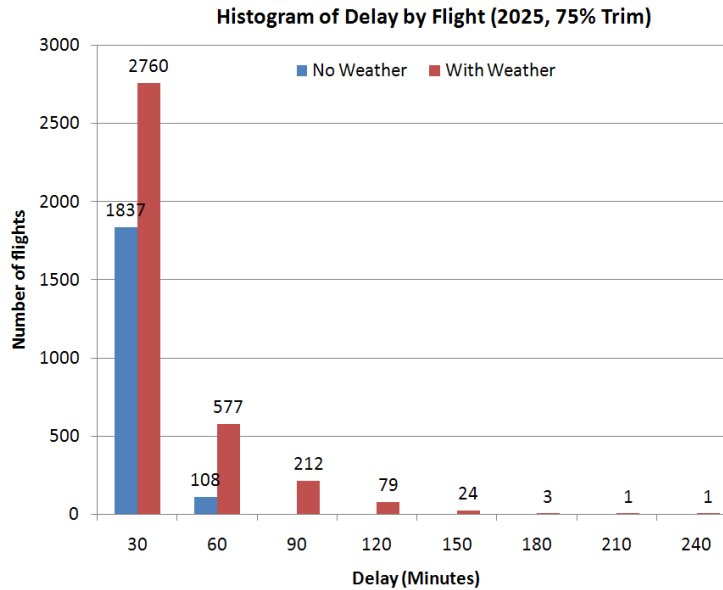


Figure 12-5. Histogram of delays (>30 Minutes) with and without weather

Figure 12-5 shows that the addition of weather significantly increased the number of flights with long delays. A comparison of delays by airports shows that weather increased average delay per flight at Chicago O’Hare (ORD) from 2 minutes to 12 minutes, at Newark (EWR) from 2 minutes to 11 minutes, and at LaGuardia (LGA) from 4 minutes to 11 minutes

Although most of the increase in delay is caused by the drop in airport capacity when thunderstorms pass directly over an airport, there is also an increase in en route delay due aircraft travelling longer routes to avoid thunderstorms. Figure 12-7 shows a histogram of the amount of airborne delay for flights in the 2025 (75%-trimmed) baseline scenario that gained more than 5 minutes of airborne delay due to weather. The data contained 1,156 flights whose airborne times increased by more than 5 minutes in the weather scenario compared to the non-weather scenario; 216 of these flights gained more than 30 minutes of airborne delay. The longest airborne delay for any flight was two hours; this is a reasonable maximum delay and comparable to the longest airborne delays that aircraft absorb in practice. There was no significant difference in delay response to weather between the baseline cases and the cases with the new vehicles.

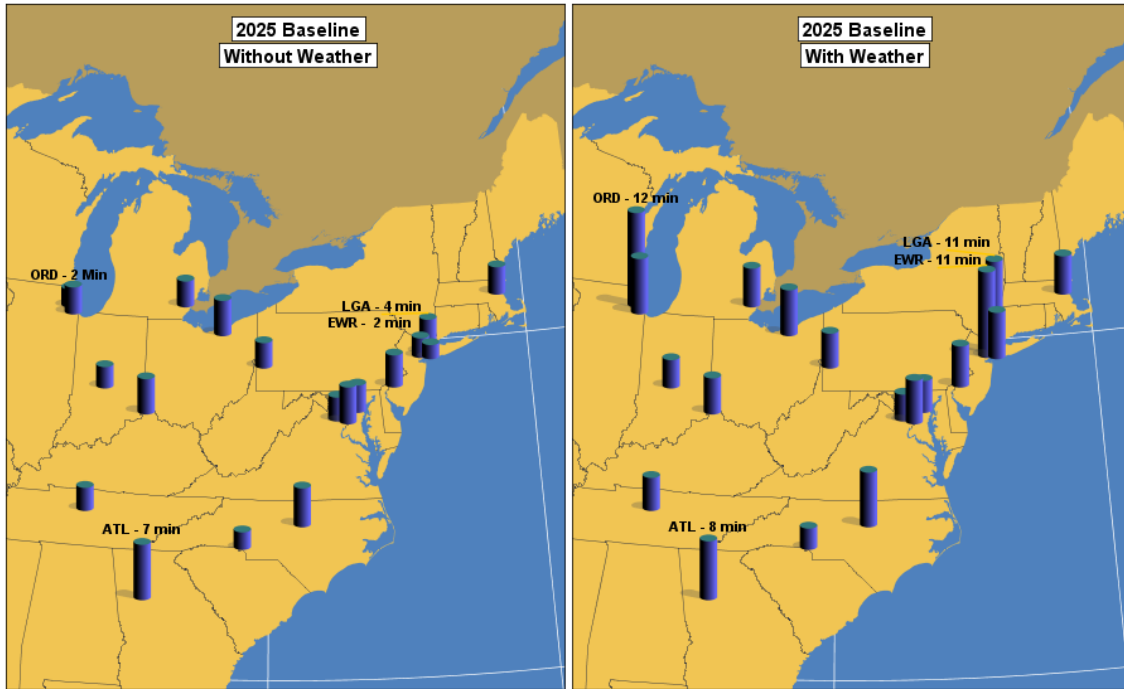


Figure 12-6. Average delay by major airport for ACES runs with and without weather.

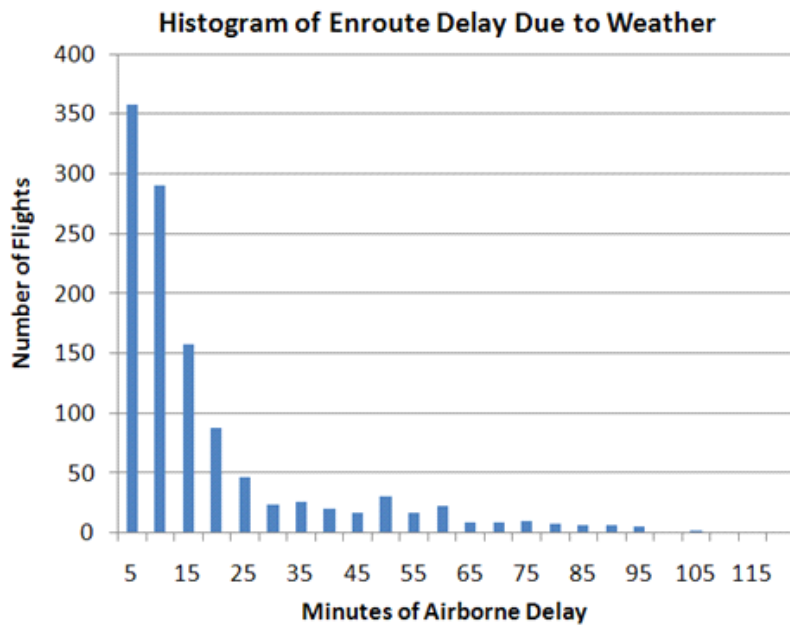


Figure 12-7. Airborne delays due to weather, 2025, 75% trim.

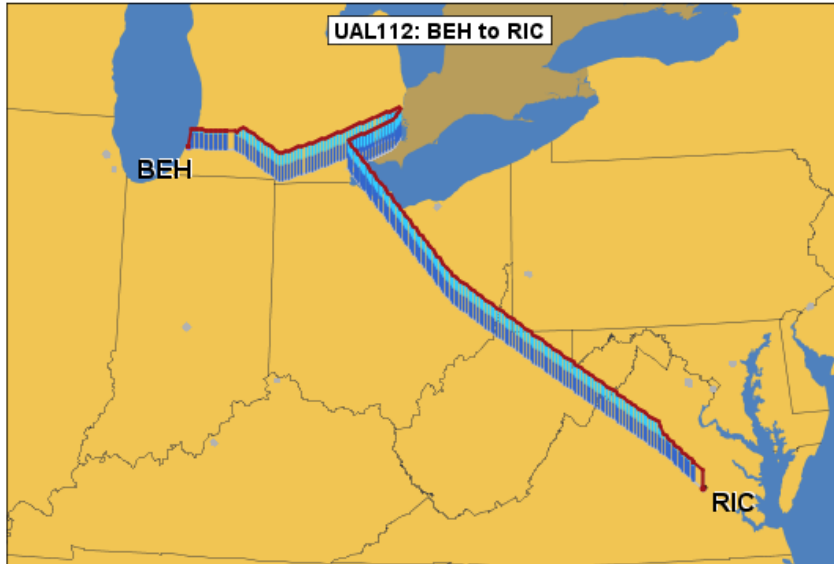


Figure 12-8. Path flown by flight UAL112 to avoid thunderstorms.

Figure 12-8 shows an example of a flight that absorbed 45 minutes of delay because a thunderstorm (not shown) blocked its path. A good feature of ACES is that, unlike statistics-based simulations, it can fly aircraft around en route obstacles and compute the resulting delay. And overall, the amount of airborne delay that ACES causes individual flights to absorb seems reasonable. Unfortunately, aircraft in ACES are not able to fly elliptical holding patterns of indefinite duration. Therefore, if an aircraft's path is blocked by a thunderstorm for a long period of time—say 30 minutes to one hour—then to absorb the delay, the aircraft will fly in one direction for half the duration of the delay before turning around and heading back to its planned route. The lack of an ability to place aircraft in holding patterns can cause aircraft to fly routes that do not resemble those of real aircraft would fly.

13. Analysis of Controller and Pilot Workload

Using the aircraft tracks produced by the ACES simulation we experimented with computing a number of metrics related to sector workload. Because ACES does not model the aircraft's flight path within 40-nm of their origin or destination airports, the analysis was restricted to en route airspace. One of the most interesting metrics that was computed from the ACES output was the number of aircraft conflicts. A conflict occurs when two aircraft flying at the same altitude are separated by less than 3 nm in terminal airspace or 5 nm in en route airspace. To avoid potential conflicts, an air traffic controller will take action to adjust the speed or heading of either or both aircraft well in advance of the conflict. Therefore the number of conflicts that a scenario produces should be a good indicator of workload for controllers and pilots. When we ran our ACES simulation we specified that the software not maneuver the aircraft to avoid conflicts. From the simulation output we tabulated the number of conflicts at both 3 and 5 nm.

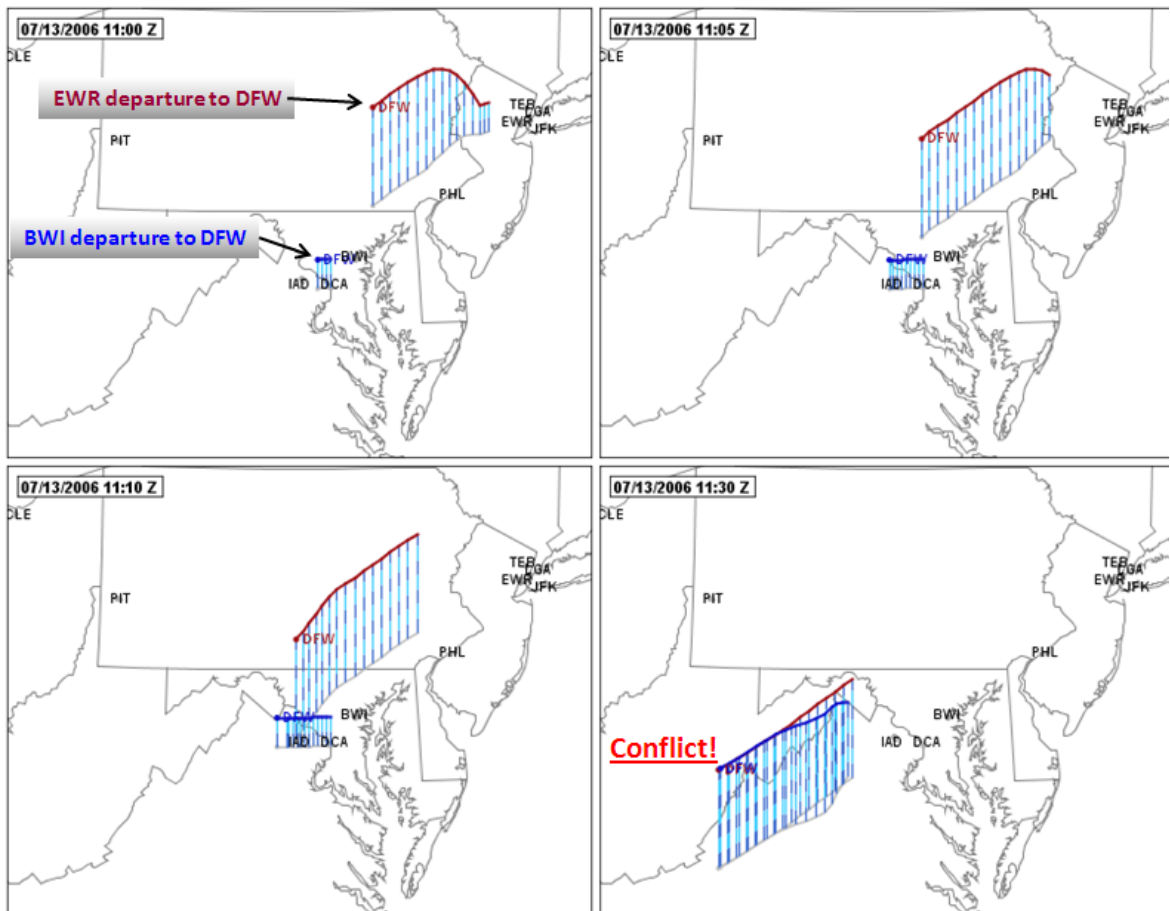


Figure 13-1. Conflict between aircraft departing from EWR and BWI Airports.

Figure 13-1 shows a common type of conflict that controllers must frequently resolve. An aircraft takes off from Newark International Airport (EWR) heading to Dallas Fort-Worth Airport (DFW). About

ten minutes later a second aircraft takes off from Baltimore-Washington International Airport (BWI) heading for DFW along the same jet route as the first. The first aircraft overtakes the second aircraft causing a conflict.

Although many conflicts occur between aircraft following the same jet route, they can also occur at points where jet routes intersect. Figure 13-2 shows the unusual case of a flight (indicated by arrow) from EWR to Phoenix Sky Harbor International Airport (PHX) that had 3-nm conflicts with seven other aircraft. The locations of the conflicts are marked by circles.

Figure 13-3 and Figure 13-4 show the locations of all 13,000 3-nm conflicts in the 2040 trimmed dataset. The conflicts appear to be evenly distributed over the most heavily travelled jet routes. The red dots in Fig. 10 show the high concentration of conflicts along routes into and out of New York.

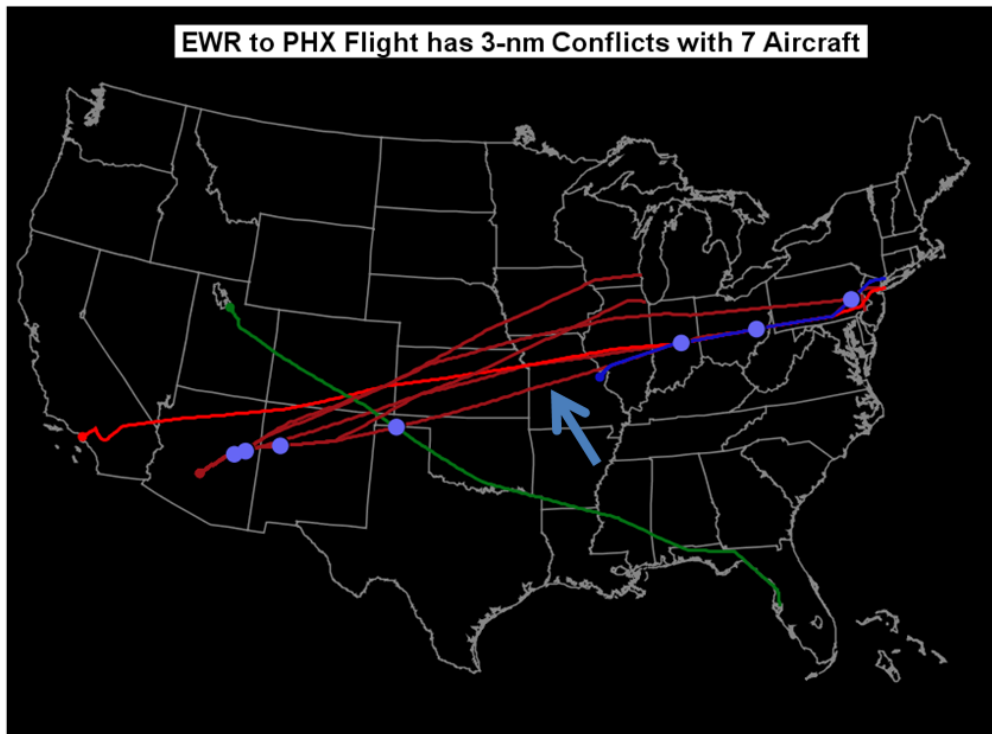


Figure 13-2. Flight from EWR to PHX with seven 3-nm conflicts.



Figure 13-4. Locations of 3-nm aircraft conflicts.

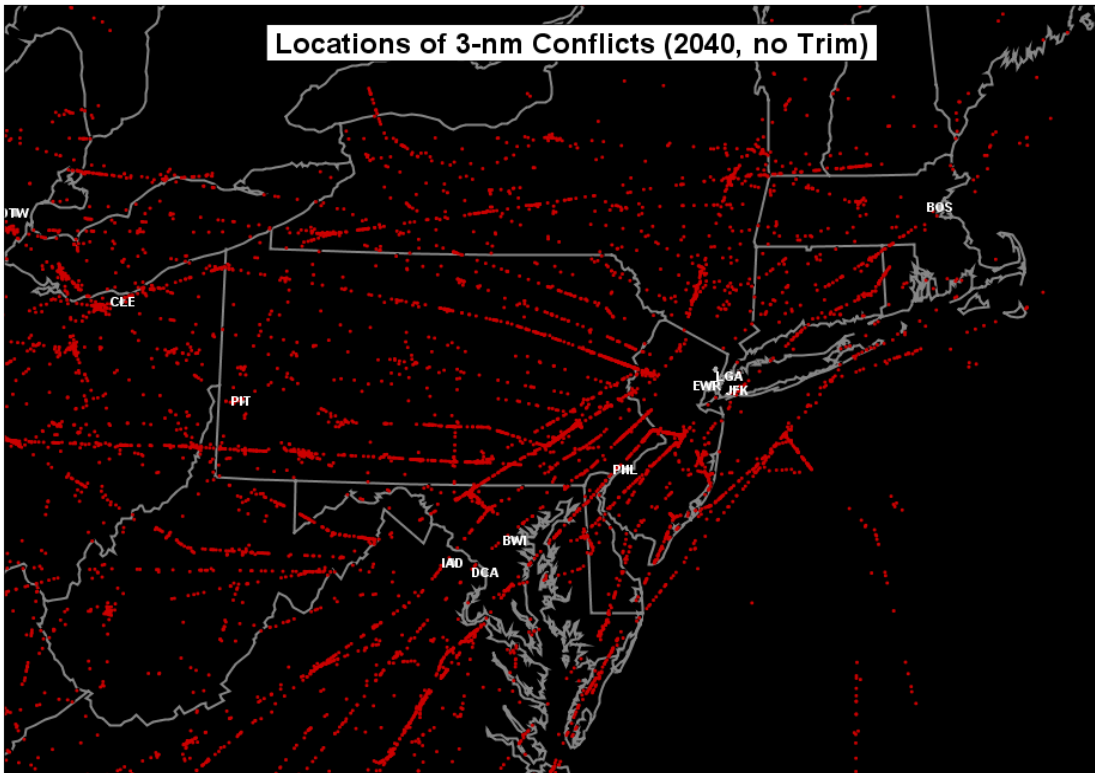


Figure 13-3. Locations of 3-nm conflicts (zoomed).

About 7% of the conflicts shown in Figure 13-3 and Figure 13-4 are byproducts of the cloning process that was used to “grow” the 2025 schedule starting from a current-day schedule. The cloning process adds flights to the current schedule by exactly copying existing flights and shifting their departure times by a minute or so, which in turn generates an artificial conflict. Most conflicts appear to be legitimate, however, and are due to aircraft sharing jet routes, intersecting flight paths, or flights converging to the same merge fix. Figure 13-5 gives a histogram of the number of 3-nm conflicts per aircraft. The distribution resembles a Poisson distribution, which is associated with random processes. For our ACES data, about 17% of aircraft would experience a 3-nm conflict without controller intervention; roughly twice this number would experience a 5-nm conflict. The untrimmed baseline scenario had 15% more flights than the 100% trimmed baseline, however the conflict rate was 30% greater.

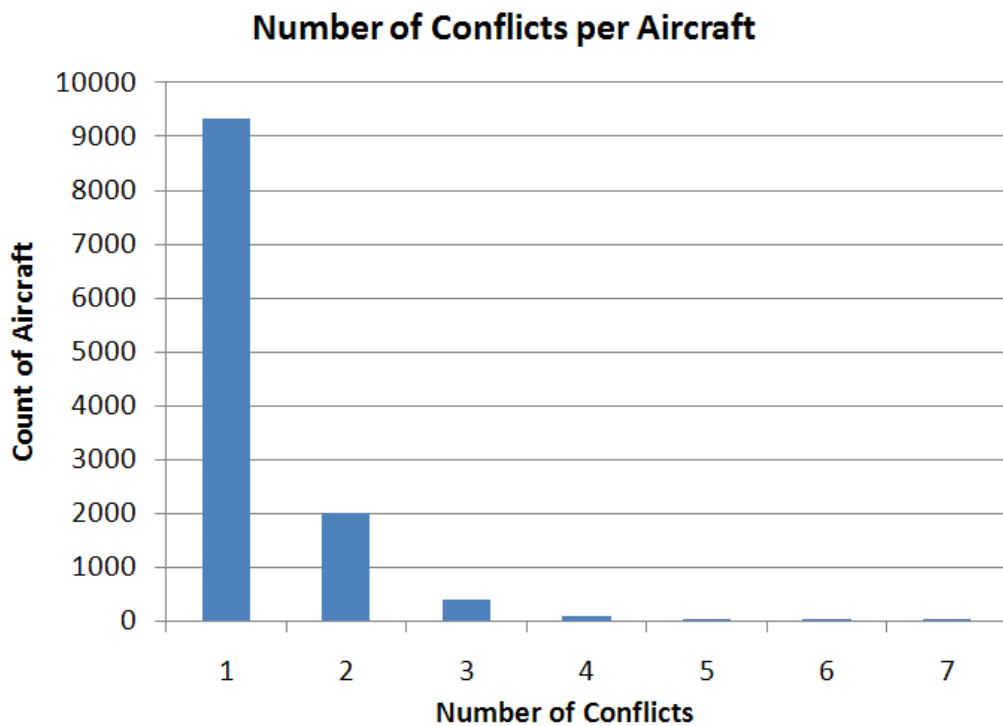


Figure 13-5. Number of 3-nm conflicts per aircraft in the 2025 trimmed

Figure 13-6 shows the number of 5-nm conflicts for the different new vehicle scenarios versus the number of flights in the 2025 scenario for the trim levels 0%, 25%, 50%, 75%, and 100%. The all-vehicle schedules shown are for trim levels 0%, 50%, and 100%. In all scenarios, conflicts increase linearly with the number of scheduled flights. The number of conflicts in the CESTOL and tiltrotor scenarios differs very little from the number in the baseline scenario. The UAS and VLJ schedules both have about 4,000 more flights than the baseline; however, neither shows a substantial increase in conflicts. The all-vehicle scenarios have about 6% more conflicts than the baseline schedules at the same trim level. The bottom line therefore is that new vehicles do not appear to contribute more to controller workload than conventional vehicles.

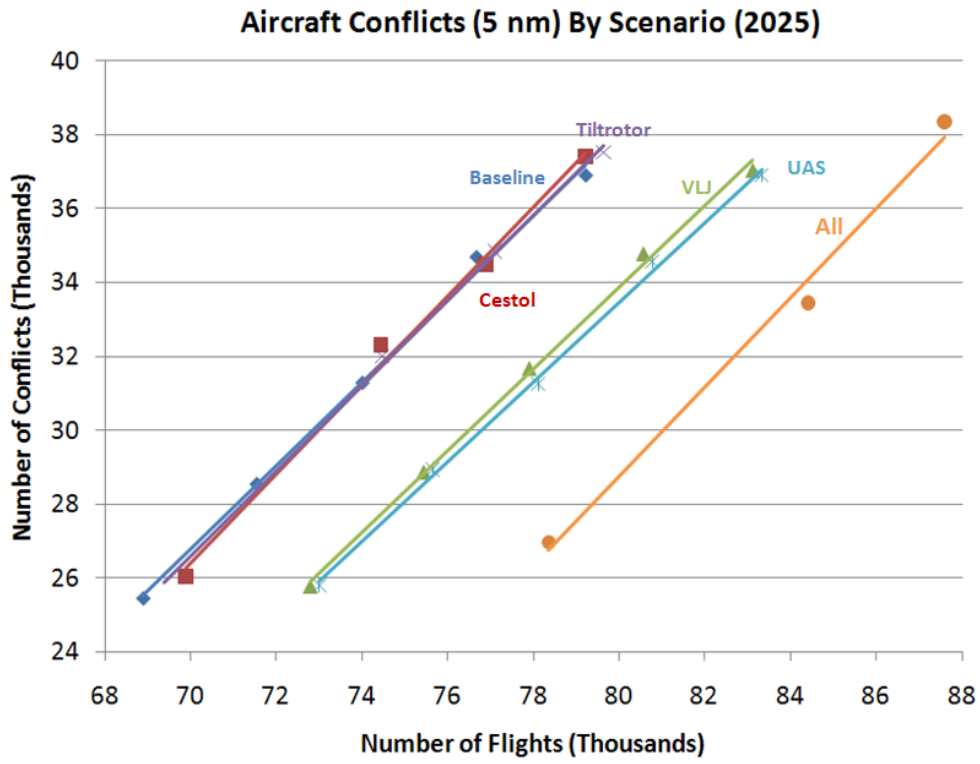


Figure 13-6. Number of 5-nm conflicts by scenario.

14. Safety

This section assesses the impact of new vehicles on the NAS from the perspective of safety and efficiency. It also highlights additional research and development issues that need to be investigated to ensure that the integration of new vehicles is seamless as NextGen becomes a reality. One product of this research is a reusable analysis infrastructure that includes a set of publicly-available safety models and analysis methods for qualitatively evaluating the safety impact of new vehicle concepts on NextGen and vice-versa.

This analysis assists with understanding key safety considerations and tradeoffs associated with the operation of advanced vehicles, including potential hazards, the effect of off-nominal conditions, and potential certification issues. It follows current safety risk management process (See Figure 14-1) to identify critical safety issues and assess safety implications.



Figure 14-1. Safety risk management process.

Our approach identifies the hazards associated with each element of the system (in this case, the elements are vehicles, rules and procedures, operating environments, stakeholder goals, and tradeoffs). The safety risk methodology determines the potential severity and likelihood of each hazard, identifies mitigation strategies for the hazards that pose the unacceptable risk, and evaluates the effectiveness of any mitigation strategies used.

The safety analysis for each vehicle is composed of the following three components:

- Identification of Known Hazards – identification of historical hazards and risks which may be exacerbated by the integration of the vehicle into NextGen.
- Identification of New Hazards – identification of new hazards peculiar to the new vehicle and its operations within NextGen.
- Analysis of Risk – an assessment that determines whether the new vehicle and its operations introduce more or less risk than is acceptable with current aircraft.

14.1. System Description

In the NextGen environment, aircraft are expected to have a wider range of operational capabilities and the ability to support varying levels of total system performance via onboard technologies. Technology will enable such capabilities including the ability to perform airborne self-separation, various spacing and merging tasks, and precise navigation and execution of four dimensional trajectories (4DTs¹). For the purposes of this project, aircraft required navigation performance (RNP) is expected to be RNP 0.3 for all vehicles operating in the NAS by the year 2025. These aircraft will also have varying levels of cooperative surveillance performance as well as enhanced flight operational performance (i.e., cruise speeds, cruise altitudes, turn rates, climb and descent rates, stall speeds).

The purpose of this safety assessment is to determine the safety hazards and risks associated with the introduction of new vehicles into the NextGen system by the year 2025. The 5M model², as depicted in Figure 14-2, was used to assist in the formulation of this system description.

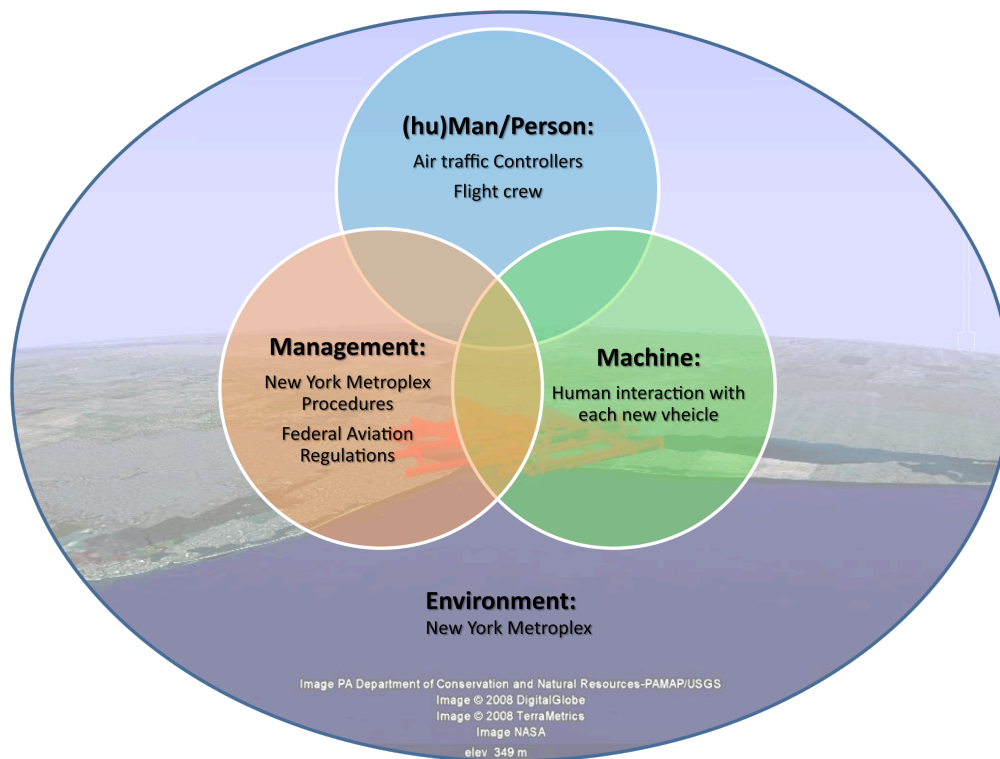


Figure 14-2. 5M Model

The scope of the assessment is limited to the operation of each new vehicle in the New York Metroplex. All nominal phases of flight (i.e., taxi, takeoff, climb, cruise, descent, approach, and landing) were examined with specific focus on human interaction (air traffic controllers and flight crew) with each new vehicle and its environment (New York Metroplex and weather conditions).

14.2. **Identified Hazards**

The safety team evaluated historical (or known) hazards through discussions with subject matter experts, examination of problem statements from the Commercial Aviation Safety Team (CAST), and examination of a safety issue database compiled from multiple stakeholders by the JPDO Safety Working Group. The stakeholders include domestic, foreign, and international aircraft manufactures, air navigation service providers, aircraft operators, and trade and safety organizations. For the purpose of this report "problem statements" and "safety concerns" will be referred to as *known hazards*. It is recognized however, that many of the safety issues or concerns identified could be considered accidents, incidents, hazards, causes, or other events. Each known hazard was evaluated with respect to whether the hazard may be exacerbated by the vehicle. If so, the known hazard was categorized and compiled in this document.

The hazards were identified through literature search and brainstorming. The safety team evaluated new hazards by reviewing areas of change identified by the Future Aviation Safety Team (FAST), safety concerns contained in the JPDO Safety Working Group safety database, and subject matter expert input. New identified hazards are compiled within this document.


The hazard identification process also included visualization of the flow of events for each phase of flight for each new vehicle. This technique helped identify the hazards in the operational environment associated with witnessed events. These hazards are listed below and associated with each vehicle. A comparison of all identified hazards, associated vehicles, and risk factors are contained in Appendix G.


14.2.1. Legend

The Safety Management System Standard developed by the JPDO Safety Working Group defines a hazard as:

Hazard – Any existing or potential condition that can lead to injury, illness, or death of a person; damage to or loss of a system, equipment or property; or damage to the environment. A hazard is a condition that is a prerequisite to an accident or incident.

For the purpose of this research project, hazards will be limited to any existing or potential condition that can lead to injury, or death of a person; or damage to or loss of the aircraft.

 **Known Hazards** – The blue triangle icon indicates a known hazard. Known hazards are historical hazards, hazards present in the current system, which may be exacerbated by or of particular concern to the integration of the new vehicle into NextGen.

 **New Hazards** – The red flag icon indicates new hazards. New hazards are unique to the new vehicles, or which are introduced as a result of their operations in NextGen.

14.2.2. CESTOL

Although each new aircraft has its own unique stability and control issues, CESTOLs are not fundamentally different from conventional, commercial jets. Historically, the departure and arrival phases of flight have posed the greatest threat to safety (see Figure 14-3), and are of particular concern with respect to the CESTOL aircraft. The phases of flight that distinguish the CESTOL from its conventional

aircraft counterpart and other operating procedures (i.e., spiral approaches, steep descents) during the phases of flight also pose safety risks. The CESTOL's performance characteristics allow it to utilize shorter runways and to perform steep and spiral approaches. The slower approach-speed creates a steeper approach without significantly increasing the descent rate. Steep approaches may be used to avoid either tall objects or high density airspace along the approach patch corridor, and to achieve short landings.

Spiral departures are rare but existed in 2008. An example of a spiral departure is the Loupe One in San Jose (see Figure 14-4). Spiral descents may be used to avoid either tall objects or high-density airspace surrounding the airport. They may also be used as a noise abatement procedure to contain the noise footprint within the airport boundary. This type of approach may have speed restrictions or crossing height restrictions. Hazards related to spiral descents, similar to spiral departures, are also associated with maintaining trajectory both vertically and laterally, which can be affected by wind conditions, equipment capability and failures, and crew situational awareness.

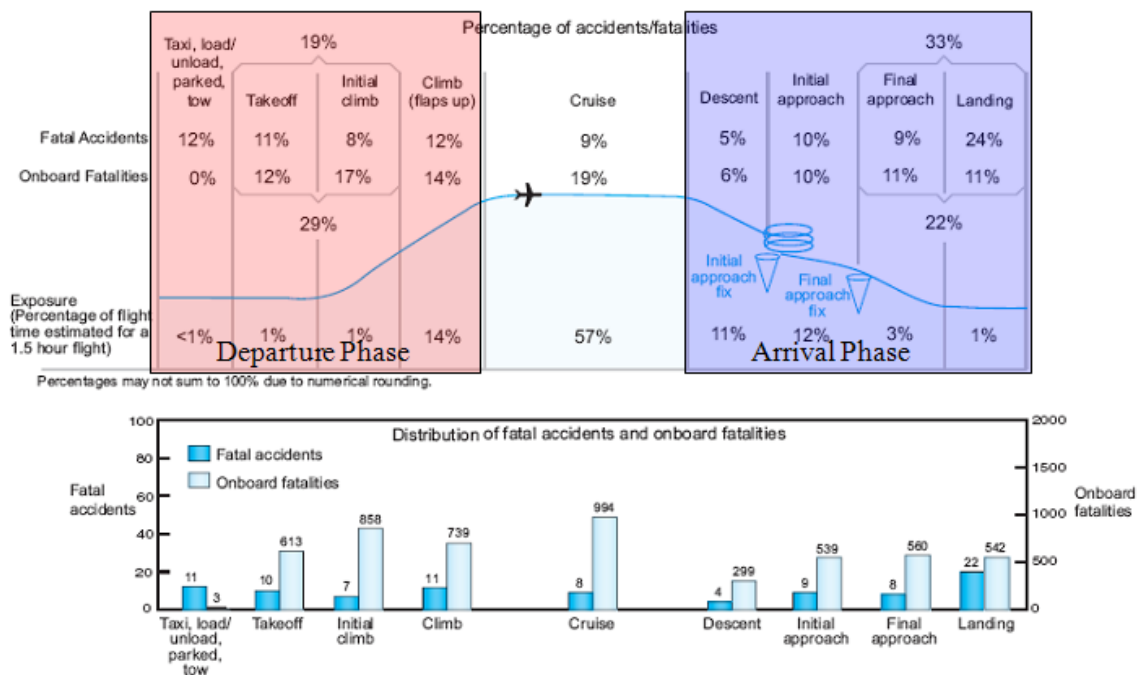


Figure 14-3. Fatal accidents and onboard fatalities by phase of flight, 1999-2008⁸.

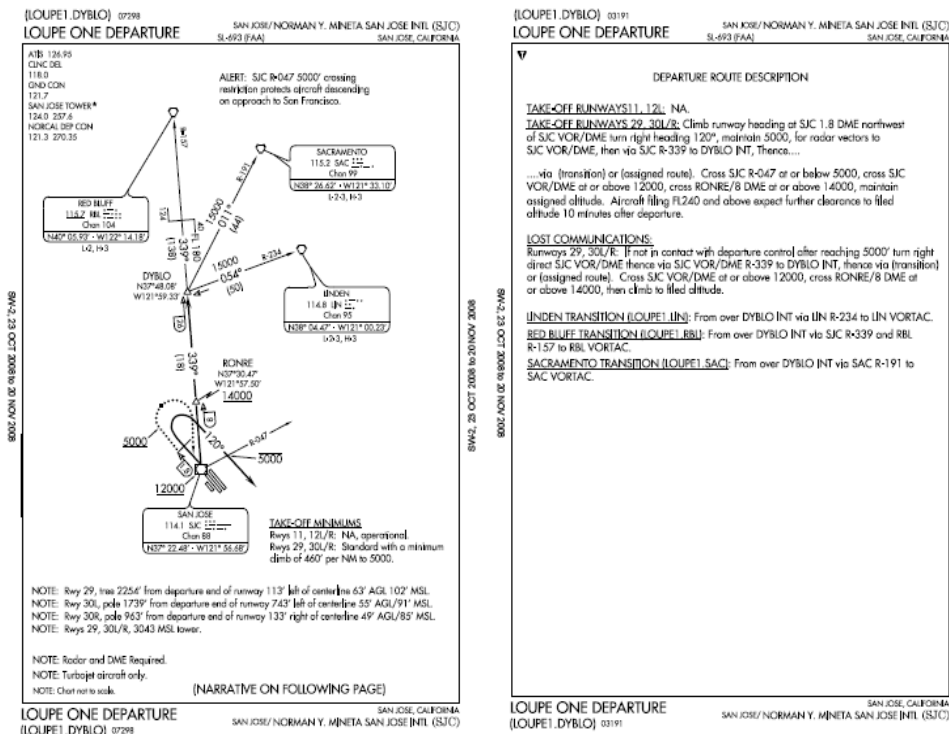












Figure 14-4. FAA - Loupe One departure^{9,10}.








This section is subdivided into five areas: performance, automation, procedures, environment, and training. In each area, hazards are grouped by observed common themes.

Performance



- Due to the slower approach speed of CESTOL aircraft, as compared to conventional aircraft, the CESTOL aircraft can execute a tighter pattern. This may significantly reduce the margin of error particularly when operating in high-density airspace.
- While not uncommon for general aviation and propeller driven aircraft, the low-wing loading of the CESTOL aircraft relative to commercial jet transports might make it more susceptible to wind gusts and thus to altitude deviations, which could lead to loss of separation from other aircraft or from the ground.
- Due to the low-wing loading, the CETSOL is susceptible to wind gusts that could result in lower passenger quality-comfort ratings resulting from increased sudden jolts, excessive ups and downs, or side-to-side motions.
- The absolute V_{stall} margin for the CESTOL aircraft is significantly lower (V_{ref} is 1.3x or less than V_s). Operating in critical phases of flight reduces the stall safety margin, impacting performance-based operations.

-  The reduced stability of the CESTOL aircraft as CG nears the aft limit at critical airspeeds (i.e., V_s , V_{so} , V_r , V_{mu}) increases the possibility of aircraft loss of control, which could lead to life/hull loss. In addition to these losses, the magnitude of such events may be compounded if they occur within the vicinity of a super-high density airport.
-  Required approach climb (go-around) capability can be risky with the CESTOL aircraft. Depending on the configuration of the aircraft and the presence of airport elements (i.e., runway layout, tree line, and buildings), CESTOL aircraft may be unable to climb readily enough to clear these obstacles. If a go-around is executed beyond a certain point on the runway, this could result in the aircraft failing to climb sufficiently to maintain adequate separation from terrain or other obstacles at the departure end of the runway, thereby resulting in potential damage or loss of aircraft and possible fatal injury to occupants or persons on the ground.
-  An engine failure in a CESTOL aircraft due to its increased thrust requirement to maintain optimal STOL capabilities may reduce flight path control precision, resulting in an increased workload for pilots and a larger noise footprint.
-  Steep-angle approaches reduce crosswind control effectiveness, which make the aircraft susceptible to landing gear side loading, ground looping, or runway excursion if crosswinds are encountered on approach.
-  A latent risk exists if CESTOL flight crew does not provide and/or maintain adequate separation during the execution of a spiral descent while in high density traffic operations, impacting trajectory-based, performance-based, and/or super-density arrival/departure operations. This may be due to the human operator expending a greater level of cognitive resources to conform to the parameters of the specified flight profile.
-  Stacking of CESTOL aircraft in the holding pattern may lead to increased controller workload to maintain separation or increased dependence on automation by both controller and pilot, thus potentially adding a vertical RNP requirement.
-  The increased descent angle of the CESTOL aircraft might lead to heightened descent or sink rates that could result in hard landings, especially if conducting steep approaches at night or during conditions of low visibility. In such instances, this could possibly leading to damage to the aircraft or injury to passengers or crew, thus impacting performance-based operations.
-  Stabilizing the aircraft during final approach may be critical and more demanding at higher sink rates, because stabilization needs to be achieved at higher altitudes given the nature of the descent profile. An unstable approach can potentially lead to undershoots, overshoots, runway excursions, or tail strikes resulting in possible damage to the aircraft or injury to passengers or crew.
-  Directional control on roll-out using the CESTOL aircraft is reduced as crosswind increases, thereby escalating the probability of runway excursion or loss of control.
-  The increased time required of the CESTOL aircraft, due to its slow speed, to rollout and change flight path could result in mid-air collisions, especially when operating in close proximity to other aircraft in the terminal area. This increases the potential for catastrophic loss of aircraft, passengers, crews, or persons on the ground.

Automation

-  If the CESTOL flight crew fails to perform a rapid deceleration speed transition correctly (by allowing the airspeed to decrease below the aircraft's stall speed due to its narrower absolute stall safety margin) upon reaching the airport boundary, the aircraft could stall, leading to potential catastrophic loss of aircraft, passengers, crews, or persons on the ground.
-  Certain CESTOL flight operations could increase the possibility of the flight crew failing to use the appropriate level of automation to configure the aircraft so as to reduce workload and complexity on the flight deck.
-  The varying complexity of approaches may lead the flight crew to excessively rely on the aircraft's automation for assistance, which in the long-term may result in the degradation of manual flight control skills.
-  Relative to the above, degraded manual flight control skills may have catastrophic consequences in instances where the automation associated to perform safety-critical tasks fails.
-  Failure of the artificial stability or control capabilities may increase the effects of wind (i.e., gusts or shear) on the aircraft and, negatively impact pilot workload during low-speed approach tasks.
-  If the CESTOL aircraft's flight management system (FMS) or the flight crew does not adequately compensate for constantly evolving wind patterns experienced as a result of steep approaches, the aircraft may violate protected airspace for the spiral descent and interfere with other traffic resulting in a possible near-midair or actual collision, particularly during super-density arrival operations.
-  The non-standardization of the command display unit (CDU) in the FMS may result in mode confusion amongst the flight crew transitioning from legacy aircraft to CESTOL. This may also result in the flight crew operating the aircraft outside of its flight envelope or intended flight operations parameters affecting performance-based operations.
-  CESTOL flight crews could succumb to a "passive command syndrome," allowing crews to unconsciously relinquish command responsibilities to automated systems momentarily, which could have disastrous consequences if it occurs when a life-saving maneuver is required.
-  Failure of the CESTOL aircraft systems to notify the flight crew of new system configuration after system(s) failure might lead to the crew's inability to recognize early trends indicating anomalous component performance.

Procedures

-  Failure to comply with speed restrictions, due to either disorientation or insufficient understanding of the unique precision required of the departure trajectory and of all its constraints, would impact trajectory-based and performance-based operations.
-  Aircraft exceeding a speed restriction might reduce its ability to maintain a turn radius tight enough to remain in the protected airspace on departure. This could result in possible mid-air collisions requiring radical maneuvering or an actual mid-air collision, especially if there is high-density airspace adjacent to or above the departure protected airspace. Exceeding maximum speeds could ultimately lead to catastrophic loss of aircraft, passengers, crews, or persons on the ground.

- 💧 Executing rapid speed changes (arrival to approach speed) coupled with rapid banking in the CESTOL aircraft in an attempt to comply with noise abatement procedures could result in the aircraft stalling, if it is allowed to decelerate below its stall speed for the bank angle demanded or if the bank angle becomes too steep for the speed being maintained. If the airspeed and bank angle changes are not sufficient the aircraft may have trouble remaining in the protected airspace for the approach that could result in possible or actual mid-air collisions with another aircraft executing an approach to or departure from another runway. Both of these conditions could lead to potential catastrophic loss of aircraft, passengers, crews, or persons on the ground.
- 💧 Unless steep approaches are segregated from standard three degree approaches, the controllers must ensure adequate or increased separation to prevent the wake from an aircraft on the steep approach from descending on the aircraft on the standard three degree approach.
- 💧 Since today's ATM systems will be in use for many years to come, there may be discrepancies between the operational concepts that were in the minds of the designers and the actual operational approaches and techniques used by newer, younger controllers having different attitudes toward automation.
- 💧 If dispatch AOC is unaware of the flight crew and/or the CESTOL aircraft capabilities, the flight could be routed to an airport or into conditions that exceed either one's capabilities or both. This could potentially lead to damage to the aircraft or injury to passengers or crew.
- 💧 If the airline/operator fails to adequately adjust to stabilized approach criteria and mandatory go-around/rejected landing policy could lead to confusion about what is a stabilized approach and when a go-around/rejected landing should be executed. This might result in short or long landing. Landing long could result in a runway excursion, which could potentially lead to damage to the aircraft or injury to passengers or crew.
- 🚩 Flight crews could become confused if CESTOL aircraft fly on the back of the power curve to affect more precise flight path control which could increase the possibility of a sink rate too great to affect a safe go-around, if required.
- 💧 Failure to comply with crossing restrictions due either to disorientation or insufficient understanding of the uniqueness of the departure trajectory and all of its constraints could possibly impact NextGen flow corridors (See Figure 14-5).

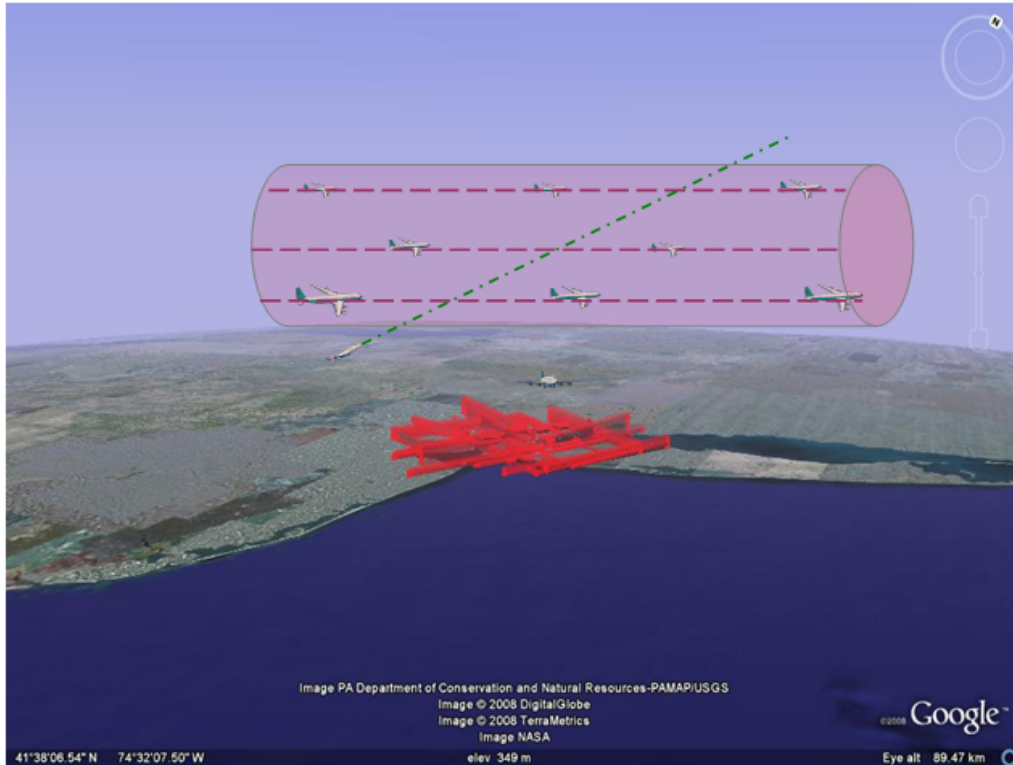


Figure 14-5. Flow corridors (Source: GA Tech/Google Earth).

- ◆ Inability to meet a crossing restriction related to obstacle or terrain clearance could result in the aircraft failing to maintain adequate separation from terrain or obstacles on the surface thus impacting performance-based operations. If the crossing restriction is for protection of other airspace, then noncompliance could result in a near or actual mid-air collision with another aircraft impacting trajectory-based operations. Both occurrences could lead to catastrophic loss of aircraft, passengers, crews, or persons on the ground.
- ◆ Aircraft failing to remain in protected airspace due to disorientation or uniqueness of departure trajectory without sufficient understanding of all the risks could impact other traffic and route structures. Additionally, aircraft outside protected airspace could result in increased controller and/or pilot workload, a near or actual mid-air collision, especially if it is a high-density air traffic corridor, subsequently impacting super-density arrival/departure operations.
- ◆ Failure of the CESTOL flight crew to maintain proper crosswind adjustment while executing a spiral approach and drifting over into another approach path, could create a collision hazard during high-density traffic operations impacting trajectory-based operations.
- ◆ The execution of rapid speed changes (arrival to approach speed) coupled with rapid banking in the CESTOL aircraft, in an attempt to comply with noise abatement procedures, could result in the aircraft stalling (if it is allowed to decelerate below its stall speed for the bank angle demanded or if the bank angle is allowed to become too steep for the speed being maintained). If the airspeed and bank angle changes are not rapid enough, the aircraft may have trouble remaining in the protected airspace on approach, which could result in a near or actual collision with another aircraft executing an approach to or departure from another runway. Both of these conditions could lead to potential catastrophic loss of aircraft, passengers, crews, or persons on the ground.

Environment









-  A CESTOL flight crew's inability to identify targets due to a steep descent angle during initial descent in high-density traffic operations might reduce the pilot's visibility (creating blind spots) due to fuselage "blanking" from the low wing configuration (if the wing is visible from the cockpit) or cockpit structural windscreen view restriction. Reduced visibility could result in near or actual mid-air collisions, leading to potential catastrophic loss of aircraft, passengers, crews, or persons on the ground.
-  Aircraft may encounter wake effects during spiral approaches if its flight path drifts into wake from other aircraft utilizing a parallel approach.
-  CESTOL aircraft operating at a high-density altitude on a hot day could result in the runway length required for takeoff to exceed the runway length available, especially at high-altitude airports. This is because CESTOL aircraft requires a decrease in thrust to generate the rapid acceleration needed for high-lift devices to work effectively. Runway excursions may result if the crew attempted to depart after calculating the runway required for takeoff, potentially leading to damage to the aircraft or injury to passengers or crew.
-  As the landing distance of the CESTOL aircraft is increased with a tailwind component and landing speed, the risk of runway excursions and rejected landings increases. The end result could force the reconfiguring of traffic operations into the airport potentially impacting super-density arrival/departure operations and increasing delays in the system.
-  Due to the steep, rapid climb-out capability of the CESTOL aircraft on departure, a latent collision hazard exists if there is a lack of visibility over the nose.
-  As payload weight increases on the CESTOL aircraft, climb performance capability is reduced, resulting in decreased end-of-runway obstacle clearance margins and a greater noise footprint during climb out along the departure flight path.
-  Rollback ice accumulation is hazardous due to slow high angle-of-attack flight operations and additional time spent maneuvering in any low-level icing conditions in the airport vicinity.
-  CESTOL aircraft operating at slow airspeeds in icy conditions with a thermal anti-ice system that does not evaporate 100% of the water on the wing's leading edge surface for an extended period of time might allow runback ice to accumulate like depicted in Figure 14-6. Ultimately, this could result in degradation of flight control effectiveness or loss of control.



Figure 14-6. Runback ice¹².

- 🚩 The windshear recovery margin is reduced with the increase in sink rate in steep angle approaches, ultimately resulting in flight crews not having the ability to climb out of a windshear encounter prior to intersecting the terrain or other objects.
- 🚩 The slower approach speeds of the CESTOL, compared to similar conventional jet transports, increases its difficulty in maintaining appropriate spacing in mixed traffic, which could cause a possible decrease in throughput impacting trajectory-based operations.
- 🔵 Aircraft inadequately compensating for changing winds in order to stay on trajectory, may increase the possibility of violating bank angles or stall margin limitations.
- 🔵 A CESTOL flight crew encountering wake turbulence during the approach could result in loss of control of the aircraft both laterally or longitudinally, which could result in failure to maintain adequate separation with terrain or other aircraft.

Training

- 🚩 CESTOL aircraft executing a manual flare from a steep approach would increase the possibility of a nose-gear landing; if not accomplished correctly, it could prompt nose-gear collapse, resulting in loss of control of the aircraft.
- 🚩 Flight crews possessing varying skills, abilities, and attitudes toward technology and automation might operate the CESTOL aircraft in ways other than intended or expected in the minds of the original designers, which could have unintended consequences impacting performance-based operations.
- 🚩 Pilots flying numerous different types of aircraft could possibly lead to habit interference, allowing for pilots to become confused between procedures of the CESTOL aircraft and others. This could also happen with new technologies deployed in the CESTOL aircraft causing confusion amongst the flight crew by interrupting certain standard prompting cues used by flight crews.

14.2.3. VLJ

Although each new aircraft has its own unique stability and control issues, VLJs are not fundamentally different from business jets and other general aviation aircraft. The safety concerns they exacerbate mainly reside in the operational domain and are associated with flight crew experience and size. It is anticipated that the majority of the VLJs will be operated as corporate jets or air taxis with professional pilots at the controls; there may also be a significant number of owner operators (non-professional pilots). While the hazards would be the same, the risks they pose would generally be higher for the non-professional pilots than for the professional pilots.

A 2002 Transportation Research Board special report (Future Flight) found that a professional crew (represented by the “air taxi” line) was approximately two times more proficient than a non-professional crew (“GA all components”). Moreover, two-pilot operations (professional crew: airline and corporate) may be three to four times more proficient than single pilot crews (air taxi). See Figure 14-7. In this figure, flight hours are estimated by FAA. Accident rates based on departures are not available because of limited data on GA departures. (Sources: TRB Future Flight, data from NTSB).

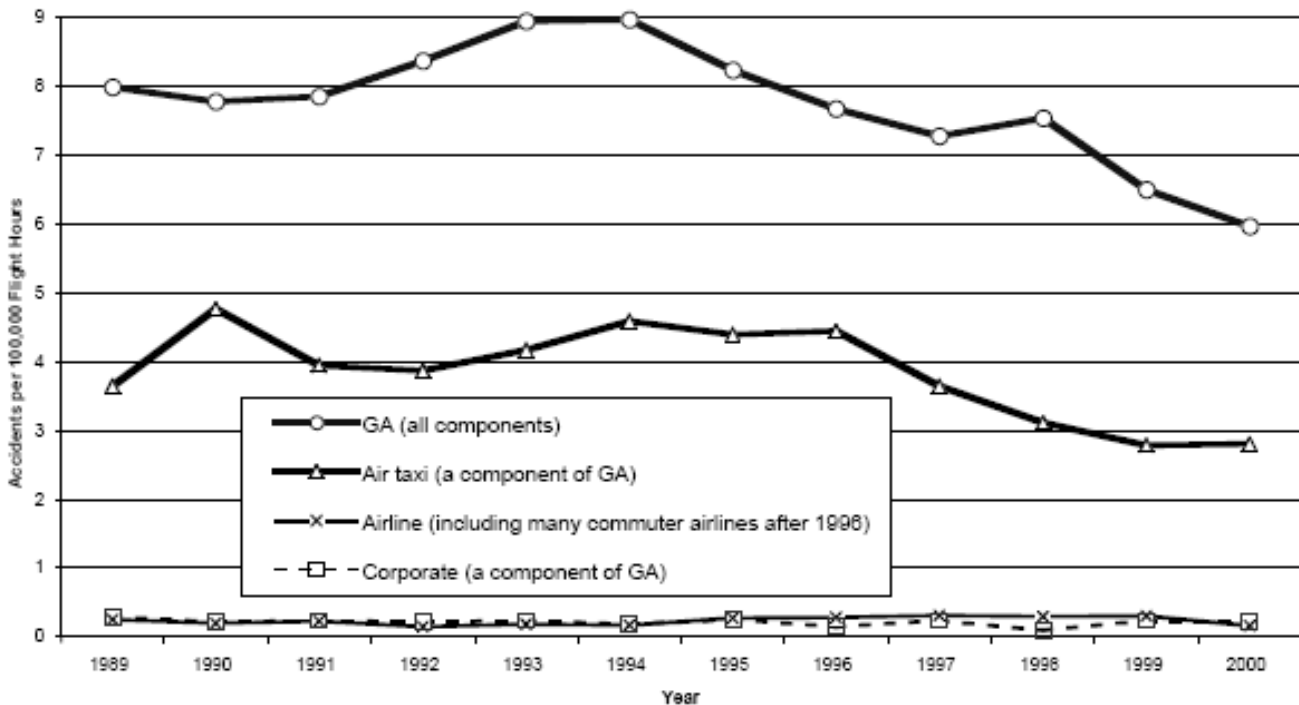


Figure 14-7. Accident trends by segments of aviation industry, 1989–2000.






The Federal Aviation Administration (FAA) requires that each US registered civil aircraft be in airworthy condition and meet the applicable airworthiness requirements for which it is certified to operate. The VLJ aircraft is evaluated for type certification under Title 14 CFR Part 23 Airworthiness Standards – Normal, Utility, Acrobatic, and Commuter Category Airplanes.

The VLJ aircraft, because of its small size, wide-altitude range, and high maneuvering capability operates in an environment not previously utilized by private pilots or single-pilot operations. The VLJ might be utilized in both commercial (air taxi) and private (general aviation (GA)) type operations, which will use both controlled and uncontrolled airports. The reduced cost of the VLJ compared to the cost of


traditional business jets make it affordable for a wide range of pilots with varying airmanship skills. While the operational hazards listed below could be associated with most jet aircraft, the merging of the commercial and GA worlds (along with dynamic pilot skill sets) exacerbates these hazards when the VLJ is exposed to this operational environment.

Historically, the departure and arrival phases of flight have posed the greatest threat to safety (see Figure 14-3). These phases continue to be of particular concern with the VLJs; not only because of crew size and experience, but also because of VLJs' ability to operate from non-towered airfields and to perform spiral approaches and steep descents.




Performance

-  Failure to become stabilized on the spiral approach could result in the aircraft not remaining in protected airspace, to undershoot or overshoot the runway, or experience excessive sink rate. These occurrences could result in the VLJ aircraft being involved in a near or actual mid-air collision or a collision with terrain or other objects, thus resulting in the possible loss of the aircraft and fatal injuries to all passengers.
-  Pilots could become distracted and encounter mode confusion while on approach in high-density traffic area, which might result in a landing on the wrong runway (parallel runway) or runway incursion with the potential to damage the aircraft or cause injury to passengers.
-  The VLJ performance (speed and ceiling) and size, makes see and avoid collision avoidance much less effective.
-  ATC unfamiliar with the VLJ aircraft's performance envelope relative to commercial and general aviation aircraft performance envelopes could lead to controllers' providing instructions that might place the aircraft and crews in an unsafe condition.
-  ATC un-familiar with the VLJ performance and single pilot operations could lead to increased pilot workload.

Automation

-  Pilots that relinquish management of the flight to automation could result in the pilot failing to recognize that an off-nominal situation is developing.

Procedures

-  Failure to program or cross check the FMS correctly could result in the aircraft not being flown on the desired flight path, thus increasing the possibility of near or actual mid-air collisions, landing off airport, or landing at the wrong airport.
-  Failure to accomplish speed transition during the spiral approach could result in the aircraft exceeding the protected airspace. If the speed is too fast, this could cause conflict with other aircraft approach paths, especially in super-density airspace resulting in decreased throughput.
-  Pilot failure to adhere to the missed approach instructions could result in the VLJ violating another aircraft's flight path and a possible near mid-air or mid-air collision causing a loss of aircraft or passengers.

- 🔹 Pilots attempting to comply with last-minute runway changes on approaches at high-density airports by attempting to re-program the FMS instead of using a lower level of automation to control the flight path, could divert their attention away from other flight tasks increasing the risk of compromising flight safety.
- 🔹 Failure of pilot to properly apply the braking technique of a VLJ aircraft not equipped with anti-lock braking systems could cause runway excursion causing bodily injury to all occupants' onboard or damage to or loss of aircraft (ASRS reports.)
- 🔹 Failure to arrest the descent could impede adequate separation from terrain resulting in possible fatal injury to all occupants onboard, persons on the ground, and a loss of the aircraft.
- 🔹 Failure to set the altimeter correctly (as a result of the pilot becoming overloaded during single-pilot operation) could cause the aircraft to descend below the assigned altitude, which could result in a near or actual mid-air collision, contact with other objects, or terrain.
- 🔹 Failure of the pilot to exercise a proper energy management technique with regard to maintaining spacing and/or adhering to separation minima in terminal airspace could possibly result in the aircraft overtaking a slower aircraft or to be overtaken by faster aircraft, which might lead to a collision.
- 🔹 Failure by the pilot to maintain adequate spacing to protect against wake turbulence when trailing larger aircraft could possibly result in a loss of the aircraft and all occupants onboard.
- 🔹 Failure by the crew to expeditiously recognize and manage an event that could cause single engine operation could result in possible loss of the aircraft and all occupants onboard.
- 🚩 During single-pilot operations, the potential for an increased headdown time with use of data link exists, which could result in loss of situational awareness possibly causing a near or actual mid-air collision. The consequences of this include a loss of the aircraft and all occupants onboard (new with data link and single-pilot operations in turbofan commercial operations).
- 🔹 Failure to level off at an assigned altitude could cause potential for a near or actual mid-air collision resulting in fatal injury to all occupants onboard or loss of the aircraft.
- 🔹 Failure to maintain a desired flight path during the spiral approach could result in the aircraft exceeding the protected airspace. This could cause conflict with other aircraft approach paths, especially in super-density airspace resulting in decreased throughput.
- 🔹 The flight crew's failure to maintain the correct spiral path on departure could result in the VLJ entering the flight of another aircraft. This could cause a near mid-air or mid-air collision. Consequently, air traffic controllers may have to expend a greater amount of effort when handling this type of aircraft, thereby reducing overall aircraft handling capacity.

Environment

- 🔹 The forecasted number of VLJs in commercial operations and their potential to operate in non-towered and non-controlled airfields may expose greater numbers of the flying public to operations without ATC support, and operations in which the pilot has de-confliction responsibility.
- 🔹 Potential for increased numbers of high-performance commercial VLJ aircraft (including training flights) operating on time-critical schedules at non-towered and non-controlled airfields increase the mix of operations and pilot skill sets. The high-performance commercial VLJ aircraft with

professionally-trained pilots and the flight on a time schedule may attempt to sequence in before a slower aircraft with student pilots resulting in an increased chance of possible mid-air collision or a loss of control of the slower aircraft.

- ◆ Pilots succumbing to information overload in the terminal environment increase their chances of losing positional awareness that could heighten the risk of near or actual mid-air collisions or aircraft contact with other objects or terrain.
- ◆ Since VLJ aircraft have the ability to operate at altitudes similar to large commercial aircraft, there is an increased possibility of encountering heavy jet turbulence while performing altitude change (pair-wise) maneuvers causing injury to passengers or crew, or loss of the aircraft from in flight breakup.

Training

- ◆ Pilots unfamiliar with or lack of adherence to reduced vertical separation minima (RVSM) procedures during transition to and from Class A airspace could result in the aircraft ascending above or descending below the assigned altitude, thus elevating collision risk.

14.2.4. LCTR

The Federal Aviation Administration (FAA) requires that each US registered civil aircraft be in an airworthy condition and meets the applicable airworthiness requirements for which it is certified to operate. The LCTR aircraft would be evaluated for type certification under Title 14 CFR Part 29 Airworthiness Standards—Transport Category Rotorcraft.












Historically, the departure and arrival phases of flight have experienced the greatest threat to safety. The phase of flight that is of particular concern with the LCTRs is transitioning from the airplane mode to rotorcraft mode on approach to landing. This section is subdivided into four areas: communicate, control, navigate, avoid, and manage. In each area hazards are further grouped based on observed common themes.

Control

For the purposes of this document control is defined as directing movement of the aircraft and monitor status.

- ◆ Certain flight operations could increase the possibility of the flight crew failing to use the appropriate level of automation to configure the aircraft so as to reduce workload and complexity on the flight deck.
- ◆ Fear the flight crew may place too much confidence in the LCTR aircraft's automation, concern that they might lose manual flying skills, could increase possibility of flight crew becoming over reliant on the automation to recover the aircraft from an unusual attitude or unusual in-flight situation.
- ◆ The non-standardization of the command display unit (CDU) in the FMS may result in mode confusion amongst the flight crew transitioning from legacy aircraft to current aircraft. This may also result in the flight crew operating the aircraft outside of its flight envelope or intended flight operations parameters affecting performance-based operations.

- ◆ Flight crews could succumb to a “passive command syndrome,” allowing crews to unconsciously relinquishing command responsibilities momentarily to automated systems, which could have disastrous results if it occurs where a life-saving maneuver is required.
- ◆ Failure of the flight crew to meet a crossing restriction could result in the aircraft failing to maintain adequate separation from terrain or obstacle on the surface, if the restriction is for obstacle or terrain clearance, impacting performance based operations. If the crossing restriction is for protection of other airspace, then failing to comply could result in a near mid-air or mid-air collision with another aircraft impacting trajectory-based operations. Both occurrences could lead to catastrophic loss of aircraft, passengers, crews or persons on the ground.
- ◆ Failure to program the FMS correctly and cross checked could result in the aircraft not being flown on the desired flight path increasing the possibility of the aircraft being involved in a near mid-air, mid-air collision, landing off airport or landing at wrong airport.
- ◆ Pilot’s failure to adhere to the missed approach instructions could result in violating another aircraft’s flight path result in a possible near mid-air or mid-air collision which could cause to loss of aircraft or all occupants onboard.
- ◆ Pilot becoming distracted and encounters mode confusion while on approach in high-density traffic area, lands on the wrong runway (parallel runway), which could result in a possible runway incursion with the potential damage to both aircraft and/or cause injury to occupants onboard.
- ◆ Pilots succumbing to information overload in the terminal environment increase their chances of losing positional awareness that could increase the possibility of becoming involved in a near mid-air, mid-air collision, contact with other objects, or terrain.
- ◆ Failure of the pilot to manage workload could result in them becoming overloaded and lose positional awareness that could increase the possibility of becoming involved in a near mid-air, mid-air collision, contact with other objects, or terrain.
- ◆ The flight crew’s failure to maintain proper approach speed and sink rate could result in the LCTR developing a high sink rate at slow airspeed which could result in the LCTR entering a vortex ring state (VRS) due to the relatively high disk loading. This could result in the LCTR developing an asymmetric VRS with uncommanded roll resulting in a possible adverse outcome if encountered a low altitude (final approach). [3]
- ◆ Failure of the flight crew to manage workload in terminal airspace could result in them becoming overloaded and lose positional awareness that could increase the possibility of becoming involved in a near mid-air, mid-air collision, contact with other objects, or terrain.
- ◆ Failure to arrest the descent could fail to maintain adequate separation from terrain resulting possible fatal injury to all occupant onboard, person on the ground, and loss of the aircraft.
- ◆ Failure to set the altimeter correctly could result in the aircraft descending below the assigned altitude which could result in a near mid-air, mid-air collision, contact with other objects, or terrain.
- ◆ Merging from above or too close to other small and slow general aviation aircraft could create a wake turbulence hazard for the trailing aircraft.

-  Pilots attempting to comply with last-minute runway changes on approaches at high density airports by attempting to re-program the FMS instead of using a lower level of automation to control the flight path could divert their attention from other flight task increasing the risk of compromising safety of the flight.
-  Pilot's failure to configure the aircraft for departure and catch it on crosscheck could result in the aircraft being involved in a runway excursion which could cause damage or loss of aircraft or injury to all occupants onboard.
-  Aircraft propulsion unit failure will result in the vehicle being unable to maintain altitude, which might result in possible near mid-air, mid-air collision with terrain or objects, and possibly another aircraft. This could ultimately result to loss of life and/or damage to property on the surface.
-  Failure to accomplish speed transition during the approach transition could result in the aircraft exceeding the separation minimums if the speed is too fast which could cause conflict with other aircraft on or merging onto approach path especially in super density airspace resulting in a increased possibility of being involved in a near mid-air, mid-air collision, thus resulting in possible loss of the aircraft and fatal injuries to all occupants onboard.
-  A simultaneous loss of an engine and drive shaft providing redundant power to the engine's prop rotor could result in a loss of control of the LCTR. This could possibly result in loss of the LCTR and all occupants onboard as well as persons on the surface. [3]
-  An undetected flight control software-defect could pose a safety risk; Combined with a hardware malfunction or failure could result in a loss of control, especially in rotorcraft mode. This could potentially result in loss of the LCTR and all occupants onboard as well as persons on the surface. [3]
-  The LCTR's relatively high disk loading makes autorotation more problematic than for equivalent weight helicopter. This could potentially result in loss of the LCTR and all occupants onboard as well as persons on the surface. [3]
-  Failure of automatic flight control system during conversion could cause loss of control which could potentially result in loss of the LCTR and all occupants onboard as well as persons on the surface.
-  Loss of conversion capability during flight could potentially result in a runway excursion which could result in loss of the LCTR, loss of all occupants onboard, and damage to property or injury to persons on the surface.
-  Negative (aft stick) trim during accelerating transition poses risk of loss of flight path performance during low-light-level or instrument condition which could potentially result in a collision hazard with other aircraft on adjacent flight paths if the LCTR deviates from its assigned flight path. This could result in loss of both vehicles, all occupants onboard as well as persons on the surface.
-  A bad signal to the flight control system could cause improper flight control response and loss of control which could result in loss of the LCTR, loss of all occupants onboard, and damage to property or injury to persons on the surface.

Navigate

For the purposes of this document the term navigate is defined as the ability to maintain actual trajectory along pre-designated routes or within assigned areas and assigned altitudes. This function relies on satellite and/or ground-based nav aids acceptable to ATC.

- Failure to level off at assigned altitude could cause potential for a near mid-air or mid-air collision which could result in fatal injury to all occupants onboard or loss of aircraft.

Avoid









For the purposes of this document the term avoid is defined as steer clear of hazardous weather, cooperative and non-cooperative aircraft, unauthorized airspace, terrain and obstacles. The LCTR maintains safe separation from cooperative traffic via ATC surveillance. This function relies on transponders, procedures, sensory systems, databases and/or other systems or methods capable of providing sufficient awareness and resolution to avoid collisions.

- Misleading transponder data being sent to other aircraft may cause possible near mid-air, mid-collision with other aircraft, terrain or objects. This incorrect data could also result in unnecessary avoidance maneuver that endangers another aircraft. This could ultimately result to loss of life or damage to property on the surface. This is of greater concern for the UAS since there would be a greater delay for a remote human to notice and compensate for the error and its potential effects.
- Incorrect data being sent to other aircraft may cause possible near mid-air, mid-air collision with other aircraft, terrain or objects. This could result in ATC being unable to direct safe separation. This could ultimately result to loss of life or damage to property on the surface.
- Air Traffic's failure to ensure appropriate separation behind aircraft that generate significant wake turbulence could result in possible loss of control. This might result in possible near mid-air, mid-collision with other aircraft, terrain or objects. This could ultimately result to loss of life or damage to property on the surface.
- Failure of the pilot to exercise proper energy management technique with regard to maintaining spacing and adhere to separation minima in terminal airspace could possibly result in overtaking slower aircraft or be overtaken by faster aircraft which could result in a near mid-air, mid-air collision.




14.2.5. UAS












Performance

- UAS propulsion unit failure will result in vehicle inability maintain altitude, which might result in possible near mid-air or mid-air collision with terrain or objects, and possibly another aircraft. This could ultimately result to loss of life and/or damage to property on the surface¹³.
- A remote pilot's loss of situational awareness while operating multiple UASs could result in possible near mid-air, mid-collision with other aircraft, terrain or objects. This could ultimately result in loss of life or damage to property on the surface.










-  Failure of the remote pilot to manage multiple instructions to multiple UASs could result in incorrect critical flight data being uploaded to the wrong UAS. As a consequence, multiple UASs could deviate from planned flight paths resulting in possible near mid-air, mid-collision with other aircraft, terrain or objects. This could ultimately result in loss of life or damage to property.
-  Failure of the remote pilot to manage multiple UASs while addressing an off-nominal condition with one UAS under his/her control could result in multiple UASs deviating from planned flight paths resulting in possible near mid-air, mid-collision with other aircraft, terrain or objects.
-  Failure of the air traffic controller to understand contingency and emergency procedures of the UAS could result in the UAS acting as a potential source of increased workload for the controller. This may have an adverse impact on the controller's ability to safely and efficiently manage traffic in the sector.
-  A remote pilot's failure to detect loss of propulsion will result in the vehicle no longer being able to maintain altitude. This could result in a mid-air or near mid-air collision if the flight crew fails to take corrective action, especially in a super-density air traffic area. This could ultimately result to loss of life or damage to property on the surface¹³.
-  A remote pilot's failure to detect loss of guidance command without alternate means to change flight path state will result in the remote pilot being unable to control the UAS through primary means. This could result in a mid-air or near mid-air collision if the remote pilot fails to switch to alternate means, particularly in a super-density air traffic area¹³.
-  Failure of the remote pilot to manage workload could result in his/her becoming overloaded and lose positional awareness, which could increase the possibility of collisions.
-  Failure of the remote pilot to be familiar with and adhere to reduced vertical separation minima (RVSM) procedures during transition to and from Class A airspace could result in the aircraft ascending above or descending below the assigned altitude elevating collision risk.
-  A remote pilot's inability to discern airborne objects from others and judge distances between those objects (especially at night) could increase the risk of collisions resulting in possible catastrophic loss of aircraft, passengers, crews, or persons on the ground.

Automation



-  Incorrect data sent to other aircraft may cause possible near mid-air, mid-air collision with other aircraft, terrain, or objects. This could result in ATC being unable to direct safe separation leading to loss of life or damage to property on the surface.¹³
-  Undetected loss of the ability to automatically respond to ATC command may result in possible near mid-air, mid-air collision with other aircraft, terrain, or objects. This might happen as UAS is operating autonomously and voice or data detection sensors fail and the ground pilot monitors fail to notice the aircraft is not responding. In such instances, this may ultimately result to loss of life or damage to property on the surface.
-  Failure of a third-party communications system between UAS and ATC could result in a loss of situational awareness and possibly affect critical flight function. This could result in a loss of control, which might ultimately result in loss of life or damage to property on the surface.

-  Total loss of control of subsystems (hydraulic/electrical) may result in a loss of control of the UAS, subsequently resulting in possible near mid-air, mid-collision with other aircraft, terrain, or objects. This could ultimately result in loss of life or damage to property on the surface.
-  Display freezes with old information could result in possible loss of control of the aircraft and the potential for damage to aircraft and persons or property on the surface.¹³
-  Failure of the UAS's autonomous system in a human-in-the-loop system could result in the remote pilot's degradation of situational awareness leading to a loss of control, fatalities, or damage to property on the surface.
-  Undetected loss of ability to translate high-level direction to specific vehicle actions would leave the remote pilot unable to control the UAS resulting in possible near mid-air, mid-air collision with other aircraft, terrain, or objects. This could ultimately result to loss of life or damage to property on the surface.¹³
-  Detected loss of ability to translate high-level direction to specific vehicle actions would leave the remote pilot unable to control UAS resulting in possible near mid-air, mid-air collision with other aircraft, terrain, or objects. This could ultimately result to loss of life or damage to property on the surface.¹³
-  Loss of ability to execute flight path commands without soft-landing flight termination function would leave the remote pilot unable to control UAS resulting in possible near mid-air, mid-air collision with other aircraft, terrain, or objects. This could ultimately result to loss of life or damage to property on the surface.¹³
-  Total loss of command and control data link function might cause the UAS to make an unpredictable maneuver with the remote pilot unable to control UAS, thus resulting in possible near mid-air, mid-air collision with other aircraft, terrain, or objects. This could ultimately result to loss of life or damage to property on the surface.¹³
-  Degraded command and control data link function resulting in an incorrect signal might cause the UAS to make an unpredictable maneuver with the remote pilot unable to control UAS resulting in possible near mid-air, mid-air collision with other aircraft, terrain, or objects. This could ultimately result to loss of life or damage to property on the surface.¹³
-  Unauthorized access of command and control data might cause the UAS to make an unpredictable maneuver with the remote pilot unable to control UAS resulting in possible near mid-air, mid-air collision with other aircraft, terrain, or objects. This could ultimately result to loss of life or damage to property on the surface.¹³
-  Undetected loss of prioritization of command and control data might cause the UAS to make an unpredictable maneuver with the remote pilot unable to control UAS resulting in possible near mid-air, mid-air collision with other aircraft, terrain, or objects. This could ultimately result to loss of life or damage to property on the surface.¹³
-  Total loss of ability to control the environment inside the UAS may cause remote pilot to take the wrong action resulting in the UAS to be operated outside its envelope resulting in possible near mid-air, mid-air collision with other aircraft, terrain or objects. This could ultimately result to loss of life or damage to property on the surface.¹³

- 🚩 Loss of ability to execute flight path commands (with soft-landing flight termination is still functioning), will result in remote pilot being unable to control the UAS. This may result in a mid-air or near mid-air if the remote pilot fails to switch to alternate means, especially in a super-density air traffic area.¹³
- 🚩 Loss of ability to translate high-level direction to specific vehicle actions (with soft-landing flight termination is still functioning), could possibly result in a remote pilot being unable to control the UAS. This may result in a mid-air or near mid-air if the remote pilot fails to switch to alternate means, especially in a super-density air traffic area.¹³
- 🚩 If UAS's primary flight control surfaces respond slowly, this may result in a pilot-induced oscillation leading to a loss of control. This could ultimately result in loss of life or damage to property on the surface.¹³
- 🚩 Failure to detect a loss of flight termination function could result in a loss of the UAS, loss of life, and/or damage to property on the service if an off-nominal situation requires the flight to be terminated.
- 🚩 Misleading information to/from the power subsystem (hydraulic/electrical) may result in loss of control of the UAS resulting in possible near mid-air, mid-collision with other aircraft, terrain, or objects. This could ultimately result to loss of life or damage to property on the surface.¹³
- 🚩 Incorrect flight path state is being presented to the pilot. The pilot will not know if the UAS is operating properly which could result in catastrophic loss of UAS, near mid-air, mid-air collision, injury to persons or damage to property on the surface.¹³
- 🚩 Misleading information in the control environment inside the UAS may cause consuming function to take the wrong action resulting in the UAS being operated outside its envelope leading to possible near mid-air, mid-air collision with other aircraft, terrain, or objects. This could ultimately result in loss of life or damage to property on the surface.¹³
- 🚩 Undetected encounters with an adverse environmental condition could lead to the UAS being operated outside its performance envelope resulting in possible near mid-air, mid-air collision with other aircraft, terrain or objects. This could ultimately result to loss of life or damage to property on the surface.¹³
- 🚩 Loss of guidance command without alternate means to change flight path, but with "soft landing" flight termination function, would render the UAS uncontrollable; yet, the "Soft Landing" function can be utilized to land the UAS safely. This could result in a mid-air or near mid-air, especially in a super-density air traffic area.¹³
- 🚩 Total loss of guidance command without alternate means to change flight path, without "soft landing" flight termination function would render the UAS uncontrollable, resulting in possible mid-air or near mid-air, especially in a super-density air traffic area. The UAS could also land in a densely populated area resulting in fatal injury to persons and damage to property on the surface.¹³
- 🚩 Failure of the UAS air traffic detection system could increase collision risk with another aircraft leading to catastrophic loss of aircraft, passengers, crew, or persons on the ground or damage to property on the surface.

-  Failure of the Situational Awareness Data Link (SADL)¹⁴ could increase the possibility of becoming involved in a near mid-air or mid-air collision with another aircraft leading to catastrophic loss of aircraft, passengers, crew, or persons on the ground or damage to property on the surface.
-  Misleading information from the UAS to the traffic information broadcast (TIS-B) system could increase the possibility of becoming involved in a near mid-air or mid-air collision with another aircraft leading possibly to catastrophic loss of aircraft, passengers, crew, or persons on the ground or damage to property on the surface.
-  Misleading information from the UAS to the Airborne Separation Assurance System (ASAS) system could increase the possibility of becoming involved in a near mid-air or mid-air collision with another aircraft leading possibly to catastrophic loss of aircraft, passengers, crew, or persons on the ground or damage to property on the surface.
-  UAS's inability to detect adverse environmental conditions could result in a loss of control, operation outside performance envelope, near mid-air, or mid-air collision with other aircraft, terrain, or objects. This could ultimately result in loss of life or damage to property on the surface.¹³
-  UAS's inability to track the relative location of adverse environmental conditions could result in a loss of control, operation outside performance envelope, near mid-air, or mid-air collision with other aircraft, terrain, or objects. This could ultimately result in loss of life or damage to property on the surface.¹³
-  UAS's inability to convey the relative location of adverse environmental conditions could result in a loss of control, operation outside performance envelope, near mid-air, or mid-air collision with other aircraft, terrain, or objects. This could ultimately result to loss of life or damage to property on the surface.¹³
-  UAS's inability to assess the relative location of adverse environmental conditions could result in a loss of control, operation outside performance envelope, near mid-air, or mid-air collision with other aircraft, terrain or objects. This could ultimately result in loss of life or damage to property on the surface.¹³
-  UAS's inability to produce corrective action commands to adverse environmental conditions could result in a loss of control, operation outside performance envelope, near mid-air, or mid-air collision with other aircraft, terrain, or objects. This could ultimately result to loss of life or damage to property on the surface.¹³
-  If UAS provides an incorrect navigation state, this could result in increased workload for ATC and remote pilots. Moreover, it could cause possible near mid-air or mid-air collisions with other aircraft, terrain, or objects. This could ultimately result in loss of life or damage to property on the surface.

Procedures

-  Remote pilot's failure to transmit intentions on UNICOM prior to entering the runway could result in a runway incursion. This could ultimately result in loss of life or damage to property on the surface.
-  Remote Pilot's failure to adhere to the missed approach instructions could result in the UAS violating another aircraft's flight path result in a possible near mid-air or mid-air collision which could cause to loss of aircraft or all occupants onboard.

- Remote Pilot's failure to adhere to pattern entry procedures at uncontrolled field could result in possible near mid-air, mid-collision with other aircraft, terrain or objects. This could ultimately result to loss of life or damage to property on the surface.
- ATC's failure to ensure appropriate separation behind aircraft that generate significant wake turbulence could result in lost links resulting in possible loss of control. This might result in possible near mid-air, mid-collision with other aircraft, terrain or objects. This could ultimately result to loss of life or damage to property on the surface.
- Remote pilot's failure to meet a crossing restriction could result in the aircraft failing to maintain adequate separation from terrain or obstacle on the surface, if the restriction is for obstacle or terrain clearance, impacting performance based operations. If the crossing restriction is for protection of other airspace, then failing to comply could result in a near mid-air or mid-air collision with another aircraft impacting trajectory-based operations. Both occurrences could lead to catastrophic loss of aircraft, passengers, crews or persons on the ground.

Environment








- Misleading transponder data being sent to other aircraft may cause possible near mid-air, mid-collision with other aircraft, terrain, or objects. This incorrect data could also result in an unnecessary avoidance maneuver that endangers another aircraft. This could ultimately result in loss of life or damage to property on the surface. This is of greater concern for the UAS since there would be a greater delay for a remote human to notice and compensate for the error and its potential effects.
- Loss of ability to communicate with the UAS could result in the ATC not being able to provide instruction, thus reducing the safety margin. For low or moderately autonomous UAS: loss of ability to communicate with the UAS human element. For the more autonomous UAS: loss of ability to communicate with the UAS aircraft.
- Failure of the UA'Ss conspicuity could increase the possibility of becoming involved in a near mid-air or mid-air collision with another aircraft leading possibly to catastrophic loss of aircraft, passengers, crew, or persons on the ground or damage to property on the surface.
- Merging from above or too close to another small and slow general aviation aircraft could result in a near mid-air or mid-air collision with another aircraft or create a wake turbulence hazard for the trailing aircraft.

14.2.6. SST






This section is subdivided into five areas: performance, automation, procedures, environment, and training. In each area hazards are further grouped by observed common themes.

Performance

- Failure of the flight crew to maintain adequate separation from another aircraft above Mach 1 could result in the SST's shock wave (sonic boom), possibly inducing a loss of control, in flight break-up, or engine failure of the other aircraft. Ultimately, this occurrence could lead to a possible catastrophic loss of the aircraft and fatal injuries to all occupants onboard.
- A flight crew's failure to recognize a breakdown in the FMS above Mach 1 could result in a rapid divergence of the SST from the planned flight path, which could increase the potential for a near mid-air or mid-air collision; thus, resulting in possible loss of the aircraft and all occupants onboard.

-  Failure of the pilot to exercise proper energy management techniques with regard to maintaining spacing and adherence to separation minima in terminal airspace could possibly result in overtaking slower aircraft, which could result in a near mid-air, mid-air collision.
-  Failure of the flight crew to respond in a timely manner to a resolution alert (RA) from the collision avoidance system (e.g. traffic collision avoidance system (TCAS)) could potentially lead to near mid-air or mid-air collision, thus resulting in possible loss of both aircraft and all occupants onboard.
-  Failure of Air Traffic Control (ATC) to be responsive to a conflict alert between an SST and another aircraft could potentially lead to near mid-air or mid-air collision, thus resulting in possible loss of the aircraft and all occupants onboard due to the potential for increased speed differential between the SST and the other aircraft.
-  Failure of the pilot to exercise proper aviating technique with regard to maintaining proper pitch (allowing the aircraft to enter a high pitch/high thrust situation) could result in flight crew reaching the back side of the power curve, especially on approach (at low airspeed). This increases the potential for stall resulting in a possible loss of control, loss of the aircraft, and fatal injuries to all occupants onboard.
-  The flight crew's lack of understanding of the operating capabilities of the SST could increase the potential of loss of control of the aircraft especially during super sonic flight.
-  Failure of the flight crew to manage workload in the terminal airspace could result in them becoming overloaded and lose positional awareness, which could increase the possibility of becoming involved in a near mid-air, mid-air collision contact with other objects, or terrain.
-  Failure to accomplish speed transition during the approach transition could result in the aircraft exceeding the separation minimums if the speed is too fast, which could conflict with other aircraft on or merging onto approach path, especially in super-density airspace.

Automation

-  Failure of the passive thermal cooling system could result in fatal temperatures in the cabin and a possible boiling of the fuel, thus resulting in potential damage and possible loss of the aircraft and injuries to all occupants onboard.¹⁶
-  Failure of the active thermal cooling could result in damage to the engine leading edge, nozzle, wing leading edge, or nose tip, thus resulting in possible loss of the aircraft and injuries to all occupants onboard.¹⁷
-  Failure of the engine inlet variable geometry center body could result in engine flameout.¹⁶
-  Failure of the variable geometry wing to extend during speed reduction transition would result in the SST having to make a faster than normal approach speed. This could result in possible damage to the aircraft and/or injury to persons or property on the surface.¹⁸
-  Undetected failure of the stability augmentation system at high velocity (above Mach 1) could result in the structural failure to the aircraft in flight leading to a possible catastrophic loss of the aircraft and fatal injuries to all occupants onboard.¹⁹

- 🚩 Undetected failure of the stability augmentation system at low velocity could result in a possible loss of control of the aircraft, thus leading to a possible loss of the aircraft and fatal injuries to all occupants onboard.¹⁹
- 🚩 Undetected failure of the flight protection envelope system at low velocity could result in a possible loss of the aircraft and fatal injuries to all occupants onboard resulting from a potential loss of control, if the flight crew attempts an abrupt maneuver.¹⁹
- 🚩 Undetected failure of the flight protection envelope system at high velocity could result in a possible catastrophic loss of the aircraft and fatal injuries to all occupants onboard resulting from a possible inflight break-up, if the flight attempts an abrupt maneuver.
- 🚩 Failure of the onboard collision avoidance system to timely detect another aircraft on a collision path with the SST could potentially result in a near mid-air or mid-air collision thus resulting in possible loss of the both aircraft and all occupants onboard.

Procedures

- 💧 The fleet operator's pairing of an inexperienced crew could increase the possibility of the SST being involved in a catastrophic event if the flight crew encountered an off-nominal or emergency situation where the event exceeded the flight crew's airmanship skills.
- 💧 Merging from above or too close to other small and slower moving aircraft (i.e., VLJ) could create a wake turbulence hazard for the trailing aircraft.

Environment














- 💧 Restricted flight deck visibility and placement of the nose landing gear aft of the flight deck could result in departing the edge of the taxiway surface during turning while taxiing.¹⁵
- 💧 Restricted flight deck visibility might result in a near mid-air or mid-air with other aircraft especially in a super density traffic area.¹⁵
- 💧 Restricted flight deck visibility might result in a collision with objects on the surface during taxi operations.¹⁵

14.2.7. Large Tiltrotor

This section is subdivided into five areas: performance, automation, procedures, environment, and training. In each area hazards are further grouped based on observed common themes.

Performance




- 💧 Flight crews could succumb to a "passive command syndrome," allowing crews to unconsciously relinquishing command responsibilities momentarily to automated systems, which could have disastrous results if it occurs where a life-saving maneuver is required.
- 💧 Failure of the flight crew to meet a crossing restriction could result in the aircraft failing to maintain adequate separation from terrain or obstacle on the surface, if the restriction is for obstacle or terrain clearance, impacting performance based operations. If the crossing restriction is for protection of other airspace, then failing to comply could result in a near mid-air or mid-air collision with another aircraft impacting trajectory-based operations. Both occurrences could lead to catastrophic loss of aircraft, passengers, crews or persons on the ground.

-  Failure to program the FMS correctly and cross checked could result in the aircraft not being flown on the desired flight path increasing the possibility of the aircraft being involved in a near mid-air, mid-air collision, landing off airport or landing at wrong airport.
-  Pilot's failure to adhere to the missed approach instructions could result in violating another aircraft's flight path result in a possible near mid-air or mid-air collision which could cause to loss of aircraft or all occupants onboard.
-  Pilot becoming distracted and encounters mode confusion while on approach in high-density traffic area, lands on the wrong runway (parallel runway), which could result in a possible runway incursion with the potential damage to either aircraft or cause injury to occupants onboard.
-  Pilots succumbing to information overload in the terminal environment increase their chances of losing positional awareness that could increase the possibility of becoming involved in a near mid-air, mid-air collision, contact with other objects, or terrain.
-  Failure of the pilot to manage workload could result in them becoming overloaded and lose positional awareness that could increase the possibility of becoming involved in a near mid-air, mid-air collision, contact with other objects, or terrain.
-  The flight crew's failure to maintain proper approach speed and sink rate could result in the LCTR developing a high sink rate at slow airspeed, which could result in the LCTR entering a vortex ring state (VRS) due to the relatively high disk loading. This could result in the LCTR developing an asymmetric VRS with un-commanded roll resulting in a possible adverse outcome if encountered at a low altitude (final approach).³
-  Failure of the flight crew to manage workload in terminal airspace could result in them becoming overloaded and lose positional awareness that could increase the possibility of becoming involved in a near mid-air mid-air collision, contact with other objects, or terrain.
-  Failure to arrest the descent could result in a lack of adequate separation from terrain resulting in possible fatal injury to all occupants onboard, persons on the ground, and a loss of the aircraft.
-  Failure to set the altimeter correctly could result in the aircraft descending below the assigned altitude, which could result in a near mid-air, mid-air collision, contact with other objects, or terrain.
-  Pilots attempting to comply with last-minute runway changes on approaches at high-density airports by attempting to re-program the FMS instead of using a lower level of automation to control the flight path could divert their attention from other flight tasks, thereby increasing flight safety risk.
-  A pilot's failure to configure the aircraft for departure and catch it on cross check could result in the aircraft being involved in a runway excursion, which could cause damage to or loss of aircraft or injury to all occupants onboard.
-  Failure to accomplish speed transition during the approach transition could result in the aircraft exceeding the separation minimums if the speed is too fast, which could cause conflict with another aircraft on or merging onto the approach path, especially in super-density airspace.
-  Failure to level off at the assigned altitude could cause potential for a near mid-air or mid-air collision, which could result in fatal injury to all occupants onboard or loss of aircraft.


- ATC's failure to ensure the appropriate separation behind aircraft that generate significant wake turbulence could result in possible loss of control. This might result in near mid-air, mid-collision with other aircraft, terrain, or objects, ultimately leading to loss of life or damage to property on the surface.
- Failure of the pilot to exercise proper energy management techniques with regards to maintaining spacing and adhering to separation minima in terminal airspace could possibly result in overtaking slower aircraft or being overtaken by faster aircraft, which heightens collision risk.

Automation


- Certain flight operations could increase the possibility of the flight crew failing to use the appropriate level of automation to configure the aircraft so as to reduce workload and complexity on the flight deck.
- The flight crew may place too much confidence in the SST aircraft's automation or they might lose manual flying skills, which could increase the possibility of the crew relying on the automation to recover the aircraft from an unusual attitude or unusual in-flight situation.
- The non-standardization of the command display unit (CDU) in the FMS may result in mode confusion among the flight crew transitioning from legacy aircraft to current aircraft. This may also result in the flight crew operating the aircraft outside of its flight envelope or intended flight operations parameters affecting performance-based operations.
- Aircraft propulsion unit failure will result in the vehicle being unable to maintain altitude, which might result in possible near mid-air, mid-air collision with terrain or objects, and possibly another aircraft. This could ultimately result to loss of life and/or damage to property on the surface.
- A simultaneous loss of an engine and drive shaft providing redundant power to the engine's prop rotor could result in a loss of control of the LCTR. This could possibly result in loss of the LCTR and all occupants onboard as well as persons on the surface.²⁰
- An undetected flight-control software defect could pose a safety risk; Combined with a hardware malfunction or failure could result in a loss of control, especially in rotorcraft mode. This could potentially result in loss of the LCTR and all occupants onboard as well as persons on the surface.²⁰
- The LCTR's relatively high disk loading makes autorotation more problematic than for equivalent weight helicopter. This could potentially result in loss of the LCTR and all occupants onboard as well as persons on the surface.²⁰
- Failure of automatic flight control system during conversion could cause loss of control which could potentially result in loss of the LCTR and all occupants onboard as well as persons on the surface.
- Loss of conversion capability during flight could potentially result in a runway excursion which could result in loss of the LCTR, loss of all occupants onboard, and damage to property or injury to persons on the surface.
- Negative (aft stick) trim during accelerating transition poses risk of loss of flight path performance during low-light-level or instrument condition which could potentially result in a collision hazard with other aircraft on adjacent flight paths if the LCTR deviates from its assigned flight path. This could result in loss of both vehicles, all occupants onboard as well as persons on the surface.

-  A bad signal to the flight control system could cause improper flight control response and loss of control which could result in loss of the LCTR, loss of all occupants onboard, and damage to property or injury to persons on the surface.
-  Misleading transponder data being sent to other aircraft may cause possible near mid-air, mid-collision with other aircraft, terrain or objects. This incorrect data could also result in unnecessary avoidance maneuver that endangers another aircraft. This could ultimately result to loss of life or damage to property on the surface. This is of greater concern for the UAS since there would be a greater delay for a remote human to notice and compensate for the error and its potential effects.
-  Incorrect data being sent to other aircraft may cause possible near mid-air, mid-air collision with other aircraft, terrain or objects. This could result in ATC being unable to direct safe separation. This could ultimately result to loss of life or damage to property on the surface.

Procedures

-  Merging from above or too close to other small and slow general aviation aircraft could create a wake turbulence hazard for the trailing aircraft.

Training

-  A pilot's failure to maintain training knowledge could harm the aircraft's performance during critical phases of flight.

14.3. ***Qualitative Assessment of Risk***

This section considers the collision risks associated with the operations of each in vehicle in cruise flight and high-density terminal areas in the NextGen air transportation system. A combination of hazard analysis techniques, including a Preliminary Hazard Analysis (PHA) and What-If analysis, were used to develop a list of hazards associated with operations with other air traffic within the NextGen air transportation system.

The severity is determined by the worst credible outcome. Table 14-1 depicts the severity classification for this study. The hazards were classified as minimal, minor, major, hazardous, or catastrophic, with minimal being the least and catastrophic being the most severe.

Table 14-1. Hazard severity classification.

Hazard Severity Classification				
Minimal 5	Minor 4	Major 3	Hazardous 2	Catastrophic 1
1) Minimal effect on operation of aircraft 2) Possible minimal injury or discomfort to passengers	1) Reduction of functional capability of aircraft but loss does not impact overall safety e.g. normal procedures 2) Possible physical discomfort to passengers	1) Reduction in safety margin or functional capability of aircraft, requiring crew to follow abnormal procedures 2) Possible physical distress on passengers 3) Possible minor injuries to passengers	Reduction in safety margin and functional capability of aircraft, requiring crew to follow abnormal procedures i.e. NMAC, system failure 2) Possible serious injury to passengers	Conditions resulting in a possible mid-air or impact with obstacle, or terrain resulting in possible hull loss, multiple fatalities, or fatal injuries

Likelihood is determined by how often one can expect the harm to occur at the worst credible severity (2).

Table 14-2. Likelihood definitions.

Likelihood Definitions				
Frequent A	Occasional B	Remote C	Extremely Remote D	Extremely implausible E
Expected to occur about every 3 months in operations	Expected to several times per year in operations	Expected to occur several times in the life of operation	Unlikely to occur, but possible in life of operation	So unlikely that it can be assumed that it will not occur in life of operation

Risk Matrix Definition²

A risk matrix offers a graphical means by which to determine risk levels. The rows in the matrix reflect previously introduced severity categories, and the columns reflect previously introduced likelihood categories. The SRM Panel assesses risk by using the risk matrix in Figure 14-8.

The risk levels used in the matrix are defined as:

High – unacceptable risk; change cannot be implemented unless the hazard’s associated risk is mitigated so that risk is reduced to a medium or low level. Tracking, monitoring, and management are required. Hazards with catastrophic effects that are caused by: 1) single point events or failures, 2) common cause events or failures, or 3) undetectable latent events in combination with single point or common cause events, are considered high risk, even if the possibility of occurrence is extremely improbable.

Medium – acceptable risk; minimum acceptable safety objective; change may be implemented, but tracking, monitoring, and management are required.

Low – acceptable without restriction or limitation; hazards are not required to be actively managed but must be documented.

A catastrophic severity and corresponding extremely improbable likelihood qualify as medium risk, as long as the effect is not the result of a single point or common cause failure. If the cause is a single point or common cause failure, the effect of the hazard is categorized as high risk and placed in the red part of the split cell in the bottom right corner of the matrix.

A **single point failure** is defined as a failure of an item that would result in the failure of the system and is not compensated for by redundancy or an alternative operational procedure. An example of a single point failure is a system with redundant hardware, in which both pieces of hardware rely on the same battery for power. In this case, if the battery fails, the system will fail.

A **common cause failure** is defined as a single fault resulting in the corresponding failure of multiple components. An example of a common cause failure is redundant computers running on the same software, which is susceptible to the same software bugs.

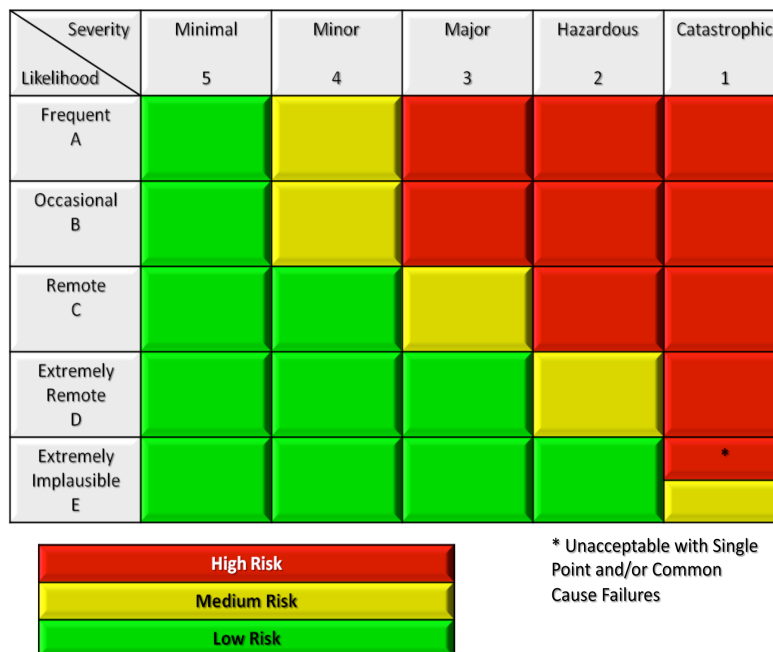


Figure 14-8. Risk matrix.

The hazards were evaluated and classified utilizing criteria in Table 14-1, and then likelihood was assessed using criteria in Table 14-2 based on subject matter expertise. The risk of each hazard was then assessed utilizing the risk matrix in

Figure 14-8. The results of the risk assessment of the hazards are recorded in Appendix G. During the identification of hazards, this study looked at only hazards that would impact NextGen, those that were unique to the particular vehicle study, and of greatest risk to the flying public. Low-risk hazards were not recorded in the initial risk assessment because the low-risk hazards could be attributed to any conventional (legacy) and posed little risk to the public.

We will now proceed to discuss specific operational risks associated with each of the new vehicles.

14.3.1. CESTOL

CESTOL Operations

The main difference between the CESTOL and vehicles operating today is increased lift, which allows it to fly at slower speeds; thus, it can take off from and land on shorter runways. Additionally, the CESTOL has a high thrust-to-weight ratio that permits a rapid acceleration to takeoff airspeed and provides for excess thrust for more precise flight-path control on approach. The slow approach speed makes steeper descent gradients possible and a more precise tracking of the touchdown point. As mentioned earlier in this report, the CESTOL design used in this study does not rely on power-augmented lift or extensive high-lift devices for its increased lift during low speed operations. Instead, the design relies on low-wing loading and a high speed slotted wing design. For the design used in this report, the area of greatest concern is the low-speed operations during approach and landing, particularly with respect to the steep approach and spiral descent. The CESTOL departures proposed for the New York Metroplex are the conventional departures with a high glide path of 10 degrees.

We will also consider:

- Approach speed versus gust margin,
- Flight path angle and rate of sink,
- Crosswinds,
- Go-around maneuver,
- Engine out.

14.3.2. Approach Speed vs. Gust Margin

According to the Federal Aviation Regulation 25.125 the approach speed must be above 1.23 times the stall speed in the landing configuration. International authorities require a factor of 1.3 times the stall speed. The more stringent 1.3 value is used here. The approach speed of the CESTOL aircraft is 105 knots (with the 1.3 factor) and the stall speed is 81 knots. The similarly sized conventional B737 aircraft has an approach speed of 134 knots and stall speed of 103 knots. These values provide the aircraft with a margin for gusts of 24 and 31 knots respectively—a difference of 7 knots. According to the NCDG at La Guardia Airport the average wind speeds are 10 – 14 mph depending on the month (data since 1954). On November 24, 2008, according to the National Weather Service the average wind speed at La Guardia was 10.5, however, the highest wind speed for the day was 24 mph and the highest gust was 31 mph. The

B737 would have been able to operate with the high gust value of 27 knots (31 mph), however, this would have been greater than the CESTOL's stall margin of 24 knots. While the CESTOL could possibly recover from the stall condition, further restricting its operations could limit it from achieving its capacity enhancing potential. Because of the risk associated with loss of control due to stall, CESTOL operations would likely be more severely affected by weather than other similarly sized aircraft.

14.3.3. Flight Path Angle and Rate of Sink

Guidance by the United Kingdom's Civil Aviation Authority indicates that approach angles up to 3.5° are considered routine, angles 3.5° to 4.5° "are unlikely to produce significant problems in normal operations," and that it is internationally accepted that approach paths 4.5° or greater "constitute steep approaches for which specific airworthiness and operational approval is required." According to the CAA guidance, "speed and flight path control become more demanding with increasing angle." However, the slower approach speeds of the CESTOL vehicle permit it to more precisely track its touchdown point, and the greater thrust-to-weight provides it with adequate residual throttle movement to make the necessary flight path corrections.

Current approach operations are 3 – 3.5° and 120 – 160 knots. Figure 14-9 shows the flight path angle and approach speed for various constant sink rates. The boxed region is roughly represents current operations, and the region above the dashed curves would be restricted do to go-around maneuvers depending on the pilot and aircraft reaction time (as determined by Hileman, and to be addressed later). The solid colored curves are lines of constant rate of sink. The Flight Safety Foundation (FSF) recommends a rate of sink (sink rate) no greater than 1,000 fpm as criteria for a stabilized approach. The approach of the CESTOL is at 104.7 knots and 5.5°, resulting in 1,016 fpm sink rate, just over that recommended by the FSF.

While there are human factors issues impacted by the steeper descent (i.e., the out the window perspective), if the sink rate is maintained at or below the FSF recommended 1,000 fpm, the crew should not be pressed for time any more than during current 3° operations. Avionics systems such as EGPWS/TAWS systems may need to be reconfigured and certified for steeper descents if these impact the rate of sink.

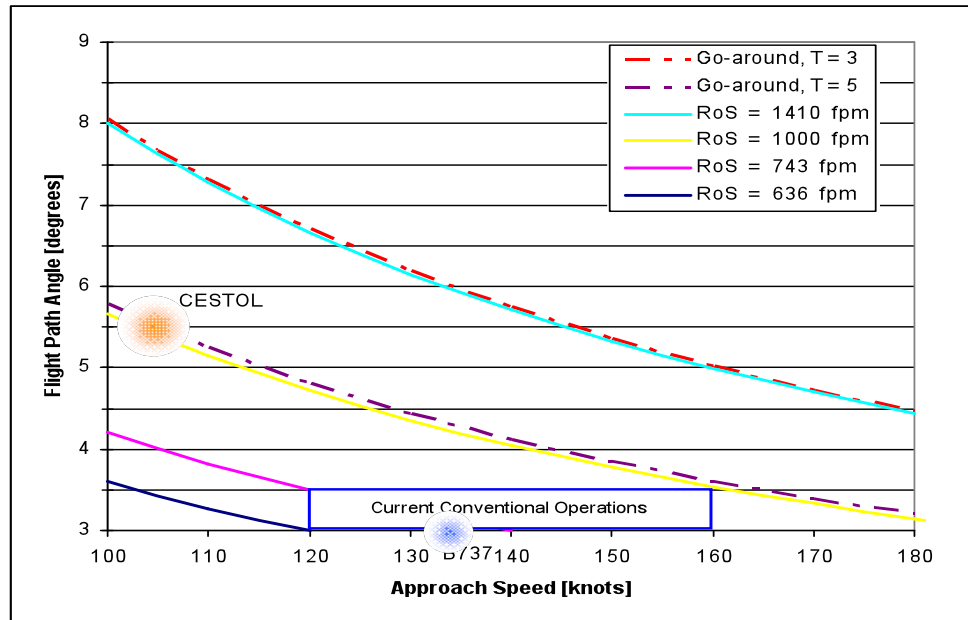


Figure 14-9. Flight path angle versus approach speed (adapted from J. Hileman by A. Hahn).

Crosswinds

Crosswinds are of particular concern with respect to the spiral approach. In a spiral, the wind will be coming from all directions, relative to the aircraft, at some point. The idea of the spiral is to maintain a circular ground track while descending from 10,000 to 1,000 feet. This can be accomplished while maintaining a constant radius by reducing the bank angle as the velocity is reduced in zero wind conditions. In order to maintain a circular ground track in real wind conditions, the bank angle and speed will have to be continuously adjusted (both decreased and increased) depending on where the aircraft is in the turn. The track in this fluid (wind) flow will not be circular.

In 2005, as reported by Hange²¹, a C-17 flew a series of tests including a $\frac{3}{4}$ radius 360° descent with a 5.5° glide path at 120 knots. The wind gusts were greater than expected and the lateral tracking of the C-17 autopilot was poor and could not be used. The lateral path was then flown manually by the pilot while the autopilot continued to be used for vertical navigation. This study by Hange found that for the operations to be performed in IMC conditions improved technologies in flight controls will be necessary to fly these approaches. When STOL operations also depend on powered-lift the cross coupling between the aerodynamics and the powered-lift system will be crucial in future integrated flight-propulsion controls. “None of the four pilots [who flew this approach] felt that the workload was too great during the SNI [simultaneous non-interfering] maneuver that it became an issue to track other traffic near the lakebed.” Hange also noted that “the need for improved RNP accuracy may force performance improvements in the control authority required by the aircraft, not just in avionics.”

Go-around Maneuver

Based on the CESTOL's performance during approach, its ability to perform a go-around is plotted in Figure 14-10. This figure shows a set of curves for performing a go-around based on the following formula:

$$DH > V_{\text{approach}} T_{\text{delay}} \sin \gamma + \frac{V_{\text{approach}}^2}{(n_{\text{limit}} - 1)g} (1 - \cos \gamma)$$

The two solid curves are for a 100 ft decision height, equivalent to that for Category II approaches, and constant aircraft and pilot reaction times (3 and 5 seconds), and a constant load factor of 1.3. The thin dashed curves are varying the load factor ± 0.1 , for a reaction time of 5 s. The thick dashed lines are for decision heights of 200 ft and 50 ft, the decision heights for CAT I and CAT III approaches respectively, and a 5 s reaction time. If the pilot/aircraft reaction time is 3 seconds then the safety constrain for the CESTOL is the 1,000 fpm sink rate (see Figure 14-11). If the 5 seconds is more the norm for this delay time for the CESTOL, then the sink rate constraint and the go-around constraint are reached almost simultaneously. Figure 14-10 shows it is possible for the CESTOL to perform the go-around maneuver given its approach flight path angle and speed (source: adapted from Hileman 2007). The CESTOL reaction time is expected to be quick since it will have "instantaneous" net thrust by closing the clamshell speed brakes.

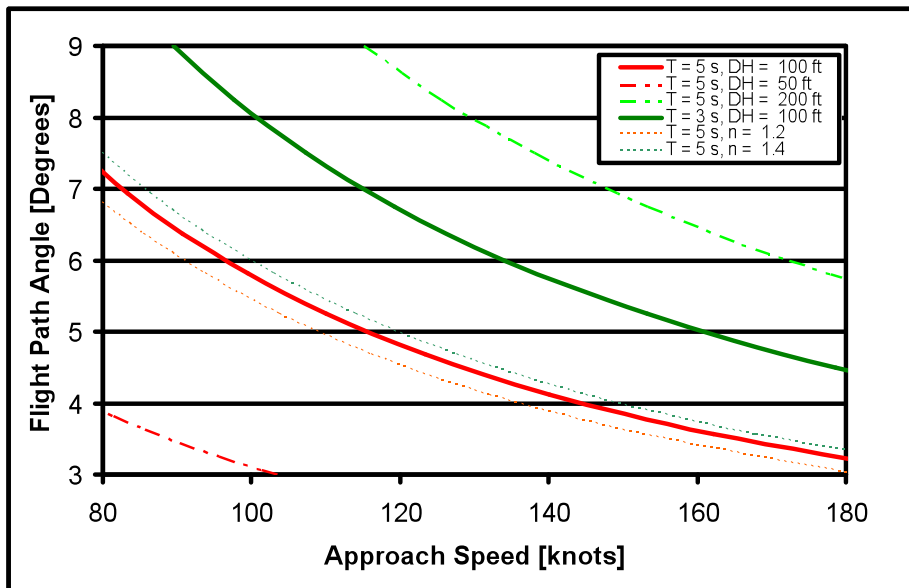


Figure 14-10. Go-around analysis results for CESTOL (red dot) and range of current operations.

Figure 14-11 shows that the decision height is a function of the rate of sink and reaction time, and is essentially constant with flight path angle. The CESTOL's minimum decision height is 100 ft.

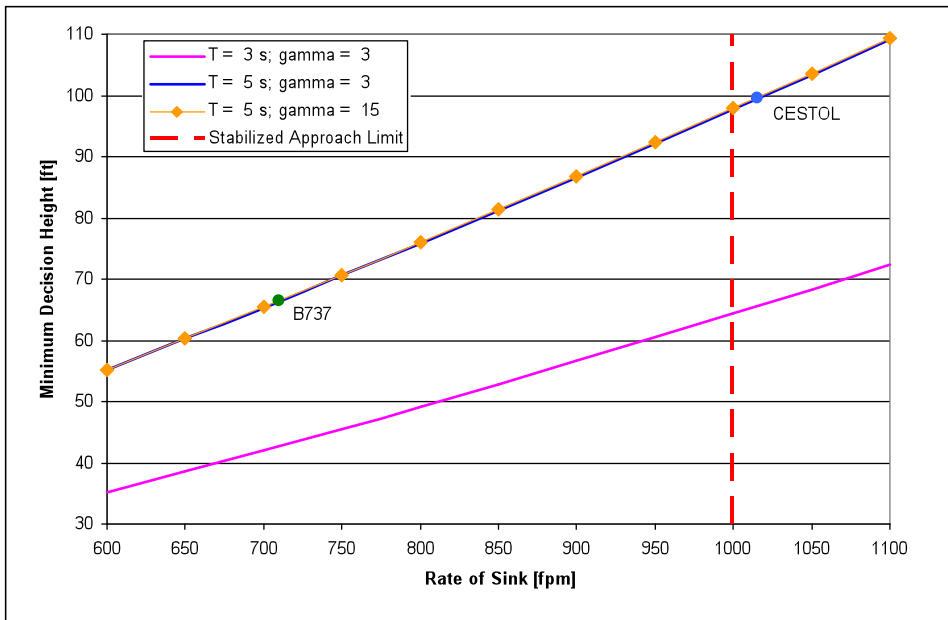


Figure 14-11. Minimum decision height as a function of rate of sink

14.3.4. Engine Out

Engine out capabilities for the CESTOL are being investigated. Of particular concern is engine out while in the spiral descent. The high thrust-to-weight ratios of STOL aircraft work to their advantage (so long as they are controllable in the asymmetric thrust configuration).

Multiple Aircraft (Traffic) Operations

This section addresses operations of multiple aircraft within the spiral, as well as interactions with other traffic flows.

14.3.5. Spiral Operations

Separation within Spiral

The spiral has a diameter of 3 nm and a total height (two 360-degree turns) of 9,000 ft. This provides for the require 3 nm lateral separation and 2,750 ft vertical separation if the trailing aircraft is half a turn behind the leading aircraft, 4,500 ft vertical separation if a full turn behind. This seems promising but the impact of RNP and corresponding vertical component will be examined for spiral operations.

Wake Turbulence

Wake turbulence transport and decay within the spiral is being considered. It does not appear that wake turbulence will be an issue for the CESTOL alone, but if the spiral is being used by mixed traffic, such as the rotorcraft and VLJs, it may still be of concern.

The hazards were evaluated and classified utilizing criteria in Table 14-1, and then likelihood was assessed using criteria in Table 14-2 based on subject matter expertise. The risk of each hazard was then assessed utilizing the risk matrix in Figure 14-8. The results of the risk assessment of the hazards are recorded in Appendix G.

14.3.6. Very Light Jets

The VLJ is a fairly conventional aircraft. The significant operational differences between the VLJ and other aircraft are that it is:

- Certified for single pilot passenger service,
- Readily accessible to a greater number of non-professional pilots,
- Significantly faster than other GA aircraft with which it will share airports and runways, and
- Sufficiently slower than commercial jet transports with which it will share both en route and terminal airspace.

VLJs will operate from both small, underutilized airports with excess runway capacity as well as from large airports. When operating from large airports VLJs will be able to utilize shorter runways not used by commercial and regional jet traffic. In addition, VLJs will be able to perform spiral descents and steep approaches.

The VLJ will encounter the same generic issues as the CESTOL in performing steep approaches and spiral descents (see CESTOL report and Figure 14-9 below). However, the VLJ has a lower wing loading (40.6 lb/sq. ft) and approach speed (~79 kts) than the CESTOL, and therefore better ability to perform the steep approaches.

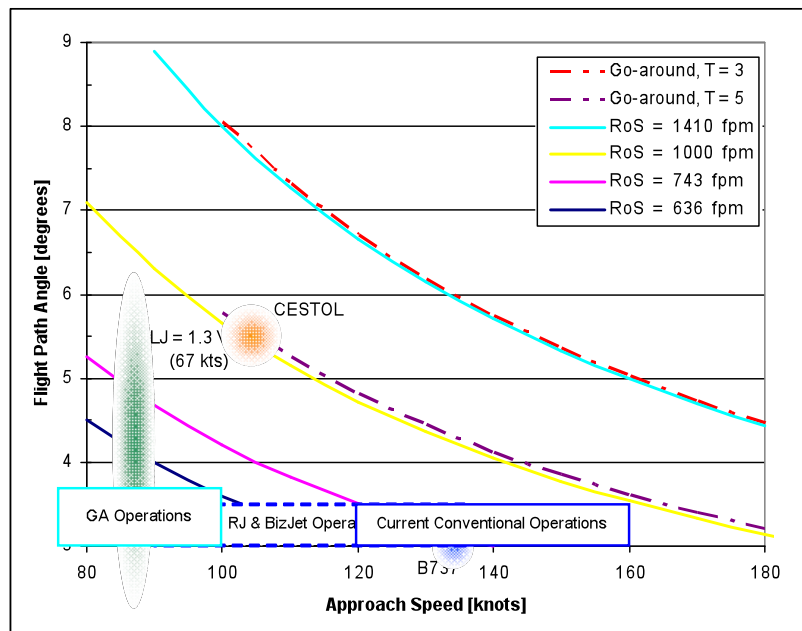


Figure 14-12. Flight path angle versus approach speed (adapted from J. Hileman by A. Hahn)

We have previously described the increased accident frequency of single-pilot operations relative to two-pilot operations and the historical accident frequency of non-professional pilots versus professional pilots. Some of the hazards associated with crew size and experience were also described. The risks associated with the potential increase in single-pilot operations and in non-professional pilot operations in these high-performance aircraft will likely be exacerbated by the performance differences between VLJs and other general aviation aircraft and between VLJs and commercial jet transports.

The hazards were evaluated and classified utilizing criteria in Table 14-1, and then likelihood was assessed using criteria in Table 14-2 based on subject matter expertise. The risk of each hazard was then assessed utilizing the risk matrix in Figure 14-8. The results of the risk assessment of the hazards are recorded in Appendix G.

14.3.7. UAS

The UAS is fully autonomous, with remote monitoring and the ability for a human pilot to intervene and remotely fly the aircraft, if needed. The human element of the UAS will monitor multiple aircraft and actively control an aircraft when necessary. The mission selected for analysis is mail and freight delivery from major distribution centers to local distribution centers. The principle operating scenario is freight forwarding from a freight operator's "spoke" airport to include the following ranges: 30-60 nm, 60-90 nm, 90-120 nm, and 120-150 nm. Due to the short distances traveled the expected maximum altitude planned would be 11,000 feet, servicing all the airports within the 150 nm radius. The number of aircraft monitored by a single individual is an area requiring further research. UASs will be operating from fairly small airports to small rural GA airports with low infrastructure. While operating into rural airports the UAS will utilize airspace with pilots with wide range of airmanship skills. The concern with operating in the environment is the pilots of lesser experience not being familiar with the UASs capabilities and limitations.

One possibility for ground control stations is the ability for a single pilot to control multiple vehicles. This feature is being actively pursued by the developers of military UASs. In this situation, new hazards arise from both an increased pilot workload and ensuring that the information presentation does not confuse the pilot about which aircraft is being controlled. Training specific to controlling multiple aircraft may be required.²²

Data link communications are of extreme importance with the operation of UASs. The concern comes with interference with communications link either unintentional or intentional means. If the control link is lost, where is the UAS going to go? If system disruptions are not being transmitted from the UAS due to an undetected communications link failure, intervention from the ground pilot could be lost. Also information such as position information from the UAS to other aircraft and ATC would not be transmitted to them if the UAS had a data link failure which could increase the risk of mid-air collision.

The hazards were evaluated and classified utilizing criteria in Table 14-1, and then likelihood was assessed using criteria in Table 14-2 based on subject matter expertise. The risk of each hazard was then assessed utilizing the risk matrix in Figure 14-8. The results of the risk assessment of the hazards are recorded in Appendix G.

14.3.8. SST

Although each new aircraft has its own unique stability and control issues, SSTs are not fundamentally different from conventional commercial jets. The SST's performance characteristics allow it to operate in supersonic (above Mach 1) flight régime, and to perform in the subsonic flight régime (approach environment). The safety concerns they highlight are mainly in the operational domain and are associated with self-separation in super-density arrival/departure (terminal) airspace, as well as en route separation, due to the speed differential between subsonic jets and SSTs operating at similar altitudes.

SSTs will operate supersonic while at cruise where it will be mixed with slower air traffic, then transition to subsonic flight for the terminal environment. The safety concerns SSTs exacerbate are mainly in the operational domain and are associated with self-separation in super-density arrival/departure (terminal) airspace as well as en route separation, due to the speed differential between subsonic jets and SSTs operating at similar altitudes.

Figure 14-13 depicts graphically the time or distance to impact. The bottom row shows the total closure rates in knots. The left hand side depicts time to impact in seconds. The colored lines depict distance in nautical miles (nm): blue = 5nm, red = 4nm, green = 3nm, and purple = 1nm. In the figure an SST and VLJ are converging head on with each other. The speed of sound at cruising altitude of most commercial jets is approximately 573 kts. The SST is cruising at 1.3 Mach (~750kts) and the VLJ is cruising at .5 Mach (~300kts). The total distance both aircraft are from each other is 3 nm. The closure rate (combined airspeed) is 1050 kts. The minimum reaction time to avoid a collision is 12.5 sec²⁴. This is represented by the red boxed "danger area".

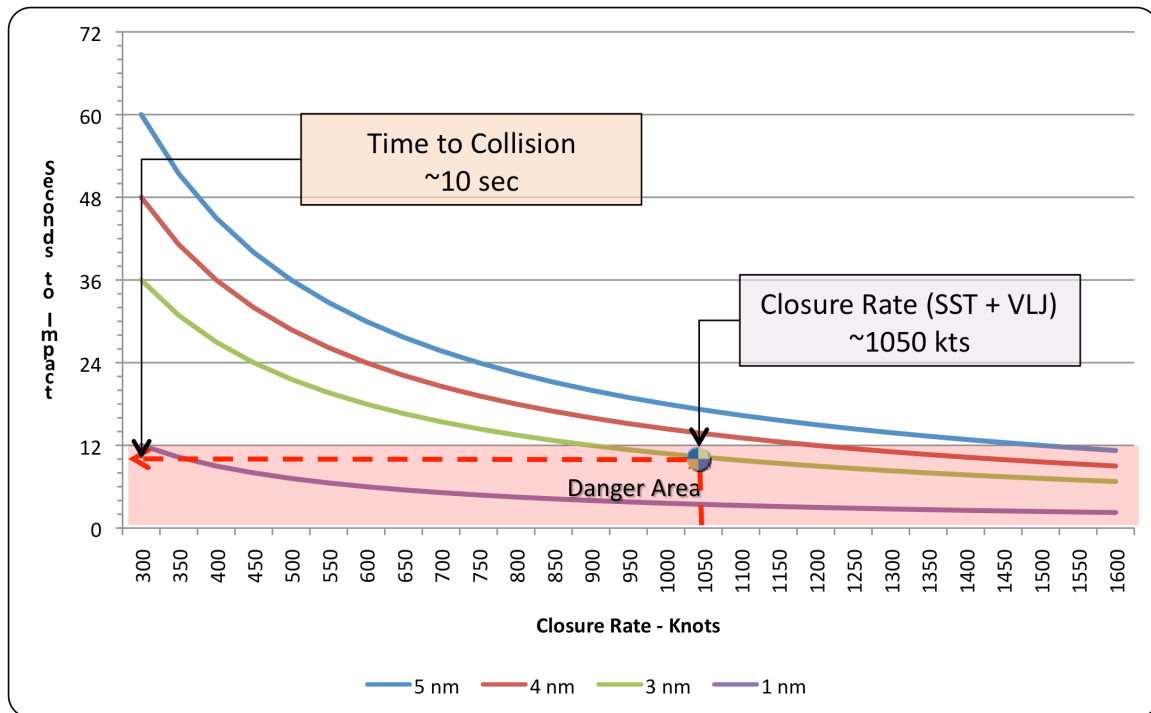


Figure 14-13. Time to collision (example).

The hazards were evaluated and classified utilizing criteria in Table 14-1, and then likelihood was assessed using criteria in Table 14-2 based on subject matter expertise. The risk of each hazard was then

assessed utilizing the risk matrix in Figure 14-8. The results of the risk assessment of the hazards are recorded in Appendix G. During the identification of hazards, this study looked at only hazards that would impact NextGen, that were unique to the particular vehicle study, and of greatest risk to the flying public. The low risk-hazards could be attributed to any conventional (legacy) and posed little risk to the public; therefore, low-risk items were not recorded in the initial risk assessment.

14.4. **Certification**

As NextGen concepts further blur the line between aircraft and Air Traffic Control (ATC) functions and responsibilities, it is envisioned that there will be greater symbiosis between the aircraft certification process and the development of ATC rules and procedures. This may result in the certification of a “vehicular package,” where the aircraft and the associated infrastructure needed to operate in a specific ATC environment are developed in parallel versus serially. Another equally important shift is to functional or “capabilities-based” certification, when greater design freedom is afforded to vehicle manufacturers regarding how specific safety-critical functionalities are incorporated into the system.

The goal of this section is to provide an overview of the envisioned aircraft certification safety management process by the year 2025. This document addresses the following three areas: Aircraft certification safety management process, new vehicle certification issues and avenues for future research as they relate to certification. The document is not intended to provide an in-depth analysis of the certification process.

14.4.1. New Vehicle Certification Issues

The dynamics of the National Airspace System (NAS) could be fundamentally changed with the introduction of new aircraft across the airframe performance spectrum. In the design of new vehicles, like any new product, there are always issues with respect to meeting and complying with certification standards. There are a wide range of issues concerning aircraft certification for each of the vehicle types listed below, but for this study only the vehicles in this NASA New Vehicle Integration NRA were examined and only within the context of each vehicle’s specific mission were their certification issues noted.

CESTOL

The gust margin poses a stall issue during approaches in gusty conditions. The CESTOL approach speed was designed to be 1.3 times the stall speed, which is the international requirement. In the CESTOL’s current configuration, its operating capability is more severely restricted by weather than other similarly sized aircraft.

The CESTOL exceeds recommended sink rate safety margin (1,000 fpm) while performing the steep approach (5.5 degrees). In the CESTOL’s current configuration, it restricts its landing capability to airports that utilize a steep approach of 5.5 degrees.

VLJ

The VLJ considered in this study is designed to be either a dual or single pilot aircraft. In the single-pilot configuration, a second pilot could be on the ground as an added safety measure to be utilized in cases of in-flight emergency and/or high workload during critical phases of flight (e.g. adverse weather,

equipment failure, medical situations). Certification decisions will have to be made on how much control or involvement the second pilot will be allowed and outlined in the certification standards. This would require the tasks to be performed by the second pilot be determined and when or under what circumstance the second pilot will become involved to assist the primary onboard.

Also what level of automation would be required to assist the primary onboard pilot in the efficient and safe operation of the VLJ? This would also have to take into account for the experience level of the pilot to determine the capabilities standards.

Another issue to consider in single pilot operations is with data link. With data link becoming a primary form of communication how much heads down time will be required to utilize this function. The heads down time could be reduced if a voice recognition and pre-canned responses to standard instructions.

With a significant number of VLJs being operated in and out of GA and non-towered airports and those mixing with less-advanced equipped aircraft, surface and airborne collision avoidance becomes an issue due to the speed disparity between GA aircraft and the VLJ.

The ability of the VLJ to perform spiral and steep approaches brings up the aspect of terrain and obstacle avoidance as well as low altitude operations issues. Standards will need to be developed which provide safety margins to avoid.

UAS

With respect to the ability of one UAS ground pilot to monitor/operate multiple UASs, what is the maximum number of UASs that one UAS pilot is able to monitor/operate? This becomes a problem when one or more of the UAS has an emergency or an off-nominal situation arises. The certification issue becomes “to what level of autonomy should the UAS have and also if there needs to be a backup ground pilot(s) to take over the other nominal operating UASs or in the case of multiple UAS emergencies having a UAS ground pilot for each troubled UAS.”

Another issue with the fully autonomous cargo UAS is its ability to safely avoid airborne hazards and during any phase of flight the ability to avoid other aircraft without querying or requiring assistance from ATC utilizing sense-and-avoid capabilities. This UAS will be operating in remote airfields with possibly low infrastructure capabilities where it will most likely encounter mixed equipage aircraft along with numerous pilots having wide ranging backgrounds and flying experience.

While operating on the airport surface, the autonomous UAS must have the ability to avoid ground hazards (i.e., fixed obstacles, other ground aircraft, and ground support equipment). The UAS also must be able to avoid airborne hazards while on the airport surface, such as avoiding a runway incursion.

In the absence of certification standards and regulations addressing UAS operations, an operator qualifications analysis should be performed to determine such standards, regulatory change requirements, future operations, and qualification requirements of the operator.

With UASs operating in population centers and possible threat of being used as a weapon of mass destruction, an analysis needs to be conducted to determine what security controls need to be developed for UAS operations.

SST

An issue with the SST is its ability to have adequate visibility out the forward flight deck windscreen. A lack of visibility restricts a pilot's ability to transition from instrument flight to visually identifying the runway environment for landing and also from maintaining visual separation from other aircraft.

The SST operated in the past as a civil transport, but was restricted from overland operation and was also waived from having to be equipped with a TCAS. Little has been accomplished in the development of TCAS for SST type aircraft. Also, the SST of the future will be operating en route with subsonic aircraft as well as in the high density arrival/departure traffic areas. This will require the supersonic aircraft to pass the subsonic aircraft both laterally and vertically. Research needs to be conducted to determine adequate safe passing distance for SST from other aircraft.

Areas for Further Research

The performance difference between VLJs and other general aviation aircraft and commercial jet transports and their associated risks posed by single-pilot operations by non-professional pilots should be examined regarding what the risks are and if there are any unintended consequences to this type of operation.

With the introduction of data link and other automated systems onboard these new complex vehicles operating in the NAS in NextGen during single-pilot operations, how much workload is placed on the pilot? If a virtual pilot is used to off-set some of the workload, what tasks should be allocated to the virtual pilot and what type of equipage would be needed to adequately perform the tasks assigned? An analysis needs to be conducted to ascertain the answers to these types of questions and to determine what unintended consequences might result from this type of operation.

The introduction of supersonic aircraft into the NAS in NextGen will introduce super and subsonic aircraft into the en-route and terminal airspace. This will require the supersonic aircraft to pass the subsonic aircraft both laterally and vertically. Research needs to be conducted to determine adequate safe-passing distance by SST and other aircraft.

As duties and responsibilities merge and change ownership with the implementation of NextGen, further study should be focused on the interaction of the OEMs, operators, and the FAA to determine the most efficient and effective process(es) to continue improving the aircraft certification process. This could include defining and developing architecture for determining capabilities required for operating safely in a particular operational environment based on the business case the operator would like to pursue.

It would be worthwhile to determine the policies and regulation changes that would be required to convert to a capabilities-based certification process. In addition, it is important to examine the development of a process of transitioning legacy aircraft into a continued airworthiness process based on a capabilities-based environment.

Given the absence of certification standards and regulations addressing UASs, operations, and operator qualifications, analyses should be performed to determine the standards, regulatory change requirements, future operations, and qualification requirements of the operator.

With UASs to be operating at low infrastructure airports, a safety assessment should be conducted to determine the risks associated with operations including taxiing, arriving, and departing lead by pilots with wide-ranging airmanship skills.

With UASs operating in population centers and the possible threat of them being used as a weapon of mass destruction, an analysis needs to be conducted to determine what security controls should be developed and instituted for UAS operations.

With the transition from the current system to NextGen being a significant change from modern operations, a more proactive safety management system with a database management process that focuses on accurately identifying precursors to potential accident is needed to ensure high degree of safety expected by the public. An analysis needs to be performed to identify hazards that may arise from unusual combinations of factors that may not individually present a significant hazard to enhance safety data collection and monitoring systems.

With currently safety database management systems containing enormous amounts of narrative data, rich with unknown information, there is a need for a way to extract and visualize information, link concepts, answer questions, and cluster similar data to identify hidden patterns. An analysis is needed to determine if natural language processing techniques would best be suited to text mining aviation safety data. If so, which techniques or combination of techniques would provide to most efficient and effective?

The aviation industry is changing to a more capability driven environment. OEMs are adopting a through-life support concept in which they are taking on responsibility of complete technical management of a fleet of aircraft, including maintenance, training support, spares logistics, and engineering management of the fleet for operators and operators owning a mixed manufacturer fleet makes the aircraft maintenance management system of an operator increasingly complex. A safety assessment is needed to identify hazards to assess risk, develop mitigation strategies, and monitor the incorporation of through-life support to study its impact on aviation maintenance safety.

With the introduction of new vehicles into the NAS in NextGen, operators will be transitioning legacy aircraft pilots to these vehicles. An analysis needs to be conducted on the impact of pilot workload when interacting with the new aircraft systems.

Research should be conducted to examine how equipage impacts provision of desired services by ATC to NAS stakeholders. The notion of best-equipped, best-served is ambiguous because it does not clearly delineate the various services that stakeholders may be interested in. Hence, more effort may need to be invested in determining the direct impact that equipage has on the range of services of interest to all users of the NAS. In doing so, tradeoffs can be clearly identified and stakeholders may be able to better understand the benefits/costs associated with equipage as it relates to services such as efficiency, accessibility etc.

Future research should focus on the impact that crew vehicles of various types have on a controllers' ability to provide safe and expeditious service during routine/non-routine operations. Many new crew vehicles require special procedures such as Spiral approaches for VLJ/CESTOL aircraft. In such instances, controllers may have to alter the way in which traffic is managed to account for aircraft that demonstrate performance characteristics that varying considerably from the 'norm' and dictate the usage

of specialized procedures. An assessment of how such alteration impacts controller performance is desirable, as is the development of policies/procedures that mitigate the potential negative impact of having to accommodate aircraft that require varying handling procedures.

One possibility for UAS ground control stations is the ability for a single virtual pilot to control multiple vehicles. An analysis needs to be conducted into new hazards which could arise from both an increased pilot workload and ensure that the information presentation does not confuse the pilot about which aircraft is being controlled.

The hazards identified in the safety study were grouped into five areas (performance, automation, procedures, environment, and training) and through the safety risk assessment a number of hazards were determined to be high risk. These high-risk hazards might be mitigated through several different strategies, but with having limited information on the new vehicles, further research needs to be conducted as the vehicle concepts mature to determine which strategy or strategies could best be employed to mitigate those risks.

During spiral approaches, given the turning radius needed to keep the operation 'tight,' a higher level of attention may be required by the controller who is sequencing traffic. This leads to two separate issues: 1) which controller has responsibility for this, terminal or tower, and how does it impact his/her ability to manage other traffic in the area given the scanning distance associated with the operation. 2) What is the impact of sustained normal and abnormal operations in such instances on controller workload?

14.5. **Safety Glossary**

Term	Definition
Air Navigation Service Provider (ANSP)	An organization responsible for and authorized to provide air traffic management (ATM) services; communications, navigation, and surveillance (CNS) services; meteorological services for air navigation; and aeronautical information services. ¹
Air Traffic Management (ATM)	The dynamic, integrated management of air traffic and airspace safely, economically, and efficiently through the provision of facilities and seamless services in collaboration with all parties. ¹
Aircraft accident	An occurrence associated with the operation of an aircraft which takes place between the time any person boards the aircraft with the intention of flight and all such persons have disembarked, and in which any person suffers death or serious injury, or in which the aircraft receives substantial damage. ²⁸
Automatic	The execution of a predefined process without intervention. ⁴
Autonomous	Not controlled by others or outside forces, Independent judgment. ⁴
Autorotation	The condition of the helicopter flight during which the main rotor is being driven by aerodynamic forces with no power from the engines. ²⁹
CESTOL	Aircraft designed to takeoff in a relatively short distance, climb quickly, cruise optimally, and land in a relatively short distance
Data link	A term referring to all links between the aircraft and the control station. It includes the command, status, communications and payload links. ⁴
Fatal Injury	Any injury which results in death within 30 days of the accident. ²⁸
Flight Crew	The individual or group of individuals responsible for the control of an individual aircraft while it is moving on the surface or while airborne. ¹
Flight Management System	A system that manages aircraft's performance and route navigation. ³⁰

Term	Definition
Function	The action or actions which an item is designed to perform. ⁴
Hazard	Any existing or potential condition that can lead to injury, illness, or death of a person; damage to or loss of a system, equipment or property; or damage to the environment. A hazard is a condition that is a prerequisite to an accident or incident. (JPDO Safety Working Group)
Spiral Descent	An approach where 360 degree turns are accomplished while descended to remain within the airport boundary until landing.
Spiral Departure	A departure in which 360 degree turns are accomplished while climbing to remain within the airport boundary until reaching a specified altitude.
Human Factors	The discipline concerned with the understanding of interactions among humans and other elements of a system. It applies theory, principles, data, and other scientific methods to system design to optimize human well-being and overall system performance. ¹
Incident	An occurrence other than an accident, associated with the operation of an aircraft, which affects or could affect the safety of operations. ²⁸
Inflight termination	Refers to systems, procedures, or functions for immediate ending a flight. ⁴
Known Hazards	Historical hazards, hazards present in the current system, which may be exacerbated by the integration of the new vehicle into NextGen.
Metropolplex	A group of two or more adjacent airports whose arrival and departure operations are highly interdependent. ¹
Minor Injury	Any injury that is neither fatal nor serious.
Near Mid-air Collision	When the separation of one aircraft from another is less than 500 feet.
New Hazards	Hazards to which the new vehicles are exposed, or which their operations introduce into NextGen.
Off-nominal Condition	Any condition or situation that deviates from the normal state of operation(s) of a system or systems. (e.g. inflight emergency)
Operator	Any person who causes or authorizes the operation of an aircraft, such as the owner, lessee, or bailee of an aircraft. ²⁸

Term	Definition
Overshoot	When the chosen flight path is flown above the required glide path to where the vehicle lands beyond its intended point of touch down.
Required Navigation Performance	A statement of the navigation performance accuracy necessary for operation within a defined airspace. RNP Operations introduce the requirement for on-board navigational performance monitoring and alerting. ¹
Runway Excursion	Any aircraft having a loss of directional control either on takeoff or landing which exits a runway other than a designated exit point (e.g. pilots conducting other than full length operations from wrong intersection or overshoot an approach).
Runway Incursion	Any occurrence at an airport involving the incorrect presence of an aircraft, vehicle or person on the protected area of a surface designated for the landing and take-off of aircraft. ³¹
Safety Assurance	The independent oversight function that tests, evaluates, and certifies, as necessary, products and processes to ensure that they are safe for the public and stakeholders. ¹
Safety Management System (SMS)	The process that provides a systematic method for managing safety. The four components of an SMS are policy, architecture, assurance, and safety promotion. ¹
See-by-wire system	A system providing for variable gain in both visible and nonvisible spectra (i.e., radar and infrared), enhanced visibility and safety at night and in adverse weather. ¹⁵
Sense-and-Avoid (SAA)	The ability of onboard UAS enabling technology to determine when other aircraft are operating within certain vertical and horizontal parameters of the UAS and then autonomously maneuvers the UAS to avoid any conflict or provides the UAS flight controller with data that is used to determine whether or not necessary for the flight controller to maneuver the UAS to avoid conflict, a mechanical equivalent to “see-and-avoid”. ³²
Shared Situational Awareness (SSA)	The sharing of information among the processes and applications that constitute the information services function to the stakeholders in the system. ¹
Serious Injury	Any injury which: (1) Requires hospitalization for more than 48 hours, commencing within 7 days from the date of the injury was received; (2) results in a fracture of any bone (except simple fractures of fingers, toes, or nose); (3) causes severe hemorrhages, nerve, muscle, or tendon damage; (4) involves any internal organ; or (5) involves second- or third-degree burns, or any burns affecting more than 5 percent of the body surface. ²⁸

Term	Definition
Situational Awareness	Refers to a service provider or operator's ability to identify, process, and comprehend important information about what is happening with regard to the operation. Airborne traffic situational awareness is an aspect of overall situational awareness for the flight crew of an aircraft operating in proximity to other aircraft. ¹
Spiral Approach	An approach where 360 degree turns are accomplished while descended to remain within the airport boundary until landing.
Spiral Departure	A departure in which 360 degree turns are accomplished while climbing to remain within the airport boundary until reaching a specified altitude.
Steep Descent	Any descent which is greater than 3.0 degrees (e.g. 5.5 degrees).
Tailstrike	An approach having a high pitch angle could result in the aircraft's to contact the runway prior to the main landing gear on landing or if the nose is overrated during takeoff.
Undershoot	When the chosen flight path is flown below the required glide path to where the vehicle lands short of its intended point of touch down. This results in landing short of the runway
Unmanned Aircraft System	A pilotless aircraft is flown without a pilot-in-command onboard and is either remotely or fully controlled from another place (ground, another aircraft, space) or programmed and fully autonomous. The UAS includes the pilotless vehicle, control system, and operator. ¹
Unstabilized Approach	An approach that is not stable before reaching 1,000 feet above airport elevation in IMC or 500 feet above airport elevation in VMC.
Vortex Ring State (VRS)	Phenomenon wherein the combination of low forward speed and high rate of descent causes the upward flow of air around a rotor to approach the same velocity as the downwash produced by the rotor. When this happens, the rotor loses lift, and addition of power makes the lift loss worse. ²⁰

14.6. **References**

1. Federal Aviation Administration. Concept of Operations. *Next Generation Air Transportation System*. Washington, DC : Joint Planning and Development office, 2007. Version 2.0.
2. FAA Air Traffic Organization. Air Traffic Safety Management System Manual. *FAA*. [Online] May 2008. [Cited: June 10, 2009.] http://www.faa.gov/airports_airtraffic/air_traffic/publications/media/ATOSMSManualVersion2-1_05-27-08_Final.pdf. Version 2.1.
3. National Business Aviation Association (NBAA). Very Light Jet Training Guidelines. *National Business Aviation Association*. [Online] National Business Aviation Association, July 22, 2009. [Cited: July 22, 2009.] <http://www.nbaa.org/ops/safety/vlj/>.
4. RTCA. Operational Services and Environment Description. s.l. : RTCA, DRAFT. SC-203.
5. United States Government Accountability Office. Unmanned Aircraft Systems: Federal Actions Needed to Ensure Safety and Expand Their Potential Uses within the National Airspace System. Washington : United States Government Accountability Office, 2008. GAO-08-511.
6. Cessna. Caravan Family. *Cessna*. [Online] Cessna, March 05, 2009. [Cited: March 05, 2009.] <http://www.cessna.com/caravan.html>.
7. *LCTR2 Design Study and Aeromechanics Analyses*. Cecil W. Acree, Jr. s.l. : NASA Ames Research Center, 2008.
8. Boeing Commercial Airplanes. *Statistical Summary of Commercial Jet Airplane Accidents Worldwide Operations 1959 - 2008*. Seattle : Aviation Safety Boeing Commercial Airplanes, 2009.
9. Federal Aviation Administration. Loupe One Departure. *National Aeronautical Charting Office*. [Online] July 22, 2009. [Cited: July 22, 2009.] <http://naco.faa.gov/d-tpp/0908/00693LOUPE.PDF>.
10. Loupe One Departure (Cont.). *National Aeronautical Charting Office*. [Online] July 22, 2009. [Cited: July 22, 2009.] http://naco.faa.gov/d-tpp/0908/00693LOUPE_C.PDF.
11. Janic, Dr. Milan. Eastern Region - 31st Annual Conference Presentations. *Federal Aviation Administration Airports*. [Online] July 22, 2009. [Cited: July 22, 2009.] http://www.faa.gov/airports/eastern/airports_news_events/hershey/media_30/Innovative%20Procedures%20for%20Runway%20Capacity.ppt.
12. Whalen, Edward A., Broeren, Andy P. and Bragg, Michael. *Characteristics of Runback Ice Accretions and Their Aerodynamic Effects*. Urbana : Federal Aviation Administration, 2007. DOT/FAA/AR-07/16.
13. Hayhurst, Kelly J., et al. Preliminary Considerations for Classifying Hazards of Unmanned Aircraft Systems. Hampton, VA : NASA, 2007.
14. DeGarmo, Matthew T. Issues Concerning Integration of Unmanned Aerial Vehicles in Civil Airspace. McLean, Virginia : MITRE, 2004. MP 04W0000323.

15. Robins, A. Warner, et al. *Concept Development of a Mach 3.0 High-Speed Civil Transport*. Hampton, VA : NASA, 1988. NASA TM 4058.
16. Domack, Christopher S., et al. *Concept Development of a Mach 4 High-Speed Civil Transport*. Hampton, VA : NASA, 1990. NASA TM 4223.
17. Douglas Aircraft Company. *Study of High-Speed Civil Transports*. Langley, VA : NASA, 1989. NASA CR 4235.
18. Apogee Aeronautics Corporation. *USRA High Speed Civil Transport*. Pomona, CA : California State Polytechnic University, 2005. NASA-CR-192041.
19. Boeing Commercial Airplane. *High-Speed Civil Transport Study*. Langley, VA : NASA, 1989. NASA CR 4233.
20. Dailey, John R., et al. *Report of the Panel to Review the V-22 Program*. Arlington : Department of Defense, 2001.
21. Hange, Craig and Eckenrod, Dennis. *Assessment of a C-17 Flight Test of an ESTOL Transport Landing Approaching for Operational Viability, Pilot Perceptions and Workload, and Passenger Ride Acceptance*. s.l. : American Institute of Aeronautics and Astronautics.
22. Hayhurst, Kelly J., et al. *Unmanned Aircraft Hazards and Their Implications for Regulation*. s.l. : Digital Avionic Systems Conference, 2006.
24. Federal Aviation Administration. *Pilots' Role In Collision Avoidance. Advisory Circular*. Washington : Federal Aviation Administration, 1983. AC 90-48C.
25. National Academy of Sciences. *Improving the Continued Airworthiness of Civil Aircraft: A Strategy for the FAA's Aircraft Certification Service*. Washington : National Academy Press, 1998. ISBN: 0-309-06185-7.
26. Ward, Yvonne and Graves, Andrew. *Through-Life Management: The Provision of Integrated Customer Solutions By Aerospace Manufacturers*. Bath, United Kingdom : University of Bath School of Management, 2005.
27. Webb, Luke and Bil, Cees. *Performance-Based Through Life Support: A model for the Future*. Melbourne, Australia : American Institute of Aeronautics and Astronautics, 2009. AIAA 2009-1640.
28. National Transportation Safety Board. *Title 49 Code of Federal Regulation Part 830*. Washington, DC : National Transportation Safety Board, 2008.
29. Montgomery, John R. *Sikorsky Helicopter Flight Theory for Pilots and Mechanics*. s.l. : United technologies Sikorsky Aircraft, 1964.
30. Brown, Gary V. *Encyclopedia of Technical Aviation*. New York, Chicago, San Francisco, Lisbon, London, Madrid, Mexico City, Milan, New Delhi, San Juan, Seoul, Singapore, Sydney, Toronto : McGraw-Hill, 2003. 0-07-140213-6.
31. Federal Aviation Administration. FAA Order JO 7110.65S. *Air Traffic Control*. Washington, DC : AJR-0 , 2008.

32. American Institute of Aeronautics and Astronautics. *Recommended Practice Terminology for Unmanned Aerial Vehicles and Remotely Operated Aircraft*. Reston : American Institute of Aeronautics and Astronautics, 2004. AIAA R-103-2004.

15. Avionics

Significant avionics upgrades are necessary to handle advanced vehicle operations in the NextGen Air Transportation System. In this section we identify the on-board technology for manned and unmanned aircraft that are anticipated to be available for our advanced vehicles around the 2018 to 2025 timeframe during which our advanced vehicles will first be introduced into the NAS. We describe the services and infrastructure that will be available in the NextGen Air Transportation System (ATS) and identify the airborne technology enhancements that can mitigate many of the potential hazards generated by the utilization of advanced vehicle performance capabilities on missions within the future NextGen ATS. Similar to the NextGen avionics roadmap developed by the JPDO Aircraft Working Group, we map the required hazard-mitigation avionics against the operational capabilities listed in the NextGen Implementation plan.

The avionics roadmaps defined here for our five advanced vehicles focus on the avionics required to avoid or mitigate the potential hazards that may occur when these advanced vehicles enter future NextGen airspace. Additional avionics capabilities are listed that will enable our advanced vehicles to take advantage of the NextGen services and benefits allotted to equipped aircraft. For this avionics roadmap, we assume an initial operational capability (IOC) of 2025 for our advanced vehicles.

Unique aircraft performance characteristics, combined with the specific mission defined for these advanced vehicles, enable a wide range of airspace users and stakeholders to access a more efficient NextGen Air Transportation System (ATS). Technology advances in ground and airborne systems enable more efficient use of the shared airspace and ground based resources.

A wide range of avionics capabilities is needed to support flight operations across various airspace and airports in the 2025-2040 timeframe. For instance, as shown in Table 15-1 below, the CESTOL, LCTR and SST operate missions in the busy metroplexes across our nation while the missions defined for the VLJ and UAS result in flight operations into untowered or low infrastructure airports.

High glide slope climb or descent operations and spiral approach or departure capabilities of the CESTOL and VLJ vehicles enable the use of shorter runways across our NAS. Avionics equipage onboard our advanced vehicles are needed to enable the vehicles to take advantage of their unique capabilities, and avoid the hazards that this capabilities can potentially create (e.g., wake turbulence, loss of situation awareness...). As each aircraft supports different aspects of our future NAS, the different pieces of an overall avionics roadmap for flight operations into the NextGen airspace of the 2025-2040 timeframe were put into place.

Table 15-1 NextGen ATS utilization due to unique vehicle missions & capabilities

	CESTOL	VLJ	UAS	LCTR	SST
Airports					
Low infrastructure / untowered	✓	✓	✓		
High density / metroplex	✓			✓	✓
Landing site					
Crossing runways	✓	✓			✓
Closely spaced parallel					

runways					
Short runways	✓	✓	✓		
Helipad / Vertiport					
Airspace					
Controlled	✓	✓	✓	✓	✓
Uncontrolled		✓	✓		
Oceanic					✓
Piloted					
Onboard	✓	✓		✓	✓
Remote backup		✓	✓		
Performance					
Supersonic					✓
Subsonic	✓	✓	✓	✓	✓
VTOL				✓	
STOL	✓	✓			

15.1. **Avionics to gain access to NextGen Services**

Each vehicle will be equipped with avionics systems or upgrades to gain the benefits granted to equipped aircraft operating in the NextGen ATS.

15.1.1. NextGen ATS assumptions for 2025-2040

The airspace and infrastructure assumptions for the NextGen ATM environment of 2025 through 2040 impact vehicle operations within the mission we have identified. Key enablers for the NextGen ATS include Performance Based Navigation, Trajectory-Based Operations (TBO), a shift from tactical to strategic Separation Management, Net-centric Operations and digital data communication (Data Comm).

15.1.2. Performance Based Navigation

The NextGen ATS will be based on 4D RNAV flight path management in core areas and RNP RNAV in non-core areas. RNP and flexible, accurate RNAV flight paths will be used for terminal area, approach and missed approach procedures. RNAV will be used to address numerous operational conditions such as parallel runways operations, adjacent runways, crossing runways, nearby runways at adjacent airports, and terrain or noise limited runway operations. This will include emission and noise reducing operations such as continuous descent arrivals (or profile descents). In the ATM system for 2025 and beyond, we will see the transition from today's flight plans to RNP RNAV trajectory-based flight plans negotiated with ATC. New procedures that take advantage of the new vehicle performance and avionics capabilities will be developed to enhance traffic integration of the advanced vehicle into the terminal environment. Optimal profile descents (i.e., continuous descents approaches) will help alleviate fuel costs and enhance the advanced vehicle business viability.

15.1.3. Trajectory-based Operations (TBO)

4-D navigation and control will allow properly equipped aircraft to file 4-D flight plans and integrate seamlessly into the NAS. Aircraft that fly in trajectory-based airspace will navigate along 3D or 4D (position, altitude and time) specified trajectory, within a time tolerance along a series of trajectory waypoints. Negotiation of user-preferred trajectories will optimize fleet operations, minimize fuel usage

and emissions, and increase throughput at the nation's busiest airports.

15.1.4. Separation Management

Alternate separation methods will be in place with separation responsibility delegated to the aircraft for specific situations. Merging and spacing operations, In Trail Spacing and passing, and separation flight path management will be normal operating procedures for aircraft flying in the NAS. ADS-B OUT for fleet management, procedure compliance, and surveillance services as well as ADS-B IN for separation, spacing, merging, surface operations will be in place. Minimum separation standards may be reduced to increase system capacity. Airborne separation and delegation procedures and technologies and adherence to 4D trajectories will provide the means by which the advanced vehicles can safely separate themselves from other aircraft.

15.1.5. Net-Centric Operations and the Shared System Wide Information Management System (SWIM)

Our advanced vehicles will be consumers and providers of data stored in SWIM. SWIM will be the centralized system for trajectory management, weather data, airspace restrictions, weather hazards and information, and real-time obstacle data. (e.g., balloons, sky divers, etc). SWIM facilitates the integration of the advanced vehicles into the NAS by sharing the intended trajectory and current position of the advanced vehicle with other airspace users. SWIM will also integrate databases, both storing data and providing a link to other stored data such as wind, temperature or other data gathered during a vehicles' ascent and descent. Convective weather forecasts and reports stored in SWIM can also be accessed by the aircraft or Airline Operating Center (AOC) for planning and rerouting purposes. SWIM will facilitate flight operations near military, restricted, or other hazardous airspace by providing aircraft with dynamic updates on the number and size of restricted, sensitive (e.g., noise sensitive areas) or "no fly" zones sensitive locations.

15.1.6. Data Communication

Data communications in 2025 will primarily be conducted via datalink with voice communication largely limited to special advisories and emergency situations. Data communication will transition from a voice based ATC communication system to a data driven system integrated with automation in support of NextGen. Communications between the flight crew of our advanced vehicles and ATC will be dominated by electronic data exchanges which require operator acknowledgement and approval prior to execution. These trajectory clearances will be automatically fed into the onboard flight management system. Besides shared data exchange with SWIM, the on-board communications technology will be utilized for flight trajectory negotiations, data exchange for distributed decision making and digital audio/video transmissions.

Roadmap

Future Comm Study: Communication Evolution Overview

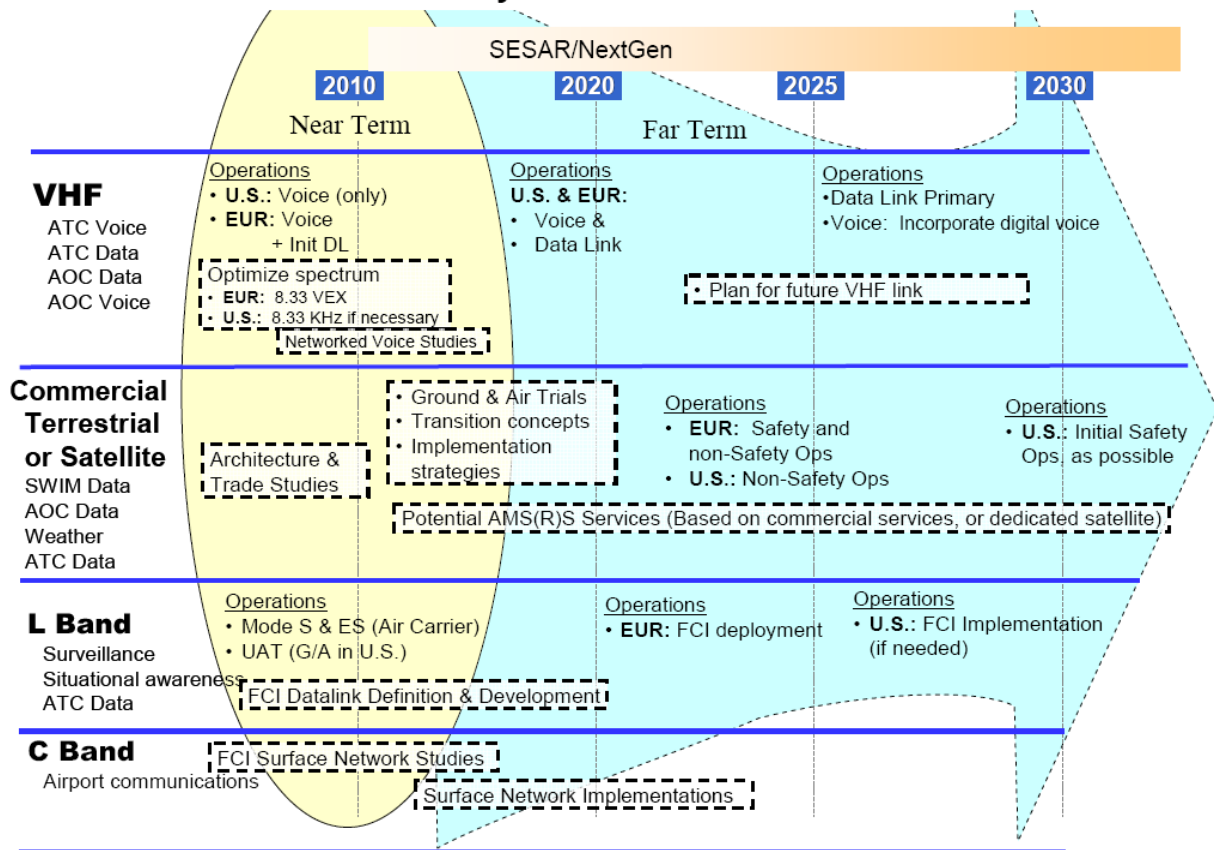


Figure 15-1 Future communication study – AP17 Final Conclusions and Recommendations

As we incrementally move to a NextGen ATS, the following advances in DataComm will be made:

DataComm Segment 1 (~2012-2017) will be similar to the EU DataComm Link2000+ program.

Applications/services expected to be supported include:

- ATN CPDLC (including DCL), ADS-C, and Data Link Operational Terminal Information Service (D-OTIS^{cxviii})
- FANS CPDLC, ADS-C
- ARINC 623 DCL and Data Link Automatic Terminal Information Service (D-ATIS)

Initial TBO and basis ASAS operations are introduced in enroute and the terminal airspace.

DataComm Segment 2 (2017-2022) will see the introduction of Datalink security. By 2017-2022, Performance based airspace rules will be in effect and all aircraft, including UA, flying in performance based airspace will be data communications equipped. Intent data from aircraft enables conformance management of negotiated 4D trajectories. SWIM will become available in this time segment.

The FAA recognizes that datalink security is a key technology enabler for advanced datalink-enabled applications/services, particularly Trajectory-based Operations. In order to accelerate Data comm. security, an evolutionary introduction of datalink security capability is planned for by the FAA with an early, phased introduction of security in Segment 1 so that security is not on the critical path for a successful Segment 2.

By 2022-2027, NextGen Trajectory Based Operations will be in place and Performance based airspace expands to all domains (but not necessarily all airspace). Performance based airspace rules will be in effect and all aircraft in performance based airspace will be data communications equipped. Data will be the required means of communication. (FAA, 2008).

Existing avionics equipment will need to be augmented and additional functionality must be installed on our advanced vehicles to gain access to the “best equipped, best served” capabilities and services provided by NextGen. For example, the FMS will need to be enhanced in several areas. To analyze, negotiate and execute user preferred trajectories, legacy FMS need to be enhanced with functionality to enable dynamic 4D flight planning & negotiations, Time Of Arrival Control (TOAC) in taxi, climb, cruise and descent, graphical flight planning and high integrity VNAV.

To support reduced emissions flights, FMS need to be able to predict, compute and execute enhanced CDA's, reduced noise and emissions cost index flights and continuous climbing cruise or unrestricted climbs. The future FMS will be enhanced with additional time-based trajectory clearance uplinks and trajectory intent data downlinks or broadcasts. To enhance the accuracy of the predicted trajectory (intent), the FMS will need to be modified to store and utilize data gathered from onboard sensors/radar and external weather sources (e.g., 4D weather cube). A move towards grid based weather modeling and probabilistic weather depiction may lead to a more detailed representation of weather in the FMS. Separation Management functionality will require a tighter integration with the surveillance and collision avoidance systems (i.e., Airborne Separation Assurance Surveillance (ASAS) functionality) to support situation awareness and altering functions, or delegated separation maneuvers such as merging and spacing with optimal profile descents, or self separation for complex maneuvers in the terminal area.

15.2. ***Safety challenges and hazards***

Differences between fixed-wing aircraft and helicopters, manned or unmanned vehicles, supersonic or subsonic transports are associated with the specific missions and operations executed by our advanced vehicles. Depending on how these operations and missions are executed, they may drive certain hazard events. Safety hazards due to the unique maneuvering capabilities and missions executed by our advanced vehicles must be mitigated for safe aircraft operations.

15.3. ***Hazards to be mitigated by avionics***

No vehicle will be immune to the hazards caused by wake vortices, convective weather, or low altitude operations. Additional hazards that each advanced vehicle could potentially be exposed to include loss of situation awareness, loss of flight path performance, and unstablized approaches. The hazards associated with operations from low infrastructure airports, or high density airports depended on the missions that the vehicles were chosen to.

Table 15-2. Advanced vehicles and the hazards they are especially susceptible to

Hazardous Conditions		CESTOL	VLJ	UAS	LCTR	SST
1	Unstabilized Approach	✓	✓	✓	✓	
2	Loss of Flight Path Performance	✓		✓	✓	✓
3	Convective Weather High bank angle, steep approaches, spirals	✓	✓	✓	✓	
4	Loss of Separation Minima (Airborne) <i>Low infrastructure or uncontrolled airports</i> <i>High density airports</i> <i>Unpiloted vehicle</i>	✓	✓	✓	✓	✓
5	Loss of Separation Minima (Surface) <i>High density airports</i>	✓				✓
6	Loss of command or control			✓		
7	Wake turbulence	✓	✓	✓	✓	✓
8	Loss of Situation Awareness (Manned AC) <i>Cockpit windscreen view restrictions</i> <i>Pilot workload</i>	✓	✓		✓	✓
9	Loss of Situation Awareness (Unmanned AC) <i>Loss of situation awareness datalink</i>			✓		

15.3.1. Unstabilized approach

Unstable approaches significantly increase the risk of runway excursions, runway undershoots or overshoots or tail strikes. An unstabilized approach can also lead to impact with ground objects, terrain or airspace infringement resulting in possible damage to the aircraft or injury to passengers or crew. Runways equipped with ILS precision approach instrumentation and wind anemometers add ‘Precision’ to the Non Precision Approach. Non-precision approaches into low infrastructure airports increase the likelihood of a safety incident due to unstabilized approach.

15.3.2. Loss of flight path / navigation performance

Loss of flight path performance during low-light-level or instrument condition could potentially result in a collision hazard with other aircraft on adjacent flight paths if the advanced vehicle deviates from its assigned flight path. There is an increased risk of airspace violations and mid-air collisions when executing low RNP (e.g., 0.1) or spiral approaches in close proximity to other aircraft or terrain at a high density airport.

15.3.3. Convective weather

Severe weather is a factor in about one-third of all aircraft accidents, turbulence is the leading cause of injury to passengers and crew members, and 40 percent of flight delays are caused by bad weather. Severe weather not only increases the probability of icing, it also impacts the flight safety of aircraft by reduction in visibility, increases in wind, windshear, turbulence and the hazards due to thunderstorms (gusts, downbursts...) or thunderstorm avoidance (e.g., rerouting). Undetected encounters with adverse environmental conditions can lead to aircraft operating outside their performance envelope resulting in possible near mid-air, or mid-air collision with other aircraft, terrain or objects. All aircraft are

susceptible to convective weather. However, aircraft operating at low altitudes, at slow approach speeds, high bank angles or without the benefits of ATC services will be especially susceptible to severe weather.

15.3.4. Loss of separation minima

Failure of the pilot to maintain spacing and adhere to separation minima in high density terminal airspace could result in overtaking slower aircraft or be overtaken by faster aircraft which could result in a near mid-air, or mid-air collision. For instance, failure of the SST to transition between supersonic and subsonic speeds during the approach transition could result in the aircraft exceeding the separation minimums if the speed is too fast which could cause conflict with other aircraft. Lack of infrastructure support on the ground at regional, rural, or non-towered airports contribute to separation hazards for advanced vehicle flight operations. Non-precision approaches, the absence of surface radar, weather data, and possibly ATC services, are key contributors to potentially higher incidents of these accidents.

15.3.5. Loss of command or control

Total loss, degraded performance, or unauthorized access to the command and control data link might cause the Unmanned Aircraft (UA) to make an unpredictable maneuver with the remote pilot unable to control the UA, resulting in possible near mid-air or mid-air collision with other aircraft, terrain or objects.

15.3.6. Wake turbulence

Failure to ensure appropriate separation behind aircraft that generate significant wake turbulence could result in possible loss of control. This might result in possible near mid-air, or mid-collision with other aircraft, terrain or objects. This could ultimately result in loss of life or damage to property on the surface.

Aircraft taking off and landings at low speeds and high angle of attack, or in STOL or VTOL mode must be very cognitive of the wake vortices they generate as well as the vortices generated by the aircraft surrounding them, especially when operating at high density airports or on parallel or crossing runways.

15.3.7. Loss of Situation Awareness – Manned aircraft

Human factors issues (increased pilot reliance on automation, situation awareness) caused by higher glideslope, steeper sink rate, earlier go-around decision points, spiral operations and recovery during emergency situations must be mitigated for our advanced vehicles. Pilots succumbing to information overload in the terminal environment increase their chances of losing positional awareness and could increase the possibility of becoming involved in a near mid-air collisions or contact with other objects or terrain.

Collision hazards also exist due to the steep, rapid climb-out capability of the VLJ and CESTOL aircraft on departure, or steep descent on approach when wing configuration or cockpit windscreen view restrictions could result in a near mid-air or mid-air collision. Windscreen view restrictions also exist for the SST. A fixed wing SST will require this advanced vehicle to land at a high angle of attack (hence less visibility) to create a higher lift since the wing is designed for subsonic cruise and is not as efficient in subsonic flights. For a swing-wing configuration, the SST design requires the addition of a boom at the nose of the aircraft which also reduces the out-of-the-window visibility for the SST flight crew. LCTR

VTOL operations restrict the pilot's visibility of the airspace or terrain directly above or below this advanced vehicle.

15.3.8. Loss of Situation Awareness – Unmanned aircraft

The loss or degradation of the situation awareness datalink between the unmanned aircraft and the UAS ground pilot will result in the loss of situation awareness by the ground pilot. For a fully autonomous UA, near mid-air or mid-air collision with other aircraft, terrain or objects can result due to loss of the situation awareness datalink, especially when combined with unpredictable UA maneuvers or off-nominal situations.

15.4. *Avionics for Hazard Mitigation*

On-board avionics will be part of the solution to mitigate the hazards associated with advanced vehicle operations. Airspace procedures, pilot and controller training and ground-based technology will contribute other essential parts of the hazard mitigation strategy. The avionics critical to safe advanced vehicle operations must aid the pilot to maintain situation awareness during spiral operations, avoid terrain and airspace infringements, facilitate surface operations during STOL operations, avoid wake vortex and hazardous weather conditions and ensure highly accurate climb and descent profiles during simultaneous approach and departure operations.

Our advanced vehicle take off and landing capabilities, autonomous or supersonic flight operations and new operating procedures at busiest airports will stress various concepts developed for NextGen, including controlled time of arrival and delegated separation. For instance, spiral or steep approaches and departures will require self-separation operations in the terminal area. Existing avionics equipment will need to be augmented and additional functionality must be installed on our advanced vehicles to enable their unique performance capabilities in the NextGen ATS. For example, current Traffic Collision Avoidance System (TCAS) functionality will have to be reconfigured as it is insufficient to handle closure rates of supersonic flights or spiral approaches in the proximity of standard approaches. As the roadmap shown below indicates, a significant number of avionics upgrades will be necessary to handle advanced vehicle operations in our future enroute and terminal environment.

15.5. *Advanced Vehicles Avionics Roadmap*

We have mapped the safety hazards identified for our advanced vehicles as well as the onboard avionics that can be used to mitigate these hazards against the operational capabilities defined in the NextGen Implementation Plan. The NextGen Implementation Plan has categorized the aircrafts-specific operational capabilities in terms of the following categories, or capability groups:

- Safety Enhancements
- Trajectory-Based Operations – Published Routes/Procedures
- Trajectory-Based Operations – Negotiated Routes
- Aircraft Separation
- Low-visibility Approach/Departure/Taxi
- ATM Efficiencies

The NextGen Implementation Plan also identifies unique safety-related technologies, such as collision avoidance, terrain awareness, and alerting for higher density and closer proximity operations. Similar to the operational capability descriptions used in the NextGen Implementation Plan, the required avionics functionality needed for safe aircraft operations for our advanced vehicles are described in terms of the operational capabilities within the above capability groups/categories.

The advanced vehicle avionics roadmap shown below in Table 15-3 includes the estimated timeframe for the availability of the onboard technology. In line with the timeframes used in the NextGen implementation plan and the Aircraft roadmap, near term capabilities are expected to be available by the end of 2011, mid-term capabilities are expected between 2012 and 2018, while far-term capabilities are from 2019 to 2025.

Table 15-3 Advanced Vehicles Avionics Roadmap

Capability Group/Category	Operational Capability	Hazardous Situation	Avionics Functionality	Time frame
Safety enhancement / hazard avoidance & mitigation	Enhanced Low Altitude Operations	Impact with terrain due to unstable approach or pilot loss of situation awareness	Enhanced Ground Proximity Warning System (E-GPWS) / Terrain Awareness and Warning System (TAWS) enhancements combined with higher integrity / resolution terrain databases to reduce Controlled Flight into Terrain (CFIT). E-GPWS integrated with 3D RNP. ^{cxix} Enhanced and Synthetic Vision System (ESVS)	Near term

Capability Group/Category	Operational Capability	Hazardous Situation	Avionics Functionality	Time frame
	Weather Avoidance	Severe weather, icing, windshear, etc.	Weather radar integrated with E-GPWS. E-GPWS / TAWS enhancements: Assisted Recovery Systems (ARS) Flight Information Services-Broadcast (FIS-B), moving map, SWIM weather forecast uplinks	Mid term
			Aircraft datalinks (e.g., DataComm, Air-Traffic Network (ATN)/ Connection Less Network Protocol (CLNP), Internet Protocols (IP), Future Air Navigation System (FANS). Airborne weather detection and avoidance system	Far Term
	Airspace, Terrain and Obstacle avoidance	Impact with ground objects, airspace infringement due to unstablized approach, loss of flight path performance or pilot loss of situation awareness	Improved Terrain Database, Improved Obstacle Database, Moving Map Synthetic and Enhanced Vision Systems (SVS/EVS) E-GPWS enhancements ¹	Near term
			E-GPWS integrated with 3D RNP	Mid term

Capability Group/Category	Operational Capability	Hazardous Situation	Avionics Functionality	Time frame
	Airborne Collision Avoidance	Near-mid-air collision due to loss of flight path performance or pilot loss of situation awareness (high density airports)	CDTI	Near term
			RNP, VNAV guidance	Near to Mid term
			E-GPWS / TAWS enhancements (e.g., Assisted Recovery System)	
			ADS-B In, TCAS Enhancements	Mid to Far term ^{cxx}
			Integrated surveillance and collision avoidance systems	
	Surface Collision Avoidance (Aircraft-based)	Runway incursions ^{cxxi} at large metroplex airports. Runway excursions ^{cxxii} , runway overruns ^{cxxiii} or underruns ^{cxxiv} due to unstable approaches. Collisions during taxi operations.	Use of on-board radar to detect other aircraft, vehicles and obstacles on the runway, taxiway, or vertiport.	Near term
			E-GPWS enhancements	
			Surface Moving Map with own ship position ^{cxxv} , Cockpit Display of Traffic Information (CDTI)	
			Runway Incursion Alerting to Cockpits, ASDE-X.	Mid term
			Surface indication and alerting systems using ADS-B In, Out	Mid to far term
	Wake avoidance & mitigation	Wake vortex turbulence during mixed fleet ops	Global Navigation Satellite Systems (GNSS), ADS-B OUT	Mid Term

Capability Group/Category	Operational Capability	Hazardous Situation	Avionics Functionality	Time frame
			ADS_B In	Mid to Far term
			AC-based wake vortex detection (system and sensors).	Far term
TBO Published Routes /Procedures	3D RNP Arrival and Departure Operations	Near-mid-air collision or airspace infringement due to loss of flight path performance. (e.g., during steep or spiral approach & departure ops)	Heads Up Display (HUD), Enhanced Vision System (EVS), GPS Landing System (GLS)	Near to mid term
			RNP RNAV, Vertical Navigation (VNAV) guidance, Data Link (DL), Flight Management System (FMS), E-GPWS integrated with 3D RNP.	Mid term
	Reduced Oceanic Separation – Altitude change Pair-wise maneuvers (incl. Oceanic In-trail climb and descent)	Near-mid-air collisions due to loss of separation minima	RNP-4, ADS-C, ADS-B In/OUT, CDTI, FIS-B, Initial Data Link (FANS 1/A+)	Near to Mid term
TBO Negotiated Routes	Trajectory Clearance with RTA and Downlink of Expected Trajectory	Near-mid-air collision due to loss of flight path performance	4D FMS, FANS 2/B, Time Of Arrival Control (TOAC), Secure comm. (UAS)	Mid term
Aircraft Separation	Merging and Spacing (Efficient Metroplex Merging and Spacing)	Near-mid-air or mid-air collision due to loss of separation minima in metroplex	RNAV, ADS-B In, CDTI	Near to Mid Term
	Flight-deck merging and spacing -- using optimized profile descents	Near-mid-air or mid-air collision in high traffic environments	RNAV, ADS-B In, CDTI, Data Link (FANS 1/A+, FANS 2/B, ATN)	Near to Mid term

Capability Group/Category	Operational Capability	Hazardous Situation	Avionics Functionality	Time frame
	Delegated Separation in Flow Corridors.	Near-mid-air or mid-air collision due to loss of separation minima / loss of pilot situation awareness of surrounding traffic	ADS-B In, CDTI	Far Term
	Self-Separation - Self-Separation Airspace	Near-mid-air or mid-air collision due to loss of separation minima	4D FMS, Datalink (FANS 1/A+, FANS 2/B, ATN), CDTI, ADS-B In, ASAS	Far Term
Low-Visibility Approach/ Departure/ Taxi	Low-Visibility Approach, Landing, Take-Off	Flight into terrain or obstacles during IMC	E-EGPWS / TAWS enhancements, LPV.	Near term
			ADS-B, ESVS, CDTI, HUD, GLS	Mid term
ATM Efficiencies	Data Link Departure Taxi Clearance and Pre-departure Clearance Revisions Data Link En Route Clearance Delivery and Frequency Changes Data Link Arrival Taxi Instructions		D_TAXI	Mid term

15.6. **Operational Capability: Enhanced Low Altitude Operations**

15.6.1. **Ensuring Stable Approaches**

Unstable approaches significantly increase the risk of runway excursions^{cxvii}. Accident statistics have shown that risk of runway excursion is even greater than runway incursion or confusion. Smart use of existing and new cockpit approach tools and aids can help the pilot plan and execute a stable approach. Runways equipped with ILS precision approach instrumentation, wind anemometers and the use of a Flight Management System (FMS) adds 'Precision' to the Non Precision Approach. The FMS can support a vertical descent profile or constant angle approach.

The use of auto-flight control, auto-throttle on approach, and situational awareness tools such as Heads-Up Displays (HUD), Enhanced Vision Systems (EVS)/ Synthetic Vision Systems (SVS) Enhanced Vision Systems (EVS)/ Synthetic Vision Systems (SVS) displays and advisory systems with altitude callouts and flare altitude calls, help encourage the advanced vehicle pilot to execute a stable approach and a safe transition to the runway.

FMS

The FMS today can be pre-programmed for a nominal approach and vertical profile. The FMS can be used to guide the pilot on a constant descent profile that targets a nominal three degree approach angle. FMS modifications will be required to enable STOL operations from non-standard runway take-off locations, as well guide the pilot on non-nominal (spiral, or high glide slope) operations.

Future approach and departure procedures will provide containment integrity minima for VNAV and Time of Arrival Control. VNAV will provide stabilized approach paths and help reduced CFIT on approaches.

Situation Awareness tools

The management of the information such as terrain data, chart data on-board sensor data, navigation data weather data, communication (both secure and non-secure), obstacle data and real time updates are the key to providing optimal situational awareness to the advanced vehicle crew.

HUD's help the pilot acquire and maintain a stable approach. The HUD also helps the visual transition in acquiring the touchdown zone. SVS transfer HUD symbology to a heads down presentation, overlaying the Attitude Display and Navigation display. Like the HUD, an SVS helps the pilot during approach and landing transition by augmenting the pilot's situational awareness of the outside world based on runway, obstacle and terrain data.

Advisory Systems

Automatic Dependent Surveillance – Broadcast (ADS-B) equipment, and a Class B Terrain Awareness and Warning System (TAWS) are optional equipment on today's aircraft. Existing Enhanced Ground Proximity Warning Systems (E-GPWS) /Terrain Awareness and Warning System (TAWS) computers can be augmented with multiple algorithms to provide advisories to the flight crew with no change to the aircraft hardware or installation or cockpit interface. Example E-GPWS enhancements include the stable approach monitor, or SAM, RAAS advisories, or deep landing or long landing advisories.



Figure 15-2 SVS Display displays the Burbank Airport at 200 feet

Stable Approach Monitor (SAM)

A simple monitor aural/visual monitor can be used to encourage stable approaches and SOPs. This simple monitor is designed to be quiet and invisible for stable approaches that adhere to operators SOPs. One such monitor scans the reference approach airspeed and the nominal approach angle to a particular runway and if prescribed values are exceeded, an aural/visual advisory can be given. Most, if not all of these signals and data bases, exist in E-GPWS computers. The software for this monitor can be hosted in existing E-GPWS computers without any hardware change and no or minimum change to the aircraft installation or cockpit. Envelopes for excess reference approach speeds and for steep angles to the runway are set by the operator and also set to minimize unwanted advisories found in real world environments.

Each advisory is given only twice aurally, and a stroke or raster text is presented on the Navigation Display (ND). If the aircraft is not stabilized by the time that the aircraft has reached a prescribed altitude above the runway, an “Unstable-Unstable” advisory can be given. During approach, if the tailwind exceeds prescribed values, an advisory can be given. (The wind can be derived from existing E-GPWS signals).

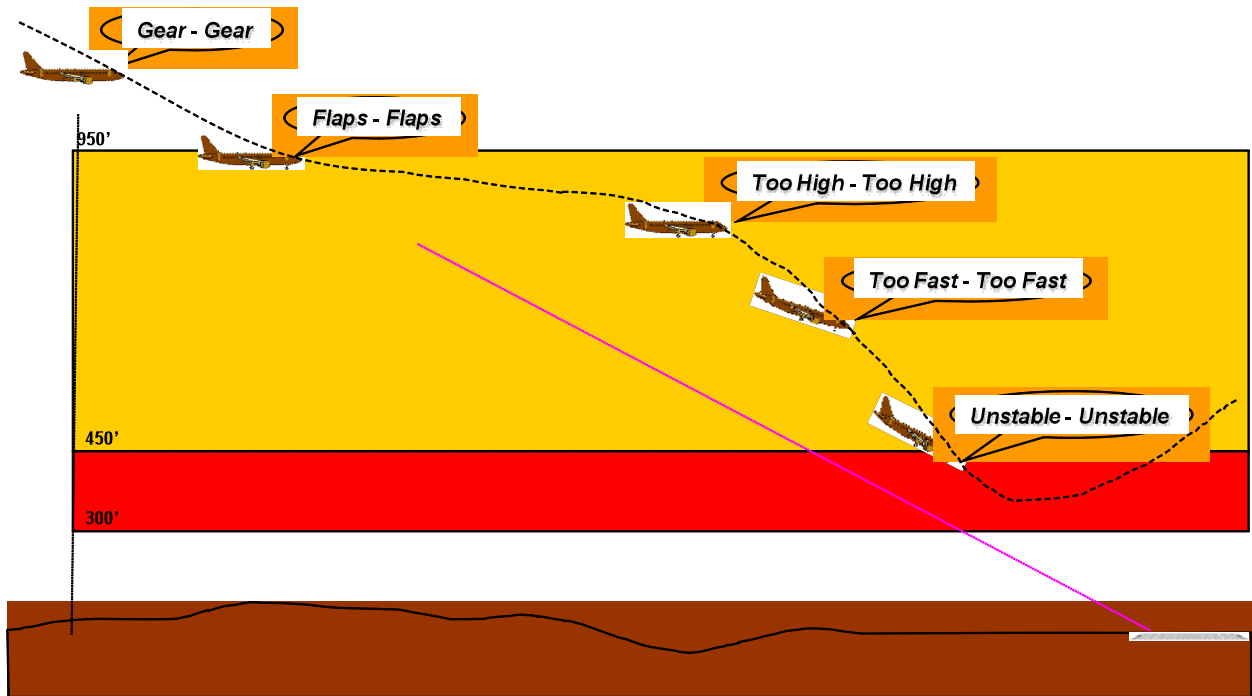


Figure 15-3 SAM advisories for unstable approach

Long (or Deep) Landing Advisories

A large number of runway overruns occur when the aircraft lands long beyond the nominal touchdown zone, or flares too long, often with a wet or contaminated runway. Simple advisories can be given for a landing-long situation by combining information on the runway length from the runway database, the aircraft's GPS position, aircraft weight on wheels or distance above the runway.

Deep landing or long landing advisories occur when the aircraft has not touched down by a specified location. This location is either a fixed distance relative to the runway threshold, or a percentage of the runway length. Distance remaining callouts can be initiated following deep landing advisories for additional situation awareness until touchdown. RAAS distance remaining callouts remain unchanged.

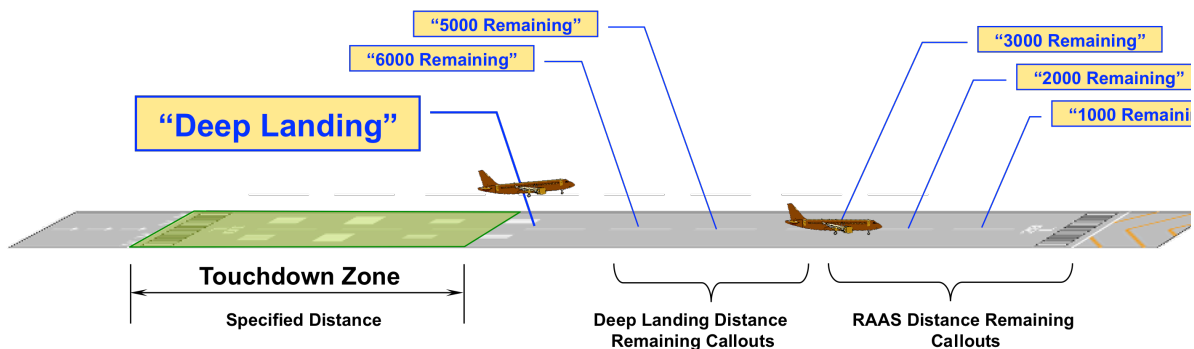


Figure 15-4 Deep Landing Advisories

The SmartRunway™ and SmartLanding™ products received Federal Aviation Administration (FAA) Technical Standard Order (TSO) approval in September 2009. The SmartRunway and SmartLanding technologies were developed to reduce runway accidents at crowded airports. SmartRunway provides visual and aural alerts to pilots about runway and taxi locations and SmartLanding informs pilots of unstable approaches and long landings, when an aircraft lands too far down the runway to safely stop. SmartRunway is the most recent version of RAAS and SmartLanding is the latest version of the SAM enhancement to E-GPWS.

SmartRunway and SmartLanding address the \$1 billion cost of runway excursions and incursions to the commercial flight industry. This new software provides added situational awareness at increasingly crowded airports while reinforcing standard operating procedures.

15.7. ***Operational Capability: Weather Avoidance***

15.7.1. Severe weather detection and avoidance

In order to avoid hazardous weather conditions (windshear, hail, icing), by 2020 the advanced vehicle will be able to take advantage of ground-to-air weather data exchange with SWIM and weather data exchange with surrounding aircraft. Besides shared data exchange with SWIM, the on-board communications technology will also be utilized for the light/trajectory negotiation, data exchange for distributed decision making and real-time fleet optimization.

Airborne weather detection and avoidance systems will combine this externally retrieved weather data such as uplinked data (winds aloft, ground based radar observations, ground-based lightning sensors with data gathered from its own aircraft: airborne weather radar, INU/GPS, icing, temperature, pressure sensors and turbulence instrumentation, measurement, and interpretation. On-board weather radar will provide complete 3-D volumetric weather acquisition, and detection of windshear and turbulence. The maximum detection range for weather and the ground map will be at least 320nm, a 40 nm or greater range for turbulence, and a detection range of at least 5 nm for windshear.

The airborne weather detection and avoidance systems will provide the pilot with automatic flight path based hazard assessment, vertical profile and constant altitude analysis modes, earth curvature correction, and internal terrain based ground clutter extraction. Hazardous weather conditions will be displayed to the flight crew and 3D Aural alerts will help the pilots to avoid strategic weather, maneuver earlier for rerouting due to weather (e.g., icing, windshear), avoid tactical hazardous weather, and minimize turbulence.

This integrated weather data will be utilized by the flight management system to model and store the wind and temperature data across the flight trajectory. Accurate wind and temperature data is essential during the climb and descent phases of flight where the advanced aircraft may perform spiral approaches and departures, operate at higher descent rates, and must stay within a limited airspace defined within RNP RNAV and VNAV procedures.

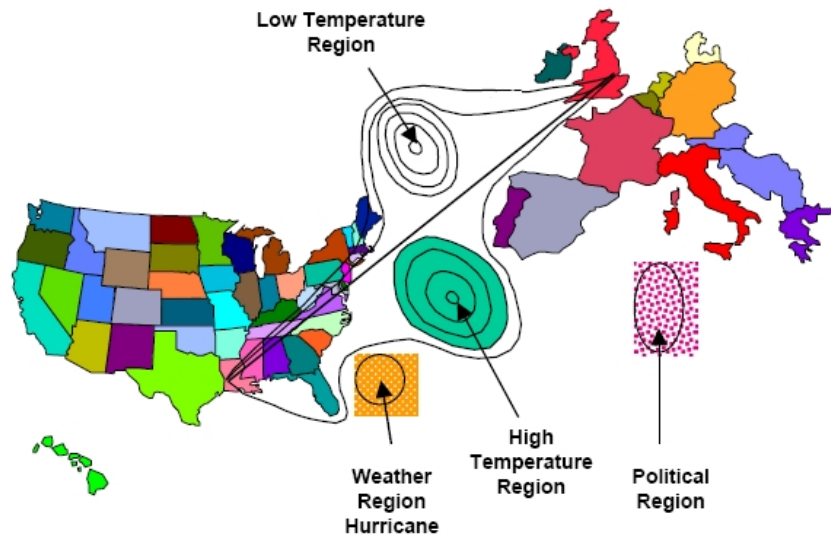


Figure 15-5 Dynamic, optimal in-flight rerouting around hazards (Baize, 1999)

The onboard lateral optimization functionality, provided by the Flight Management system or EFB, will compute a fuel and/or time optimized route that avoids weather, environmentally sensitive regions, and enables the dynamic rerouting around non-standard events. If rerouting due to hazardous weather is deemed necessary, modification to the aircraft flight path can be requested from ATC.

Future [Assisted Recovery Systems](#) can anticipate in-flight dangers like windshear, or any rapidly changing wind currents posing danger to aircrafts,. ARS can automatically maneuver the aircraft in response to a windshear alert from the airplane's weather radar system.

Technology advances in severe weather detection and avoidance can be seen in product such as the IntuVue™ family of weather radar products. IntuVue™ radar provides flight crews with accurate, real-time information to assess approaching weather systems and determine a safe, efficient way to avoid thunderstorms, turbulence, windshear and other potentially hazardous weather conditions. Unlike conventional airborne weather radars which scan a relatively small area and need to be manually adjusted by the pilot, IntuVue automatically scans the airspace from the ground up to 60,000 feet, out to a range of at least 320 nautical miles. The system creates a highly accurate, continuously updated view of all the weather and turbulence in the vast airspace the radar scans. IntuVue also uses a high-resolution Enhanced Ground Proximity Warning System terrain database to automatically eliminate ground clutter that conventional radars can mistake for weather returns.

15.8. **Operational Capability: Terrain, Airspace and Obstacle Avoidance**

Safe advanced vehicle operations will require flight path protection, which will be achieved via a combination of procedure design, flight path integrity, and reliable terrain and obstacle alerting.

Enhanced Vision Systems (EVS)/ Synthetic Vision Systems (SVS) technology can aid the advanced vehicle in terrain and airspace avoidance during spiral approaches and departures in high density or terrain-challenged airspace as well as during simultaneous take off and landing operations on crossing runways. Pilots must retain situational awareness during these high workload operations and the

EVS/SVS terrain avoidance, alerting and situation awareness display tool may provide the time-critical information necessary to keep the advanced vehicle pilot from infringing into safety hazardous threat areas.

E-EGPWS/TAWS functionality will interact with 3D RNP arrival, approach and departure functionality, to provide sufficient terrain predictive alerting yet avoid nuisance alerts when the aircraft is in terrain/obstacle challenging low-RNP. Future SVS/EVS systems will recognize when the aircraft is in compliance with the intended RNP procedure, and warn the flight crew when failure to follow a defined procedure introduces a potential terrain or obstacle collision threat.

15.9. ***Operational Capability: Airborne Collision Avoidance***

Improvements in the hardware and software of airborne collision avoidance systems are actively researched, developed, flight tested by the aircraft suppliers and OEM's. Aircraft suppliers are assessing the advanced vehicle avionics architectures to integrate products (e.g., TCAS, Transponder, DME) in an effort to reduce hardware equipment volume, antennas, cabling, etc. TCAS/Transponder products have already been integrated today, in preparation for broadcasting of ownship ADS-B data and receiving ADS-B data from surrounding aircraft.

Aircraft suppliers are also developing software to enhance the performance of the existing onboard collision-warning devices they manufacture. Enhanced TCAS research and development is on-going by MITRE, L3, Honeywell and other corporations. The TCAS RA maneuvering system is currently in the final stages of development, and may be ready for aircraft installation by early 2010. The E-GPWS Assisted Recovery System, initially developed for Airbus aircraft, may become standard equipment on fixed wing and rotor-winged aircraft.

15.9.1. Assisted Recovery Systems (ARS)

Assisted recovery system (ARS) is an E-GPWS enhancement that uses the automatic flight control system in fly-by-wire aircraft to override pilots who set a course that would enter restricted airspace, fly into terrain, hazardous weather or on a collision course with airborne or ground based objects.

Flight tests of the system were conducted in April 2005 with a United Airlines A319 in airspace near Monterrey, California. The automatic flight controls can be reprogrammed to assume control of the airliner, rather than simply give the pilot a warning. The system has also been tested in flight aboard a Beech Aircraft Corp's Beech King Air twin turboprop aircraft.

The automatic recovery system is an upgrade to the E-GPWS, which uses a worldwide terrain database to alert pilots to obstacles such as mountains, man-made obstacles or terrain. Automatic recovery will require modifications to the E-GPWS terrain database. E.g., "virtual keep-out areas," such as restricted airspace above the White House can be added into flight computers equipped with the E-GPWS terrain database.

The system gives the pilot a warning as the aircraft enters a buffer zone around potential dangers. The Assisted Recovery system gives the pilots a few seconds to respond to a terrain or obstacle warning. If

the pilot does not respond to alerts given by the system by initiating a correcting maneuver within a predefined response time, the ARS software commands the aircraft's flight control system to maneuver, avoiding the danger. Once the danger has passed, the system returns control to the pilots. (Trimble, 2005)

The new avionics software can also anticipate in-flight dangers like windshear, or any rapidly changing wind currents posing danger to aircrafts,. ARS can maneuver the aircraft in response to a windshear alert from the airplane's weather radar system. The system can also assist the pilots by maneuvering the aircraft to avoid collision with another aircraft. (Perone, 2004).

In Europe, politicians and regulators are looking to mandate software changes provided by Assisted Recovery Systems. Airbus intends to start installing them on aircraft coming out of the factory by mid-2009. Boeing is also expected to incorporate the changes in its production lines. (Pasztor, 2008).

15.9.2. TCAS RA Maneuvering System

TCAS II, the second and current generation of instrument warning TCAS, is installed on the majority of commercial aviation aircraft. TCAS II generates Resolution Advisories (RA) which are direct, vocalized instructions to the pilot on how to avoid impending danger.

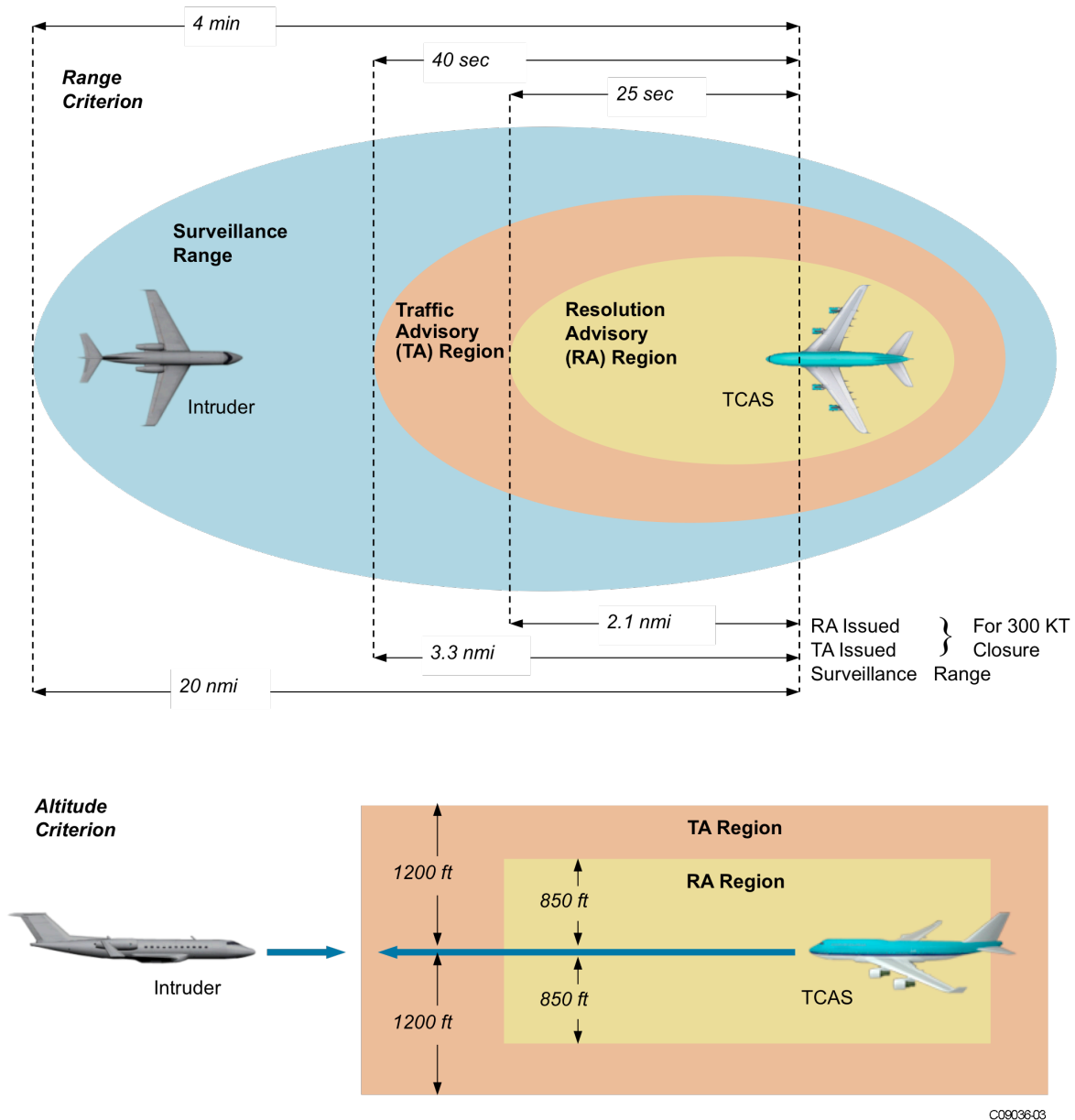


Figure 15-6. TCAS Advisory Regions

Airbus has developed an automatic TCAS RA Maneuver System, similar to the assisted recovery system enhancement for EGPWS. The TCAS RA Maneuver System will be installed on Airbus 380, 350, 330/340 and 320 aircraft. This automated maneuvering system is an indispensable avionics addition to UA, where the time to impact is short, and communication delays to the remote pilot are a concern. Note: According to the appendix 1 of AC 20-131B draft and subsequent AC 20-151 advisory circular, “The TCAS II RA algorithms are based on the pilot initiating the initial 0.25 g acceleration maneuver within approximately 5 seconds. Pilot response is expected within approximately 2.5 seconds if an additional RA is issued.”

15.9.3. ADS-B In

ADS-B In is a highly anticipated future technology for airborne traffic awareness and safety applications. The ADS-B system enables airplanes to transmit critical information on their location, speed, and altitude to other planes in their vicinity and to ground stations connected to air traffic control centers. The system uses Global Positioning System (GPS) technology to determine an airplane's exact location and whether it's climbing, descending, or turning, broadcasting this data in real time. Armed with this information, pilots can maintain situational awareness of other aircraft around them, allowing for safer and more efficient flights. (ADS-B, 2008)

ADS-B offers pilots important tools including the following:

Air-to-air surveillance capability

Surveillance of remote or inhospitable areas lacking radar coverage

Reduced separation and greater predictability in departure and arrival times

Improvement of airlines' ability to manage traffic and aircraft fleets

Real-time traffic, weather, and aeronautical information in the cockpit

Air taxi services, air ambulance services, and air delivery services have operated in Alaska for years without the benefit of surveillance radars where bad weather, harsh geography, and inadequate equipment contributed to high accidents rates. VLJs or UA flying into low infrastructure airports will benefit from ADS-B technology in a manner similar to the small aircraft flying into Alaska.

CDTI

The CDTI is the pilot's interface to the surveillance system. CDTI functions are composed of a traffic display function, associated control functions, annunciation functions, and alert functions. The CDTI traffic display function can present information on a dedicated display device or a shared/multi-function display (MFD) device. It depicts traffic information relative to own-ship. Additional information about the traffic (for example, ground speed, distance, closure rate) can also be presented. Traffic information may be obtained from one or more sources; e.g., automatic dependent surveillance broadcast (ADS-B), traffic information service (TIS), and the surveillance part of the traffic alert and collision avoidance system (TCAS). This information is processed by the Airborne Surveillance and Separation Assurance Processing (ASSAP) function and is sent to the CDTI. The CDTI will facilitate advanced vehicle flight operations by providing:

Enhanced visual acquisition and visual approaches

In-trail (or lead) climb and descent in non-radar airspace (en route, and remote)

In-trail (or lead) climb and descent to co-altitude in non-radar airspace (en route, and remote).

Far-term, the CDTI applications will provide improved safety, efficiency, flexibility, and, capacity by providing the airborne crew with:

Improved traffic situational awareness

Improved visual traffic acquisition

Facilitate the positive identification of traffic
Reduced probability of loss of the visual contact
Aid in judgments of closure and encounter geometry and spacing
Increased access to more efficient altitudes and tracks.

15.9.4. Traffic Surveillance System

A Traffic Surveillance system developed for the any of the new vehicles must meet the needs of future surveillance and ADS-B initiatives, including Airborne Separation Assurance System (ASAS), Cockpit Display of Traffic Information (CDTI), and Traffic Computer (TC). Traffic Surveillance system applications include:

- Enhanced Traffic Situational Awareness, both airborne and on the surface.
- Enhanced Visual Separation on approach
- Enhanced Visual Acquisition for See & Avoid
- Enhanced Sequencing and Merging and Crossing and Passing Operations
- In-Trail Procedures in oceanic airspace

15.10. *Operational Capability: Surface Collision Avoidance (Aircraft-based)*

The advanced vehicle must be able to avoid ground hazards (Ground-to-Ground) such as fixed obstacles, other ground aircraft, as well as ground support equipment during taxi operations in the airfield environment. While on the ground, the advanced vehicle must be able to avoid airborne hazards (Ground-to-Air), i.e., avoid runway incursion by clearing final before taking the active runway.

For safe operation on and near the runway, we should supplement current flight crew procedures by providing an onboard system that includes an electronic map of the airport surface, displays relevant surface and airborne traffic, indicates runway occupancy during normal operations, and provides caution and warning alerts for predicted collisions with aircraft or vehicles on the runway surface.

Runway Incursion Alerting to Cockpits

At our nation's airports, investment in runway infrastructure, runway signage, runway traffic lights, ASDE-X, multi-lateration, surface movement radar, and ADS-B are implemented to help reduce runway incursion/confusion risks. Existing and future cockpit runway awareness tools for the pilot also aim to reduce the risks of runway incursion/confusion and ground-based obstacle collision. Through the utilization of ADS-B-In, onboard displays and alerting functions, airborne technology can identify and alert the advanced vehicle pilot of runway occupancy and potential incursions. Cockpit technologies to reduce runway incursion/confusion risks include:

Moving Map Display (own aircraft position) in the cockpit.

Runway advisories (aural and visual).

Wrong runway take-off aural and visual warning (intent from Flight Management System or data linked ATC clearance).

Extending ASDE-X warnings to the cockpit.

TAWS/E-GPWS enhancements: utilizing ADS-B and runway position information to provide advisories and alerts.

Use of radar on the ground to detect runway and taxiway obstacles such as other aircraft, or vehicles, and construction equipment.

Moving Map Airport Displays

For runway awareness, a very valuable tool for the pilot is a visual moving map display with own aircraft position shown for orientation and the display evolving to show data linked ATC taxi clearance. Moving maps can be displayed on the cockpit MFD or on an Electronic Flight Bag (EFB). Class III EFBs are fully integrated into the aircraft and located directly in front of the pilot. However, they are very expensive (>\$100K). Class II displays are far less expensive (<\$25K), but most are located in areas not directly in front of the pilot.

An extensive database is required to support the moving map display and its multiple functions. The database requirements climb exponentially as more airport detail is added.

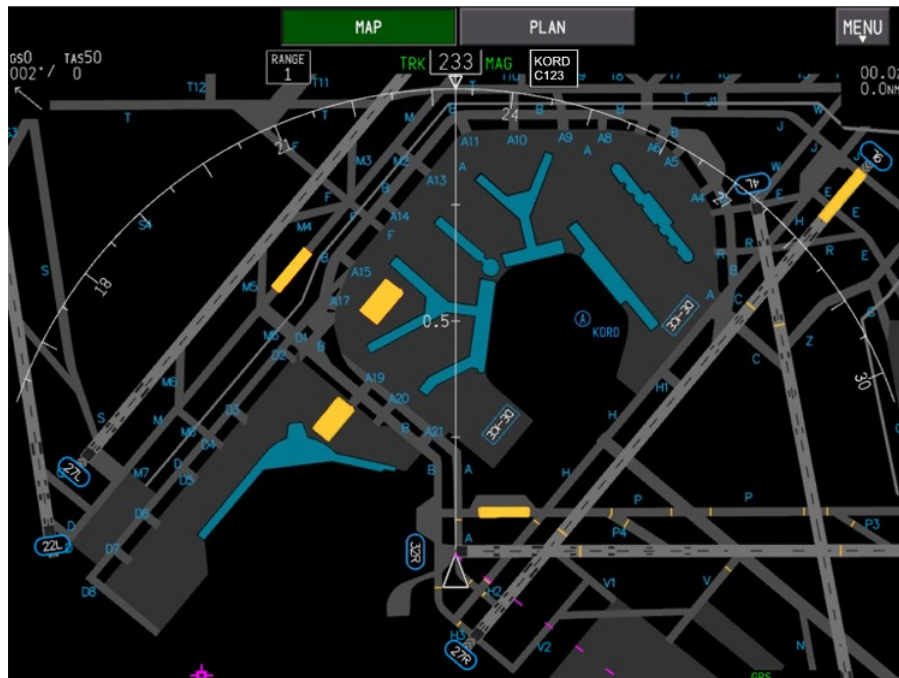


Figure 15-7 Taxi map -- Boeing 787 Navigation Display while on the ground at KORD

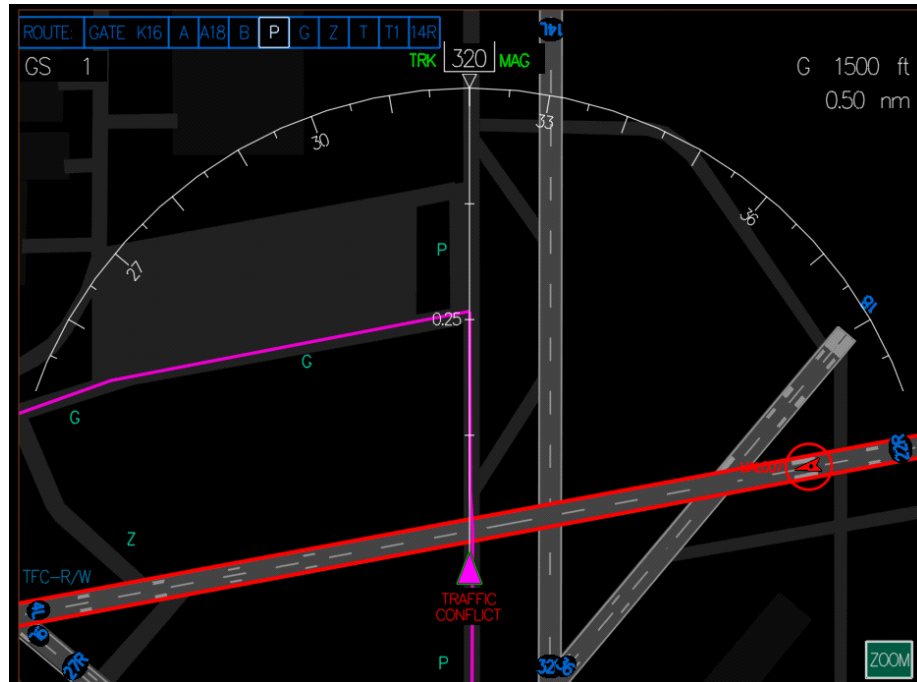


Figure 15-8 Taxi map display of datalinked taxi routes with traffic

Research into traffic display onto airport taxi maps is ongoing. For instance, the operations R&D project at Boeing is investigating the display of datalinked taxi routes combined with active traffic as a growth feature for the B787 and B747-8. Figure 15-7 and Figure 15-8 depict existing and future airport moving maps for Boeing aircraft.

Surface indication and alerting systems

The latest FAA-funded ADS-B trials by ACSS^{cxvii} in Philadelphia have advanced surface area indication and management beyond the airport map with ownship and other traffic to visual and aural alerts to pilots of potential ground conflicts. The management of aircraft in the airport surface environment has been advanced beyond simple visual awareness to actual alerts of potential runway conflicts via airport surface conflict detection using ADS-B In and ADS-B Out where on-board ADS-B transponders and GPS are used to broadcast ownship position and velocity to ground stations and similarly equipped aircraft. Surface awareness information can be displayed on an electronic fight bag or built-in cockpit displays. For instance, the depiction of the cleared digital taxi path on a multipurpose control display unit is envisioned for future surface alerting systems.

The widespread use of surface area moving maps is expected; Airbus plans to provide that technology on its aircraft by 2011. The more complicated alerting solutions are not expected to be available before 2013-14. The challenges of developing the more advanced alerting systems, based on the accuracy and integrity of the aircraft position reported through ADS-B, should be addressed by the time the advanced vehicles enter our NAS.

Extending ASDE-X warnings to the cockpit.

The challenge for VLJ and UA operations is the absence of ground infrastructure at many of the non-towered airports they utilize. Runway incursion alerting technology that is airport independent will help mitigate accidents risks for these aircraft, especially valuable at airports with poor ground infrastructure, data and services.

Honeywell International and Sensis Corporation, in coordination with the FAA, demonstrated a technology that can detect and communicate potential runway incursions directly to an aircraft cockpit, alerting the flight crew of a potential incident. The cockpit advisory technology sends potential ground, arrival or departure conflicts directly to pilots as an audible alert using a Mode-S data link and an existing modified TCAS unit in the aircraft. The audible alert in the cockpit is generated by Sensis' Airport Surface Detection Equipment Model X (ASDE-X) Safety Logic, and is provided to pilots at the same time that ASDE-X transmits the information to air traffic controllers. The runway incursion cockpit advisory technology uses existing ground and avionics systems, limiting the likely equipment changes to only software modifications. Currently, surveillance detection equipment notifies air traffic controllers of potential incursions and then controllers must relay the information to pilots via voice, resulting in less than optimal response time.

By December 2008, ASDE-X was in use at 14 airports and will be installed at the top 35 airports by the end of 2010.

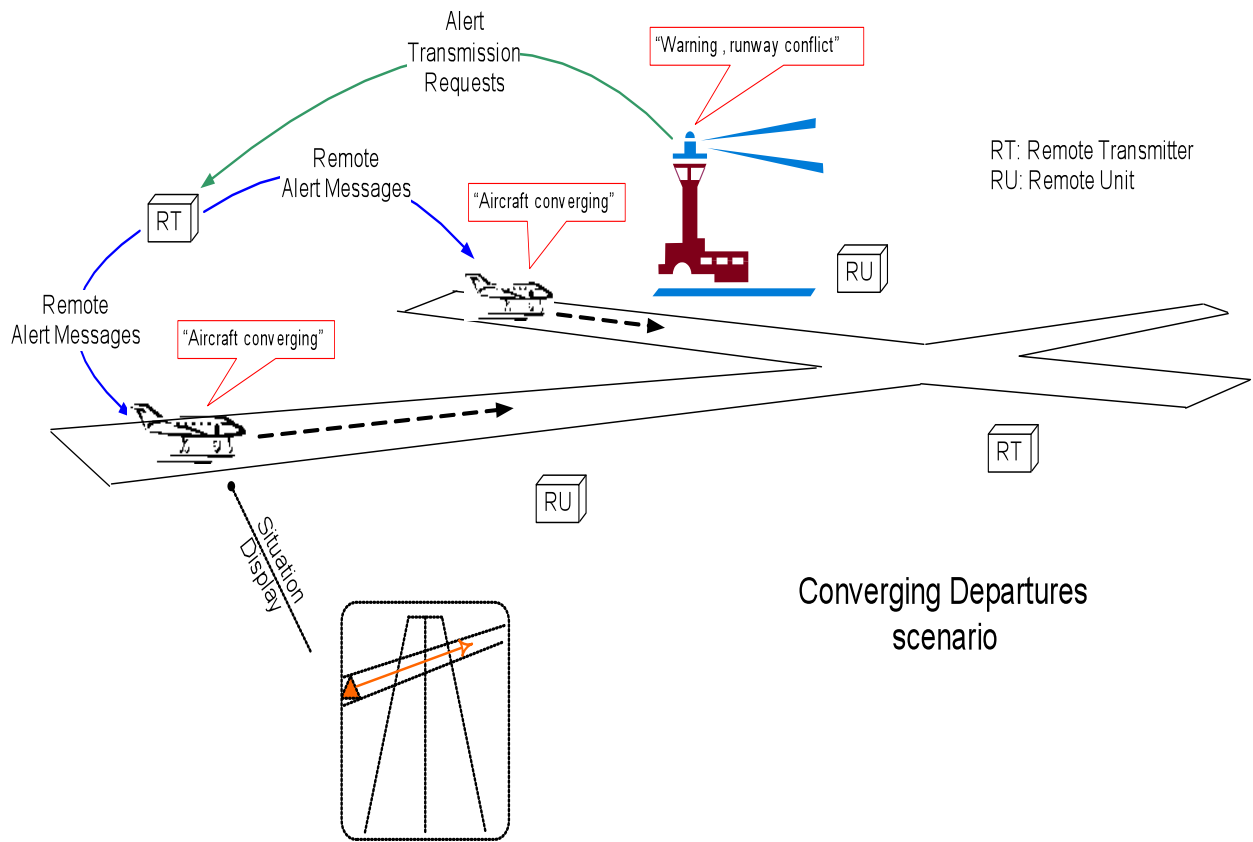


Figure 15-9 Ground-based ASDE-X Alerts to Cockpits

ADS-B Applications on the Ground

ADS-B In technology can also provide benefits on the ground. When combined with runway and taxiway data bases and GPS position, it can provide awareness of other equipped ADS-B aircraft and used as a Runway Traffic Advisory System (R-TAS) type of aircraft safety system. R-TAS can provide timely alerting-warnings for potential runway incursions and collisions. Flight demonstrations of this concept have been demonstrated using multiple aircraft.

The great advantage of R-TAS type of aircraft safety system is that it can be utilized at all of the airports in the world. It operates independent of airport infrastructure and ATC.

R-TAS algorithms can be hosted on any aircraft equipped with E-GPWS/TAWS.

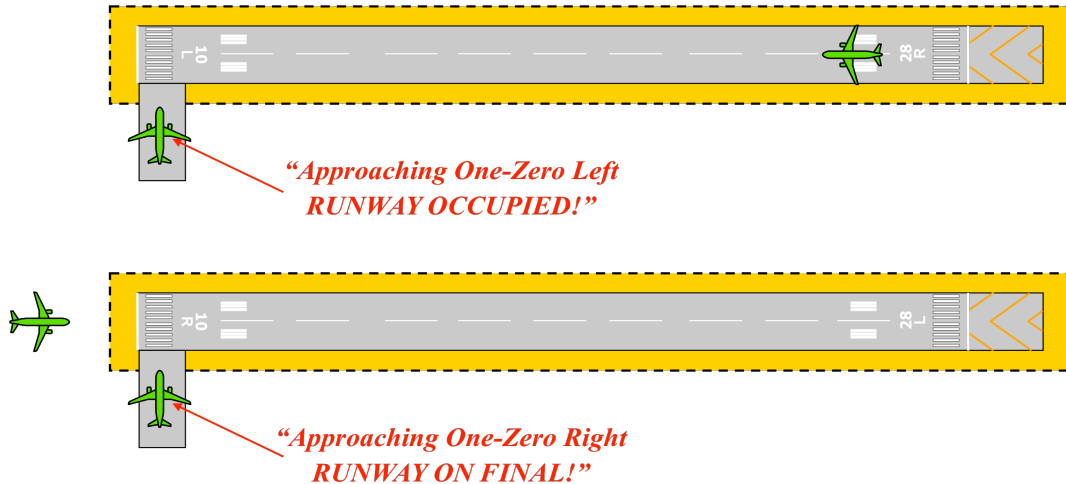


Figure 15-10 Runway Safety: using ADS-B In with RAAS and E-GPWS/TAWS

The Use of on-board Radar to Detect other Aircraft, Vehicles and Obstacles on the Runway

The use of millimeter radar (24 or 72GHz) in a ground mapping mode can be used to detect other aircraft, ground vehicles or obstacles on the runway.

The great advantage of on-board radar is that the advanced aircraft can generate the needed obstacle information (including foreign object debris) independent of equipment external to the aircraft. Other aircraft, ground vehicles or construction equipment do not have to be fitted with ADS-B nor the airport fitted with radar or ASDE-X equipment. Source: (Bateman, Don, 2008)

Runway Awareness and Advisory System (RAAS)

The Runway Awareness and Advisory System is a low cost aural awareness system which can be hosted in existing E-EGPWS /TAWS computers installed on most worldwide aircraft. RAAS uses the GPS position utilized by E-EGPWS, a validated runway database and a 'virtual' box in software that surrounds the runway. This 'virtual' box approximates the ICAO runway holding line. The existing aural interface of the existing E-EGPWS is used and no change to hardware or aircraft wiring is required.

RAAS provides position awareness and alert advisories with respect to the runways and can provide awareness to a possible short runway for take-off or landing. RAAS can also advise of a possible inadvertent take-off or landing on a taxiway. RAAS can also advise the pilot of the distance (in meters or feet) remaining to stop.

RAAS can be very effective to help reduce runway confusion and for inadvertently take-off or landing on a taxiway or runway that is possibly too short (as determined by the operator).

Currently, RAAS is installed on some 2,000 business, and airline aircraft. Eight airline operators have installed RAAS certified by both the FAA and EASA on 800 plus aircraft while another 1,200 business aircraft are fitted.

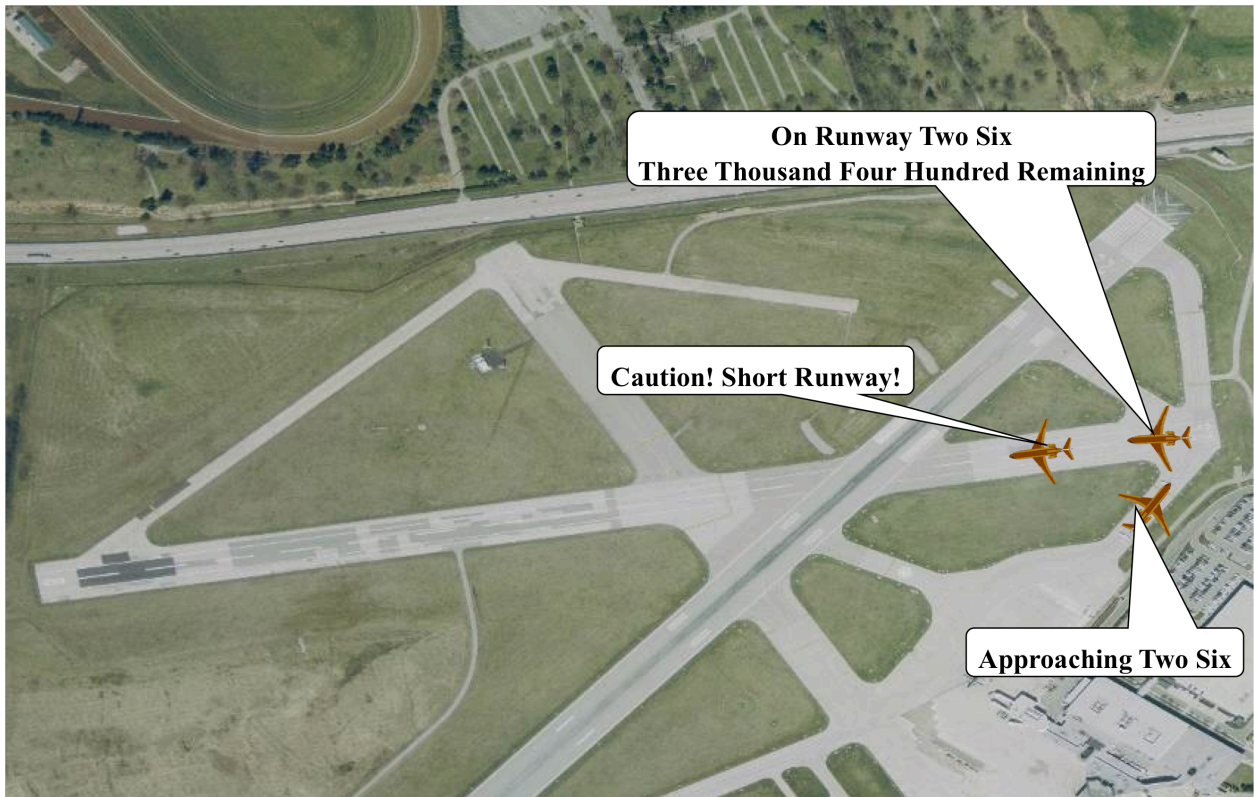


Figure 15-11 Runway confusion on take off

Wrong Runway Take-Off Visual and Aural Warning

A cockpit warning can be given for a possible wrong runway take-off. This assessment can be made by combining data on the runway selected for take-off (entered into the FMS), the current aircraft position, runway data, and throttle advancement. This warning can be tied into the Master or Central Warning System

15.11. ***Operational Capability: Wake avoidance & mitigation (Aircraft-based)***

Wake detection and avoidance is critical during simultaneous take off and landing operations, especially when operating on crossing runways. Today the impact of wake turbulence is mitigated procedurally by maintaining minimum separation based on aircraft weight combinations (large trailing heavy, heavy trailing small, etc.). However, for flight operations at non-towered airports, ATC will not provide this protection. Ideally, airborne wake vortex detection systems available to the advanced aircraft in the 2018 – 2040 timeframe will detect and display wake vortices and provide cockpit advisories to the pilots.

For the 2025-2040 timeframe, wake vortex detection and mitigation technologies developed for military applications will be available in commercial aircraft to improve performance in weather and wake vortex detection. Wake Vortex free approach will be achieved via dynamic adjustment of aircraft spacing, based on the strength of the vortex of the preceding aircraft, detected by on-board sensors and displayed to the pilot. Aircraft will be able to determine the wake vortex characteristic they generate and broadcast this information by data link to neighboring aircraft. This enables the aircraft to dynamically

adjust the aircraft spacing (either automatically, or via input by the pilot) based on the actual strength of the vortex of its predecessor.

ADS-B information on wake vortex category, as well as aircraft position, velocity and altitude information may also be useful in the determination and avoidance of wake vortices generated by leading aircraft. As a first step, preliminary discussions about leveraging ADS-B merging and spacing applications into wake vortex management are occurring today. In the development this new wake vortex management capability sensors on the aircraft transmitting velocity and position to the ground could instantaneously uplink to an aircraft behind. That instant transmission would allow the trailing aircraft to calculate if increased separation is necessary.

15.12. ***Operational Capability: 3D RNP Arrival and Departure Operations***

The flight deck in the midterm timeframe will provide the pilot with integrated flight displays where vertical and horizontal flight profiles are displayed, and vertical and horizontal containment limits are indicated. VLJ and CESTOL execution of spiral descents, approaches, or departures, can be defined much like RNP procedures today, using vertical and horizontal flight profiles with vertical and horizontal containment limits. The aircraft FMS will need to monitor the containment limits and alert the pilot when the containment limits are exceeded. The pilot will be notified when the aircraft will not be able to comply with the containment integrity requirements specified in the approach/descent procedure or any part of the flight trajectory where these limits are used to contain the flight trajectory of the aircraft.

Renegotiation of the RNP RNAV or VNAV containment or RTA-constraint window will need to be initiated with ATC if the aircraft can no longer maintain its negotiated contract. This negotiation process will occur over datalink, and may be automated between the airborne and ground based systems in NextGen.

More flexible trajectory definitions will need to be available for the definition of climb and descent profiles. The FMS will be augmented to able to specify multiple descent profiles such as the ability to overtake a leading aircraft, perform vertical offset maneuvers to avoid conflicts or execute a spiral descent or climb maneuver. Flight trajectory constraints, traditionally specified on waypoints, may be augmented by time varying RNP limits/boundaries on trajectory segments, including segments that are part of the spiral procedure segments.

The aircraft will be certified to fly RNP RNAV limits as small as 0.1 nm, and VPPL of 160ft or below, accuracy which will be essential to the advanced aircraft while conducting final approach, spiral and other highly precise operations.

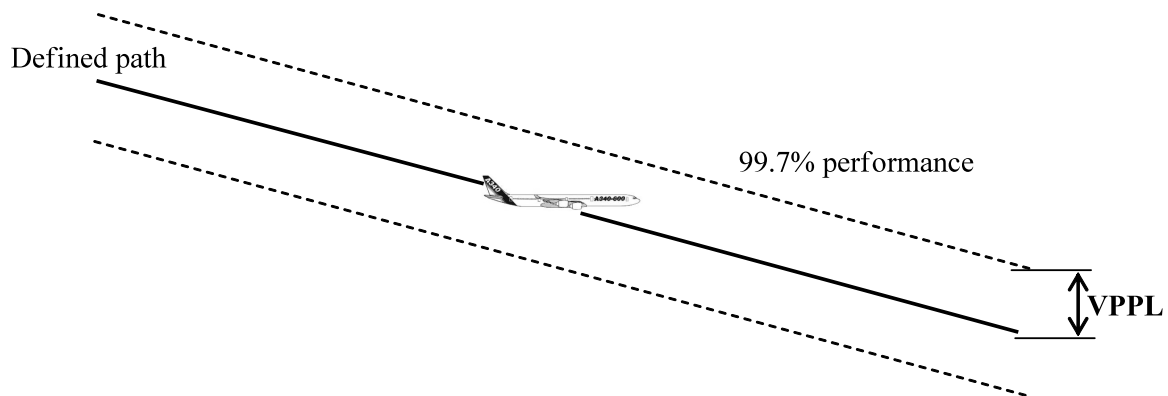


Figure 15-12 Vertical Path Performance Limit (VPPL)

Future approach and departure procedures will provide containment integrity minima for VNAV and Time of Arrival Control. VNAV will provide stabilized approach paths and reduced CFIT on approaches. The navigation system will provide data to enable the generation of command signals for autopilot/flight director/CDI. A measured value of path steering error (PSE), together with the other system error budgets, shall be used to monitor system compliance to RNP RNAV requirement. RNP VNAV will provide temperature compensation to the vertical path altitudes when the altimetry source temperature is colder than or warmer than ISA temperature.

Containment limits for special operations such as holding procedures or spiral operations (with more restrictive RNP types) may be affected by abnormal environmental conditions (e.g. unusually high winds). The utilization of blended internal and external weather data in the navigation function will minimize this source of containment loss.

The CDU, navigation display, the FMS and PFD will provide the flight crew with enhanced capabilities and graphics to minimize manual insertion and control errors, improved situation awareness, RNP monitoring and alerting, straight-forward indication of equipment failure and a reduced exposure to operational errors (e.g., containment errors). Graphical display of emergency procedures or missed approach maneuvers will also be available, and important to the advanced vehicle aircrew.

15.13. ***Operational Capability: Reduced Oceanic Separation – Altitude Change Maneuvers***

Pair-wise separation requirements for altitude changes in oceanic airspace are reduced for RNP-4 and FANS 1/A capable aircraft. Improvements in communications, navigation, surveillance and air traffic management systems have enabled Performance Based Navigation (PBN) Separation Reductions which allow major separation reductions in the oceanic environment. When equipped with the necessary ADS technology, RNP capable aircraft can be safely separated at much closer distances than aircraft that do not meet the RNP requirements. Reduced Vertical Separation Minimum (RVSM) allows the vertical spacing of equipped aircraft to be reduced from 2000ft to 1000ft in airspace where the RVSM standard has been implemented. Oceanic RVSM allows aircraft to fly closer to fuel efficient altitudes and execute smaller (1,000 foot step) climbs, which require less fuel.

User preferred oceanic profiles for capable aircraft will be more accessible through pair-wise altitude change maneuvers with ground-based separation responsibility. Aircraft-to-aircraft oceanic longitudinal and lateral spacing is reduced (e.g., to 10-15 nm) during altitude change maneuver. Pair wise maneuvers (e.g. in-trail climbs and descents) are enabled through the use of improved oceanic cooperative surveillance information. If equipped with Automatic Dependent Surveillance-Contract (ADS-C) and satellite-based communication to provide surveillance to the controller who provides ground-based separation assurance, spacing can be reduced to 15 nm. If equipped with Automatic Dependent Surveillance-Broadcast (ADS-B) Out/In, on-board displays and algorithms (i.e., CDTI) for observation by a pilot, and satellite-based communication for position reporting to the controller, spacing can be reduced to 10 nm during this delegated self-separation maneuver. In either case, the surveillance information provided to the controller is required in order to gain controller clearance for the initiation of the maneuver.

“Availability of user preferred oceanic profiles is further increased through reduction of horizontal spacing to below 30 nm for pair wise co-altitude maneuvers between capable aircraft. Co-altitude maneuvers, such as passing a similar-speed aircraft, have much longer risk exposure times than altitude change maneuvers, and thus carry a higher collision risk and communication uncertainties play a significant role in defining safe separation standards.”

These pair-wise maneuvers rely on RNP, satellite-based data communications, and either increased ADS-C update rate or ADS-B. “ (JPDO, October 2008)

To conduct altitude change pair wise maneuvers, key enablers such as RNP-4, ADS-C, ADS-B In/OUT, CDTI, FIS-B, Initial Data Link (FANS 1/A+) must be installed on the aircraft. Existing avionics systems will need to be updated to enable pair-wise maneuvers. The surveillance system, displays and communication system will require enhancements currently not available on existing air transport systems.

Surveillance system upgrades: At a minimum, the TCAS must be capable of ADS-B In capability (receive and send to display ADS-B information) and provide enhanced information (ITP distance computation). This requires a link to cockpit displays. It is recommended that the TCAS also provides some level of automation to ease ITP initiation criteria assessment, avoid unnecessary requests (which would be rejected by the controller) and automatically send ITP information to the communication systems to prepare a maneuver request to the controller. The traffic computer can provide system automation to optimize the flight crew workload and the success rate of ITP procedure and can pro-actively provide information to identify ITP opportunity to the flight crew. For instance, automation can support criteria assessment (overall ITP feasibility status, ground speed differential, ADS-B quality) will minimize pilot workload.

The communication system must be updated to carry new specific ITP messages which will need to be added to the ICAO message set. By 2013, these will be pre-formatted free text. By 2020, new CPDLC messages will facilitate the request and approval of ITP.

The Flight Management System does not need to be updated provided that it can display performance data such as a ‘recommended max altitude’ computed on the basis of a 300 ft/min minimum climb. The pilot is required to check this information as one of the initiation criteria.

For certifiable solutions, cockpit displays must be updated with the following architectural options: MCDU for pilot entries and queries, and either a Navigation display, EFB or vertical display for the display of traffic and route information.

15.14. ***Operational Capability: Trajectory Clearance with RTA and Downlink***

The aircraft Flight Management System can provide high precision RNAV/VNAV and Time of arrival control (TOAC) at waypoints along the flight trajectory. It can receive, evaluate and insert datalinked 4D route clearances into the actively controlled-to trajectory, and compute the aircraft intent, i.e., predicted flight trajectory, to be downlinked to the ground (SWIM, ATC) and broadcasted to the surrounding aircraft.

In the 2025 timeframe trajectory clearances will be uplinked to the aircraft via datalink (CPDLC). These clearances may specify RTA constraints or one or more points on the planned trajectory, or may give the aircraft the ability to execute these maneuvers via delegated separation.

15.14.1. 4D Trajectory Data Link (4DTRAD)

4DTRAD enables the negotiation and synchronization of trajectory data between ground and air systems. This includes the exchange of 4 dimensional clearance and intent information such as lateral, longitudinal, vertical and time or speed information for the whole airborne trajectory. As depicted in Figure 15-13 below, the 4DTRAD service consists of the following operating methods:

- Air/Ground Synchronization of aircraft's 4D trajectory;
- Ground- ground co-ordination/notification of the 4D trajectory;
- Uplink of a clearance covering the coordinated constraints;
- Downlink of a clearance request
- Monitoring for conformance to the constraints in the 4D clearance

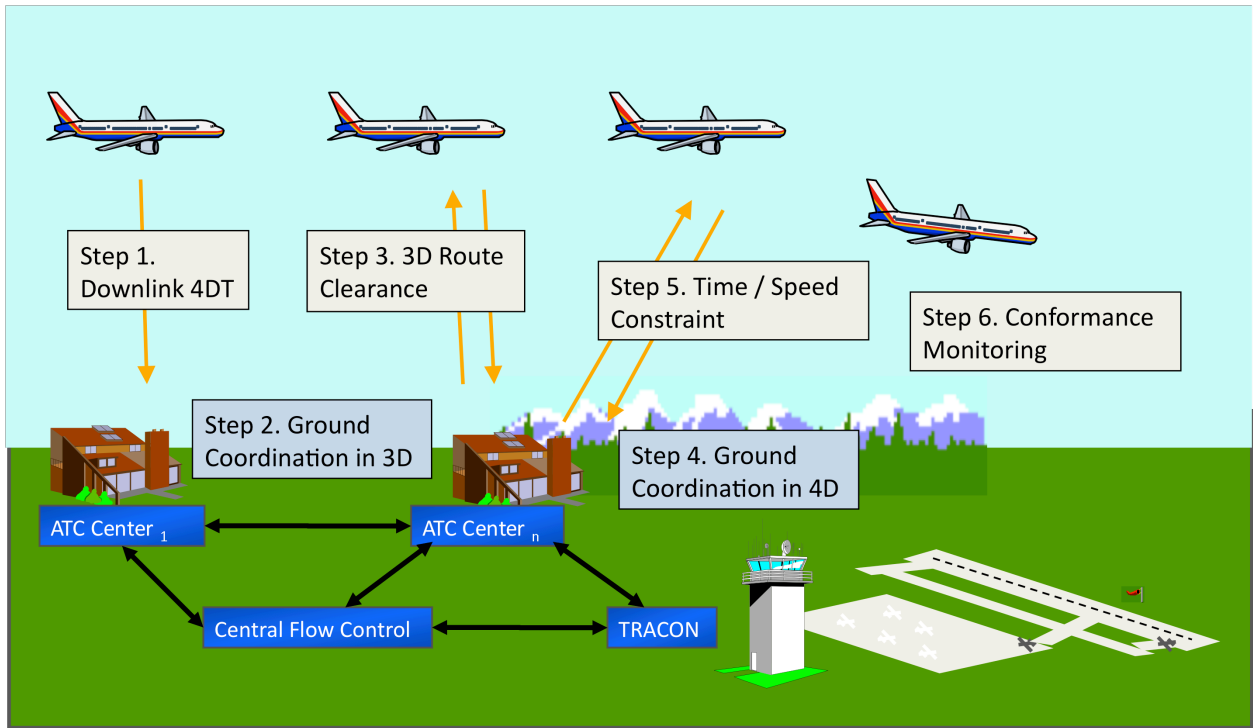


Figure 15-13 4DTRAD negotiation

The 4DTRAD service includes three main capabilities that can be used independently or in concert, depending upon their availability and applicability in specific airspace and aircraft.

Controller Pilot Data Link Communications (CPDLC), software application messages and exchanges as they relate to the amendment of an aircraft's airborne trajectory (through ATC clearances),

Automatic Dependent Surveillance Contract (ADS-C), Extended Projected Profile (EPP), for downlink of aircraft trajectory intent and other relevant information.

The aircraft's capability to meet route, altitude, speed and time constraints as issued in 4DTRAD clearances.

CPDLC will allow controllers and the aircraft to exchange complex route clearances that can be loaded directly into onboard avionics. The CPDLC capability will provide the controller with the ability to specify the desired route for aircraft, including altitude, time or speed constraints as needed to reduce the potential variability of the aircraft trajectories. The SC214/WG78 activity is defining an enhanced message set for CPDLC which will include new messages to support 4DTRAD.

ADS-C EPP will provide the controller with a downlink of the aircraft's predicted trajectory, including the vertical path with speed schedule and predicted times along the trajectory. This standard is now in final coordination within the ICAO Operational Data Link Panel, and the SC214/WG78 group is proposing some additions to the draft standard.

Downlinked 4D Trajectory (via ADS-C EPP).

The 4D trajectory data downlinked from the aircraft is the detailed user preferred trajectory. The ADS-C EPP report describes one possible collection of useful airborne trajectory data that can be downlinked. The ADS-C EPP report includes the following information:

Waypoints, both lateral route waypoints and vertical computed waypoints (T/D, decel points, crossover altitude, etc.)

Altitude, time, and speed predictions at each waypoint

Constraints in the flight plan (altitude, speed, and time constraints) (can be part of published procedures or part of ATC clearances)

Gross weight (approximate)

Min/Max ETA at several waypoints specified by ATC

Predicted ground speed profile, forecasted and sensed environmental conditions, and distances along the lateral path can be used by the FMS to calculate the ETA at downstream waypoints. Additionally, an earliest/latest time window associated with the RTA waypoint can be computed based on flying max/min allowable speed to the waypoint; this time window can be provided to ATC over datalink using an enhanced ADS-C functionality at waypoints specified by ATC.

Air-ground negotiation / synchronization of 3D trajectory

If the trajectory needs to be changed for air traffic considerations, then the ground agreed route with altitude constraints will be uplinked to the aircraft with a CPDLC clearance. The FMS will analyze the implications of the ground proposed trajectory and will either accept or reject it. If the CPDLC clearance is accepted, the clearance is engaged in the FMS, and the updated 4DT is downlinked to the ground. The ground will process and share the trajectory. If the reason for the rejection can be downlinked by the advanced aircraft, it may help the ground system to define a more feasible trajectory modification, which can subsequently be accepted by the advanced aircraft.

As appropriate, the aircraft will load the meteorological data for the modified route to ensure that the predicted times and speeds are accurate.

Air/ground negotiation of time constraint

After the 3D route has been synchronized, the 4th dimension (time / speed) may need to be adjusted to fit with arrival flow management, or to keep aircraft trajectories strategically separated. The ATC responsible for the advanced aircraft issues the time constraint clearance to our advanced vehicle. The FMS reviews the implications of the ground proposed time constraint and will either notify the pilot if this clearance can be met in lieu of the existing trajectory constraints and aircraft performance characteristics.

The ATC ground system can uplink to the aircraft the desired conflict-free trajectory consisting of a 2D lateral route, altitude constraints, and required times of arrival at key waypoints. The avionics reduces the uncertainty in the flown trajectory by applying feedback control onboard the aircraft to track the desired trajectory. If 4D accuracy is required, ATC can specify time constraints at key points in the trajectory and these can be met by the avionics adjusting the airspeed flown based on the onboard

trajectory predictions. Essentially, this approach helps alleviate the need for perfectly eliminating the sources of trajectory prediction error by observing the effects of the errors and taking corrective action.

Today, the FMS cannot accept a pre-defined vertical path, such as a descent path. Instead, altitude constraints are used to specify the path implicitly, combined with FMS standards that define what the FMS can do with these constraints. In the 2020+ timeframe, ATC may uplink multiple proposed trajectories and allow the aircraft to select the most optimum for its mission and corporate objectives.

Conformance monitoring

The flight continues its progression in accordance with the agreed route and constraints.

The aircraft will downlink updated 4DT as the flight progresses, as specified by the ADS-C contract; the contract may include periodic updates and event-based updates, such as predicted speed, time, or altitude deviating beyond specified thresholds.

RTA / TOAC

Many FMS systems today already have the ability to automatically modify the aircraft speed profile during cruise to meet an RTA constraint. The use of this capability has the potential to further reduce controller workload by having the aircraft autonomously make speed adjustments to meet the RTA that would otherwise require controller intervention. However, the FMS RTA systems fielded today can only adjust the aircraft speed profile while the aircraft is prior to the top-of-descent point. Once the aircraft is in descent the present day FMSs cannot automatically adjust the descent speed to meet an RTA point low in the descent phase. The most useful location to place an RTA crossing point is at the Initial Approach Fix, late in the descent phase. So, the present day FMS RTA systems fall short of accurately controlling the time of arrival in the terminal phase of flight.

An airborne control system for achieving waypoint crossing time constraints at multiple waypoints, in any flight phase, is feasible and practical. Placing the feedback control system in the aircraft has the potential to reduce controller workload for time-based Air Traffic Management systems. Airborne RTA also makes concepts such as Continuous Descent Approaches and Tailored Arrivals more practical in moderate traffic density by ensuring that the aircraft will enter the terminal area traffic at a known time, enabling the associated environmental and economic benefits associated with these concepts – reduced fuel consumption, noise, and aircraft delay. RTA reduces the uncertainty in the FMS-flown trajectory by applying feedback control onboard the aircraft to meet the specified waypoint arrival time(s).

The time of arrival control (TOAC) available to the advanced aircraft will enable ATC to specify multiple waypoints in the climb, cruise, enroute and descent flight phases to more precisely control the advanced aircraft's flight along the negotiated trajectory, thereby ensuring safe separation from surrounding traffic. The TOAC accuracy will improve over today's system since blended weather (esp. wind and temperature) data will be available to the FMS for its trajectory prediction and trajectory guidance functionality.

The requirements for the full, long-term solution are still being discussed in the standards committees, and may not be finalized until the after the NextGen and SESAR operational concepts are mature in the next several years. Aspects such as uplink to the aircraft of wind and temperature data at multiple

altitudes at waypoints along the aircraft route, as well as downlink of min/max ETAs at selected waypoints, are not supported by current datalink messages, and a means of communicating these data will be required in the long term.

15.15. ***Aircraft Separation***

Enhanced surveillance and new procedures enable the ANSP to delegate aircraft-to-aircraft separation. Improved display avionics and broadcast positional data provide detailed traffic situation awareness to the flight deck. When authorized by the controller, pilots will implement delegated separation between equipment aircraft using established procedures. Delegated separation operations planned for NextGen include delegated Separation for Specific Operations or Complex Operations, Delegated Separation in Flow Corridors, and Reduced Oceanic Separation – Co-Altitude Pair-wise Maneuvers. (FAA, Delivering NextGen Trajectory Based Operations, 2009)

Advanced airborne navigation technologies such as flight planning, flight management, flight guidance, flight control, and aircraft state sensing will enable aircraft to execute accurate flight trajectories and assist with self-separation maneuvers. Improved navigation accuracy will permit a reduction in the separation standards used in oceanic and remote areas.

Delegated separation operations may give rise to hazardous conditions for the SST, at altitudes where their speeds may be significantly higher than the aircraft surrounding them. The resulting high closure rates will impact existing safety equipment onboard the aircraft, and the reaction time remaining for the pilot, or automation to avert a collision. The existing collision avoidance algorithms and surveillance algorithms will need to be updated to handle supersonic flight. For instance, the TCAS surveillance algorithms do not handle closure rates greater than 1200 knots and existing collision avoidance algorithms evaluation (Monte Carlo -etc) were not done with supersonic aircraft in the model. At Mach 1.6, existing algorithms will have to be modified to handle this higher closure rate. Strategic conflict detection and resolution (CD&R) functionality combined with automated tactical CD&R may be required to avert collisions at supersonic speeds.

15.16. ***Operational Capability: Merging and Spacing***

Avionics to aid the pilot in safe and Efficient Metroplex Merging and Spacing operations are needed to avoid the possibility of the loss of separation minima's or (near) mid air collision.

Aircraft funneled into the same airport may be cleared to merge and self separate using onboard traffic and navigation displays. A leading aircraft may follow a negotiated trajectory, while trailing aircraft maintain a specified time or distance behind the leading aircraft. The time separation between the two aircraft is calculated by the ATM automation system based on wake vortex considerations, runway occupancy time estimates, and regulatory separation requirements. A trailing aircraft must adjust its spacing requirement to take real-time wake vortex from the leading aircraft into account. Enhanced algorithms for merging and spacing requiring additional information such as arrival routes, final approach speed, and wake vortex class are under investigation at NASA Langley Research Center (Krishnamurthy 2005).

During merging and spacing operations, flights follow speed guidance to meet an absolute time using their onboard equipment until they come into ADS-B range of their lead-aircraft. The lead aircraft provides state and trajectory information using ADS-B to assist the trailing aircraft in maintaining the desired separation. Once they are in ADS-B range, flights follow relative spacing guidance. Spacing guidance is based on a trajectory-based spacing algorithm. The self-spacing system provides the trailing aircraft with guidance cues to the autopilot/auto throttle and the pilot displays while the flight crew maintains situational awareness by use of a CDTI display. After their top of descent, flights follow a published CDA to the final merge fix and the runway.

“For the sequencing and merging application, it is desirable for the system to have a broadcast uplink capability. A back-up system for GNSS needs to be selected to allow higher accuracy navigation even in the presence of GNSS outages. A method of fusing surveillance data from multiple sensors needs to be selected and a networked surveillance system needs to be developed. The optional extensions of ADS-B that support the transmission of intent information need to be required and fielded widespread. An ubiquitous TCAS-equivalent capability will be needed by all participating aircraft.” (Morgenstern2006)

15.16.1. Merging and Spacing using Optimized Profile descents

The emissions research conducted by ATAC on this NASA NRA indicates that SST emissions are worse than the emissions from commercial jets in the terminal area. Thus it is essential that SST's are allowed to execute optimal descent profiles into high traffic environments to minimize the fuel burn during descent. Since the SST will fly at subsonic speeds while operating in the terminal area or at altitudes frequented by subsonic transports, the SST will be no more vulnerable to hazards during this maneuver than traditional subsonic aircraft.

Procedures for Continuous Descent Approach (CDA) and Optimized Profile Descents (OPD) are being fielded today to allow aircraft to approach moderately dense terminal areas while flying efficient, near-idle descent trajectories that save fuel, and reduce emissions and noise. (Shresta, 2009). CDA procedures are a compromise between allowing the FMS to fly an unconstrained optimal descent and ATC procedures for optimizing the throughput of the airspace. (Sprong, 2008). Future flight management systems will combine the execution of CDAs with time of arrival control (TOAC) to optimize the fuel and cost savings for the operator while still meeting the aircraft trajectory constraints dictated by ATC.

15.17. **Operational Capability: Delegated Separation in Flow Corridors**

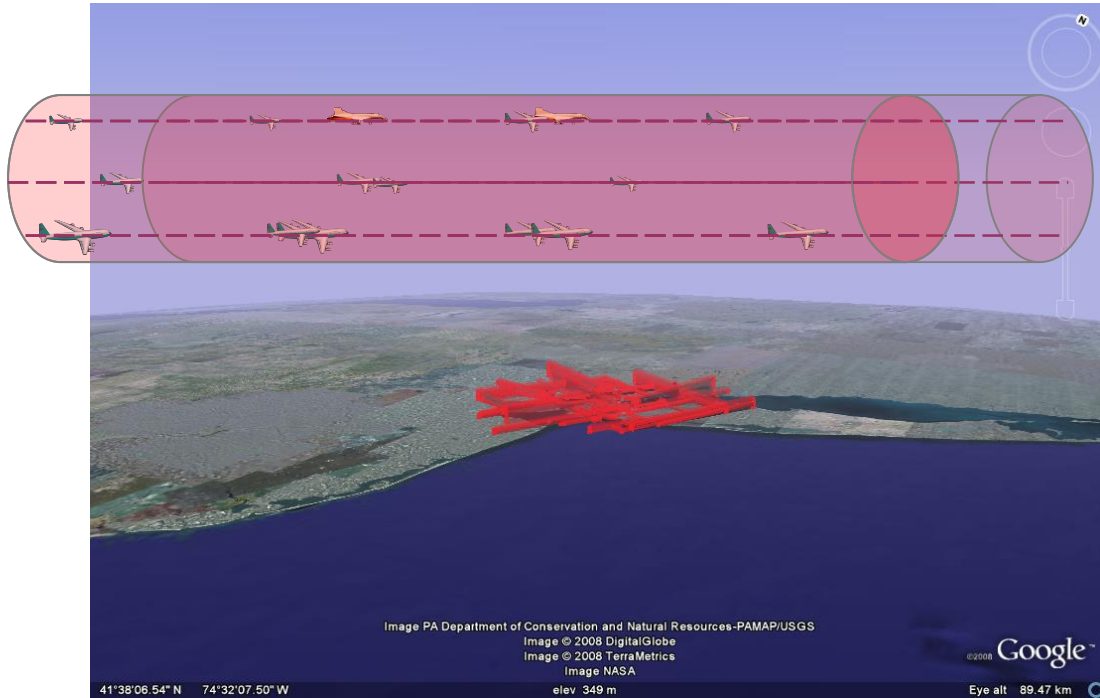


Figure 15-14 Enroute Traffic Flow

Flow corridors can be considered interstate highways in the sky that contain parallel streams of aircraft where aircraft are self-separating. ATC and the flight crew will require tool support for the delegation of self-separation operations and the negotiation of the end of self-separation in flow corridors. This includes tool support for entry slot identification, 4DT constraint specification, negotiation and monitoring, and exit negotiation for flow corridors.

15.18. **Operational Capability: Self-Separation - Self-Separation Airspace**

Airborne self separation (SSEP) in self separation airspace (SSA) is an operational capability not anticipated until the far term timeframe. During SSEP, the flight crew is responsible for separation from other aircraft and other obstacles while continuing to adhere to flow management constraints. During the self separation operations, the flight crew will have several new and/or modified responsibilities:

- Separation assurance from other aircraft.
- Trajectory Management:
- Tactical de-confliction
- Avoidance of high complexity areas
- Avoidance of Weather Hazard Area (WHA) and Restricted Airspace Area (RAA)
- Overall trajectory optimization
- CTA/RTAs compliance.
- Monitoring of data communications.

15.18.1. Airborne self separation scenario

A typical airborne self separation flight may have the following progression: An aircraft takes off from the airport and climbs through the departure TMA, where the traffic flow is controlled by the Air Navigation Service Provider (ANSP) responsible for aircraft separation. A 4D flight trajectory has been negotiated and approved by ATC before take-off. When leaving the departure TMA, the responsibility for separation is shifted from the ANSP to the flight crew.

During self separation operations, the flight crew can modify the aircraft trajectory without negotiation with any ANSP, provided that defined autonomous flight rules are satisfied and that the Controlled Time of Arrival (CTA) at the destination TMA will be achieved. If there is a need to modify the CTA constraints, this change must be negotiated with the ANSP in control of the destination TMA. In Self Separation Airspace (SSA), the aircraft does not need to follow any predefined airway structure.

Within SSA, flight and weather data will be exchanged among aircraft via data link, with voice communications only in emergency situations. Each aircraft flying in SSA continuously broadcasts aircraft state vector and if possible trajectory intent data to allow surrounding aircraft to predict its planned trajectory.

Onboard avionics will aid the flight crew in preventing a Loss of Separation (LoS). Avionics for collision avoidance (preventing a collision in the case of LoS) is identical for aircraft operating in SSA or in ATC-managed airspace. All conflicts should be solved using the onboard conflict management functionality, with ACAS only as a safety backup.

To ensure separation and onboard trajectory management tasks, the SST flight crew will need onboard avionics support to monitor the aircraft surroundings and help the flight crew to detect and resolve conflicts.

When a conflict is detected within a time-to-separation loss that allows for longer-term conflict resolution (CR), the onboard equipment will propose a solution, which is then assessed by the flight crew. When the solution is approved by the flight crew, the flown trajectory is updated and the aircraft broadcasts its new state and intent information. When time-to-separation loss is imminent, the collision avoidance system will take precedence and direct crew alerting followed by possible automated maneuvering will occur to prevent the imminent collision.

When the aircraft approaches its destination TMA, the responsibility for separation is shifted back from the flight crew to the ANSP and the self-separation part of the flight is terminated. (Casek, Petr; Gelnarova, Eva, 2009)

15.18.2. Avionics to enable airborne self separation

Self separation operations are enabled by cooperative airborne surveillance, data communication and by onboard automation that monitors traffic, detects potential conflicts, provides situation awareness and conflict avoidance solutions to the flight crew. An integrated set of functionality will be required onboard our advanced vehicle to support trajectory-based operations combined with aircraft self-separation.

The advanced vehicle flight crew will require new decision support tools which will help reduce pilot workload, provide additional situation awareness and enhance the longevity of the conflict avoidance solution (i.e., prevent secondary conflicts, avoid conflicts with all obstacles in the timeframe considered). Traffic surveillance and navigation information will be displayed to facilitate informed pilot decision making, and easy maneuver execution.

Data communication and surveillance will be key enablers of SSEP operations. Data exchanged during the SSEP operation may be divided into three main types:

- Data broadcasted by the autonomous aircraft (ADS-B).
 - Broadcasted state information in the form of State Vector and Identifier (which is part of Mode Status) and Air Referenced Velocity Report (DO-260A) (all SL).
 - Air-Air data links State Vector Accuracy, Update Interval and Acquisition Range Requirements meet the Equipage class A3 (DO-242A)
- Information provided to/by a ground supporting system (SWIM). SWIM is expected to work in two models: pull model, when data are sent to user upon request, and push model, when data (e.g., Wx) is periodically sent.
- Voice communication which will remain the backup means of communication in nonstandard or emergency situations.

Airborne Separation Assurance System

The Airborne Separation Assurance System will combine trajectory management and conflict management functionality to provide the flight crew with conflict detection and resolution functionality for both strategic and tactical flight modes.

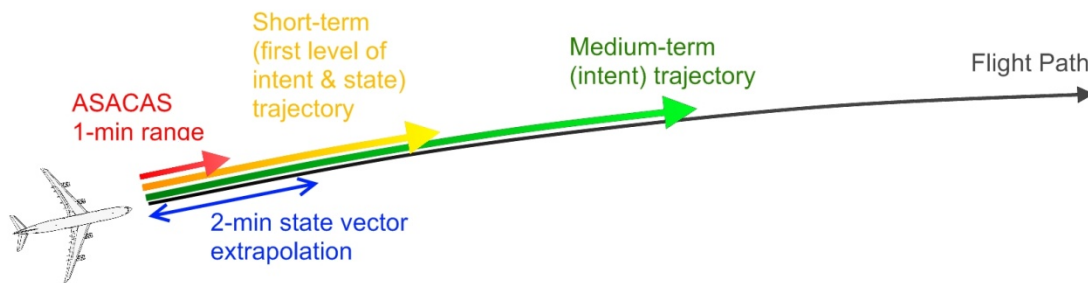


Figure 15-15 CD&R methods and their associated time-to-Loss of separation.

Long term trajectory management (TM) is focused beyond 20 minutes. Using Long Term Area Conflict Detection (LTACD), long term TM will provide the pilot with trajectory modifications that that will avoid potential future traffic conflicts and dynamic weather hazards.

Conflict management provides detection and resolution of conflicts with traffic and well-defined area hazards, and provides the flight crew with alerting and situation enhancement. A typical, nominal time horizon for strategic conflict management is 10 to 20 minutes.

Intent-based conflict detection and Alerting

The nominal look-ahead time for intent-based CD is 10 minutes. This time horizon provides more than adequate time for alerting and strategic conflict resolution (CR) in highly complex and constrained scenarios (Wing, 2009).

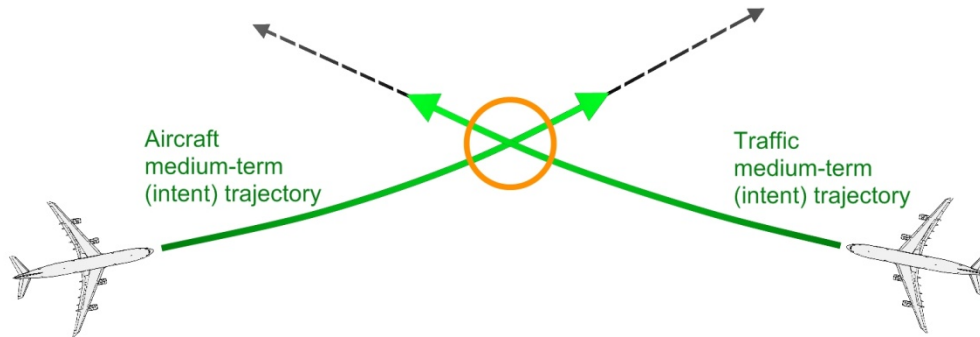


Figure 15-16 Medium term, intent-based Conflict Detection

Strategic Intent-based Conflict Resolution

Strategic Intent-based Conflict Resolution provides CR options for the flight crew in terms of modifications to the FMS active route. The resolutions provide separation from all aircraft and reconnect to the original route while keeping the aircraft on the negotiated 4D trajectory and pre-existing trajectory constraints. SICR is the primary and preferred method for conflict resolution, as it allows the aircraft to remain in the strategic flight mode (i.e., FMS-coupled) throughout the resolution maneuver.

Tactical Intent-based Conflict Resolution

When normal flight operations cannot be conducted in a strategic flight mode, e.g., amidst dynamic convective weather, conflict resolution and obstacle avoidance may become highly tactical as the flight crew maneuvers around hazards they identify visually and via onboard weather radar. When the strategic function cannot find a solution or when time is short, tactical intent-based conflict resolution functionality uses shorter look-ahead horizons to find viable solutions using tactical operations. Flight crews frequently adapt to this situation by flying in tactical guidance modes that provide more agile decision-making, and maneuvering without heads-down time. Tactical Intent-based Conflict Resolution support tactical flight modes without giving up some of the advantages of strategic conflict management, such as longer look-ahead horizons, the ability to separate from all nearby traffic, and the use of available intent data from traffic and from the ownship.

State-based CD&R

Intent-based conflict management is complemented by independent and parallel state-based conflict detection (SBCD) and state-based conflict resolution (SBCR) functionality. SBCD uses only state-vector data for detecting conflicts. State-based systems limitations include short time horizons, unutilized intent data, including even limited ownship intent in the form of target states, and they can handle only one conflict aircraft during conflict resolution. However, by not using intent, state-based approaches are immune to intent-based faults such as non-conformance and blunders (Wing, 2009).

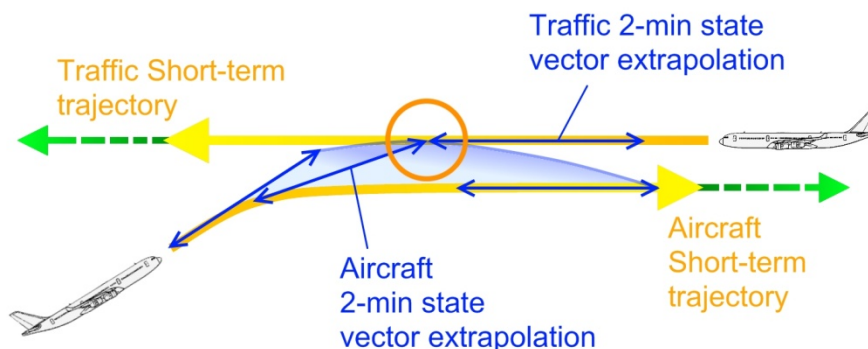


Figure 15-17 Short term, state based conflict detection and resolution maneuvers.

ASAS Self separation as an advanced separation mode will require new data-links (L band, SATCOM, ADS-B), high integrity trajectory management, synthetic vision and a comprehensive conflict management system. Key enablers include ADS-B In, OUT, CDTI, ADS-C, surveillance sensors, dual GNUS for Navigation and VDLM2, VHF, SATCOM for Communication. System dependencies include the FMS (RNAV/ RNP), TCAS and SWIM.

15.19. **Operational Capability: Data Link Clearance Delivery and Taxi instructions**

15.19.1. Data Link Taxi Clearance (D-TAXI)

The D-TAXI service provides datalink communication between the aircraft and the Air Traffic Service (ATS) system in order to obtain the necessary clearances to proceed between any two points on the airport surface (e.g., between the hanger or gate and the runway).

D-TAXI is used for start-up, push-back, and taxi clearances as well as special airport operations such as taxiing to/from a de-icing area. D-TAXI may also be used to provide pre-departure and pre-arrival information related to the expected taxi route.

D-TAXI clearances are usually provided in response to a request by the aircraft, but may also be initiated by the ATS controller or automation. A D-TAXI clearance may be requested and/or issued while the aircraft is in the approach pattern, or after the aircraft has landed.

D_TAXI requests over ATN are “request/reply” services where the aircraft submits a D_TAXI clearance request over datalink. The aircraft avionics can communicate directly with the automation in the control tower to make the request. When the D_TAXI clearance has been received from ATS, the aircraft receives a clearance (e.g., start-up). When the aircraft can comply with the start-up clearance, the flight crew responds with a WILCO and proceeds with the cleared operation. Various other communication sequences between the US and ATSU system can occur, as listed in the RTCA SC-214/EUROCAE WG-78 Air traffic Services Safety and Interoperability Requirements document.

15.20. **Operational Capability: Increase access and throughput at uncontrolled airports**

Advanced airborne technologies will be needed to safely and efficiently conduct flight operations at airports with minimal or insufficient ground infrastructure. New airborne technologies such as EVS/SVS, HUD, auto land systems, airborne avionics for GBAS Cat II/III (more stringent CAT-II/III precision approach and landing), or integrated GNSS / INS or GNSS/AHRS systems will pave the way for VLJs and UA to take greater advantage of small, non-hub airports and runways.

15.21. **Operational Capabilities: Low-Visibility Approach, Landing, Take-Off**

15.21.1. Enhanced and Synthetic Vision Systems (ESVS)

EVS and SVS technology will aid the crew of advanced aircraft in night and low visibility operations into low infrastructure airports where airport lighting may not be installed. Pilots must retain situational awareness during these high workload operations and the EVS/SVS terrain avoidance, alerting and situation awareness display tool may provide the time-critical information necessary to keep the advanced aircraft pilots from infringing into safety hazardous threat areas. On-board enhanced and synthetic vision systems will also be available to support surface movement operations and improve approach and departure operations. The crew will be provided with an integrated, synthetic, graphical view of the flight path and terrain. The SVS/EVS systems will use terrain imagery from the terrain database, and process

raw sensor data from the air data computer (ADC), inertial reference system (IRS), and global positioning system (GPS) in order to produce smooth PFD symbology displays and real-time moving synthetic view terrain images to enable safe approach and ground operations. Figure 15-18 depicts an IPFD display as the aircraft approaches an airport for landing.



Figure 15-18 IPFD during landing

The on-board Synthetic Vision System available in the 2020 timeframe will integrate the Synthetic Vision (SV) Primary Flight Display system with the Enhanced Ground Proximity Warning System (E-GPWS), or TAWS. The terrain threat information from the E-GPWS system will be displayed with synthetic vision terrain background in a coordinated 3D perspective-view and 2D lateral map format for improved situation awareness. The flight path based display symbology will provide unambiguous information to flight crews for recovery and avoidance with respect to threats (terrain, obstacles, and restricted flight areas). The SV based display will also help the flight crew maintain situational awareness, prevent blunders in low visibility situations, and further prevent the accident chain that typically precedes control flight into terrain (CFIT) accidents. The IPFD display will clearly show where the potential conflicts will be for the current flight path well ahead of triggering E-GPWS events. It will offer an increased lead time for hazard detection thus reducing the likelihood of operating an aircraft into hazardous situations during impaired situational awareness. The flight path based symbology displayed with the terrain threat areas will show the recovery path clearly for the current flight conditions.

The TAWS functionality will interact with the RNP arrival, approach and departure functions, to provide sufficient terrain predictive alerting yet avoid nuisance alerts when the aircraft is in terrain/obstacle challenging low-RNP. The integrated SVS/EVS system will recognize when the aircraft is in compliance with the intended RNP procedure, and warn the flight crew when failure to follow a defined procedure introduces a potential terrain or obstacle collision threat.

Honeywell has started flight testing a technology that merges the view of an infrared enhanced-vision system (EVS) with that of a synthetic-vision system (SVS) to give pilots a new way of seeing the world at

night or in poor visibility using a Cessna Citation V and a Sovereign fitted with forward-looking IR sensors and its SmartView SVS . The integrated EVS/SVS system will be available for installation on aircraft around the 2012 to 2013 time frame, and will not require the use of a head-up display. Rockwell Collins has started testing a similar technology for its developmental Pro Line Fusion cockpit. Developers of this new technology hope that the combination of SVS and EVS may results in the FAA permitting lower approach minimums for aircraft installed with this integrated EVS/SVS system. Current rules let EVS/HUD-equipped airplanes descend to 100 feet on straight-in precision instrument approaches if the pilot can see the runway environment with the EVS. (Pope, September 10, 2009).

15.21.2. Localizer Performance with Vertical Guidance (LPV)

Most business aircraft operations are conducted from non Instrument Landing System (ILS) airports which restrict incoming aircraft to non precision approaches. Using non precision approaches in less than desirable weather conditions can result in a missed approach due to low ceilings and may force the aircraft to divert to an alternate airport with better weather minimums. Localizer Performance with Vertical Guidance (LPV) approaches, accomplished with a WAAS GPS receiver, allow minimums as low as 200 feet Above Ground Level (AGL) and visibility minimums as low as one-half mile before a missed approach must be executed. LPV approaches provide operators with fuel savings due to reduced diversions to alternate airports. The fuel and cost savings are significant considering the amount of airports that do not have ILS installed.

15.21.3. GPS/Global Navigation Satellite System Landing System (GLS)

GBAS enables the aircraft to execute precision approaches to all runways ends. Honeywell and Air services Australia have developed the GLS system, a Ground-Based Augmentation System (GBAS) that correlates GPS signals received on the ground to correct any errors in the data from the satellites. GLS is a procession approach type, much like ILS. GLS approaches and augmentation signals are transmitted from a VHF ground station to the airplanes MultiMode Receiver (MMR). The MMR computes localizer and glide slope deviations using the uplinked approach coordinates and the augmented GPS lateral and vertical positions.

The FMS stores GLS approaches in the navigation database. The aircraft executes the GLS approach in the FMS and auto-tunes the VHF channel on the GBAS ground station. The FMS can use the augmented GPS position to improve the Actual Navigation Performance (ANP) for RNAV operations. The onboard autopilot must also be upgraded to reflect this new mode. The approach path information can also be broadcast to the aircraft. If an airport creates a new approach (e.g., displaced threshold due to construction), the aircraft can utilize the approach. It provides the aircraft with better navigation performance (improved EPU) when it receives Position, Velocity and Time (PVT) information from GBAS.

Several airports around the world already have prototype systems installed include Memphis (Tenn.) International; Atlantic City (N.J.) International (near the FAA's William J. Hughes Technical Center); and airports at Bremen, Germany, and Malaga, Spain. The on-board avionics make it possible for the aircraft to fly Cat. 1 approaches to a 200-ft. decision altitude. The GLS system will be improved to provide Cat. 2 (100 ft.) and 3 (near zero-zero) landings in the years to come. FAA Cat. 3 certification is expected in about 2012.

737 NGs are already equipped with the Rockwell Collins multi-mode receivers needed for the aircraft to fly a GLS and Honeywell has recently developed the airborne equipment needed to fly a GLS for the Gulfstream G650.

The TAWS functionality will interact with the RNP arrival, approach and departure functions, to provide sufficient terrain predictive alerting yet avoid nuisance alerts when the aircraft is in terrain/obstacle challenging low-RNP. The integrated EGPWS system will recognize when the aircraft is in compliance with the intended RNP procedure, and warn the flight recovery system (and the remote pilot) when failure to follow a defined procedure introduces a potential terrain or obstacle collision threat.

15.22. **Avionics Bibliography**

ADS-B. (2008, August). Retrieved December 2008, from MITRE Aviation:
http://www.mitre.org/news/digest/aviation/08_08/av_adsb.html

Agency, N. S. (2008). *NSA Suite B Cryptography*. Retrieved February 2009, from National Security Agency Central Security Service: http://www.nsa.gov/ia/programs/suiteb_cryptography/index.shtml

Alfredo Colon et al. (2009). Unmanned Aerial Systems Safety Analysis: New Hazards Identification.

Alfredo Colon. (2008). Very Light Jet Safety -- New Hazards.

Andrew R. Lacher, David R. Maroney, Dr. Andrew D. Zeitlin. (2007). *UNMANNED AIRCRAFT COLLISION AVOIDANCE –TECHNOLOGY ASSESSMENT AND EVALUATION METHODS*. McLean, VA, USA: The MITRE Corporation.

Bateman, Don. (2008). A Review of Some Technology Aids to Support the Flight Safety Foundation Runway Safety Initiative. *61st Annual International Air Safety Seminar (IASS) Flight Safety Foundation*.

Casek, P. et al. (2008). Safety, Complexity and Responsibility based design and validation of highly automated Air Traffic Management. Framework 6 Programme.

C. Tiana, R. H. (2006). Fused enhanced and synthetic vision systems (EVS/SVS) for low-visibility operations. *Proc. SPIE 6559*.

C. W. Acree, J. H. (2008). Performance Optimization of the NASA Large Civil Tiltrotor. *IPLC*.

Captain J Leslie Robinson, N. P. Very Light Jets Impacts on NAS Operations. *Consortium for Aviation System Advancement (CASA) web site*:
http://www.casa.aero/adminUploads/TheVeryLightJet_ATCA.pdf.

Cessna Caravan. (n.d.). Retrieved February 16, 2009, from Cessna Aircraft Company:
<http://www.cessna.com/caravan.html>

Colon, Alfredo. (2009). Civil Tiltrotor Safety Analysis: Initial Hazards Identification.

Croft, J. (2008, May 30). *UAV Autonomy - Flying sense*. Retrieved March 2009, from Flight International: <http://www.flightglobal.com/articles/2008/05/30/224349/uav-autonomy-flying-sense.html>

Data Communications Program Overview – Air/Ground Connectivity for the Next Generation Air transportation System (NextGen). (2008., January 5). FAA.

Eclipse 500 Operation Features. (n.d.). Retrieved 12 15, 2008, from Eclipse Aviation: <http://www.eclipseaviation.com/eclipse500/operation/features.php>

Egozi, A. (2008, April 02). Israel's Aeronautics prepares unmanned D-Jet. *Flight International* .

Eurocontrol. (2009, May 15). *Mitigation of Wake Turbulence Hazard*. Retrieved July 13, 2009, from SKYbrary wiki: http://www.skybrary.aero/index.php/Mitigation_of_Wake_Turbulence_Hazard

FAA. (2008, January 5). Data Communications Program Overview – Air/Ground Connectivity for the Next Generation Air transportation System (NextGen).

FAA to Publish Nearly 100 RNAV/RNP Procedures in 2007. (2007). Retrieved from Flt Tech Online: <http://www.fltteconline.com/Current/FAA%20to%20Publish%20Nearly%20100%20RNAV-RNP%20Procedures%20in%202007.htm>

Frederick Wieland, J. S. (2009). Implications of New Aircraft Technology on the Next Generation Air transportation System. *ATM*.

Gang He, T. F. (2008). Synthetic Vision Primary Flight Displays for Helicopters. *SPIE*.

GAO. (2007). VERY LIGHT JETS - Several Factors Could Influence Their Effect on the National Airspace System. <http://www.gao.gov/cgi-bin/getrpt?GAO-07-1001>.

Heimerl, L. (2009, February 27). *Modeling Tool Advances Rotorcraft Design*. Retrieved July 13, 2009, from NASA Scientific and Technical Information (STI): http://www.sti.nasa.gov/tto/Spinoff2007/t_2.html

Holmes, B. (2008). Implementing Next-Generation Air Transportation System Technologies. *Proceedings of the 26th International Conference on the Aeronautical Sciences*. Anchorage, Alaska.

Holmes, B. (2008). Very Light Jets. *NASA Annual Meeting*.

Honeywell claims new software helps avoid air collisions. (2005, September 9). *Xinhua News Agency*.

Hughes, D. (2008, October 20). Honeywell Civil Air Navigation Innovation Nears Completion. *Aviation Week & Space Technology* , p. 53.

ICAO. Manual for the ATN using IPS Standards and Protocols (Doc 9896). ICAO.

James Stack, J. C. (2004, 11 24). *Helicopter Wake Vortices*. Retrieved 7 13, 2009, from http://www.me.berkeley.edu/fml/projects/helicopter_wake.html

JPDO, A. W. (October 2008). NextGen Avionics Roadmap, version 1.0. FAA.

JPDO, J. P. (13 June 2007.). CONCEPT OF OPERATIONS FOR THE AIR TRAFFIC MANAGEMENT OPERATIONS NEXT GENERATION AIR TRANSPORTATION SYSTEM (NEXTGEN) CHAPTER 2 VERSION 2.0.

Lampe, S. (n.d.). *navigation and autoflight*. Retrieved May 7, 2009, from AircraftMech: <http://www.aircraftmech.com/avio.html>

M. Hebel, K. B. (2006). Imaging sensor fusion and enhanced vision for helicopter landing operations. *Proc. SPIE 6226*.

M.L. Cummings, J. P. (2006). Human Performance Considerations in the Development of Interoperability Standards for UAV Interfaces. *Moving Autonomy Forward Conference 2006*. Lincoln, UK.

Matthew DeGarmo and Gregory M. Nelson. Prospective Unmanned Aerial Vehicle Operations in the Future National Airspace System , MITRE public release, case #04-0936. MITRE.

(2004). MK XXII Helicopter –Enhanced ground Proximity Warning System Pilot’s Guide .

N. Yonemoto, e. a. (2003). Obstacles detection and warning for helicopter flight using infrared and millimeter wave. *Proc. SPIE 5081*, (pp. 31-38).

Neale, M. (12/12/07). UAS Control and Communications System Technology Roadmap, SC-203 Position paper IP-WG2-003-A, rev A. RTCA.

Pasztor, A. (2007, December 20). New Technology Helps Pilots Avoid Runway Collisions. *The Wall Street Journal* , p. D8.

Pasztor, A. (2008, November 7). U.S. News: rise in Collision Hazards For Planes Spurs Changes. *The Wall Street Journal* , p. A4.

Perone, J. R. (2004, June 3). Honeywell tests air-crash system. *Business, The Start-Ledger*

Pope, S. (September 10, 2009). Honeywell’s SVS/EVS Could Yield Lower Minimums. *Avionics* .

RTCA, S.-2. (2009, January 09). SC-203 RW0001_Requirements baseline.

RTCA, S.-2. (n.d.). *SC-203 Unmanned Aircraft Systems*. Retrieved February 2009, from RTCA: <http://www.rtca.org/comm/Committee.cfm?id=45>

RTCA, S.-2. U. (2007). UAS CONTROL AND COMMUNICATIONS LINK SPECTRUM CONSIDERATIONS. Washington D.C.: RTCA Inc.

SPG Media, L. Eclipse 500 Very Light Jet, USA. <http://www.aerospace-technology.com/projects/eclipse-avi/>.

Team, I. I. (2009). Third International Helicopter Safety Symposium (IHSS 2009). Retrieved from www.ihst.org.

Tom McGuffin and Karl Klewer. (2007, October 10-11). Honeywell presentation at the Link 2000+ Wide scale Implementation Workshop.

Trimble. (2005, September 20). Recovery system will override pilot. *Flight International* .

TRW. (n.d.). *TRW Begins Flight Testing Stage for Automatic Landing Of U.S. Army's Hunter UAV*. Retrieved May 5, 2009, from <http://www.sncorp.com/news/hunter.html>

United States Government Accountability Office. (2008). *Unmanned Aircraft Systems: Federal Actions Needed to Ensure Safety and Expand Their Potential Uses within the National Airspace System*. Washington, D.C.: United States Government Accountability Office.

WAAS-FMS. (2009). *WAAS Capable GPS and FMS System Solutions for your Aircraft - Utilizing LPV Approach Capability and RNP Procedure Technology*. Retrieved September 18, 2009, from WAAS FMS: <http://www.waasfms.com/>

Weber, R., Blom, H., & Casek, P. (2008). Safe, airborne self-separation operations in tomorrow's airspace? *International System Safety Conference*. Vancouver.

Weber, Rosa. (2008). *Avionics Roadmap for CESTOL Aircraft in NextGen*.

Wing, D. J. (2005). A Potentially Useful Role for Airborne Separation in 4D-Trajectory ATM Operations. *AIAA-2005*.

Wing, D. V. (2009). *Airborne Tactical Intent-Based Conflict Resolution Capability*. 9th AIAA Aviation Technology, Integration, and Operations Conference (ATIO). Hilton Head, SC: AIAA.

cxviii Datalink service that provides OTIS (combined ATIS and NOTAM), ATIS, NOTAM or VOLMET reports.

cxix Mid-term for LCTR

cxx Mid-term if the FAA reauthorization bill is enacted which requires the FAA to accelerate planned timelines for integrating Automatic Dependent Surveillance-Broadcast (ADS-B) technology into the NAS, requiring the use of "ADS-B Out" on all aircraft by 2015 and "ADS-B In" on all aircraft by 2018. If not, ADS-B In will be available in the far term.

cxxi Runway incursion: Any occurrence at an airport involving the incorrect presence of an aircraft, vehicle or person on the protected area of a surface designated for the landing and take-off of aircraft. (Source: FAA).

cxxii Runway excursion: Any aircraft having a loss of directional control either on takeoff or landing which exits a runway other than a designated exit point (e.g. pilots conducting other than full length operations from wrong intersection or overshoot an approach).

cxxiii Runway overrun: When the chosen flight path is flown above the required glide path to where the vehicle lands beyond its intended point of touch down.

cxxiv Runway underrun: When the chosen flight path is flown below the required glide path to where the vehicle lands short of its intended point of touch down. This results in landing short of the runway.

cxxv Mid term for LCTR.

cxxvi Runway excursion: Any aircraft having a loss of directional control either on takeoff or landing which exits a runway other than a designated exit point (e.g. pilots conducting other than full length operations from wrong intersection or overshoot an approach).

cxxvii ACSS is a joint Honeywell, L-3 Communications-Thales joint venture funded by the FAA surveillance and broadcast services office.

16. Environmental Impacts

New vehicle concepts in the NextGen airspace can be evaluated in terms of energy and environmental impact areas at three levels of resolution: are vehicle, regional, and national. For this study, regional and national can alternatively be thought of as metroplex and system-wide, respectively. The environmental impact areas we consider are noise, air quality, and climate. It is important to account for the different categories of environmental impacts as the mix of effects and stakeholders impacted varies across them. Climate impacts, for example, are realized globally whereas noise impacts are mostly felt by people who live in the immediate vicinity of airports. The metrics and assessment tools of relevance also vary across the different categories. For instance, calculating climate impacts at the system-wide level requires an integrated climate model capable of evaluating impacts on the global scale, whereas impacts at the vehicle level can be determined from aircraft characteristics and first principles.

In order to capture the range of environmental impacts and spatial resolutions, a set of environmental assessment metrics have been defined that are relevant to the study, as detailed in Table 16-1.

Table 16-1. Environmental impact metrics.

Level	Environment			
	Energy	Noise	Air Quality	Climate
NATIONAL / SYSTEM-WIDE	Sum of the energy consumed by operations between all airports normalized by revenue payload-distance carried on those flights	Sum of the % change in population exposure to X dB DNL due to operations at all airports	Sum of % change in premature mortality due to total PM _{2.5} exposure due to operations at all airports (considering emissions of PM, NO _x , and SO _x)	Change in time-integrated, globally averaged surface temperature change due to operations at and between all airports (considering emissions of CH ₄ , N ₂ O and CO ₂ that result from fuel production and combustion emissions of CO ₂ , H ₂ O, NO _x , SO _x , and PM, as well as formation of contrails-cirrus clouds)
REGIONAL / METROPLEX	Sum of the energy consumed by all operations at metroplex / terminal area / airport normalized by payload-distance carried on those flights	Change in population exposure to X dB DNL due to all operations at metroplex / terminal area / airport	Change in premature mortality due to total PM _{2.5} exposure due to all operations at metroplex / terminal area / airport (considering emissions of PM, NO _x , and SO _x)	Change in life cycle greenhouse gas emissions (described at the national level) due to all operations at metroplex / terminal area / airport
VEHICLE	Energy consumed by individual aircraft operation normalized by available revenue payload-distance carried	Change in population exposure to X dB LA _{max} due to a single aircraft operation	Change in emissions of PM, NO _x , and SO _x due to a single aircraft operation	Change in life cycle greenhouse gas emissions (described at the national level due to a single aircraft operation)

Although all of these metrics could be determined using the modeling tools available, time constraints required that a reduced subset be examined, and hence the environmental impact analysis focused on three important elements of this metrics table: system-wide climate (only combustion emissions); metroplex air quality in terms of changes to ambient PM2.5 concentration; and metroplex noise. The tool that enables us to calculate the target metrics in these sectors and also allows us to monetize impacts is the Aviation environmental Portfolio Management Tool-Impacts (APMT-Impacts), described in the next section.

16.1. APMT-Impacts

When exploring aviation policy options, policy makers have historically regulated the environmental impact of aviation by setting noise and emissions certification standards. However, it is becoming increasingly important to evaluate the complex interdependencies among aviation’s impact on climate, air quality and noise. Knowing how these impacts interact and evolve in the future is vital when it comes to designing effective and sustainable environmental policies. APMT-Impacts—developed and run by MIT—is a component of the FAA’s Aviation Environmental Tools Suite that uses a flexible, probabilistic framework for estimating the physical and socio-economic environmental impacts of aviation. The structure and components of the FAA’s Aviation Environmental Tools Suite are depicted in Figure 16-1.

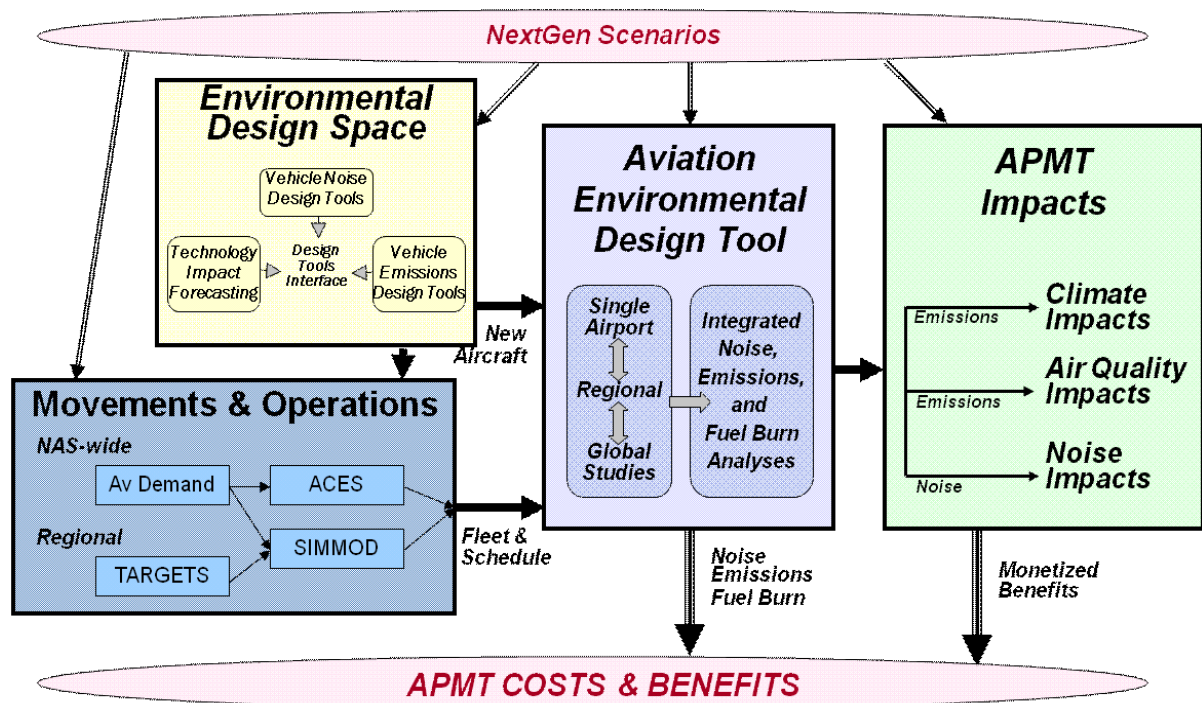


Figure 16-1. FAA Aviation Environmental Tools Suite.

For this project, APMT-Impacts uses noise and emissions inventories produced in the Aviation Environmental Design Tool (AEDT) as the primary inputs. Since uncertainty with many aviation effects is high, APMT-Impacts rigorously tracks and explicitly presents uncertainty associated with the aviation effects analyzed and the impact valuation methods used. Monte Carlo analyses are performed in order to

present ranges on output values while formal uncertainty analyses are performed to determine the most influential assumptions for each metric.

APMT-Impacts presents the effects of a policy or scenario in terms of physical impacts, such as those given in Table 16-1, as well as in monetary terms, allowing for a direct comparison between benefits and costs. For noise, APMT-Impacts yields both the number of people exposed to a given noise level and the net present value of the housing depreciation. For air quality, APMT-Impacts calculates the incidences of premature mortality as well as the net present value of the health risks associated with the increase in ambient particulate matter. For global climate change, APMT-Impacts provides both the globally-averaged surface temperature change and the net present value of the socio-economic damages that result.

In the following sections, we first present a system-wide climate analysis, an analysis of the impact on the air quality in the NYC metroplex, and an examination of the noise impacts in the NYC metroplex for the candidate technologies in this study.

16.2. Climate Analysis (System-wide Scale)

Aviation emissions impact the radiative balance of the planet through effects that are diverse in terms of the time and spatial scales involved. The impact pathway for aviation-induced climate change starts with direct emissions of CO₂, NO_x, H₂O, SO_x, HC, and soot and ends with societal impacts as shown in Figure 16-2.

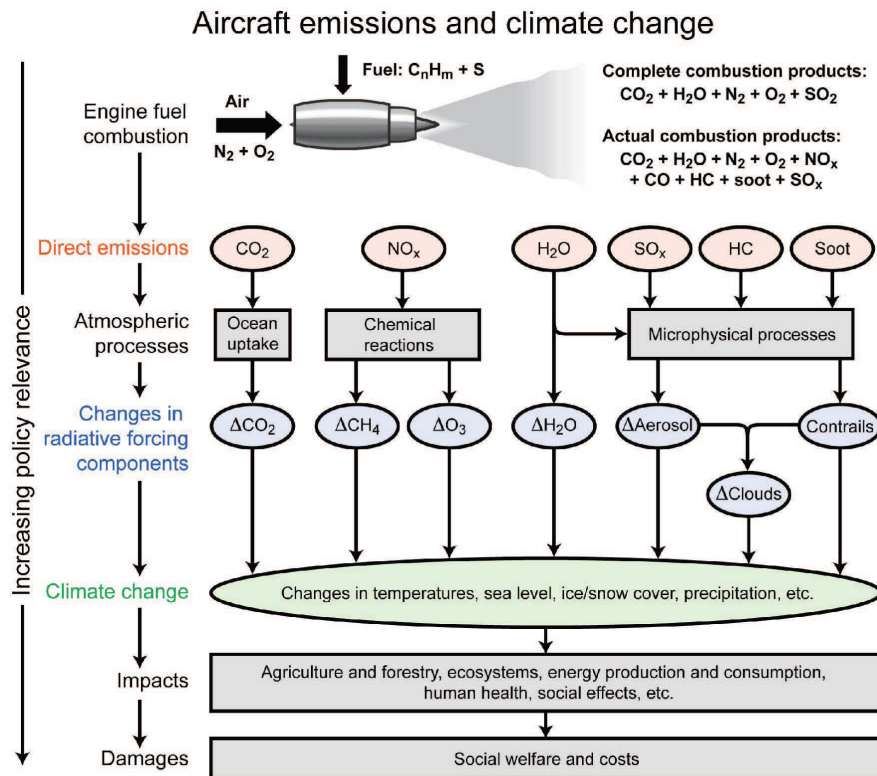


Figure 16-2. Aviation climate impacts pathway (from Wuebbles et al., 2007^{cxxviii})

The effect of aviation on climate can be measured by changes in indicators such as surface temperature, sea level, precipitation patterns, ice or snow cover, etc. Surface temperature is a commonly used metric to relate the impacts on humans as well as global biological systems. Some examples of these impacts include effects on agriculture, energy production, ecosystems, and so on. Estimating these hard-to-grasp impacts can be difficult and often involves making ethical judgments, especially when estimating societal damage in monetary units. Still, as one proceeds from emissions to estimating societal impacts, the information becomes increasingly relevant and understandable to those who need to make decisions and hence it is important to consider the complete pathway illustrated in Figure 16-2.

Climate impact valuation in APMT-Impacts borrows heavily from prior work on anthropogenic climate change, estimating physical and economic impacts for various aviation effects (CO₂, NO_x on methane, NO_x on ozone, water, sulfates, soot, and contrails/aviation-induced cirrus). The APMT-Impacts Climate Module uses reduced-order methods based on the work by Hasselmann et al.^{cxxxix}, Sausen et al.^{cxxx}, Fuglesvedt et al.^{cxxxix}, and Shine et al.^{cxxxii}. The module relates changes in fleet-level aviation emissions to globally-averaged radiative forcing (RF) and surface temperature change. Figure 16-3 provides a schematic that graphically explains the processes behind the APMT-Impacts Climate Module.

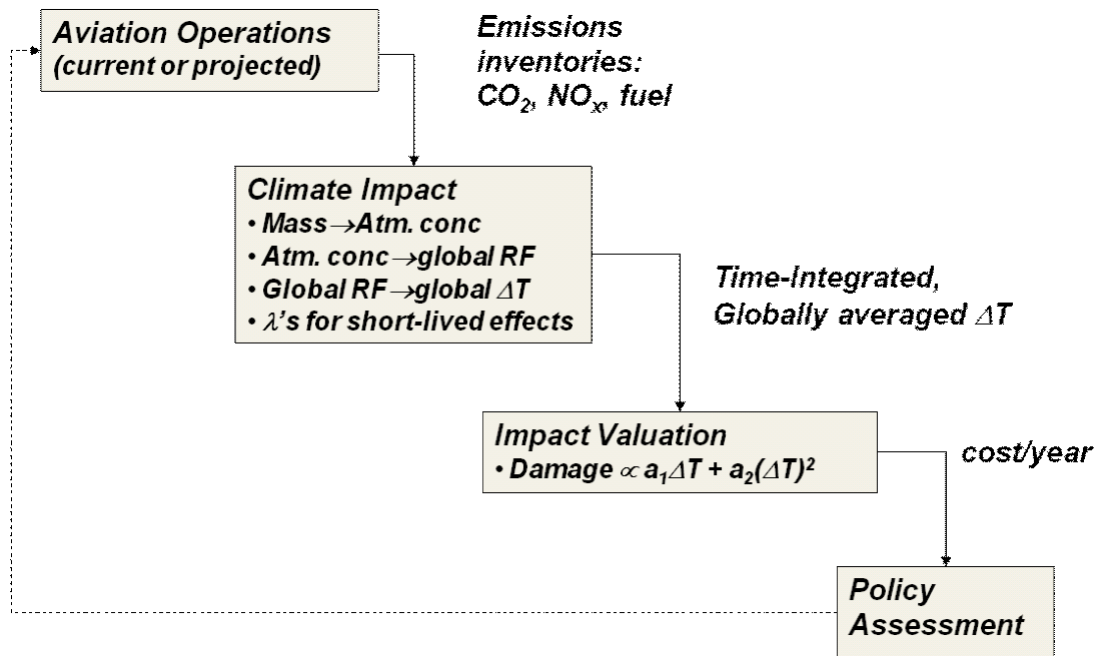


Figure 16-3. APMT-Impacts Climate Module (from Marais et al.^{cxxxiii})

Atmospheric concentrations of CO₂ are calculated using impulse response functions derived from complex carbon cycle models. RF due to CO₂ is calculated as a logarithmic function of concentration changes. RF for non-CO₂ effects is scaled according to most recent estimates from Sausen et al.^{cxxxiv}, Wild et al.^{cxxxv}, Stevenson et al.^{cxxxvi}, and Hoor et al.^{cxxxvii}. A simplified temperature response model by Shine et al.⁵ completes the physical impact modeling pathway. Lastly, different damage functions and discount rates are used to explore the health, welfare, and ecological costs in terms of percent change of world GDP and net present value of damages. A detailed description of the APMT Climate Module is presented in Marais et al.⁶ and Jun^{cxxxviii}.

For this study, we assessed the climate impact of eight different NextGen scenarios. We ran a case for each of the new vehicle concepts—CESTOL, VLJ, UAS, LCTR, and SST—in addition to “all vehicle,” baseline, and CESTOL-specific baseline cases. For climate impacts, the primary metrics of interest are time-integrated, globally-averaged surface temperature change and net present value of damages. Since we are interested in knowing the impact of each of the vehicles relative to a baseline case without those new vehicle concepts, our focus is on presenting the change in these metrics from the baseline to the policy scenarios. The main inputs to the model are fuel burn, CO₂ emissions (which scale directly from fuel burn), and NO_x emissions. These inputs were generated in AEDT for three years—2025, 2040, and 2086 (equating to 3X traffic)—for all cases except the VLJ and SST. No VLJs were flown for the year 2086 and SSTs were not introduced until 2040. APMT interpolates the inputs between the three out years and calculates results for the entire scenario. Fuel burn and NO_x emissions are plotted for all cases in Figure 16-4 and Figure 16-5.

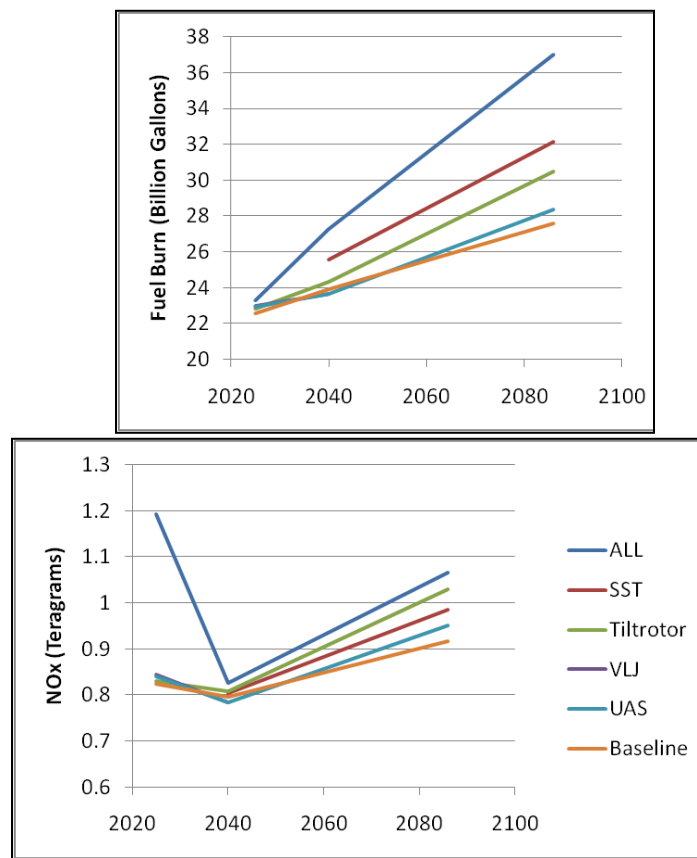


Figure 16-4. Yearly fuel burn and NO_x emissions for new vehicle scenarios.

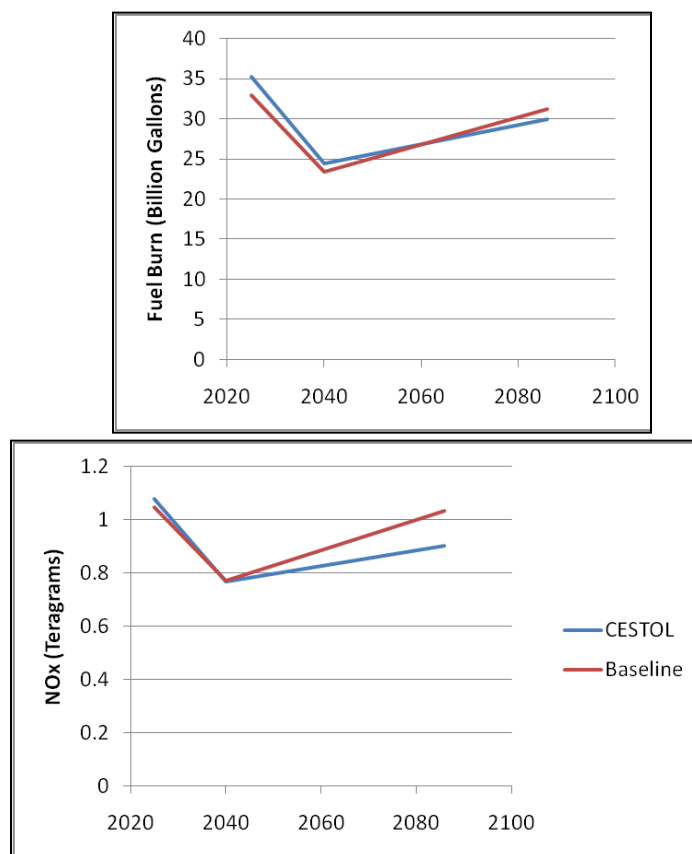


Figure 16-5. Yearly fuel burn and NO_x emissions for CESTOL scenarios.

For all of the cases, the results are determined by the inputs and their underlying assumptions. Further information on the details of the scenarios and their underlying assumptions can be found in earlier sections of this report. It is clear from Figure 16-4 that all non-CESTOL cases burn more fuel than the baseline because they represent additional flights. The CESTOL case in Figure 16-5 has its own particular baseline scenario due to a business shift that was made for the CESTOL concept where some baseline flights were being replaced with CESTOL aircraft.

For climate impacts, uncertainty for a given change in fuel burn and NO_x emissions is captured by calculating low, mid, and high output metrics for a range of input assumptions. Nominally, the analysis is conducted using Monte Carlo methods and the results represent the mean of several thousand runs. For the low and high case, several significant inputs are fixed at the lower and upper bounds of their distributions. Table 16-2 lists the primary assumptions used in the climate analysis for this study. The rationale behind the values and ranges used in the model can be found in Marais et al. (2007)⁶.

Table 16-2. Climate assumptions for new vehicle study.

Climate Assumptions	Low	Mid	High
Climate sensitivity	2K	Triangular distribution (mode, range) [3.0, 2.0-4.5] K	4.5K
NO _x -related effects	Stevenson et al. RF values (2004)	Discrete uniform distribution: Wild, Stevenson, Hoor et al (2009) values	Wild et al. RF values (2001)
Short-lived effects radiative forcing [Cirrus, Sulfates, Soot, H ₂ O, contrails]	[0, 0, 0, 0, 0, 0] mW/m ²	Triangular distribution (mode, range) [30 (0 – 50), -3.5 (-10-0), 2.5 (0-10), 2.0 (0-6.0), 10 (0-30)] mW/m ²	[50, 80, -10, 10, 6, 30] mW/m ²
Background scenario	IPCC SRES A1B	IPCC SRES A1B	IPCC SRES A1B
Damage coefficient	5% value of distribution	Normal distribution on DICE 2007 (mean = 0.002839, std = 0.0013)	90% value of distribution
Discount rate	3%	3%	3%

The choice of discount rate merits further discussion. Discounting methods are used for converting future monetary impacts into present day terms and the selection of a discount rate is a topic of debate among economists. Three percent is chosen as a midrange value in line with EPA practice^{cxix}. Discount rate choice—largely a decision maker preference—can have a large influence on the calculation of net present value (NPV), or the total present value of a time series of climate damages. For the purposes of looking at changes compared to a baseline, however, a single discount rate ought to be suitable unless there are significant changes in short- versus long-lived effects (since these are influenced differently by different levels of discounting). Not listed in the table is the fact that impacts are calculated 800 years out from the emission years so as to capture the full lifetime of CO₂ emissions in the atmosphere.

Climate impact results are first presented for all cases except the CESTOL and CESTOL baseline. Figure 16-6 depicts the difference in deltaT-years, i.e. the total time-integrated temperature change due to the new vehicle scenario minus that due to the baseline scenario. Figure 16-7 shows change in NPV in a similar fashion. The error bars in each figure represent the low and high estimates while the red vertical mark represents the midrange estimate.

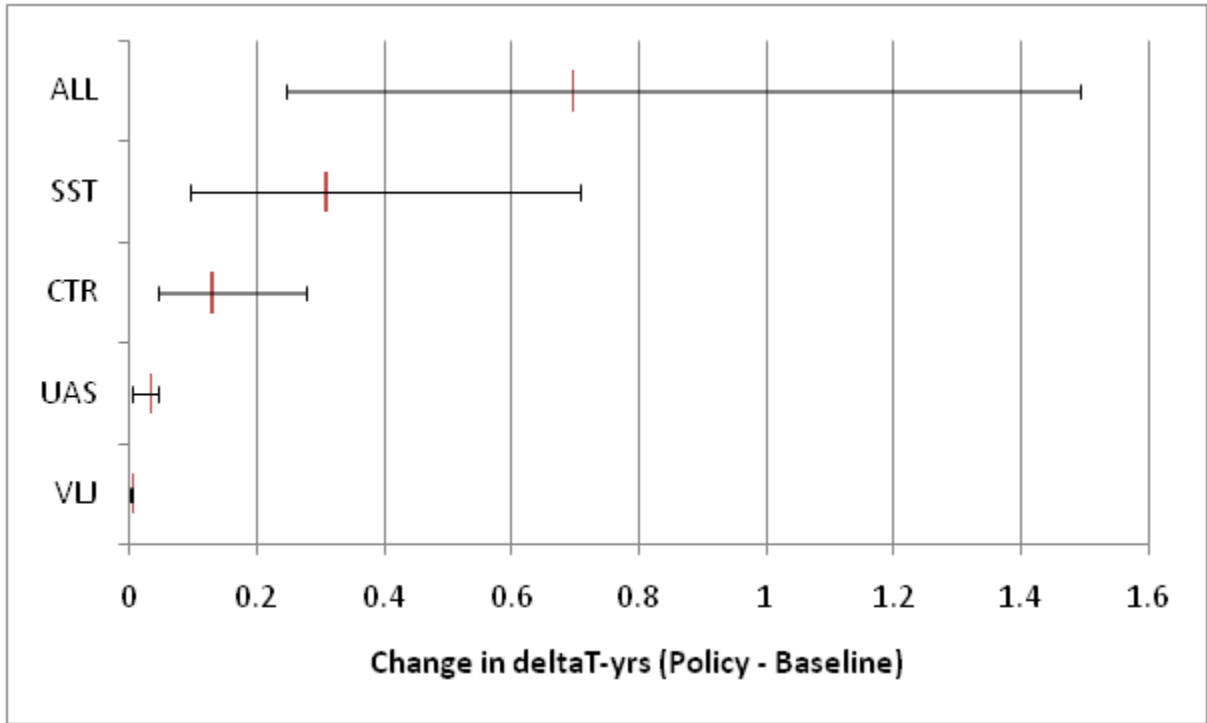


Figure 16-6 Difference in time-integrated temperature change (K; policy – baseline)

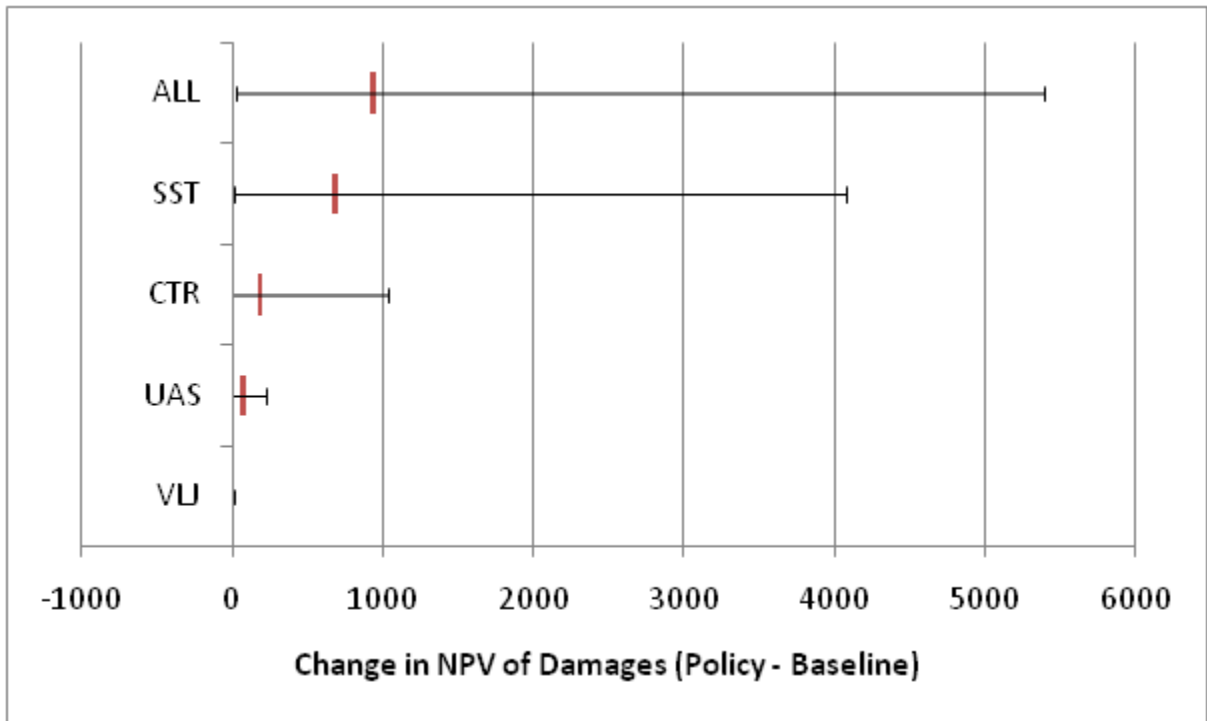


Figure 16-7 Difference in net present value (2005 US\$; policy – baseline).

Both physical and economic metrics demonstrate how climate impact tracks with fuel burn, to first order. Vehicles that burn much fuel, like the SST and LCTR, result in a larger increase in temperature

and, consequently, monetized damages. The SST also has an increased impact on climate due to a heightened warming influence of water vapor emitted in the stratosphere. To account for this effect, radiative forcing due to SSTs in the scenario was scaled by a factor of five, which was derived from the IPCC’s study on high-speed civil transports^{cxl}. Vehicles that account for a small percentage of overall system-wide fuel burn, such as the UAS and VLJ, lead to smaller changes in climate impacts relative to the baseline scenario.

Results for the CESTOL case are presented in Figure 16-8 and Figure 16-9. For this scenario, the changes and output metrics were calculated with respect to a CESTOL-specific baseline scenario.

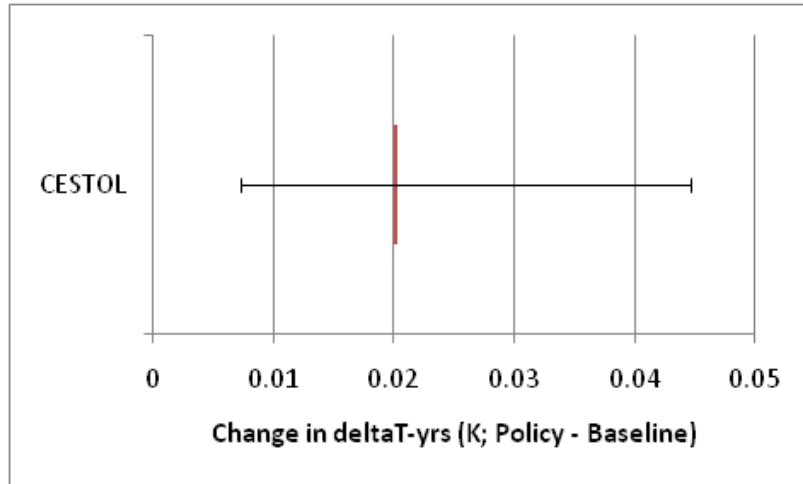


Figure 16-8. CESTOL temperature impact (policy – baseline)

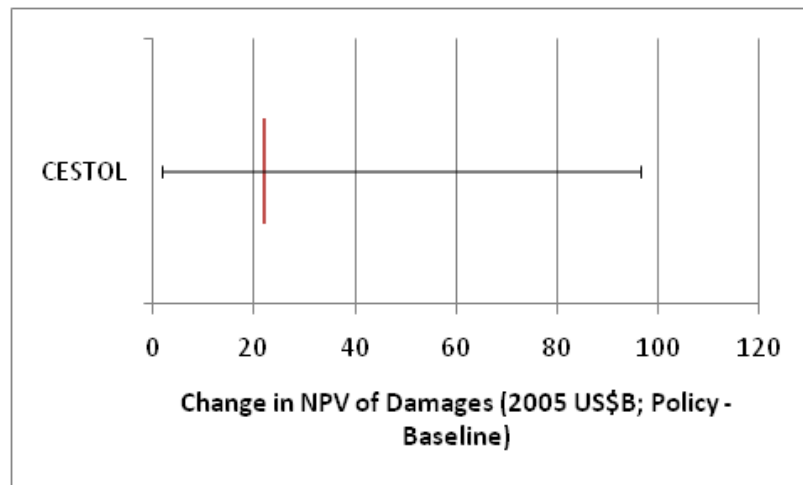


Figure 16-9. CESTOL monetized damages (policy–baseline).

The CESTOL’s increase in the climate metrics is not surprising considering that the CESTOL case results in an additional 63.5 teragrams of total fuel burn, and hence 200 Tg more CO₂, as compared to the baseline. The overall impact of the CESTOL case, however, is more in line with the lower overall impact of the VLJ and UAS cases as opposed to the high damages associated with the LCTR and SST vehicles. Because the CESTOL is not a purely additive case, the answer is particularly sensitive to underlying

assumptions in the design of the scenario. A slightly different fleet mix or replacement scenario could certainly change the result, and thus the results presented here ought to be considered in tandem with a clear understanding of how each scenario was defined.

16.3. ***Air Quality Analysis (Metropolitan scale)***

Airborne particulate matter is the focus of the air quality analysis due to its detrimental effect on human health^{cxli}. To properly assess the impacts of any scenario on society, it is therefore essential that ambient PM concentration is chosen to be one of the key metrics, and the focus is on particulate matter that is less than 2.5 μm in aerodynamic diameter, or $\text{PM}_{2.5}$, because that has been shown to have the most significant health impact. Aircraft engines emit particulate matter in the form of elemental carbon or soot, known as primary PM. However, $\text{PM}_{2.5}$ is also created from the reaction of pre-cursor gases of NO_x , SO_x and unburned hydrocarbons with other species in the atmosphere to form secondary PM and the mass of this secondary PM exceeds that of primary PM^{cxlii}.

While APMT-Impacts has an air quality modeling capability, the research team did not use this module for this analysis. Instead, we developed an approach to air quality modeling that takes advantage of higher fidelity tools that are better suited for air quality impact analysis at the regional scale as required for assessment of the metropolitan case.

The first step was to obtain a set of emission inventories for the aircraft flying into and out of the New York City metropolitan area. As explained in earlier sections of this report, the demand for air travel was modeled and a schedule of operations was generated. For the purposes of air quality modeling, the schedule of operations was generated for a single representative day for each year of simulation.

The aircraft are then "flown" using AEDT to obtain aircraft performance along its flight path. The aircraft performance is translated into emissions macro-species such as unburned hydrocarbons (HC), NO_x , SO_x and primary particulate matter (PM). The emission inventories are generated for each segment of the flight path of every aircraft, thereby allowing spatial and temporal resolution of the inventories in terms of quantities and locations of the emissions. Although emissions at cruise could impact surface air quality, this study only considered emissions for flight segments below 10,000ft. This limits the emissions to only those that occur during the landing and takeoff (LTO) cycle.

The emissions for a single day of operations were expanded to support a full 2-month period of simulation by utilizing daily emissions scaling factors. We chose the months of February and July to represent a typical month from the winter and summer seasons respectively. This is done to minimize computational time while still being able to provide good insight into the effects of aviation on the environment. The scaling factors were derived from an earlier PARTNER NextGen project between UNC and CSSI^{cxliii}. The scaling factor provides a historical variation in the number of operations at each airport in the NYC metropolitan area. The scaling factors are provided for the two months (60 days) of simulation as well as an additional 10 days spin-up period that is required to correctly model the initial chemical conditions in the atmosphere from background sources, that are then dissipated.

These emissions inventories were input to CMAQ (Community Multi-scale Air Quality model), an EPA developed, three-dimensional, Eulerian chemical-transport model. CMAQ requires a comprehensive set of inputs – gridded meteorological inputs (derived from either MM5 or WRF), emissions inputs from

all natural and anthropogenic sources (using the SMOKE model), photolysis rates, and initial and boundary conditions. For each time step and grid cell, CMAQ calculates the change in chemical concentration based on advection, diffusion, chemical formation, removal of each species and the given emissions^{cxliv}. The output of interest with respect to air quality modeling is the concentration of ambient PM_{2.5}. CMAQ predicts the mass of various chemical components of PM_{2.5}, i.e., ammonium, sulfate, nitrate, elemental carbon and organic carbon (primary and secondary). We ran the Mesoscale Meteorological (MM5) model for February and July 2005 at a 12-km resolution over the Eastern U.S. to prepare gridded hourly meteorological inputs to drive CMAQ.

The emissions inventories as obtained from AEDT only include macro-species, as defined earlier. In order to carry out detailed chemistry and obtain an accurate distribution of PM concentration, the macro-species have to be speciated into distinct chemicals. The speciated emissions are then temporally and spatially allocated in the three-dimensional space surrounding the NYC metroplex with an hourly time resolution. The grid is resolved vertically until the lower stratosphere, even though the aircraft emissions data are capped at 10,000ft; this accounts for convective winds that circulate vertically from the upper atmosphere.

The last step before performing the dispersion and chemical modeling using CMAQ is to incorporate background emissions. Background emissions refer to emissions from other anthropogenic and biological sources such as factories, ground transportation and vegetation. Inclusion of these sources is essential to a complete modeling of air quality, because there may be complex reactions involving emissions from aviations and background species that already exist in the atmosphere. The background emissions were obtained from EPA's National Emissions Inventory (NEI) (<http://www.epa.gov/oar/data/neidb.html>) for the year 2005, and processed through SMOKE to prepare CMAQ-ready emissions inputs.

We prepared the chemical initial and boundary conditions for these simulations from existing 36-km CMAQ simulations performed by UNC under PARTNER research over the Continental U.S. This ensured that the background conditions in the atmosphere were realistic of ambient conditions to enable the incremental assessment due to aviation for the NYC Metroplex analysis.

The present air quality study leverages previous research that examined the contribution of aviation to the concentration of ambient PM. Air quality modeling efforts over Atlanta (ATL), Chicago (ORD) and Providence (PVD) by Arunachalam et al. (2008) provide a foundation for the current research¹⁶. Figure 16-10 illustrates the grid domain that was previously developed and leveraged here. The domains are labeled in such a way that the boundaries that are depicted on the map contain grid cells of specified size; for example, the entire North American region bounded by the thin black box is divided into grid cells that are 36-km square. This grid is used for APMT-impacts analyses of aviation's air quality impact. The 12-km modeling domain was utilized to model the air quality impacts over the NYC metroplex. Important processes such as the grid generation, background inventory processing, and meteorological data processing from prior modeling activities were leveraged here. Ideally, a smaller region with a more refined grid (at 4 km resolution), similar to that associated with ATL or PVD, would have been used; such an analysis is recommended for follow-on work.

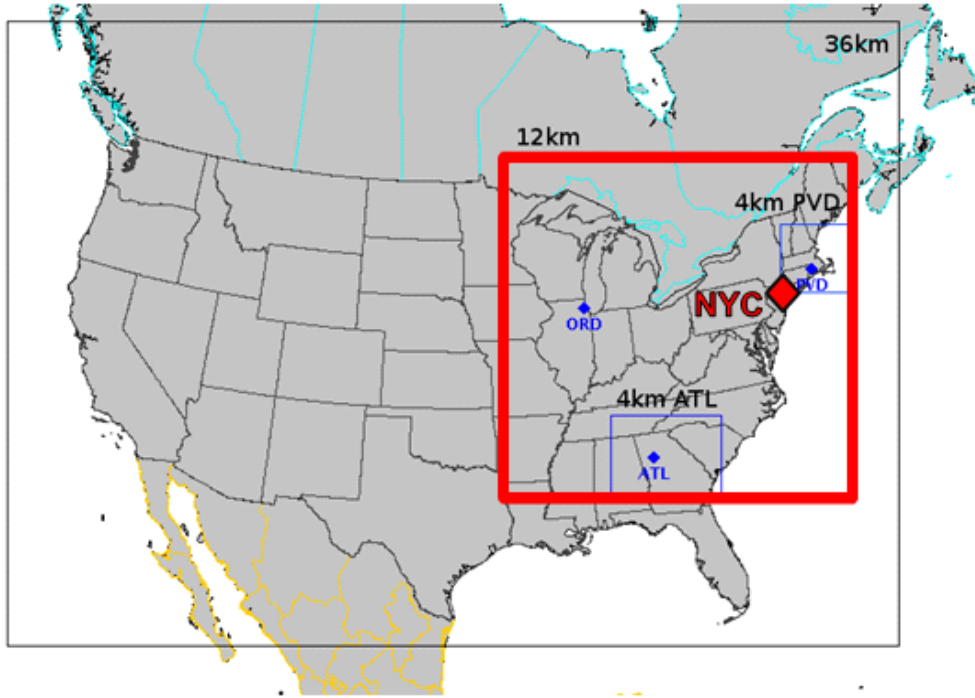


Figure 16-10 Multi-scale modeling domain used in Arunachalam et al.¹⁶

The air quality analysis over the NYC metroplex and the surrounding regions considered operations at the following eight airports: Kennedy (JFK), Newark (EWR), LaGuardia (LGA), Teterboro (TEB), Stewart (SWF), Westchester (HPN), Republic (FRG) and Islip (ISP). The inclusion of just these eight airports skews the results somewhat because the CESTOL business-shift scenario moved some flights from major airports to satellite airports that are not among these eight, resulting in a net decrease in flights in the New York metroplex. The modeling domain extended far beyond the metroplex area, as shown in Figure 16-10, to assess the impacts on air quality at downwind distances in the surrounding region.

The focus of the analysis was on the impacts of NextGen airspace on the concentration of $PM_{2.5}$ in the NYC region (i.e. with no new aircraft technologies being introduced). The number of flights into and out of the NYC metroplex was held constant. In follow-on work, the effects of future year emissions scenarios or incorporating advanced technologies (such as CESTOL aircraft in the fleet mix) on air quality could also be studied.

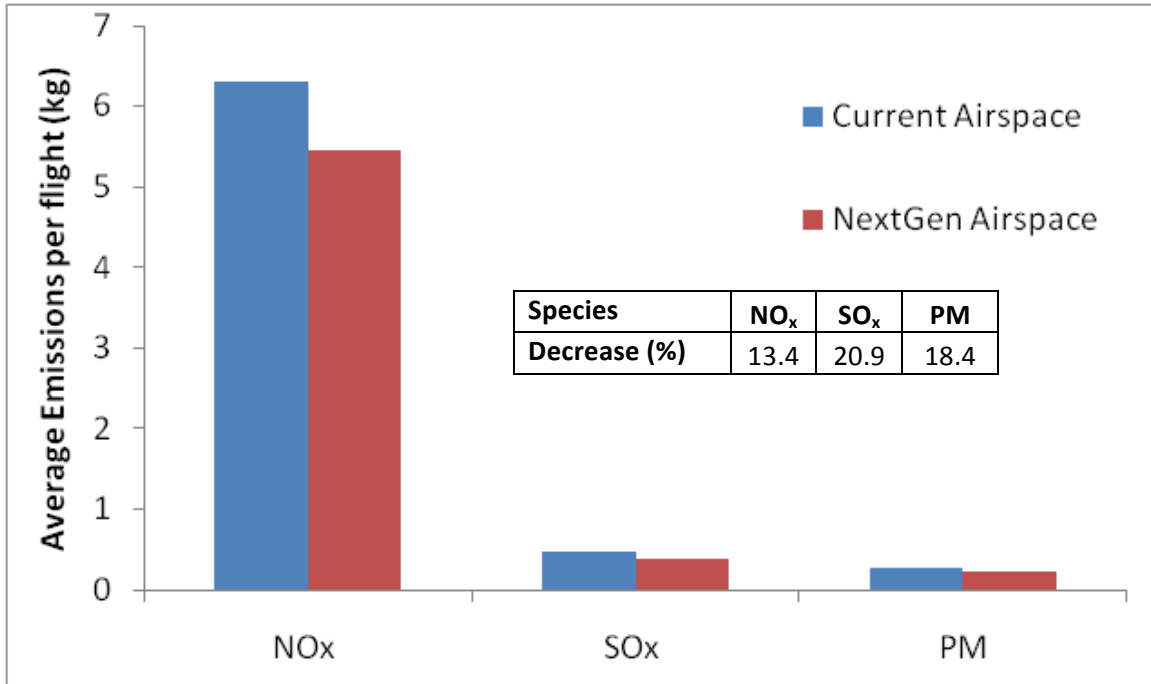


Figure 16-11. AEDT emissions data for Conventional airspace and NextGen airspace.

Figure 16-11 presents the emission data (average per flight as output from AEDT) for both the current airspace (baseline) case and the NextGen airspace case. It is evident that the advanced operations within the NextGen airspace have a beneficial impact on the average emissions. This is further quantified by the inset table in Figure 16-11, which presents the percentage decrease relative to the baseline Conventional Airspace emissions.

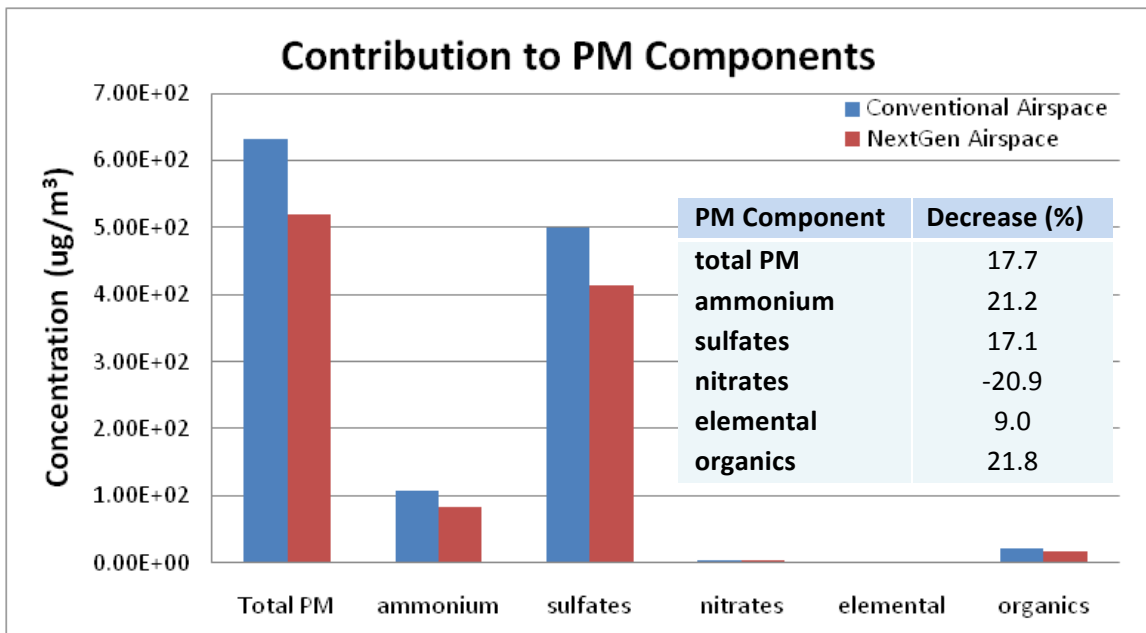


Figure 16-12. Contribution to PM Species for Conventional and NextGen airspace.

The bar chart in Figure 16-12 shows the contribution of Landing and Takeoff (LTO) operations in the New York Metroplex region to the various components of total ambient PM as predicted by CMAQ. The data are averaged over the two-month simulation period. The NextGen airspace leads to a 17.7% decrease in total ambient PM, when compared to the conventional airspace. A similar trend exists for most of the components of PM, with the exception of PM nitrates which increases in the NextGen scenario.

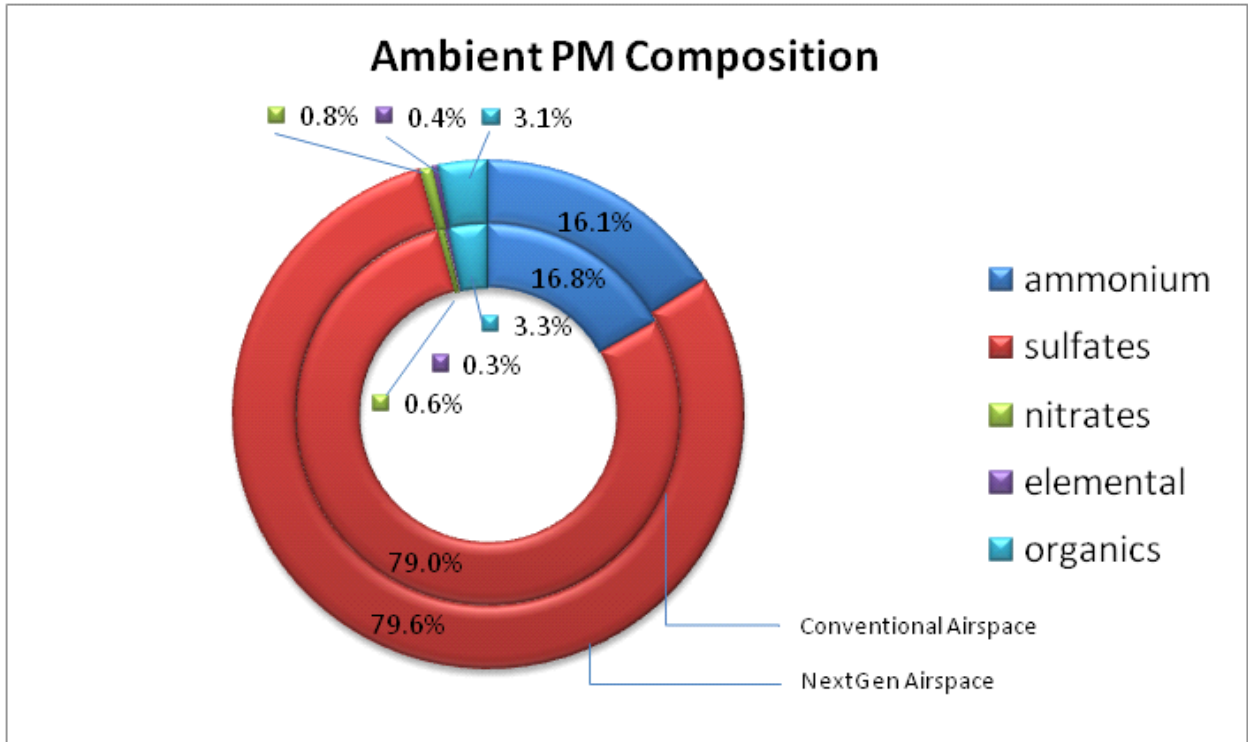


Figure 16-13. Composition of PM in conventional and NextGen airspace scenarios.

The pie chart in Figure 16-13 illustrates how the composition changes for both Conventional and NextGen scenarios. Adopting the NextGen airspace leads to slight differences in the aviation contribution to makeup of ambient PM. PM Sulfates continues to form the majority of the PM in the NextGen case, and makes up a higher percentage of the total than in the Conventional scenario. This occurs despite a 17.1% decrease in absolute PM Sulfate concentration. The percentage composition of PM Nitrates and elemental PM also increases, albeit by very small percentage points.

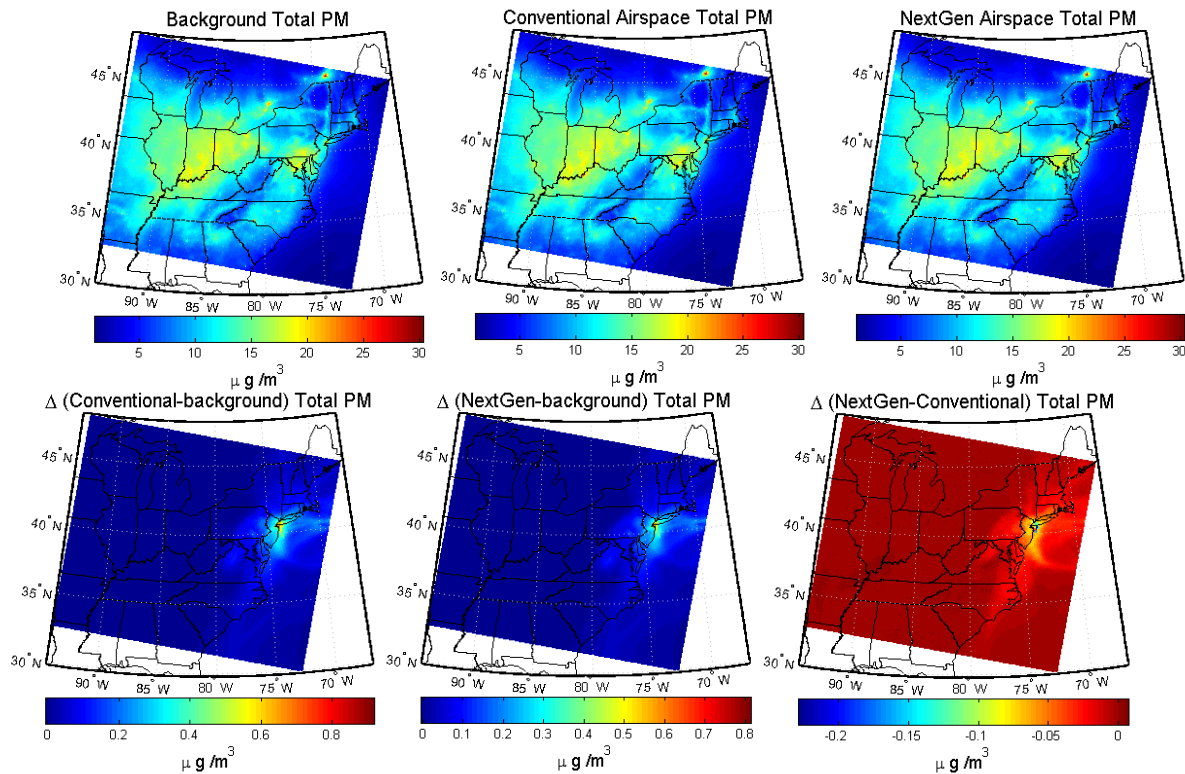


Figure 16-14. Ambient concentration of total PM over domain.

Total ambient PM concentrations are overlaid onto a map of the CMAQ modeling domain in Figure 16-14. The top row shows the total PM predicted by CMAQ for each of the 3 emissions scenarios that we modeled, and the bottom row shows the differences in total PM between the various scenarios. The data were averaged over the two-month computational period, and represents the average contribution to total ambient PM. As seen in the bottom row of Figure 16-14 which shows the difference plots of CMAQ scenarios, much of the aviation-related PM is propagated towards the east over Long Island NY and south over New Jersey. The significance of the NextGen airspace is seen in the bottom row third plot, which illustrates the difference in aviation related contribution to PM between the Conventional and NextGen scenarios. The NextGen scenario leads to an overall decrease in ambient PM, a significant portion of which occurs over the heavily populated land masses of New York and New Jersey. It is important to realize that changes in PM concentration over populated land masses (as opposed to sparsely populated or oceanic environments) yield the greatest benefit in terms of human health. In this respect, it is evident that the NextGen airspace could have a significant benefit in terms of air quality health impacts relative to the baseline case. Future studies could be performed to quantify these benefits in terms of weighting the decrease by population densities, and examining potential health impacts that arise as a result.

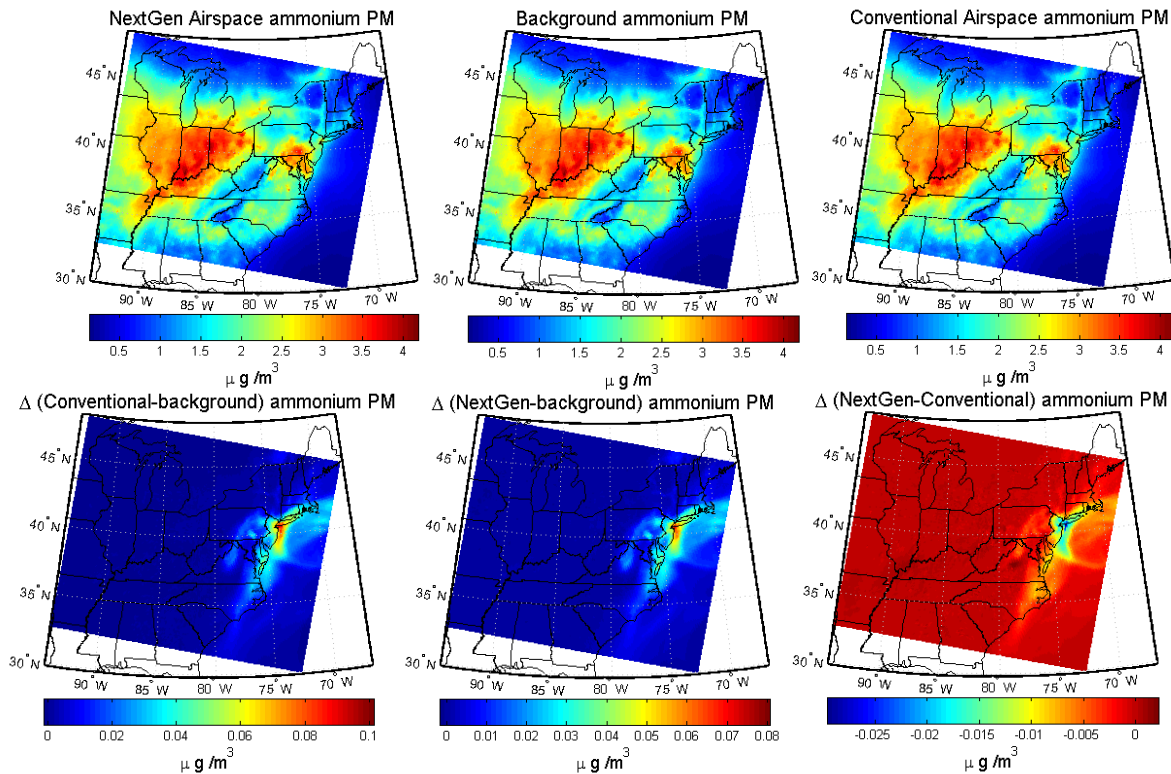


Figure 16-15. Ambient concentration of PM Ammonium over domain.

Because PM sulfates are the largest contributor to total PM, their spatial distribution is largely similar to Figure 16-14. The contribution from PM Elemental Carbon, PM Nitrates and PM Organics are relatively small, and do not yield any further insight into the propagation of PM in the region. However, it is informative to examine the distribution of PM Ammonium, the second largest contributor of Total PM. From the difference plots shown in Figure 16-15, it is observed that aviation activity in the NYC metroplex has a more far-reaching effect over the region. Both Conventional and NextGen airspace Landing and Takeoff (LTO) activity affects ambient PM Ammonium as far as northern North Carolina and southern Massachusetts on the coast, and as far inland as Virginia and Pennsylvania. The NextGen airspace has a positive effect in terms of the decrease in PM Ammonium, although most of the change is seen only in the coastal regions.

Figure 16-16 plots total ambient PM concentration as a function of approximate radius from the NYC metroplex. The datum was assumed to be Manhattan [Latitude 40.77° N, Longitude 73.98° W]. This location is chosen in order to provide a good approximation of the air quality over the densely populated regions of NYC. Also, since the modeling domain comprises a structured conformal grid, the “radial” distances are approximated based on the number of cells from the center cell (which contains the above-mentioned coordinates).

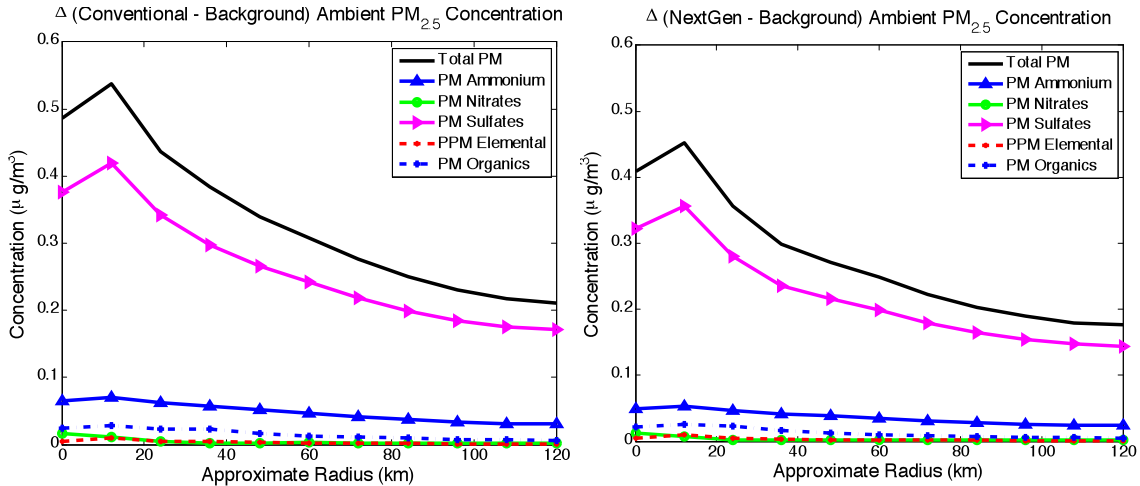


Figure 16-16. Ambient PM_{2.5} concentration in baseline (left) vs. NextGen operations (right).

The aviation related PM concentrations increase initially, and then drop gradually as the distance from Manhattan increases. The spike in PM concentration in the first 12 km is attributed to the fact that the major airports that are modeled (JFK, LGA and EWR) are situated surrounding the assumed center of the metroplex; a large fraction of the aircraft emissions would be located close to these major airports, subsequently causing a high concentration of PM in those areas. Ambient surface level PM concentrations decrease as aircraft climb away from the airports, leading to the gradual drop that is observed as the radius increases. It should be noted that the conventional scenario represents, on average, a 2.7% increase in total PM over the local NYC background emissions. The NextGen airspace results in a slightly lower 2.2% increment. These levels are highly sensitive to a number of factors including meteorological conditions and other sources of background emissions.

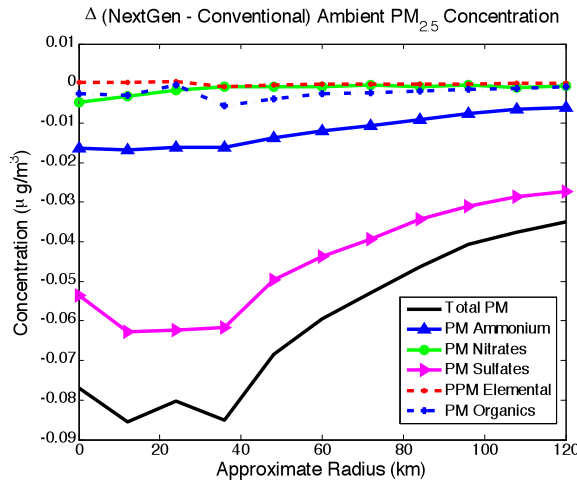


Figure 16-17. Delta (NextGen-Conventional) PM radial concentrations.

In Figure 16-17, the difference between the NextGen and Conventional scenarios is quantified. The greatest decrease occurs close to the airports, roughly between 12 and 36 km from the center of NYC. The decrease becomes less pronounced at locations further away from the center. As mentioned earlier, the

effects of the decrease in PM concentrations should be quantified in terms of health impacts, and is the recommendation for future work.

16.4. **Noise Analysis (Metroplex Scale)**

Aircraft noise has a number of direct effects on residents near airports. The most well-known effect is general annoyance, but there is evidence that aviation noise also contributes to sleep disturbance, learning impairment, and certain cardiovascular diseases (e.g. hypertension)^{cxlv}.

The APMT-Impacts Noise Module computes the environmental impact of aircraft noise through physical metrics such as population exposure to a given noise level and the number of people highly annoyed. APMT uses day-night average noise level (DNL) contours around airports as inputs and overlays them on population and housing data grids from the 2000 SF3 US Census^{cxlvi}. The population exposed is calculated as the number of people inside a specific contour, or noise level. The physical effects of aircraft noise can be monetized through hedonic pricing which reveals individuals' value of noise by examining the price of complementary market goods that are related to noise, such as house prices. A Noise Depreciation Index (NDI), derived from revealed preference analyses, is used to estimate housing depreciation due to noise. The NDI is a coefficient relating the percentage loss in housing price to a unit decibel change in noise. Currently, the Noise Module uses Nelson's meta-analysis of NDI estimates at 23 different airports in the United States and Canada^{cxlvii}. A more thorough description of the APMT Noise Module can be found in Kish (2008)^{cxlviii}.

For this study, the noise impacts in the New York City metroplex were examined for two cases. In the first case, we examined the impact of current day vehicles operating in conventional airspace compared to the impact of current day vehicles operating in NextGen airspace, as described in an earlier section of this report. In the second case, the impact of the CESTOL scenario compared to a baseline case was assessed. Noise contours generated in AEDT were used as inputs to the model. The AEDT contours were generated from results from capacity and delay simulations performed by ATAC using the publicly available airport and airspace simulation model, SIMMOD.

The analysis was run for a day of operations in the year 2007 at the following eight airports in the NYC metroplex: EWR, JFK, LGA, TEB, SWF, HPN, ISP, FRG. The assumptions used for the calculation are shown in Table 16-3. The rationale behind the values chosen is described in Kish (2008)²¹.

Table 16-3. Mid-range noise input assumptions.

Noise Assumptions	Mid-range
Noise Depreciation Index	Normal distribution mean = 0.65%/dB, std = 0.10%/dB
Background Noise Level	Triangular distribution (mode = 52.5, range = 50-55) dB
Housing Growth Rate	Historic distribution
Significance Level	55 dB
Contour Uncertainty	Triangular distribution (mode = 0, range = -2 to 2) dB

Using the mid-range assumptions in Table 16-3, the conventional scenario exposes approximately 1.42 million people and the NextGen scenario exposes approximately 1.05 million people to sound levels in excess of 55 dB DNL. In other words, the NextGen airspace results in 370,000 fewer people exposed to this noise level. In terms of monetized damages, the results are also positive: the NextGen scenario nominally results in a \$180 million reduction in housing value loss and rent changes compared to the conventional airspace scenario (year 2005 USD).

The second case that was assessed was the noise impact of the CESTOL vehicle. For this analysis, the noise impacts were calculated for two scenarios over a time frame from 2025 to 2086. As discussed in earlier sections of the report, the two scenarios include similar evolution of the fleet with the exception that the “CESTOL” case includes the introduction of the CESTOL while the “Baseline” does not. Again, the analysis was conducted for operations at the eight airports in the NYC metroplex previously identified. As calculated using the assumptions listed in Table 16-3, the yearly population exposed to greater than 55 dB DNL is presented in Figure 16-18.

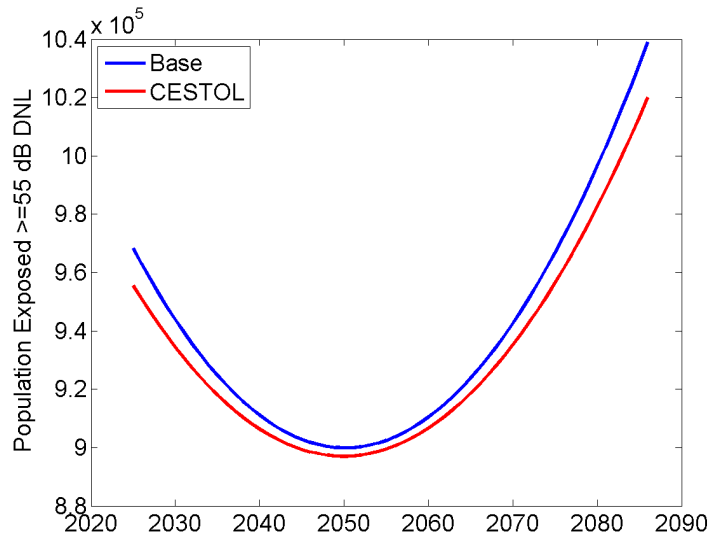


Figure 16-18. Yearly population exposed (CESTOL case).

In total, the CESTOL case exposes 462,000 fewer people to a noise level of 55 DNL as compared to the baseline case over the full scenario time frame. Consequently, the CESTOL case also reduces losses from housing value depreciation and rent changes by \$220 million with respect to the baseline (2005 USD).

16.5. ***Caveats on Environmental Analysis***

An important point to make when considering the environmental results presented here is that they depend strongly on assumptions embedded within the noise and emissions inventories that were analyzed. For instance, the processes of demand modeling, demand trimming, fleet evolution, fleet mix, and vehicle design all heavily influence both the generation of performance data as well as the resulting impact analysis. These factors should be carefully considered when interpreting results. Additionally, APMT-Impacts does not model potentially important items either for lack of scientific understanding or model fidelity. For instance, the health impacts of noise and broader economic impacts of noise—e.g. through delayed airport expansion—are unknown at this time. Also, the APMT-Impacts climate model does not incorporate some potentially important climate feedbacks or threshold events, nor does it account for regionalized impacts. The air quality modeling does not consider the impact of cruise emissions and the analysis presented herein did not examine the health impact on the general population (this is typically included in an APMT-Impacts analysis). All things considered, the information presented in this report is intended to provide general insights into the environmental impact of the candidate new vehicles in NextGen.

16.6. ***Summary of Findings and Potential Follow-on Work***

System-wide climate impacts assessments have been conducted for scenarios with the new vehicle technology candidates. Each of the new vehicle scenarios caused greater damage to the global climate relative to the relevant baseline scenario in terms of both time-integrated surface temperature change and monetized damages due to the higher fuel burn and emissions. The SST, Tiltrotor, and all-vehicle

scenarios are particularly detrimental due to fuel burn levels much greater than the baseline case. The SST has an increased adverse impact on climate due to effects unique to flight in the stratosphere. The remaining cases—VLJ, UAS, and CESTOL—have smaller impact on climate because they account for a small percentage change in total fuel burn relative to the baseline.

A metroplex-scale air quality analysis was performed over the NYC region, for the Conventional Current Airspace as well as for the NextGen Airspace. The NextGen scenario produces fewer emissions from the airspace activity compared to the Conventional airspace, and the effects of this reduction in emissions manifest themselves in an overall decrease in PM concentrations in the NYC region. In particular, the reduction in PM Ammonium is observed far beyond the local NYC metroplex area, extending further along the coasts and inland. The reduction in PM due to the NextGen airspace has the greatest effect close to the airports, the decrease becoming less pronounced as the distance from the datum increases.

Noise was assessed at the NYC metroplex level in order to independently assess the impacts of the advanced technologies of the CESTOL vehicle and the advanced operations and airspace design enabled through NextGen (without any advanced vehicle concepts). Both scenarios led to a reduction in total population exposed to a given noise level and in monetized damages in the form of housing value depreciation.

During the course of the environmental analysis, the research team identified a few potentially valuable areas of research for follow-on work. Firstly, with regard to the air quality analysis, it would be valuable to refine the grid to 4 km instead of 12 km so as to provide better resolution over the NYC metroplex. A similar air quality analysis for the 2025 to 2086 CESTOL scenario could prove insightful. While this report only presented regional assessments for air quality and noise, APMT-Impacts is capable of conducting system-wide analyses in these domains. Given the required input data, the research team could analyze the impact of each of the new vehicles in terms of system-wide noise and air quality in a similar manner to the analysis of global climate change. In terms of climate modeling, it would be worthwhile to conduct a comprehensive examination of the CESTOL and N150 entering the fleet independently, rather than a scenario with both vehicles, so as to avoid the strong influence of fleet mix on results. Lastly, the climate assessment of the SST could be improved through a more detailed study of existing literature on the impact of flying in the stratosphere with a particular focus on the treatment of water vapor and ozone.

cxxviii Wuebbles, D. J., M. Gupta, & M. Ko, “Evaluating the Impacts of Aviation on Climate Change,” *EOS*, 88, 157-160, 2007.

cxxix Hasselmann, K., S. Hasselmann, R. Giering, V. Ocana, & H. V. Storch, “Sensitivity Study of Optimal CO₂ Emission Paths Using a Simplified Structural Integrated Assessment Model (SIAM),” *Climactic Change*, 37(2):345 – 386, Oct 1997.

cxxx Sausen, R. & U. Schumann, “Estimates of the Climate Response to Aircraft CO₂ and NO_x Emissions Scenarios,” *Climactic Change*, 44(1-2):27 – 58, Jan 2000.

-
- cxxxix Fuglesvedt, J. S., T. K. Berntsen, O. Godal, R. Sausen, K. P. Shine, & T. Skodvin, “Metrics of Climate Change: Assessing Radiative Forcing and Emission Indices,” *Climactic Change*, 58(3):267 – 331, June 2003.
- cxliii Shine, K. P., J. S. Fuglesvedt, K. Hailemariam, & N. Stuber, “Alternatives to the Global Warming Potential for Comparing Climate Impacts of Emissions of Greenhouse Gases,” *Climactic Change*, 68(3): 281 – 302, Feb 2005.
- cxliiii Marais, K., S. P. Lukachko, M. Jun, A. Mahashabde, & I. A. Waitz, “Assessing the Impact of Aviation on Climate,” *Meteorologische Zeitschrift*, 17:157 – 172, 2008.
- cxliiii Sausen, R. et al., “Aviation Radiative Forcing in 200: An Update on IPCC (1999),” *Meteorologische Zeitschrift*, 14:555 – 561, 2005.
- cxliiii Wild, O., M. J. Prather, & H. Akimoto, “Indirect Long-term Global Radiative Cooling from NO_x Emissions,” *Geophysical Research Letters*, 28(9):1719 – 1722, 2001.
- cxliiii Stevenson, S. D. et al., “Radiative Forcing from Aircraft NO_x Emissions: Mechanisms and Seasonal Dependence,” *Journal of Geophysical Research*, 109(D17307), 2004.
- cxliiii Hoor, P. et al., “The Impact of Traffic Emissions on Atmospheric Ozone and OH: Results from QUANTIFY,” *Atmospheric Chemistry and Physics*, 9:3113 – 3136, 2009.
- cxliiii Jun, M., “Uncertainty Analysis of an Aviation Climate Model and an Aircraft Price Model for Assessment of Environmental Effects,” S.M. Thesis, Massachusetts Institute of Technology, 2007.
- cxliiii “Technical Support Document on Benefits of Reducing GHG Emissions,” US EPA, 12 June 2008.
- cxli Penner, J.E., IPCC Working Groups I, III, and Vienna Convention for the Protection of the Ozone Layer Scientific Assessment Panel, “Aviation and the Global Atmosphere: a special report of IPCC Working Groups I and III in collaboration with the Scientific Assessment Panel to the Montreal Protocol on Substances that Deplete the Ozone Layer,” Cambridge University Press, Cambridge, NY, 1999.
- cxli Rojo, J. J., “Future Trends in Local Air Quality Impacts of Aviation,” S.M. Thesis, Massachusetts Institute of Technology, 2007.
- cxliii Michael Graham, Melissa Ohsfeldt, Gayle Ratliff, Christopher Sequeira, Terence Thompson, Theodore Thrasher, Ian Waitz. “*Aircraft Impacts on Local and Regional Air Quality in the United States*,” Final report of PARTNER Project 15. October 2009. Report No. PARTNER-COE-2009-002
- cxliiii Arunachalam, S. et al., “An Improved Method to Represent Aviation Emissions in Air Quality Modeling Systems and their Impacts on Air Quality,” In Proceedings of the 13th Conference on Aviation, Range and Aerospace Meteorology, New Orleans, LA, Jan 2008.

cxliv Byun, D. W., & K. L. Schere, "Review of the Governing Equations, Computational Algorithms, and Other Components of the Models-3 Community Multiscale Air Quality (CMAQ) Modeling System," US Environmental Protection Agency, Office of Research and Development, 2006.

cxlv "Transport-related Health Effects with a Particular Focus on Children: Noise," Transport, Health and Environment Pan-European Programme (THE PEP), WHO, 2004

cxlvi "2000 Census Rent Data Used in Calculation of FY2005 FMRS," HUD, <http://www.huduser.org/datasets/fmr/CensusRentData/>, 31 March 2005.

cxlvii Nelson, J. P., "Meta-analysis of Airport Noise and Hedonic Property Values: Problems and Perspectives," Journal of Transport Economics and Policy, 38 (1), pp. 1-28, 2004.

cxlviii Kish, C., "An Estimate of the Global Impact of Commercial Aviation Noise," S.M. Thesis, Massachusetts Institute of Technology, June 2008.

17. Metrics

This section describes an approach for assessing the impact of integrating new vehicle concepts into the NAS. The approach, based on control theory, utilizes International Civil Aviation Organization (ICAO) Key Performance Areas (KPAs), and can be extended to a wide range of performance and trade-off assessments at varying levels of fidelity. To illustrate the approach, three key trade studies between two performance areas of system performance, environment and safety are utilized. An array of trade-offs and potential research goals that might be of interest to NASA in the future are also summarized.

17.1. *Previous Research*

Previous studies have compiled metrics based on research conducted by organizations such as NASA, FAA, MITRE, and Eurocontrol. Allendoerfer and Galusha¹ survey the existing literature to compile and classify metrics in use by industry. These authors not only provide a reference to the design and execution of many baseline studies, but also discuss metrics suitable for assessing system performance and workload. Casso and Kopardekar² present a comprehensive set of metrics addressing human factors and human performance. A compilation of performance measures and measurement techniques used by researchers can be found in Hadley, Guttman, and Stringer³. Throughout Air Traffic Management (ATM) literature, many metrics are used to evaluate performance-related aspects of concepts, operations, and procedures. Bradford, Brown, and Blucher⁴ examine the current use and understanding of metrics within the US airspace system. Some research has also been conducted to develop frameworks useful for performance measurement and assessment. Williams, Bradford, Liang, Post, and Pomeret⁵, for example, present a metrics taxonomy and a common framework for measuring performance. Breuing, Bradford, and Liang⁶ describe an approach to standardizing performance measurements. Preliminary studies presented in Bonnefoy and Hansman⁷ address the impact of introducing vehicles, such as very light jets (VLJ) into the NAS. Xu, Baik, and Trani⁸ examine new noise and emission impacts more recently introduced by operations associated with the Small Aircraft Transportation System (SATS).

The metrics framework developed by the Williams team⁵ addresses discrepancies and ambiguities common in ATM performance measurement that have resulted when diverse organizations named metrics and developed their own specifications for them. Our proposed framework accounts for different levels of performance evaluation and, based on performance requirements and organizational goals, provides a useful roll-up of measures. The effort described in this paper builds on some of the ideas of the Williams team to propose a new framework; we used a trade study approach that can assess the impact of integrating new vehicle concepts into the NAS. As mentioned above, this approach draws upon concepts from control theory, utilizes ICAO KPAs, and can be extended to perform a wide range of performance and trade-off assessments of varying levels of fidelity. We have illustrated our approach using examples drawn from multiple studies and we further propose other trade-offs and research goals of possible future interest to NASA.

17.2. *Approach*

The NAS is a complex, dynamically changing system comprised of numerous airports, airspace classes, air traffic control facilities, and other resources. Primary users of the system include aircraft operators and air carriers, and their associated flights. User behaviors are constrained by approved operational procedures and performance characteristics of the vehicles they operate. The characteristics of

these NAS resources and operational procedures represent the system itself, whereas the traffic demand and vehicle performance characteristics serve as inputs to the system. Traffic (the collective performance of all flights) and the system's response to the demands imposed by traffic can be captured as outputs. As a result, system performance is driven by user and ATM system needs.

The ICAO and civil aviation authorities of individual countries have established standards that clearly define limits for accepted safety and environmental impacts. These standards cannot be violated, and may require fine-tuning of demand and vehicle performance characteristics (inputs) to ensure safe and environmentally friendly NAS operations. Other aspects of performance, however, are clearly *outcomes*. While performance aspects may reach unacceptable levels (e.g., very large delays), internationally accepted standards are lacking for outcomes, and they remain unregulated.

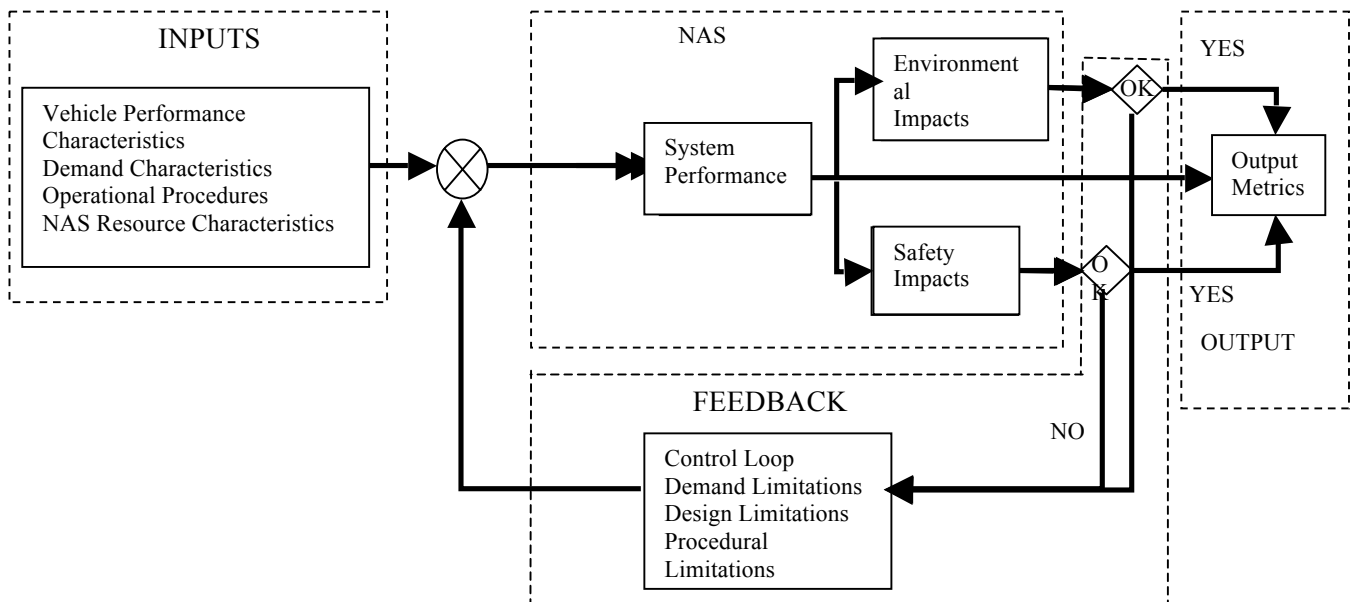


Figure 17-1: Simplified representation of the NAS as a system with dynamic behavior

A simplified representation of the NAS as a system characterized by dynamic behavior is illustrated in Figure 17-1 above. This depiction also provides a foundation for the proposed methodology used to study trade-offs between system performance, safety, and environmental impacts. The significance of this control-theory-based approach lies in its ability to fine-tune the characteristics of demand and user behavior. This capability provides a control mechanism with the potential to achieve the desired performance outcomes and ultimately meet performance targets (e.g., regulatory targets). This framework provides for a multi-step assessment methodology to determine if an acceptable (though not necessarily optimal) resolution is possible. It is proposed, through a series of controlled and iterative adjustments to demand characteristics (e.g., volume and fleet mix), operational procedures, or vehicle design characteristics, that researchers can meaningfully assess and fine tune system performance as well as environmental and safety impacts. However, in the research effort described here, only demand characteristics are varied as a means to provide a control mechanism.

It is important to note that this proposed approach does not exactly follow control theory approach. NAS is an adaptive system in which operational procedures and characteristics of its elements can and do adapt as a result of overall system performance. Consequently, even though operational procedures truly belong inside the NAS domain, they are used as inputs to the proposed approach.

Key metrics used for each of the performance areas yield outcomes that are computed by the modeling infrastructure established for this research effort. The following tools are utilized:

- Demand modeling: AvDemand (developed by Sensis Corporation)
- Aircraft design modeling: Environmental Design Space (EDS)
- Procedure design modeling
- New vehicle procedure “fly ability” validation: Terminal Area Route Generation, Evaluation, and Traffic Simulation (TARGETS)
- NAS-wide fast-time simulation: Advanced Concept Evaluation System (ACES), Future ATM Concepts Evaluation Tool (FACET), and MIT Extensible Air Network Simulation (MEANS)
- Airport and multi-airport impact modeling: the Airport and Airspace Simulation Model (SIMMOD)
- NAS-wide airport and airspace impact visualization: AvAnalyst (developed by Sensis Corporation)
- Spacing and ATC Workload: Time-Domain Analysis Simulation for Advanced Tracking (TASAT)
- Environmental impact modeling: Aviation Environmental Design Tool (AEDT), Aviation Environmental Portfolio Management Tool (APMT), and PC-Boom (the U.S. Air Force's sonic boom modeling tool)

The above set of tools provides the necessary modeling infrastructure to conduct the trade studies using the iterative approach presented in Figure 17-1. Vehicle performance characteristic summary tables, drawn from Base of Aircraft Data (BADA), appear in our calculations along with demand modeling (AvDemand). Operational procedures also are used as inputs to conduct NAS-wide simulations in FACET or ACES that help to determine system performance. Outputs from these and other required inputs can be used in AEDT and APMT to study environmental impacts and/or computed through SIMMOD and Performance Data Analysis and Reporting System/Georgia Tech (PDARS/GT) safety models to study safety impacts. If outcomes are unsatisfactory, any design, procedure, or demand restrictions can be reprocessed; continuous processing may continue until acceptable safety and environmental performance is achieved.

We defined and categorized the metrics produced by these tools relative to their contribution toward understanding system performance, environmental, and safety impacts on the NAS. Some of the metrics clarify performance directly, often referred to as performance indicators (or, simply indicators). Typically, indicators are used to set performance targets and measure the effectiveness of meeting such targets. In fact, as stipulated by ICAO International⁹, “Performance indicators are defined in order to quantify the degree to which performance objectives are being, and should be, met. When describing performance indicators, one must define what and how measurements will be obtained (through supporting metrics) and combined to produce an indicator.” The inherent information value of individual metrics, however,

may be insufficient to clarify performance. As a result, they may need to be combined with results from other metrics in order to clarify the direction and magnitude of their impact on performance.

Further, we have sought to determine many cause-effect relationships between, and among, the metrics and to illustrate the connectivity found in these relationships. We created diagrams to help visualize the type and extent of impact propagation that can result from a change in the system inputs, characteristics of the system itself, or a control action. More importantly, these diagrams provide a means to better understand the metrics and the processes that affect more than just one area of performance. They provide the basis for building trade-offs between system, safety, and environmental performance. Additionally, these diagrams point out gaps in metric definition and availability that might be useful in future trade assessments. In some instances, identified gaps have resulted from the lack, rather than availability, of metric definition; in other words, tools being used in this research effort may produce data necessary to generate a metric, but that particular metric has not yet been defined and evaluated. Although these metrics have been introduced into the initial metrics list, they actually flag gaps both in definition and availability. Such gaps have been documented and will be presented in later sections of this document.

The approach described above is generic and can be applied to any class of vehicle. In fact, it can be extended to any *combination* of vehicle classes—as well as to other types of NAS-wide studies. This approach provides for local, regional, and system-wide impact assessments and can be extended both to high and low fidelity investigations. The relevant metrics may constitute the only differentiator needed to integrate critical details related to the objectives of a specific analysis: such a differentiator may be applicable only to a distinct vehicle class, scope of analysis, or some other underlying important consideration.

17.3. **Key Performance Areas (KPA) and Key Performance Indicators (KPI)**

The focus of this section is to assess the impact of new vehicles on the NAS and to better understand their impacts on system, safety, and environmental performance. System performance is considered according to several subcategories that relate to ICAO KPAs and allow for a more precise understanding of overall performance. For the purpose of establishing worldwide standards in performance measurements, ICAO¹⁰ has identified the following eleven service expectations, also referred to as the KPAs: Access and Equity, Capacity, Cost Effectiveness, Efficiency, Environment, Flexibility, Global Interoperability, Predictability, Participation, Safety, and Security.

Our assessment of the applicability of these KPAs and their corresponding performance indicators are summarized below. We considered Global Interoperability, Participation, and Security KPAs outside the scope of this effort, but we maintained Environment and Safety as distinct performance categories. We also looked at the effects of the remaining six KPAs under a single category we called System Performance. While we presented the KPAs as they have been defined by ICAO in the context of the current effort, we identified the specific indicators for a corresponding KPA. Next we identified the KPI(s) for each of the KPAs, such that they were meaningful and provided an accurate reflection of performance. KPIs were selected based on intuition, years of experience and involvement with the ICAO ATM Requirements and Performance Panel, and by consulting with industry experts and other literature search. For example, the Efficiency KPA captured how cost effective the ATM system has proven to be from a single flight perspective. The KPI that effectively provided a means to measure efficiency,

therefore, has been the particular operating cost that could be incurred due to extra or additional (above nominal) fuel burn as a result of additional (beyond nominal) flight time. In the same vein, we addressed the need to meet current and future demand levels using the KPA capacity. Throughput provided us a measure of how much demand was successfully met and accommodated by the ATM system, and has thus far been a good indicator for measuring capacity. We plan to continue to fine-tune and refine the KPIs presented below through experimentation and simulation studies.

17.3.1. Access & Equity

Access and equity KPA ensures that all airspace users have access to ATM resources to meet their operational requirements and that the shared use of the airspace by the different users can be achieved safely. The global ATM system must also ensure equity for all users with access to the given airspace or service.

Key Performance Indicators:

- Percent of re-routed flights by user category and by cause of the re-routing: number of re-routed flights divided by the total number of flights using the resource (e.g., by user category, by cause of re-routing)
- Percent of delayed flights by user category and by cause of the delay: number of flights delayed by total number of flights using the same resource (e.g., by user category, by cause of delay)
- Percent of additional flights that are realized by user category: number of additional flights divided by the total number of flights using the same resource (e.g., by user category)
- Available seat miles (ASM): number of seats available multiplied by the number of miles flown (e.g., per day, per year)
- Operational availability: number of service hours relative to the maximum service hours for a facility/resource (considers all outage time except for improvements, expressed as a percent)

17.3.2. Capacity

Capacity KPA addresses the ability of the ATM system to meet current and future airspace user demands.

Key Performance Indicators:

- NAS, sector or airport throughput: number of realized operations per unit time of interest (e.g., 15-min bin, hour, annual)
- Annual service volume: a five year moving average throughput for the top 35 OEP airports
- Number of flights using a resource: number of flights (cumulative) using the same resource (sector, center, airspace segments) in a specified period of time (e.g. flights/year, flights/hour, flights/15-min interval)

17.3.3. Cost Effectiveness

Cost effectiveness KPA addresses the need of the ATM system to preserve resources, while balancing the interests of the varied ATM users. When evaluating any proposal to improve the ATM quality of service, the cost of the service needs to be considered.

Key Performance Indicators:

- Cost of service provision: captures the cost of service provision from the ATC perspective (includes staffing and other relevant costs)

17.3.4. Efficiency

Efficiency KPA addresses the operational and economic cost effectiveness of gate-to-gate flight operations from a single-flight perspective.

Key Performance Indicators:

- Additional flight time (delay): difference between the actual and the planned flight time (e.g., for a whole flight, phase of flight, within a specified resource) in minutes
- Additional fuel burn: difference between the actual and the planned fuel burn (e.g., for a whole flight, phase of flight, within a specified resource) in pounds
- Direct Operating Cost (DOC): captures the cost of operations from a single-flight perspective in dollars
- Additional DOC: difference between the planned DOC and the actual DOC from a single flight perspective in dollars
- Payload distance flown: the product of the payload and the distance flown between origin and destination airport (kg.km)

17.3.5. Environment

Environment KPA addresses the need to protect the environment from gaseous emissions, noise, and other environmental impacts from the implementation and operation of the global ATM system.

Key Performance Indicators:

- Payload Fuel Energy Intensity (PFEI) of aircraft operation in terms of total fuel energy consumed per payload distance flown in MJ/kg-km or MJ/tonne-km
- Emissions below 3,000ft: NO_x, SO_x, PM, CO and HC: annualized inventory of listed emissions at each airport of interest in the US; includes all of the modes of flight below the mixing height, both departure and arrival; kg/yr
- Full flight emissions^{cxlix}: CO₂, NO_x, SO_x, PM, and H₂O: annualized inventory of listed emissions for the entire US; includes all of the modes of flight, and typically takes the entire flight for either international departures or arrivals or both; kg/yr
- Terminal noise contour area: 65,60,55 dB Day-Night Average Sound Level (DNL) terminal noise contour area in nm (e.g., by airport)
- Noise population exposure: number of people cumulatively exposed to 65, 60 , 55 dB DNL noise contours (e.g., by airport)

- Number of premature mortalities due to particulate matter (PM)_{2.5} exposure: number of premature deaths resulting from emissions below 3000 ft^{cl}
- Globally averaged surface temperature change per year resulting from the change in radiative forcing (RF) due to aviation emissions in degrees Celsius
- Monetary impact total: net monetized value resulting from global surface temperature change, premature mortality, and noise exposure (%GDP; dollars)

17.3.6. Flexibility

Flexibility KPA addresses the ability of all airspace users to modify flight trajectories dynamically, and adjust arrival and departure times, to exploit operational opportunities as they occur.

Key Performance Indicators:

- Percent of user requests granted: number of user requests that are granted divided by the total number of user requests (e.g., type of request)
- Percent of flights with shorter routes due to increased access to airspace previously not available: ratio of number of flights with shorter routes and the total number of flights (e.g., per day, per year)

17.3.7. Global Interoperability

Global Interoperability KPA addresses the need for global standards and uniform principles to ensure the technical and operational interoperability of ATM systems.

Key Performance Indicators: not considered in the current research effort.

17.4. *Predictability*

Predictability KPA addresses the ability of the airspace users and ATM service providers to provide consistent and dependable levels of performance

Key Performance Indicators:

- Distribution (variance, standard deviation) of delay: histogram of the distribution of flights by delay bins (e.g., for a specified airport, sector, market-pair)
- Distribution (variance, standard deviation) of fuel burn by a vehicle type on a given market: standard deviation of fuel burn (e.g., by vehicle type)

17.4.1. Participation

Participation KPA addresses the need for the continual involvement of the ATM community in the planning, implementation, and operation of the system to ensure that the evolution of the global ATM system meets the needs of the community.

Key Performance Indicators: not considered in the current research effort.

17.4.2. Safety

Safety KPA addresses the risk, prevention, occurrence and mitigation of air traffic accidents. Safety is of the highest priority and ATM plays a vital role in ensuring overall aviation safety. Uniform safety standards, together with risk and safety management practices, must be systematically applied to the ATM system.

Key Performance Indicators:

- Number of separation violation events: count of loss of separation events, Traffic Alert and Collision Avoidance System (TCAS) alerts on a specified time period, per specified operation, etc.
- Number of conflicts and resolution maneuvers: count of conflicts and resolution maneuvers in a specified period of time or per specified operation
- Fatalities per accident category: number of accidents or incidents leading to fatalities (e.g., per accident category, by airport, per year)
- Propensity: captures the likelihood of a safety significant event to occur during normal operations
- Resilience: captures the ability to respond to perturbations or accommodate change while minimizing the potential adverse impacts and keeping the impact local

17.4.3. Security

Security KPA addresses the need to protect against threats that stem from intentional acts (e.g., terrorism) or unintentional acts (e.g., human errors, natural disaster) affecting aircraft, people or ground installations.

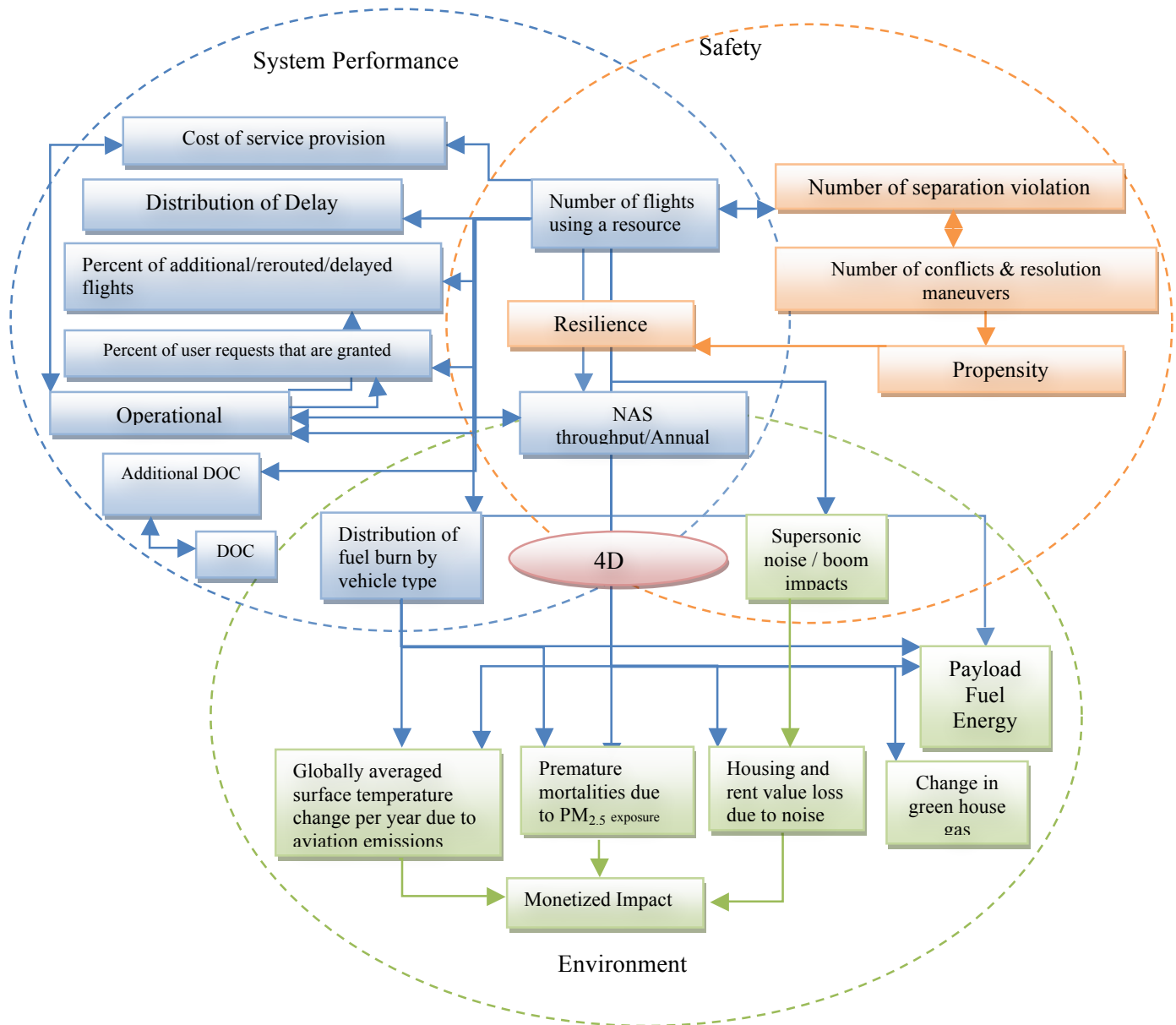
Key Performance Indicators: not considered in the current research effort.

17.5. High-Level Metrics Framework

In establishing the high level metrics framework, the cause-effect relationships were studied through detailed investigation of the requested and realized 4D trajectories. Note that the 4D trajectory is not a metric, but simply a construct that provides for connectivity between system, safety, and environmental performance in the absence of indicators that provide a direct link to contributing metrics. Figure 17-2 illustrates cause-effect connectivity between selected KPIs to present a high level metrics framework that captures system, safety, and environmental performance outcomes.

It is important to point out that Figure 17-2 captures only some of the high level (or societal level) performance indicators proposed for each of the performance areas considered in this research effort. The list of metrics that is actually produced by the available tools or can be computed for these indicators is considerably longer. In other words, many of these indicators connect via cause-effect relationships with other metrics; some of these extended diagrams are presented later.

The Venn-diagram in Figure 17-2 captures the interaction between the three performance areas of interest: system performance, safety and environment. Each circle of the color-coded diagram represents one of the performance areas. Three colors – blue (system performance), orange (safety) and green (environment) – are used. KPIs represent the influences and interactions among the three areas.



Overlapping regions represent indicators that relate to more than one performance area.

Metrics Classification Levels

The metrics used to evaluate performance and conduct trade studies in this research effort capture and represent performance at several hierarchical levels. Classification can be based on geographical location, such as national, regional airport, regional terminal, and vehicle, where metrics can be aggregated to provide the higher-level impacts; alternatively, classification can be based on socio-economic impacts, such as societal, operational, and vehicle level).

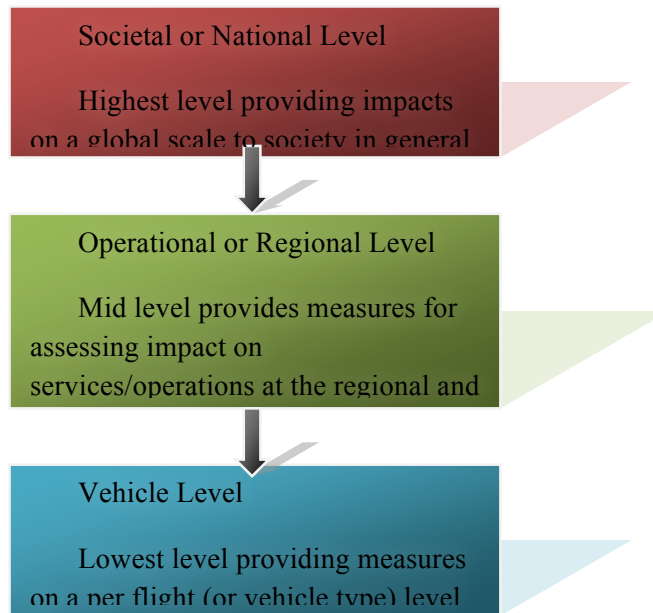


Figure 17-3: Metrics classification levels

For the purpose of this study, the metrics are classified into three levels (as depicted in Figure 17-3):

Level 1, Societal or National Level—captures metrics with socio-economic considerations or aggregated results that provide impacts on a global or national scale to society in general. This stratum represents the highest level of abstraction and is of particular interest to regulatory and governmental organizations

Level 2, Operational or Regional Level—provides mid-level measures for assessing impacts at system-wide or regional (including airport) levels, but with a focus on services and operations. This stratum provides finer granularity than the previous level, and is of particular interest to local authorities, service providers, and NAS users.

Level 3, Vehicle Level—captures metrics relevant to any lower-level assessments that may be needed. It comprises the lowest stratum and provides metrics at the finest granularity. It provides performance measurements at the individual flight (or vehicle type) level, and is of particular interest to service providers and NAS users.

The classification scheme established above allows metrics to be rolled up or down to support selective and multiple analyses from the highest to the lowest level.

17.5.1. Trade Studies Simulation Design

As presented in Figure 17-4, the simulation setup proposed for conducting the trade studies follows a simplified representation of the NAS as a system with dynamic behavior. This control-theory-based simulation design allows for iterative tests in which any of the input variables can also be used as control variables. For instance, the design allows one to determine vehicle design limitations with respect to the

performance characteristics required for operating in the entire NAS or in a part of it. In this example, the NAS is described through the characteristics of its resources (e.g., airports, airspace, facilities). Additionally, the demand characteristics and operational procedures are assumed to be reasonable for a given set of vehicle performance characteristics. In each of the iterations, performance outputs are evaluated for a constant set of vehicle performance characteristics, and any required adjustments are determined and implemented via the control loop. Ultimately, any limitations in vehicle performance characteristics that result in unacceptable performance outcomes are determined; these may include speed, altitude, rate-of-climb, and other limitations for operating in a given part of the NAS. The example below illustrates the design's ability to provide for the wide range of assessments and fine-tuning that may be needed to evaluate new vehicle types, procedures, technologies, and concepts of operations.

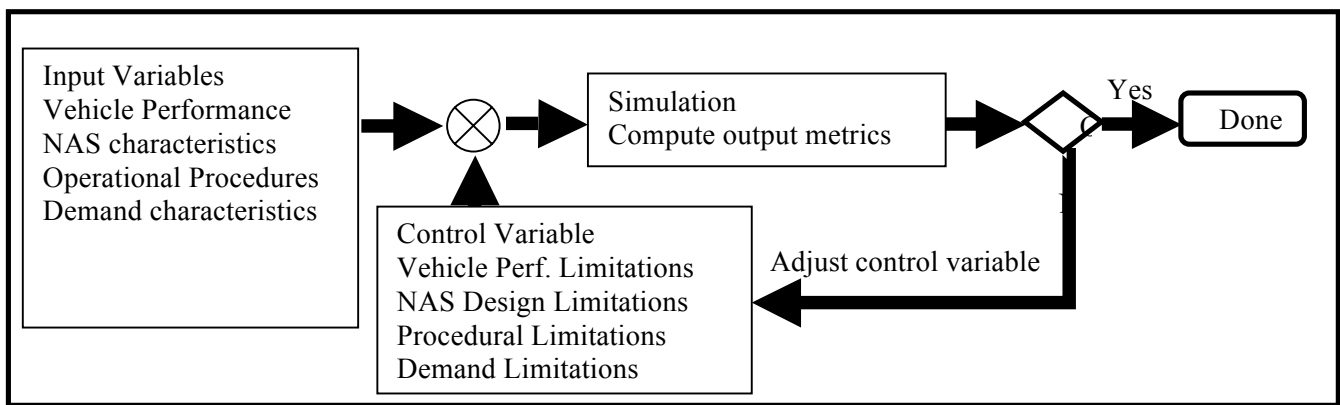


Figure 17-4: Simulation design to enable iterative runs to deliver acceptable outcomes

A two-fold increase in air traffic operations is expected by 2025¹¹. Additionally, the number of operations is expected to continue to increase and reach a three-fold increase by 2059¹². Therefore, it is important not only to consider the impact of increased demand, but also to ensure a mechanism for assessing how this demand increase can be safely accommodated with acceptable environmental impacts.

Although iterative runs will not be performed across the range of simulations conducted as part of this effort, the simulations will use demand characteristics as an input variable to the system. Traffic volume, fleet mix, and geometry of the flown trajectories will be fine-tuned prior to the actual simulations (in addition to the static inputs required to conduct the simulation) to represent sensible demand characteristics forecasted for the three demand levels of interest. The output of these simulations will allow the corresponding impact onto NAS performance to be assessed.

Input Variables:

- Static Inputs
 - Aircraft performance – BADA performance specifications
 - Airport and airspace characteristics – resource availability and limitations in their use
 - Operational procedures – restrictions in user behavior

- Variable Inputs
 - Demand characteristics – desired or restricted schedules and trajectories

Traffic volume, fleet mix, geometry of flown/desired trajectories as forecasted for the years of 2025, 2040 and 2086 with conventional as well as new vehicles integrated will be used.

Control Variables

- None

Outputs

- KPIs and other metrics required to assess system performance, environmental and safety impacts.

17.5.2. Key Trade Studies Used In This Research Effort

Three key trade studies were identified that provided individual feasible bases for conducting our research. They included trading between impacts onto Capacity and Environment KPAs, Capacity and Efficiency KPAs, and Capacity and Predictability KPAs. Our use of each of these studies provided valuable insight into the trade space.

A description of supporting trade studies is provided in this Section. Numerous other examples of trade studies that may be of interest to future NASA research efforts are examined in Section: Other Trade Studies Proposed to NASA for Future Research.

17.5.3. Trade-off #1: Capacity vs. Environment

This trade study examines the impact of a change in traffic flow characteristics on capacity and environment. It assumes that safety considerations are satisfied through implementation of appropriate separation standards and procedural restrictions. The Capacity vs. Environment trade-off study utilizes a multi-level metrics interaction diagram elaborated in Section: High-Level Metrics Framework, and provides a hierarchical method for evaluating trade-offs between the capacity and environment KPAs at the national, airport/regional, and vehicle assessment levels. The underlying experiment design supporting this trade study provides a feedback loop for capturing the adaptable and dynamic nature of the NAS by introducing the iterative fine-tuning of traffic flow characteristics. The full fine-tuning capability was not utilized in this research effort; however, a single run-through was performed to illustrate the approach and its potential. Please refer to the Approach Section for a complete description of the approach.

Research Goals

- Capacity vs. Environment trade-offs will be studied using both NAS-wide and regional (New York Metroplex region) simulations. There are two key research goals supported by this trade study:
- Research goal #1: Examine the impact of changes in traffic flow characteristics on the environment at the airport / regional level. In particular, this study addresses the following questions:

- What are the environmental impacts of increased demand?
- Can the additional volume (by vehicle class) and new overall characteristics of demand be accommodated without adverse environmental impacts?
- Is there a need to restrict the operations to meet environmental constraints?
- Research goal #2: Examine the impact of changes in en route traffic flows on the environment. For example:
 - What are the environmental impacts of increased demand?
 - Can the additional volume (by vehicle class) and new overall characteristics of demand be accommodated without adverse environmental impacts?
 - Is there a need to restrict operations in some manner to meet environmental constraints?

Cause-Effect Relationships

The representative indicators capturing performance within the capacity and environment KPAs and the cause-effect relationships of the supporting metrics are illustrated in Figure 17-5. The underlying relationships shown in Figure 17-5 were developed through intuition and experience, as well as by using metric definitions and other available supporting information such as evaluation method. Capacity impacts trickle down to the environment through the time individual aircraft spend in the air, by the aviation emissions that pollute the atmosphere as a result of fuel burn, and by the efficiency with which all the aircraft within the system can be accommodated (the relationship between demand from flights and system capacity leading, with the consequence of congestion when the former exceeds the latter). For example, the number of aircraft entering airports, as well as the amount of airborne holding they incur when arrival demand exceeds airport capacity has a direct relation to the noise contours and population exposure levels (noise impacts) in the terminal area.

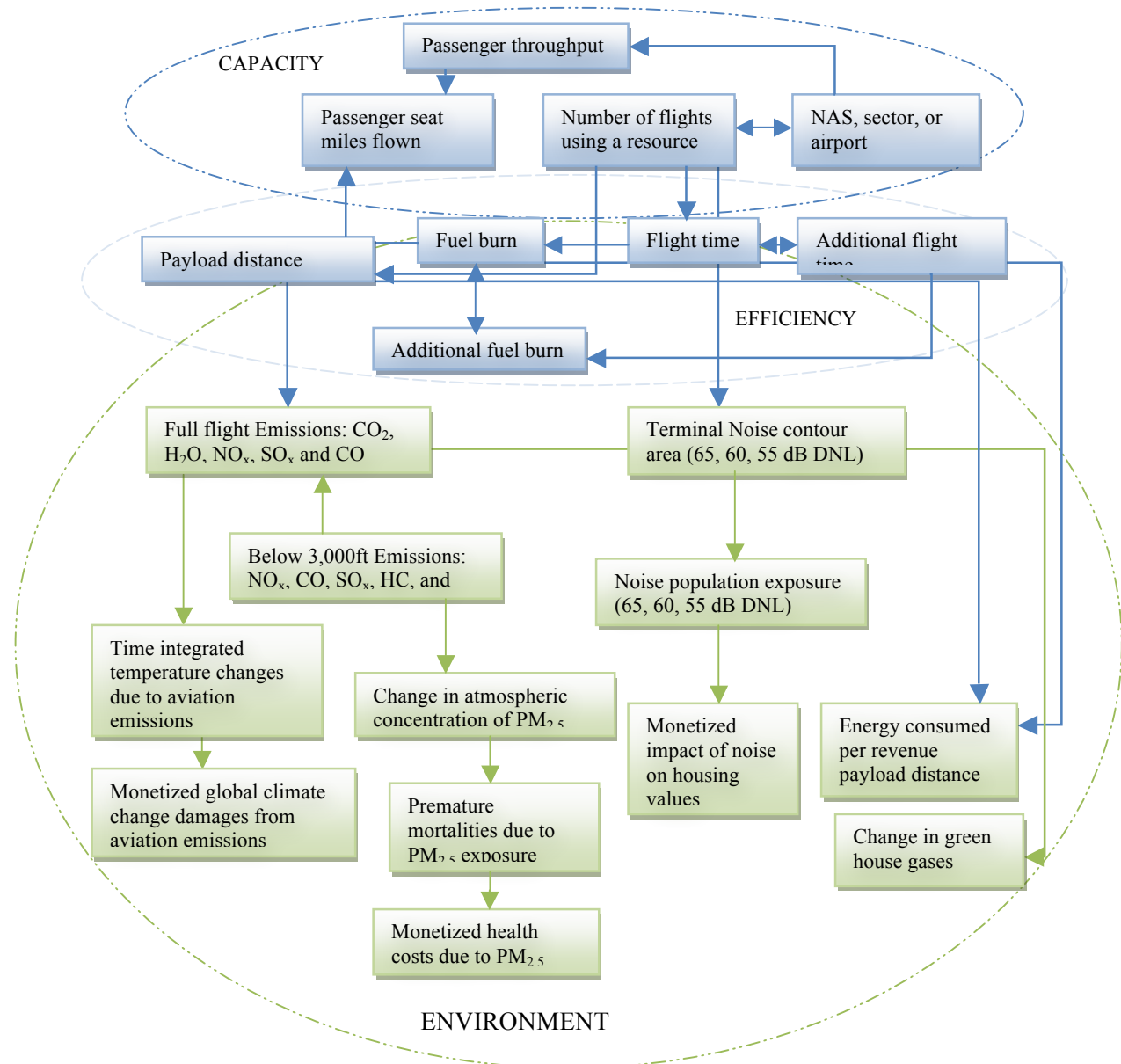


Figure 17-5: Cause-effect relationships for Capacity vs. Environment trade study

Aviation emissions due to fuel burn (and excess fuel burn owing to excess flight time induced by inefficiency and delay) in the terminal area (below 3000ft) affect the concentration of pollutants (such as PM_{2.5}) leading to premature mortality (air quality impacts). Fuel burn impacts over the full mission cause change in green house gas emissions and global temperature changes (climate change).

Performance Outputs

Based on the cause-effect relationships established in Figure 17-5 and the metrics classifications developed in the Metrics Classification Levels section, KPIs supporting the Capacity vs. Environment trade study will be identified for each of the three assessment levels discussed above. These indicators are presented for system-wide and regional assessments.

Experiment Design

The tools (along with the flow of information and order of usage) that will be used to conduct this trade study are shown in Figure 17-6, which also outlines an analysis process to study system-wide and regional impacts.

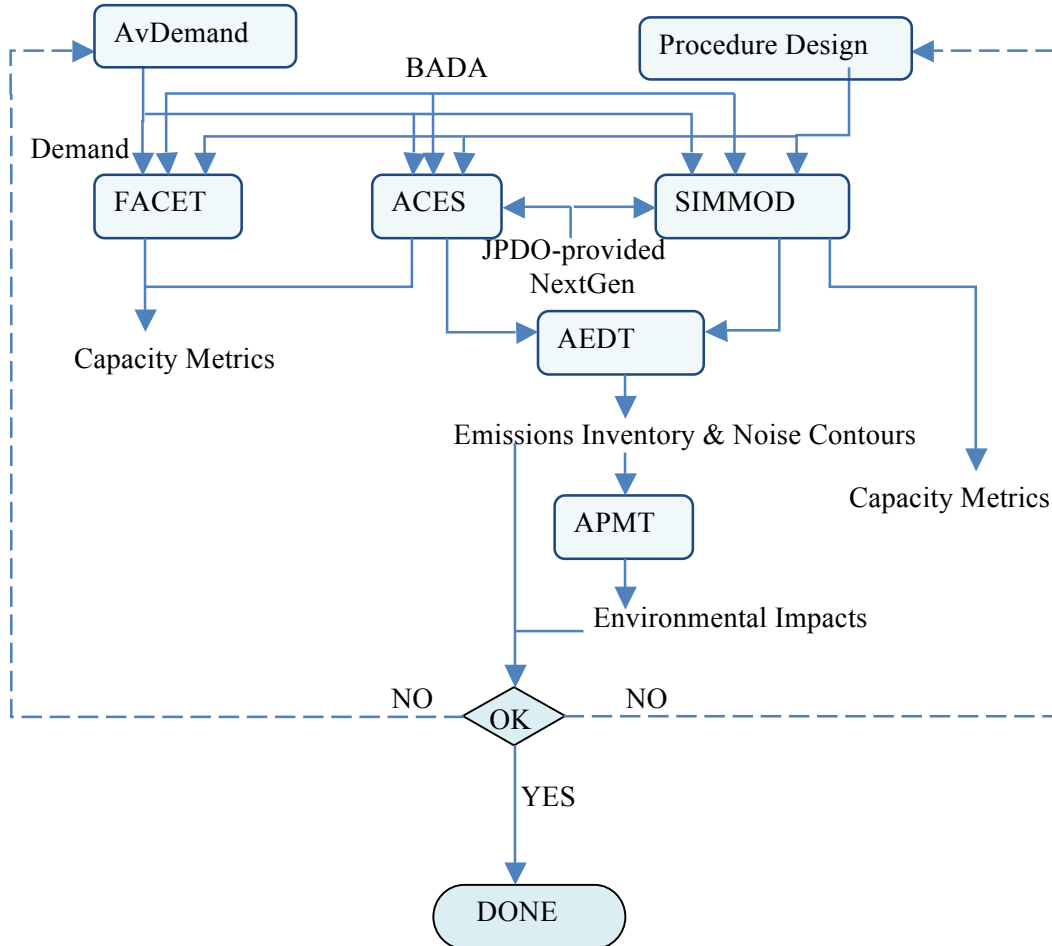


Figure 17-6: Experiment design with iterative loops for trade study #1

Table 17-1: Capacity vs. Environment performance outputs for system-wide and regional analysis

Level	Capacity	Environment			
		Energy Efficiency	Noise	Air Quality	Climate
NATIONAL	<p>1) % change in available passenger seat miles between all airports</p> <p>2) % change in cargo transport miles between all airports</p> <p>3) % change in number of flights between all airports</p>	<p>1) Sum of the energy consumed by operations between all airports normalized by revenue payload-distance carried on those flights</p>	<p>1) Sum of the % change in population exposure to X dB DNL due to operations at All airports</p>	<p>1) Sum of % change in premature mortality due to total PM_{2.5} exposure due to operations at all airports (considering emissions of PM, NOx, and SOx under 3,000 ft)</p>	<p>1)% change in time-integrated, globally averaged surface temperature change due to operations at and between all airports (considering emissions of CO₂, H₂O, NO_x, SO_x, and PM, as well as formation of contrails-cirrus clouds)</p>
REGIONAL	<p>1) % change in available passenger seat miles at Metroplex / terminal area / airport</p> <p>2)% change in cargo transport miles at Metroplex / terminal area / airport</p> <p>3) % change in number of flights at Metroplex / terminal area / airport</p>	<p>1) Sum of the energy consumed by all operations at Metroplex / terminal area / airport normalized by payload-distance carried on those flights</p> <p><i>Airport-level energy efficiency metric included for sake of completeness, only has marginal value</i></p>	<p>1)% change in population exposure to X dB DNL due to all operations at Metroplex / terminal area / airport</p>	<p>1) % change in premature mortality due to total PM_{2.5} exposure due to all operations at Metroplex / terminal area / airport (considering emissions of PM, NOx, and SOx under 3,000 ft)</p> <p><i>MIT evaluating potential to conduct this analysis</i></p>	<p>1) % change in greenhouse gas emissions due to all operations at Metroplex / terminal area / airport (considering emissions of CO₂, H₂O, NO_x, SO_x, and PM).</p>

VEHICLE	1) % change in available passenger seat miles using this vehicle (relative to the total number of operations) 2) % change in cargo transport miles using this vehicle (relative to the total number of operations) 3) % change in number of flights using this vehicle (relative to the total number of operations)	1) Energy consumed by individual aircraft operation normalized by available revenue payload-distance carried	1) % change in Population Exposure to X dB max due to a single aircraft operation	1) % change in emissions of PM, NOx, and SOx due to a single aircraft operation	1) % change in greenhouse gas emissions (CO ₂ , H ₂ O, NOx, SOx, and PM) due to a single aircraft operation
----------------	---	--	---	---	---

On the national level, outputs from AvDemand (demand levels and fleet mix), EDS (BADA aircraft performance models), and Procedure Design models will be used in ACES and FACET to conduct NAS-wide simulations to assess airport and airspace system performance. 4D trajectory outputs from ACES and FACET will then be used in AEDT environment models to compute environmental impacts (noise and emission metrics displayed in table above). Finally, outputs from AEDT will be used by APMT models to calculate environmental impacts.

Regional airspace and airport impact studies will be conducted using SIMMOD, which will draw upon outputs from AvDemand, EDS, and Procedure Design models to generate 4D regional trajectories; the trajectories will then be employed to conduct regional environmental impact studies using AEDT environmental models. Outputs from AEDT will be used in APMT models to calculate environmental impacts. In addition, PC-Boom will be run to determine the noise impacts from supersonic vehicle integration.

If resulting environmental impacts (noise, emissions and monetary) are unsatisfactory, then traffic flow characteristics (demand levels and fleet mix) and/or procedure designs will be adjusted and this process will continue until acceptable levels of environmental impacts are achieved. While the proposed approach allows for demand characteristics adjustment and/or procedures in an iterative process until desirable outcomes are achieved, it should be noted that in the current research effort, only different demand scenarios will be used to conduct the simulations necessary to generate performance outputs.

Sample Dashboard Graphics

The graphs below represent notional examples. On the highest level, radar graphs will be used to simultaneously capture the impacts and changes to KPIs from each of the Capacity and Environmental categories so that trade-offs and interdependencies between them can be visualized. Figure 17-7 provides a sample radar graph of the comparison of the key indicators highlighting environmental impacts for four different demand scenarios at the national level.

Figure 17-8 provides a sample radar graph for comparison of environmental impacts at the airport level. The radar graphs in Figure 17-7 and

Figure 17-8 display all the key metrics identified for the capacity vs. environment trade study at the relevant classification level. It should be noted that the acceptable direction of change (increasing or decreasing) for a given metric has to be taken into consideration when interpreting the radar graphs. In addition, the following graphs will be produced for the system-wide and regional analysis:

- %change in throughput vs. % change in population exposure to 55 DNL
- %change in throughput vs. % change in population exposure to 65 DNL
- %change in throughput vs. % change in premature mortality due to PM exposure from aviation emissions
- %change in throughput vs. % change in CO₂ emissions
- %change in throughput vs. % change in energy per available seat mile
- %change in throughput vs. % change in time integrated mean temperature due to aircraft emissions
- %change in emissions affecting air quality, namely NO_x, SO_x, PM, CO, and HC for top five airports

Gaps in Metrics

Gaps in the current set of metrics have been identified based on initial examination of the existing tools and models and the metrics that can be computed by those models. The identified set of metric gaps addresses the following issues:

- Rotorcraft noise (airport impacts)
- Supersonic noise/boom (en-route impacts)
- Uncertainty in the impact of short-lived aviation emissions on global climate change (e.g. the impact of contrails and contrail-cirrus)

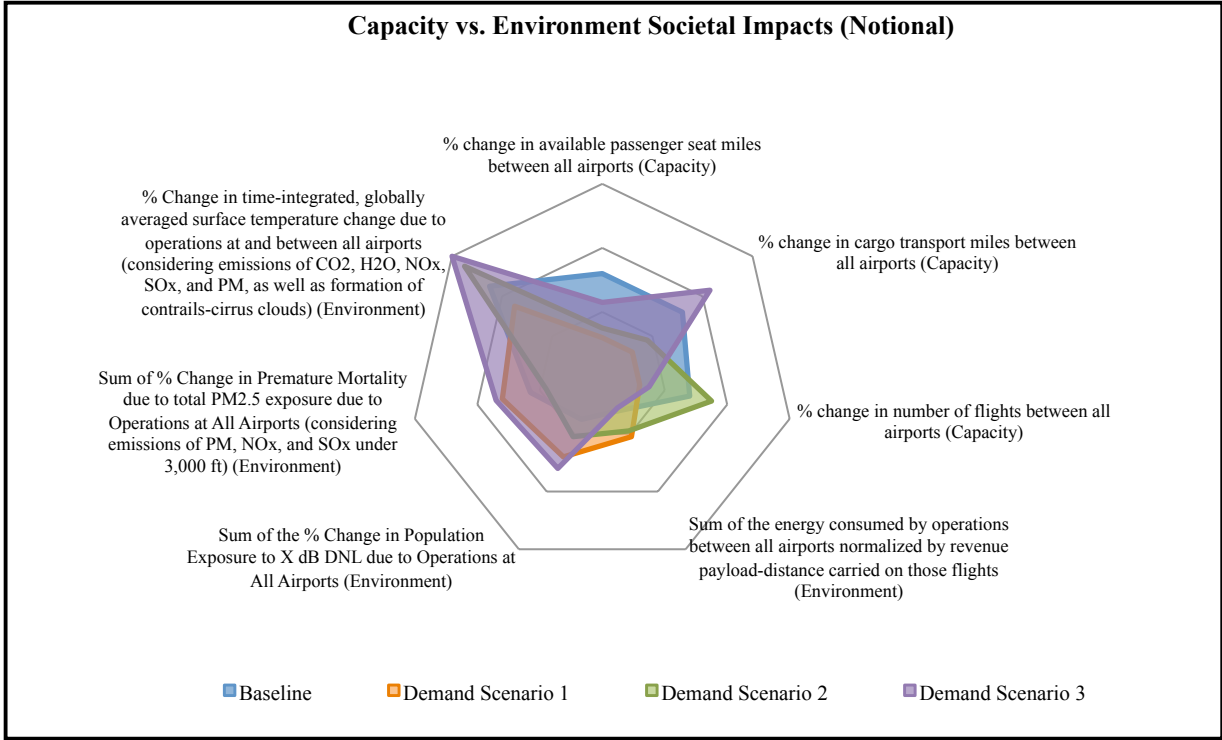


Figure 17-7: Radar graph of Capacity vs. Environment national level impacts (notional)

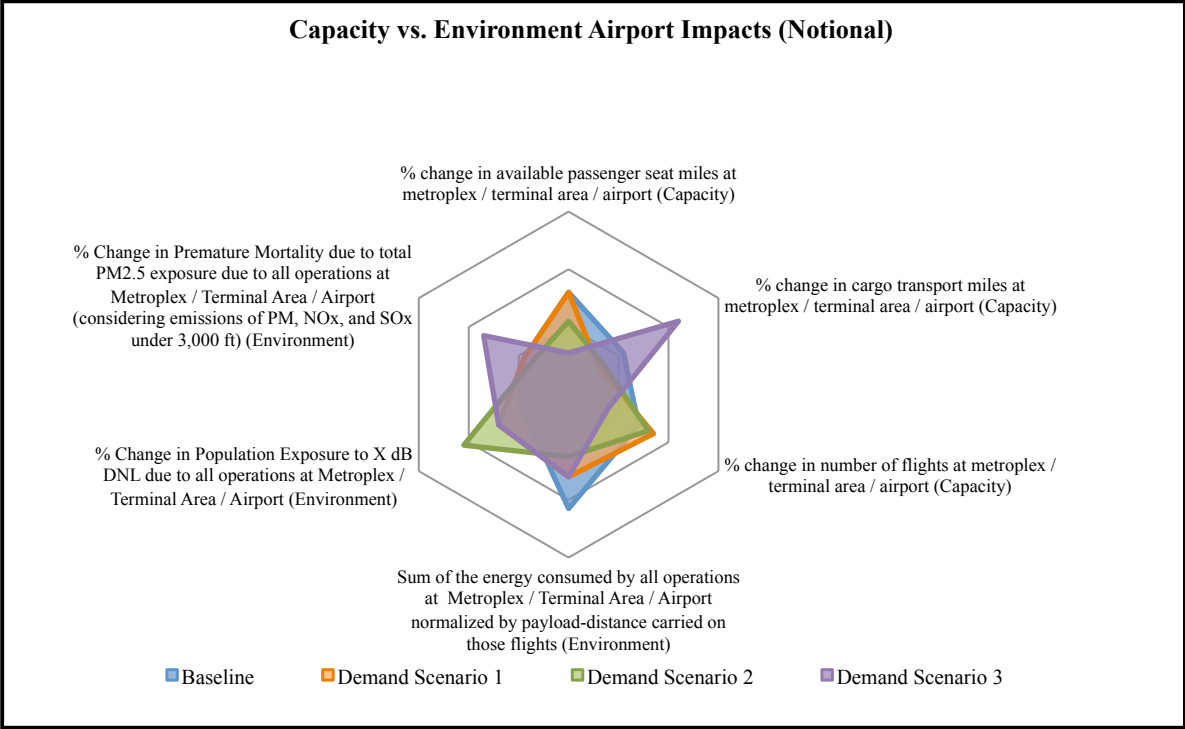


Figure 17-8: Radar graph of Capacity vs. Environment airport level impacts (notional)

17.5.4. Trade-off #2: Capacity vs. Efficiency

This trade study assesses the impact of changes in traffic flow characteristics on capacity and flight efficiency. An assumption is made that safety considerations will be inherent in the analysis through application of appropriate separation standards and procedural restrictions. The Capacity vs. Efficiency trade study helps evaluate trade-offs between capacity and efficiency. As in the previous trade study, a multi-level metrics framework is utilized to perform the analysis at the national, airport, and vehicle level.

Research Goals

A key research goal considered in this trade study is: Research goal #3: Determine the impact of changes in traffic characteristics at a given airport based on airport throughput and performance. In particular, this trade study addresses the following questions:

- Can the additional volume (by vehicle class) and new overall characteristics of demand be accommodated without any adverse effect on flight efficiency (safety is embedded through implementation of appropriate separation standards and procedural restrictions)?
- Is there a need to restrict the number of operations by a vehicle class in some manner (e.g., time of day, number of operations, access to airport by airport type and geographic location) with a goal of improving the overall airport throughput and performance?
- What other operational procedures and improvements can be incorporated to improve the overall airport throughput and performance with minimal impact on flight efficiency?

Cause-Effect Relationships

The representative indicators capturing performance within the KPAs of capacity and flight efficiency used in this trade study and the cause-effect relationships of the supporting metrics are illustrated in Figure 17-9. Capacity limitations have a direct impact on the efficiency of operations in the NAS. Highly congested areas or areas of bad weather can lead to longer flight times and greater fuel burn, causing an increase in airline operating costs. The key indicators providing a measure of the efficiency of the ATM system are flight time and fuel burn. The monetary impact of capacity constraints on efficiency is directly measured through the change in the operating costs incurred by the user, change in maximum payload capability afforded to the user, and revenue accrued through the change in passenger seat miles flown.

Performance Outputs

Based on the metrics relationships established above and the key indicators identified, Table 17-2 provides a summary of the output metrics chosen to analyze this trade study. As indicated previously, efficiency is measured in terms of the direct operating costs, individual aircraft flight time, and fuel burn-- while impacts of capacity are measured in terms of throughput and passenger seat miles flown

Experiment Design

Existing tools and models that will be used to conduct this trade study are shown in Figure 17-10. Arrows indicate both the order in which the tools will be used and the direction of the flow of information. System-wide capacity and efficiency metrics listed in Table 17-2 will be outputs of NAS-

wide simulations run in the FACET and ACES models, while regional capacity and efficiency metrics will be outputs of SIMMOD runs. If the performance outputs are unsatisfactory or can be improved further, demand characteristics and/or procedures will be adjusted for better outcomes.

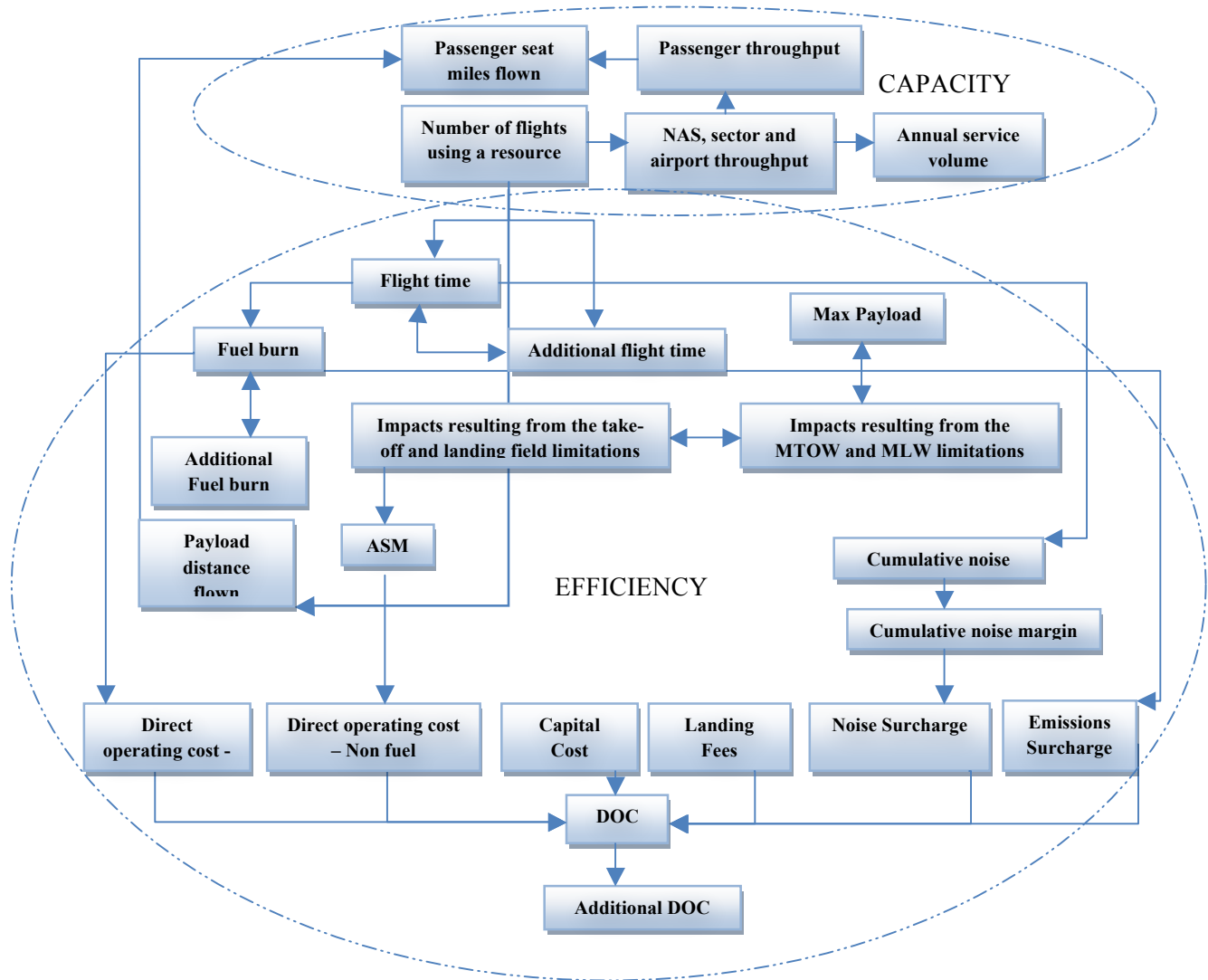


Figure 17-9: Capacity vs. Efficiency cause-effect relationships

Sample Dashboard Graphics

Figure 17-11 provides a notional radar graph of the comparison of the key indicators highlighting capacity and efficiency trade-offs for four different demand scenarios at the airport level. The radar graphs display all the key metrics identified for the Capacity vs. Efficiency trade study at the relevant classification level. It should be noted that the acceptable direction of change (increasing or decreasing) for a given metric has to be taken into consideration when interpreting the radar graphs.

In addition, the following graphs will be produced for the system-wide and regional analysis:

- %change in throughput vs. % change in direct operating cost for operations at all airports (or Metroplex airports for regional analysis)

- %change in throughput vs. % change in maximum payload for operations at all airports (or Metroplex airports for regional analysis)
- % change in maximum payload by airline and/or freight company
- % change in flight time by vehicle type
- % change in fuel burn by vehicle type

Table 17-2: Capacity vs. Efficiency performance metrics for trade study #2

Level	Capacity	Efficiency
NATIONAL	1) % change in available passenger seat miles between all airports 2) % change in cargo transport miles between all airports 3) % change in number of flights between all airports	1) % change in passenger delay (passengers per aircraft * aircraft delay) 2) % Change in GDP due to passenger delay
REGIONAL	1) % change in available passenger seat miles at Metroplex/ Terminal Area / Airport 2) % change in cargo transport miles at Metroplex/Terminal Area/Airport 3) % change in number of flights at Metroplex / Terminal Area / Airport	1) % change in direct operating costs (DOC) for operations at all Metroplex / Terminal Area / Airport <i>Metric cannot be computed at this time but is included here as potential metric for future research efforts</i> 2) % change in max payload for operations at all Metroplex/Terminal Area/ Airport 3) % change in passenger delay (passengers per aircraft * aircraft delay)
VEHICLE	1) % change in available passenger seat miles using this vehicle (relative to the total number of operations) 2)% change in cargo transport miles at using this vehicle (relative to the total number of operations) 3) % change in number of flights using this vehicle (relative to the total number of operations)	1)% change in individual aircraft flight time between origin destination pairs by vehicle type 2)% change in individual aircraft fuel burn between origin destination pairs by vehicle type 3)% change in individual aircraft flight time between origin destination pairs for all other vehicle types 4)% change in individual aircraft fuel burn between origin destination pairs for all other vehicle types

Gap in Metrics:

Based on preliminary research of the existing tools, models, and metrics, a set of gaps in the metrics computed by those tools was identified. The following metrics were determined to be useful indicators for future research in studying the impacts of new vehicles within a NextGen context.

- Aircraft size trends (impact of decreasing aircraft size, increasing passenger volume, increasing load factors, flight cancellations)
- Lost revenue for a carrier due to a limited or prohibited access to an airport

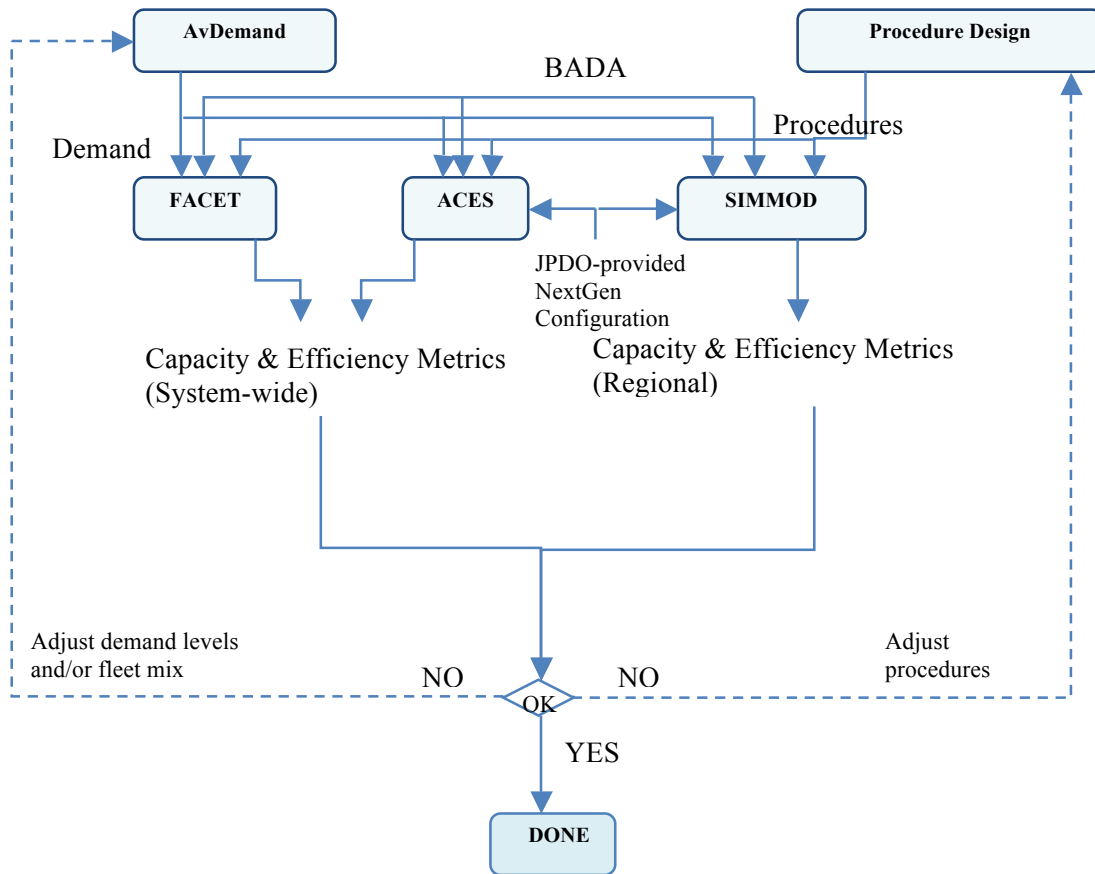


Figure 17-10: Experiment design with iterative loops for trade study #2

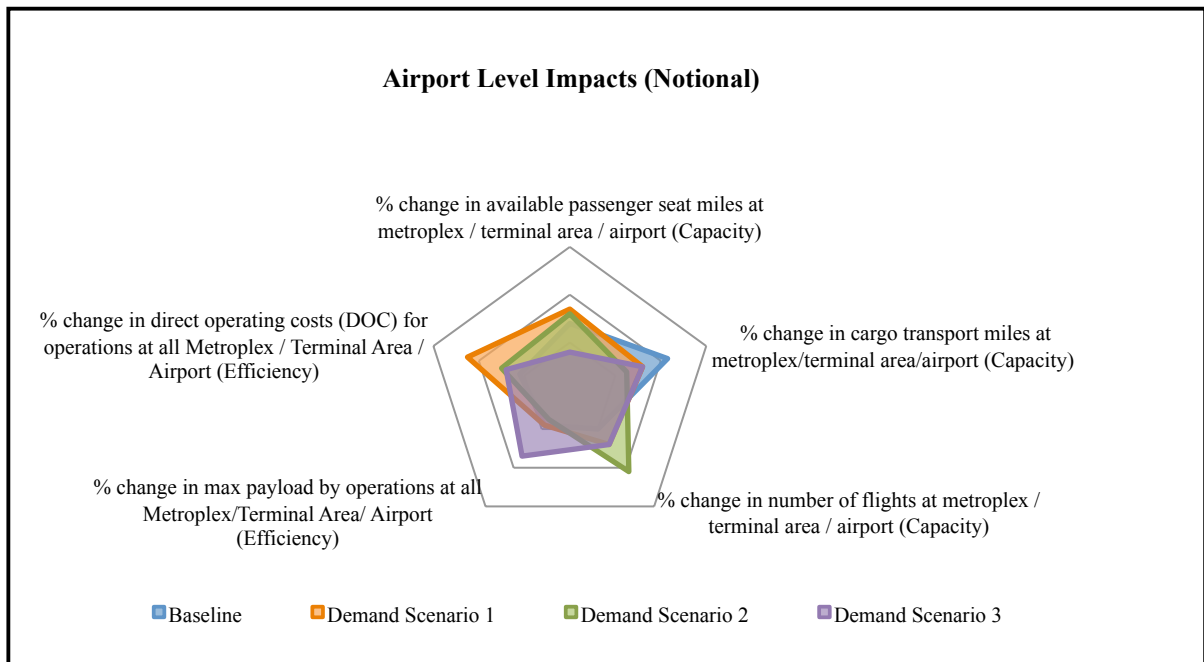


Figure 17-11: Radar graph of Capacity vs. Efficiency airport level impacts (notional)

A metric that captures impact of schedule restrictions:

- If an additional flight is added to the schedule, what is the additional gain for that carrier? Can that gain be sufficiently captured by determining increase in revenue?
- If that flight causes others to be delayed or perturbed in some manner, how can the overall effect be accurately assessed (e.g., their gain vs. others' loss)?

17.5.5. Trade-off #3: Capacity vs. Predictability

The following study assesses the impact of the predictability of traffic flow characteristics on airspace and airport throughput and performance. Safety considerations are assumed to be inherent in the analysis through application of appropriate separation standards and procedural restrictions. The Capacity vs. Predictability trade study enables the evaluation of impacts of capacity constraints on the predictability of ATM services. Historically, delay has been considered the key metric in efficiency analysis and statistical distribution of delay provides a good measure to conduct predictability analysis.

Research Goals

The key goal identified for the study of the impact of changes in traffic flow characteristics on capacity and predictability and the trade-offs possible between the two KPA is:

- Research goal #4: Determine the level of operations that the system can accommodate that will not exceed a given level of arrival delay (e.g., On-Time Gate Arrivals – captures flights that arrive at the gate less than 15 minutes after the scheduled gate arrival time).
 - What operational procedures can be incorporated to bring delay to acceptable levels?

Cause Effect Relationships

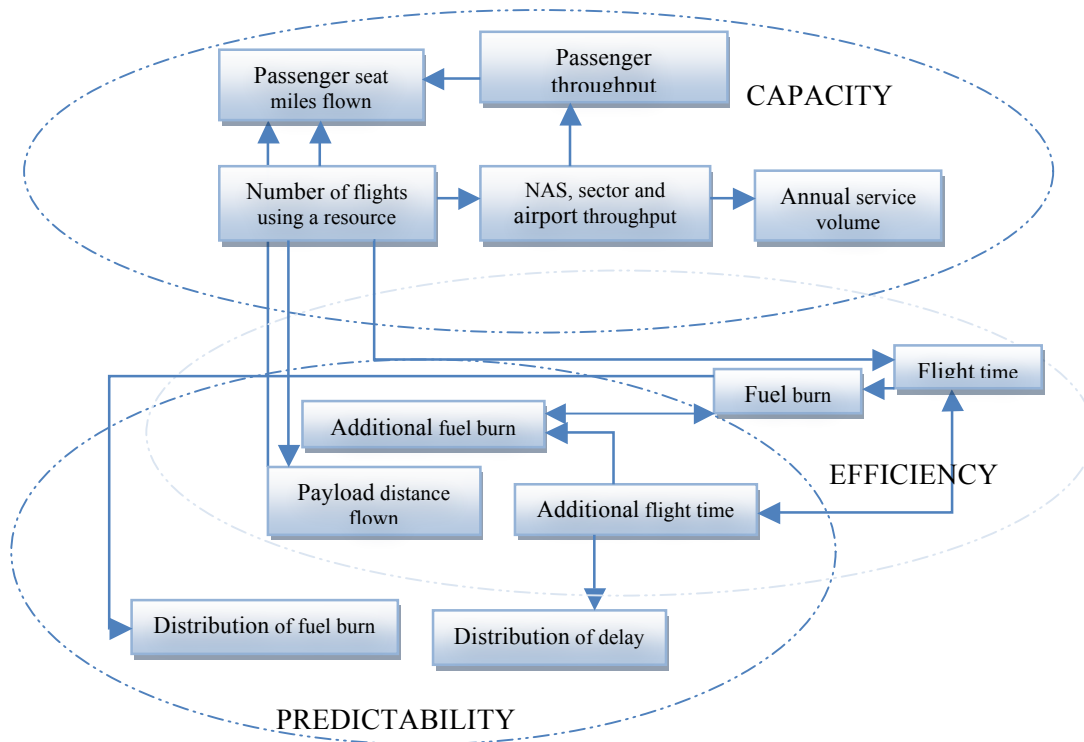


Figure 17-12: Capacity vs. Predictability cause-effect relationships

- The representative indicators capturing performance within the KPAs of capacity and predictability used in this tradeoff study and the cause-effect relationships of the supporting metrics are illustrated in Figure 17-12.

As noted previously, distribution (standard deviation) of delay provides a valuable measure for predicting the performance of the ATM system and distribution (standard deviation) of fuel burn is another good measure for predicting the efficiency of the system from the user perspective.

Performance Outputs

Based on the cause-effect relationships established above and key indicators noted, the performance metrics helpful in understanding the trades between the KPAs Capacity and Predictability are listed in Table 17-3 (Performance).

Experiment Design

The tools, along with the order of usage and the flow of information, are outlined in Table 17-3. (Performance) outputs for the two key performance areas of capacity and predictability are produced via NAS-wide simulation in FACET and ACES while regional metrics are output through simulation runs in SIMMOD. As noted previously, demand characteristics can be adjusted to fine tune the required system performance.

Table 17-3: Capacity vs. Predictability performance metrics for system-wide and regional analysis

Level	Capacity	Predictability
NATIONAL	1) % change in available passenger seat miles between all airports 2) % change in cargo transport miles between all airports 3) % change in number of flights between all airports	1) % change in the standard deviation of delay for operations between all airports 2) % change in the standard deviation of fuel burn for all operations between all airports 3) % change in the standard deviation of passenger delay for operations between all airports
REGIONAL	1) % change in available passenger seat miles at Metroplex / Terminal Area / Airport 2) % change in cargo transport miles at Metroplex/Terminal Area/Airport 3) % change in number of flights at Metroplex / Terminal Area / Airport	1) % change in standard deviation of delay for operations at all Metroplex / Terminal Area / Airport 2) % change in the standard deviation of fuel burn for operations at all Metroplex/Terminal Area/ Airport 3) % change in the standard deviation of passenger delay for operations at all Metroplex/Terminal Area/Airport
VEHICLE	1) % change in available passenger seat miles using this vehicle (relative to the total number of operations) 2) % change in cargo transport miles at using this vehicle (relative to the total number of operations) 3) % change in number of flights using this vehicle (relative to the total number of operations)	1) % change in individual aircraft additional flight time 2) % change in individual aircraft additional fuel burn 3) % change in delay per passenger

The following graphs will be produced for the system-wide and regional analysis:

- %change in throughput vs. % change in standard deviation of delay for operations at all airports (or Metroplex airports for regional analysis)
- %change in throughput vs. % change in standard deviation of fuel burn for operations at all airports (or Metroplex airports for regional analysis)
- % change in standard deviation of delay for top five airports (Metroplex airports for regional analysis)
- % change in standard deviation of fuel burn by airline for top five airports (Metroplex airports for regional analysis)
- % change in additional flight time by vehicle type
- % change in additional fuel burn by vehicle type

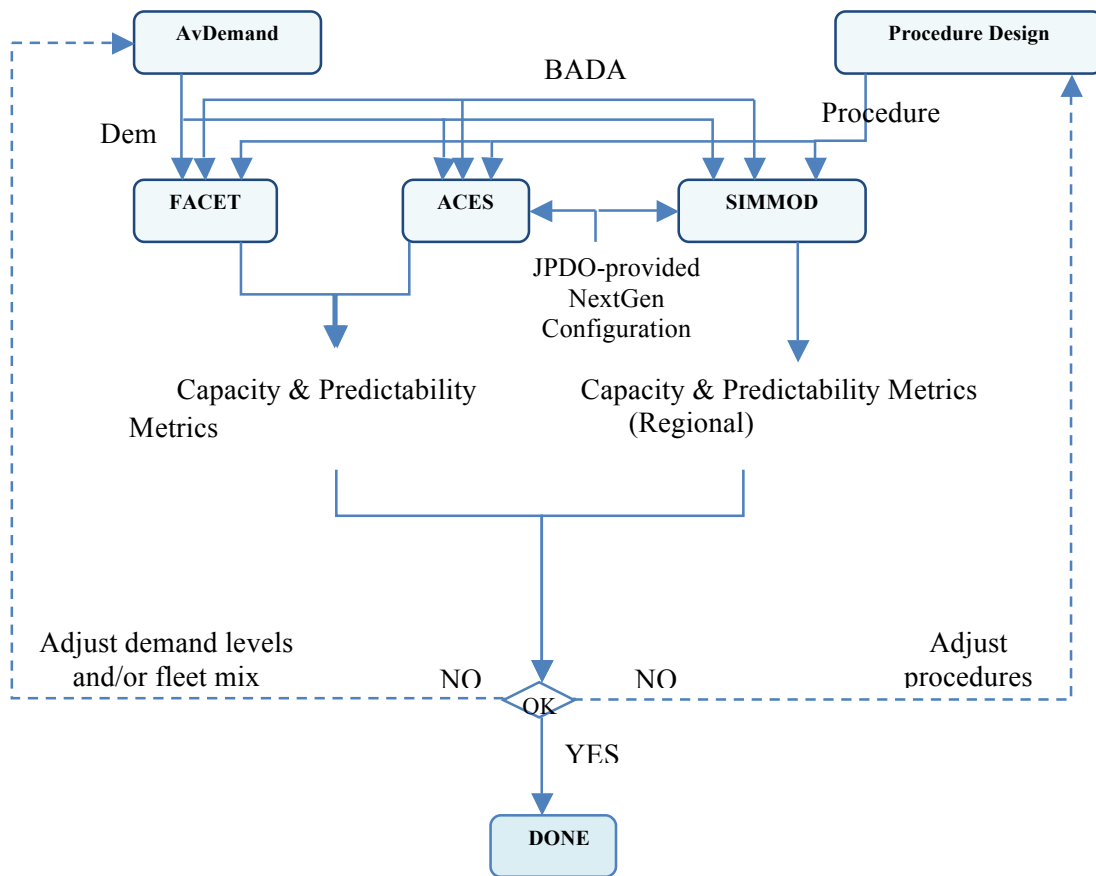


Figure 17-13: Simulation design with iterative loops for trade study #3

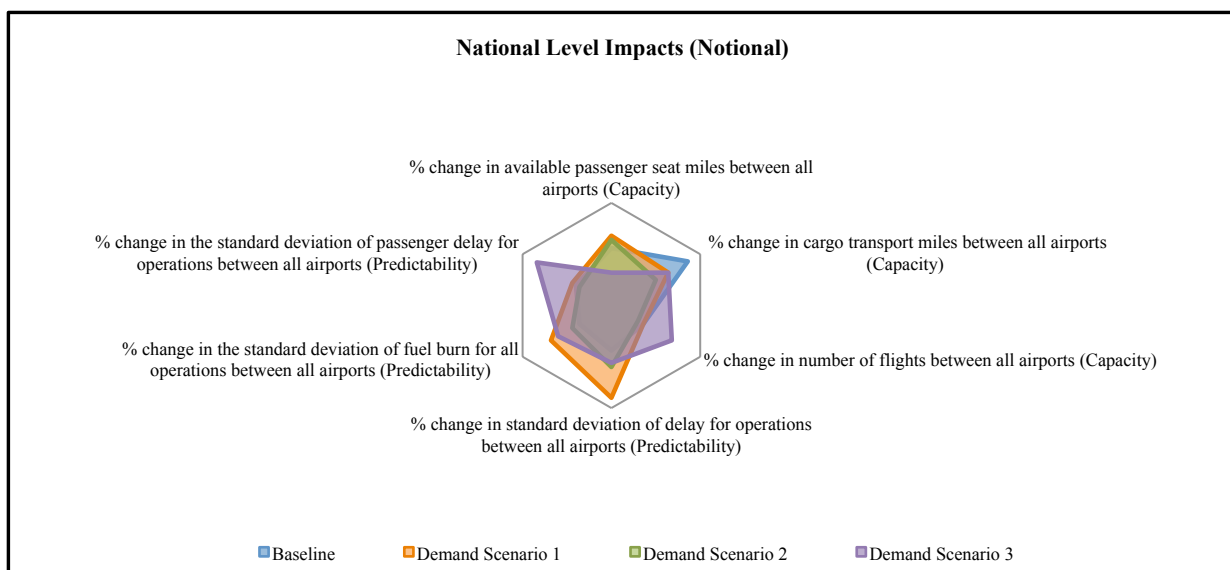


Figure 17-14: Capacity vs. Predictability national level impacts (notional)

Gaps in metrics:

Weather plays the predominant role in disrupting air traffic. While most occurrences of delay are largely attributed to weather, there is still a lack of appropriate metrics that incorporate weather forecast impacts on predicting system performance.

17.6. Other Trade Studies Proposed to NASA for Future Research

Trade studies not brought into the current research effort, but potentially useful for future research to NASA, are summarized in this section. The items presented below are categorized according to trades comprising the three KPAs referred to throughout this document: namely, system performance, environment and safety. Sub trades spanning any two of the three performance areas are also provided. For each trade listed below, only demand characteristics are shown as the control variable. However, it would certainly be possible in most cases to use airspace or procedure design (or a combination of one or more of the three characteristics) as the control mechanism.

Other significant key trades to assess NextGen improvements include the trades between Noise and Emissions, Capacity, Environment and Safety, Flexibility, Access and Equity, and Predictability. In the analysis thus far, safety was assumed to be inherent in the system through the application of proper

separation procedures and regulations. For a complete understanding of the bounds of the system as a whole, it is necessary to consider trades that include safety as well.

17.6.1. Trade space #4: Capacity vs. Environment vs. Safety

This trade study assesses the impact of variation in traffic flow characteristics on capacity, environment and safety, and the trades that are possible among the three key performance areas of system performance, environment, and safety. The Capacity vs. Environment trade study was presented in Section: Trade-off #1: Capacity vs. Environment. A Capacity vs. Safety trade study and a Capacity vs. Environment vs. Safety are presented here. Table 17-4 (Performance) provides the performance metrics for Safety while Capacity and Environment were already presented in Table 17-1 (Environment).

Trade space #4.1 Capacity vs. Safety

The following trade studies capture the impact of variation in traffic flow characteristics on capacity and safety and the trades that can be achieved between the two. Refer to Table 17-1 (Environment) and Table 17-4 (Performance) for the performance outputs for the two KPAs Capacity and Safety.

Research goal #5: Determine the restrictions in traffic flow characteristics that will improve capacity without negative impacts on safety.

Trade space #4.2: Capacity vs. Environment vs. Safety

Research goal #6: Determine the impact of variations in traffic flow characteristics that provides reasonable throughput with acceptable levels of safety and environmental impacts.

Performance outputs for Capacity and Environment can be found in Table 17-1 (Environment) and Safety metrics in Table 17-5 (Safety)

17.6.2. Trade space #5: Flexibility vs. Access & Equity vs. Predictability

The following set of trades captures the impacts of traffic flow characteristics on flexibility, access and equity, and predictability and the trades that are possible among and between the three performance areas. Table 17-5 (Safety) provides the performance outputs for this trade study.

Table 17-4: Safety performance metrics for system-wide and regional analysis

Level	Safety
NATIONAL	1) Propensity <i>There is no mechanism to quantify and measure this metric at this time.</i> 2) % change in fatalities by accident category
REGIONAL	1) % change in separation violation errors at Metroplex / Terminal Area/ Airport 2) % change in number of conflicts and resolution maneuvers at Metroplex/Terminal Area/Airport
VEHICLE	1) % change in fatalities by vehicle type

Trade space #5.1: Flexibility vs. Access & Equity

The following trade study assesses the impacts of variations in user behavior on airport and airspace access. Refer to Table 17-5 (Performance) for the performance outputs related to the Flexibility and Access & Equity KPAs:

Research goal #7: Determine the impact of flexibility of user behavior on access to airports and airspace:

What percentage of flights are re-routed and/or delayed (by vehicle category and cause of re-routing) due to allowing user flexibility in selection of routes, and/or arrival/departure times?

Can additional flights (by user category) be accommodated when ensuring flexibility in user preferences for routes and/or arrival/departure times?

What levels of flexibility (e.g., route changes) can be accommodated without deteriorating access to airports and airspace?

Trade space #5.2: Flexibility vs. Predictability

The following trade study assesses the impact of variations in user behavior on predictability. Refer to Table 17.5 (Performance) for the performance outputs for the two KPAs: Flexibility and Predictability.

Research goal #8: Determine the impact of flexibility of user behavior on predictability:

What are the impacts of flexibility on delay? How many levels of flexibility can be supported while keeping delay to acceptable levels?

What are the benefits accrued by the flights that are allowed flexibility in route selection and/or arrival/departure times? What is the cost effectiveness in terms of fuel burn distribution per vehicle type? Per class of vehicles?

Trade space #5.3: Flexibility vs. Access & Equity vs. Predictability

Building on the two trade studies presented above, this study addresses the impact of flexibility on access to airspace and airport resources while maintaining acceptable levels of delay (predictability). Refer to Table 17-5 (Performance) for the performance outputs of Flexibility, Predictability, and Access & Equity KPAs:

Research goal #10: Determine the impact of flexibility in user behavior on airport and airspace access and predictability:

What levels of flexibility can safely be accommodated while enabling an increase in access to airports and airspace and maintaining acceptable levels of delay?

Can additional flights be introduced by increasing flexibility of users in route selection and/or choice of arrival/departure times while keeping delay to acceptable levels?

What percentage of flights are delayed and/or re-routed due to inaccessibility of airspace/airport due to flights with flexible schedules restricting access to certain airspace/airport resources?

17.6.3. Trade space #6: Flexibility vs. Environment vs. Capacity vs. Safety

This trade study assesses the impact of traffic flow characteristics on flexibility and the trades that are possible among flexibility, capacity, and environment and safety. Performance outputs to be computed for this trade study are presented in Table 17.1 (Environment), Table 17-4 (Safety), and Table 17-5 (Performance).

Trade space #6.1: Flexibility vs. Capacity

The impact of variation in traffic flow characteristics on flexibility and capacity and the trades that can be achieved between them is presented here. Performance outputs for this study can be found in Table 17-1 (Environment) and Table 17-5 (Performance).

Research goal #11: Determine the impact of flexibility in user behavior onto airspace and airport capacity and throughput. In particular, this trade study addresses the question:

How much flexibility can be accommodated without negative impact on capacity?

Trade space #6.2: Flexibility vs. Environment

The following trade study assesses the impact of flexibility in user behavior on environment.

Research goal #12: Determine the impact of flexibility in user behavior onto airspace and airport environment.

Performance outputs for this trade study can be found in Table 17-1 (Environment) and Table 17-5.

Trade space #6.3: Flexibility vs. Safety

The following trade study assesses the impact of flexibility onto safety.

Research goal #13: Determine the impact of flexibility in user behavior onto safety.

Performance outputs for this trade study can be found in Table 17-4 (Safety) and Table 17-5 (Flexibility).

Trade space #6.4: Flexibility vs. Environment vs. Safety

This trade study assesses the impact of traffic flow characteristics on flexibility of user behavior while enabling acceptable levels of safety and environmental performance.

Research goal #14: Determine the impact of variations in traffic flow characteristics on user flexibility with acceptable levels of safety and environmental performance.

Performance outputs for this trade study can be found in Table 17-1 (Environment), Table 17-4 (Safety) and Table 17-5 (Flexibility).

17.6.4. Trade Space #7: Access & Equity vs. Environment vs. Safety

The following trade studies assess the impact of variation in traffic flow characteristics on access and equity and the trades possible among access and equity, environment and safety.

Trade space #7.1: Access & Equity vs. Efficiency

The following trade study assesses the impact of variation in traffic flow characteristics (demand levels and fleet mix), efficiency and the ability to provide fair access and equity in service to all vehicle classes.

Research goal #15: Determine restrictions in traffic flow characteristics that provide for fair access and equity in service of all of the vehicle classes.

Performance outputs for this trade study can be found in Table 17-5 (Access & Equity) and Table 17-2 (Efficiency)

Trade space #7.2: Access & Equity vs. Predictability

The following trade study assesses the impact of traffic flow characteristics on access to airports and airspace resources and predictability.

Research goal #16: Determine the impact of variations in traffic flow characteristics on airport and airspace access and predictability

What are the impacts on delay due to additional flights realized by users?

Performance outputs for this trade study can be found in Table 17-5 (Access & Equity and Predictability).

Trade Space #7.3: Access & Equity vs. Environment

The following trade study assesses the impact of variation in traffic flow characteristics (demand levels and fleet mix) on environmental impacts and the ability to provide fair access and equity in service to all vehicle classes

Research goal #17: Determine restrictions in traffic flow characteristics that provide fair access and equity in service while maintaining acceptable levels of environmental impacts

Performance outputs for this trade study can be found in Table 17-1 (Environment) and Table 17-5 (Access & Equity).

Trade space #7.4: Access & Equity vs. Safety

The following trade study assesses the impact of variation in traffic flow characteristics (demand levels and fleet mix) on safety and the ability to provide fair access and equity in service to all vehicle classes.

Research goal #18: Determine restrictions in traffic flow characteristics that provide for fair access and equity in service of all of the vehicle classes with acceptable levels of safety.

Performance outputs for this trade study can be found in Table 17-4 (Safety) and Table 17-5 (Access & Equity).

Trade Space #7.5: Access & Equity vs. Environment vs. Safety

The following trade study assesses the impact of variation in traffic flow characteristics (demand levels and fleet mix) on safety and environmental impacts while providing fair access and equity in service to all vehicle classes.

Research goal #19: Determine restrictions in traffic flow characteristics that provide fair access and equity in service to all vehicle classes while maintaining acceptable levels of safety and environmental impacts.

Performance outputs for this trade study can be found in Table 17-1 (Environment), Table 17-4 (Safety) and Table 17-5 (Access & Equity).

Table 17-5: Flexibility, access and equity, and predictability metrics for various levels of analysis.

Level	Flexibility	Access & Equity	Predictability
NATIONAL	<p>1) % change in number of user requests that are granted for operations at all airports</p> <p>2) % change in the number of flights that change routes and improve travel time for operations at all airports</p>	<p>1) % change in number of flights that are negatively impacted for operations at all airports</p> <p>2) %change in number of flights that are re-routed by user category for operations at all airports</p> <p>3) %change in additional flights that are realized by user category for operations at all airports</p>	<p>1) % change in the distribution of delay for operations between all airports</p> <p>2) % change in the distribution of fuel burn for all operations between all airports</p> <p>3) % change in the distribution of passenger delay for operations between all airports</p>
REGIONAL	<p>1) % change in number of user requests that are granted for operations at Metroplex/ Terminal Area/ Airport</p> <p>2) % change in the number of flights that change routes and improve travel time for operations at Metroplex/Terminal Area/ Airport</p>	<p>1) % change in number of flights that are negatively impacted for operations at all airports in Metroplex/Terminal Area/Airport</p> <p>2) %change in number of flights that are re-routed by user category for operations at all airports in Metroplex/Terminal Area/Airport</p> <p>3) %change in additional flights that are realized by user category for operations at all airports in Metroplex/Terminal Area/Airport</p>	<p>1) % change in distribution of delay for operations at all Metroplex / Terminal Area / Airport</p> <p>2) % change in the distribution of fuel burn for operations at all Metroplex/Terminal Area/ Airport</p> <p>3) % change in the distribution of passenger delay for operations at all Metroplex/Terminal Area/Airport</p>
VEHICLE	<p>1) %change in the number of times a flight changes route</p>	<p><i>Metric not defined</i></p>	<p>1) % change in individual aircraft additional flight time</p> <p>2) % change in individual aircraft additional fuel burn</p> <p>3) % change in delay per passenger</p>

17.6.5. Trade space #8: Predictability vs. Environment vs. Safety

The following trade study assesses the impact of variation in traffic flow characteristics on predictability and the trades possible among predictability, safety and environment.

Trade space#8.1: Predictability vs. Environment

The following trade study assesses the impact of predictability of traffic flow characteristics on the environment (noise and emissions).

Research goal #20: Determine the impact of predictability of traffic flow characteristics onto environmental impacts at airports and en-route airspace.

Performance outputs for this trade study can be found in Table 17-1 (Environment) and Table 17-5 (Predictability).

Trade space #8.2: Predictability vs. Safety

The following trade study assesses the impact of predictability of traffic flow characteristics on the safety of the NAS.

Research goal #21: Determine the impact of predictability of traffic flow characteristics onto safety.

Performance outputs for this trade study can be found in

Table 17-4 (Safety) and Table 17-5 (Predictability).

Trade space #8.3: Predictability vs. Environment vs. Safety

The following trade study assesses the impact of predictability onto environment and safety

Research goal #22: Determine the impact of predictability of traffic flow characteristics onto safety and environment.

Performance outputs for this trade study can be found in Table 17-1 (Environment), Table 17-4 (Safety) and Table 17-5 (Predictability).

17.6.6. Trade Space #9: Efficiency vs. Environment vs. Safety

The following trade study assesses the impact of variation of traffic flow characteristics on efficiency while providing acceptable levels of safety and environmental impacts.

Trade Space #9.1: Efficiency vs. Environment

The following trade study assesses the impact of variation of traffic flow characteristics on efficiency while providing acceptable levels of environmental impacts.

Research goal #23: Determine the restrictions in traffic flow characteristics to provide efficient operations for all vehicle classes while enabling acceptable levels of environmental impacts.

Performance outputs for this trade study can be found in Table 17-1 (Environment) and Table 17-2 (Efficiency).

Trade Space #9.2: Efficiency vs. Safety

The following trade study assesses the impact of variation of traffic flow characteristics on efficiency while providing acceptable levels of safety impacts.

Research goal #24: Determine the restrictions in traffic flow characteristics to provide efficient operations for all vehicle classes while enabling acceptable levels of safety impacts.

Performance outputs for this trade study can be found in Table 17-4 (Safety) and Table 17-2 (Efficiency).

Trade Space #9.3: Efficiency vs. Environment vs. Safety

The following trade study assesses the impact of variation of traffic flow characteristics on efficiency while providing acceptable levels of safety and environmental impacts.

Research goal #25: Determine the restrictions in traffic flow characteristics to provide efficient operations for all vehicle classes while enabling acceptable levels of safety and environmental impacts.

Performance outputs for this trade study can be found in Table 17-1 (Environment), Table 17-2 (Efficiency) and Table 17-4 (Safety).

17.6.7. Trade space #10: Environment vs. Safety

The following trade study assesses the impact of variation of traffic flow characteristics on environment and safety and the trades that are possible between the two.

Research goal #26: Determine the impact of variations in traffic flow characteristics onto safety that provides acceptable levels of environmental impacts.

Performance outputs for this trade study can be found in Table 17-1 (Environment) and Table 17-4 (Safety).

17.6.8. Trade space #11: Noise vs. Emissions

The following study considers possible trade-offs in noise levels and emissions using traffic flow characteristics as the control mechanism. Table 17-6 provides the performance outputs for this trade study.

Research goal #27: Determine the trade-off potential between noise and emissions (by vehicle class and airport type).

Table 17-6: Noise vs. Emissions performance metrics for system-wide and regional analysis

Level	Environment	
	Noise	Emissions
NATIONAL	1) Sum of the % Change in Population Exposure to X dB DNL due to Operations at All Airports	1) Sum of % Change in Premature Mortality due to total PM _{2.5} exposure due to Operations at All Airports (considering emissions of PM, NO _x , and SO _x under 3,000 ft)
REGIONAL	1)% Change in Population Exposure to X dB DNL due to all operations at Metroplex / Terminal Area / Airport	1) % Change in Premature Mortality due to total PM _{2.5} exposure due to all operations at Metroplex / Terminal Area / Airport (considering emissions of PM, NO _x , and SO _x under 3,000 ft) <i>MIT evaluating potential to conduct this analysis</i>
VEHICLE	1)% Change in Population Exposure to X dB DNL max due to a single aircraft operation	1)% Change in emissions of PM, NO _x , and SO _x due to a single aircraft operation

17.7. Metric Gaps

The research suggests that the gaps in metrics stem from a lack of understanding of the underlying processes (environment: supersonic noise boom, capacity: airspace capacity as a function of severe weather impacts), a lack of modeling capabilities that would provide their evaluation (safety: resilience, flexibility: number of options), or from a lack of both of these. An initial summary of metric gaps for the key performance areas is provided in Table 17-7.

It should be noted that the ability to conduct the full range of assessments that will be required to understand the impacts of the vehicles associated with this study may require fine-tuning of the existing metrics. Given the ‘virtual’ nature of the vehicles, procedures, and airspace associated with this study, the

metrics of the existing models are likely to be sufficient for the level of detail required at this point in understanding the issues associated with their integration into the NAS. However, as the various attributes of the vehicles, airspace, and procedures become better understood, either further-tuning or new metrics may be required to support the required level of understanding. Additionally, new analysis methods, models, and metrics may be needed to evaluate these vehicle types, procedures, and technologies as the range of operational concepts becomes better defined and understood. It is likely that the concepts of operations associated with the three demand set timeframes (i.e., 2025, 2040, and 2059) used in this effort will not only be considerably different from the present, but also different from each other as well. This will no doubt require new metrics, and/or potentially a revision of the KPA categories and underlying analytical framework and associated modeling infrastructure.

Table 17-7: Identified gaps in metrics

KPA	Metric Gaps	Comments
Access and Equity	Equity Metric	Captures the equity of the treatment of, and the impacts across, various users, operators, etc.
Capacity	Airspace capacity as a function of severe weather impacts	Change in airspace capacity resulting from severe weather impacts (as a function of severity, location and size of impacts)
Efficiency	Aircraft size trends	Metric that captures impact of changes in aircraft size, passenger and payload volume, and load factors
	Lost revenue and other schedule restrictions impacts	Flight cancellations, lost revenue and other impacts caused by a limited or prohibited access to an airport or other schedule restrictions
Environment	Other than air quality and noise related metric; for instance, water quality metrics	Limit or reduce significant impacts associated with non-air quality and noise related environmental impacts
	En-route supersonic noise/boom impacts	
	Rotorcraft noise (airport impacts)	
	Uncertainty and corresponding impacts of short-lived aviation emissions on global climate change (e.g. the impact of contrails and contrail-cirrus)	
Flexibility	Ability to accommodate preferred airport selection (origin and/or destination)	Captures the ability of different vehicle class operators to serve their preferred markets out of the preferred airports
	Number of options (routes)	Number of available routes or trajectory options
Predictability	Predictability of 4D trajectory	Captures accuracy in executing planned 4D trajectories
Safety	Resilience	Captures the ability to respond to perturbations while minimizing the potential adverse impacts and keeping the impact local (related to Flexibility: Number of options)

17.8. **Future Research Capabilities Provided to NASA**

The current research effort uses a single pass through the models to compute the performance outputs for different demand scenarios. As illustrated in Section: Approach, the proposed approach supports an iterative feedback mechanism to fine tune the inputs needed to reach acceptable performance outputs. Only demand characteristics are used to assess the impact of new vehicle integration. For a complete analysis, demand, as well as airspace characteristics and vehicle design characteristics must be considered. Enhancements to existing tools and models are necessary to circumvent gaps in existing metrics and limitations in tools and models expected to conduct the simulations.

17.9. **Conclusions**

A control theory based approach was presented to study the impacts of new vehicle integration into the NAS with emphasis on system performance, safety, and environmental impacts. The method presented is generic and can be used to investigate other operational impact assessments as well as for system-wide, regional, or local analysis. The approach focuses on performance, safety, and environmental impact assessment. It also accounts for fine-tuning of demand characteristics, airspace procedures, and vehicle performance/design characteristics that may be required for achieving desired performance outputs.

For the most part, our research indicates that system performance, safety, and environmental impacts can be captured using well understood metric specifications and existing tools. In some cases, however, we were able to identify metric gaps that stem from a lack of understanding of underlying processes (example: supersonic noise/boom), a lack of modeling capabilities that would facilitate their evaluation (example: flexibility/number of options), or from a lack of both of these elements.

The research indicates that cause-effect relationships between metrics can be effectively used for capturing impact propagation and enabling trade-off analyses between different performance aspects. Furthermore, the metrics framework is more than just an effective means of capturing impact propagation across performance areas: the concept also can be helpful in rolling up performance outcomes from lower- to higher-levels of performance assessment. (Examples of this latter capability might involve rolling-up outcomes from the regional to national, the vehicle to the operational, or the operational to societal levels.)

Further research is needed to better understand the complexities involved with using iterative run-scenarios and analyses that enable fine-tuning of demand characteristics, airspace procedures, or vehicle performance/design characteristics to deliver desired performance outcomes; however, the necessary foundation was developed and successfully used to support low fidelity assessments performed under the Advanced Vehicle Concepts and Implications for NextGen NRA.

17.10. **References**

1 K.R. Allendoerfer and J. Galushka, "Air Traffic Control System Baseline Methodology," DOT/FAA/CT-TN99/15, June 1999.

2 N. Casso and P. Kopardekar, “Air Traffic Management System Development and Integration (ATMSDI),” Dec. 2001.

3 G.A. Hadley, J.A. Guttman, and P.G. Stringer, “Air Traffic Control Specialist Performance Measurement Database,” June 1999.

4 S. Bradford, L.M. Brown, and M.J. Blucher, “Use of Performance Metrics in Airspace Systems: US Perspective,” 2nd USA/Europe Air Traffic Management R&D Seminar, Dec. 1998.

5 A. Williams, S. Bradford, D. Liang, W. Post, and J.M. Pomeret, “Common Metrics Framework for ATM Performance Assessment and Monitoring,” Digital Avionics Systems Conference, DASC 04, 2004.

6 T. Breuing, S. Bradford, and D. Liang, “Standardizing Performance Metrics,” 5th USA/Europe Air Traffic Management R&D Seminar, June 2003.

7 P.A. Bonnefoy, and R.J. Hansman, “Investigation of the Potential Impacts of the Entry of Very Light Jets in the National Airspace System,” MIT International Center for Air Transportation (ICAT) Report 2006-02.

8 Y. Xu, H. Baik, and A. Trani, “A Preliminary Assessment of Airport Noise and Emissions Impacts Induced by Small Aircraft Transportation System Operations,” 6th AIAA Aviation Technology, Integration and Operations Conference (ATIO) Sept. 2006.

9 ICAO Secretariat, “Performance Based Transition Guidelines,” Version 0.51 March 2007.

10 International Civil Aviation Organization (ICAO), “Global Air Traffic Management Operational Concept,” DOC 9854 AN/458, 2005.

11 ACI-NA Environmental Committee, FAA Office of Environment & Energy, “NextGen Environmental Goals and Targets,” Sept. 2008.

12 D. Schleicher, E. Wendel, and A. Huang, “Demand Loading Analysis for a 3x NextGen Future,” 7th AIAAATIO Conference, Belfast, UK, 2007.

17.11. **Metrics Definitions**

Additional DOC: difference between the planned DOC and the actual DOC from a single flight perspective in dollars

Additional flight time (delay) : difference between the actual and the planned flight time (e.g. for a whole flight, phase of flight, within a specified resource) in minutes

Additional fuel burn: difference between the actual and the planned fuel burn (e.g. for a whole flight, phase of flight, within a specified resource) in lbs

Annual service volume: a five year moving average throughput for the top 35 OEP airports

Annualized Fuel Burn Inventory for the US: Annualized (or other time scale) inventory of fuel burn for the entire US; includes all of the modes of flight and typically takes the entire flight for either international departures or arrivals, but not both.

ASM: measure of an airline's total product offering (seats*miles flown)

Aircraft sizing trends: Metrics to measure the impacts of decreasing aircraft size, increasing passenger volume, delays, flight cancellations etc

Below 3,000ft emissions: NO_x, CO₂, SO_x, H₂O and PM: annualized inventory of listed emissions at each airport of interest in the US; includes all of the modes of flight below the mixing height, both departure and arrival in g or Gg; kg/yr

Cost per Available Seat Mile (CASM): cost efficiency and useful compared to RASM is useful in marginal unit measures [operating costs/ASM]

Cumulative Noise: the cumulative certification noise at sideline, flyover and approach in dB.

Cumulative Noise Margin: the noise margin to chapter 4 limit in EPN dB by sideline, flyover and approach

Capital Cost: costs incurred in the purchase of land, buildings, construction and equipment to be used in the production of goods or the rendering of services.

Cargo transport miles: the total cargo carried normalized by the total flight time

Cost of service provision: captures the cost of service provision from the ATC perspective (includes staffing and other relevant costs)

Cardiopulmonary Ailments (number of people, \$): Number of cases of, and monetized valuation of the number of cases of, cardiopulmonary ailments resulting from emissions below 3000'

Change in green house gas emissions – the change in green house gas emissions from the nominal

Change in noise exposure at given point (duration and DNL)

Chronic Bronchitis (number of people, \$): Number of cases of, and monetized valuation of the number of cases of, chronic bronchitis resulting from emissions below 3000'

Change in atmospheric concentration of PM_{2.5}: change in concentration of PM_{2.5} for a specified region (e.g. airport), for a specified time of day

Controlled flight into terrain (CFIT): In flight collision with terrain, water, or obstacle without indication of loss of control. [CICTT] Number of such events per time period, typically in years.

Conflict: Existing or pending situations between tracked targets (known IFR or VFR aircraft) that require his/her immediate attention/action.

Direct Operating Cost – Nonfuel: Direct cost of maintaining and operating the aircraft not including fuel costs [Operating cost/(Avail Seats or Avail Payload * Distance)]

Direct Operating Cost – Fuel: Fuel cost, per distance of operating vehicle [Fuel burn*Fuel price/(Avail Seats or Avail Payload * Distance)]

DOC+I: Sum of ownership cost and operating costs [DOC + Capital Cost/(Avail Seats or Avail Payload * Distance)]

Distribution (variance, standard deviation) of delay: histogram of the distribution of flights by delay bins (e.g. for a specified airport, sector, market-pair)

Distribution (variance, standard deviation) of fuel burn by a vehicle type on a given market: standard deviation of fuel burn (e.g. by vehicle type)

Damages and monetary impact due to CO₂, NO_x/Methane, NO_x/O₃ short, NO_x/O₃ long, Soot, Sulphates, Water Vapor, Contrails, Induced Cirrus, Total – damages and monetized damages, resulting from global surface temperature change (%GDP, dollars)

Dynamic density: Dynamic density is a measure of controller workload and sector capacity that uses various factors in a regression equation to estimate the complexity of an en route airspace condition for a specified time-period

Dynamic density prediction error: Difference between predicted dynamic density and the measured/observed dynamic density value for a specified time period.

Energy consumed per revenue payload distance: energy consumed by individual aircraft normalized by available revenue payload distance carried

Emissions Surcharge – additional cost incurred based on emissions certification for the vehicle

ER visits due to asthma (number of people, \$): Number of, and monetized valuation of the number of, ER visits due to Asthma resulting from emissions below 3000'

Forecast lead time: Metric for assessing skill in forecasting onset of IFR events

Full flight emissions: NO_x, PM, CO₂, SO_x, HC: annualized inventory of listed emissions for the entire US; includes all of the modes of flight, and typically takes the entire flight for either international departures or arrivals or both in g or Gg; kg/yr,

Flight time: Duration of the flight (total or for a specified phase/portion of the flight)

Fuel burn per RPM: Fuel burn per revenue passenger mile

Fuel burn per RTM: Fuel burn per cargo transport mile

Fuel burn: Weight of fuel consumed during a flight (or a specified portion of the flight)

Fatalities per accident category: Number of fatalities per accident category over a given time period, typically years *Globally averaged surface temperature change* per year resulting from the change in radiative forcing (RF) due to aviation emissions in degrees Celsius

Housing value and rent loss: Loss in housing value and rent loss due to noise in the vicinity of airports

Impacts resulting from the take-off and landing field limitations: metric that captures airports (or runways) that the vehicle can use considering its take-off and landing field requirements (e.g. by vehicle class, by operator type)

Impacts resulting from the MTOW and MLW limitations: metric that captures airports (or runways) that the vehicle can use considering its maximum take-off and landing weight limitations (e.g. by vehicle class, by operator type)

Impacts resulting from the perception of intangibles: A metric that captures impacts resulting from the intangibles such as perception of comfort, safety, etc.

Inherent Aircraft Vulnerabilities: Failure or malfunction of an aircraft system or component - other than the powerplant. [CICCT] Number of such events per time period, typically in years.

ICAO LTO Emissions – based on ICAO Landing and Takeoff (LTO) cycle, characteristics engine emissions. Is influenced by the fuel burn of the vehicle

Landing Fee: landing and handling fees based on maximum take-off and sometimes maximum landing weight (e.g. by airport, by time of day)

Load Factor: RPMs/ASMs

Loss of control in flight (LOC-I): Loss of aircraft control while in flight (takeoff to touchdown). [CICCT] Number of such events per time period, typically in years.

Market Share: airline ASMs/total ASMs (at airport or in market)

Monetary impact total: Net monetized value resulting from global surface temperature change, premature mortality, and noise exposure (%GDP; dollars)

Monetized health costs due to PM_{2.5} exposure: net monetized health costs due to exposure to PM_{2.5} (e.g. for a specified airport) in dollars

Max Payload: The maximum allowed payload by vehicle class and operation type

Minor Restricted Activity Days (number of days, \$): Number of, and monetized valuation of the number of, MRADs resulting from emissions below 3000'

Mid-air collision (MAC): Collisions between aircraft in flight. Number of such events per time period, typically in years.

Near- Midair Collision (NMAC): An incident associated with the operation of an aircraft in which the possibility of collision occurs as a result of proximity of less than 500 feet to another aircraft, or a report is received from a pilot or flight crewmember stating that a collision hazard existed between two or more aircraft.

Noise Surcharge: surcharge based on noise certification value or noise margin and weight by airport

Number of flights requesting a service –total number of flights requesting service in a specified period of time and for a specified resource.

NAS, sector or airport throughput: number of realized operations per unit time of interest (e.g., 15-min bin, hour, annual)

Number of flights using a resource: cumulative count of the number of flights using the same resource (sector, center, airspace segments) in a specified period of time (e.g. flights/year, flights/hour, flights/15-min interval)

Noise population exposure (65, 60, 55 dB DNL): number of people cumulatively exposed to 65, 60 , 55 dB DNL noise contours (e.g. by airport)

Number of premature mortalities due to PM_{2.5} exposure – number of and monetized valuation of number of premature deaths resulting from emissions below 3000 ft.

Number of flights requesting service: Total number of flights requesting service in a specified period of time and for a specified resource (cumulative count)

Number of flight plans impacted by weather: Total number of flights with flight plans/trajectories overlapping with severe weather cell forecasts

Number of actual flights impacted by weather: Total number of flights flying sub-optimal profiles due to bad weather. In this case, depending on the available information, sub-optimal profiles can refer to any profile that is different from the optimal or flight-planned flight profiles

Number of flights impacted by TMI's or GDP: Number of flights impacted by a Traffic Flow Management Initiative or Ground Delay Program.

Number of people annoyed: Number of people annoyed due to noise in the vicinity of airports

Number of sleep awakenings: Number of sleep awakenings due to noise in the vicinity of airports

Number of students exposed: Number of students exposed to certain levels of noise in the vicinity of airports

Number of people exposed to sonic boom: total count of people exposed to sonic boom by region (by time of day, hourly, daily, annual)

Number of noise related events: total count of noise related events by airport, region or NAS (by time of day, hourly, daily, annual)

Number of options: Number of available routes or trajectory

Operational availability – captures service hours relative to the maximum service hours for a facility/resource (considers all outage time except for improvements; expressed as a percent).

Operational errors: Number or rate per year of occurrences attributable to an element of the air traffic system in which: (1) Less than 90% of the applicable separation minima results between two or more airborne aircraft, or less than the applicable separation minima result

Operational deviation: Number or rate per year of occurrences that attributable to an element of the air traffic system which did not result in an Operational Error (OE) as defined in FAAO 7210.56C, Para 5-1-1, e, (1), (2), (3), but: (1) Less than the applicable separation minima

Other intangibles' impacts: A metric that captures impacts resulting from other (easier to evaluate?) intangibles such as airport access, security procedures, rent-a-car availability, etc.

Passenger seat miles flown: number of passengers per flight multiplied by the number of miles flown for that flight (e.g. average per day, total for NAS, airport, region)

Passenger throughput: total number of passengers flown (e.g. NAS, per airport, per time of day)

Passenger delay: computed as the product of the total delay per flight and the total number of passengers

Percent of additional flights that are realized by user – number of additional flights divided by the total number of flights using the same resource (e.g. by user category).

Percent of re-routed flights by user category and by cause of re-routing – number of re-routed flights divided by the total number of flights using the resource (e.g. by user category, by cause of re-routing)

Percent of delayed flights by user category and by cause of delay – number of flights delayed by total number of flights using the same resource (e.g. by user category, by cause of delay).

Percent of flights that were negatively impacted

Percent of user requests granted: number of user requests that are granted divided by the total number of user requests (e.g. type of request)

Percent of flights with shorter routes due to increased access to previously unavailable airspace: number of flights with shorter routes divided by the total number of flights using the same airspace.

Propensity: captures the likelihood of a safety significant event occurring during normal operations.

Payload distance flown: the distance between origin and destination flown (nm)

Payload fuel energy efficiency: Productivity (payload distance flown) per unit fuel energy consumed

Premature mortality, infants (number of people, \$): Number of, and monetized valuation of number of, premature infant deaths resulting from emissions below 3000'

Premature mortality, adults (number of people, \$): Number of, and monetized valuation of number of, premature adult deaths resulting from emissions below 3000'

Propensity: The likelihood of a safety significant event occurring during normal operations.

Pilot deviations: Number of actions of pilots that result in the violation of a Federal Aviation Regulation or a North American Aerospace Defense (Command Air Defense Identification Zone) tolerance per year or per number of operations.

Revenue per Available Seat Mile (RASM): indicates profitability and revenue generating ability gives information about marginal units [operating income/ASM]

Resilience: captures the ability to respond to perturbations or accommodate change while minimizing the potential adverse impacts and keeping the impact local

Revenue: Revenue Collected from operation, function of demand and payload range capability

Revenue/ASM: [Revenue/(Avail Seats or Avail Payload * Distance)]

Rotorcraft noise level and exposure area: Metrics that capture the distinct characteristics of the rotorcraft noise profiles

Respiratory illness (number of people, \$): Number of cases of, and monetized valuation of the number of cases of, respiratory illness resulting from emissions below 3000'

Resource utilization: Safe and efficient use of available airport or airspace capacity

Runway incursions: Any occurrence at an aerodrome involving the incorrect presence of an aircraft, vehicle or person on the protected area of a surface designated for the landing and take-off of aircraft. [FAA, ICAO, CICTT]

Runway excursions: A veer off or overrun off the runway surface. [CICTT]

Risk of an event: Risk or probability that a certain type of event will occur in a certain period of time or for a certain operation type.

Runway collision: Collision between aircraft on the runway. Number of such events per time period, typically in years.

Sector overload – flights – number of flights in excess of sector capacity or the difference between the actual number of flights in the sector and its capacity.

Sector overload – sectors – number of sectors where demand exceeds capacity in a specified time period.

Schedule restrictions impact – more information is required to develop direct relationships. But in general this metric is affected by the number of flights using a resource.

Sonic boom level and exposure area: Metrics that capture the level and full noise area for supersonic flights

Separation violation (loss of separation): Occurrence in which two or more aircraft in-flight come closer than the separation minima.

Terminal noise contour area: 65,60,55 dB DNL terminal noise contour area in nm² (e.g. by airport)

Turn Times: minutes/tail number, or minutes per arriving and departing flight

Wake turbulence encounter (TURB): Fatal in flight wake vortex encounter. Number of such events per time period, typically in years.

Yield: offers amount of revenue per revenue paying passenger mile, or how much money the operator gets from carrying passengers [system yield = passenger revenue/ total RPMs]

17.12. **Complete Metrics Framework**

Building on the ideas evolved in the high level metrics diagram displayed in Figure 17-2, a complete metrics framework was developed for the full set of metrics (existing as well as identified gaps in current models). The complete metrics framework was developed expanding on the high level metrics framework. Each of the three key performance areas was further sub-divided into individual categories. A description of each of these performance areas and sub-categories is provided next. See Figure 17-1 for the complete framework diagram. Refer to the Metrics Definitions section for a description of the metrics considered in this research effort.

System Performance

System performance comprises the six key performance areas: namely, Access & Equity, Capacity, Cost Effectiveness, Efficiency, Flexibility and Predictability. Each of the sub-categories is explored to greater depth in the subsections below. For each sub-category referred to in the previous paragraph, relationships established among key indicators from that category, as well as those in overlapping or other categories, are provided along with a discussion of established relationships.

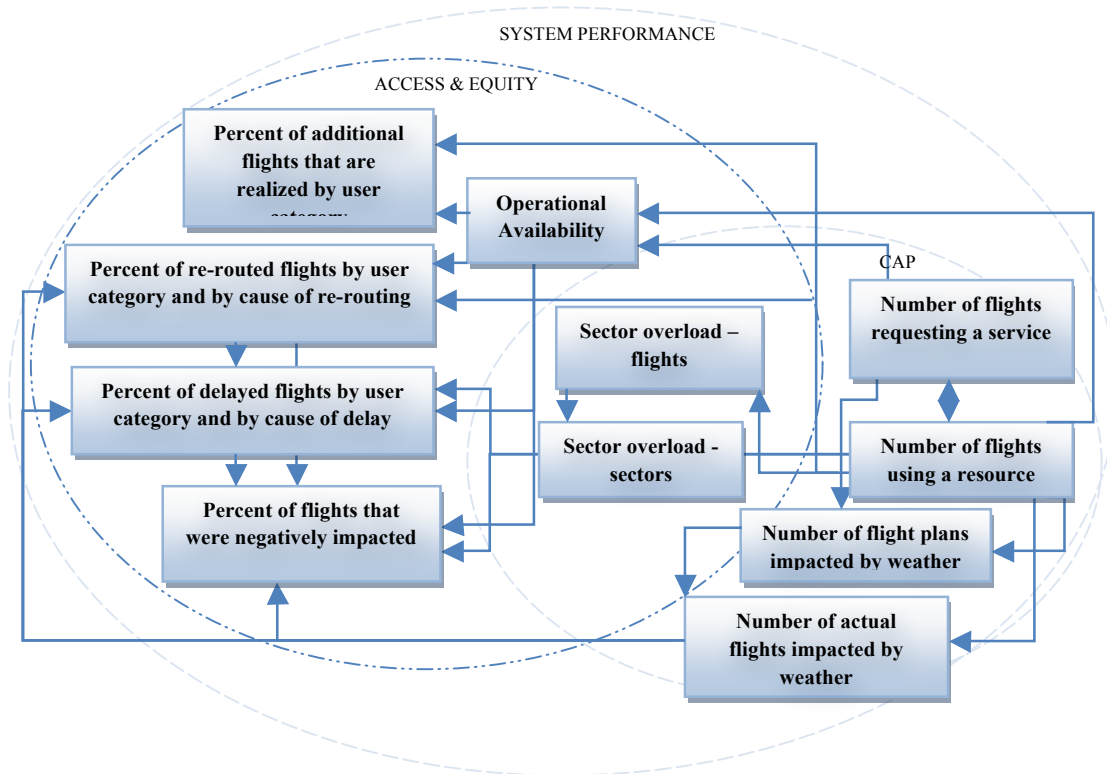


Figure 17-15: Access & Equity cause-effect relationships

Access & Equity

Access & Equity ensures that all airspace users have access to ATM resources to meet their operational requirements and that the shared use of the airspace by the different users can be achieved safely. Figure 17-15 displays the key relationships for the key indicators for this performance area.

Capacity

To meet current and future airspace user demands, the global ATM system needs to increase capacity (with due consideration to environmental impacts) without adversely affecting safety and minimizing restrictions on traffic flow. A good measure of capacity is throughput, as measured by the number of flights using a given resource. This, in turn is directly influenced by the number of flights requesting a service. Figure 17-16 provides the key relationships for the capacity metrics.

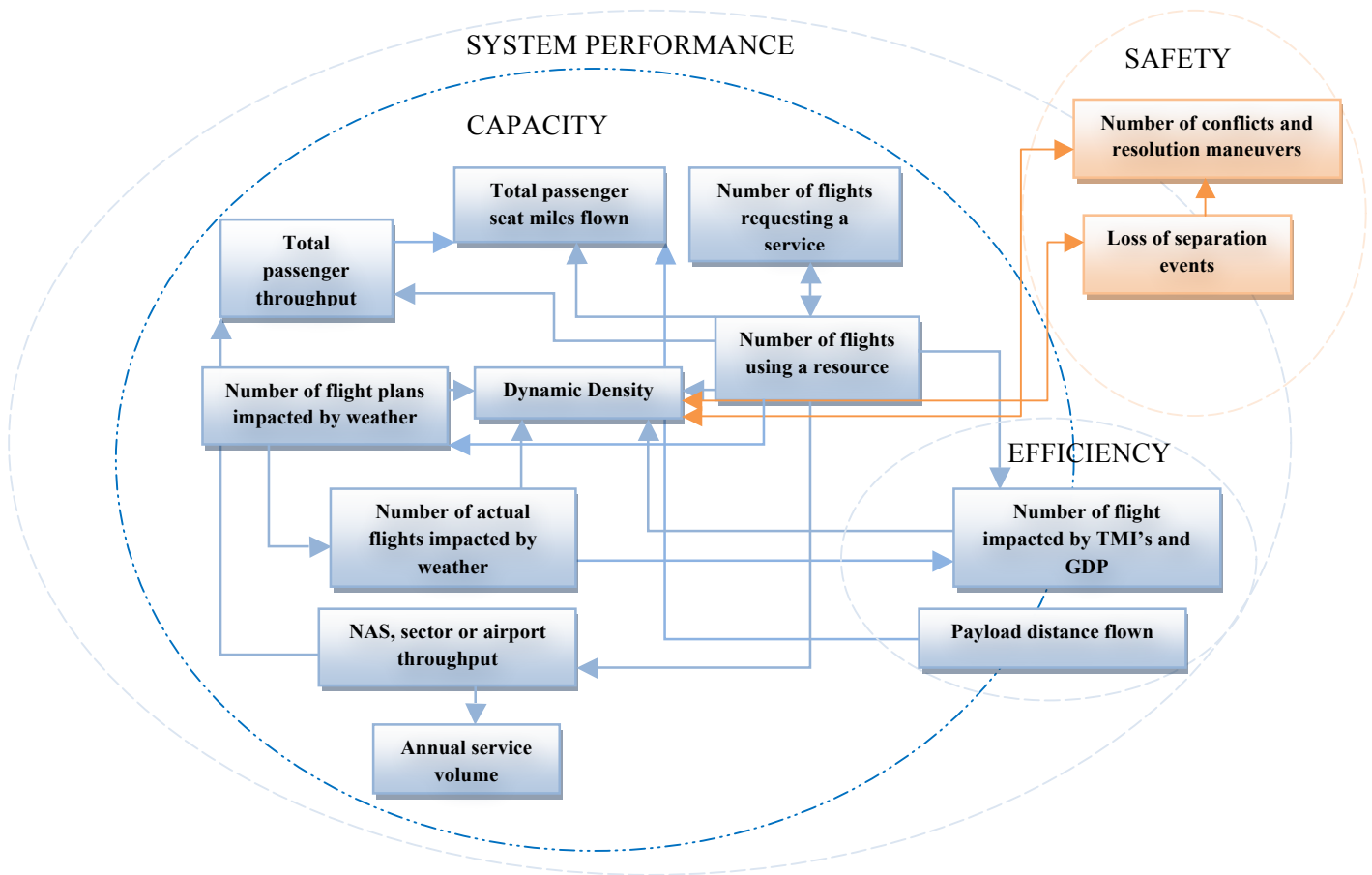
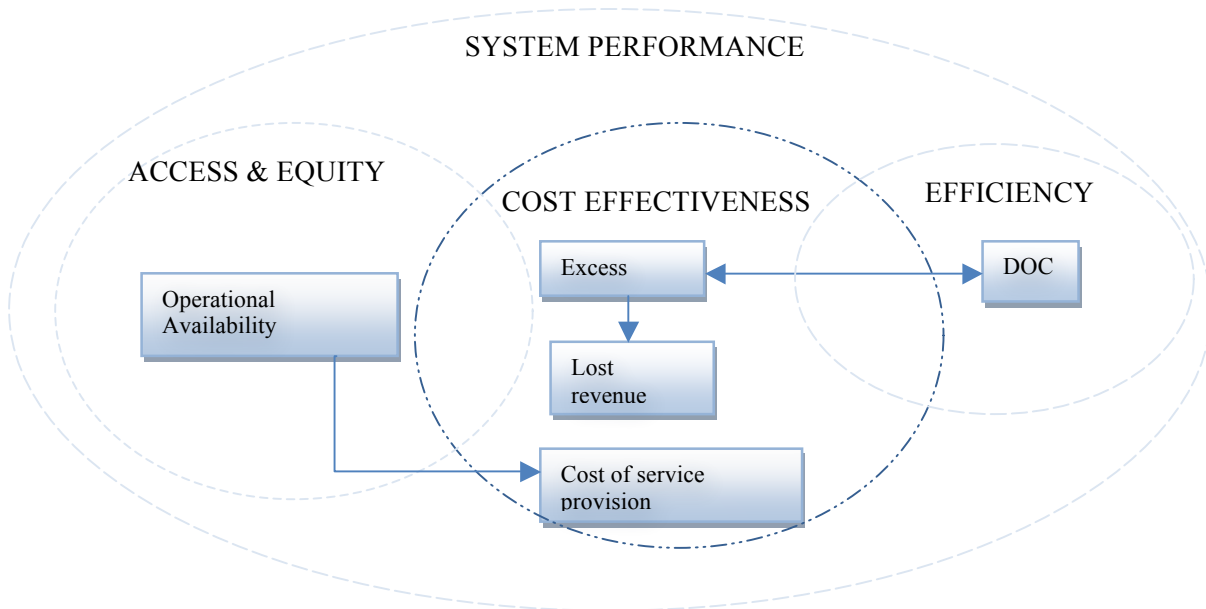


Figure 17-16: Capacity metrics cause-effect relationships

Cost Effectiveness

Cost effectiveness addresses the need of the ATM system to be cost effective, while balancing the interests of the varied ATM users. While evaluating any proposal to improve the ATM quality of service, the cost of the service needs to be considered. Figure 17-17 provides a summary of key cost effectiveness metrics relationships.



Efficiency

Efficiency addresses the operational and economic cost effectiveness of gate-to-gate flight operations from a single flight perspective. Efficiency can be measured in terms of a combination of direct operating costs (as determined by adding up all the individual costs such as landing fees, emissions surcharge, noise surcharge as well as any other operating costs), flight time (or additional flight time), and fuel burn (or additional fuel burn). Additional flight time influences the distribution of delay in the system and introduces a chain of effects. Flight time (and/or additional flight time) impacts terminal noise, which, in turn, triggers the noise surcharge. Fuel burn (and/or additional fuel burn) impacts terminal emissions, which triggers the emissions surcharge. Figure 17-19 provides the relationships among the key indicators for efficiency.

Flexibility

Flexibility addresses the ability of all airspace users to modify flight trajectories dynamically and adjust arrival and departure times to exploit operational opportunities as they occur. Flexibility indicators are chiefly those that enable the user to exercise flexibility in using a resource. Figure 17-21 displays the flexibility metrics relationships.

Predictability

Predictability addresses the ability of the airspace users and ATM service providers to provide consistent and dependable levels of performance. Metrics that measure predictability include distribution of delay and distribution of fuel burn. Delay results from additional (or excess) flight time. Aircraft sizing trends influence the number of flights using a resource and vice versa. Figure 17-20 displays the relationships among the predictability indicators.

Environment

Environment addresses the need to protect the physical environment from gaseous emissions, noise and other environmental issues related to the implementation and operation of the global ATM system. Environmental impacts are further sub-categorized into air quality, climate change and noise impacts.

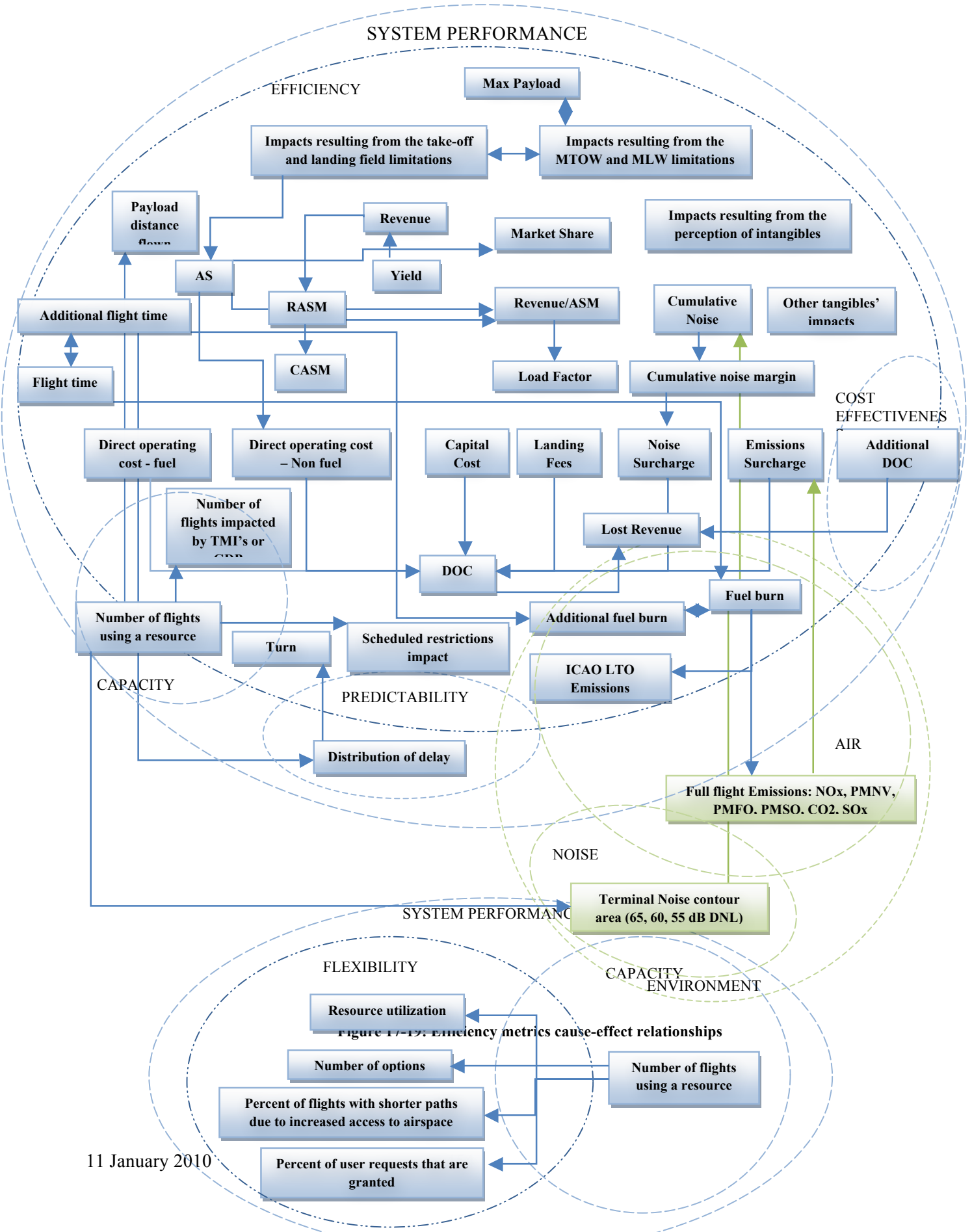


Figure 17-21: Flexibility metrics cause-effect relationships

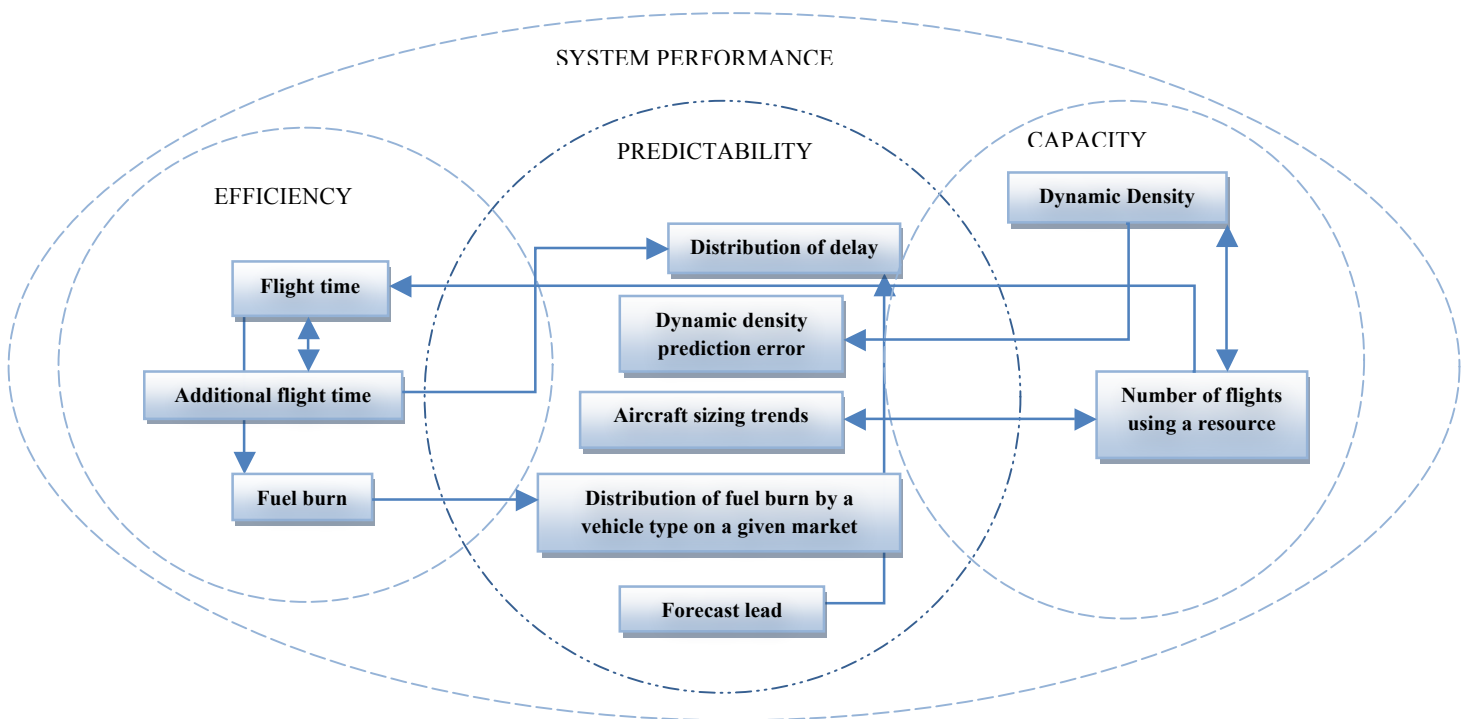


Figure 17-20: Predictability metrics cause-effect relationships

Air Quality

Air quality impacts are measured by aviation emissions such as nitrates, sulphates, and hydrocarbons affecting concentrations of PM_{2.5}, ozone and hazardous air pollutants that can lead to the incidence of premature mortality and morbidity. Performance indicators to measure air quality impacts at the lowest level are those measuring individual aviation emissions as a result of fuel burn in the atmosphere. The interaction of these emissions affects the concentration of particle matter and leads to more societal

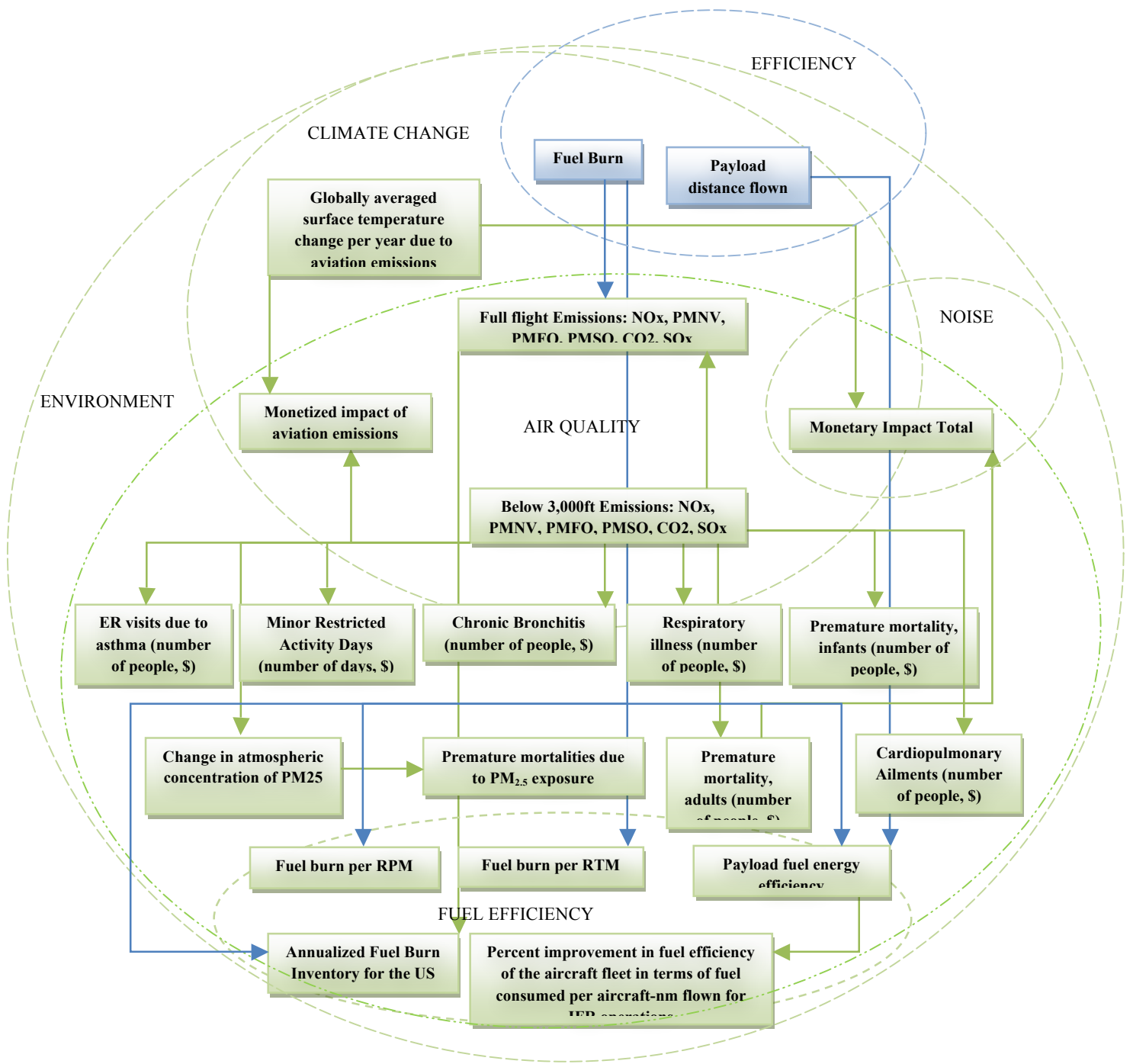


Figure 17-22: Air Quality metrics cause-effect relationships

impacts on populations leading to medical ailments and emergency room visits that result in premature mortality. Figure 17-22 provides the air quality metrics relationships.

Climate Change

Aviation emissions such as CO₂, NO_x, SO_x, Soot, contrails, water vapor result in changes in atmospheric concentration of CO₂, CH₄, O₃, H₂O, aerosols and so on leading to climate change impacts such as global temperature changes, sea level changes and other climate impacts. Climate change impacts are ultimately triggered by aviation emissions as a result of fuel burn in the atmosphere. Figure 17-23 displays the cause-effect relationships among the climate change metrics.

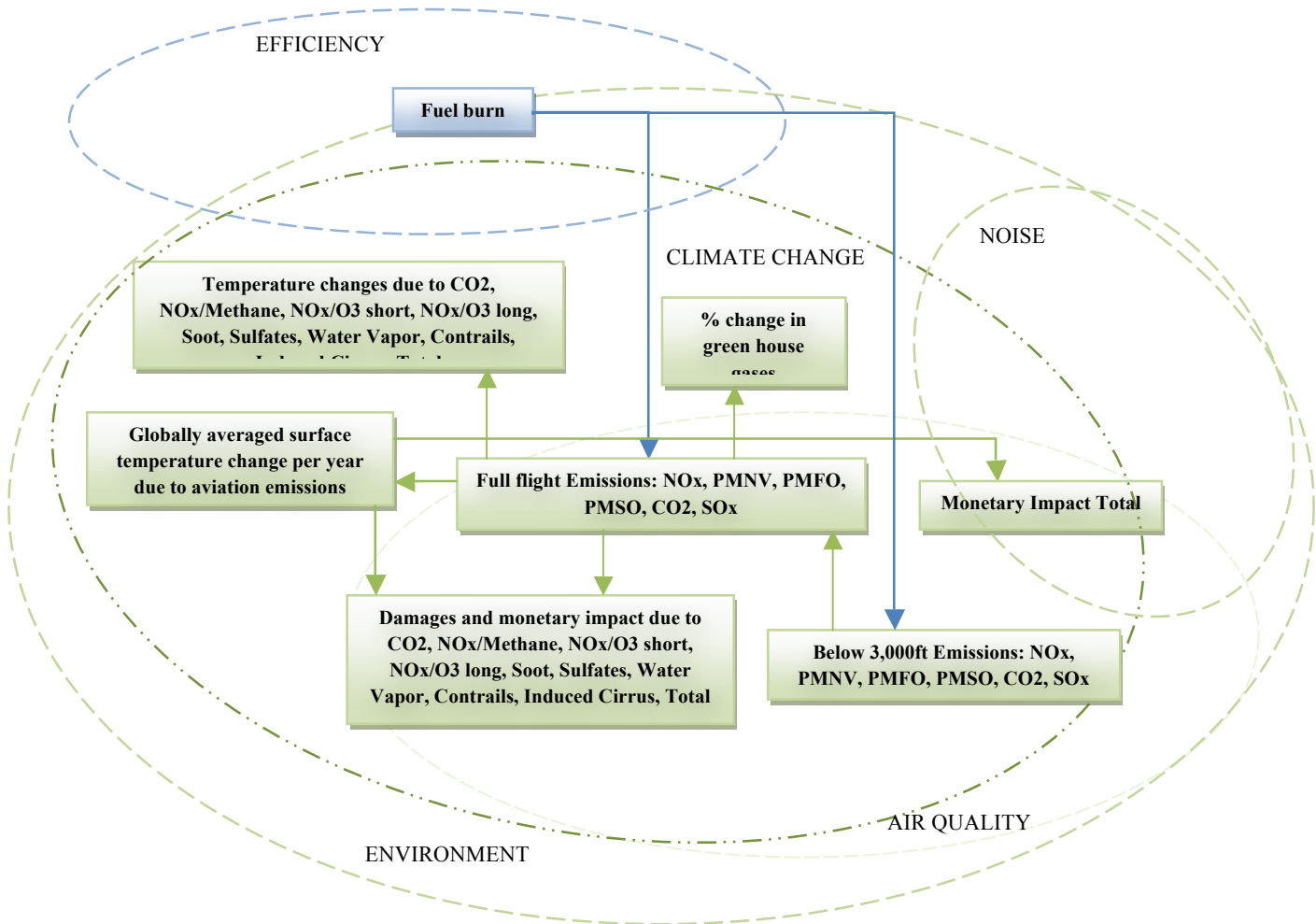


Figure 17-23: Climate change metrics cause-effect relationships

Noise

Noise is influenced by the Day Night Noise Level, the number of operations, and the exposure level. Aircraft, rotorcraft and supersonic noise impacts are measured by the number of people exposed, the noise contours and exposure level. As with aviation emissions, aviation noise ultimately results from flight time (and or excess flight time). Figure 17-24 provides the relationships among the noise metrics.

Fuel (Energy) Efficiency

Metrics that enable measuring overall energy efficiency fall into this category. See Figure 17-25 for details

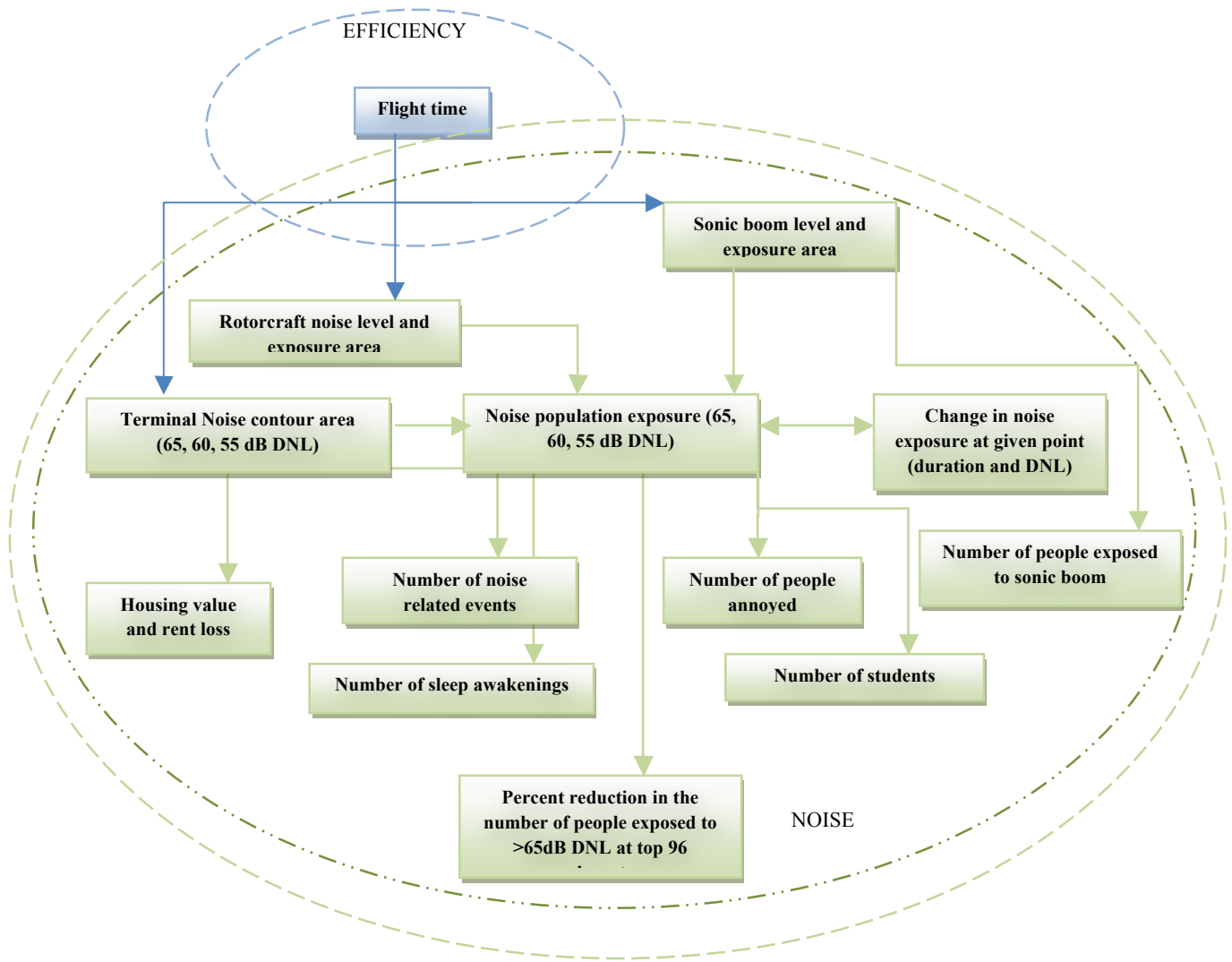


Figure 17-24: Noise metrics cause-effect relationships

Safety

Safety is of highest priority and ATM plays a vital role in ensuring overall aviation safety. Uniform safety standards, risk and safety management practices must be systematically applied to the ATM system. Safety metrics are further sub-categorized into human performance errors and accident risk.

Human Performance Error

Errors resulting from pilot or controller actions (such as pilot deviations, operational errors, and operational deviations leading to accidents and/or increasing risk of accidents) are sub-categorized as human performance errors. The number of flights using a resource affects the number of conflicts as well as the nature of resolution maneuvers necessary to avoid the conflicts. The dynamic density affects operational deviations and operational errors, conditions that, in turn, can lead to loss of separation events and pilot deviations. Factors that increase risk and lead to fatal accidents include system component

failures/malfunctions, wake turbulence encounter, runway incursions, runway excursions, and mid-air collisions.

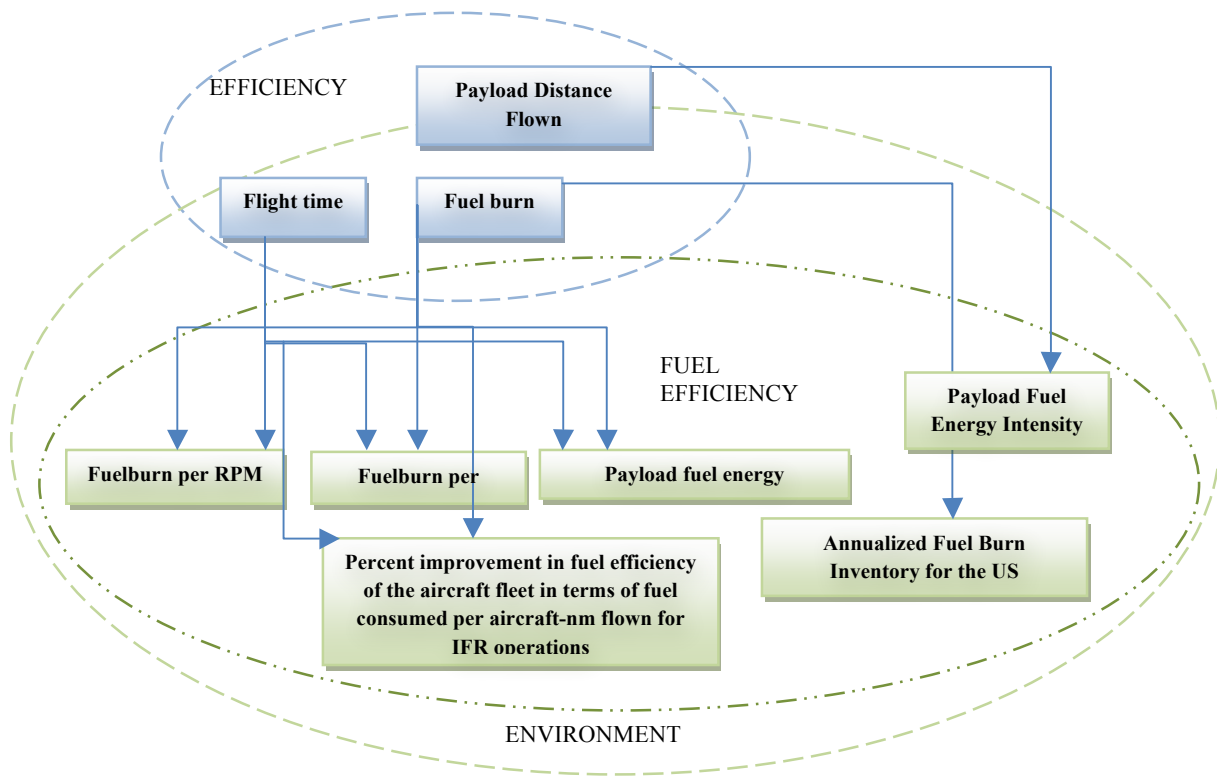


Figure 17-25: Fuel Efficiency metrics cause-effect relationships

Inherent aircraft vulnerabilities can lead to loss of control in flight. Likewise, loss of separation can set up conditions causing aircraft to encounter wake turbulence. Any risks such as system failures, loss of separation, and types of conflict can increase the risks to safety. Figure 17-26 illustrates the cause-effect relationships for human performance error metrics.

Accident Risk

All other metrics measuring the actual occurrence of accidents or the computation of risk or probability of occurrence of safety significant events leading to accidents are sub-categorized under accident risk metrics. Figure 17-27 provides the cause-effect relationships for the accident risk metrics.

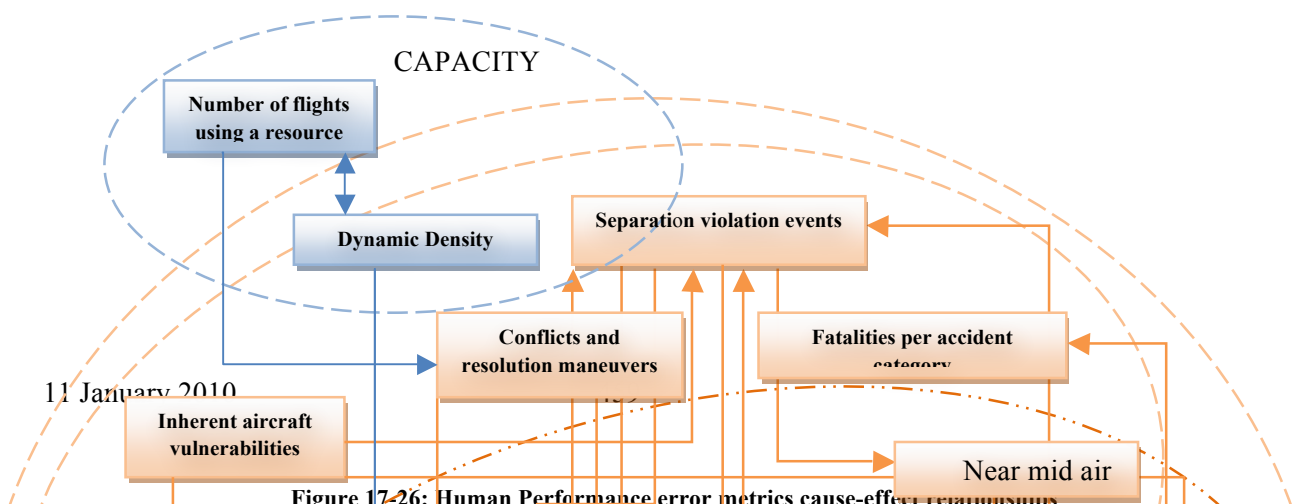


Figure 17-26: Human Performance error metrics cause-effect relationships

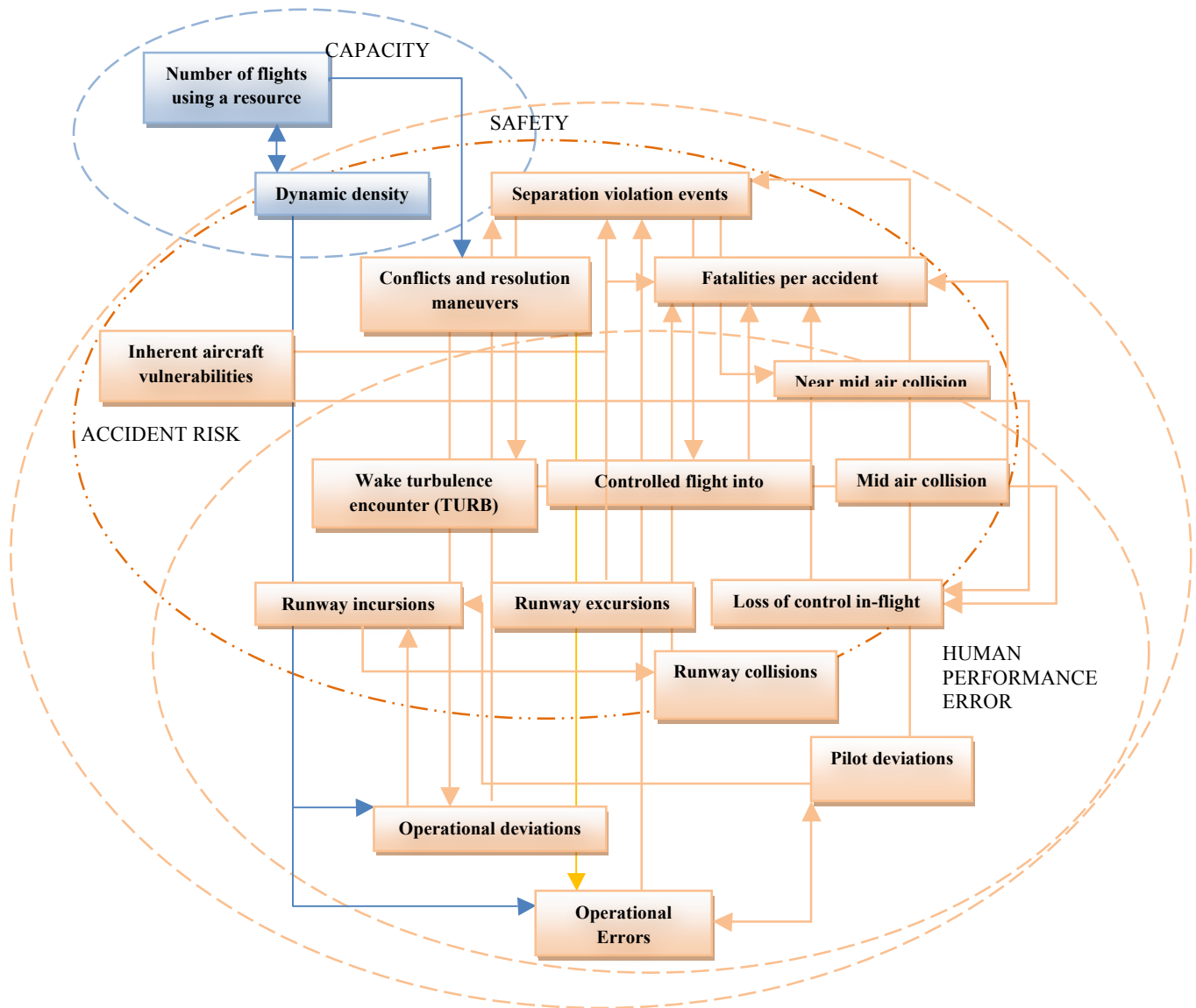


Figure 17-27: Accident Risk metrics cause-effect relationships

cxlix If alternative fuels are being analyzed, then it is imperative that both fuel production and fuel combustion be examined in what is commonly known as a “well-to-wake” fuel life cycle analysis.

cl Recent research indicates that emissions above 3,000 ft may also have an appreciable impact on human health.

18. Suggested Topics for Future Research

The analysis capability developed under this project—including the tools, framework, and team assembled for this effort—can provide significant value beyond new vehicle assessments. One major objective of the study is to provide recommendations for further research to NASA’s Aeronautics Research Mission Directorate (ARMD). This includes guidance for airspace systems research to the Airspace System Program (ASP), vehicle technology research to the Fundamental Aeronautics Program (FAP), recommendations to the Aviation Safety Program (AvSP), and research topics for the new Integrated System Research Program (ISRP). The key challenge in the current research has been not the new vehicles themselves, but understanding the new operations they enable and the concomitant impact the NextGen and the environment. This section summarizes the team’s recommendations.

18.1. *Policy Implementation Studies*

Best equipped, best served (BEBS): There is significant interest in the concept of moving to a service model for which “best-equipped, best-served” replaces “first-come, first-served” in highly congested markets. This change in priority could have major impacts on the performance of the NAS. The NVNRA framework would be an excellent platform to study ways this policy could be carried out in terms of the ramifications to capacity and delay, as well as to safety and the environment. This study would provide initial data regarding the recent RTCA Task Force 5 assessment of BEBS. Other types of service models could be assessed as well.

Distributed Metroplex Airport Access: Although not a written policy, the current approach to airport and runway infrastructure investment favors adding runways at major congested hub airports rather than improving reliever airports as a means of increasing system capacity. However, past studies have shown that one Metroplex runway adds only a few percent to the nation’s capacity during an era when increases of 150 to 300 percent are needed (and the likelihood of building 150 to 300 more runways is nil). Although the so-called reliever airports in the major Metroplex areas represent underutilized capacity for meeting regional needs, existing aircraft performance and scheduled air carrier hubbing business models are not aligned with a concept to use such airports. The NVNRA framework could provide the tool to study vehicle, airspace, and airport policies and related technology policies that lead to alternative approaches to meeting national air mobility needs; specifically, by more efficiently incorporating the underutilized reliever airports in meeting capacity requirements. The framework developed in this project includes the ability to measure the noise and emissions impact in addition to the capacity.

NextGen Investment Tradeoff: NextGen investments will cost billions of dollars over the next decade. Much of this investment will go to technologies and infrastructure to improve capacity in specific ways, such as adding runways and other capabilities to increase runway throughput at congested airports (e.g. airports with closely spaced parallel runways). Our current study demonstrated that some new vehicle types, such as LCTR, could provide significant increased capacity at major hub airports through the vehicle’s unique capabilities to take off and land without impacting the main runways. Future research could analyze the investment tradeoff between adding conventional runways and technology for more operations on the conventional runway as opposed to enabling and manufacturing new unique vehicles to operate independent of the runways. It might turn out, for example, that providing subsidies for the new vehicles would be more cost effective than squeezing additional capacity out of existing long runways.

18.2. **Transition Studies**

Partial Vehicle Equipage: The current study of new vehicles (and most JPDO studies) of NextGen evaluate NAS performance after NextGen is fully completed and assumes all vehicles are equipped for NextGen operations. A topic that is ripe for study involves looking at points in the future in which vehicles and the ATM system have only partial equipage. An equipage modeling study could be combined with the policy study “*Best-equipped, best-served*” to understand the implications of that policy and the likely system performance at something like 25%, 50%, 75%, and 100% equipage. This study would evaluate mixes of conventional and new vehicle classes, along with varied performance-based capabilities for aircraft and airports.

NextGen Capability Value: Because most existing studies assume NextGen at the end-state, there are no studies that identify which groupings of systems within NextGen have significant value to certain users, markets, or business models. Some efforts identify the earliest systems for implementation—essentially low-hanging fruit—but do not analyze the benefits by user-groupings of partial implementation of certain NextGen systems. For example, can airlines use CESTOL aircraft to make spiral descents to major airports with less than “full NextGen” implementation? If so, does a business case exist with adequate NextGen and vehicle technologies so that introduction of this aircraft can take place earlier than 2025? Is there some subset, or subsets, of NextGen capabilities that will provide a disproportionate benefit, such as gaining 75% of the capacity increase benefit for only 25% of the investment? This study would build a matrix of NextGen operating capabilities benefits and different potential fleet mixes along a timeline for early implementation to gain insights into possible alternate deployment schedules.

JPDO OI Impact on New Vehicles: The transition to NextGen is driven by a series of Operational Improvements developed by the JPDO, the implementation of which are now the responsibility of the FAA NextGen Integration and Implementation Office. Their focus is on the “mid-term” 2018 NextGen capability. Because NASA’s role is primarily to develop the accelerated implementation of farther-term technologies, a review of all the OIs and their implications for new vehicles should be conducted to determine if crucial OIs should be accelerated.

18.3. **Airport Studies**

Ground Side Traffic Impact: Increased demand for air travel will require additional passenger terminal space, gates, etc. Several of the new vehicles already studied (e.g. CESTOL and LCTR) may facilitate significantly more passengers at existing congested airports than anticipated with only conventional aircraft, increasing the strain on airport and highway assets beyond runways and taxiways. This study would evaluate the impact of additional gate and passenger terminal requirements under a variety of scenarios. The study could be done as a relatively high-level initial NAS aggregate assessment. It could also be done at a detailed level, focusing on individual airports, or with very high fidelity at one or more airports where we closely evaluate the ground side including parking, road and rail access. Even though the boundaries of the FAA and NASA charters end at the airport curb, and states bear the burden of providing highway access to serve airports, this study would be valuable in revealing ground-side issues requiring attention on- and off-airport.

18.4. **Safety Studies**

Safety in Transition: The transition from the current system to NextGen is currently not well understood and has not been studied. In such an environment there will be mixed-equipage considerations, airports with different levels of capabilities, new vehicles of different maturity levels, and airspace in transition. The heterogeneity of the system makes for a rich research environment for safety issues. We have configured agent-based models to study safety (as reported at the 2nd workshop). These models can be configured to study a mixed-equipage environment and determine levels of safety—probabilities of airspace violations, runway incursions, separation violations. This study would explore the potential safety implications of the implementation of NextGen capabilities.

Software for Trajectory Based Operations: Trajectory Based Operations represent one of the major promises for NextGen airspace efficiency and capacity. While the various concepts for trajectory management are emerging, early planning on TBO management software verification and validation (V&V) R&D is timely. This task would develop the R&D strategies for TBO software V&V.

Off Nominal Analysis: The initial study evaluated a few safety aspects of “off nominal,” the avionics required, and a few convective weather scenarios. However, many of the NextGen concepts involve significantly reduced margins, including closer spacing of aircraft in distance and time, reduced reaction time for pilots and controllers, and significantly more reliance on automation. These and many other NextGen implications could be much more fully analyzed for both the potential benefit of the concept and the potential risks and possible mitigations of the concepts. This study could identify dozens of technology and human factors research requirements as well as quantify the relative disruption impact of NAS disturbances such as terrorist attacks, pandemic outbreaks, environmental disaster operations, and extended power outages and itemize the ATC automation and avionics infrastructure ramifications.

Hazardous Impact Analysis: Evaluation of different hazardous conditions and how they impact different vehicles and systems, quantity and quality of impact (e.g. loss of satellite coverage could impact many vehicles, different failures impact different numbers of ground and airborne systems.)

4D Conformance Monitoring: Current conformance monitoring is generally limited to simple horizontal situations, such as parallel closely spaced runway approaches. As we move to complex, curved continuous-descent approaches the conformance monitoring will need to encompass complex 4D trajectory monitoring. A first step would be to develop a vertical conformance monitoring capability. As the approach becomes more and more complex (such as the spiral approach proposed in this study for the CESTOL aircraft), which controller has responsibility to monitor the aircraft? How does this effect workload?

4D Safety Analysis: In the future all aircraft are to be flying on negotiated 4D Trajectories that are conflict-free for some period into the future. When a major ATM system failure occurs there is a natural safety feature under this operating paradigm in that the aircraft are currently all on conflict-free trajectories. However, how long will they remain conflict-free? Sources of error (e.g. winds) and unpredictable aspects (e.g. convective weather or other system failures) will eventually create conflicts. An important issue is to characterize this 4DT safety: How long are the trajectories conflict free? What situations accelerate the probabilistic nature? What types of failures exacerbate and accelerate the

degradation of 4DT Safety? What are the strategies for recovery as the ATM monitoring systems come back online?

18.5. **Environmental Studies**

Improved Environmental Analysis of Current Vehicles: Although significant results were completed under the existing study on the existing five vehicles, there were many areas that could benefit from additional research to gain significantly better insight into the environmental impacts. The following projects would provide relatively short-term activities and deliverables that would ensure we get the maximum value out of the work that has already been accomplished.

- Detailed Air Quality (AQ) and noise analysis of all of the new vehicle concepts in the NY metroplex. Under the current project and schedule, we will only have analyzed a few simple cases such as the change in operations. This additional more detailed environmental analysis could be accomplished with the existing NY metroplex simulation data in an additional 3-6 months.
- A system-wide analysis of the change in noise and AQ impacts from each of the new vehicles. The current report will only have system-wide climate impacts, not noise or AQ.
- A comprehensive examination of two cases. In one, we examine the impact of N150 aircraft entering the fleet and in the other we look at the impact of CESTOL entering the fleet. Our CESTOL scenario has both of these aircraft in it, so it is very hard to examine the relative contribution of each.
- A system-wide examination of the environmental impacts of the SST design. This is a 3-6 month effort that would leverage the existing literature to further examine the climate and ozone impacts of an SST flying in the stratosphere.

Most Environmentally Friendly, First Served: There is a growing investment at both NASA and FAA in achieving significantly decreased environmental impact. One concept would be to provide operational priority to those operators who can provide decreased environmental impact. This could be provided and studied in many ways. An example approach would be to provide priority at any cue to the more environmentally friendly aircraft (e.g. ramp spot or take off cue position for departure, arrival flow order for arrival). Another example would be lower noise impact priority. These kinds of policies could have system-wide environmental benefit or detriment depending on many factors. This study would investigate a variety of strategies and evaluate the impact of these strategies on capacity and environment.

18.6. **Vehicle Studies**

FAP Vehicle Analysis: The Fundamental Aeronautics Program (FAP) is developing and analyzing (in house and through NRA contractor teams) various specific future vehicle designs for near, mid, and far term (N+1, N+2, and N+3). This design activity is occurring for three classes of vehicles that would impact the NAS: subsonic, rotary wing, and supersonic. The current new vehicle analysis was performed on vehicles selected and specified by the New Vehicle NRA teams. This study would perform a similar NAS impact analysis but utilizing the NASA (and NASA contractor) specified vehicles beyond those in the current scope.

JPDO and NASA Goal Alignment: The JPDO has specific goals for overall system impact, such as environmental impact. The NASA FAP currently has goals for future (N+1, N+2, and N+3) subsonic, rotary wing, and supersonic vehicle performance. The alignment between these goals is not clearly

understood. This study would use the JPDO defined goals (starting with environmental) and model the FAP future vehicles from the vehicle goals (e.g. N+1 environmental impact) and determine the required fleet deployment dates and rates to achieve the JPDO goals. This would provide feedback and advocacy to the NASA programs (Especially FAP and ISRP/ERA) on the R&D priorities needed to meet national goals and provide a mechanism to develop future research goals and the analysis data to advocate future research goals.

Refine Existing Vehicle Modeling and Simulation: The Current study modeled CESTOL, LCTR, VLJ, UAS Freight Forwarding, and SST vehicles. Many aspects of this study could be refined and improved dramatically, ranging from better surface and terminal modeling to more accurately assess CESTOL and LCTR throughput benefits to better JPDO baseline environmental modeling to understand the environmental impact of the new vehicles. The first phase would be identifying the most valuable improvements in the analysis methods and then perform the complete performance and environment analysis again. The vehicles could be refined based on this feedback loop along with more detailed business case analysis. This study would produce a modeling and simulation roadmap of requirements and approaches for NextGen vehicles and infrastructure performance, costs, and environmental effects.

Alternate Powered Aircraft Impact: Energy costs and environmental impact are becoming stronger drivers in aviation system design. Research is underway in a variety of alternate power plants for a variety of vehicles. Fuel cells and battery-powered alternatives are being developed and marketed for UASs and general aviation. Conceptually, the current Cessna Caravan sized UAS for freight forwarding needs only a range of approximately 200nm and could have time to recharge batteries between flight segments. This capability is within the range of near future technology and would greatly reduce emissions and noise. We propose designing and analyzing a variety of all-electric vehicles for a set of particular business models. In this study, the ASDL would design the vehicle with the ensuing performance and impact analyses conducted using existing and emerging tools (e.g., AEDT), including procedure design, metroplex analysis, system-wide analysis, and environmental analysis.

Military UAS in the NAS: This is a real “NowGen” issue and growing daily. The analysis framework could be used to analyze the impact of large scale military UAS use of the NAS for transition, training, etc. This study would produce a system-level impact assessment of a range of UAS fleet size and utilization rate scenarios on NAS performance, workloads, costs, safety, and capacity.

Improved CESTOL: The CESTOL we designed for the current NRA is limited to 100 passengers. The 100 passenger market is not nearly as lucrative as the 150 passenger market. However, designing a CESTOL that can takeoff/land in a 3,000 foot runway and carries 150 passengers is a design challenge, but one that the team is willing to tackle. The 100-pax design is easier, as the airplane is lighter and its takeoff/landing requirements are less. This study would expand on the current results to explore the scalability of the CESTOL concepts upward in passenger size.

Improved LCTR: The LCTR that was studied vehicle has a 1,000-nm range. For the high-volume short-haul markets, we discovered that a 500-nm range is sufficient to generate enough business to support the vehicle. In addition, the 90-passenger vehicle presents significant design and operational risks, making a smaller size much more feasible. In this study, we propose designing and analyzing the smaller 500-nm LCTR, which because of its reduced weight, noise, fuel consumption, and power requirements is more likely to be feasible for airport surface operations.

New Vehicle: Airships: A large heavier-than-air airship that is slow, efficient, and quiet has an interesting business case, for transporting passengers as well as heavy cargo. Such a vehicle has been the topic of feasibility studies by Lockheed Martin and the DoD in recent years. This study would undertake an evaluation of the impact of the NextGen NAS of this category of vehicle, which is not part of the current study.

New Vehicle: Spacecraft: Several commercial human-occupied, space-launch systems are coming on[line in the next few years for both tourism and re-supply of the International Space Station . Space vehicles will soon become a part of the future NAS. Any analysis of the impact of new vehicles must also include the impacts of the daily operation of space flights on NextGen NAS operations to address the following questions such as: How will daily civilian spaceflight operation impact existing NAS operations? What procedures and processes must be incorporated to limit restrictions on normal operations? What are the safety implications of daily civilian spaceflight operations in the NAS?

18.7. **Major Model Improvements / Studies**

Aircraft Environmental Design Tool (AEDT): This tool represents a significant step forward in the modeling of system-level effects of technology and operational strategies affecting noise and emissions. The maturation of the use of this tool requires both human and software system advancements. On the human side, we need a community of government, industry and academic engineers, analysts, and policy-makers skilled in applying the tool to the challenges of the 21st century. On the software side, we need continuing refinement of the fidelity of the modeling capability to account for non-average, non-Gaussian, non-linear effects that can be expected to dominate in the system outcomes from new technologies and significant operational changes. The current industry perspective is one of skepticism about the utility of tools such as AEDT for policy or regulatory action, and agreement that the tool can be of great value for comparative, differential design studies. This study would build on the progress in development and use of AEDT to help validate and demonstrate the use of AEDT for informing policy and for engineering design tradeoff analyses.

Improved Analysis of Surface Operations: The concept of trajectory-based operations is intended to extend down to include surface operations (see programs on Surface Tactical Flow and Surface Conformance Monitor in BLI 1A11 of the Capital Investment Plan). High-resolution surface-modeling of the airports in a Metroplex is required to accurately measure the performance of the overall terminal area, as well as the related effects of surface traffic management on the performance of the entire NAS. Currently our surface modeling is limited to statistical abstractions: average taxi-out and taxi-in times, and average gate occupancy and turn-around times. We believe the lack of fidelity in the surface modeling is likely the most pronounced modeling inaccuracy in our current studies. Several higher fidelity terminal and surface models have been in development for ACES. We recommend utilizing the new TME software to implement a major metroplex (e.g. NY) to evaluate the differences in performance between the existing study and a new study utilizing the enhanced surface modeling. Another option would be to improve SIMMOD to ensure it has enough resolution to model the surface in great detail, for example it would be relatively easy to add gate and taxiway usage modeling. In either case, surface observations from PDARS and from ASDE-X can be used to configure and validate the surface models.

Improved Tail Connectivity and Schedule Generation: According to the Bureau of Transportation Statistics more than one-third of all delay in 2009 was due to “Late Aircraft.” That is, passengers are delayed not because of a problem at their destination, but because the aircraft they are flying on got delayed sometime earlier in the day. To capture this propagated delay it is therefore crucial that aircraft in simulations fly tail-connected itineraries. This is airline proprietary information today so is unavailable in existing schedules. To assign tail-numbers to the flights to the JPDO-provided future schedules we used what’s known as a “greedy” algorithm. This algorithm is only moderately successful in creating tail-connected itineraries for the flights in the database. Whereas an airline typically flies 6-8 flights per day with a single airframe, our processing achieves only half this number. This means we significantly underestimate the amount of propagated delay. We would create improved algorithms to generate aircraft itineraries that more closely resemble those flown by airlines today. These algorithms would seek to execute a given schedule with the minimum number of airframes. It would also be worthwhile to investigate adjusting the arrival and departure times in the JPDO-provided schedules to make it easier to create efficient tail-connected itineraries. The schedules that would be created would be usable in any NAS-simulation that can track tail-numbers and would provide more accurate estimates of propagated delay and fleet size. Airlines design their schedules to maximize the usage of their fleet. A tail-connection algorithm that schedules too few flights per airframe per day will either overestimate the number aircraft needed to fly a given schedule or underestimate the number of flights that a given fleet can complete in one day. This study would enable much more accurate studies into the challenges in disruption management (irregular operations) that are feasibly manageable in a NextGen world.

Optimized Enroute Trajectory Impact: Most flights today still follow jet routes. Our current NextGen studies all grow future schedules based on a seed day of today’s traffic, including today’s routing along jet routes. It is anticipated under NextGen that flights would fly wind optimized direct routing on all longer distance flights, perhaps all flights. Will this wind optimized individual routing create fundamental new problems in the airspace? Will there be more conflicts or fewer conflicts? How much fuel will this save? This study would investigate a broad set of impacts based on individual flights flying individually optimized routes in place of today’s jet routes.

Enhanced Experimental Design: The terminal airspace experimental design could be improved to make it easier to identify and isolate the impacts of the different types of vehicles. In the current study, the future year flight demand schedules were optimized for the modeling of operations at the NAS-level. However, this does not provide the necessary resolution required to measure terminal airspace impact. Particularly, point performance demand sets of predicted future operations with their numerous underlying assumptions do not provide the necessary structure needed to identify specific vehicle operating characteristics and their impact. We recommend the development of a new experimental matrix and demand sets that are optimized to analyze performance in the terminal area and to make it easier to isolate the impact of individual independent variables, and use these new demand sets for a new round of simulation runs and analysis.

Determine Metroplex Capacity: In our initial study we developed a new NY and DC terminal airspace design that decoupled arrival and departure paths for different airports and runways in the metroplex regions. This provided significantly more capacity. In the initial study we used the JPDO forecast baselines including schedule and fleet mix (with some updates). We did not attempt to assess what the realistic capacity of these redesigned metroplex areas is. This study would develop a wide variety of

different future schedules with different realistic fleet mixes and different business models such as arrival and departure push timing and use of regional airports vs. hubs. From this study we should be able to characterize the maximum capacity of the metroplex and to provide significant insight into the impacts on capacity depending on how you chose to utilize the airports and airspace. We will also evaluate environmental and safety implications of the different options.

Off-nominal scenario model improvement: The current study only included one off-nominal scenario, which focused on one particular pattern of inclement weather. In order to better capture and analyze the sensitivity of proposed future vehicles and operations, a lot more different scenarios should be designed, modeled and analyzed.

Weather Impact: Most existing system studies focus on VFR operations; some studies in recent years evaluate a few aspects of airport or en-route convective weather. One of the main presumptions in NextGen is that operations under adverse weather will be very close to clear weather performance levels. This study would evaluate several days of bad convective weather to determine the impact on performance of a NextGen NAS compared to VFR conditions and to develop an understanding of what aspects of NextGen are crucial to enabling reliable and predictable behavior under these bad convective weather periods.

NextGen Capabilities Not Analyzed: Several key NAS capacity enhancing capabilities in NextGen were not analyzed in this study as they had no direct impact on the specific new vehicles selected for this study. Additional studies could be performed specifically on these capabilities to quantify the benefits of the capability and to determine what new vehicles or vehicle capabilities would be needed or benefit from these capabilities. Examples include closely spaced parallel runways and paired approach operations.

NextGen Flow Control: Current TFM flow control methods are basically ground holds and Miles In Trail (MIT) restrictions. Implementation of these and especially determining when and how to remove these constraints is problematic today. Under the NextGen paradigm, aircraft are expected to operate on individually negotiated 4D trajectories (flight plans). When the system is forecast to have greater demand than capacity, how will flow control be implemented? What will be measured and become the trigger to invoke flow controls? How will it be determined to disengage flow control?

TFM Individual Flight Impact: Current Under a NextGen environment, from a flow control standpoint it is anticipated that actions will be performed on individual flights rather than flows of flights. Even today you can analyze what is likely to be the impact of individual flight, you can look at the impact each flight is likely to have on each sector as well as the airports/runways it is operating from. The TFM system could evaluate which flights was the most “damaging” to the system every day and look for patterns. What if the same flight from X to Y is causing the most impact most days? What would be the impact of holding or rerouting that flight significantly instead of impacting a lot of other flights a little? Could major delay reductions be accomplished by changing only a few flights? Initial work has already been performed by the JPDO IPSA team on this subject using the PNP platform, this effort could go toward analyzing if such a TFM system could be used in the near future to provide significant benefit to system performance.

Improved Terminal/Metroplex Demand Data: One of the factors that made the analysis of the terminal airspace challenging was the many variables that changed in the different demand cases. To

identify and isolate the impacts of each vehicle, the terminal airspace experimental design needs further development. Future year flight demand schedules that are sufficient for modeling operations at the NAS-level may not provide the necessary resolution required to measure terminal airspace impact. Point performance demand sets of predicted future operations with their numerous underlying assumptions do not provide the necessary structure needed to identify specific vehicle operating characteristics and their impact.

Appendix A. Acronym List

Acronym	Expansion
ACARS	Aircraft Communications Addressing and Reporting System
ACES	Advanced Concept Evaluation System
ADS-B	Automatic Dependent Surveillance-Broadcast
ADS-C	Automatic Dependent Surveillance-Contract
AEDT	Aviation Environmental Design Tool
AIAA	American Institute of Aeronautics and Astronautics
ANSP	Air Navigation Service Provider
APMT	Aviation Environmental Portfolio Management Tool
ARINC	Aeronautical Radio Incorporated
ARS	Assisted Recovery System
ARTCC	Air Route Traffic Control Center
ASAS	Airborne Separation Assurance System
ASDE-X	Airport Surface Detection Equipment, Model X
ASDL	Aerospace Design Laboratory
ATC	Air Traffic Control
ATIO	Aviation Technology, Integration and Operations
ATM	Air Traffic Management
ATN	Aeronautical Telecommunication Network
ATS	Air Transportation System
BADA	Base of Aircraft Data
CAST	Commercial Aviation Safety Team
CDA	Continuous Descent Arrival
CDTI	Cockpit Display of Traffic Information
CDU	Command Display Unit
CESTOL	Cruise Efficient Short Take Off and Landing
CFIT	Controlled Flight into Terrain
CMU	Communications Management Unit
CPDLC	Controller Pilot Data Link Communications
DL	Datalink
DNL	Day-Night Average Sound Level
DOC	Direct Operating Cost
D-TAXI	Data Link TAXI
EDS	Environmental Design Space
ESTOL	Extremely Short Takeoff and Landing
ESVS	Enhanced and Synthetic Vision Systems
ETA	Estimated Time of Arrival
EVS	Enhanced Vision Systems
FAA	Federal Aviation Administration

FACET	Future ATM Concepts Evaluation Tool
FANS	Future Air Navigation System
FAST	Future Aviation Safety Team
FIS-B	Flight Information Service-Broadcast
FMS	Flight Management Systems
FSF	Flight Safety Foundation
GA	General Aviation
GBAS	Ground Based Augmentation System
GLS	GPS Landing Systems
GNSS	Global Navigation Satellite System
GPS	Global Positioning System
GT	Georgia Tech
HMI	Human-Machine Interface
HUD	Head Up Display
ICAO	International Civil Aviation Organization
IFR	Instrument Flight Rules
ILS	Instrument Landing System
IMC	Instrument Meteorological Conditions
JPDO	Joint Planning and Development Office
KIAS	Knots Indicated Air Speed
KPA	Key Performance Areas
LCTR	Large Civil Tiltrotor
LNAV	Lateral Navigation
MCL	Minimum Capabilities List
MEANS	MIT Extensible Air Network Simulation
MEL	Minimum Equipment List
NAS	National Airspace System
NASA	National Aeronautics and Space Administration
NMAC	Near Mid-Air Collision
OEM	Original Equipment Manufacturer
PBN	Performance Based Navigation
PDARS	Performance Data Analysis and Reporting System
PFD	Primary Flight Display
PFEI	Payload Fuel Energy Intensity
PM	Particulate Matter
RAAS	Runway Awareness and Advisory System
RF	Radiative Forcing
RNAV	Area Navigation
RNP	Required Navigational Performance
RTA	Required Time of Arrival

SATCOM	Satellite Communications
SATS	Small Aircraft Transportation System
SBAS	Space Based Augmentation System
SIMMOD	Airport and Airspace Simulation Model
SMAD	System Modeling and Analysis Division
SST	Super Sonic Transport
STOL	Short Takeoff and Landing
SUA	Special Use Airspace
SVS	Synthetic Vision Systems
SWIM	System-Wide Information Management
TARGETS	Terminal Area Route Generation, Evaluation, and Traffic Simulation
TASAT	Time-Domain Analysis Simulation for Advanced Tracking
TAWS	Terrain Awareness System
TBO	Trajectory Based Operations
TCAS	Traffic Collision Avoidance System
TOAC	Time Of Arrival Control
TRACON	Terminal Radar Approach Control
UA	Unmanned Aircraft
UAS	Unmanned Aerial System
UAT	Universal Access Transceiver
VLJ	Very Light Jet
VMC	Visual Meteorological Conditions
VNAV	Vertical Navigation

Appendix B. AEDT Notes

The software used for the environmental impacts analysis, the Aviation Environmental Design Tool (AEDT) is a new product currently under development by the FAA with a team of companies under Volpe leadership. AEDT is intended to replace several disparate tools currently used in industry with a single unified product. AEDT was in the early stages of development at the onset of our research project but the FAA sponsor and Volpe team agreed to accelerate the specific features we needed and provide direct support to our team as “alpha” users of the software. Hence, our analysis relied on a specifically-built software version. The following paragraphs highlight our experiences using this alpha-test version of the software.

As we were simulating nation-wide traffic and some runs included up to 3 times today’s traffic the AEDT flight preprocessor performance was found to be very slow. To give a rough estimate of the scaling, it takes only seconds to process several thousand flights, about 20 minutes for about 15,000 flights, and about 10 hours for about 50,000 flights. Our solution was to split the datasets depending on the number of flights. We also created an automated process to efficiently process the large number of datasets expected for this research.

Incomplete meteorological data for airports was also a problem. For instance, we found during testing that 21 airports had missing weather station meteorological data such as relative humidity. As a workaround, the AIRPORT database was searched for the closest alternative weather stations and the data replaced accordingly. This turned out to be relatively complex, because there were thirteen data sets to process: twelve monthly and one annual.

The availability and quality of data for airport-specific information was a problem as well. In most cases, we were able to substitute “best available” or equivalent information as necessary.

An unexpected challenge was the incomplete flight tracks provided by ACES for flights with international arrivals or departures. By design, the AEDT flight preprocessor would discard flights that were missing either arrival or departure airport information. Sensis developed a tool that would artificially add the appropriate state messages for most of these. However, some small percentage of flights was still missing a full set of information. This was, however, easily omitted by the nature of the relational queries in SQL server. The other problem that needed to be remedied at this stage, but only became more obvious after much more testing of the data and the final results, was that some takeoff and landing pairs were associated with two trajectories. This resulted in anomalous results for those flights, which were therefore excluded from the analysis.

Some of the vehicles, most notably the tiltrotor, also presented unique challenges. It is technically necessary to use a combination of helicopter-like and airplane-like performance modeling during different phases of flight for this type of vehicle. However, the helicopter-like functionality was deemed too complex to be ready in time for our analysis. Hence, we decided to model the tiltrotor using a modified fixed-wing model in the hover phases that would mimic the flight path, fuel-burn and emissions reasonably well.

Similarly, the supersonic transport exceeded the limits of the current modeling methods used. After some testing, however, it became apparent that the analysis would still be valid for supersonic flight with

the exception of the subsonic-supersonic transition. This behavior had to be artificially induced and was limited to the ground-track-only mode (i.e. not with radar trajectory equivalents).

These kinds of problems are to be expected when utilizing a new piece of complex code that is still in development. We would like to thank the FAA and Volpe personnel who worked diligently with us to resolve these issues to a point where we could conclude the research. Without their help and dedication we could never have completed this study.

Appendix C. ACES Notes

This section documents the ACES software configuration for all simulations. We also discuss issues with the flight trajectory simulation, inconsistencies in the airport capacity file, software changes, and anomalies in the output data.

C.1. ACES Configuration

The input settings for the simulations are shown in Figure C-1. The main difference between simulations is the flight data set.

Figure C-1. Auto-Configure Properties (ACP) settings for simulations.

System Settings	
Start/Stop Dates	July 13, 2006 07:00 GMT July 14, 2006 23:00 GMT
Scenario	No scenario files were used except for the bad weather simulations (weather date: 27 July 2007).
Terminal Area Modeling	
Airport Taxi Times	Airport taxi times were derived from ASPM data for 2007.
Airport State	No state files were used except for the bad weather simulations (weather date: 27 July 2007).
Airport Capacity	Input file featured the fully-implemented NextGen airport capacities developed by JPDO.
Airport TFM Parameters	Default inputs were used.
Surface Traffic TFM Parameters	Not used. The focus of the simulations was system-wide and not confined to a specific airport.
Surface Traffic ATC Parameters	Not used. The focus of the simulations was system-wide and not confined to a specific airport.
Arrival Fix Spacing	This feature was not used. Evaluation of the feature indicated little or no benefit in its use while increasing the duration of simulations. Some flights in a data set can trigger assertions failures when this feature is enabled (see page 479).
Surface Traffic Limitations	Not used. The focus of the simulations was system-wide and not confined to a specific airport.
Arrival/Departure Fix Spacing	Enabled. This feature enforces arrival and departure time separation within the terminal area.
En-Route Modeling	
Sector Grid	Default input file was used.
Center Boundary	Default input file was used.
Low Sector	Input file featured the fully-implemented NextGen airspace capacities developed by JPDO.
High Sector	Input file featured the fully-implemented NextGen airspace capacities developed by JPDO.
Super High Sector	Input file featured the fully-implemented NextGen airspace capacities developed by JPDO.
Delay Maneuvers	This feature was not used. Evaluation of the feature indicated little or no benefit in its use while increasing the duration of simulations.

Collision Detection and Resolution	This feature was not used. Evaluation of the feature suggested it does not work properly in the version of ACES used for our simulations.
Advanced Airspace Concepts	Not used.
Flight Modeling	
AOC Operation	Tail-tracking only.
Data Set	The turn-around time was set to 45-minutes for all flights.
Environment	
Wind	Disabled.

C.2. Flight Trajectory Simulation

The 4-D trajectory generator for the en-route environment in ACES is the Multi-Purpose Aircraft Simulation (MPAS). For reasons discussed below, MPAS was not suitable to model the CESTOL, LCTR, and SST aircraft without workarounds.

The slow CESTOL descent rate caused MPAS to reject a large number of flights. The descent modeling method in MPAS is based on typical aircraft profiles that descend at higher rates. We developed a process where we reduced the cruise speed of CESTOL aircraft to reduce the number of rejections by MPAS. Subsequently, the arrival times for these flights were recomputed to account for the new cruise speed. This process reduced the number of rejected CESTOL aircraft in simulations to less than 1-percent of the input flight schedules.

We faced a similar situation while integrating the LCTR aircraft. The LCTR can land and take off vertically. We found that the flight equations in MPAS are not suited to handle aircraft with extremely low lift coefficient ratios during takeoff and landing such as in CTRs. Unsurprisingly, most of the CTRs in the flight schedules ended up being rejected by ACES. Our solution was to use a C-130 aircraft as replacement for the LCTR in the en-route environment. We set the cruise speed and altitude figures for flights in the schedule agreed with the expected LCTR cruise performance (i.e. LCTR in airplane mode).

Finally, we conducted several experiments to integrate the SST aircraft into ACES. The target cruise speed and altitude for the SST was Mach 1.6 and 51,000 feet, respectively. However, we were unable to arrive at a satisfactory aircraft parameters model that would fly the expected profile in ACES. Our workaround was to fly the aircraft in the schedule at subsonic cruise speeds and altitudes. Then, we post-processed the output SST tracks from ACES to conform to the design climb, cruise, and descent profile for this aircraft type.

C.3. Airport Capacities

The ACES simulations conducted for the New Vehicles research (NVNRA) used an airport capacity file developed by the JPDO in the summer of 2008. The file contains arrival, departure, and total capacity rates for a number of airports in both IFR and VFR conditions for the fully implemented NextGen airspace system. Through the course of developing weather scenarios for use in our research, we noted that IFR airport capacities exceeded the VFR rates in several cases (see Figure C-2 for a comparison of total capacity rates only).

Figure C-2. IFR Vs. VFR Total Rates

Airport_ID	VFR_Rate_Total	IFR_Rate_Total	Delta
KATL	229	294	-65
KAUS	160	175	-15
KDTW	213	231	-18
KFLL	126	252	-126
KLAS	104	120	-16
KMKE	153	240	-87
KMSP	188	191	-3
KORD	342	458	-116
KSAN	63	68	-5
KSDF	129	134	-5
KSEA	123	165	-42
KBLV	156	158	-2
KILG	156	158	-2
KOPF	156	158	-2
KYIP	156	158	-2

We analyzed the arrival, departure and total rates for IFR and VFR states for all airports in the airport capacity file. The IFR rate was changed to equal the VFR rate whenever the IFR rates were higher than the VFR rates. We chose to leave the VFR rates unchanged to avoid re-doing previous simulations.

C.4. Software Issues

We found that a large number of domestic flights (i.e. within continental US) were terminated by ACES at the arrival fix whenever the fix for the airport was outside the airport's ARTCC boundary. As a result, flights would "disappear" at the arrival fix position (see figure 1). ACES software developers submitted a fix for this bug (SCR-1257) which will be available in a future software release. We chose to implement the code change in our software version due to its low complexity. Afterwards, we ran small and large simulations and compared the results to prior baselines generated with ACES 5.0. We verified that the software change produced the expected results without introducing new problems.

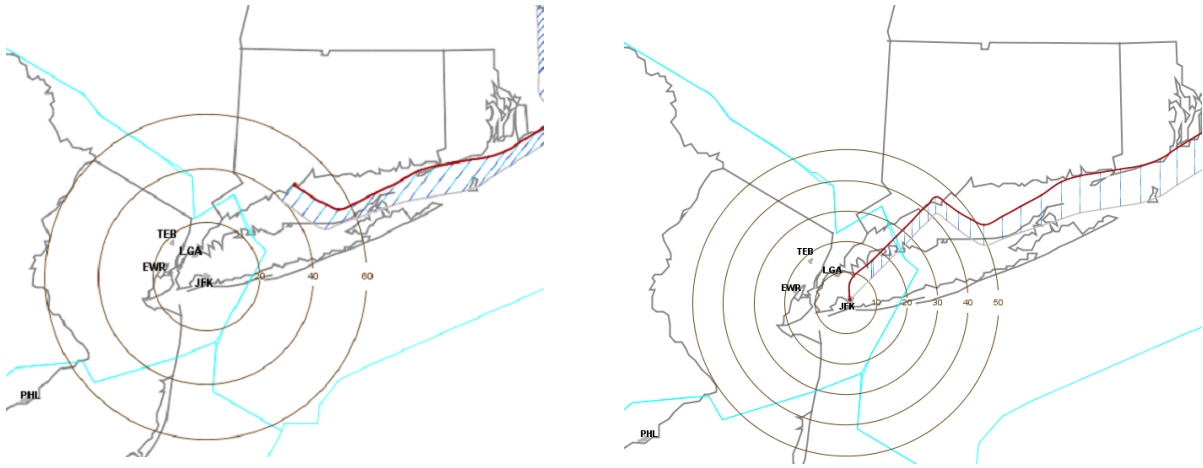


Figure C-3. Flight trajectory for flight between BOS and JFK.

C.5. Output Data Anomalies

Assertion Failure “Crossing out of ARTCC”

This assertion error occurs when a flight crosses into a neighboring ARTCC boundary at a stage where this behavior is not expected. In the figure below, the turn was prompted by bad weather in the simulation.

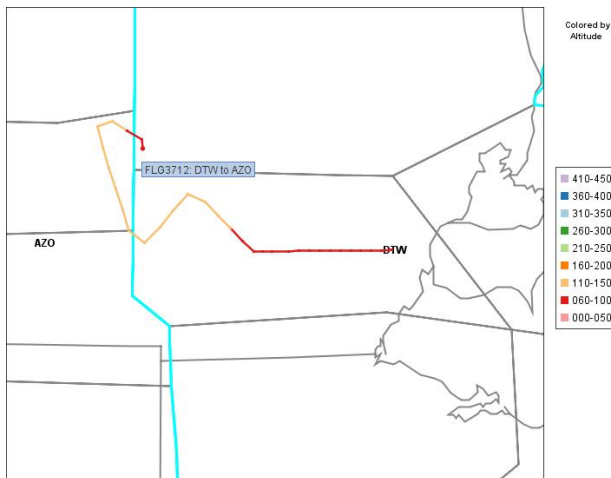


Figure C-4. Flight crossing into neighboring ARTCC

Our workaround is to start ACES without `-ea` option in the `aces.prop` file. It is also possible to eliminate the flight and re-run the simulation.

Aircraft Separation Anomalies Using Runway Model

The runway model (i.e. enhanced terminal) model in ACES provided incorrect separation between successive runway operations. The number of incorrect separation episodes was about 4.3% of all flights for one simulation.cli

Tail-tracking Anomalies

We found that the tail-connectivity feature in ACES did not work properly for some simulations. We identified two modes of failure: 1) tail-connected flights in ACES took off earlier than the specified turn-around time, and 2) flights took off before tail-connected flight landed at the airport. The number of flights affected by this behavior was under 1%.

Overloaded International Sectors

ACES did not constrain the flow of international flights into the US for our largest simulations. As a result, the number of arriving aircraft in sectors bordering the continental US airspace was very high compared to the sector MAP value (Figure C-5). Based on input we received from ACES developers, we tested the same scenario with the simulation switch “Perform Delay Maneuvers” enabled. However, the results from the two simulations were indistinguishable.

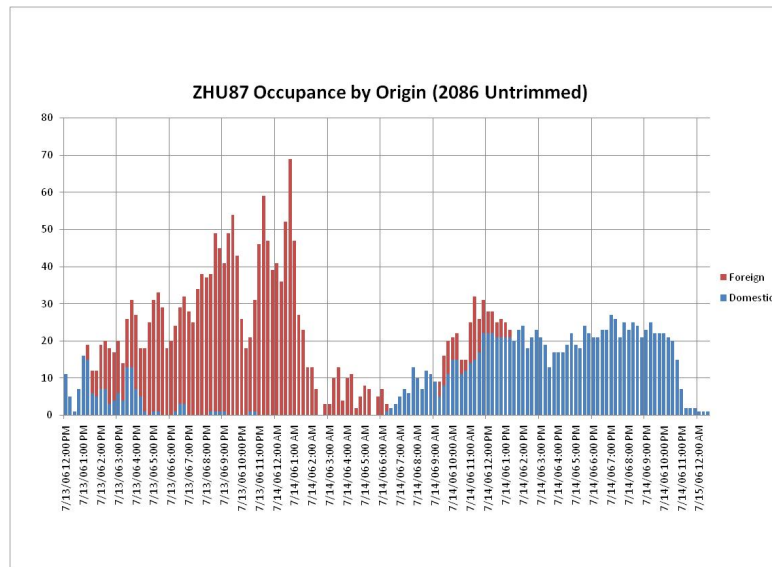


Figure C-5. Aircraft counts for one sector as a function of time.

Differences in FdsStaticDataMessage and FlightTimeDataMessage Tables

ACES outputs simulation statistics in the RunConfiguration.txt file found in the “Batch_Job” directory for every simulation. We routinely found small discrepancies between the counts in the RunConfiguration.txt file and the counts in the output database. See Figure C-6. for an illustration. These flights appear to enter the US airspace but their arrival and departure airports are not inside the US boundary.

Database Table	Flight Counts	RunConfiguration.txt Counts	Difference
fdsStaticDataMessage	98,317	98,317	0
flightTimeDataMessage	97,952	98,317	365

Figure C-6. Flight Counts in Sample Output Tables clii

C.6. References

CDRL 17.3 Airspace Concept Evaluation System (ACES) Software User Manual, 29 September 2006

cli job_312_ldc_20090818_202015_nv2_xxxx_2040_baseline_potomac_100p (reston4)

cli job_403_ldc_20090903_141506_nv2_vlj1_2086_treatment_100p (reston4)

Appendix D. Procedure Analysis Using TARGETS

All the arrival and departure procedures for the project can be implemented as a single route in TARGETS. The concept of a procedure in TARGETS is primarily for combining RNAV leg segments and generating official paper work. Flyability and simulations can be developed on routes as well as procedures so there is no need to apply an extra step of creating procedures. We call them procedures but in TARGETS terminology they are simply routes. For convenience connecting to the runways we also use the route transition tool. The common and en route drawing tools will generate warnings when connecting to a runway. The generic route drawing tool can also be used for these procedure designs. Two important notes: 1. always draw routes in the direction of travel. If you don't, the route cannot be "reversed" so it must be deleted and re-drawn. Always set the arrival or departure mode before drawing. This can be corrected in the route properties dialog.

D.1. Spiral Arrival

The spiral approach in this initial investigation is designed for two complete traversals of the spiral circumference. We investigated two forms of a spiral procedure creation process in TARGETS. One involves using straight segments, defaulting to track-to-fix (TF) legs, and the other involves using the radius-to-a-fix (RF) legs which are fixed radius turns. The straight leg segment approach was tested first knowing that it would be the easiest to implement. There are known limitations of RF leg creation in TARGETS and improvements are currently being investigated. The RF leg based procedure is the preferred implementation. Feedback from this analysis will assist in defining the needed improvements.

TF Leg Spiral Arrival

The straight segment TF leg or pseudo-spiral contains waypoints at four corners of the 1.5 nm radius around the waypoint that is centered on the spiral location. In this design the aircraft enters the spiral at 10,000 feet at 180 kts. The spiral exit is at the entry point of the 5 nm final approach at 1000 feet at 110 kts. Details of the route design and speed and altitude restrictions are shown in Figure 2-3. The spiral procedure can be moved to accommodate other scenarios and the results will be the same. The route drawing process is relatively simple and involves using the TARGETS measurement tools to place the waypoints and then "connecting the dots" using the route drawing tool and the snap-to feature of TARGETS. A range box with a radius of 0.3 nm. was added to the route to provide a visual reference for the 0.3 RNP value of the procedure. There are multiple waypoints at each corner as the flight path traverses the spiral radius two full times on the descent.

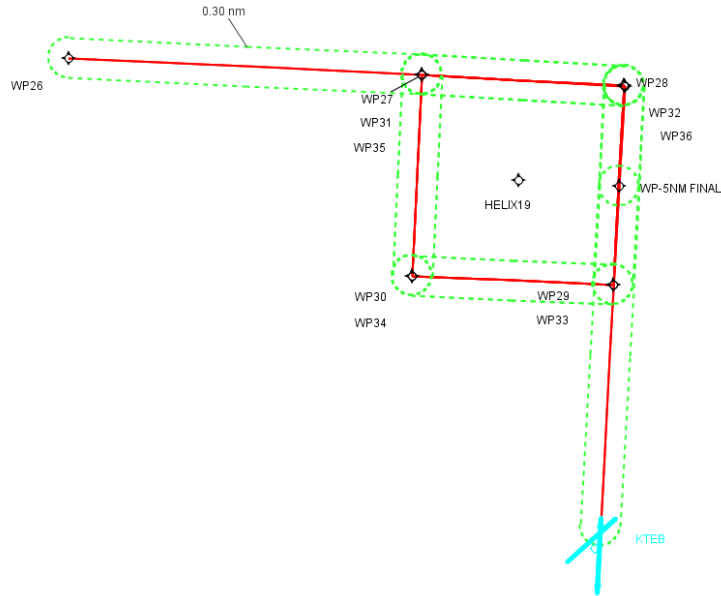


Figure D-1. Overview of the straight segment TF leg spiral arrival.

Flyability on the TF leg spiral arrival was successful with the performance values described in the aircraft performance sections below. However, the flyability track was irregular (shown in blue below). The inner most tracks occur first. As the aircraft slows and descends, TARGETS appears to be able to better follow the defined tracks.

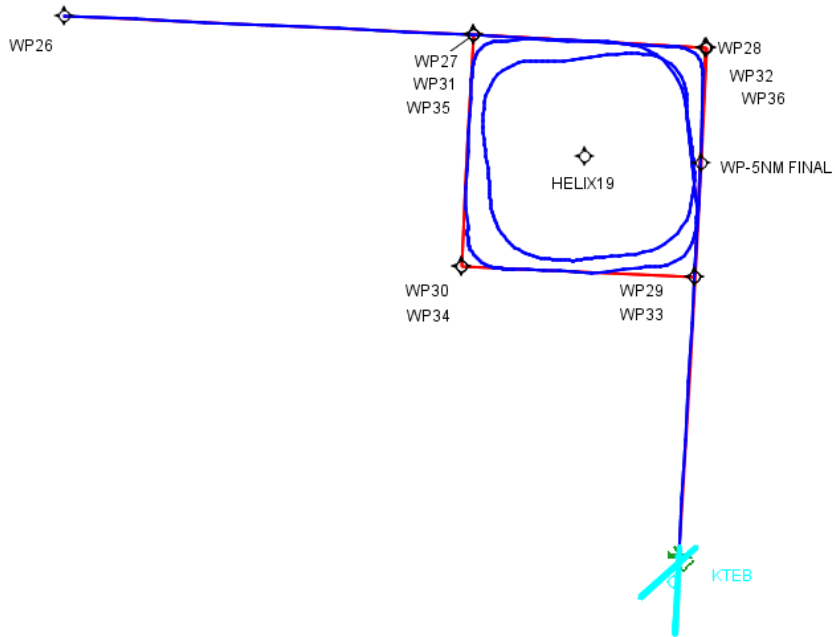


Figure D-2. Depicts flyability on the straight segment TF leg spiral arrival.

Inner lines are flown first on the descent.

Details of the TF leg spiral arrival route segments are shown below.

Leg #	Leg Type	Waypoint	Turn Type	Alt Restr 1	Alt Restr 2	Spd Restr	MEA	Dist (nm)	Hdg/Crs Magnetic	Hdg/Crs True	Turn Dir	Rec Nava
1	IF	WP26		12000		190		0.00				
2	TF	WP27	FLY_BY	10000		180	Not Initialized	5.34	104.63	092.63	CLOSEST	
3	TF	WP28	FLY_BY	9500		170	Not Initialized	3.05	105.11	093.11	CLOSEST	
4	TF	WP29	FLY_BY	9000		175	Not Initialized	3.00	195.10	183.10	CLOSEST	
5	TF	WP30	FLY_BY	8000		165	Not Initialized	3.04	284.58	272.58	CLOSEST	
6	TF	WP31	FLY_BY	7000		155	Not Initialized	3.03	014.84	002.84	CLOSEST	
7	TF	WP32	FLY_BY	6000		145	Not Initialized	3.05	105.11	093.11	CLOSEST	
8	TF	WP33	FLY_BY	5000		135	Not Initialized	3.00	194.97	182.97	CLOSEST	
9	TF	WP34	FLY_BY	4000		125	Not Initialized	3.04	284.58	272.58	CLOSEST	
10	TF	WP35	FLY_BY	3000		115	Not Initialized	3.03	014.84	002.84	CLOSEST	
11	TF	WP36	FLY_BY	2000		110	Not Initialized	3.06	105.15	093.15	CLOSEST	
12	TF	WP-SNM FIN/	FLY_BY	1000		110	Not Initialized	1.51	194.96	182.96	CLOSEST	
13	TF	KTEB:RW19:1	FLY_BY	50		100	Not Initialized	5.13	195.19	183.19		

Figure D-3. Details of the TF leg spiral arrival with speed and altitude restrictions.

By default TARGETS will descend and decelerate as quickly as possible on arrival, which is not typical aircraft behavior. When only initial and ending speeds and altitudes are supplied, TARGETS descended and decelerated to the end values about half way through the spiral descent. To provide a more continuous descent, speed and altitude restrictions are specified at each leg segment. TARGETS does have a mode called “expedite arrivals” that will postpone descent and deceleration until necessary to make a particular restriction but it works best in simulation mode while sometimes causing invalid failures in flyability analysis.

Segment #	Fix	Leg	Type	Alt	Spd	Turn	Segment Length	Flyability Length	Time to Fly	Extra Dist needed for dAlt	Extra Dist needed for dSpd	End Course	ΔHdg	End Alt	ΔAlt	Gradient (ft/nm)	End Speed	ΔSpd	
1	WP26	IF	INITIAL	P	P	P	--	--	--	--	--	104.63	--	12000	--	--	190.0	--	N
2	WP27	TF	STRAIGHT	P	P	P	5.35	5.35	H 00 M 01 S 30.00	--	--	104.63	0.0	10000	-2000	-373.49	180.0	-10	N
3	WP28	TF	STRAIGHT	P	P	P	1.63	2.63	H 00 M 00 S 29.00	--	--	105.11	0.48	9500	-500	-189.8	170.0	-10	N
4			FLY BY	P	P	P	1.75	--	H 00 M 00 S 37.00	--	--	195.1	89.99	9500	0	--	170.0	0	N
5	WP29	TF	STRAIGHT	P	P	P	0.44	1.37	H 00 M 00 S 08.00	--	--	195.1	0.0	9057	-443	-323.11	175.0	5	N
6			FLY BY	P	P	P	1.63	--	H 00 M 00 S 34.00	--	--	284.58	89.48	9000	-57	--	175.0	0	N
7	WP30	TF	STRAIGHT	P	P	P	0.39	1.08	H 00 M 00 S 07.00	--	--	284.58	0.0	8690	-310	-287.52	173.6	-1	N
8			FLY BY	P	P	P	1.59	--	H 00 M 00 S 35.00	--	--	14.84	90.26	8000	-690	--	165.0	-9	N
9	WP31	TF	STRAIGHT	P	P	P	0.61	1.09	H 00 M 00 S 12.00	--	--	14.84	0.0	7509	-491	-449.41	162.6	-2	N
10			FLY BY	P	P	P	1.27	--	H 00 M 00 S 31.00	--	--	105.11	90.28	7000	-509	--	155.0	-8	N
11	WP32	TF	STRAIGHT	P	P	P	0.94	1.29	H 00 M 00 S 20.00	--	--	105.11	0.0	6249	-751	-584.58	151.0	-4	N
12			FLY BY	P	P	P	1.16	--	H 00 M 00 S 31.00	--	--	194.97	89.85	6000	-249	--	145.0	-6	N
13	WP33	TF	STRAIGHT	P	P	P	1.24	1.24	H 00 M 00 S 29.00	--	--	194.97	0.0	5005	-995	-800.76	139.2	-6	N
14			FLY BY	P	P	P	1.03	--	H 00 M 00 S 30.00	--	--	284.58	89.61	5000	-5	--	135.0	-4	N
15	WP34	TF	STRAIGHT	P	P	P	1.66	1.66	H 00 M 00 S 43.00	--	--	284.58	0.0	4000	-1000	-603.94	125.0	-10	N
16			FLY BY	P	P	P	0.81	--	H 00 M 00 S 26.00	--	--	14.84	90.26	4000	0	--	125.0	0	N
17	WP35	TF	STRAIGHT	P	P	P	1.91	1.91	H 00 M 00 S 55.00	--	--	14.84	0.0	3000	-1000	-522.94	115.0	-10	N
18			FLY BY	P	P	P	0.68	--	H 00 M 00 S 24.00	--	--	105.15	90.31	3000	0	--	115.0	0	N
19	WP36	TF	STRAIGHT	P	P	P	2.1	2.1	H 00 M 01 S 06.00	--	--	105.15	0.0	2000	-1000	-475.9	110.0	-5	N
20			FLY BY	P	P	P	0.6	--	H 00 M 00 S 22.00	--	--	194.96	89.81	2000	0	--	110.0	0	N
21	WP-36M ...	TF	STRAIGHT	P	P	P	1.18	1.18	H 00 M 00 S 38.00	--	--	194.96	0.0	1000	-1000	-844.99	110.0	0	N
22	KTEB/RW...	TF	STRAIGHT	P	P	P	5.11	5.11	H 00 M 03 S 01.00	--	--	195.19	0.24	50	-950	-185.96	100.0	-10	N

Figure D-4. Details of the flyability run on the TF leg spiral approach.

The FAA criteria checking that runs automatically during flyability fails on leg length calculation but this is to be expected with such an experimental procedure. FAA criteria check failures will be ignored for this project. The 90 degree turns at 180 kts would require a minimum of 5 nm. leg length to pass current FAA criteria defined for leg lengths in the 8260.54A criteria and the Feb 19, 2009 Memorandum for Performance Based Navigation Instrument Procedure Minimum Segment Length Standard.

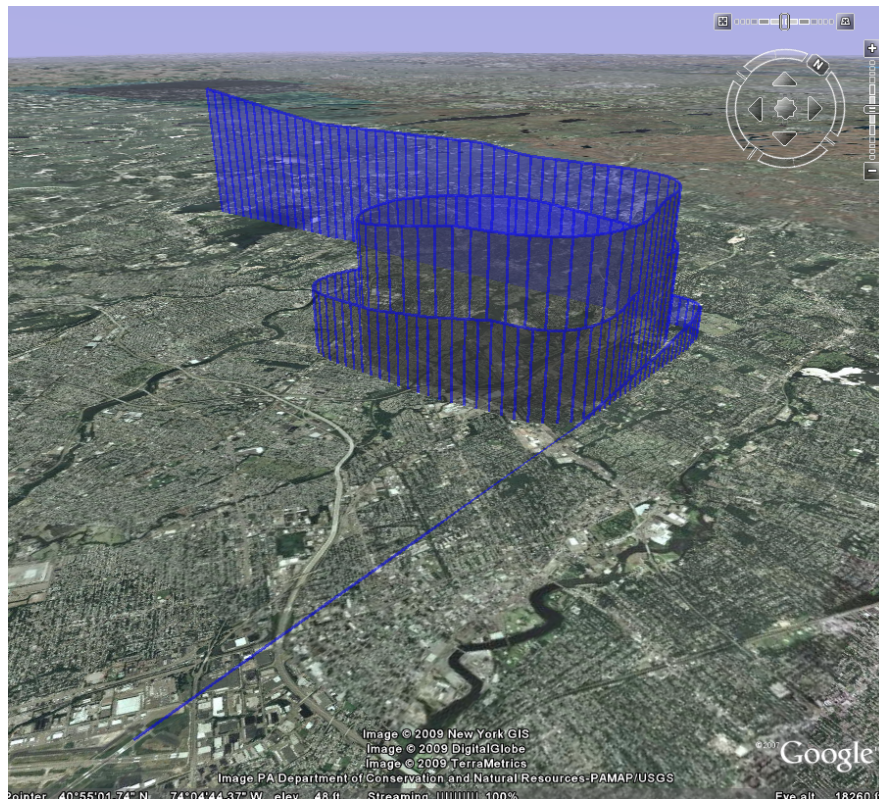


Figure D-5. The TF leg spiral approach flyability in Google Earth.

RF Leg Spiral Arrival

RF legs in TARGETS can be implemented using the SAAAR (Special Aircraft Aircrew Authorization Required) approach prototype tool or by drawing a route and converting existing TF legs to RF legs in the route properties dialog. Ideally, the spiral could be specified using one or two RF legs per complete rotation of the spiral. After some experimentation we were able to establish a consistent method of generating multiple RF legs in a route. But the near 360 degree RF leg was not well behaved. We found that using four 180 degree RF legs was a viable technique. This procedure does not have a 90 degree angle between the entry and exit legs but it could be recreated for such a requirement.

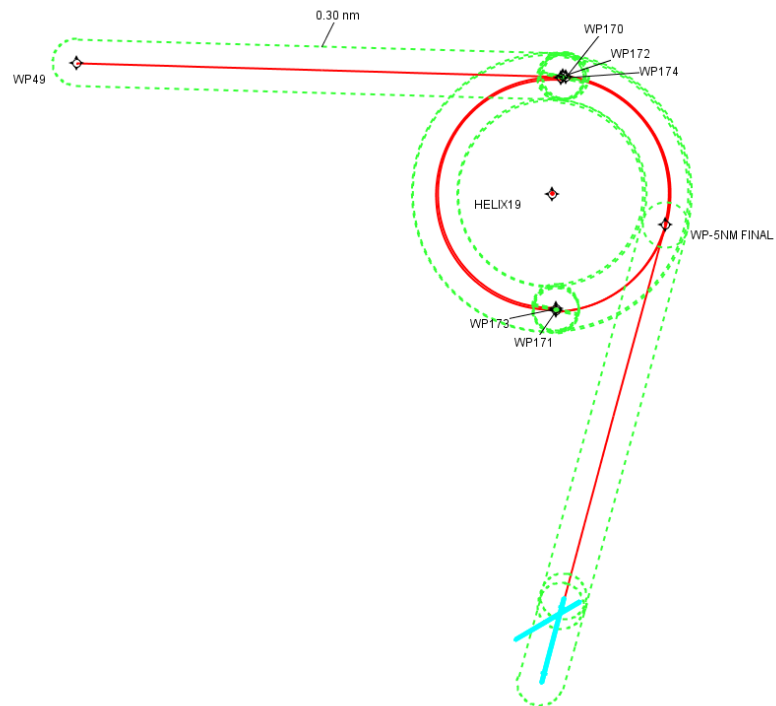


Figure D-6. Spiral approach implemented using TARGETS Route tool and substituting RF legs.



Figure D-7. Spiral approach using RF legs viewed in Google Earth.

The SAAAR approach prototype tool was also used to implement the spiral approach using 3 RF legs. See Figure D-8. This tool draws the approaches backwards. We used two RF legs that are almost 360 degrees each from the exit point and one initial RF to enter the first quarter turn of the spiral. It would also be possible to generate the approach with a series of 180 degree RF legs as in the previous route based technique. One drawback using the SAAAR tool was that there are short TF legs between the RF legs. The TF legs also contain incorrect turn directions which could not be changed. This limitation may be able to be resolved with more investigation into the tool. The primary limitation is that the altitudes are pre-calculated based on FAA TERPS criteria and there does not appear to be a way to specify the altitudes during the descent.

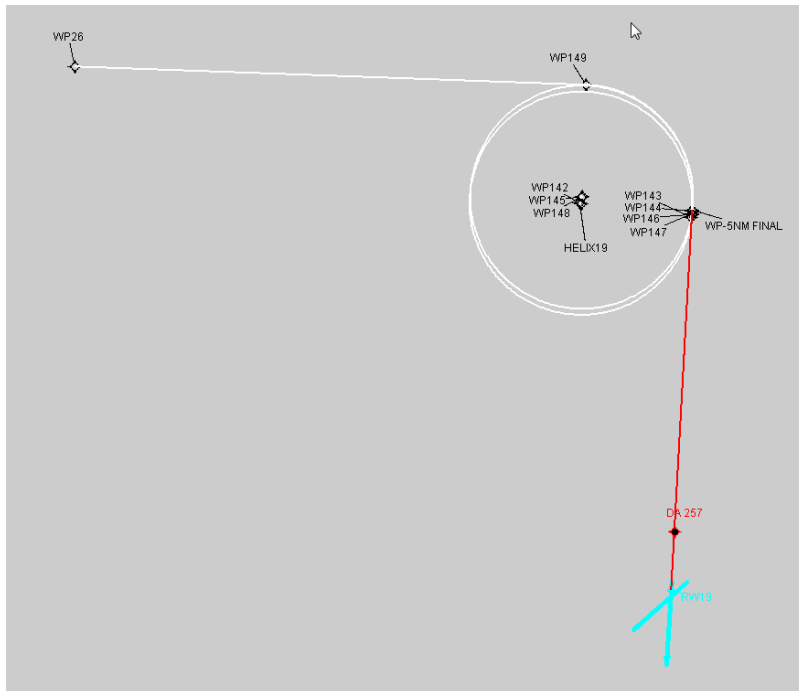


Figure D-8. Spiral approach implemented using the TARGETS SAAAR Prototype tool.

Flyability on the RF leg is not viable in its current state in TARGETS. The example below used the RF route example described above.

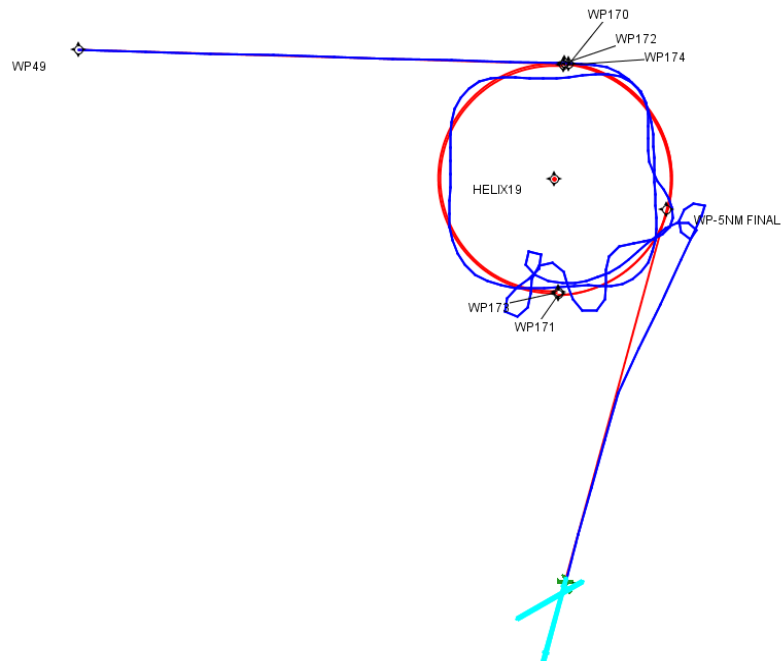


Figure D-9. Flyability of five sequential RF legs.

D.2. Spiral Departure

A pseudo spiral departure was created using the four corner posts of the spiral as flyby waypoints. Flyability using the experimental aircraft was successful. Speed and altitude restrictions were required to create a gradual ascent. A climb gradient of 1000 ft/nm was applied. An energy share factor of 90/10 climb/acceleration was required. Based on the length of the route to 10000 feet a climb gradient of approximately 357 feet should be sufficient. This is similar to what was seen on the arrival.

A spiral departure consisting of RF legs was also constructed but was not flyable similar to the RF leg spiral approach.

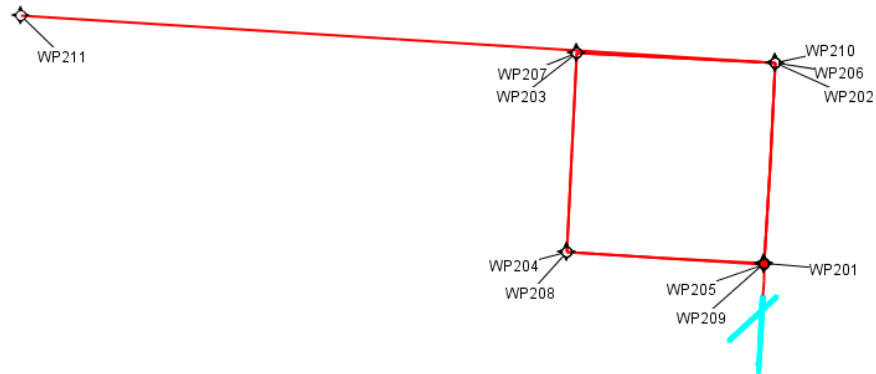


Figure D-10. The pseudo spiral departure constructed with TF legs.

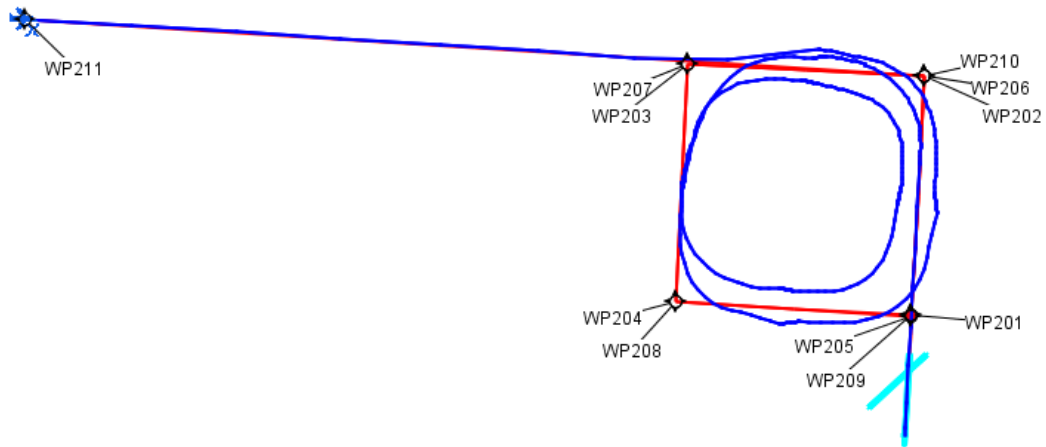


Figure D-11. Flyability on the pseudo spiral using the CESTOL aircraft.

Route Properties : RW01

Route Name: RW01 Route/Transition Type: SID Runway Transition

Airport: KTEB (Magnetic Variation: W12.00) Runway: RW01

Route Magnetic Variation: W 12.00

Properties Display Properties

Leg #	Leg Type	Waypoint	Turn Type	Alt Restr 1	Alt Restr 2	Spd Restr	MEA	Dist (nm)	Hdg/Crs Magnetic	Hdg/Crs True	Turn Dir
1	VA			+520			Not Initialized	0.48	015.19	003.19	CLOSEST
2	DF	WP202	FLY_BY	2000			Not Initialized	3.02	015.19	003.19	CLOSEST
3	TF	WP203	FLY_BY	3000			Not Initialized	3.00	285.00	273.00	CLOSEST
4	TF	WP204	FLY_BY	4000			Not Initialized	3.00	195.00	183.00	CLOSEST
5	TF	WP205	FLY_BY	5000		180	Not Initialized	2.99	105.30	093.30	CLOSEST
6	TF	WP206	FLY_BY	6000			Not Initialized	3.02	015.19	003.19	CLOSEST
7	TF	WP207	FLY_BY	7000			Not Initialized	3.00	285.00	273.00	CLOSEST
8	TF	WP208	FLY_BY	8000			Not Initialized	3.00	195.00	183.00	CLOSEST
9	TF	WP209	FLY_BY	9000			Not Initialized	2.99	104.95	092.95	CLOSEST
10	TF	WP210	FLY_BY	10000		200	Not Initialized	3.00	015.19	003.19	CLOSEST
11	TF	WP211	FLY_BY				Not Initialized	11.42	285.69	273.69	

Buttons: Append Leg, Insert Leg, Remove Leg, Create Transitions, Check Flyability, Export to Spreadsheet File

Buttons: Help, Ok, Apply, Cancel

Figure D-12. Altitude and speed restrictions on the pseudo spiral departure.

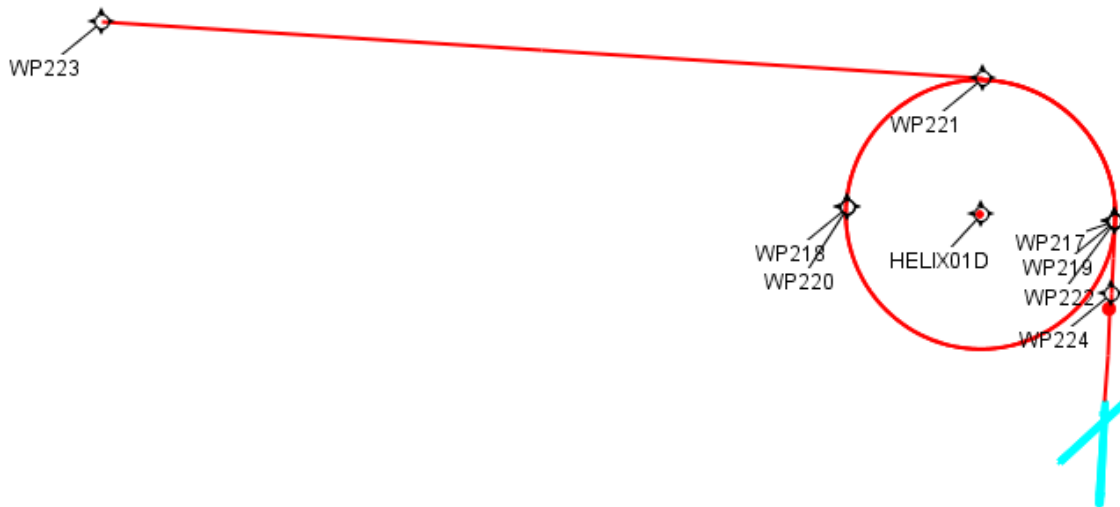


Figure D-13. The spiral departure constructed with RF legs.



Figure D-14. The RF leg spiral departure in Google Earth.

D.3. Applying Wind in TARGETS

Use the menu Project Data/New Wind command to create new winds. In the first dialog specify the wind name and direction and speed at the desired altitudes. Select Compute to observe the wind applied at each altitude and select Ok to save the new wind values.

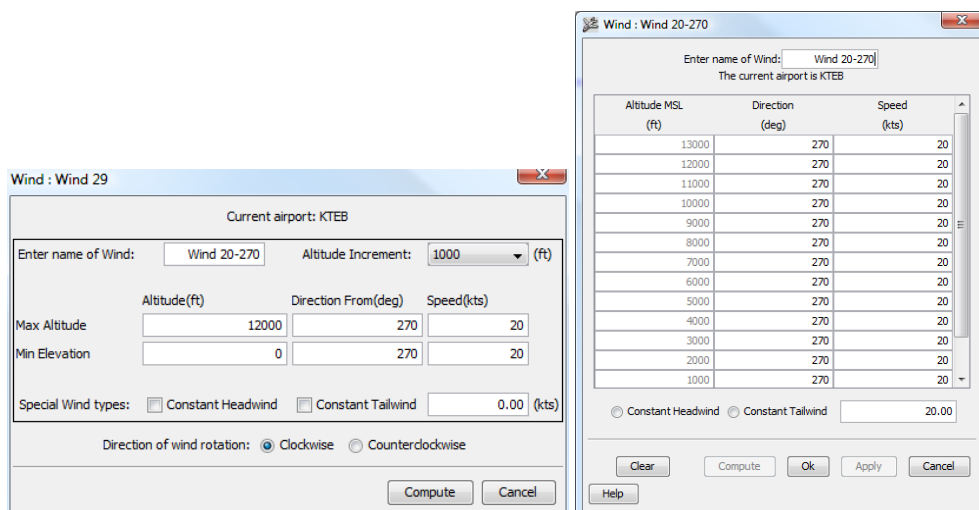


Figure D-15. Wind definition dialogs.

Open the properties of a flyability parameter set and select the newly defined wind. Then run the flyability on the route using the specified flyability parameter set.

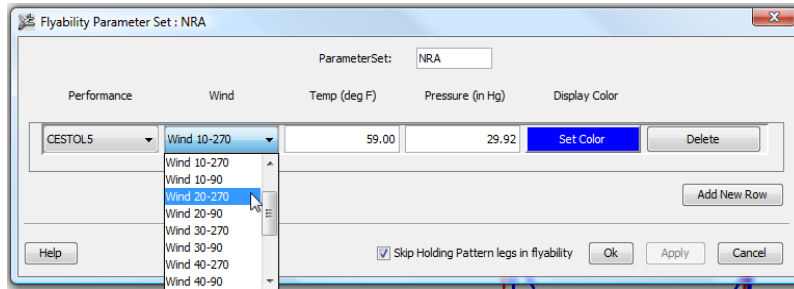


Figure D-16. Setting wind in the flyability parameter set properties dialog.

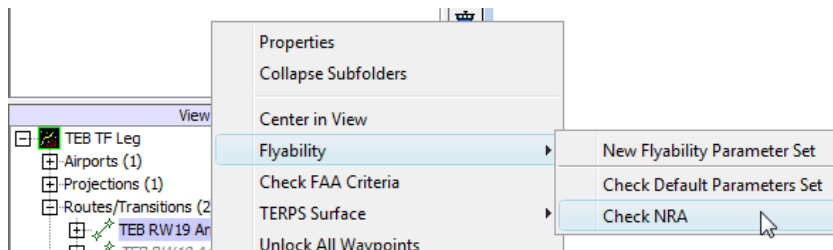


Figure D-17. Command to run the flyability on a user defined flyability parameter set.

Initial winds were defined for 90 and 270 directions to verify the definition of the wind and the impact it has on the flyability. A wind heading of 270 at 20 kts produced the results show in Figure 4-4. The aircraft is pushed to the west as expected. The opposite occurred for a wind heading of 90.

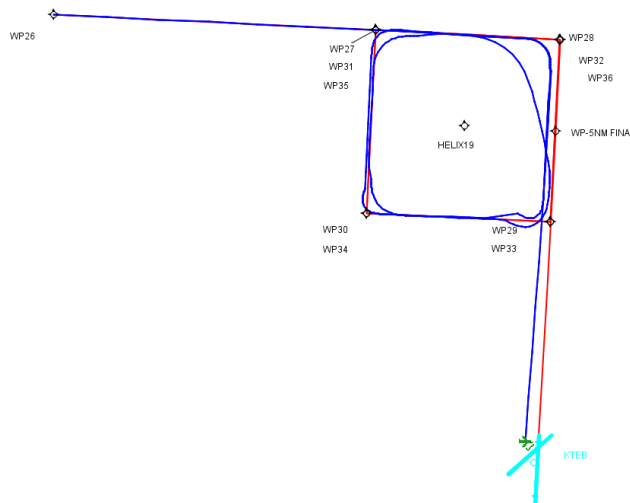


Figure D-18. A wind heading of 270 at 20 kts pushes the aircraft to the west as expected.

The deviation is most notable on the final approach.

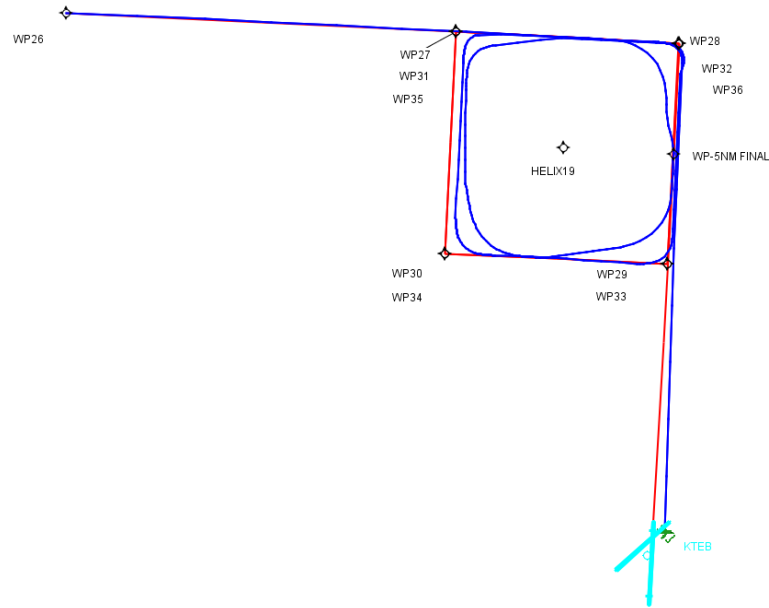


Figure D-19. A wind heading of 90 at 20 kts pushes the aircraft to the east as expected.

The deviation is most notable on the final approach.

Wind was applied to flyability on the pseudo spiral arrival since that route can be flown in TARGETS. Winds of 270 and 90 in increments of 10 kts from 10 to 70 were flown separately. This first route flown has speed restrictions at each waypoint which more accurately reproduces a continuous descent. A wind of 10- to 60 kts from 270 generated a failure, “Failed speed constraint”. A wind from 270 at 70 kts generated a failure, “Unable to join outbound leg after completion of flyby turn”. For a wind of just 10 kts from 90 a failure occurred due to speed restrictions. This appears to be an unexplainable inconsistency.

Since 90 wind failures were speed constraints, the same winds were flown on the pseudo spiral route that only had initial and ending restrictions. The failure to join the outbound leg occurred at 40 kts. The 30 kts flyability passes but its depiction in TARGETS raises questions as to whether it really should be passing since the aircraft is far from the runway. This occurs because TARGETS has a tolerance of 1 nm and in Figure 4-6 the aircraft position is .75 nm perpendicular to the runway end. The 1 nm tolerance may be acceptable on an RNAV procedure but may not be for an RNP approach or for actually landing on the runway. This tolerance level is currently not a user-adjustable value in TARGETS, but a preference is generally easy to add. If the tolerance was set to .3 nm (.3 RNP) then the 30 kts flyability would be a failure. The 20 kts wind would pass since its runway position is less than .3 nm. See the following figures.

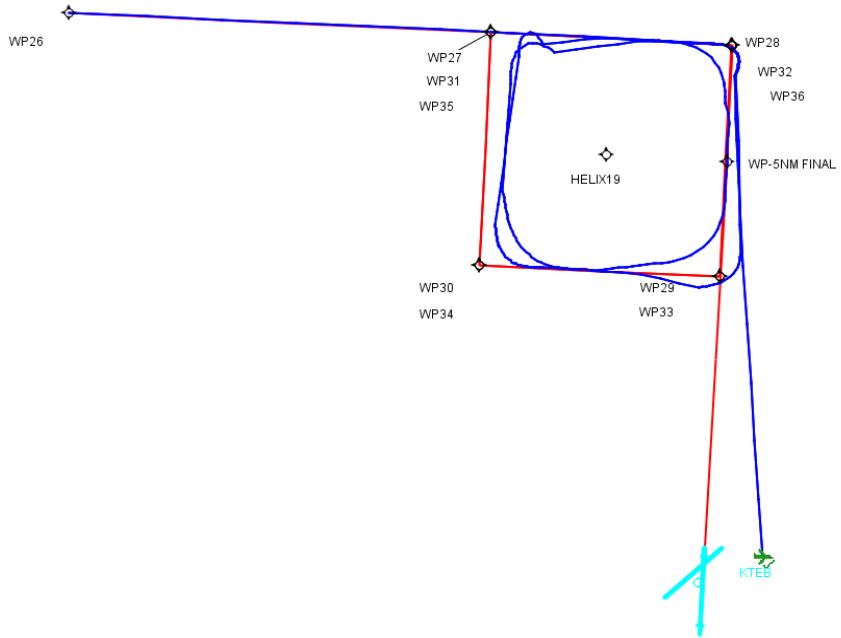


Figure D-20. Wind from 90 at 40 kts fails.

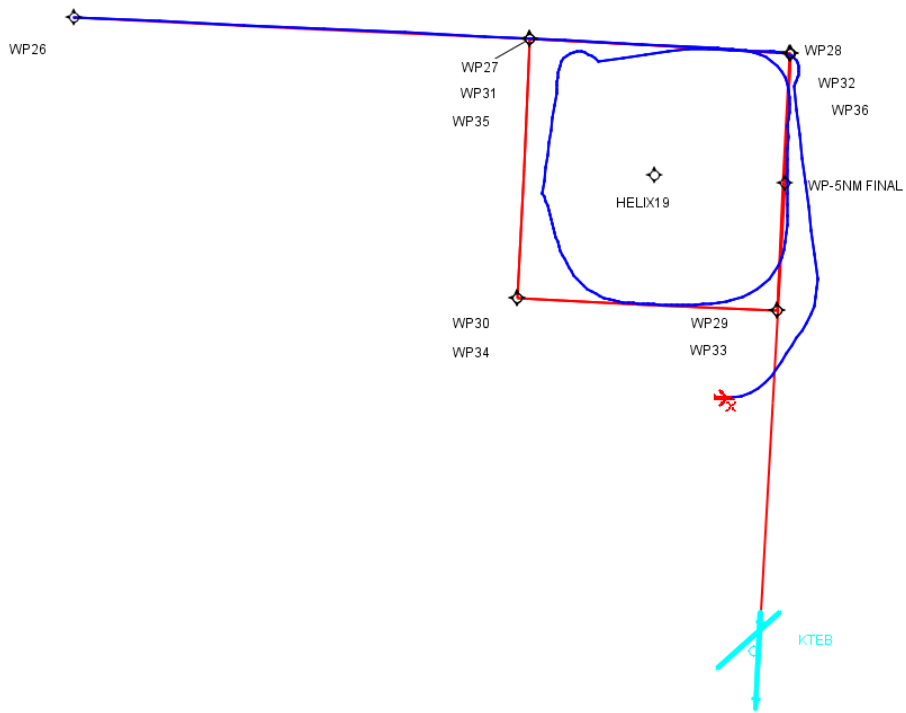


Figure D-21. Wind from 90 at 30 kts passes.

When the 270 wind was applied flyability passed at 50 kts and below and failed at 60 kts and the failure was “Unable to join outbound leg”. When the 90 wind was applied flyability passed at 40 kts and below and failed at 50 kts with the same outbound leg failure.

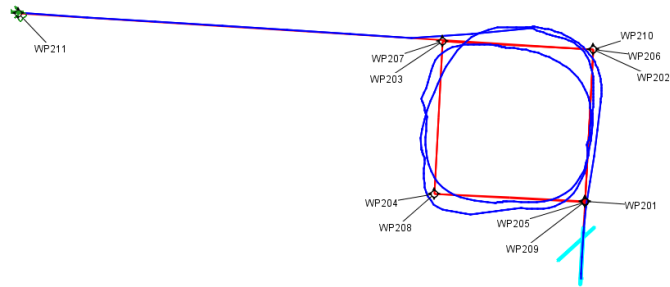


Figure D-22. Wind on spiral departure from 90 at 40 kts passes.

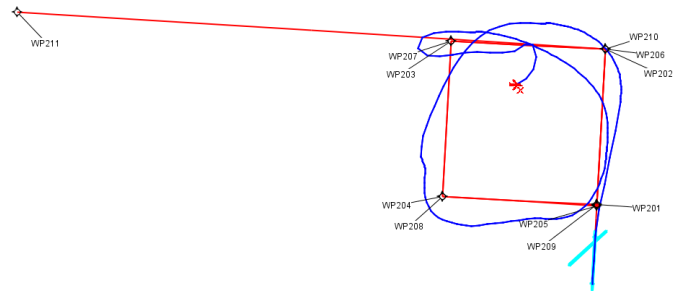


Figure D-23. Wind on spiral departure from 90 at 50 kts fails.

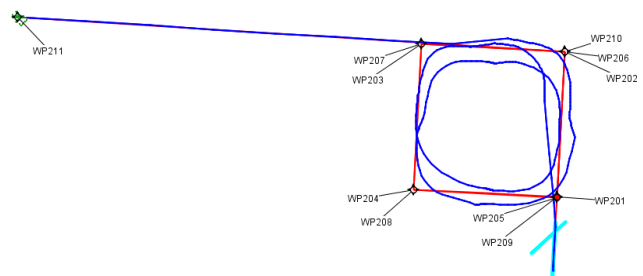


Figure D-24. Wind on spiral departure from 270 at 50 kts passes.

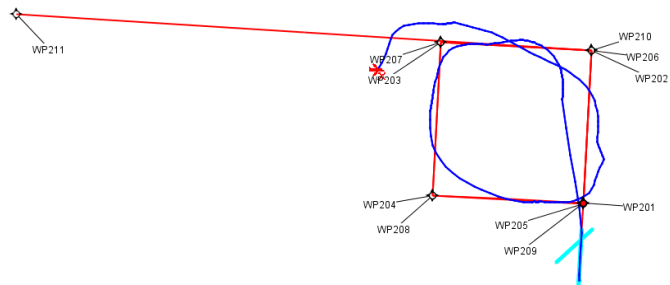


Figure D-25. Wind on spiral departure from 270 at 60 kts fails.

D.4. TARGETS Aircraft Performance

CESTOL Aircraft Performance

A CESTOL configuration was generated using the data provided by Georgia Tech. The 1000 feet/nm descent gradient was required to pass flyability.

CESTOL	Value used	Comments
Engine	Large Jet	
Maximum takeoff weight	97,500 lbs	for 2000 nmi range
Maximum landing weight	83,300 lbs	for the 2000 nmi mission, not the maximum structural landing weight
Cruise altitude	35,000 ft	
Cruise speed	264 kts	M0.78, 449 KTAS, 264 KIAS/KCAS
Takeoff speed	117 kts	
Landing speed	95 kts	10 + 1.3*stall speed 64.7 kts
Takeoff acceleration	280 kts/min	the average acceleration up to 35 feet obstacle – 280 kts/min
Roll rates	3 degrees	average acceleration up to 10000 ft – 23.2 kts/min
Climb gradient	1000 ft/nmi	no value provided
Energy Share Factor (ESF)	90/10	between liftoff and 35 feet obstacle - 239 ft/nmi
Descent gradient	1000 ft/nmi	between 35 feet obstacle and 10,000ft - 780 ft/nmi (more than required)
Bank angle	25 degrees	no values provided
Average deceleration	50 kts/min	between 35,000ft and 10,000ft – 200 ft/nmi
		below 10,000 ft – 3,000 ft – 505 ft/nmi; below 3,000ft – 585ft/nmi

Figure D-26. CESTOL Performance in TARGETS.

VLJ Performance

A VLJ configuration was generated with the data provided by Georgia Tech. The spiral approach flyability passed once the 1000 feet/nm descent gradient was applied.

VLJ	Value used	Comments
Engine	Turbofan	
Maximum takeoff weight	5,750 lbs	for 750 nmi range
Maximum landing weight	5,500 lbs	for the 750 nmi mission, not the maximum structural landing weight
Cruise altitude	35,000 ft	
Cruise speed	346 kts	M0.6, 346 KTAS, 200 KIAS/KCAS;
Takeoff speed	85.9 kts	
Landing speed	92.6 kts	10 + 1.3*stall speed 63.5 kts
Takeoff acceleration	202.4 kts/min	the average acceleration up to 35 feet obstacle – 202.4 kts/min average acceleration up to 10000 ft – 13.7 kts/min
Roll rates	3 degrees	no value provided
Climb gradient	1000 ft/nmi	between liftoff and 35 feet obstacle – 442.3 ft/nmi
Energy Share Factor (ESF)	90/10	between 35 feet obstacle and 10,000ft – 823.1 ft/nmi; no values provided
Descent gradient	1000 ft/nmi	between 35,000ft and 12,000ft – 379.9 ft/nmi
Bank angle	25 degrees	below 12,000 ft – 4,700 ft – 507.1 ft/nmi; below 4,700ft – 586.0 ft/nmi;
Average deceleration	50 kts/min	

The screenshot shows the 'Aircraft Performance : VLJ' window. The 'Performance Name' is 'VLJ'. Under 'Attributes', 'S' is selected. 'Weight Class' is 'L', 'Engine Type' is 'Jet/Turboprop', and 'Equipment' is 'NON-RNAV'. Performance parameters are set as follows: Cruise Altitude (35000.00), Max Takeoff Weight (5.75), Takeoff Speed (85.90), Takeoff Acceleration (202.40), Cruise Speed (200.00), Max Landing Weight (5.50), Landing Speed (92.60), and Roll Rate (3.00). Under 'Values by Altitude', 'Gradient' is selected with an 'Altitude Increment' of 10000. Temperature is 59.00 and Pressure is 29.92. The 'Values at Standard Temp and Pressure' table is shown below.

Max Alt MSL (ft)	Climb Grad (ft/nm)	ESF (Climb/Accel)	Accel Rate (kts/min)	Descent Grad (ft/nm)	ESF (Descent/Decel)	D R (kts)
0.00	1000.00	90/10	202.40	1000.00	90/10	
10000.00	1000.00	90/10	13.70	1000.00	90/10	

Under 'Values by Speed', 'Bank Angle' is selected with a 'Speed Increment' of 500. The table shows Bank Angle values of 0.00 and 25.00 degrees at 0.00 and 500.00 kts respectively.

Buttons at the bottom include Help, Ok, Apply, Copy, Export, Reset, and Cancel. A note at the bottom states: 'NOTE : All speeds are indicated airspeeds.'

Figure D-27. VLJ Performance in TARGETS.

UAS Performance

A UAS configuration was generated with the data provided by Georgia Tech. The spiral approach flyability passed once the 1000 feet/nm descent gradient was applied.

UAS	Value used	Comments
Engine	Turboprop	
Maximum takeoff weight	8,785 lbs	for 400 nmi range
Maximum landing weight	8,500 lbs	for the 400 nmi mission, not the maximum structural landing weight)
Cruise altitude	15,000 ft	
Cruise speed	141 kts	M0.283, 177 KTAS, 141 KIAS/KCAS
Takeoff speed	81.7 kts	
Landing speed	88.4 kts	10 + 1.3*stall speed 60.3 kts
Takeoff acceleration	211.6 kts/min	the average acceleration up to 50 feet obstacle – 211.6 kts/min
Roll rates	3 degrees	average acceleration up to 10000 ft – 13.6 kts/min; no value provided
Climb gradient	1000 ft/nmi	between liftoff and 50 feet obstacle – 414.5 ft/nmi
Energy Share Factor (ESF)	90/10	between 50 feet obstacle and 10,000ft – 399.7 ft/nmi; no values provided
Descent gradient	1000 ft/nmi	between 15,000ft and 10,000ft – 301.7 ft/nmi
Bank angle	25 degrees	below 10,000 ft – 3,000 ft – 329.4 ft/nmi; below 3,000ft – 318.4ft/nmi;
Average deceleration	50 kts/min	

The screenshot shows the 'Aircraft Performance : UAS' dialog box. The 'Performance Name' is 'UAS'. Under 'Attributes', 'S' and 'RNAV' are selected. 'Weight Class' is 'L', 'Engine Type' is 'Jet/Turboprop', and 'Equipage' is 'NON-RNAV'. The 'H' and 'Jet' options are also visible. Performance values are: Cruise Altitude (15000.00), Max Takeoff Weight (8.79), Takeoff Speed (81.70), Takeoff Acceleration (211.60), Cruise Speed (141.00), Max Landing Weight (8.50), Landing Speed (88.40), and Roll Rate (3.00). The 'Values by Altitude' section has 'Gradient' selected with an altitude increment of 10000. Temperature is 59.00 and pressure is 29.92. The 'Values at Standard Temp and Pressure' table is shown below.

Max Alt MSL (ft)	Climb Grad (ft/nm)	ESF (Climb/Accel)	Accel Rate (kts/min)	Descent Grad (ft/nm)	ESF (Descent/Decel)	D R (kts)
0.00	1000.00	90/10	211.60	1000.00	80/20	
10000.00	1000.00	90/10	13.60	1000.00	80/20	

The 'Values by Speed' section has 'Bank Angle' selected with a speed increment of 500. The table shows Bank Angle values of 25.00 degrees for speeds of 0.00 and 500.00 kts.

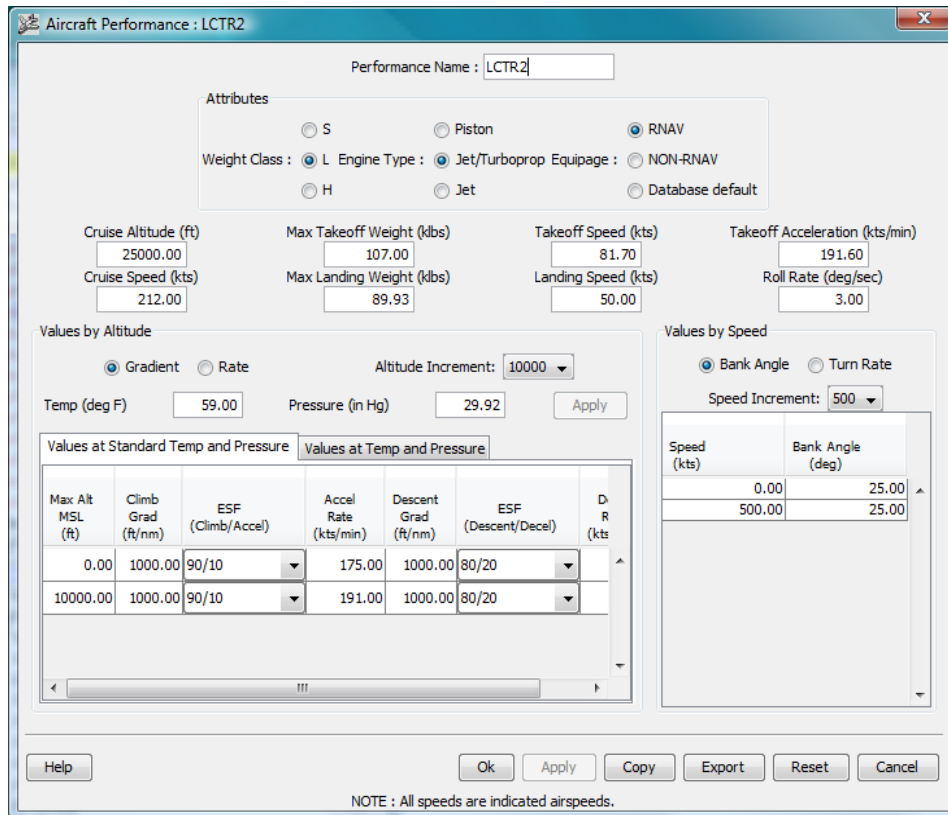
Buttons at the bottom include Help, Ok, Apply, Copy, Export, Reset, and Cancel. A note at the bottom states: 'NOTE : All speeds are indicated airspeeds.'

Figure D-28. UAS Performance in TARGETS.

Tiltrotor (LCTR2) Performance

A tilt rotor configuration was generated with the data provided by Georgia Tech. The spiral approach flyability passed once the 1000 feet/nm descent gradient was applied.

Tilt Rotor	Value used	Comments
Engine	Turboshaft	4 engines
Maximum takeoff weight	107,104 lbs	for 1200 nmi range
Maximum landing weight	89,934 lbs	for the 1200 nmi mission, not the maximum structural landing weight
Cruise altitude	25,000 ft	
Cruise speed	212 kts	M0.51, 310 KTAS, 212 KIAS/KCAS
Takeoff speed	81.7 kts	75-deg nacelle tilt with 55% power setting);
Landing speed	50 kts	75-deg nacelle tilt
Takeoff acceleration	191.6 kts/min	the average acceleration up to 35 feet obstacle – 175.1 kts/min (75-deg nacelle tilt with 55% power setting) average acceleration up to 6,000 ft – 191.6 kts/min (nacelle conversion from 75-deg to 0-deg occurs at 1,000~2,000 ft altitude)
Roll rates	3 degrees	no value provided
Climb gradient	1000 ft/nmi	between liftoff and 35 feet obstacle - 351 ft/nmi between 35 feet obstacle and 6,000ft – 515.8 ft/nmi (nacelle conversion from 75-deg to 0-deg occurs during 1,000~2,000 ft altitude)
Energy Share Factor (ESF)	90/10	no values provided
Descent gradient	1000 ft/nmi	between 25,000ft and 7,000ft – 200 ft/nmi below 7,000 ft – 2,000 ft – 296.4 ft/nmi; below 2,000ft – 451.5ft/nmi (nacelle conversion from 0-deg to 75-deg occurs at 2,000 ft altitude)
Bank angle	25 degrees	Bank angle: 45 deg (80 kts forward speed with nacelle tilt of 60 deg. This is the design limit condition.)
Average deceleration	50 kts/min	
		*Note on nacelle tilt: 0-deg for airplane mode and 90-deg for helicopter mode



Performance Name : LCTR2

Attributes

S Piston RNAV

Weight Class : L Engine Type : Jet/Turboprop Equipage : NON-RNAV

H Jet Database default

Cruise Altitude (ft) 25000.00 Max Takeoff Weight (klbs) 107.00 Takeoff Speed (kts) 81.70 Takeoff Acceleration (kts/min) 191.60

Cruise Speed (kts) 212.00 Max Landing Weight (klbs) 89.93 Landing Speed (kts) 50.00 Roll Rate (deg/sec) 3.00

Values by Altitude Gradient Rate Altitude Increment: 10000

Temp (deg F) 59.00 Pressure (in Hg) 29.92 Apply

Values at Standard Temp and Pressure Values at Temp and Pressure

Max Alt MSL (ft)	Climb Grad (ft/nm)	ESF (Climb/Accel)	Accel Rate (kts/min)	Descent Grad (ft/nm)	ESF (Descent/Decel)	D/R (kts)
0.00	1000.00	90/10	175.00	1000.00	80/20	
10000.00	1000.00	90/10	191.00	1000.00	80/20	

Speed (kts) Bank Angle (deg)

0.00	25.00
500.00	25.00

Help Ok Apply Copy Export Reset Cancel

NOTE : All speeds are indicated airspeeds.

Figure D-29. Tiltrotor Performance in TARGETS.

Appendix E. Safety Analysis of the CESTOL Spiral Approach

E.1. Introduction

The CESTOL spiral approach is not in widespread use today and therefore deserves special attention from the perspective of safety. Therefore, this section examines failures that could occur during the CESTOL spiral approach that could compromise safety. Topics considered include the impact of realistic steady-state wind conditions on the ability of the flight crew to revert to manual control. Pilot intervention may be a result of wind conditions which exceed the limitations of the Flight Management System (FMS), a generator or electrical failure in which equipment providing input to the FMS is lost, a failure of navigational inputs to the FMS, or a degraded state of the FMS itself. The constantly changing relative wind to which the aircraft is exposed during the spiral descent makes maintaining a planned trajectory of a spiral approach under manual control a challenge to the pilots. This is exacerbated by the CESTOL aircraft's low wing loading relative to the one of conventional jet transports, which makes it more susceptible to wind disturbances. The ability of the flight crews and vehicles to maintain adequate control to accomplish a safe landing, and maintain adequate separation from other traffic flows is assessed. Specifically, attention is given to the assessment of the likelihood of a hazardous drift of the spiral trajectory towards a neighboring path of vehicles operating from adjacent runways and airspace.

E.2. Analytic Approach

The complex dynamics and level of interactions taking place within such an environment such as the National Airspace System (NAS) makes it difficult to capture the behavior of every single entity (e.g., pilots, air traffic controllers, etc.) using classical approaches (e.g., differential equations or centralized control architectures). To this end, the agent-based paradigm has risen as a result of a shift in attention from individual systems and entities, to their, inherent interactions and the environment in which they operate. Many systems intrinsically are or have further evolved into large and complex architectures of interoperable parts and players, examples of which can be found in many domains, from complex ecosystems¹ or virtual societies^{2,3} to the global economy^{4,5} or airlines' economic strategy⁶ to the system-of-systems concept.

Some characteristics of these types of networks are the presence of open boundaries evolving in time, internal heterogeneity and high quantitative dimensionality. As a consequence, unified or centralized approaches may not be appropriate, as they are better suited to describe closed and well structured systems. As an alternative, agent-based techniques exploit the idea of distribution by focusing on the system constituents and their behavioral rules at the microscopic level, thus allowing the network's dynamics and the components' integration to emerge at the macroscopic level. Improved system-level robustness, adaptability, and self-organization are some of the resulting features that make agents appealing to engineering integration and management of complex infrastructures. In order to accomplish its objective, an agent interacts with other agents and the environment by exhibiting a host of qualities such as reactivity, proactivity, sociability, learning, in-time evolution, and others. Interactions and heterogeneity within a system generate the need for communication protocols and schemes to optimally resolve conflicts and/or enhance inter-agent coordination, for which various solutions have been proposed in the literature.

In the context of the NAS, its modeling is characterized by the interaction of various heterogeneous entities, e.g., aircraft, control towers, or various personnel, spatially distributed. Besides the intrinsic complexity of such a system, an interesting point being raised at the simulation phase is the difference in time scale among the various entities: a physics-based calculation may require a fine time step to guarantee adequate accuracy, while a discrete-in-time event will need to be updated less frequently. As observed by Lee et al.⁷, this issue of different time granularity works against the possibility of asynchronous simulation and forces synchronization, especially in the presence of stochastic events for which event time is not known a priori. As an alternative, in order to guarantee consistency of results, asynchronous simulation with partial resynchronization is suggested, where information and data updates are predicted and occur when necessary. Disruptions or unforeseen events can cause a series of cascading effects which call for time critical decisions. However, decisions may be hard to agree upon when many competing players are involved.

An attempt at modeling such circumstances is provided in⁸, where the agent-based model IMPACT (Intelligent agent-based Model for Policy Analysis of Collaborative Traffic flow management) was employed to simulate the decision-making process involving airlines and traffic control authorities in response to weather-based schedule changes. Harper et al.⁹ have also conducted similar studies with a focus on the human element in the context of decision making. Pilots, airline dispatchers and traffic controllers are all modeled using the same agent structure, made up of three units: air traffic situation assessor, collaborative decision making element, and plan executor, respectively in charge of collecting and processing current data, resolving traffic issues, and performing plan changes. The SAMPLE (Situation Assessment Model of Pilot-in-the-Loop Evaluation) agent-based architecture for modeling human behavior has been integrated in the FACET (Future Air Traffic Management Concepts Evaluation Tool) environment and principled negotiation has been employed as a means to provide coordination and resolve conflicts between aircraft⁹, where a solution is sought by providing communal advantages for all the interested parties. The goal of the study was to establish the need, if any, for negotiation in a complex environment where responsibilities and decisions were decentralized and distributed among the parties, as would be needed for the implementation of the free-flight concept.

E.3. Spiral and Spiral Descents

Spiral, or spiral, descents are being evaluated as noise abatement procedures and as a means for alleviating high-density airspace surrounding the airport. This type of approach may contain speed restrictions, crossing height restrictions, or lateral constraints linked to airport configuration. Concerns with these types of descents are associated with maintaining trajectory both vertically and laterally, and with the impact of wind conditions, equipment limitations and failures, and crew situational awareness in a high workload environment. Illustrated in Figure E-1 is the redesigned arrival and departure routes for four airports in the New York metroplex, including the spiral arrivals. This airspace redesign assumes all traffic is capable of RNP 0.3, vectoring is minimized with adequate metering, and slower traffic is segregated from nominal flows. The spiral descents were originally envisioned as noise abatement maneuvers, were designed with constant bank angle (decreasing radius) assuming no wind, and were located over the airport to minimize the impact on surrounding communities. They were moved off the airport to allow for missed approaches and avoid interference with other traffic. The bank angle was allowed to vary while the radius was set to a fixed value to better accommodate engine-out conditions and

other failures. Consideration is now being given to specify only the exit criteria to allow the flight crew and FMS more flexibility.

Assuming a constant-radius spiral the CESTOL aircraft enters the 1.5 nm radius spiral at 10000 ft above the airport elevation, at 180 kts, and with a 25° bank angle, and exits the spiral at 1000 ft above the airport elevation, at 110 kts, and with than a $\sim 4^{\circ}$ bank, at 1.5 to 3 nm from the runway threshold (Figure E-2). The extra 1.5 nm or 3 nm to the runway threshold is to allow for stabilization on the glidepath as well as on the localizer. Aircraft are expected to be in full landing configuration by the time they exit the spiral.

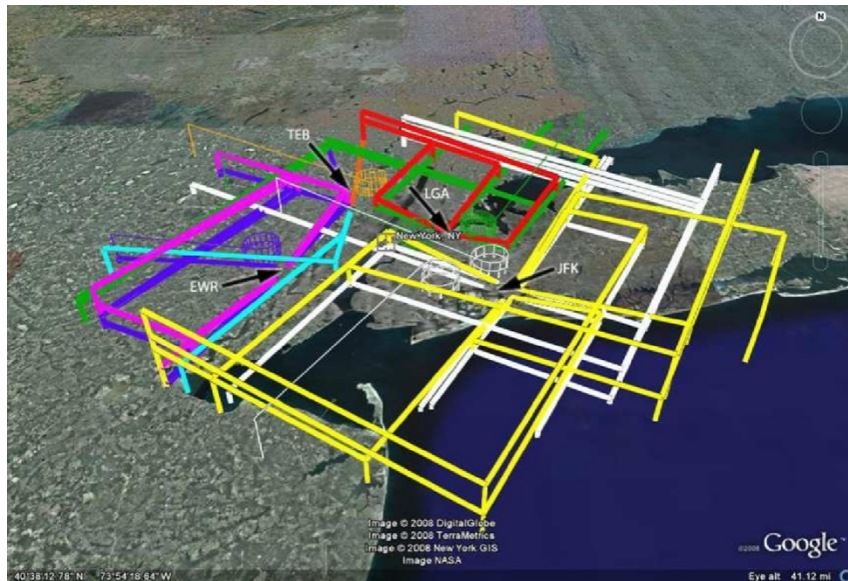


Figure E-1. Decoupled arrival and departure routes for four New York metroplex airports¹¹

E.4. Modeling environment and assumptions

The agent-based simulation approach has demonstrated its efficacy and easy implementation in modeling diverse complex systems, and has been herein adopted to conduct an initial assessment of the safety of the novel spiral landing procedure in the context of CESTOL. The landing procedure has been developed using the freeware multi-agent simulation environment NETLOGO^{12, 13} (version 3D Preview 5) from the Northwestern University.

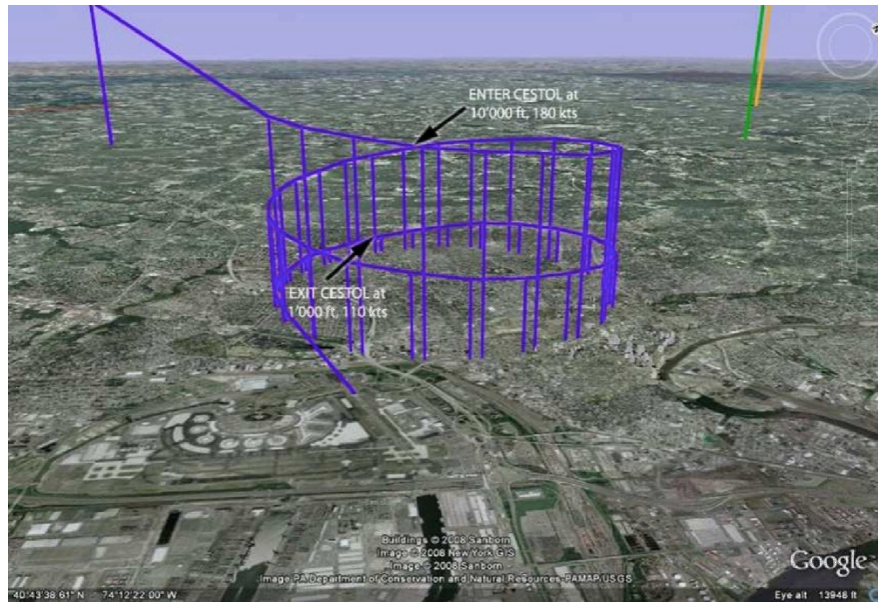


Figure E-2. Spiral approach¹¹

The following specific scenario was taken into consideration: a CESTOL aircraft plans to descend with a flight path angle of -5.5° and a calibrated airspeed which decreases linearly with altitude. In the case of spiral descent, the turn radius is a function of load factor, flight path angle, and magnitude of the vehicle's ground speed is treated as dependent performance parameter, whereas it is treated as a requirement and kept constant for an spiral descent. Two extreme possible situations can be identified in terms of safety for the surrounding air traffic. In the first case, the flight management system is assumed to be fully functional and capable of compensating for any external disturbance (e.g., wind) for the aircraft to land safely and as expected along its designated flight path. In the second situation, a failure in the flight management system forces the pilot to perform the landing procedure manually, hence his/her qualifications, training, recent experience, level of fatigue, and overall ability to compensate for disturbances may become critical in terms of safely landing the aircraft consistently and reliably without creating an unstabilized approach or causing a conflict with other traffic. This second scenario is at the basis of the study conducted herein on plausible hazard scenarios for the CESTOL spiral-landing procedure.

The main assumptions feeding into the agent-based simulation environment developed for this research study consist of the following:

- Interaction with other approaches: only the probability of the intrusion into the airspace designated for the neighboring approaches is estimated (no interactions are considered, such as evasive maneuvers by the aircraft whose airspace is invaded).
- Aircraft model: it is solely based on kinematics rules, where the vehicle's state vector includes only its inertial position, flight path angle γ , bank angle ϕ , and heading ψ .
- The trajectory is divided in three segments:
 - Spiral trajectory at $\gamma = -5.5$, constant turn radius $R = 1.5$ nm, and linear V_C profile ($V_C = 180$ kts, $\phi = 25^\circ$ at 10000 ft, $V_C = 110$ kts, $\phi \approx 4^\circ$ at 1000 ft); furthermore, the

- vehicle will exit at the established altitude regardless of its position and orientation with respect to the runway;
- Stabilization/transition phase: γ around -1° with path decided by pilot's based on vehicle's location when exiting the spiral;
- Conventional landing where the flight path angle γ is not to drop below -3° .
- The aircraft is subject to the following performance constraints:
 - The load factor $n = \cos(\gamma)/\cos(\phi)$ is not to exceed the limit of 1.15 during the spiral;
 - During the transition phase, the bank angle γ is not to exceed $\pm 20^\circ$ and the turn radius R must be greater than or equal to $1.5 R_{\min}$.
- Modeling of the wind velocity W : the time-invariant wind profile is assumed to depend only on the altitude z . At each simulation, a representative profile is constructed using a weighted sum of measured wind data, i.e., $W = \sum_j c_j W_j$. The time-varying nature of the wind can be modeled assuming distinct random weights C_j for each of the vehicles.
- Pilot's compensation: in order to account for the time delay (τ) in the pilot's response, the true airspeed V at any given altitude z is adjusted to compensate for the wind velocity W measured at the altitude $z - \tau \sin(\gamma) V_I$. During the spiraling phase, the flight path angle γ is never allowed to drop below -6.5° due to the wind effect, as it is assumed that the pilot would become aware of such a steep descent and would respond more promptly. Finally, for the results presented in this research study, no compensation of cumulative velocity drift has been included. At low altitudes, however, it may be hypothesized that visual cues may become available to the pilots to alert them of large incurring drifts in the trajectory.

E.5. Results

In order to assess the risk level associated with vehicle-separation violation in the presence of an spiral landing, two sources of uncertainty have been modeled and their effects investigated. The first one consists of the wind forecast error, modeled via rescaling and rotation of nominal wind profiles according to Gaussian distributions $N(\mu, \sigma)$. Illustrated in Figure 4 is the nominal wind velocity profile used as baseline for this study, and obtained through linear interpolation of measurement data. The information on the wind velocity $W = [W_N, W_E, W_D]^T$ has been expressed with respect to a North-East-Down (NED) reference frame with its local-north direction parallel to the runway, with additional assumption that W_D is equal to zero. The second source of error relates to the pilot's response time delay τ , which was characterized by means of a lognormal distribution $L(\mu_L, \sigma_L)$.

The airport environment considered herein is composed of two parallel runways, one of which is utilized for conventional landings, whereas the other is dedicated to those vehicles performing spiral approaches. The probability $P_{\text{violation}}$ that two approaching/landing airplanes will violate the minimum-separation safety requirement can be expressed as follows:

$$P_{\text{violation}} = P_{\text{FMS failure}} \times P_{\text{helix drift}} \times P_{\text{other aircraft}} \quad (1)$$

where $P_{\text{FMS failure}}$ is the probability of a FMS failure, $P_{\text{helix drift}}$ is the probability that the spiraling descending aircraft will drift away from its nominal course, and $P_{\text{other aircraft}}$ is the probability that

another airplane will be in its vicinity. Given the layout of the landing site, depicted in Figure E-4, attention was given to the term $P_{\text{helix drift}}$ within Eq.(1), i.e., the probability that a vehicle on a drift spiral will invade the airspace reserved to other incoming aircraft by crossing the centerline in between the two runways. The hazard scenarios for CESTOL aircraft have been investigated by means of a Monte Carlo representation of the disturbances associated with the wind conditions and pilot reactions to the wind conditions themselves in the presence of a degraded FMS, where both sources of uncertainty were treated as independent random inputs. The wind nominal profile of Figure E-3 has been randomized for each vehicle by assuming a wind intensity's amplification factor $\kappa \sim N(\mu = 1, \sigma = 0.1)$, and a forecast error on the wind direction sampled through $N(\mu = 0, \sigma = 5)$. As regards the pilot's response, the time delay $\tau \sim L(\mu L = 10 \text{ sec}, \sigma L = 10 \text{ sec})$, with a constraint on its maximum allowed sampled value set equal to 20 sec to avoid unrealistic lags.

Depicted in Figure E-5 is a screenshot of the simulation environment highlighting both conventional and spiral landing procedures. All aircraft enter their respective landing approach at the same location, but each of them experiences a different wind which ultimately leads to a different response from the pilot and, in the case of spiral descents, to a unique stabilization trajectory. Shown in Figure E-6 to Figure E-8 are the results for three wind scenarios, namely south-west, cross and tail wind. It can be observed that even in the presence of mild winds with intensity on the order of ~ 20 kts, significant drift of the spiral may occur, as in the case of the cross-wind scenario. In case of wind and aircraft speed of the same order of magnitude, a very quick response from the pilot is needed to contain the spiral drift, which may otherwise lead to impractical landing scenarios. Accumulated drift without pilot intervention, however, may become unrealistic as the pilot will eventually realize to be off course. Since the model did not include any logics to compensate for cumulative effects, the aforementioned scenarios were discarded in the post-processing of the simulation results. Of course, the amount of "invasion" of the adjacent air space will also depend on the position at which an aircraft enters and exits the spiral. Even relaxing the exit condition by allowing the aircraft to abandon the spiral at an altitude other than 1000 ft in favor of a better alignment with the runway may help the pilot better assess his/her position through visual cues and thus control the drift more successfully. In some of the investigated scenarios, the effect of wind exhibited rather minor sensitivity with respect to the response delay. This was the case for tail as well as head wind in which conditions the flight path angle was the aircraft's parameter affected the most.

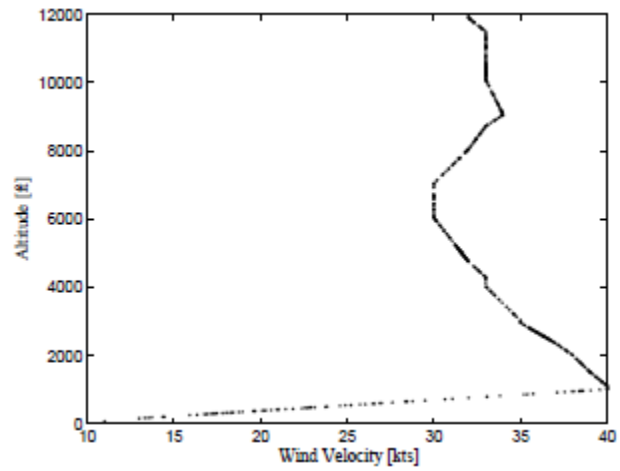


Figure E-3. Nominal wind profile.

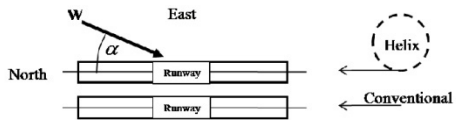


Figure E-4. Planar layout of the landing site.

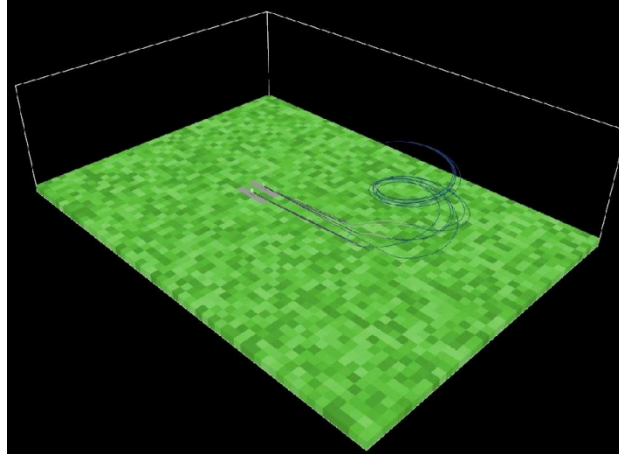
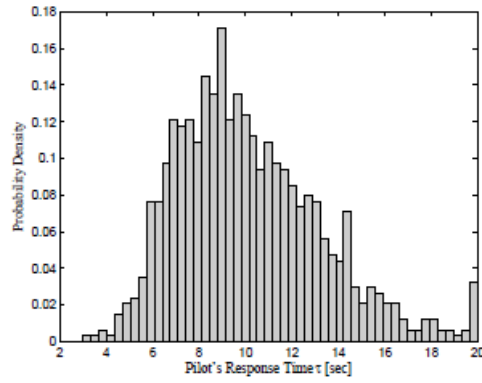
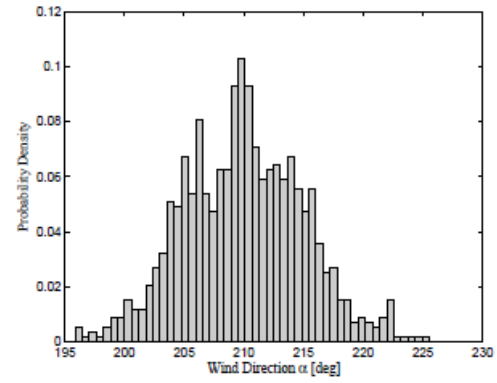


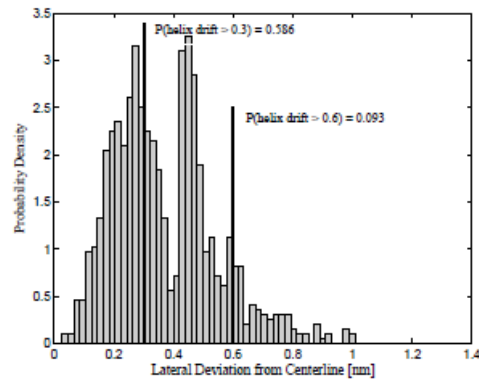
Figure E-5. Conventional and spiral landing trajectories in the presence of varying wind.



(a) $\tau \sim L(\mu_L = 10 \text{ sec}, \sigma_L = 10 \text{ sec})$

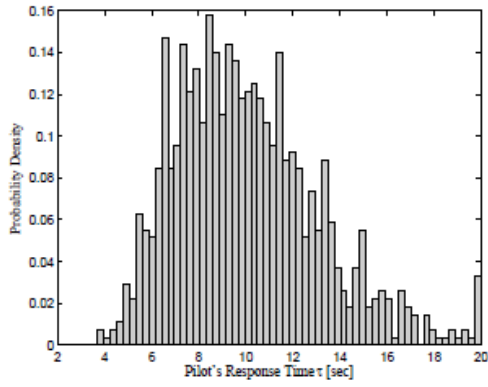


(b) $\alpha \sim N(\mu = 210^\circ, \sigma = 5^\circ)$

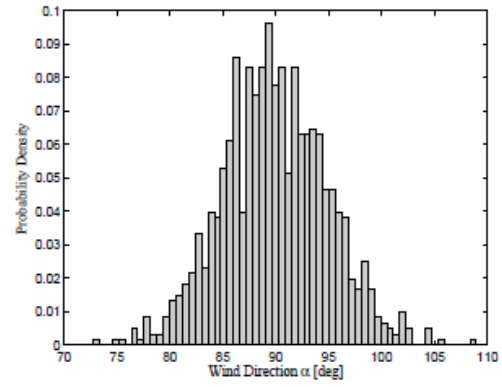


(c) $P_{helix \text{ drift}}$

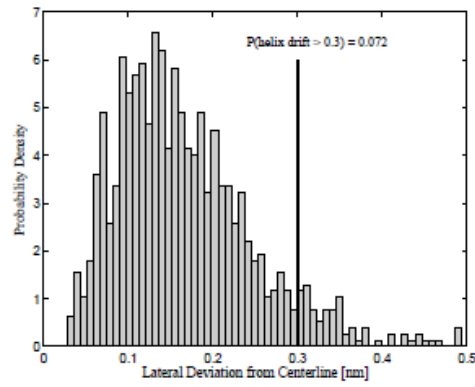
Figure E-6. Separation violation hazard in the presence of a south-west wind.



(a) $\tau \sim L(\mu_L = 10 \text{ sec}, \sigma_L = 10 \text{ sec})$

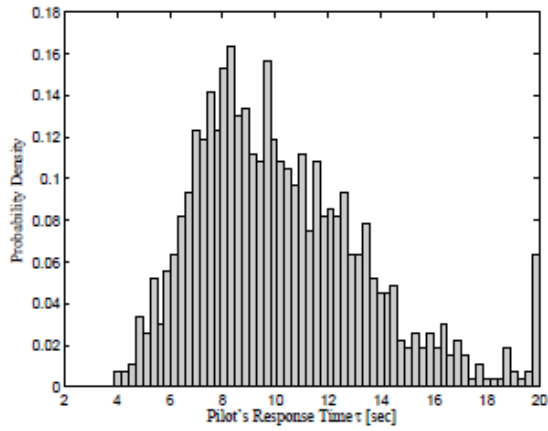


(b) $\alpha \sim N(\mu = 90^\circ, \sigma = 5^\circ)$

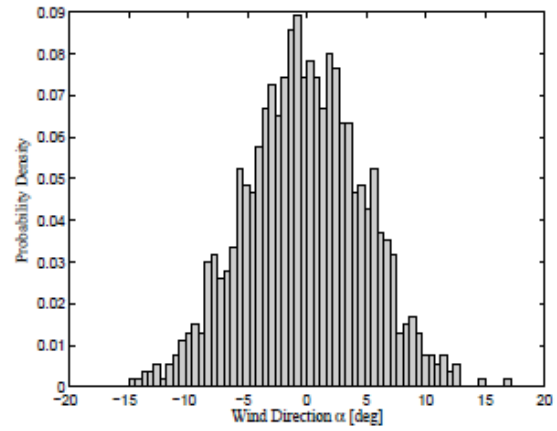


(c) $P_{helix\ drift}$

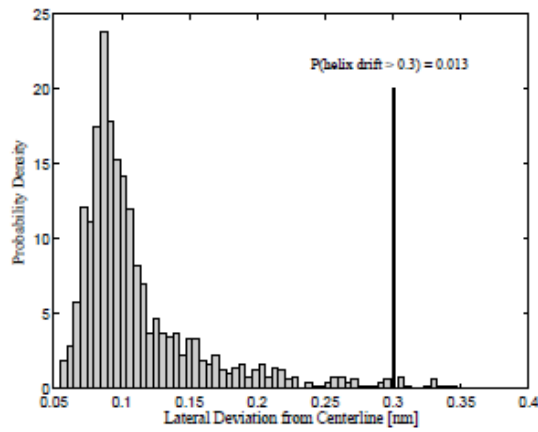
Figure E-7. Separation violation hazard in the presence of a cross wind.



(a) $\tau \sim L(\mu_L = 10 \text{ sec}, \sigma_L = 10 \text{ sec})$



(b) $\alpha \sim N(\mu = 0^\circ, \sigma = 5^\circ)$



(c) $P_{helix \text{ drift}}$

Figure E-8. Separation violation hazard in the presence of a tail wind.

E.6. Conclusions

Spiral landing scenarios for CESTOL aircraft were considered and modeled to assess the hazards induced by trajectory drift and consequent invasion of the air space dedicated to other incoming traffic. The investigation was conducted using agent-based simulation approach, since it provides a suitable framework to investigate combined effects occurring at different levels associated with the complex dynamic system NextGen, the air-traffic procedures, and the vehicle characteristics.

Results have shown that the combination of cross and head winds provide the most adverse scenario for airspace invasion and inter-vehicle separation violation since it may lead to very high probabilities of drifting away from the expected trajectory even in the presence of moderate wind velocities. Of course, a risky scenario may be exacerbated further depending on the corrections applied by the pilots and their timing.

As part of future research steps, the model provides results which can be used to fine-tune the air traffic procedures to avoid or mitigate potential hazards (e.g., increased flexibility in terms of exiting the spiral, or permitting some path deviation inside the spiral so that a correct position may be easily attained upon leaving the spiral trajectory). Missed approaches and go-around scenarios shall also be included within the simulation together with a more thorough mapping between the model logics and realistic pilot responses. Finally, additional players and sources of uncertainty and failure such as air traffic controllers and communication protocols shall be captured within the framework, thus exploiting further the modeling capabilities of agent-based approaches. In particular, the interactions among the aircrafts from several neighboring approach segments will be considered (for example, the possibility of evasive maneuvers if the possibility of space separation violation is detected).

E.7. Nomenclature

z	Altitude
Ψ	Heading
Φ	Bank angle
γ	Flight path angle
V_I	Inertial speed
V	True airspeed
V_C	Calibrated airspeed
N	Load factor
R	Turn Radius
R_{\min}	Minimum allowed turn radius
W	Wind vector velocity
W_N, W_E, W_D	Wind velocity components in the NED frame
\hat{W}	Measured wind velocity
A	Wind direction in the NE plane
K	Amplification factor for wind speed
T	Pilot's response time delay
P_E	Probability of event E's occurrence
$N(\mu, \sigma)$	Normal distribution
$L(\mu_L, \sigma_L)$	Lognormal distribution

E.8. References

1. Bonabeau, E. and Meyer, C., "Swarm Intelligence: a whole new way to think about business," *Harvard Business Review*, May 2001, pp. 107–114.
2. Epstein, J. and Axtell, R., *Growing artificial societies: social science from bottom up*, Brookings Institution Press, Washington, D.C., USA, 1991.
3. Parker, M., "What Is Ascape and Why Should You Care?" *Journal of Artificial Societies and Social Simulation*, Vol. 4, No. 1, 2001.
4. Icosystem Corporation, <http://www.icosystem.com>, 2009, Cambridge, MA, USA.
5. Bonabeau, E., "Agent-based modeling: Methods and techniques for simulating human systems," *Proceedings of the National Academy of Sciences*, Vol. 99, No. 3, May 2002, pp. 7280–7287.
6. Niedringhaus, W., "An Agent-based Model of the Airline Industry," The Mitre Corporation, 2000, McLean, VA, USA.
7. Lee, S., Pritchett, A., and Goldsman, D., "Hybrid Agent-based Simulation for analyzing the National Airspace System," *Proceedings of 33rd Winter Simulation Conference*, Arlington, VA, USA, 2001, pp. 1029–1036.
8. Campbell, K., Cooper, W., Greenbaum, D., and Wojcik, L., "Modeling Distributed Human Decision-Making in Traffic Flow Management Operations," *Third USA/Europe Air Traffic Management Research and Development Seminar*, Naples, Italy, June, 13-16 2000.
9. Harper, K., Guarino, S., White, A., and M., H., "An Agent-Based Approach to Aircraft Conflict Resolution with Constraints," *AIAA Conference on Guidance, Navigation and Control*, Monterey, CA, USA, 2000.
10. Hollingsworth, P., Kirby, M., Ran, H., Dufresne, S., and Sung, W., "Advanced Vehicles Modeling for the Next Generation Air Transportation System (NextGen Vehicle Integration NRA)," *9th AIAA Aviation Technology, Integration, and Operations Conference (ATIO)*, Hilton Head, South Carolina, 21 - 23 Sep 2009, pp. AIAA–2009–7119.
11. Nagle, G., Elliot, M., and Clarke, J.-P., "New York Metro Airspace Redesign," *9th AIAA Aviation Technology, Integration, and Operations Conference (ATIO)*, Hilton Head, South Carolina, 21 - 23 Sep 2009, pp. AIAA–2009–7069.
12. Wilensky, U., *NetLogo*. <http://ccl.northwestern.edu/netlogo>, 2009, Evanston, IL, USA.
13. Sklar, E., "Software review: NetLogo, a multi-agent simulation environment," *Artificial Life*, Vol. 13, No. 3, 2007, pp. 303–311.

Appendix F. Calculation of Fuelburn and Emissions Using AEDT

The environmental analysis in this study was performed using the Aviation Environmental Design Tool (AEDT). Although still in development, AEDT represents a confluence of legacy regulatory and analysis tools such as the Integrated Noise Model (INM), the Noise Integrated Routing System (NIRS), and the Environmental Design Space (EDMS) as well as the System for assessing Aviation's Global Emissions (SAGE) and the Model for Assessing Global Exposure to the Noise of Transport Aircraft (MAGENTA). AEDT is a data driven environmental analysis tool that relies on mostly manufacturer supplied certification data and internationally accepted standardized method to compute the noise^{cliii} and emissions of aviation. This is done by computing noise and/or emissions for a complete flight, comprising take-off, en route, and landing, for a specific airframe and engine. The alpha application^{cliv} that was created for use in this study comes with databases for aircraft (FLEET)^{clv} and airports (AIRPORT)^{clvi} that supply vehicle and engine specific information as well as airport and airport specific weather data. ACES was the source of the trajectory and flight information for the systemwide environmental analysis.

The linking of ACES and AEDT meant that the vehicle specific data created in the vehicle design effort had to be imported into the FLEET database as well as the import of the ACES provided flight and trajectory information. Both processes were automated with software tools. The vehicle import tool was developed at Georgia Tech, whereas the ACES connectivity was developed at Volpe and was included in the AEDT alpha application.

F.1. ACES Data Preprocessing

The provided preprocessor^{clviiiclviii} is a standalone executable that was automated via a Python script to provide automated linkage from ACES to the AEDT MOVEMENTS database. However, this assumes that the ACES MySQL server is accessible on a local network. This was not the case in this analysis. Therefore Sensis provided Georgia Tech with comma separated value (CSV) files compressed onto DVD-Rs via FedEx. This necessitated modifying the Python scripts to account for the change in source location and format.

After the first preprocessing trials it became evident that the preprocessor scales badly with the number of flights, probably due to scaling issues with the flight information matching algorithms. To give a rough estimate of the scaling, it takes only seconds for several thousand flights, about 20 minutes for about 15,000 flights, and about 10 hours for about 50,000 flights. Datasets over about 80,000 flights will run up to the 32bit .NET application memory limit. Changing the Windows memory management and modifying the executable can alter this. However, in practice this is not a good path to take since the preprocessor will take much too long to be usable.

The solution was to split the datasets, which exceed 100,000 flights in some cases. In this case they were split into four pieces. The requirement was, however, that the process be automated due to the number of runs desired. Furthermore, the preprocessor requires three pieces of information per flight, the takeoff, landing, and state messages to be present. So the data had to be split up such that each of the four pieces contained all three pieces consistently in the same sub-piece of the entire dataset. The easiest way to accomplish this is via a relational database, so the automated scripts that were developed first use the SQL bulk copy command to transfer all of the ACES MySQL exported files back into SQL server. Then a set of queries is used to split the dataset into four pieces of each the takeoff, landing, and state messages.

At this state it became also apparent that not all flights have all three pieces of required information. Primarily, this was the case due to one end of the flight being at an airport outside of the US airspace simulated by ACES. Sensis developed a tool that would artificially add the appropriate state messages for most of these. However, some small percentage of flights was still missing a full set of information. This was, however, easily omitted by the nature of the relational queries in SQL server. The other problem that needed to be remedied at this stage, but only became more obvious after much more testing of the data and the final results, was that some takeoff and landing pairs did get associated with two trajectories. This did result in very anomalous results for those flights, so they were excluded at this point of processing also.

Once the data was split into four, it was then re-exported into comma-separated value files. The sets of four times three files were then scripted to be processed each separately by the preprocessor. At the end of each preprocessor run, the outputs were copied into a staging copy of the AEDT MOVEMENTS database, where each subsequent copy was then merged into the FLIGHT, FLIGHT_TRAJECTORY and OD_PAIR tables such as to ensure continuity of the index numbering and foreign key links as well as uniqueness of the origin and destination pairs.

This method allowed automated importing of runs in under one hour per run, as well as conditioning the data as already mentioned and additionally properly adjusting the taxi times to the expected unit of seconds and fixing some inconsistencies created by some of the ACES post processing tools such as runway assignments to anything but “0L” and “0R,” which signify unknown runway assignment. There was also a required replacement of NULL entries in the input data in columns not used, at least according to the preprocessor application ADD, with “0”.

F.2. Database Modifications

The default system databases had to be modified in order to accommodate this particular type of analysis as well as the peculiarities of the data contained within it. The two primary databases that had to be adjusted for data content were the FLEET and the AIRPORT database. The MOVEMENTS and the EVENTRESULTS^{clix} databases primarily had to be adjusted for structure to facilitate the analysis of many datasets as well as expedite the analysis of the raw results.

F.3. FLEET Database

The primary data modification to the FLEET database was obviously the import of the new vehicle definitions as defined by the scenarios to be analyzed. Additionally, vehicle models representative of the N+1 and N+2 vehicle goals for the 150 and 300 seat classes based on modified reference vehicles were also imported.

After the first trials of the preprocessor, it became evident that there were a large number of failures that stemmed from missing aircraft types. ACES uses an aircraft-naming scheme based on the ICAO AC_TYPE. However, version 2.2.3 of the FLEET database uses ACCODE as well as an ICAO engine UID. Therefore, a mapping table exists in the FLEET database to allow this translation to occur. This mapping table is based primarily on commercial jet fleet information and as such was lacking mappings for quite a few smaller and general aviation aircraft. These mappings were added to minimize the number of rejected flights.

After much analysis, it also became obvious that a number of small aircraft were substituted to several Piper aircraft terminal performance definitions due to lack of available data. However, these definitions lack throttle setting definitions, which in turn makes the emission modeling method (Boeing Fuel Flow Method v2)^{clx} not usable because it depends on knowledge of throttle setting. This required modifying the substitutions appropriately to similar other available terminal performance definitions. This was necessary for almost a dozen small aircraft, which affected almost five percent of the flights in the datasets. These flights would otherwise be dropped from the analysis. This substitution, while only an approximation, at least allows a significant amount of flights to be retained through the analysis.

F.4. AIRPORT Database

During testing it also became apparent that all flights to certain airports did not get processed at all. After some investigation there was a set of 21 airports that had missing weather station meteorological data such as relative humidity. Therefore, the AIRPORT database was searched for the closest other weather station and replaced the missing data with duplicates of the closest other weather station. This turned out to be relatively complex, because there are thirteen (twelve monthly and one annual) sets of data.

Additionally, it turned out that most data fields in the airport information table (APT_MAIN) had to be filled out otherwise the airport did not get processed. This meant replacing state and other naming information for a relatively small set of airports.

The final pieces of data that were missing primarily for international airports were runway locations as well as elevation data. This was actually a problem for over 300 airports. As it turned out, however, fixing only a small number of this fixed the vast majority of airports since there are many that were only affected by a single flight. However, locating the runway end position data became another quite large problem. This is due to the lack of publicly available databases for this type of information. So for most of the airports Google Earth was used to estimate the runway location as much as possible.

F.5. MOVEMENTS Database

This database holds the flight and trajectory information to be processed through AEDT. Initial testing revealed that it is not possible to change the name or add indices to hold multiple scenario data at the same time, which would have facilitated running many scenarios.

In order to work around this problem, the three primary information tables were replaced with synonyms that represent a way to have a static entry point into the database which can be dynamically altered to point to any desired scenario. The final workflow consisted of having the preprocessor fill a staging set of tables, followed by moving this data into a scenario specific set of tables, which basically consisted of the default names with a scenario number added to the end of the name. The synonyms with the default names, which take the place of actual tables with the default names, then can be changed as needed to perform analysis runs on any desired scenario. This was the only change to this database.

F.6. EVENTRESULTS Database

Similar to the MOVEMENTS database, it was not possible to make any changes to the primary structure of the EVENTRESULTS database. However, again similar to the MOVEMENTS database, the primary tables that in this case hold the raw encoded results data were replaced by synonyms pointing to

the scenario specific actual tables which also had the regular names with an added scenario number appended.

It also turned out to be advantageous to actually add a second set of synonyms with slightly different names, which simultaneously can point to different raw results tables for the purpose of unpacking the results without interfering with a run. This turned out to be quite useful because several tasks could be performed simultaneously.

It also turned out to be necessary to adjust the provided stored procedures to work with the synonyms. Furthermore, the stored procedures were at times prone to causing exceptions in the code, which unpacks the raw results. This was caused by invalid results that some analysis runs would produce for certain single pieces of data. The stored procedures had to be modified to handle these exceptions so that a single spurious result would not block unpacking results for an entire scenario.

F.7. Workflow

Once initial testing of the primary executable was completed and additional development, which was done to facilitate processing a large number of scenario runs, was finished, a set of scripts was developed to automate the entire workflow.

In order, these scripts perform the following steps on the database server in order to generate the raw results:

- Move flight and trajectory data from staging tables into final scenario specific holding tables
- Clear scenario specific EVR_COMBINED table
- Drop all synonyms specific to the executable
- Create all synonyms pointing to scenario specific tables for running the executable

Then on the compute node:

- Ensure run specific configuration file is in place
- Run executable
- Retrieve log file
- Run automated error parse to generate statistics

After this the run is complete. On the Georgia Tech database server and one compute node on the same local network a systemwide emissions run depending on the number of flights will take from about one hour to just over two hours for about 100,000 flights and about 24 hours for a systemwide noise run.

The next workflow is to unpack the raw results and create the proper views to aggregate and format the results into the data format required by APMT.

The workflow steps are as follows:

- Drop all synonyms specific to the unpacking of results
- Create synonymns for unpacking for the scenario to be processed
- Run stored procedure to get performance results
- Run stored procedure to get emissions results
- Or run stored procedure to get accumulated emissions results to produce default results tables
- Drop scenario specific performance, emissions, and noise results tables
- Rename default results tables to scenario specific table

- Add scenario specific primary keys based on event id and segment number to improve results query performance
- Create scenario specific view joining the scenario specific performance and event tables zeroing negative results
- Create scenario specific view joining the scenario specific emissions and event tables zeroing negative results
- Create scenario specific view joining the performance and emissions results on a flight and segment basis and joining the ACCODE identifier. This is also the entry point for verification and validation of the results, because it allows flight by flight and segment by segment comparisons and analysis.
- Create scenario specific view summing the previous view by ACCODE for the entire scenario and format columns in the right order for APMT and filtering for US only flights
- Query the final view and export to excel
- For noise results, the unpacked scenario specific results table can be directly accessed to create contours

F.8. Scenarios

This section will not repeat any scenario-specific details or descriptions; instead this section will focus on scenario specific details of the AEDT runs that were performed as well as showing results.

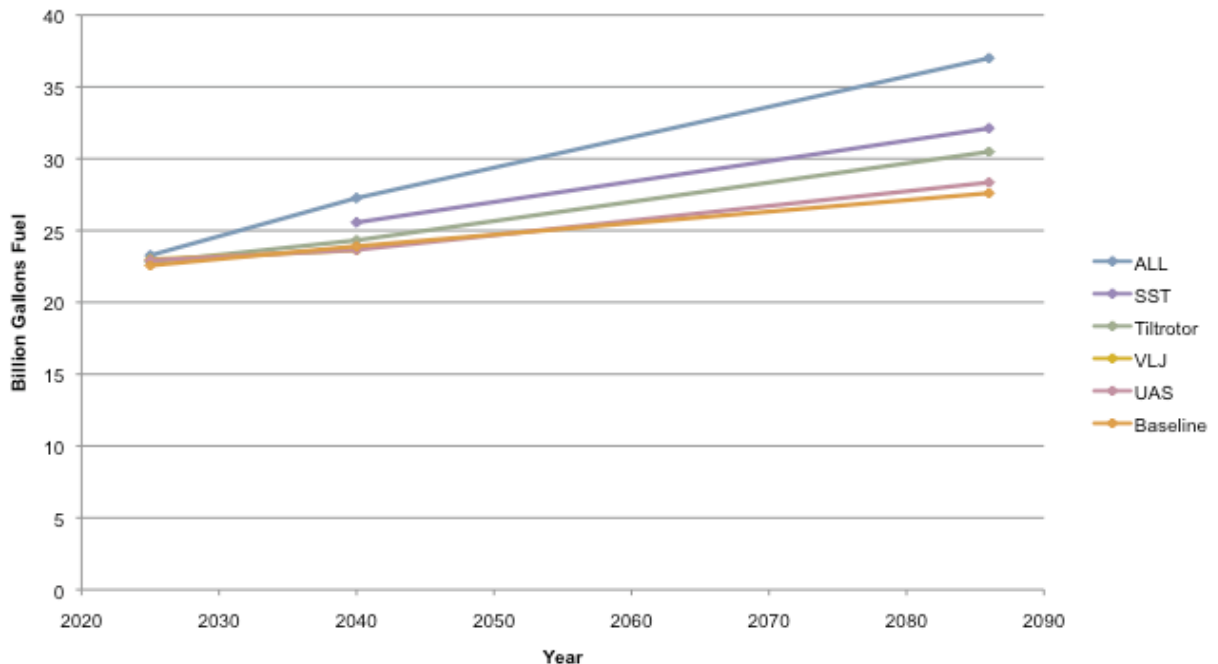


Figure F-1. Scenario Annualized Comparison

Figure F-1 shows an annualized comparison of the results on an annualized basis in billion gallons. The raw systemwide totals are by default provided in kilograms for fuel and grams for all other emissions. The time scaling depends on the input flight set, which in this case was a set of daily flights in the NAS as projected into the future.

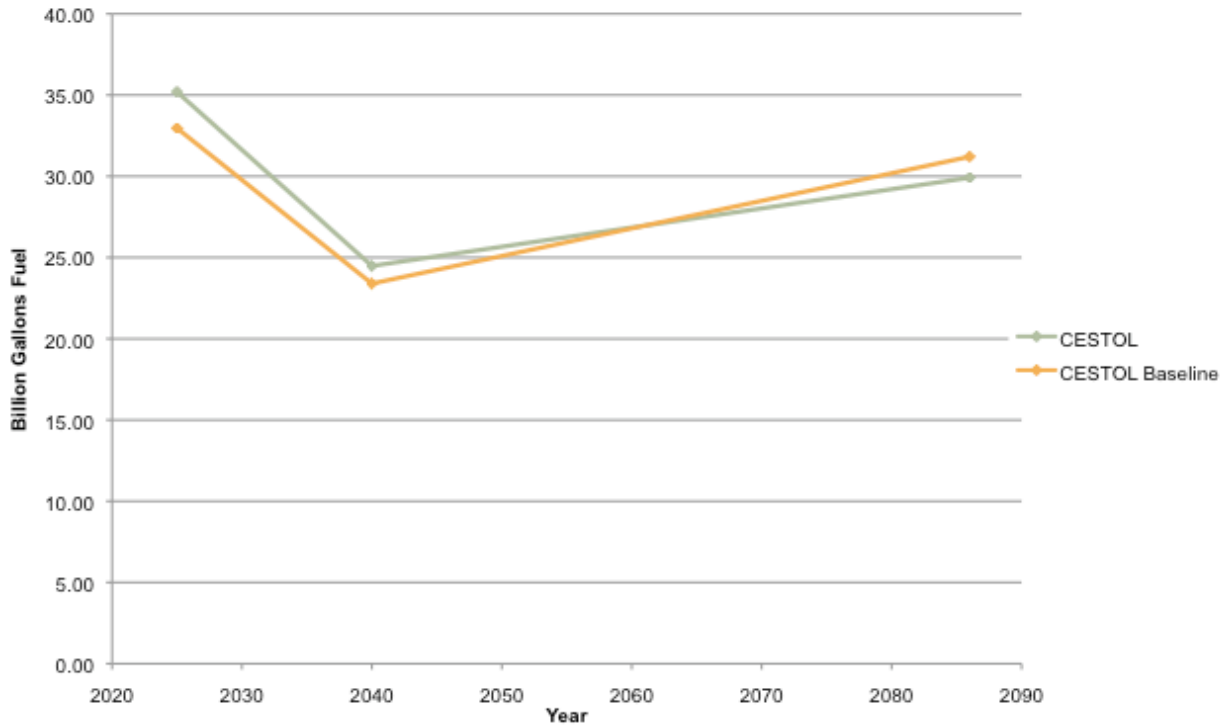


Figure F-2. CESTOL Scenario Annualized Comparison

The CESTOL scenarios obviously require further explanation. As shown in Figure F-2 the fuelburn drops between the 1.4x (2025) and the 2x (2040) scenario runs and only slightly recovers slightly for the 3x (2086) run. This is primarily due to the phase-in of the narrow body replacement vehicle (N150) that was introduced into the fleet to some small degree in the 2025 runs but then essentially replaces the entire existing fleet of narrowbody aircraft. This leads to dramatic reductions in fuelburn even while increasing the number of flights. The CESTOL scenario has more fuelburn overall in general because of the added flights that are possible due to the capacity improvements achieved by the vehicle capabilities offered by the CESTOL.

The order of the scenarios switches for the 2086 year due to the way the CESTOL is used as a smaller vehicle and being also slightly less efficient than the N150. This is reflected in the number of flights, which are shown in Figure F-3 and Figure F-4.

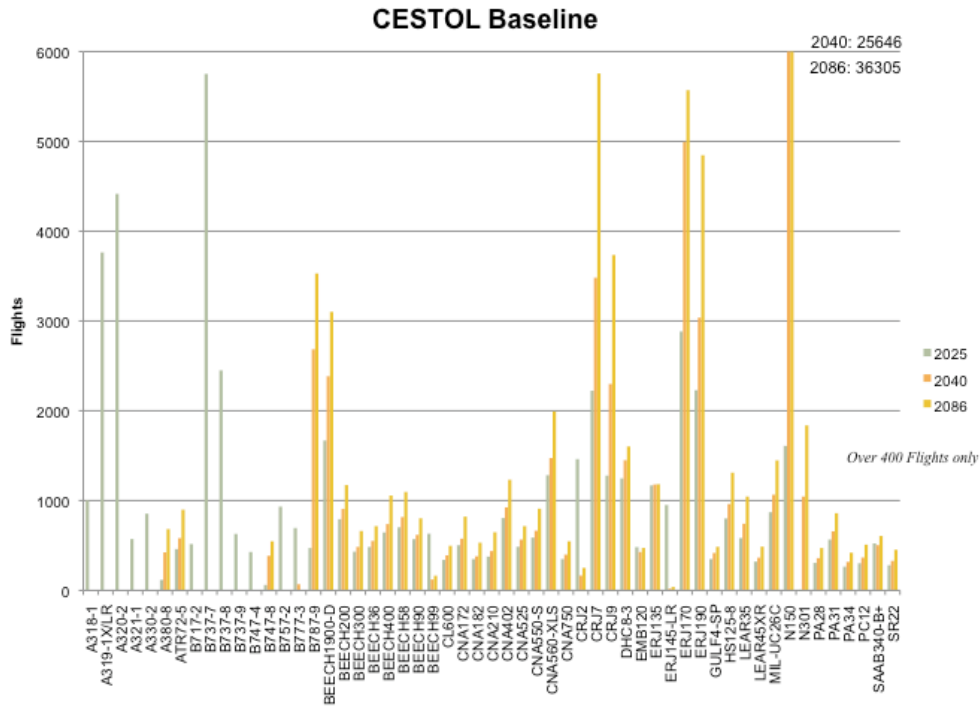


Figure F-3. CESTOL Baseline Number of Flights

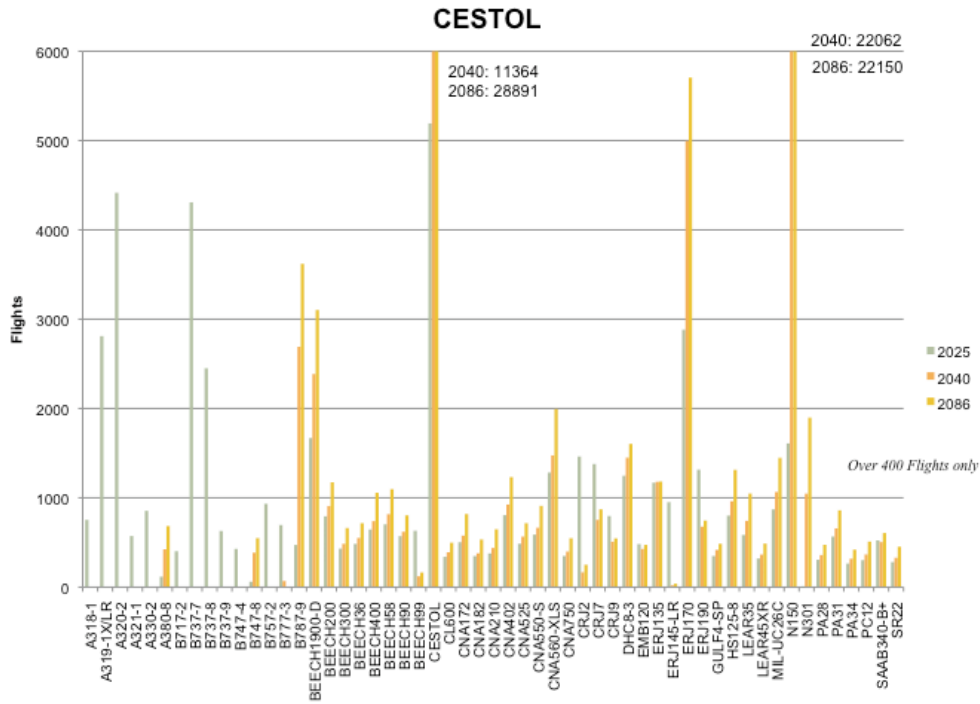


Figure F-4. CESTOL Number of Flights

F.9. Baseline

Processing the baseline scenario had no specific challenges outside of the ones described previously.

Year	AC Category	Fuelburn (kg)	NOx (g)	% Fuelburn	% NOx
2025	Small Twin Aisle	3.18E+07	4.36E+08	17%	19%
	Single Aisle	9.71E+07	1.08E+09	51%	48%
	Regional Jet	2.25E+07	2.23E+08	12%	10%
	Large Twin Aisle	1.42E+07	2.56E+08	8%	11%
	Large Quad	1.24E+07	1.68E+08	7%	7%
	General Aviation	1.10E+07	9.37E+07	6%	4%
	Total	1.89E+08	2.26E+09		
2040	AC Category	Fuelburn (kg)	NOx (g)	% Fuelburn	% NOx
	Small Twin Aisle	2.97E+07	4.06E+08	15%	19%
	Single Aisle	9.61E+07	9.01E+08	48%	41%
	Regional Jet	2.84E+07	2.89E+08	14%	13%
	Large Twin Aisle	2.05E+07	2.87E+08	10%	13%
	Large Quad	1.25E+07	1.82E+08	6%	8%
	General Aviation	1.32E+07	1.16E+08	7%	5%
Total	2.00E+08	2.18E+09			
2086	AC Category	Fuelburn (kg)	NOx (g)	% Fuelburn	% NOx
	Small Twin Aisle	3.69E+07	5.06E+08	16%	20%
	Single Aisle	1.00E+08	9.30E+08	43%	37%
	Regional Jet	3.18E+07	3.21E+08	14%	13%
	Large Twin Aisle	2.77E+07	3.49E+08	12%	14%
	Large Quad	1.71E+07	2.52E+08	7%	10%
	General Aviation	1.73E+07	1.50E+08	7%	6%
Total	2.31E+08	2.51E+09			

Figure F-5. Baseline Categorized Fuelburn and NOx Results

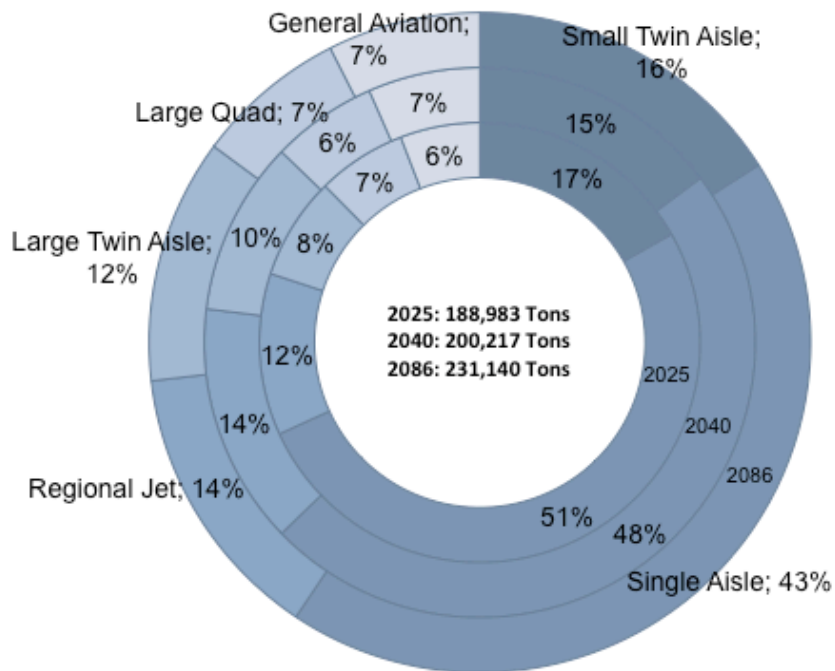


Figure F-6. Baseline Fuelburn

F.10. VLJ

Because the VLJ is based on an existing airframe, processing the VLJ scenario had no unique challenges.

Year	AC Category	Fuelburn (kg)	NOx (g)	% Fuelburn	% NOx
2025	Small Twin Aisle	3.21E+07	4.43E+08	17%	19%
	Single Aisle	9.87E+07	1.10E+09	51%	48%
	Regional Jet	2.30E+07	2.30E+08	12%	10%
	Large Twin Aisle	1.44E+07	2.61E+08	7%	11%
	Large Quad	1.26E+07	1.71E+08	7%	7%
	General Aviation	1.14E+07	9.91E+07	6%	4%
	VLJ	3.46E+05	1.39E+06	0.2%	0.1%
	Total	1.93E+08	2.31E+09		
2040	AC Category	Fuelburn (kg)	NOx (g)	% Fuelburn	% NOx
	Small Twin Aisle	2.92E+07	4.01E+08	15%	19%
	Single Aisle	9.48E+07	8.88E+08	48%	41%
	Regional Jet	2.79E+07	2.80E+08	14%	13%
	Large Twin Aisle	2.02E+07	2.84E+08	10%	13%
	Large Quad	1.23E+07	1.79E+08	6%	8%
	General Aviation	1.29E+07	1.13E+08	7%	5%
	VLJ	5.70E+05	2.26E+06	0.3%	0.1%
Total	1.98E+08	2.15E+09			

Figure F-7. VLJ Categorized Fuelburn and NOx Results

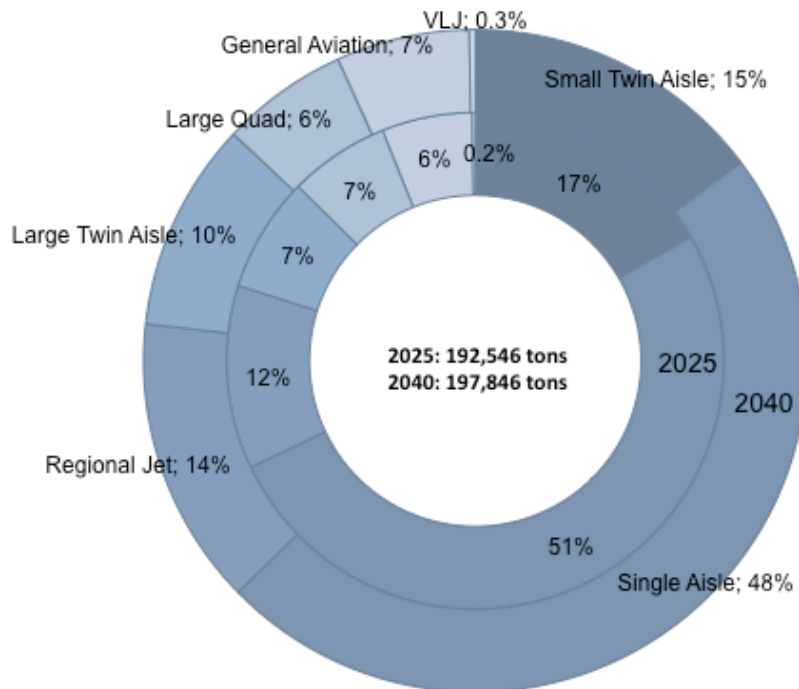


Figure F-8. VLJ Fuelburn

F.11. UAS

The UAS scenario had some difficulty in importing the vehicle definition into the FLEET database, because the import tool had not been validated for propeller aircraft and had to be modified slightly.

The emissions run itself presented some unique challenges that actually required debugging the performance computations^{clxi} because a large number of UAS flights would fail due to trajectory problems. After some investigation it became apparent that this was caused by the UAS never leaving the terminal area and in many cases never climbing over 10,000 ft. This is important because the performance calculations operate differently if that happens due to the switch of performance model that happens at that altitude. This caused problems following the trajectories with takeoffs and landings. Tests were run to try and switch the computation mode such that this would not happen by changing the default runway assignment to a nonexistent runway based on airport location, however this led to the problem that the way the trajectories were generated used these same coordinates as end points, which leads to an interpolation error between the start or end of the trajectory and the start or end of the takeoff or landing roll if they are the same since the difference becomes zero.

Therefore, this fix actually increased the number of dropped flights for this aircraft. So the final decision was to in the end use the same computation mode as in the other scenario runs to not distort the analysis while keeping the performance computation errors to a minimum.

Year	AC Category	Fuelburn (kg)	NOx (g)	% Fuelburn	% NOx
2025	Small Twin Aisle	3.20E+07	4.42E+08	17%	19%
	Single Aisle	9.84E+07	1.10E+09	51%	48%
	Regional Jet	2.29E+07	2.29E+08	12%	10%
	Large Twin Aisle	1.44E+07	2.61E+08	8%	11%
	Large Quad	1.26E+07	1.71E+08	7%	7%
	General Aviation	1.14E+07	9.91E+07	6%	4%
	UAS	2.91E+05	1.01E+06	0.2%	0.0%
	Total	1.92E+08	2.30E+09		
2040	AC Category	Fuelburn (kg)	NOx (g)	% Fuelburn	% NOx
	Small Twin Aisle	2.91E+07	3.98E+08	15%	19%
	Single Aisle	9.49E+07	8.87E+08	48%	41%
	Regional Jet	2.81E+07	2.85E+08	14%	13%
	Large Twin Aisle	2.04E+07	2.85E+08	10%	13%
	Large Quad	1.23E+07	1.79E+08	6%	8%
	General Aviation	1.30E+07	1.14E+08	7%	5%
	UAS	2.85E+05	9.87E+05	0.1%	0.0%
Total	1.98E+08	2.15E+09			
2086	AC Category	Fuelburn (kg)	NOx (g)	% Fuelburn	% NOx
	Small Twin Aisle	3.77E+07	5.20E+08	16%	20%
	Single Aisle	1.03E+08	9.73E+08	44%	37%
	Regional Jet	3.24E+07	3.29E+08	14%	13%
	Large Twin Aisle	2.84E+07	3.59E+08	12%	14%
	Large Quad	1.77E+07	2.68E+08	7%	10%
	General Aviation	1.75E+07	1.55E+08	7%	6%
	UAS	2.95E+05	1.02E+06	0.1%	0.0%
Total	2.37E+08	2.60E+09			

Figure F-9. UAS Categorized Fuelburn and NOx Results

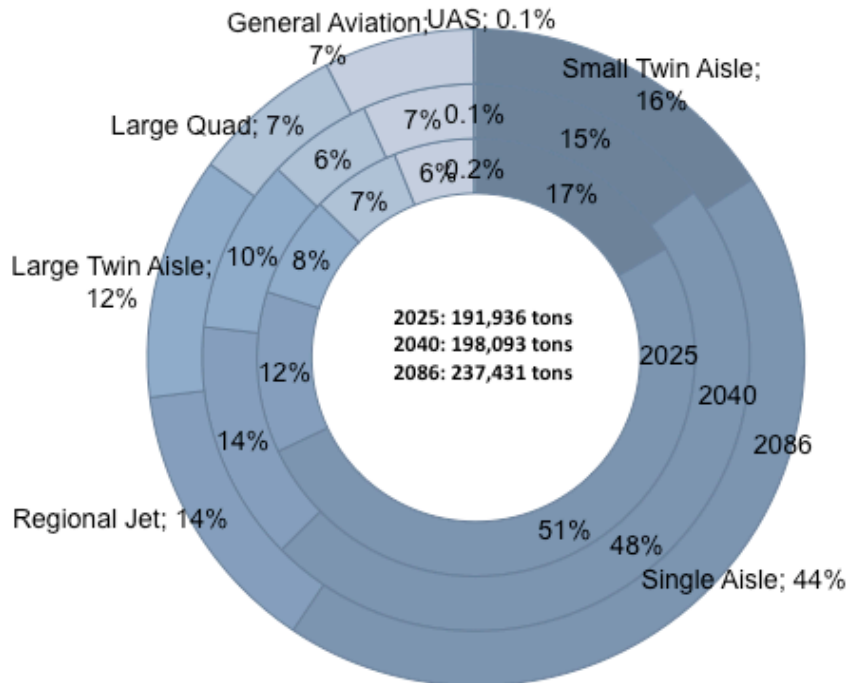


Figure F-10. UAS Fuelburn

F.12. LCTR

The tiltrotor was subject to the same propeller model import modifications as the UAS. So once this was updated accordingly, this presented no issue. The only remaining issue of concern was the high fuel burn in the terminal area flight phases. This actually lead to an iteration on the vehicle representation in AEDT as well as more sanity checks, where it was confirmed that the powered lift phases do burn a lot of fuel.

Year	AC Category	Fuelburn (kg)	NOx (g)	% Fuelburn	% NOx
2025	Small Twin Aisle	3.15E+07	4.31E+08	16%	19%
	Single Aisle	9.49E+07	1.05E+09	50%	46%
	Regional Jet	2.21E+07	2.20E+08	12%	10%
	Large Twin Aisle	1.42E+07	2.56E+08	7%	11%
	Large Quad	1.23E+07	1.67E+08	6%	7%
	General Aviation	1.11E+07	9.52E+07	6%	4%
	CTR	4.79E+06	5.64E+07	3%	2%
	Total	1.91E+08	2.28E+09		
2040	AC Category	Fuelburn (kg)	NOx (g)	% Fuelburn	% NOx
	Small Twin Aisle	2.89E+07	3.96E+08	14%	18%
	Single Aisle	9.02E+07	8.33E+08	44%	38%
	Regional Jet	2.73E+07	2.75E+08	13%	12%
	Large Twin Aisle	1.99E+07	2.75E+08	10%	12%
	Large Quad	1.21E+07	1.78E+08	6%	8%
	General Aviation	1.27E+07	1.09E+08	6%	5%
	CTR	1.26E+07	1.48E+08	6%	7%
Total	2.04E+08	2.21E+09			
2086	AC Category	Fuelburn (kg)	NOx (g)	% Fuelburn	% NOx
	Small Twin Aisle	3.74E+07	5.15E+08	15%	18%
	Single Aisle	9.10E+07	8.32E+08	36%	29%
	Regional Jet	2.80E+07	2.80E+08	11%	10%
	Large Twin Aisle	2.83E+07	3.58E+08	11%	13%
	Large Quad	1.77E+07	2.67E+08	7%	9%
	General Aviation	1.72E+07	1.49E+08	7%	5%
	CTR	3.57E+07	4.21E+08	14%	15%
Total	2.55E+08	2.82E+09			

Figure F-11. LCTR Categorized Fuelburn and NOx Results

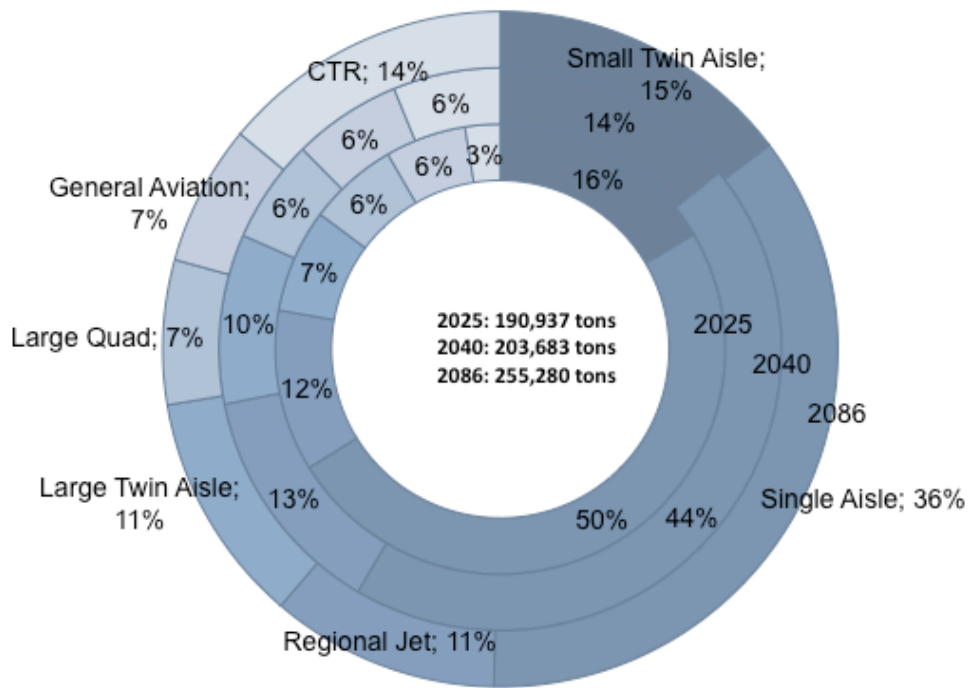


Figure F-12. LCTR Fuelburn

F.13. SST

The SST presented a unique challenge for the representation in the BADA and SAE 1845 models since they do not support supersonic operations. After some initial testing, however, it became evident that the equations could work with certain limitations where subsonic and supersonic flight could not be supported by the same model outside of adjusting the cruise altitudes.

It was also confirmed that the performance calculations would successfully and accurately support this type of flight. However, once the trajectory data from the ACES post-processor was received it became evident that this did not work. After some effort discovering the reason for this, it became evident that the relatively simple trajectories primarily consisting of a simple low altitude point and then jumping to supersonic cruise at 51,000 ft would not work.

The reason for this is that the aircraft as designed does not have enough thrust to directly follow a flight path that is based on a linear interpolation of a low altitude point and a high altitude cruise condition.

However, the aircraft is nonetheless capable of supersonic flight. It simply requires a very specific trajectory in which it transitions from subsonic to supersonic to achieve this. After some consideration, a series of scripts was developed to export all of the 367 and almost 800 flights in the SST scenarios such that they could be run in the test executable used to check the designs behavior in AEDT. This executable would allow flying a simple ground track extracted from the ACES like trajectory provided such that it could follow its desired altitude profile such as to enable supersonic cruise. This worked quite well. The results of this analysis were then merged back with the AEDT alpha executable results for the SST and the all-vehicle scenarios.

Year	AC Category	Fuelburn (kg)	NOx (g)	% Fuelburn	% NOx
2040	Small Twin Aisle	2.85E+07	3.89E+08	13%	18%
	Single Aisle	9.44E+07	8.85E+08	44%	40%
	Regional Jet	2.80E+07	2.83E+08	13%	13%
	Large Twin Aisle	1.94E+07	2.70E+08	9%	12%
	Large Quad	1.18E+07	1.70E+08	5%	8%
	General Aviation	1.27E+07	1.11E+08	6%	5%
	SST	1.93E+07	9.57E+07	9%	4%
	Total	2.14E+08	2.20E+09		
2086	AC Category	Fuelburn (kg)	NOx (g)	% Fuelburn	% NOx
	Small Twin Aisle	3.55E+07	4.86E+08	14%	19%
	Single Aisle	1.01E+08	9.53E+08	41%	37%
	Regional Jet	3.23E+07	3.27E+08	13%	13%
	Large Twin Aisle	2.65E+07	3.33E+08	11%	13%
	Large Quad	1.68E+07	2.55E+08	7%	10%
	General Aviation	1.72E+07	1.47E+08	7%	6%
	SST	1.73E+07	9.15E+07	7%	4%
Total	2.47E+08	2.59E+09			

Figure F-13. SST Categorized Fuelburn and NOx Results

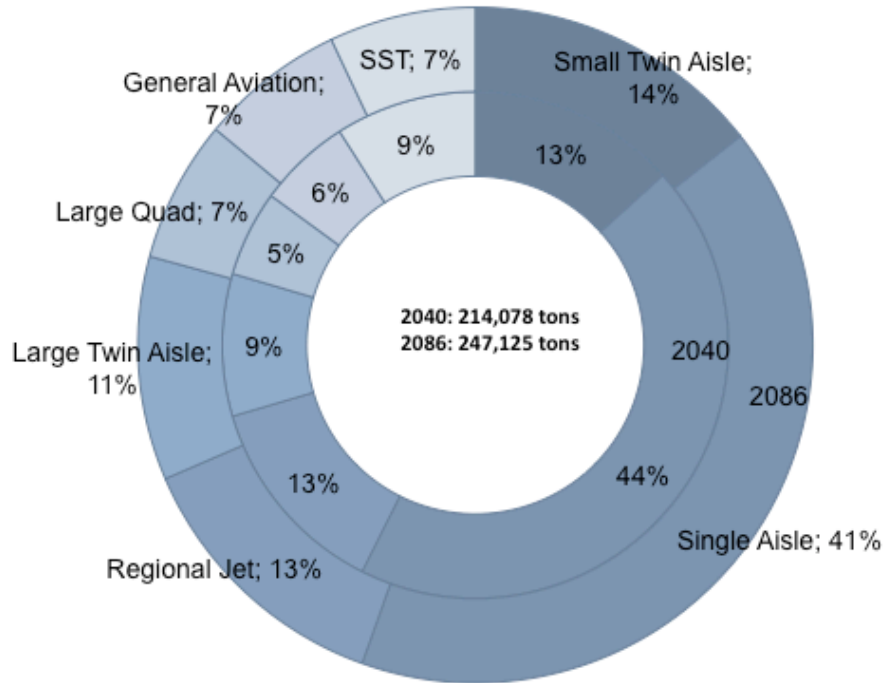


Figure F-14. SST Fuelburn

F.14. All-Vehicles

The scenario with all vehicles presented no additional challenges as compared to the vehicle specific scenarios. The SST flights were processed again separately and then merged back with the rest of the results.

Year	AC Category	Fuelburn (kg)	NOx (g)	% Fuelburn	% NOx
2025	Small Twin Aisle	3.21E+07	4.42E+08	16%	19%
	Single Aisle	9.13E+07	1.01E+09	47%	44%
	Regional Jet	2.01E+07	2.02E+08	10%	9%
	Large Twin Aisle	1.45E+07	2.62E+08	7%	12%
	Large Quad	1.26E+07	1.71E+08	6%	8%
	General Aviation	1.14E+07	9.91E+07	6%	4%
	SST	0.00E+00	0.00E+00	0%	0%
	UAS	2.90E+05	9.91E+05	0.1%	0.0%
	VLJ	3.50E+05	1.40E+06	0.2%	0.1%
	CTR	4.75E+06	5.59E+07	2%	2%
	CESTOL	7.61E+06	3.52E+07	4%	2%
	Total	1.95E+08	2.27E+09		
	2040	AC Category	Fuelburn (kg)	NOx (g)	% Fuelburn
Small Twin Aisle		2.85E+07	3.89E+08	13%	18%
Single Aisle		8.62E+07	7.91E+08	40%	36%
Regional Jet		2.03E+07	2.07E+08	9%	9%
Large Twin Aisle		1.96E+07	2.73E+08	9%	12%
Large Quad		1.17E+07	1.72E+08	5%	8%
General Aviation		1.26E+07	1.09E+08	6%	5%
SST		8.88E+06	4.59E+07	4%	2%
UAS		2.95E+05	1.02E+06	0.1%	0.0%
VLJ		5.76E+05	2.31E+06	0.3%	0.1%
CTR		1.27E+07	1.49E+08	6%	7%
CESTOL		1.66E+07	7.61E+07	8%	3%
Total		2.18E+08	2.22E+09		
2086	AC Category	Fuelburn (kg)	NOx (g)	% Fuelburn	% NOx
	Small Twin Aisle	3.53E+07	4.85E+08	12%	17%
	Single Aisle	8.36E+07	7.62E+08	29%	27%
	Regional Jet	2.11E+07	2.13E+08	7%	8%
	Large Twin Aisle	2.64E+07	3.34E+08	9%	12%
	Large Quad	1.67E+07	2.54E+08	6%	9%
	General Aviation	1.70E+07	1.48E+08	6%	5%
	SST	1.73E+07	9.04E+07	6%	3%
	UAS	2.87E+05	9.97E+05	0.1%	0.0%
	VLJ	5.84E+05	2.34E+06	0.2%	0.1%
	CTR	2.80E+07	3.30E+08	10%	12%
	CESTOL	4.18E+07	1.94E+08	15%	7%
	Total	2.88E+08	2.82E+09		

Figure F-15. ALL Vehicles Categorized Fuelburn and NOx Results

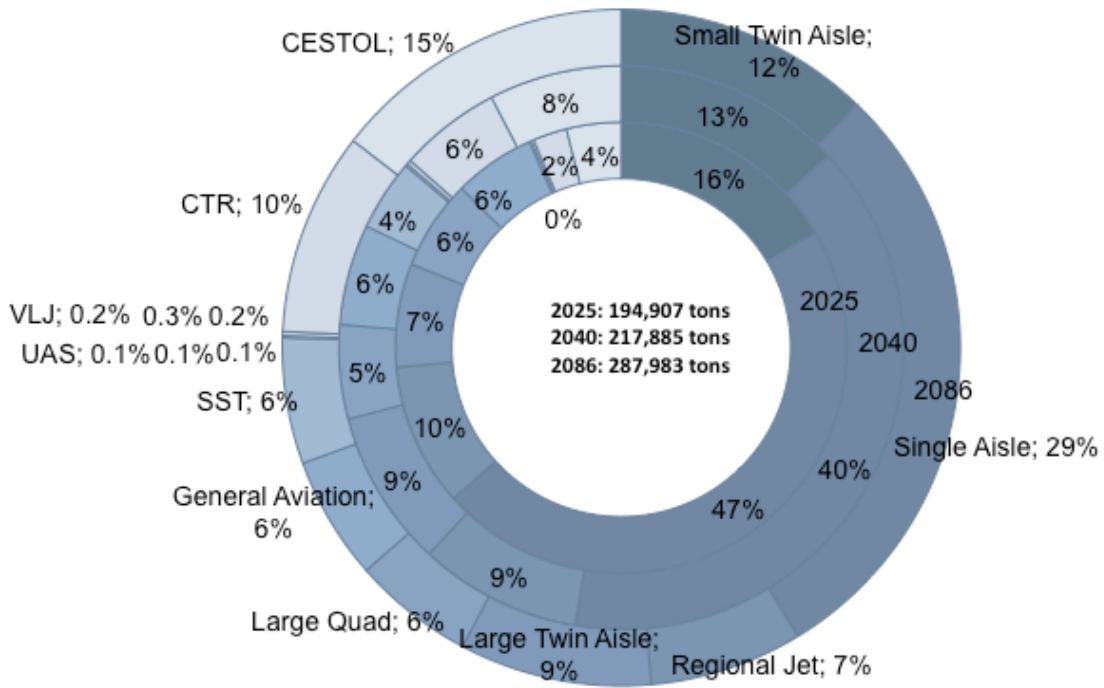


Figure F-16. All-vehicle fuelburn

F.15. CESTOL Baseline

The CESTOL baseline scenario is a specially constructed baseline that presented no special challenges as compared to the regular baseline scenario.

Year	AC Category	Fuelburn (kg)	NOx (g)	% Fuelburn	% NOx
2025	Small Twin Aisle	4.39E+07	5.22E+08	16%	18%
	Single Aisle	1.43E+08	1.40E+09	52%	49%
	Regional Jet	2.68E+07	2.53E+08	10%	9%
	Large Twin Aisle	3.98E+07	4.39E+08	14%	15%
	Large Quad	1.20E+07	1.58E+08	4%	6%
	General Aviation	1.08E+07	9.66E+07	4%	3%
	Total	2.76E+08	2.87E+09		
2040	AC Category	Fuelburn (kg)	NOx (g)	% Fuelburn	% NOx
	Small Twin Aisle	2.82E+07	3.83E+08	14%	18%
	Single Aisle	9.47E+07	8.86E+08	48%	42%
	Regional Jet	2.91E+07	2.93E+08	15%	14%
	Large Twin Aisle	1.97E+07	2.72E+08	10%	13%
	Large Quad	1.18E+07	1.69E+08	6%	8%
	General Aviation	1.23E+07	1.09E+08	6%	5%
Total	1.96E+08	2.11E+09			
2086	AC Category	Fuelburn (kg)	NOx (g)	% Fuelburn	% NOx
	Small Twin Aisle	3.60E+07	4.90E+08	14%	17%
	Single Aisle	1.25E+08	1.21E+09	48%	43%
	Regional Jet	3.93E+07	3.94E+08	15%	14%
	Large Twin Aisle	2.70E+07	3.39E+08	10%	12%
	Large Quad	1.72E+07	2.48E+08	7%	9%
	General Aviation	1.68E+07	1.53E+08	6%	5%
Total	2.61E+08	2.83E+09			

Figure F-17. CESTOL Baseline Categorized Fuelburn and NOx Results

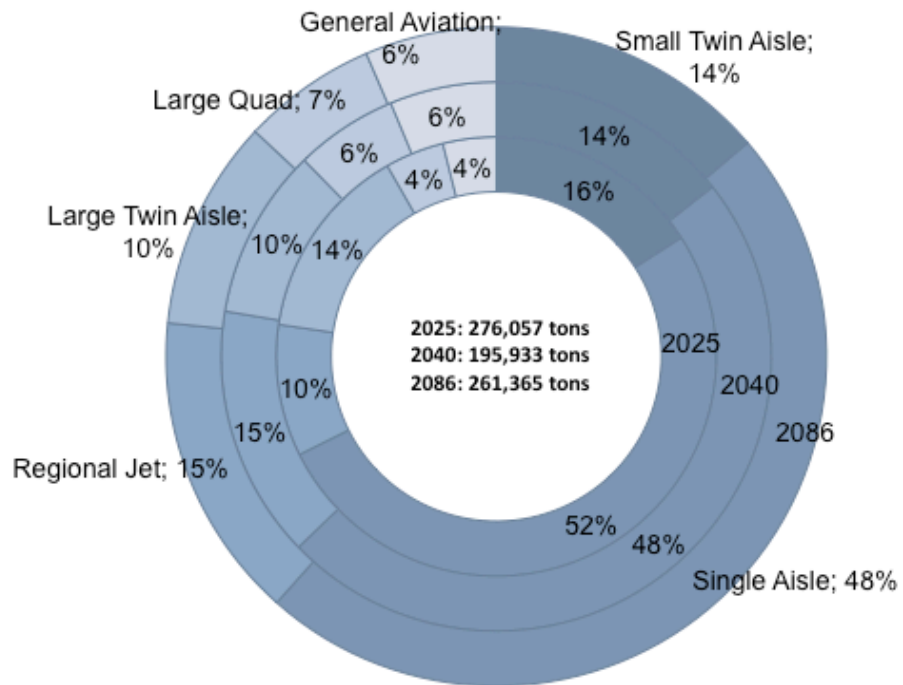


Figure F-18. CESTOL Baseline Fuelburn

F.16. CESTOL

The CESTOL vehicle scenario also did not have any additional work that needed to be performed, since the vehicle very much behaves like a conventional commercial jet aircraft.

Year	AC Category	Fuelburn (kg)	NOx (g)	% Fuelburn	% NOx
2025	Small Twin Aisle	5.33E+07	6.13E+08	18%	21%
	Single Aisle	1.47E+08	1.37E+09	50%	46%
	Regional Jet	2.15E+07	2.04E+08	7%	7%
	Large Twin Aisle	4.16E+07	4.85E+08	14%	16%
	Large Quad	1.18E+07	1.56E+08	4%	5%
	General Aviation	1.06E+07	9.39E+07	4%	3%
	CESTOL	8.86E+06	3.79E+07	3%	1%
	Total	2.95E+08	2.96E+09		
2040	AC Category	Fuelburn (kg)	NOx (g)	% Fuelburn	% NOx
	Small Twin Aisle	2.96E+07	4.02E+08	14%	19%
	Single Aisle	9.21E+07	8.49E+08	45%	40%
	Regional Jet	2.10E+07	2.14E+08	10%	10%
	Large Twin Aisle	2.06E+07	2.85E+08	10%	14%
	Large Quad	1.23E+07	1.75E+08	6%	8%
	General Aviation	1.23E+07	1.05E+08	6%	5%
	CESTOL	1.72E+07	7.84E+07	8%	4%
	Total	2.05E+08	2.11E+09		
2086	AC Category	Fuelburn (kg)	NOx (g)	% Fuelburn	% NOx
	Small Twin Aisle	3.57E+07	4.89E+08	14%	20%
	Single Aisle	8.82E+07	8.13E+08	35%	33%
	Regional Jet	2.33E+07	2.38E+08	9%	10%
	Large Twin Aisle	2.75E+07	3.45E+08	11%	14%
	Large Quad	1.69E+07	2.44E+08	7%	10%
	General Aviation	1.68E+07	1.53E+08	7%	6%
	CESTOL	4.23E+07	1.96E+08	17%	8%
	Total	2.51E+08	2.48E+09		

Figure F-19. CESTOL Categorized Fuelburn and NOx Results

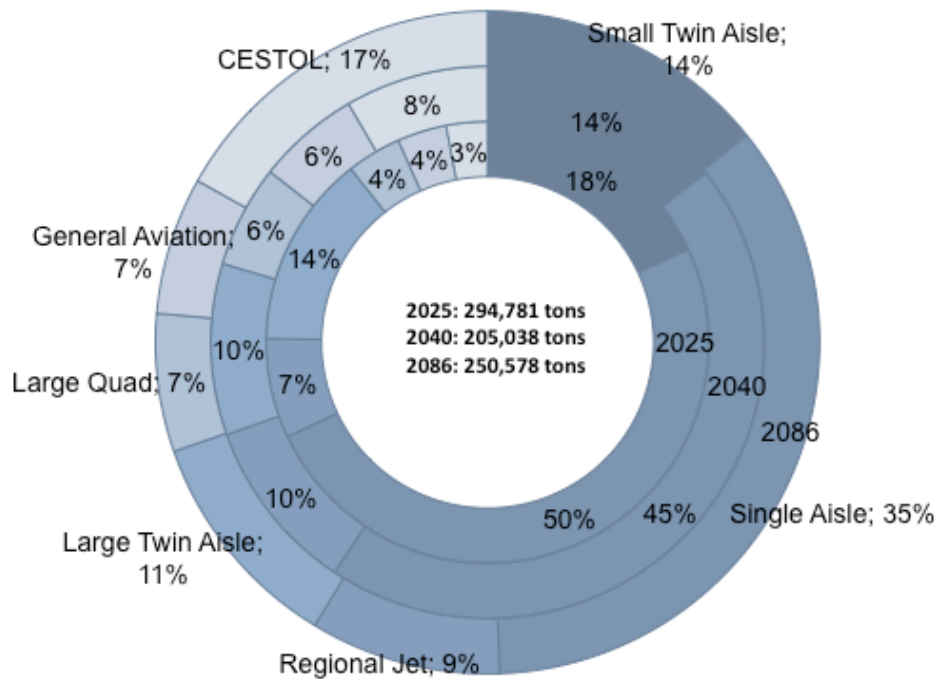


Figure F-20. CESTOL Categorized Fuelburn and NOx Results

F.17. Lessons Learned

The consistent issues with matching aircraft names and models as well as airport information challenges as well as format conversion make the execution of the environmental analysis difficult. Outside of these data issues it is actually relatively easy to execute a systemwide environmental analysis with this new generation of environmental tool.

The results—especially with regards to fuelburn and NO_x—demonstrate the importance of how the fleet and assignment of aircraft to flights is evolved over time, especially how new technology aircraft are introduced, while replacing existing aircraft, and how this interacts with the size of the aircraft operated on certain flights. This demonstrates the need to introduce a “family” of aircraft to account for the size differences within a certain class of aircraft. Otherwise, the introduction of a new aircraft will significantly distort the environmental characteristics of the overall fleet.

This report also only shows a small fraction of the results, which in total amount to ~400 Gb of data. Overall, this was a significant effort to demonstrate the first time through a complex tool chain and many lessons were learned about how to best define the scenarios to maximize the amount of information that can be extracted from the environmental results.

Table F-1. Overview of Baseline Scenario Error Statistics

Treatment	takeoffs	flights	Percent imported	Known APM losses	% APM Loss	Known AEM losses	% AEM Loss	All Exec. Errors	% Exec Errors	performance	emissions	Percent loss
2025_job654_nv2_cestnl_final	64146	62778	97.87%	1143	1.78%	3067	4.78%	4814	7.50%	57585	55189	13.96%
2040_job657_nv2_cesto_final	76719	74787	98.30%	1303	1.71%	3499	4.60%	5401	7.10%	72048	67411	11.39%
2086_job658_nv2_cesto_final	106348	104581	98.34%	1773	1.67%	4666	4.39%	7267	6.83%	99166	95374	10.32%
job_752_CTR2_2025_treatment_100p	63657	62545	98.25%	711	1.12%	374	0.59%	1673	2.63%	61237	60688	4.38%
job_748_CTR2_2040_treatment_100p	73326	72065	98.28%	826	1.13%	435	0.59%	1953	2.66%	69078	69163	5.08%
job_749_CTR2_2086_treatment_100p	91379	89606	98.06%	1219	1.33%	638	0.70%	2803	3.07%	86534	86115	5.76%
job_1_VL11_2025_treatment_100p	67068	66588	97.79%	755	1.13%	374	0.56%	1759	2.62%	64385	64035	4.52%
job_3_VL11_2040_treatment_100p	78361	76362	97.45%	889	1.13%	435	0.56%	2090	2.67%	73482	73923	5.66%
job_4_UAS1_2025_treatment_100p	67258	66087	98.26%	1512	2.25%	374	0.56%	3292	4.89%	63939	63575	5.48%
job_5_UAS1_2040_treatment_100p	75922	74599	98.26%	1624	2.14%	435	0.57%	3564	4.69%	71432	71503	5.82%
job_7_UAS1_2086_treatment_100p	92188	90417	98.08%	2017	2.19%	638	0.69%	4413	4.79%	87661	87118	5.50%
job_24_ALL_2025_treatment_100p	72590	71043	97.87%	1561	2.15%	374	0.52%	3389	4.67%	68959	68604	5.49%
job_55_ALL_2040_treatment_100p.tar.gz	88227	86136	97.63%	1722	1.95%	435	0.49%	3774	4.28%	82172	82553	6.43%
job_68_ALL_2086_treatment_100p.tar.gz	119188	116610	97.84%	2255	1.89%	638	0.54%	4889	4.10%	112620	112428	5.67%
job_43_SST1_2040_treatment_100p.tar.gz	71831	70568	98.24%	826	1.15%	435	0.61%	1953	2.72%	68055	68162	5.11%
job_57_SST1_2086_treatment_100p.tar.gz	88099	86391	98.06%	1271	1.39%	638	0.72%	2801	3.18%	84015	82917	5.88%

Table F-2. Overview of Vehicle Scenario Error Statistics

Baseline	takeoffs	flights	Percent imported	Known APM losses	% APM Loss	Known AEM losses	% AEM Loss	All Exec. Errors	% Exec Errors	performance	emissions	Percent loss
2025_job655_nv2_cestol_baseline_100p	64161	62802	97.88%	1136	1.77%	3066	4.78%	4801	7.48%	58449	55990	12.74%
2040_job656_nv2_cestol_baseline_100p	76119	74441	97.80%	1288	1.69%	3499	4.60%	5379	7.07%	69731	66204	13.03%
2086_job659_nv2_cestol_baseline_100p	106516	102585	96.31%	1706	1.60%	4664	4.38%	7190	6.75%	99800	95238	10.59%
job_651_XXXX_2025_baseline_100p	63165	62053	98.24%	711	1.13%	374	0.59%	1674	2.65%	59713	59528	5.76%
job_653_XXXX_2040_baseline_100p	71830	70567	98.24%	825	1.15%	435	0.61%	1952	2.72%	69200	68802	4.22%
job_680_XXXX_2086_baseline_100p	88095	86390	98.06%	1222	1.39%	638	0.72%	2801	3.18%	82536	82624	6.21%
job_651_XXXX_2025_baseline_100p	63165	62053	98.24%	711	1.13%	374	0.59%	1674	2.65%	59713	59528	5.76%
job_653_XXXX_2040_baseline_100p	71830	70567	98.24%	825	1.15%	435	0.61%	1952	2.72%	69200	68802	4.22%
job_651_XXXX_2025_baseline_100p	63165	62053	98.24%	711	1.13%	374	0.59%	1674	2.65%	59713	59528	5.76%
job_653_XXXX_2040_baseline_100p	71830	70567	98.24%	825	1.15%	435	0.61%	1952	2.72%	69200	68802	4.22%
job_680_XXXX_2086_baseline_100p	88095	86390	98.06%	1222	1.39%	638	0.72%	2801	3.18%	82536	82624	6.21%
2025_job655_nv2_cestol_baseline_100p	64161	62802	97.88%	1136	1.77%	3066	4.78%	4801	7.48%	58449	55990	12.74%
2040_job656_nv2_cestol_baseline_100p.tar.gz	76119	74441	97.80%	1288	1.69%	3499	4.60%	5379	7.07%	69731	66204	13.03%
2086_job659_nv2_cestol_baseline_100p.tar.gz	106516	102585	96.31%	1706	1.60%	4664	4.38%	7190	6.75%	99800	95238	10.59%
2040_job653_nv2_baseline_100p.tar.gz	71830	70567	98.24%	825	1.15%	435	0.61%	1952	2.72%	69200	68802	4.22%
job_680_XXXX_2086_baseline_100p.tar.gz	88095	86390	98.06%	1222	1.39%	638	0.72%	2801	3.18%	82536	82624	6.21%

Table F-3. Overview of Aircraft Category Mappings.

ACCODE	CATEGORY	ACCODE	CATEGORY	ACCODE	CATEGORY
A300B2-2	Small Twin Aisle	CL300	General Aviation	HS125-1000	General Aviation
A300C4-6	Small Twin Aisle	CL600	Regional Jet	HS125-6	General Aviation
A310-3	Single Aisle	CL604	Regional Jet	HS125-8	General Aviation
A318-1	Single Aisle	CNA150	General Aviation	HS125-9	General Aviation
A319-1X/LR	Single Aisle	CNA172	General Aviation	IAI1124A	General Aviation
A320-2	Single Aisle	CNA182	General Aviation	IAI1125	General Aviation
A321-1	Single Aisle	CNA206	General Aviation	IAI1126	General Aviation
A330-2	Small Twin Aisle	CNA208	General Aviation	J31	Regional Jet
A330-3	Small Twin Aisle	CNA210	General Aviation	J32-EP	Regional Jet
A340-3	Large Quad	CNA310	General Aviation	JETSTAR-II/731	General Aviation
A340-6	Large Quad	CNA340	General Aviation	LC40	General Aviation
A380-8	Large Quad	CNA402	General Aviation	LC41	General Aviation
AC500	Regional Jet	CNA414	General Aviation	LCTR2-01	CTR
AEROSTAR	General Aviation	CNA421	General Aviation	LEAR24	General Aviation
AN26	Regional Jet	CNA425	General Aviation	LEAR25	General Aviation
ATR42-320	Regional Jet	CNA441	General Aviation	LEAR28	General Aviation
ATR72-5	Regional Jet	CNA500	General Aviation	LEAR31	General Aviation
aUAS	UAS	CNA501	General Aviation	LEAR35	General Aviation
aVLJ	VLJ	CNA525	General Aviation	LEAR40	General Aviation
B707-1	Single Aisle	CNA550-5	General Aviation	LEAR45XR	General Aviation
B717-2	Single Aisle	CNA552	General Aviation	LEAR55	General Aviation
B737-7	Single Aisle	CNA560-XLS	General Aviation	LEAR60	General Aviation
B737-8	Single Aisle	CNA650	General Aviation	MD11	Small Twin Aisle
B737-9	Single Aisle	CNA680	General Aviation	MIL-C130	Regional Jet
B747-4	Large Quad	CNA750	General Aviation	MIL-P3	Regional Jet
B747-8	Large Quad	COMMANDER690	General Aviation	MIL-UC26C	Regional Jet
B757-2	Small Twin Aisle	COMMANDER980/1000	General Aviation	MOONEY-M20K	General Aviation
B757-3	Small Twin Aisle	CRJ1	Regional Jet	MU2	General Aviation
B767-2ER	Small Twin Aisle	CRJ2	Regional Jet	MU300	General Aviation
B767-3	Small Twin Aisle	CRJ7	Regional Jet	N150	Single Aisle
B767-4	Small Twin Aisle	CRJ9	Regional Jet	N301	Large Twin Aisle
B777-2ER	Large Twin Aisle	CV640	Regional Jet	P180	General Aviation
B777-3	Large Twin Aisle	DC3	Regional Jet	P68	General Aviation
B777-3ER	Large Twin Aisle	DHC8-1	Regional Jet	PA24	General Aviation
B787-9	Small Twin Aisle	DHC8-3	Regional Jet	PA27	General Aviation
BAE146-RJ70	Regional Jet	DHC8Q-2	Regional Jet	PA28	General Aviation
BEECH100	General Aviation	DIAMOND-DA40	General Aviation	PA31	General Aviation
BEECH18	General Aviation	DO328-1	Regional Jet	PA31T	General Aviation
BEECH19	General Aviation	DO328JET	Regional Jet	PA32	General Aviation
BEECH1900-D	Regional Jet	EMB110	Regional Jet	PA34	General Aviation
BEECH200	General Aviation	EMB120	Regional Jet	PA42	General Aviation
BEECH23	General Aviation	ERJ135	Regional Jet	PA46T	General Aviation
BEECH300	General Aviation	ERJ145-LR	Regional Jet	PC12	General Aviation
BEECH36	General Aviation	ERJ170	Regional Jet	PIPER32	General Aviation
BEECH400	General Aviation	ERJ190	Regional Jet	PREMIER	General Aviation
BEECH55	General Aviation	FAL100	General Aviation	SA226	General Aviation
BEECH58	General Aviation	FAL200	General Aviation	SA26	General Aviation
BEECH60	General Aviation	FAL2000EX	General Aviation	SAAB2000	Regional Jet
BEECH65	General Aviation	FAL50-EX	General Aviation	SAAB340-B+	Regional Jet
BEECH80	General Aviation	FAL900C	General Aviation	SABR65	General Aviation
BEECH90	General Aviation	GLOBALEXPRESS	General Aviation	SABR80	General Aviation
BEECH99	General Aviation	GRUMMAN-AA5	General Aviation	SC7-3A-1	General Aviation
CASA212-4	Regional Jet	GRUMMAN-GA7	General Aviation	SD360-3	Regional Jet
CESSNA150	General Aviation	GULF1	General Aviation	SOCATA-TB20	General Aviation
CESSNA172RG	General Aviation	GULF2-SP	General Aviation	SR20	General Aviation
CESSNA303	General Aviation	GULF3	General Aviation	SR22	General Aviation
CESSNA337	General Aviation	GULF4	General Aviation	SST01	SST
CESSNA404	General Aviation	GULF4-SP	General Aviation	TBM700	General Aviation
CESSNAR182	General Aviation	GULF5	General Aviation		
CESTOL	CESTOL				

cliii Boeker, E., “AEDT Algorithm Description Document, Aircraft Acoustics Module, Version 2.1,” Prepared for FAA, February 2008.

cliv Hansen, A., Gerbi, P., Regan, G., Roof, C., Rose, D., Wilson, A., “AEDT alpha-Application User’s Guide, Version 0.1,” Prepared for FAA, June 2009.

clv Hall, C., Smith, D., Soucacos, P., Hansen, A., Nwokeji, P., Regan, G., “AEDT Database Description Document, Fleet Database, Version 2.2.3,” Prepared for FAA, November 2008.

clvi Baker, G., “AEDT Database Description Document, Airport Database, Version 1.5.5,” Prepared for FAA, April 2009.

clvii Malwitz, A., Roof, C., Hansen, A., “AEDT Algorithm Description Document, ACES/Simmod Data Conversion Module, Version 1.0.1,” Prepared for FAA, December 2008.

clviii Malwitz, A., Roof, C., Hansen, A., “AEDT Interface Control Document, ACES/Simmod Data Conversion Module, Version 1.0.1,” Prepared for FAA, December 2008.

clix Baker, G., Hansen, A., Malwitz, A., Roof, C. “AEDT Database Description Document, Results Database, Version 0.1.0,” Prepared for FAA, March 2009.

clx Malwitz, A., Soucacos, P., “AEDT Algorithm Description Document, Aircraft Emissions Module, Version 1.4,” Prepared for FAA, August 2009.

clxi Dinges, E., “AEDT Algorithm Description Document, Aircraft Performance Module, Version 2.7.0,” Prepared for FAA, August 2008.

This page intentionally left blank.

Appendix G. Safety Hazards Table

Hazard Description	Known Hazard	New Hazard	Phase of Operation	Possible Effect(s)	Title	Likelihood of Occurrence	Risk Level (only vehicles affected)					
							CESTOL	VLJ	UAS	SST	LCTR	
Aircraft executes a tighter spiral pattern to achieve a slower approach speed than conventional aircraft.	x		Approach	near mid-air collision (NMAC)	Hazardous	Extremely remote, based on SME analysis	Medium					
Aircraft susceptible to wind gusts due to low-wing loading.		x	Takeoff, Climb, Cruise, Descent, Approach, Landing, Missed Approach, Go-Around, Emergency Landing	Reduced passenger ride quality comfort rating resulting from frequent sudden jolts, excessive ups and downs, or side-to-side motions	Major	Remote, based on SME analysis	Medium					

Hazard Description	Known Hazard	New Hazard	Phase of Operation	Possible Effect(s)	Title	Likelihood of Occurrence	Risk Level (only vehicles affected)					
							CESTOL	VLJ	UAS	SST	LCTR	
The absolute V _{stall} margin for the aircraft is limited (V _{ref} is 1.3x or less than V _s).		x	Takeoff, Climb, Cruise, Descent, Approach, Landing, Missed Approach, Go-Around, Emergency Landing	Operating in critical phases of flight reduces the stall safety margin, thus impacting performance-based operations	Major	Remote, based on SME analysis	Medium					
Pilots experiencing disorientation or lacking sufficient understanding of the unique precision required of the departure trajectory and its constraints may fail to comply with speed restrictions.	x		Climb, Cruise, Descent, Approach	Decreased performance capability with respect to trajectory-based and performance-based operations	Hazardous	Remote, based on SME analysis	High	High				

Hazard Description	Known Hazard	New Hazard	Phase of Operation	Possible Effect(s)	Title	Likelihood of Occurrence	Risk Level (only vehicles affected)				
							CESTOL	VLJ	UAS	SST	LCTR
Exceeding speed restrictions.	x		Climb, Cruise, Descent, Approach	Aircraft traveling at high speed may not be able to maintain a tight turn radius and remain in protected airspace on departure. This could result in a near mid-air requiring radical maneuvering or an actual mid-air collision, especially if there is high-density airspace adjacent to or above the departure protected airspace. Additionally, expected throughput could be negatively affected.	Hazardous	Remote, based on SME analysis	High	High			

Hazard Description	Known Hazard	New Hazard	Phase of Operation	Possible Effect(s)	Title	Likelihood of Occurrence	Risk Level (only vehicles affected)				
							CESTOL	VLJ	UAS	SST	LCTR
Aircraft experiencing rapid speed changes (i.e., arrival to approach speed), coupled with rapid banking in an attempt to comply with noise abatement procedures.	x		Descent and Approach	The aircraft could stall, if it 1) is allowed to decelerate below its minimum stall speed for the bank angle or 2) if the bank angle becomes too steep to be maneuvered at the current rate of speed. In turn, the aircraft may go outside of protected airspace or experience a collision risk	Hazardous	Remote, based on SME analysis	High	High			

Hazard Description	Known Hazard	New Hazard	Phase of Operation	Possible Effect(s)	Title	Likelihood of Occurrence	Risk Level (only vehicles affected)				
							CESTOL	VLJ	UAS	SST	LCTR
Upon reaching the airport boundary while performing a spiraling descent, flight crew fails to perform a rapid deceleration speed transition correctly, allowing the airspeed to decrease below the aircraft's stall speed due to its narrower absolute stall safety margin	x		Approach	The aircraft could stall, leading to potential catastrophic loss of aircraft, passengers, crews, or persons on the ground.	Major	Remote, based on SME analysis	Medium	Medium			
Flight crew unable to identify targets on a steep descent angle caused by fuselage "blinking," from the low-wing configuration (if the wing is visible from the cockpit), or a cockpit structural windscreen view restriction.	x		Descent and Approach	Reduced pilot visibility because of blind spots.	Hazardous	Remote, based on SME analysis	High				

Hazard Description	Known Hazard	New Hazard	Phase of Operation	Possible Effect(s)	Title	Likelihood of Occurrence	Risk Level (only vehicles affected)				
							CESTOL	VLJ	UAS	SST	LCTR
Aircraft flies into wake encounter during spiral approaches.	x		Approach	Loss of control	Major	Remote, based on SME analysis	Medium	Medium			
Flight crew fails to use the correct automation procedures to configure the aircraft.	x		Takeoff, Climb, Cruise, Descent, Approach, Landing, Missed Approach, Go-Around, Emergency Landing	Loss of individual or crew situational awareness	Major	Remote, based on SME analysis	Medium	High	Medium	Medium	Medium
Flight crew places too much confidence in the aircraft's automation capabilities.	x		Takeoff, Climb, Cruise, Descent, Approach, Landing, Missed Approach, Go-Around, Emergency Landing	Loss of situational awareness, loss of positional awareness	Major	Remote, based on SME analysis	Medium	High	Medium	Medium	Medium

Hazard Description	Known Hazard	New Hazard	Phase of Operation	Possible Effect(s)	Title	Likelihood of Occurrence	Risk Level (only vehicles affected)				
							CESTOL	VLJ	UAS	SST	LCTR
Aircraft lands on short runway (less than 3,000 feet) with a tailwind.	x		Landing	Runway Excursion, Rejected landing and subsequent reconfiguring of traffic operations into the airport potentially impacting super-density arrival/ departure operations, increasing system delays	Major	Remote, based on SME analysis	Medium	Medium			

Hazard Description	Known Hazard	New Hazard	Phase of Operation	Possible Effect(s)	Title	Likelihood of Occurrence	Risk Level (only vehicles affected)					
							CESTOL	VLJ	UAS	SST	LCTR	
Possible aircraft instability as CG moves toward aft limit at critical airspeeds.		x	Takeoff, Climb, Cruise, Descent, Approach, Landing, Missed Approach, Go-Around, Emergency Landing	Loss of control	Hazardous	Extremely Remote, based on SME analysis	Medium					
Insufficient approach climb (go-around) capability due to certain configurations of the aircraft, flight profiles, and runways.		x	Go-Around	Loss of control	Hazardous	Extremely Remote, based on SME analysis	Medium					

Hazard Description	Known Hazard	New Hazard	Phase of Operation	Possible Effect(s)	Title	Likelihood of Occurrence	Risk Level (only vehicles affected)				
							CESTOL	VLJ	UAS	SST	LCTR
Insufficient flight deck visibility during steep rapid climb out.	x		Takeoff, Climb, Cruise, Descent, Approach, Landing, Missed Approach, Go-Around, Emergency Landing	Lack of pilot visibility over the nose	Hazardous	Remote, based on SME analysis	High			High	
Reduced climb performance capability of aircraft as payload weight increases.		x	Climb	A decrease in the end-of-runway obstacle clearance margin and an increase in noise footprint during climb out along the departure flight path	Major	Remote, based on SME analysis	Medium				
While executing a spiral approach, the aircraft may experience reduced flight path control	x		Approach	An ncrease in pilot workload and noise footprint	Hazardous	Extremely Remote, based on SME analysis	Medium	Medium			

Hazard Description	Known Hazard	New Hazard	Phase of Operation	Possible Effect(s)	Title	Likelihood of Occurrence	Risk Level (only vehicles affected)				
							CESTOL	VLJ	UAS	SST	LCTR
precision.											
While executing a steep approach, the aircraft may experience reduced flight path control precision.		x	Approach	A reduction in flight path control precision increasing pilot workload and noise footprint.	Hazardous	Extremely Remote, based on SME analysis	Medium				

Hazard Description	Known Hazard	New Hazard	Phase of Operation	Possible Effect(s)	Title	Likelihood of Occurrence	Risk Level (only vehicles affected)					
							CESTOL	VLJ	UAS	SST	LCTR	
Failure of the aircraft system stability or control augmentation		x	Takeoff, Climb, Cruise, Descent, Approach, Landing, Missed Approach, Go-Around, Emergency Landing	An increase in wind effects (i.e., gusts or shear) on the aircraft creating greater pilot workload during low-speed approach task by decreasing both static and dynamic stability. Touchdown accuracy may also be decreased.	Hazardous	Extremely Remote, based on SME analysis	Medium					
Rollback ice accumulation on aircraft while operating at slow speed, high angle-of-attack flight operations such as holding, and additional time spent maneuvering in			Maneuvering	Loss of control	Hazardous	Remote, based on SME analysis	High					

Hazard Description	Known Hazard	New Hazard	Phase of Operation	Possible Effect(s)	Title	Likelihood of Occurrence	Risk Level (only vehicles affected)				
							CESTOL	VLJ	UAS	SST	LCTR
any low-level icing conditions.											
Operating an aircraft with an improper thermal anti-ice system that does not evaporate 100% of the water on the wing leading edge surface for an extended period of time, particularly at slow airspeeds.		x	Takeoff, Climb, Cruise, Descent, Approach, Landing, Missed Approach, Go-Around, Emergency Landing	Loss of control	Hazardous	Extremely Remote, based on SME analysis	Medium				

Hazard Description	Known Hazard	New Hazard	Phase of Operation	Possible Effect(s)	Title	Likelihood of Occurrence	Risk Level (only vehicles affected)				
							CESTOL	VLJ	UAS	SST	LCTR
A non-standardized command display unit (CDU) in the FMS due to a lack of configuration standards.	x		All	System mode confusion and possibly operating the aircraft outside of its flight envelope or intended flight operations parameters.	Major	Remote, based on SME analysis	Medium	High		Medium	Medium
Limited crosswind control effectiveness while executing steep approach in crosswind conditions.			Takeoff and Landing	Runway excursion, nose landing gear side-loading, and ground looping	Hazardous	Remote, based on SME analysis	High				
A nose- gear landing while executing a manual flare from steep approach.			Approach	Potential nose gear collapse, loss of control, ground loop	Hazardous	Remote, based on SME analysis	High				

Hazard Description	Known Hazard	New Hazard	Phase of Operation	Possible Effect(s)	Title	Likelihood of Occurrence	Risk Level (only vehicles affected)					
							CESTOL	VLJ	UAS	SST	LCTR	
Failure to recover from windshear on steep approach.			Approach	The inability to climb-out of a windshear encounter, thus impacting terrain or other obstacles	Catastrophic	Extremely Remote, based on SME analysis	High					
The slower approach speeds of the CESTOL compared to similar conventional jet transports.		x	Approach	Possible difficulty in maintaining spacing in mixed traffic	Hazardous	Remote, based on SME analysis	High					
Flight crews possessing varying skills, abilities, and attitudes toward technology and automation.	x		All	Operation of the aircraft in ways other than intended or expected by the original designers, which could lead to damages or fatalities.	Major	Remote based on SME analysis	Medium	High				

Hazard Description	Known Hazard	New Hazard	Phase of Operation	Possible Effect(s)	Title	Likelihood of Occurrence	Risk Level (only vehicles affected)					
							CESTOL	VLJ	UAS	SST	LCTR	
Degradation of pilot manual flying skills due to a reliance on flight deck automation.		x	All	A crew's inability to adequately fly the aircraft in the event of automation malfunction or failure	Hazardous	Remote, based on SME analysis	High					
Because of the many types of aircraft introduced in NextGen, pilots may confuse the operations of one aircraft for another incorrectly.	x		All	Old habits or training interfering with new aircraft operations	Major	Remote, based on SME analysis	Medium	High	Medium	Medium	Medium	Medium
Flight crew unconsciously relinquishes command responsibilities momentarily to automated systems (passive command syndrome).	x		All		Major	Remote, based on SME analysis	Medium	High		Medium	Medium	Medium

Hazard Description	Known Hazard	New Hazard	Phase of Operation	Possible Effect(s)	Title	Likelihood of Occurrence	Risk Level (only vehicles affected)					
							CESTOL	VLJ	UAS	SST	LCTR	
Failure of the [CESTOL] aircraft systems to notify the flight crew of new system configuration changes.		x	All	Crew fails to recognize early trends indicating anomalous component performance		Extremely Remote, based on SME analysis	Medium					
Flight crew flying on the back side of the power curve affecting precise flight path control due to steeper approach and departure path angles.	x		Climb and Approach	Classically trained crews might become confused, thereby increasing the possibility of a sink rate too great to perform a safe go-around, if required	Hazardous	Extremely Remote, based on SME analysis	Medium	High				

Hazard Description	Known Hazard	New Hazard	Phase of Operation	Possible Effect(s)	Title	Likelihood of Occurrence	Risk Level (only vehicles affected)				
							CESTOL	VLJ	UAS	SST	LCTR
The [CESTOL] aircraft's flight management system (FMS) or the flight crew does not adequately compensate for changing winds during the descent.		x	Takeoff, Climb, Cruise, Descent, Approach, Landing, Missed Approach, Go-Around, Emergency Landing	Protected airspace violations, NMAC, or mid-air collision	Catastrophic	Remote, based on SME analysis	High				
Flight crew inadequately compensates for changing winds with respect to its expected trajectory.		x	Takeoff, Climb, Cruise, Descent, Approach, Landing, Missed Approach, Go-Around, Emergency Landing	Violation of bank angles or stall margin limitations	Catastrophic	Extremely Remote, based on SME analysis	High				
Flight crew failure to comply with crossing restrictions.	x		Climb and Descent	Adverse impacts on flow corridors setup in NextGen, NMAC, or mid-air collision	Catastrophic	Remote, based on SME analysis	High	High	High	High	High

Hazard Description	Known Hazard	New Hazard	Phase of Operation	Possible Effect(s)	Title	Likelihood of Occurrence	Risk Level (only vehicles affected)				
							CESTOL	VLJ	UAS	SST	LCTR
Aircraft fails to remain in protected airspace.	x		Climb, Descent, Approach, Maneuvering	Violation of protected airspace, NMAC, or mid-air collision	Catastrophic	Remote, based on SME analysis	High	High	High		
Failure of the [CESTOL] flight crew to maintain proper crosswind adjustment while executing a spiral approach.		x	Approach	Drifting over into another approach path, NMAC, or mid-air collision	Catastrophic	Remote, based on SME analysis	High				
Executing rapid speed changes (arrival to approach speed) coupled with rapid banking in the CESTOL aircraft (in an attempt to comply with noise abatement procedures).		x	Approach	Aircraft may stall	Hazardous		Medium				

Hazard Description	Known Hazard	New Hazard	Phase of Operation	Possible Effect(s)	Title	Likelihood of Occurrence	Risk Level (only vehicles affected)					
							CESTOL	VLJ	UAS	SST	LCTR	
Wake turbulence encounters on approach.	x		Takeoff, Climb, Cruise, Descent, Approach, Landing, Missed Approach, Go-Around, Emergency Landing	Loss of control of the aircraft both laterally or longitudinally	Hazardous	Remote, based on SME analysis	High					
Limited directional control on roll-out (CESTOL only) with increasing crosswind component.		x	Landing	Runway excursion or loss of control	Hazardous	Remote, based on SME analysis	High					
Aircraft fails to maintain adequate separation from merging traffic of steep and stand simultaneous approaches to same runway.		x	Approach	Loss of separation, NMAC, mid-air collision	Catastrophic	Remote, based on SME analysis	High					

Hazard Description	Known Hazard	New Hazard	Phase of Operation	Possible Effect(s)	Title	Likelihood of Occurrence	Risk Level (only vehicles affected)					
							CESTOL	VLJ	UAS	SST	LCTR	
Incorrect use of the automated air traffic management system.		x	N/A		Hazardous	Extremely Remote, based on SME analysis	Medium					
the Dispatcher is unaware of the flight crew and the aircraft's skills due to a lack of understanding of the CESTOL's capabilities.		x	N/A	Exceeding either the flight crew's or aircraft's capabilities (or both)	Major	Remote, based on SME analysis	Medium					
Airline/operator fails to establish adequate stabilized approach criteria and mandatory go-around/rejected landing policy.		x	N/A	Crew confusion, runway incursion, runway excursion	Hazardous	Extremely Remote, based on SME analysis	Medium					
Failure to program the FMS correctly and cross check.	x		All	The aircraft may deviate from the desired flight path	Hazardous	Extremely Remote, based on SME analysis	Medium	Medium		Medium	Medium	Medium

Hazard Description	Known Hazard	New Hazard	Phase of Operation	Possible Effect(s)	Title	Likelihood of Occurrence	Risk Level (only vehicles affected)				
							CESTOL	VLJ	UAS	SST	LCTR
An aircraft that fails to adhere to the missed approach instructions could result in the aircraft violating another aircraft's flight path.	x		Missed Approach	Violation of protected airspace, undershoots or overshoots the runway, excessive sink rate, which could result in the VLJ aircraft being involved in a near mid-air, mid-air collision, impact with terrain, or other objects.	Catastrophic	Extremely Remote, based on SME analysis	High	High	High	High	High
Aircrafts lands on the wrong runway (parallel runway).			Landing	runway incursion, runway excursion	Hazardous	Extremely Remote, based on SME analysis	Medium	High	Medium	Medium	Medium

Hazard Description	Known Hazard	New Hazard	Phase of Operation	Possible Effect(s)	Title	Likelihood of Occurrence	Risk Level (only vehicles affected)				
							CESTOL	VLJ	UAS	SST	LCTR
Flight crew fails to self-separate at non-towered and non-controlled air fields.			Climb, Descent, Approach, Maneuvering, Landing	NMAC, mid-air collision	Catastrophic	Extremely Remote, based on SME analysis		High	High		
Potential for increased numbers of high performance aircraft operating on time-critical schedules at non-towered and non-controlled airfields increase the mix (including training flights) of operations and pilot skill sets. The high performance VLJ, with professionally trained pilots on a schedule may need to squeeze in before a slower aircraft with student pilots.			N/A	NMAC, mid-air collision	Catastrophic	Remote, based on SME analysis		High			

Hazard Description	Known Hazard	New Hazard	Phase of Operation	Possible Effect(s)	Title	Likelihood of Occurrence	Risk Level (only vehicles affected)				
							CESTOL	VLJ	UAS	SST	LCTR
Pilot succumbs to information overload in the terminal environment.	x		Takeoff, Climb, Descent, Approach, Landing	Loss of positional awareness, loss of situational awareness	Hazardous	Extremely Remote, based on SME analysis	Medium	High	Medium	Medium	Medium
Pilot fails to manage workload.	x		All	Loss of situational awareness	Hazardous	Extremely Remote, based on SME analysis	Medium	High	Medium	Medium	Medium
Pilot falls behind in completing required tasks	x		All	Loss of control, loss of situational awareness	Hazardous	Extremely Remote, based on SME analysis	Medium	High	Medium	Medium	Medium
Pilot attempts to comply with last-minute runway changes on approaches at high-density airports by attempting to re-program the FMS, instead of using a lower level of automation to	x		Landing	Loss of control, runway incursion, runway excursion	Hazardous	Extremely Remote, based on SME analysis	Medium	High	Medium	Medium	Medium

Hazard Description	Known Hazard	New Hazard	Phase of Operation	Possible Effect(s)	Title	Likelihood of Occurrence	Risk Level (only vehicles affected)				
							CESTOL	VLJ	UAS	SST	LCTR
control the flight path.											
Pilot fails to configure the aircraft for departure and catch it on crosscheck.			Takeoff	Loss of control	Hazardous	Extremely Remote, based on SME analysis	Medium	High	Medium	Medium	Medium
Pilot fails to properly apply breaking technique of an aircraft not equipped with anti-lock breaking systems.		x	Landing	Loss of control, runway excursion	Hazardous	Remote, based on SME analysis		High			
Pilot fails to arrest the descent.	x		Descent, Approach, Landing	CFIT	Catastrophic	Extremely Remote, based on SME analysis	High	High	High	High	High

Hazard Description	Known Hazard	New Hazard	Phase of Operation	Possible Effect(s)	Title	Likelihood of Occurrence	Risk Level (only vehicles affected)				
							CESTOL	VLJ	UAS	SST	LCTR
Pilot fails to set the altimeter to correctly.	x		Takeoff, Climb, Cruise, Descent, Approach, Landing, Missed Approach, Go-Around, Emergency Landing	CFIT	Hazardous	Extremely Remote, based on SME analysis	Medium	High	Medium	Medium	Medium
Pilot fails to adhere to reduced vertical separation minima (RVSM) procedures during transition to and from Class A airspace.	x		Climb, Cruise, Descent	NMAC, mid-air collision	Catastrophic	Extremely Remote, based on SME analysis		High			
Pilot fails to exercise proper energy management technique with regard to maintaining spacing and adhering to separation minima in terminal airspace.	x		Takeoff, Climb, Cruise, Descent, Approach, Landing, Missed Approach, Go-Around, Emergency Landing	NMAC, mid-air collision	Catastrophic	Extremely Remote, based on SME analysis		High			

Hazard Description	Known Hazard	New Hazard	Phase of Operation	Possible Effect(s)	Title	Likelihood of Occurrence	Risk Level (only vehicles affected)				
							CESTOL	VLJ	UAS	SST	LCTR
Failure to maintain adequate spacing to protect against wake turbulence when trailing larger aircraft .	x		Climb, Cruise, Descent, Approach	NMAC, mid-air collision	Catastrophic	Extremely Remote, based on SME analysis		High			
Aircraft merges from above or too close to other small, slow-moving aircraft.	x		Climb, Cruise, Descent, Approach, Maneuvering	NMAC, mid-air collision	Catastrophic	Extremely Remote, based on SME analysis		High		High	
Flight crew fails to expeditiously recognize and/ or properly manage an event causing a single engine flameout.		x	Takeoff, Climb, Cruise, Descent, Approach, Landing, Missed Approach, Go-around, Emergency Landing	Loss of control	Catastrophic	Extremely Remote, based on SME analysis		High			
In single-pilot operations, there is a potential for increased headdown time with use of data	x		All	Loss of situational awareness	Hazardous	Remote, based on SME analysis		High			

Hazard Description	Known Hazard	New Hazard	Phase of Operation	Possible Effect(s)	Title	Likelihood of Occurrence	Risk Level (only vehicles affected)				
							CESTOL	VLJ	UAS	SST	LCTR
link.											
Aircraft fails to level off at assigned altitude.	x		Climb, Descent	NMAC, mid-air collision	Catastrophic	Extremely Remote, based on SME analysis	High	High	High	High	High
Failure to maintain desired flight path during the spiral approach	x		Approach	NMAC, mid-air collision	Catastrophic	Extremely Remote, based on SME analysis	High	High			
Flight crew fails to maintain the correct spiral path on departure.	x		Approach	NMAC, mid-air collision	Catastrophic	Extremely Remote, based on SME analysis	High	High			

Hazard Description	Known Hazard	New Hazard	Phase of Operation	Possible Effect(s)	Title	Likelihood of Occurrence	Risk Level (only vehicles affected)				
							CESTOL	VLJ	UAS	SST	LCTR
Since VLJ aircraft have the capabilities of operating at altitudes of large commercial aircraft, there is the possibility of it encountering heavy jet turbulence while performing altitude change (pair-wise) maneuvers.		x	Climb and Descent	Loss of control	Hazardous	Extremely Remote, based on SME analysis		Medium			
Failure to adequately space trailing aircraft from a leading VLJ to account for the VLJ's runway occupancy when taxing off a long runway.		x	Cruise	Loss of control	Major	Remote, based on SME analysis		Medium			
ATC is unfamiliar with the VLJ aircraft's performance envelope relative to commercial and general aviation aircraft performance		x	All	NMAC, mid-air collision	Catastrophic	Extremely Remote, based on SME analysis		High			

Hazard Description	Known Hazard	New Hazard	Phase of Operation	Possible Effect(s)	Title	Likelihood of Occurrence	Risk Level (only vehicles affected)				
							CESTOL	VLJ	UAS	SST	LCTR
envelopes.											
Misleading transponder data is being sent to other aircraft.	x		Takeoff, Climb, Cruise, Descent, Approach, Landing, Missed Approach, Go-Around, Emergency Landing	NMAC, mid-air collision	Catastrophic	Extremely Remote, based on SME analysis	High	High	High	High	High
Inability to communicate with the UAS.		x	All	NMAC, mid-air collision	Catastrophic	Remote, based on SME analysis			High		
Remote pilot fails to transmit intentions on UNICOM, prior to entering the runway.		x	Takeoff	NMAC, mid-air collision	Catastrophic	Remote, based on SME analysis			High		

Hazard Description	Known Hazard	New Hazard	Phase of Operation	Possible Effect(s)	Title	Likelihood of Occurrence	Risk Level (only vehicles affected)				
							CESTOL	VLJ	UAS	SST	LCTR
Incorrect data is being sent to other aircraft.	x		All	NMAC, mid-air collision	Catastrophic	Extremely Remote, based on SME analysis	High	High	High	High	High
Undetected loss of ability to automatically respond to ATC command.		x	All	Loss of situational awareness , loss of control	Catastrophic	Extremely Remote, based on SME analysis			High		
A third-party communications system fails between UAS and ATC.		x	All	Loss of situational awareness , loss of control	Catastrophic	Extremely Remote, based on SME analysis			High		
Total loss of control power of subsystems (hydraulic/electrical).		x	All	Loss of control	Catastrophic	Extremely Remote, based on SME analysis			High		

Hazard Description	Known Hazard	New Hazard	Phase of Operation	Possible Effect(s)	Title	Likelihood of Occurrence	Risk Level (only vehicles affected)				
							CESTOL	VLJ	UAS	SST	LCTR
Remote pilot fails to adhere to the missed approach instructions, which could result in the UAS violating another aircraft's flight path.		x	Missed Approach	NMAC, mid-air collision	Catastrophic	Extremely Remote, based on SME analysis			High		
Display freezes with old information.		x	All	loss of situational awareness	Hazardous	Extremely Remote, based on SME analysis			Medium		
Propulsion unit fails during critical phase of flight	x		Takoff, Approach, Missed Approach, Go-Around, Landing, Emergency Landing	Loss of control	Hazardous	Extremely Remote, based on SME analysis	Medium	Medium	Medium	Medium	Medium
ATC fails to ensure appropriate separation behind aircraft.	x		Climb, Cruise Descent, Approach, Landing	NMAC, mid-air collision	Catastrophic	Extremely Remote, based on SME analysis	High	High	High	High	High

Hazard Description	Known Hazard	New Hazard	Phase of Operation	Possible Effect(s)	Title	Likelihood of Occurrence	Risk Level (only vehicles affected)				
							CESTOL	VLJ	UAS	SST	LCTR
UASs autonomous system fails in a human-in-the-loop system.		x	All	Loss of situational awareness	Hazardous	Extremely Remote, based on SME analysis			Medium		
Remote pilot fails to detect loss of propulsion.		x	All	Vehicle no longer is able to maintain altitude	Hazardous	Extremely Remote, based on SME analysis			Medium		
Undetected loss of ability to translate high-level direction to specific vehicle actions.		x	All	Loss of control	Hazardous	Extremely Remote, based on SME analysis			Medium		
Detected loss of ability to translate high-level direction to specific vehicle actions.		x	All	Loss of control	Hazardous	Extremely Remote, based on SME analysis			Medium		

Hazard Description	Known Hazard	New Hazard	Phase of Operation	Possible Effect(s)	Title	Likelihood of Occurrence	Risk Level (only vehicles affected)				
							CESTOL	VLJ	UAS	SST	LCTR
Inability to execute flight path command without soft landing flight termination function.		x	Climb, Cruise, Descent, Approach, Landing	Loss of control	Catastrophic	Extremely Remote, based on SME analysis			High		
Total loss of command and control data link functionality.		x	All	Loss of control	Catastrophic	Extremely Remote, based on SME analysis			High		
Degraded command and control data link functionality.		x	All	Loss of control	Hazardous	Extremely Remote, based on SME analysis			Medium		
Unauthorized access of command and control data.		x	All	Loss of control	Catastrophic	Extremely Remote, based on SME analysis			High		

Hazard Description	Known Hazard	New Hazard	Phase of Operation	Possible Effect(s)	Title	Likelihood of Occurrence	Risk Level (only vehicles affected)				
							CESTOL	VLJ	UAS	SST	LCTR
Undetected loss of prioritization of command and control data		x	All	Loss of control	Hazardous	Extremely Remote, based on SME analysis			Medium		
Total loss of ability to control the environment inside the UAS.		x	All	?	Catastrophic	Extremely Remote, based on SME analysis			High		
The remote pilot fails to detect loss of guidance command without alternate means to change flight path state.		x	Climb, Cruise, Descent, Approach, Landing, Missed Approach, Go-Around, Emergency Landing	Loss of control	Catastrophic	Extremely Remote, based on SME analysis			High		

Hazard Description	Known Hazard	New Hazard	Phase of Operation	Possible Effect(s)	Title	Likelihood of Occurrence	Risk Level (only vehicles affected)				
							CESTOL	VLJ	UAS	SST	LCTR
Inability to execute flight path commands, but soft landing flight termination is still functioning.		x	Climb, Cruise, Descent, Approach, Landing, Missed Approach, Go-Around, Emergency Landing	Flight termination executed	Hazardous	Extremely Remote, based on SME analysis			Medium		
Inability to translate high-level direction to specific vehicle actions, but soft landing flight termination is still functioning.		x	Climb, Cruise, Descent, Approach, Landing, Missed Approach, Go-Around, Emergency Landing	Flight termination executed	Hazardous	Extremely Remote, based on SME analysis			Medium		

Hazard Description	Known Hazard	New Hazard	Phase of Operation	Possible Effect(s)	Title	Likelihood of Occurrence	Risk Level (only vehicles affected)				
							CESTOL	VLJ	UAS	SST	LCTR
UAS's primary flight control surfaces respond slowly.		x	Takeoff, Climb, Cruise, Descent, Approach, Landing, Missed Approach, Go-Around, Emergency Landing	Pilot induced oscillation, loss of control	Hazardous	Extremely Remote, based on SME analysis			Medium		
Failure to detect a loss of flight termination function.		x	All	Loss of control	Catastrophic	Extremely Remote, based on SME analysis			High		
Misleading information is sent to/from the power subsystem (hydraulic/electrical).		x	All	Loss of control	Hazardous	Extremely Remote, based on SME analysis			Medium		
Incorrect flight path state is presented to the pilot.		x	All	Loss of situational awareness	Hazardous	Extremely Remote, based on SME analysis			Medium		

Hazard Description	Known Hazard	New Hazard	Phase of Operation	Possible Effect(s)	Title	Likelihood of Occurrence	Risk Level (only vehicles affected)				
							CESTOL	VLJ	UAS	SST	LCTR
Misleading information exists in the control environment inside the UAS.		x	All	Loss of situational awareness	Hazardous	Extremely Remote, based on SME analysis			Medium		
UAS provides incorrect navigation state.		x	All	Increased ATC and remote pilot workload	Hazardous	Extremely Remote, based on SME analysis			Medium		
Loss of guidance command without alternate means to change flight path, but with “soft landing” flight termination.		x	Takeoff, Climb, Cruise, Descent, Approach, Landing, Missed Approach, Go-Around, Emergency Landing	Loss of control	Catastrophic	Extremely Remote, based on SME analysis			High		

Hazard Description	Known Hazard	New Hazard	Phase of Operation	Possible Effect(s)	Title	Likelihood of Occurrence	Risk Level (only vehicles affected)				
							CESTOL	VLJ	UAS	SST	LCTR
Total loss of guidance command without alternate means to change flight path, without “soft landing” flight termination function.		x	Takeoff, Climb, Cruise, Descent, Approach, Landing, Missed Approach, Go-Around, Emergency Landing	Loss of control	Catastrophic	Extremely Remote, based on SME analysis			High		
Remote pilot is unable to discern objects and judgedistances between objects (especially at night).		x	All	NMAC, mid-air collision	Catastrophic	Remote based on SME analysis			High		
UASs conspicuity fails.		x	All	NMAC, mid-air collision	Catastrophic	Extremely Remote, based on SME analysis			High		

Hazard Description	Known Hazard	New Hazard	Phase of Operation	Possible Effect(s)	Title	Likelihood of Occurrence	Risk Level (only vehicles affected)				
							CESTOL	VLJ	UAS	SST	LCTR
UAS air traffic detection system fails.		x	All	NMAC, mid-air collision	Catastrophic	Extremely Remote, based on SME analysis			High		
Situational Awareness Data Link (SADL) [18] fails.		x	All	Loss of situational awareness	Hazardous	Extremely Remote, based on SME analysis			Medium		
Misleading information is sent from the UAS to the traffic information broadcast (TIS-B) system.		x	All	Loss of situational awareness	Hazardous	Extremely Remote, based on SME analysis			Medium		
Misleading information is sent from the UAS to the Airborne Separation Assurance System (ASAS).		x	All	NMAC, mid-air collision	Catastrophic	Extremely Remote, based on SME analysis			High		

Hazard Description	Known Hazard	New Hazard	Phase of Operation	Possible Effect(s)	Title	Likelihood of Occurrence	Risk Level (only vehicles affected)				
							CESTOL	VLJ	UAS	SST	LCTR
UAS is unable to detect adverse environmental conditions.		x	All	Loss of situational awareness, loss of control	Hazardous	Extremely Remote, based on SME analysis			Medium		
UAS is unable to track relative location of adverse environmental conditions.		x	All	Loss of situational awareness	Hazardous	Extremely Remote, based on SME analysis			Medium		
UAS is unable to convey relative location of adverse environmental conditions.		x	All	Loss of situational awareness	Hazardous	Extremely Remote, based on SME analysis			Medium		
UAS is unable to assess relative location of adverse environmental conditions.		x	All	Loss of situational awareness	Hazardous	Extremely Remote, based on SME analysis			Medium		

Hazard Description	Known Hazard	New Hazard	Phase of Operation	Possible Effect(s)	Title	Likelihood of Occurrence	Risk Level (only vehicles affected)				
							CESTOL	VLJ	UAS	SST	LCTR
UAS is unable to produce corrective action commands to adverse environmental conditions.		x	All	Loss of control	Hazardous	Extremely Remote, based on SME analysis			Medium		
Remote pilot loses situational awareness while operating multiple UASs.		x	All	Loss of situational awareness, NMAC, mid-air collision	Catastrophic	Extremely Remote, based on SME analysis			High		
Remote pilot fails to manage multiple instructions from various UASs.		x	All	Loss of situational awareness, NMAC, mid-air collision	Catastrophic	Extremely Remote, based on SME analysis			High		
Remote pilot fails to manage multiple UASs while addressing an off-nominal condition with one UAS under his/her control .		x	All	Loss of situational awareness, loss of control	Catastrophic	Remote, based on SME analysis			High		

Hazard Description	Known Hazard	New Hazard	Phase of Operation	Possible Effect(s)	Title	Likelihood of Occurrence	Risk Level (only vehicles affected)				
							CESTOL	VLJ	UAS	SST	LCTR
Air traffic controller fails to understand contingency and emergency procedures of UAS.		x	All	Loss of situational awareness	Major	Remote, based on SME analysis			Medium		
Restricted flightdeck visibility and placement of the nose landing gear aft of the flight deck.		x	Taxi	Loss of situational awareness, runway excursion	Major	Remote, based on SME analysis				Medium	
The flight crew over rotates the aircraft on takeoff, which could result in the empennage (tailstrike) colliding with the runway surface.	x		Takeoff	Tailstrike	Hazardous	Extremely Remote, based on SME analysis				Medium	
Failure of the Passive thermal cooling failure.		x	Cruise	Fatal temperatures in the cabin and possible boiling of fuel	Hazardous	Extremely Remote, based on SME analysis				Medium	

Hazard Description	Known Hazard	New Hazard	Phase of Operation	Possible Effect(s)	Title	Likelihood of Occurrence	Risk Level (only vehicles affected)				
							CESTOL	VLJ	UAS	SST	LCTR
Active thermal cooling failure.		x	Cruise	Damage to the engine leading edge, nozzle, wing leading edge, or nose tip	Hazardous	Extremely Remote, based on SME analysis				Medium	
Failure of the engine inlet variable geometry center body.		x	Takeoff, Climb, Cruise, Descent, Approach, Landing, Missed Approach, Go-Around, Emergency Landing	Flameout	Hazardous	Extremely Remote, based on SME analysis				Medium	
Variable geometry wing fails to extend during speed reduction transition		x	Descent, Approach, Landing, Missed approach, Go-Around, Emergency Landing	Faster than normal approach speed, runway excursion	Hazardous	Extremely Remote, based on SME analysis				Medium	

Hazard Description	Known Hazard	New Hazard	Phase of Operation	Possible Effect(s)	Title	Likelihood of Occurrence	Risk Level (only vehicles affected)				
							CESTOL	VLJ	UAS	SST	LCTR
Undetected failure of the stability augmentation system at high velocity above Mach 1.		x	Cruise	Structural failure	Catastrophic	Extremely Remote, based on SME analysis				High	
Flight crew fails to maintain adequate separation from other aircraft above Mach 1		x	Cruise	Loss of control of other aircraft	Catastrophic	Extremely Remote, based on SME analysis				High	
Undetected failure of the stability augmentation system at low velocity.		x	Takeoff, Climb, Cruise, Descent, Approach, Landing, Missed Approach, Go-Around, Emergency Landing	Loss of control	Hazardous	Extremely Remote, based on SME analysis				Medium	

Hazard Description	Known Hazard	New Hazard	Phase of Operation	Possible Effect(s)	Title	Likelihood of Occurrence	Risk Level (only vehicles affected)				
							CESTOL	VLJ	UAS	SST	LCTR
Undetected failure of the flight protection envelope system at low velocity.		x	Takeoff, Climb, Cruise, Descent, Approach, Landing, Missed Approach, Go-Around, Emergency Landing	Loss of control	Hazardous	Extremely Remote, based on SME analysis				Medium	
Undetected failure of the flight protection envelope system at high velocity.		x	Cruise	In flight break-up	Catastrophic	Extremely Remote, based on SME analysis				High	
Flight crew fails to recognize a failure of the FMS above Mach 1.		x	Cruise	Loss of positional awareness, NMAC	Hazardous	Extremely Remote, based on SME analysis				Medium	

Hazard Description	Known Hazard	New Hazard	Phase of Operation	Possible Effect(s)	Title	Likelihood of Occurrence	Risk Level (only vehicles affected)				
							CESTOL	VLJ	UAS	SST	LCTR
Pilot fails to exercise proper energy management technique with regard to maintaining spacing and adhering to separation minima in terminal airspace.	x		Takeoff, Climb, Cruise, Descent, Approach, Landing, Missed Approach, Go-Around, Emergency Landing	Loss of separation, NMAC	Hazardous	Extremely Remote, based on SME analysis	Medium	High	Medium	Medium	Medium
Flight crew fails to respond in a timely manner to a resolution alert (RA) from the collision avoidance system (e.g. traffic collision avoidance system (TCAS))		x	Takeoff, Climb, Cruise, Descent, Approach, Landing, Missed Approach, Go-Around	Loss of separation, NMAC, mid-air	Catastrophic	Extremely Remote, based on SME analysis				High	

Hazard Description	Known Hazard	New Hazard	Phase of Operation	Possible Effect(s)	Title	Likelihood of Occurrence	Risk Level (only vehicles affected)				
							CESTOL	VLJ	UAS	SST	LCTR
Onboard collision avoidance system fails to timely detect another aircraft on a collision path with the SST.		x	Takeoff, Climb, Cruise, Descent, Approach, Landing, Missed Approach, Go-Around	Loss of separation, NMAC, mid-air	Catastrophic	Extremely Remote, based on SME analysis				High	
Air Traffic Control (ATC) fails to respond to a collision alert between an SST another aircraft.		x	Takeoff, Climb, Cruise, Descent, Approach, Landing, Missed approach, Go-around	Loss of separation, NMAC, mid-air	Catastrophic	Extremely Remote, based on SME analysis				High	
Pilot fails to exercise proper energy management technique with regard to maintaining proper pitch (allowing the aircraft to enter a high pitch/high thrust situation).		x	Approach	Loss of control	Hazardous	Extremely Remote, based on SME analysis				Medium	

Hazard Description	Known Hazard	New Hazard	Phase of Operation	Possible Effect(s)	Title	Likelihood of Occurrence	Risk Level (only vehicles affected)				
							CESTOL	VLJ	UAS	SST	LCTR
Flight crew lacks understanding of the operating capabilities of the SST.		x	All		Hazardous	Extremely Remote, based on SME analysis				Medium	
The operator's pairing of an inexperienced crew.		x	N/A		Hazardous	Extremely Remote, based on SME analysis				Medium	
Aircrafts fails to accomplish speed transition during the approach transition.	x		Approach	NMAC, Mid-air collision	Major	Remote, based on SME analysis	Medium	Medium	Medium	Medium	Medium
Flight crew fails to maintain proper approach speed and sink rate.	x		Approach	Loss of control	Hazardous	Extremely Remote, based on SME analysis	Medium	Medium			
A simultaneous loss of an engine and drive shaft providing redundant power to the engine's		x	All	Loss of control	Catastrophic	Extremely Remote, based on SME analysis					High

Hazard Description	Known Hazard	New Hazard	Phase of Operation	Possible Effect(s)	Title	Likelihood of Occurrence	Risk Level (only vehicles affected)				
							CESTOL	VLJ	UAS	SST	LCTR
prop rotor.											
An undetected flight control software-defect.		x	All	Loss of control	Catastrophic	Extremely Remote, based on SME analysis					High
The LCTR's relatively high disk loading makes auto-rotation more problematic than for equivalent weight helicopter.		x	All	Loss of control	Catastrophic	Extremely Remote, based on SME analysis					High
Automatic flight control system fails during conversion.		x	Approach	Loss of control	Catastrophic	Extremely Remote, based on SME analysis					High

Hazard Description	Known Hazard	New Hazard	Phase of Operation	Possible Effect(s)	Title	Likelihood of Occurrence	Risk Level (only vehicles affected)					
							CESTOL	VLJ	UAS	SST	LCTR	
Loss of conversion capability during flight.		x	All	Runway excursion	Hazardous	Extremely Remote, based on SME analysis						Medium
Negative (aft stick) trim during accelerating transition.		x	All		Catastrophic	Extremely Remote, based on SME analysis						High
A bad signal produced by the flight control system.		x	All	Loss of control	Catastrophic	Extremely Remote, based on SME analysis						High
Aircraft fails to accomplish speed transition during the spiral approach	x		Approach	NMAC, Mid-air collision	Hazardous	Extremely Remote, based on SME analysis	Medium	High				

Hazard Description	Known Hazard	New Hazard	Phase of Operation	Possible Effect(s)	Title	Likelihood of Occurrence	Risk Level (only vehicles affected)				
							CESTOL	VLJ	UAS	SST	LCTR
Aircraft fails to become stabilized on the spiral approach	x		Approach	Loss of control	Hazardous	Extremely Remote, based on SME analysis	Medium	High			
Pilot fails to recognize an off nominal situation developing due to automation complacency.	x		All	Pilot relinquishes management of the flight to the automation	Hazardous	Extremely Remote, based on SME analysis	Medium	High	Medium	Medium	Medium

Appendix H. Summary of Contents for Data DVD

The contents of the DVD Sensis Media #09-1473 included with this report are presented in this section. The names of the directories and a general explanation of the contents is shown next:

- Airport Capacity: This is the airport capacity file used in ACES simulations.
- Airport Taxi: Average taxi-in/taxi out times used in ACES simulations.
- Airspace Capacity: Sector capacity values used in ACES simulations.
- AOC Settings: Airline operations center parameter file used in ACES simulations.
- BADA: Aircraft performance models developed by Georgia Tech in various formats.
- Demand Sets: Flight schedules for each demand year and different trim levels.
- MPAS Files: Aircraft model parameters as used in ACES simulations.
- NY Metroplex Analysis: Documentation of ATAC analysis of NY metroplex.
- NY Procedures: Documentation of ATAC/Georgia Tech analysis of NY metroplex.
- Scenario Files: Marginal weather input file used in ACES weather simulations.
- Software: Software developed by Sensis for simulation output analysis.

The following is a list of the contents for each directory in the DVD:

Directory of D:\Code_Data\NY Metroplex Analysis\Electronic Appendix of Results\

VLJ\Performance\Other Charts

12/03/2009 01:33 PM <DIR> .

12/03/2009 01:33 PM <DIR> ..

09/24/2009 03:54 PM 56,266 Delay Data (VLJ airports only).xlsx

06/23/2009 10:44 AM 31,888 Delay Related Charts 20090623.xlsx

05/19/2009 05:53 PM 28,813 Demand Charts.xlsx

3 File(s) 116,967 bytes

Directory of D:\Code_Data\NY Metroplex Analysis\Electronic Appendix of Results\

VLJ\Performance\Pareto Charts

12/03/2009 01:33 PM <DIR> .

12/03/2009 01:33 PM <DIR> ..

09/24/2009 01:09 PM 461,862 Pareto 2025 CONV format all only.xlsm

09/24/2009 01:08 PM 476,353 Pareto 2025 CONV.xlsm

09/24/2009 01:07 PM 463,952 Pareto 2025 VLJ format all only.xlsm

09/24/2009 01:16 PM 478,925 Pareto 2025 VLJ.xlsm

09/24/2009 01:21 PM 462,049 Pareto 2040 CONV format all only.xlsm

09/24/2009 01:24 PM 477,211 Pareto 2040 CONV.xlsm

09/24/2009 01:25 PM 462,932 Pareto 2040 VLJ format all only.xlsm

09/24/2009 01:27 PM 478,175 Pareto 2040 VLJ.xlsm

09/24/2009 01:29 PM 462,541 Pareto 2086 CONV format all only.xlsm

09/24/2009 01:33 PM 477,849 Pareto 2086 CONV.xlsm

09/24/2009 03:48 PM 491,694 Pareto 2086 VLJ format all only.xlsm

09/24/2009 03:51 PM 478,217 Pareto 2086 VLJ.xlsm

12 File(s) 5,671,760 bytes

Directory of D:\Code_Data\NY Metroplex Analysis\Electronic Appendix of Results\

VLJ\Performance\Results Summary

12/03/2009 01:33 PM <DIR> .

12/03/2009 01:33 PM <DIR> ..

09/24/2009 03:51 PM 10,099 results summary_20090519.xlsx

1 File(s) 10,099 bytes

Directory of D:\Code_Data\NY Metroplex Analysis\Electronic Appendix of Results\

VLJ\Performance\Simulation Files

12/03/2009 01:33 PM <DIR> .

12/03/2009 01:33 PM <DIR> ..

09/24/2009 04:39 PM 28,650,624 NYMetro_NGA_Conv_2025_FT.zip

09/24/2009 04:40 PM 30,064,575 NYMetro_NGA_Conv_2040_FT.zip

09/24/2009 04:51 PM 31,865,021 NYMetro_NGA_Conv_2086_FT.zip

09/24/2009 12:30 PM 29,616,919 NYMetro_NGA_VLJ_2025_FT.zip

09/24/2009 04:00 PM 31,008,633 NYMetro_NGA_VLJ_2040_FT.zip

09/24/2009 04:02 PM 32,878,133 NYMetro_NGA_VLJ_2086_FT.zip

6 File(s) 184,083,905 bytes

Directory of D:\Code_Data\NY_Procedures

12/03/2009 01:36 PM <DIR> .

12/03/2009 01:39 PM <DIR> ..

04/09/2009 03:00 PM 118,272 NYCprocV10.xls

04/09/2009 03:00 PM 32,768 RunwayConfigV10.xls

2 File(s) 151,040 bytes

Directory of D:\Code_Data\Scenario Files

12/03/2009 01:36 PM <DIR> .

12/03/2009 01:39 PM <DIR> ..

03/13/2009 08:31 AM 67,080 weather27June2007.txt

1 File(s) 67,080 bytes

Directory of D:\Code_Data\Software

12/03/2009 01:36 PM <DIR> .

12/03/2009 01:39 PM <DIR> ..

12/03/2009 01:36 PM <DIR> ACES_AEDT

12/03/2009 01:36 PM <DIR> ACES_CTR

12/03/2009 01:36 PM <DIR> SQL

0 File(s) 0 bytes

Directory of D:\Code_Data\Software\ACES_AEDT

12/03/2009 01:36 PM <DIR> .

12/03/2009 01:36 PM <DIR> ..

12/01/2009 12:57 PM 3,722 build.xml

12/03/2009 01:36 PM <DIR> dist_something

12/01/2009 12:57 PM 85 manifest.mf

12/01/2009 12:57 PM 756 master-application.jnlp

12/03/2009 01:36 PM <DIR> nbproject

12/01/2009 12:57 PM 752 preview-application.html

12/03/2009 01:36 PM <DIR> src

12/03/2009 01:36 PM <DIR> test

4 File(s) 5,315 bytes

Directory of D:\Code_Data\Software\ACES_AEDT\dist_something

12/03/2009 01:36 PM <DIR> .

12/03/2009 01:36 PM <DIR> ..

12/01/2009 12:57 PM 6,313,225 ACES_AEDT.jar

12/03/2009 01:36 PM <DIR> lib

12/01/2009 12:57 PM 1,448 README.TXT

2 File(s) 6,314,673 bytes

Directory of D:\Code_Data\Software\ACES_AEDT\dist_something\lib

12/03/2009 01:36 PM <DIR> .

12/03/2009 01:36 PM <DIR> ..

0 File(s) 0 bytes

Directory of D:\Code_Data\Software\ACES_AEDT\nbproject

12/03/2009 01:36 PM <DIR> .

12/03/2009 01:36 PM <DIR> ..

12/01/2009 12:57 PM 37,936 build-impl.xml

12/03/2009 01:36 PM <DIR> configs

12/01/2009 12:57 PM 475 genfiles.properties

12/01/2009 12:57 PM 12,116 jnlp-impl.xml

12/01/2009 12:57 PM 2,649 project.properties

12/01/2009 12:57 PM 832 project.xml

5 File(s) 54,008 bytes

Directory of D:\Code_Data\Software\ACES_AEDT\nbproject\configs

12/03/2009 01:36 PM <DIR> .

12/03/2009 01:36 PM <DIR> ..

12/01/2009 12:57 PM 22 ACES_AEDT.properties

12/01/2009 12:57 PM 173 JWS_generated.properties

2 File(s) 195 bytes

Directory of D:\Code_Data\Software\ACES_AEDT\src

12/03/2009 01:36 PM <DIR> .

12/03/2009 01:36 PM <DIR> ..

12/03/2009 01:36 PM <DIR> com

12/03/2009 01:36 PM <DIR> META-INF

12/01/2009 12:57 PM 328 newhtml.html

1 File(s) 328 bytes

Directory of D:\Code_Data\Software\ACES_AEDT\src\com

12/03/2009 01:36 PM <DIR> .

12/03/2009 01:36 PM <DIR> ..

12/03/2009 01:36 PM <DIR> sensis

0 File(s) 0 bytes

Directory of D:\Code_Data\Software\ACES_AEDT\src\com\sensis

12/03/2009 01:36 PM <DIR> .

12/03/2009 01:36 PM <DIR> ..

12/03/2009 01:36 PM <DIR> rtc

0 File(s) 0 bytes

Directory of D:\Code_Data\Software\ACES_AEDT\src\com\sensis\rtc

12/03/2009 01:36 PM <DIR> .

12/03/2009 01:36 PM <DIR> ..

12/03/2009 01:36 PM <DIR> acesaedt

12/03/2009 01:36 PM <DIR> greatcircle

0 File(s) 0 bytes

Directory of D:\Code_Data\Software\ACES_AEDT\src\com\sensis\rtc\acesaedt

12/03/2009 01:36 PM <DIR> .

12/03/2009 01:36 PM <DIR> ..

12/01/2009 12:57 PM 10,181 Aircraftstatemessage.java

12/01/2009 12:57 PM 9,754 AirportatcscanstatsmessageListofactualfli

ghts.java

12/01/2009 12:57 PM 3,784 DbAccess.java

12/01/2009 12:57 PM 38,781 DbConvert.java

12/01/2009 12:57 PM 5,933 TerminalModelManagementDs.java

12/01/2009 12:57 PM 19,640 UserInterface.form

12/01/2009 12:57 PM 21,703 UserInterface.java

7 File(s) 109,776 bytes

Directory of D:\Code_Data\Software\ACES_AEDT\src\com\sensis\rtc\greatcircle

12/03/2009 01:36 PM <DIR> .

12/03/2009 01:36 PM <DIR> ..

12/01/2009 12:57 PM 6,688 GreatCircleMath.java

12/01/2009 12:57 PM 1,845 Waypoint.java

2 File(s) 8,533 bytes

Directory of D:\Code_Data\Software\ACES_AEDT\src\META-INF

12/03/2009 01:36 PM <DIR> .

12/03/2009 01:36 PM <DIR> ..

12/01/2009 12:57 PM 523,998 ACES_AEDT.dbschema

12/01/2009 12:57 PM 2,859,146 ACES_AEDT_1.dbschema

12/01/2009 12:57 PM 1,021 persistence.xml

3 File(s) 3,384,165 bytes

Directory of D:\Code_Data\Software\ACES_AEDT\test

12/03/2009 01:36 PM <DIR> .

12/03/2009 01:36 PM <DIR> ..

0 File(s) 0 bytes

Directory of D:\Code_Data\Software\ACES_CTR

12/03/2009 01:36 PM <DIR> .

12/03/2009 01:36 PM <DIR> ..

12/01/2009 02:21 PM 3,719 build.xml

12/01/2009 02:21 PM 85 manifest.mf

12/01/2009 02:21 PM 756 master-application.jnlp

12/03/2009 01:36 PM <DIR> nbproject

12/01/2009 02:21 PM 752 preview-application.html

12/03/2009 01:36 PM <DIR> src

12/03/2009 01:36 PM <DIR> test

4 File(s) 5,312 bytes

Directory of D:\Code_Data\Software\ACES_CTR\nbproject

12/03/2009 01:36 PM <DIR> .

12/03/2009 01:36 PM <DIR> ..

12/01/2009 02:21 PM 37,935 build-impl.xml

12/03/2009 01:36 PM <DIR> configs

12/01/2009 02:21 PM 465 genfiles.properties

12/01/2009 02:21 PM 12,116 jnlp-impl.xml

12/01/2009 02:21 PM 2,641 project.properties

12/01/2009 02:21 PM 831 project.xml

5 File(s) 53,988 bytes

Directory of D:\Code_Data\Software\ACES_CTR\nbproject\configs

12/03/2009 01:36 PM <DIR> .

12/03/2009 01:36 PM <DIR> ..

12/01/2009 02:21 PM 22 ACES_AEDT.properties

12/01/2009 02:21 PM 173 JWS_generated.properties

2 File(s) 195 bytes

Directory of D:\Code_Data\Software\ACES_CTR\src

12/03/2009 01:36 PM <DIR> .

12/03/2009 01:36 PM <DIR> ..

12/03/2009 01:36 PM <DIR> com

12/03/2009 01:36 PM <DIR> META-INF

0 File(s) 0 bytes

Directory of D:\Code_Data\Software\ACES_CTR\src\com

12/03/2009 01:36 PM <DIR> .

12/03/2009 01:36 PM <DIR> ..

12/03/2009 01:36 PM <DIR> sensis

0 File(s) 0 bytes

Directory of D:\Code_Data\Software\ACES_CTR\src\com\sensis

12/03/2009 01:36 PM <DIR> .

12/03/2009 01:36 PM <DIR> ..

12/03/2009 01:36 PM <DIR> rtc

0 File(s) 0 bytes

Directory of D:\Code_Data\Software\ACES_CTR\src\com\sensis\rtc

12/03/2009 01:36 PM <DIR> .

12/03/2009 01:36 PM <DIR> ..

12/03/2009 01:36 PM <DIR> aces_ctr

0 File(s) 0 bytes

Directory of D:\Code_Data\Software\ACES_CTR\src\com\sensis\rtc\aces_ctr

12/03/2009 01:36 PM <DIR> .

12/03/2009 01:36 PM <DIR> ..

12/01/2009 02:21 PM 3,784 DbAccess.java

12/01/2009 02:21 PM 16,446 DbConvert.java

12/01/2009 02:21 PM 5,933 TerminalModelManagementDs.java

12/01/2009 02:21 PM 18,455 UserInterface.form

12/01/2009 02:21 PM 20,351 UserInterface.java

5 File(s) 64,969 bytes

Directory of D:\Code_Data\Software\ACES_CTR\src\META-INF

12/03/2009 01:36 PM <DIR> .

12/03/2009 01:36 PM <DIR> ..

12/01/2009 02:21 PM 523,998 ACES_AEDT.dbschema

12/01/2009 02:21 PM 2,859,146 ACES_AEDT_1.dbschema

12/01/2009 02:21 PM 1,021 persistence.xml

3 File(s) 3,384,165 bytes

Directory of D:\Code_Data\Software\ACES_CTR\test

12/03/2009 01:36 PM <DIR> .

12/03/2009 01:36 PM <DIR> ..

0 File(s) 0 bytes

Directory of D:\Code_Data\Software\SQL

12/03/2009 01:36 PM <DIR> .

12/03/2009 01:36 PM <DIR> ..

12/01/2009 04:40 PM 4,156 acesConfig_runwayModel.zip

1 File(s) 4,156 bytes

Total Files Listed:

368 File(s) 1,734,500,967 bytes

237 Dir(s) 0 bytes free

REPORT DOCUMENTATION PAGE

Form Approved
OMB No. 0704-0188

Public reporting burden for this collection of information is estimated to average 1 hour per response, including the time for reviewing instructions, searching data sources, gathering and maintaining the data needed, and completing and reviewing the collection of information. Send comments regarding this burden estimate or any other aspect of this collection of information, including suggestions for reducing this burden to Washington Headquarters Service, Directorate for Information Operations and Reports, 1215 Jefferson Davis Highway, Suite 1204, Arlington, VA 22202-4302, and to the Office of Management and Budget, Paperwork Reduction Project (0704-0188) Washington, DC 20503.
PLEASE DO NOT RETURN YOUR FORM TO THE ABOVE ADDRESS.

1. REPORT DATE (DD-MM-YYYY) 11-01-2010	2. REPORT TYPE Final Report	3. DATES COVERED (From - To) 10 June 2008 – 11 January 2010
--	---------------------------------------	---

4. TITLE AND SUBTITLE Advanced Vehicle Concepts and Implications for NextGen	5a. CONTRACT NUMBER NNA08BA64C
	5b. GRANT NUMBER N/A
	5c. PROGRAM ELEMENT NUMBER N/A
	5d. PROJECT NUMBER N/A
6. AUTHOR(S) Matt Blake Jim Smith Ken Wright Ricky Mediavilla (Sensis Corporation)	5e. TASK NUMBER N/A
	5f. WORK UNIT NUMBER N/A

7. PERFORMING ORGANIZATION NAME(S) AND ADDRESS(ES) Sensis Corporation 85 Collamer Crossings East Syracuse, NY 13057	8. PERFORMING ORGANIZATION REPORT NUMBER 840-023053
---	---

9. SPONSORING/MONITORING AGENCY NAME(S) AND ADDRESS(ES) NASA Ames Research Center Janessa Langford Mail Stop 241-1 Moffett Field, CA 94035-1000 COTR – Harry Swenson M/S 210-15, TM – Philip Arcara M/S 442	10. SPONSOR/MONITOR'S ACRONYM(S) NASA
	11. SPONSORING/MONITORING AGENCY REPORT NUMBER

12. DISTRIBUTION AVAILABILITY STATEMENT

13. SUPPLEMENTARY NOTES

14. ABSTRACT
This study considers the impact of five advanced vehicles: 90-passenger large civil tiltrotors (LCTRs), unmanned aircraft systems (UASs), supersonic civil transports (SSTs), very light jets (VLJs), and cruise-efficient short takeoff and landing vehicles (CESTOLs) on NextGen in the system performance, safety and environmental domains.

15. SUBJECT TERMS

16. SECURITY CLASSIFICATION OF:			17. LIMITATION OF ABSTRACT SAR	18. NUMBER OF PAGES 597	19a. NAME OF RESPONSIBLE PERSON James A Smith
a. REPORT U	b. ABSTRACT U	c. THIS PAGE U			19b. TELEPHONE NUMBER (Include area code) 571-299-1222

1. REPORT DATE. Full publication date, including day, month, if available. Must cite at least the year and be Year 2000 compliant, e.g., 30-06-1998; xx-08-1998; xx-xx-1998.

2. REPORT TYPE. State the type of report, such as final, technical, interim, memorandum, master's thesis, progress, quarterly, research, special, group study, etc.

3. DATES COVERED. Indicate the time during which the work was performed and the report was written, e.g., Jun 1997 - Jun 1998; 1-10 Jun 1996; May - Nov 1998; Nov 1998.

4. TITLE. Enter title and subtitle with volume number and part number, if applicable. On classified documents, enter the title classification in parentheses.

5a. CONTRACT NUMBER. Enter all contract numbers as they appear in the report, e.g. F33615-86-C-5169.

5b. GRANT NUMBER. Enter all grant numbers as they appear in the report, e.g. 1F665702D1257.

5c. PROGRAM ELEMENT NUMBER. Enter all program element numbers as they appear in the report, e.g. AFOSR-82-1234.

5d. PROJECT NUMBER. Enter all project numbers as they appear in the report, e.g. 1F665702D1257; ILIR.

5e. TASK NUMBER. Enter all task numbers as they appear in the report, e.g. 05; RF0330201; T4112.

5f. WORK UNIT NUMBER. Enter all work unit numbers as they appear in the report, e.g. 001; AFAPL30480105.

6. AUTHOR(S). Enter name(s) of person(s) responsible for writing the report, performing the research, or credited with the content of the report. The form of entry is the last name, first name, middle initial, and additional qualifiers separated by commas, e.g. Smith, Richard, Jr.

7. PERFORMING ORGANIZATION NAME(S) AND ADDRESS(ES). Self-explanatory.

8. PERFORMING ORGANIZATION REPORT NUMBER. Enter all unique alphanumeric report numbers assigned by the

performing organization, e.g. BRL-1234; AFWL-TR-85-4017-Vol-21-PT-2.

9. SPONSORING/MONITORS AGENCY NAME(S) AND ADDRESS(ES).

Enter the name and address of the organization(s) financially responsible for and monitoring the work.

10. SPONSOR/MONITOR'S ACRONYM(S). Enter, if available, e.g. BRL, ARDEC, NADC.

11. SPONSOR/MONITOR'S REPORT NUMBER(S). Enter report number as assigned by the sponsoring/ monitoring agency, if available, e.g. BRL-TR-829; -215.

12. DISTRIBUTION/AVAILABILITY STATEMENT.

Use agency-mandated availability statements to indicate the public availability or distribution limitations of the report. If additional limitations/restrictions or special markings are indicated, follow agency authorization procedures, e.g. RD/FRD, PROPIN, ITAR, etc. Include copyright information.

13. SUPPLEMENTARY NOTES. Enter information not included elsewhere such as: prepared in cooperation with; translation of; report supersedes; old edition number, etc.

14. ABSTRACT. A brief (approximately 200 words) factual summary of the most significant information.

15. SUBJECT TERMS. Key words or phrases identifying major concepts in the report.

16. SECURITY CLASSIFICATION.

Enter security classification in accordance with security classification regulations, e.g. U, C, S, etc. If this form contains classified information, stamp classification level on the top and bottom of this page.

17. LIMITATION OF ABSTRACT. This block must be completed to assign a distribution limitation to the abstract. Enter UU (Unclassified Unlimited) or SAR (Same as Report). An entry in this block is necessary if the abstract is to be limited.